



UNIVERSITAT DE  
BARCELONA

## **Safety and efficacy investigations for new prenatal neuroprotective therapies. Applications in a model of intrauterine growth restriction (IUGR)**

Britta Anna Kühne



Aquesta tesi doctoral està subjecta a la llicència **Reconeixement- NoComercial – SenseObraDerivada 4.0. Espanya de Creative Commons.**

Esta tesis doctoral está sujeta a la licencia **Reconocimiento - NoComercial – SinObraDerivada 4.0. España de Creative Commons.**

This doctoral thesis is licensed under the **Creative Commons Attribution-NonCommercial-NoDerivs 4.0. Spain License.**

# DOCTORAL THESIS

to obtain the Doctoral degree at the University of Barcelona  
Doctoral Program in Biomedicine



UNIVERSITAT DE  
BARCELONA

## **Safety and efficacy investigations for new prenatal neuroprotective therapies. Applications in a model of intrauterine growth restriction (IUGR).**

FACULTY OF PHARMACY AND FOOD SCIENCES | DEPARTMENT OF PHARMACOLOGY, TOXICOLOGY  
AND THERAPEUTIC CHEMISTRY | TOXICOLOGY UNIT  
BCNATAL | FETAL MEDICINE RESEARCH CENTER

Britta Anna Kühne

A handwritten signature in blue ink, appearing to read "B. Kühne".

Directors: Dr. Marta Barenys Espadaler

A handwritten signature in blue ink, appearing to read "Marta Barenys Espadaler".

Dr. Míriam Illa Armengol

A handwritten signature in blue ink, appearing to read "Míriam Illa Armengol".

Tutor: Prof. Dr. Juan M Llobet Mallafre

A handwritten signature in blue ink, appearing to read "Juan M Llobet Mallafre".

Barcelona, 06<sup>th</sup> of September 2022



This thesis has been done in the Toxicology Unit of the Faculty of Pharmacy of the University of Barcelona together with the BCNatal group and has been funded by:

Instituto de Salud Carlos III through the project "PI18/01763" (co-funded by European Regional Development Fund, "*A way to make Europe*"), from "LaCaixa" Foundation under grant agreements LCF/PR/GN14/10270005 and LCF/PR/GN18/10310003, and from AGAUR under grant 2017 SGR n° 1531. B.A.K. received a scholarship from Fundació Bosch i Gimpera (project number: 300155). B.A.K. received a grant for short stays from the Montcelimar Foundation 2021 at IUF – Leibniz Research Institute for Environmental Medicine Düsseldorf, Germany between the 1st of October 2021 to the 30th of November 2021.



Science knows no country, because knowledge belongs to humanity,  
and is the torch which illuminates the world.

***Louis Pasteur***



## Acknowledgements

From the beginning of my PhD until today, a whole life seems to have passed. I have gained self-confidence and awareness, scientific knowledge, sense of responsibility, critical thinking, good friends, and memories, thanks to the supervision, support and friendship of several people who made my dissertation possible.

An immense thank you goes to my day-to-day supervisor Dr. Marta Barenys who made the implementation of this work possible by providing the very interesting and future-oriented topic. Because of her I was allowed to take this life path by all means. I see her as an excellent scientist who is very goal-oriented and realistic, and I was very lucky to have her as a supervisor by my side who kept me motivated throughout the whole process. Due to her comprehensive supervision, support, and encouragement during the entire doctoral period, I was able to develop myself professionally and personally to a great extent. I will be forever grateful for all the good discussions, which kept me on track and always inspired me. Without you Marta, I would not be here where I am now, thank you!

A big thank you goes to my supervisor Dr. Miriam Illa, who made the preparation of my PhD thesis possible by providing the interesting and clinically relevant topic. She gave me a direct relation of my topic to the clinic and always taught me to keep the overall view. She enthusiastically guided and supported me throughout the entire time. I am really grateful for her great inspiration and support. Thank you, Miriam!

I would especially like to thank Prof. Joan M. Llobet for his tutorship, which made my dissertation possible.

Another special thank you goes to Prof. Jesús Gomez, who always accompanied me as a working group leader and made my doctoral thesis feasible with great support throughout my entire doctoral period.

I also like to thank Dr. Eduard Gratacós, through whose support the project was made possible.

Many thanks to all my former and current colleagues Laura G., Noelia, Eli, Laia, Laura P., Paula, Mercè, Lara, Estela, Carla, Laura G., Anna M., of the GRET and BCNatal group for the help and support during my entire time and especially for the great working atmosphere with lots of fun and great conversation. A special thanks to Paula, Mercè, Lara and Estela who I had the



pleasure to supervise and who supported me with excellent lab work, many thanks also to Mercè who introduced the best jukebox. It was an incredibly fantastic time in our team, you made my time lively and unforgettable.

Another big thank goes to Prof. Ellen Fritsche and the entire AG Fritsche at IUF in Düsseldorf, through whom my stay abroad was made possible. I learned in relatively short time an incredible number of techniques. I really enjoyed the time and felt immediately comfortable with you, thank you for the great time with lots of fun.

Lastly, and with special honor, I would like to thank Joscha and my parents for their tireless support in every way, for their constant motivation and patience, and above all for the necessary support throughout my studies and doctorate. Thank you Joscha for accepting the many turbulent phases and your great understanding. You have encouraged me to face all challenges with confidence and joy.

Vielen, vielen Dank für alles! Muchísimas gracias por todo! Moltes gràcies per tot!

## Summary

Intrauterine growth restriction (IUGR) is defined as a significant reduction on fetal growth rate, resulting in a birth weight below the 10<sup>th</sup> percentile for the corresponding gestational age (Sharma et al., 2016). The prevalence accounts for 5-10% of all pregnancies, and amounts to approximately 600.000 cases in Europe, being a serious health problem worldwide (Kady and Gardosi, 2004). Placental insufficiency, the main cause of IUGR, chronically decreases the blood flow and nutrient supply to the developing fetus resulting in an adverse intrauterine environment with chronic hypoxia conditions and undernutrition. This situation results to a wide range of changes in brain development including grey (GM) and white matter (WM) injury (Esteban et al., 2010; Pla et al., 2020), which are associated with short- and long-term neurodevelopmental damage and cognitive dysfunctions (Mwaniki et al., 2012; Batalle et al., 2014; Eixarch et al., 2016). The most prevalent causes of brain damage of prenatal origin manifest as subtle neurological abnormalities. Indeed, IUGR has been proposed as the cause of one-quarter of special educational needs postnatally (Mackay et al., 2013). But currently, there is no efficient treatment which avoids deleterious consequences related to IUGR, especially in the neurodevelopmental field.

To better understand, which basic cellular processes of brain development are altered due to IUGR, we established a novel *in vitro* model based on primary rabbit neuronal progenitor cells (NPCs) (Barenys et al., 2021). IUGR was surgically induced in one uterus horn in pregnant rabbits on gestational day (GD) 25. Neural progenitor cells (NPCs) growing as three-dimensional (3D) cell aggregates known as neurospheres were obtained from rabbit pups' brains immediately after caesarean delivery at GD30. Neurospheres are able to mimic basic processes of brain development such as NPC proliferation, migration, differentiation into the brain effector cells neurons, oligodendrocytes and astrocytes, synaptogenesis, and network formation (Barenys et al., 2017; Breier et al., 2010; Gassmann et al., 2010a; Moors et al., 2009, 2007a; Schreiber et al., 2010). We revealed a significantly lower ability to form oligodendrocytes due to a slower differentiation rate in IUGR neurospheres. This result correlates very well with the clinical outcome of IUGR-generated white matter alterations. In addition, IUGR neurospheres presented an increased neurite length, which is consistent with previous *in vivo* studies (Pla et al., 2020). We have discovered for the first time that IUGR neurospheres respond differently than control to the exposure of the compound EGCG, which triggers migration alterations, and we have revealed the mechanism behind this difference: an overexpression of the adhesion molecule Integrin- $\beta$ 1 in IUGR. Because Integrin- $\beta$ 1 is implied in NPC migration but also in axonal growth and neuronal branching, this discovery gives new insights into the characterization of IUGR-induced neurodevelopmental alterations. The thesis addresses the medical necessity by assessing the safety and efficacy of the potential neuroprotective therapies

docosahexaenoic acid (DHA), melatonin (MEL), 3,3',5-triiodothyronine (T3), zinc, lactoferrin (LF) and its main metabolite sialic acid (SA), epigallocatechin gallate (EGCG) and derivatives in two different approaches: (1) exposure *in vitro* and (2) prenatal administration *in vivo*, both followed by the evaluation *in vitro*. DHA, and MEL, were identified as the best therapeutical agents for preventing/reverting impaired oligodendrogenesis caused by IUGR. LF and its main metabolite SA were revealed to reduce IUGR-induced neurite length extension. Finally, we integrated the discovered results about IUGR-induced changes in neurodevelopment into an “adverse outcome pathway” (AOP) approach and developed the putative AOP “Disrupted laminin- $\beta$ 1-integrin interaction leading to developmental neurotoxicity”. Overall, the novel neurosphere model is well suited for characterizing so far unknown neurodevelopmental effects on the cellular level induced by chemicals or IUGR. This new method opens the door to testing possible neuroprotective therapies for IUGR easily and cost-efficiently.

## Abstract

Intrauterine growth restriction (IUGR), a serious health problem worldwide, is defined as a significant reduction in fetal growth rate resulting in a birth weight below the 10<sup>th</sup> percentile for the corresponding gestational age. Placental insufficiency, the leading cause of IUGR, reduces blood flow and nutrient delivery to the developing baby, resulting in short- and long-term brain alterations and cognitive impairment. In this work, we developed for the first time an *in vitro* rabbit neurosphere model based on primary neural progenitor cells (NPCs) that mimics brain development complicated by IUGR. Neurospheres are 3D cell aggregates that represent basic neurodevelopmental processes such as proliferation, migration, differentiation, synaptogenesis, and network formation of NPCs. IUGR neurospheres exhibited a significantly reduced rate of oligodendrocyte differentiation, which correlates very well with the clinical outcome of white matter injury. In addition, neurons in IUGR neurospheres exhibited significantly prolonged neurites. We found that IUGR neurospheres respond differently from control neurospheres to the drug EGCG which induces migration alterations. This difference is due to overexpression of the adhesion molecule integrin- $\beta$ 1, which is involved in NPC migration as well as in axonal growth and neuronal branching. Through toxicological and pharmacological studies, we evaluated the safety and efficacy of potential neuroprotective therapies using the novel *in vitro* rabbit neurosphere model. DHA and MEL were identified as beneficial therapies because of their promoting effects on oligodendrocyte differentiation not only after *in vitro* exposure but also after prenatal administration during rabbit pregnancy. LF and its major metabolite SA reduced the length of elongated neurites because of a possible interaction between integrin- $\beta$ 1 and the extracellular matrix protein laminin. Finally, we integrated the obtained results into an adverse outcome pathway (AOP) by designing the putative AOP "Disrupted laminin- $\beta$ 1-integrin interaction leading to developmental neurotoxicity". Overall, the novel neurosphere model is well suited to rapidly and cost-effectively characterize unknown neurodevelopmental impairments caused by chemicals or IUGR. In future studies, it will also be important to measure the effects and safety of the tested therapies not only in terms of neurodevelopment, but also in terms of general developmental parameters.

## Extracto

El retraso del crecimiento intrauterino (RCIU), un grave problema de salud en todo el mundo, se define como una reducción significativa de la tasa de crecimiento fetal que da lugar a un peso al nacer inferior al percentil 10 para la edad gestacional correspondiente. La insuficiencia placentaria, principal causa del RCIU, reduce el flujo sanguíneo y el aporte de nutrientes al bebé en desarrollo, lo que provoca daños cerebrales y deterioro cognitivo a corto y largo plazo. En este trabajo, desarrollamos por primera vez un modelo de neuroesfera de conejo *in vitro* basado en células progenitoras neurales (CPN) primarias que imita el desarrollo cerebral complicado por RCIU. Las neuroesferas son agregados celulares en 3D capaces de reproducir procesos básicos del neurodesarrollo como la proliferación, la migración, la diferenciación, la sinaptogénesis y la formación de redes de CPNs. Las neuroesferas del grupo RCIU mostraron una tasa significativamente reducida de diferenciación de oligodendrocitos, que se correlaciona muy bien con los resultados clínico que describen lesiones de la materia blanca. Además, las neuronas de las neuroesferas IUGR mostraron neuritas significativamente más largas. Encontramos que las neuroesferas IUGR responden de forma diferente a las neuroesferas control respecto al compuesto EGCG, que induce alteraciones en la migración. Esta diferencia se debe a la sobreexpresión de la molécula de adhesión integrina- $\beta$ 1, que está implicada en la migración de las CNP, así como en el crecimiento axonal y la ramificación neuronal. Mediante estudios toxicológicos y farmacológicos, evaluamos la seguridad y eficacia de potenciales terapias neuroprotectoras utilizando el novedoso modelo de neuroesfera de conejo *in vitro*. El DHA y la MEL se identificaron como terapias beneficiosas por sus efectos promotores de la diferenciación de los oligodendrocitos no sólo tras la exposición *in vitro*, sino también tras la administración prenatal durante la gestación en conejo. La LF y su principal metabolito SA redujeron la longitud de las neuritas debido a una posible interacción entre la integrina- $\beta$ 1 y la proteína de la matriz extracelular laminina. Finalmente, integramos los resultados obtenidos en una "adverse outcome pathway" (AOP) diseñando el AOP putativo "Disrupted laminin- $\beta$ 1-integrin interaction leading to developmental neurotoxicity". En general, el nuevo modelo de neuroesferas resulta muy adecuado para caracterizar de forma rápida y rentable las alteraciones desconocidas del neurodesarrollo causadas por sustancias químicas o por la RCI. En futuros estudios, también será importante medir los efectos y la seguridad de las terapias probadas no sólo en términos de neurodesarrollo, sino también en términos de parámetros generales de desarrollo.

## Acronyms

|                  |  |
|------------------|--|
| 3D               | Three-dimensional  |
| 3R               | Replacement, refinement, and reduction   |
| A2B5             | Cell surface ganglioside epitope A2B5  |
| AO               | Adverse outcome  |
| AOP              | Adverse outcome pathway  |
| BBB              | Blood- brain barrier   |
| CA               | Cornu ammonis  |
| CC               | Corpus callosum  |
| CNPase           | 2',3'-Cyclic-nucleotide 3'-phosphodiesterase   |
| CNS              | Central nervous system   |
| C-section        | Cesarean-section   |
| CTB              | Cell titer blue  |
| D                | Decile   |
| DG               | Dentate gyrus  |
| DHA              | Docosahexaenoic acid   |
| DIO2             | Type II iodothyronine deiodinase   |
| DNT              | Developmental neurotoxicity  |
| EC               | Effective concentration  |
| ECM              | Extracellular matrix   |
| EFSA             | European Food Safety Authority   |
| EGCG             | Epigallocatechin gallate   |
| EGF              | Epidermal growth factor  |
| EPA              | U.S. Environmental Protection Agency   |
| ERK1/2           | Extracellular signal-regulated kinases   |
| FCS              | Fetal calf serum   |
| FGF              | Fibroblast growth factor   |
| Fig.             | Figure   |
| G37              | 1,4-bis[(3,4,5-trihydroxybenzoyl)oxy]naphthalene   |
| G56              | 4,4'-bis[(3,4,5-trihydroxybenzoyl)oxy]-1,1'-biphenyl   |
| GalC             | Galactocerebroside   |
| Gcl              | Granule cell layer   |
| GD               | Gestational day  |
| GFAP             | Glial fibrillary acidic protein  |
| GM               | Grey matter  |
| GW               | Gestational week   |
| HIE              | Hypoxia-ischemia   |
| IATA             | Integrated approaches to testing and assessment  |
| IC <sub>50</sub> | Half maximal inhibitory concentration  |
| ICH              | International Conferences on Harmonization of technical requirements for pharmaceuticals for human use |
| ICH-E            | ICH efficacy guideline   |
| ICH-M            | ICH multidisciplinary guideline  |
| ICH-Q            | ICH quality guideline  |
| ICH-S            | ICH safety guideline   |
| IF               | Impact factor  |
| IQ               | Intelligence quotient  |

|                |  |
|----------------|--|
| IUGR           | Intrauterine growth restriction                          |
| IVB            | In vitro battery   |
| IVH            | Intraventricular hemorrhage                              |
| KE             | Key event  |
| KER            | Key event relationship                                   |
| LF             | Lactoferrin  |
| LOAEL          | Lowest observed adverse effect level                     |
| M1             | 4-hydroxy-2-naphthyl 3,4,5-trihydroxybenzoate            |
| M2             | 3-hydroxy-1-naphthyl 3,4,5-trihydroxybenzoate            |
| MAG            | Myelin associated glycoprotein                           |
| MBP            | Myelin basic protein                                     |
| MCT8           | Monocarboxylate transporter 8                            |
| MEA            | Microelectrode array                                     |
| mEC            | Most effective concentration                             |
| MEL            | Melatonin  |
| MIE            | Molecular initiating event                               |
| MI             | Molecular layer  |
| MoA            | Mode of action   |
| MOG            | Myelin-oligodendrocyte glycoprotein                      |
| MoS            | Margin of safety   |
| MRI            | Magnetic resonance imaging                               |
| MTC            | Maximum tolerated concentration                          |
| Nano-EGCG      | EGCG PEGylated-PLGA nanoparticles                        |
| NCC            | Neural crest cell  |
| NG2            | Neuron-glia antigen 2                                    |
| NGO            | Non-governmental organization                            |
| Nkx2.2         | NK2 homeobox 2   |
| NOAEL          | No observed adverse effect level                         |
| NPCs           | Neural progenitor cells                                  |
| O1             | Oligodendrocyte Marker 1                                 |
| O4             | Oligodendrocyte Marker 4                                 |
| OA             | Open access  |
| OECD           | Organisation for Economic Co-operation and Development   |
| Olig1          | Oligodendrocyte lineage gene 1                           |
| Olig2          | Oligodendrocyte lineage gene 2                           |
| OLs            | Oligodendrocytes   |
| OPC            | Oligodendrocyte precursor cell                           |
| Pcl            | Pyramidal cell layer                                     |
| PDGFR $\alpha$ | Platelet-derived growth factor receptor A                |
| PDL            | Poly-D-Lysin   |
| PEG            | Polyethylene glycol                                      |
| PEGylated-PLGA | Polyethylene glycosylated poly (lactic-co-glycolic acid) |
| PLP            | Proteolipid protein                                      |
| PND            | Postnatal day  |
| PVL            | Periventricular leukomalacia                             |
| Q              | Quartile   |
| qAOP           | Quantitative AOP   |

|         |  |
|---------|--|
| qRT-PCR | Quantitative reverse transcription polymerase chain reaction |
| SA      | Sialic acid  |
| SC      | Solvent control  |
| Sgz     | Subgranular zone   |
| SO      | Stratum oriens   |
| SOX10   | Sry-related HMg-Box gene 10                                  |
| SR      | Stratum radiatum   |
| SVZ     | Subventricular zone  |
| T3      | 3,3',5-triiodothyronine                                      |
| T4      | Thyroxine  |
| TG      | Test guideline   |
| TH      | Thyroid hormone  |
| TI      | Therapeutic index  |
| UA      | Umbilical artery   |
| VC      | Vehicle control  |
| VZ      | Ventricular zone   |
| w/o     | Without  |
| WHO     | World Health Organization                                    |
| WM      | White matter   |
| WMI     | White matter injury  |





# Index

|       |  |     |
|-------|--|-----|
| 1     | Introduction.....  | 1   |
| 1.1   | Brain development .....  | 1   |
| 1.2   | Intrauterine growth restriction (IUGR).....  | 4   |
| 1.2.1 | Neurodevelopmental damage induced by IUGR.....   | 6   |
| 1.3   | Models of IUGR induced neurodevelopmental effects.....   | 8   |
| 1.3.1 | Rabbit IUGR model.....   | 8   |
| 1.3.2 | In vitro neurosphere model.....  | 10  |
| 1.4   | Neuroprotective strategies.....  | 12  |
| 1.4.1 | Current neuroprotective strategies .....   | 12  |
| 1.4.2 | Safety and efficacy testing.....   | 13  |
| 1.4.3 | Potential neuroprotective therapies.....   | 18  |
| 2     | Objectives of the thesis.....  | 23  |
| 3     | Material and methods .....   | 24  |
| 3.1   | Protocols for the evaluation of neurodevelopmental alterations in rabbit models in vitro and in vivo .....   | 26  |
| 4     | Results.....   | 52  |
| 4.1   | Structural Brain Changes during the Neonatal Period in a Rabbit Model of Intrauterine Growth Restriction.....  | 52  |
| 4.2   | Rabbit neurospheres as a novel in vitro tool for studying neurodevelopmental effects induced by intrauterine growth restriction.....                             | 67  |
| 4.3   | Docosahexaenoic Acid and Melatonin Prevent Impaired Oligodendrogenesis Induced by Intrauterine Growth Restriction (IUGR) .....                                   | 82  |
| 4.4   | Lactoferrin prevents adverse effects of intrauterine growth restriction (IUGR) on neurite length: investigations in an in vitro rabbit neurosphere model.....    | 102 |
| 4.5   | Comparison of migration disturbance potency of epigallocatechin gallate (EGCG) synthetic analogs and EGCG PEGylated PLGA nanoparticles in rat neurospheres ..... | 131 |
| 4.6   | Application of the adverse outcome pathway to identify changes in prenatal brain programming after exposure to EGCG .....  | 143 |

|  |     |
|--|-----|
| Summary of results .....   | 182 |
| Supervisors' report.....   | 185 |
| 5 Discussion .....   | 189 |
| 5.1 The need of new prenatal therapies.....  | 189 |
| 5.2 The rabbit in vitro neurosphere model .....  | 190 |
| 5.3 Effects of IUGR on brain development.....  | 192 |
| 5.4 Potential therapies.....   | 193 |
| 5.5 Shifting from <i>in vivo</i> to <i>in vitro</i> in DNT .....   | 196 |
| 5.6 Integration of results in an AOP framework .....   | 196 |
| 5.7 Extrapolation from in vitro to in vivo in human .....  | 198 |
| 6 Conclusions.....   | 200 |
| 7 References.....  | 202 |
| 8 Annex .....  | 226 |
| 8.1 Docosahexaenoic acid and lactoferrin effects on the brain and placenta in a rabbit model of<br>intrauterine growth restriction .....   | 226 |
| 8.2 Epigallocatechin-3-gallate PEGylated poly(lactic-co-glycolic) acid nanoparticles mitigate striatal<br>pathology and motor deficits in 3-nitropropionic acid intoxicated mice.....  | 255 |
| 8.3 Dual-drug loaded nanoparticles of Epigallocatechin-3-gallate (EGCG) / Ascorbic acid enhance<br>therapeutic efficacy of EGCG in a APPswe/PS1dE9 Alzheimer's disease mice model..... | 284 |
| 8.4 Literature review and appraisal on alternative neurotoxicity testing methods .....   | 300 |
| 8.5 Summary of short stay abroad .....   | 305 |

# 1 Introduction

## 1.1 Brain development

Brain development is one of the most sensitive and vulnerable processes during fetal development and is influenced by environmental and external factors from the first day of neurogenesis. Therefore, understanding brain development is crucial to recognize neural disturbances which may manifest in neurobehavioral disorders throughout life (Linderkamp et al., 2009; Mwaniki et al., 2012).

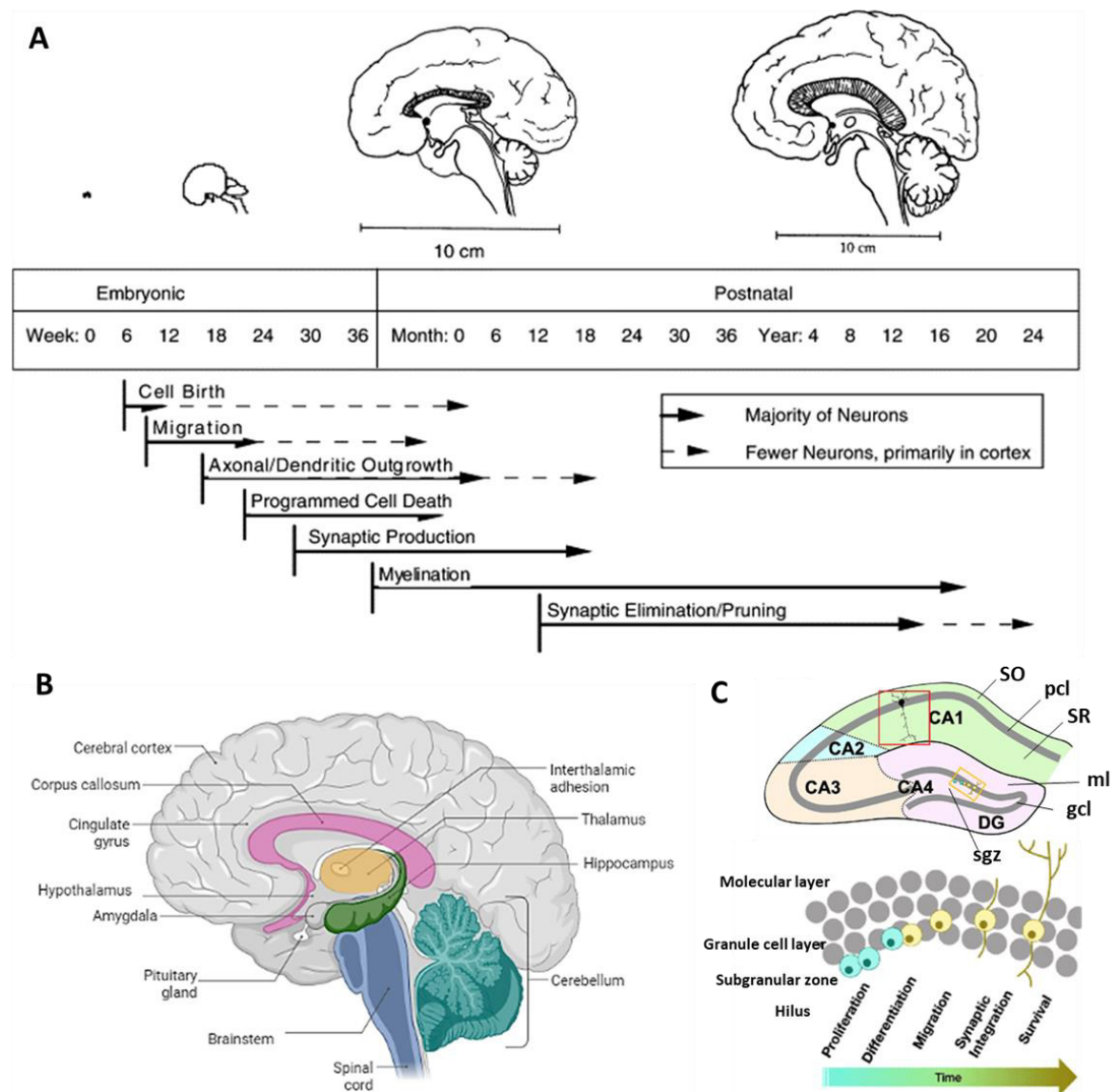


**Figure 1. A)** The stages of human brain development from Andersen (2003). **B)** Schematic lateral cross-section of a mature human brain with different brain regions indicated. Pink: Corpus callosum, yellow: Thalamus, green: Hippocampus, blue: Brainstem, cyan: Cerebellum, created in Biorender.com. **C) Upper part:** Illustration of the major sections of the hippocampus including dentate gyrus (DG) and cornu ammonis (CA) with its distinct subareas CA1-CA4; red box: CA1 pyramidal neuron with apical dendrites in stratum radiatum (SR) and basal dendrites in SO (stratum oriens). **Lower part:** Illustration of neurogenesis stages of granule neurons in the DG (yellow box in upper illustration); modified from Sheppard et al. (2019). DG: dentate gyrus; CA: cornu ammonis SO: stratum oriens; SR: stratum radiatum of CA sections; pcl, pyramidal cell layer of CA sections; gcl, granule cell layer of the DG; sgz: subgranular zone of the DG; ml: molecular layer.

Brain development is a highly controlled process, including complex and strictly regulated molecular and cellular processes lasting from the early embryonic phase until adolescence (Fig. 1, (Silbereis et al., 2016; Stiles and Jernigan, 2010)). Already after three gestational weeks in humans, the first brain structures are built with the formation of the neural plate (Stiles and Jernigan, 2010). The fusion of neural folds leading to the emergence of the neural tube is described as the starting point of early neurogenesis, which will develop after massive proliferation five vesicles of the future brain: telencephalon, diencephalon, mesencephalon, metencephalon and myelencephalon (Linderkamp et al., 2009). During these early vesicle stages, the wall of the neural tube comprises the ventricular zone (VZ) that builds a layer of neuroepithelial cells, a type of primary neural progenitors from which all neurons and microglia of the central nervous system (CNS) including astrocytes and oligodendrocytes (OLs) derive (Silbereis et al., 2016). During the expansion time, neuroepithelial cells generate apical radial glial cells attached to the basal lamina, which undergo mitotic symmetric or asymmetric divisions (Fernández et al., 2016). The symmetric differentiation includes the division into two neurons while the asymmetric division produces either new apical radial glial cells or progenitor cells that differentiate into neurons or glial cells (Fernández et al., 2016; Huttner and Kosodo, 2005). At this timepoint, a further neurogenic proliferative compartment generates young neurons expanding above the VZ to the subventricular zone (SVZ) (Silbereis et al., 2016). Radial glial cells extend very long processes through the SVZ developing a scaffold of glial fibers, which allows young neurons to travel to distant positions along the cortical surface, this process is called radial migration (Borrell and Götz, 2014; Fernández et al., 2016). Migrating neurons arriving at the cortical plate forming six deep-seated cortical layers containing different types of neurons, whereas subsequent migrating neurons construct more superficial layers of the cortex (Stiles and Jernigan, 2010). Once neurons have migrated to their final location, they detach from radial fibers and continue to differentiate. Immature neocortical neurons begin to extend axons and elaborate complex dendritic branching followed by synaptogenesis and axon myelination to build a neuronal network (Silbereis et al., 2016; Stiles and Jernigan, 2010). Synaptogenesis follows a specific spatiotemporal sequence and continues during the first 2 postnatal years with rapid formation and overproduction of synapses with an ensuing refinement of synaptic connections by elimination and pruning (Susan L. Andersen, 2003; Silbereis et al., 2016). Whereas neural progenitor cells (NPCs) from the SVZ differentiate into multiple distinct neuronal subtypes, radial glial cells in the central brain area ‘hippocampus’ develop a single type of neurons, the granule neurons (Rolando and Taylor, 2014). The hippocampus is located in the inner region of the temporal lobe, which belongs to the limbic system responsible for learning, memory, and spatial navigation as well as regulation of emotional reactions (Yassa, 2020). A detailed description of hippocampus’ anatomy is illustrated in Fig. 1C. The neurogenesis of hippocampal granule neurons is dynamic and responds to physiological and pathological stimuli throughout life (Rolando and Taylor, 2014).

Astrocytes and OL precursor cells (OPCs) are derived from radial glial cells in mid-gestation, whereas OLs migrate and mature predominantly during the first 3 postnatal years in humans (Howard et al., 2008; Jakovcevski et al., 2009). Postnatally, glial progenitor cells proliferate while migrating outwards into overlying white matter (WM) and cortex, striatum, and hippocampus where they continue to differentiate into astrocytes and OPC (Stiles and Jernigan, 2010). OLs are myelinating cells with filamentous myelin wrapping and isolating axons from neurons, mainly found in the developing WM and less abundant in grey matter (GM) of the brain cortex (Kuhn et al., 2019). OLs undergo several maturation stages until they reach their postmitotic myelinating stage guided by axonal and/or astrocytic signals (Baumann and Pham-Dinh, 2001). The OL lineage begins with OPCs developing Pre-OLs over immature OL to non-myelinating mature OLs until myelinating mature OLs recognized by markers specific for different maturation stages (Fig. 2, (Jakovcevski et al., 2009; Kuhn et al., 2019)).

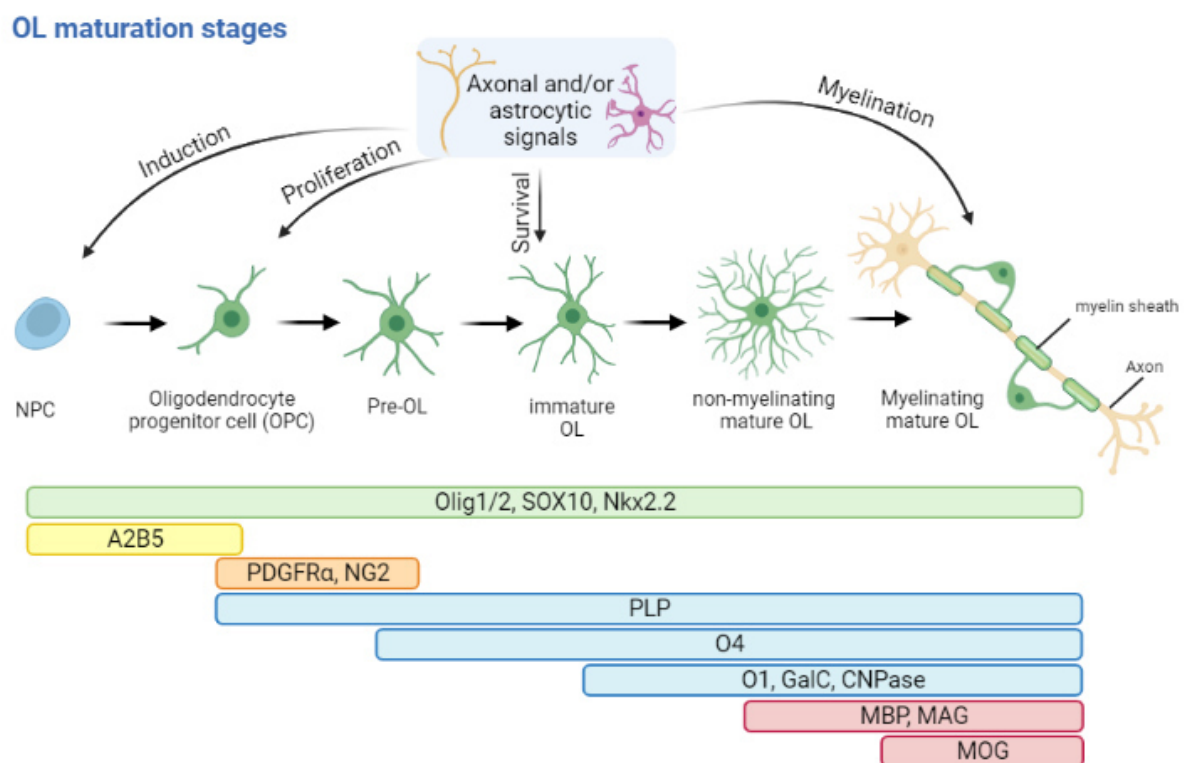


**Figure 2.** Oligodendrocyte (OL) maturation stages from neuronal progenitor cells (NPCs) until myelinating mature OL including lineage marker and axonal and astrocytic signals. *Olig1* and *2*, *Sox10* and *Nkx2.2* are expressed in all stages of the OL lineage. *A2B5* is expressed only in NPC and OPC, while *PDGFR $\alpha$*  and *NG2* are early markers for OPC and Pre-OL. *PLP*, *O4*, *O1*, *GalC* and *CNPase* are involved in the differentiation phase from progenitor to mature OLs. The marker *MBP* is already expressed in mature pre-myelinating OLs, while *MOG* is only expressed in the late mature myelinating OLs. NPC: neuronal progenitor cell; OPC: oligodendrocyte progenitor cell; OL: oligodendrocyte; *PDGFR $\alpha$* : platelet-derived growth factor receptor A; *NG2*: neuron-glia antigen 2; *PLP*: proteolipid protein; *CNPase*: 2',3'-Cyclic-nucleotide 3'-phosphodiesterase; *MBP*: myelin basic protein; *MAG*: myelin associated glycoprotein; *MOG*: myelin-oligodendrocyte glycoprotein; *GalC*: galactocerebroside. Created in Biorender.com; adapted from (Barateiro and Fernandes, 2014; Baumann and Pham-Dinh, 2001; Kuhn et al., 2019).

As mentioned, embryonic brain development is a highly regulated process controlled by multiple factors and cellular mechanisms acting as signaling pathways, second messengers, or receptors, consistent with specific spatiotemporal expression patterns of transcription factors. Each developmental process of the brain is especially susceptible towards external stimuli and already a minor impact of chemicals or diseases might lead to enormous adverse outcomes (Grandjean and Landrigan, 2014; Mwaniki et al., 2012; Volpe, 2000).

## 1.2 Intrauterine growth restriction (IUGR)

Intrauterine growth restriction (IUGR) is a significant health issue worldwide with a prevalence of 5-10% of all pregnancies, approximately 30 million newborns worldwide and 600.000 cases in Europe (Kady and Gardosi, 2004; Tolcos et al., 2017). It is defined as a significant reduction of the fetal growth rate leading to a birth weight below the 10<sup>th</sup> percentile for the corresponding gestational age and is one of the most common causes of poor perinatal and long-term outcomes (Figueras and Gratacos, 2017; Sharma et al., 2016).

Causes of IUGR include maternal, fetal, placental, or genetic reasons or a combination of these factors (Sharma et al., 2016). Maternal factors comprise the age of the mother, smoking, maternal health, infection, or previous pregnancy affected with IUGR (Sharma et al., 2016). There is also a strong association with early-onset IUGR resulting secondary to maternal preeclampsia, which is defined by an increased diastolic blood pressure (Figueras and Gratacos, 2017; Figueras and Gratacós, 2014; Marasciulo et al., 2021; Pedroso et al., 2018). Fetal factors include chromosomal abnormalities, multiple gestation, or congenital infections (HIV, Syphilis, Malaria) (Sharma et al., 2016). However, the main cause of IUGR is placental insufficiency, which chronically reduces the blood flow and nutrient supply to the fetus leading to fetal development under chronic hypoxia. Fetal umbilical cord oxygen is related to the babies' birth size and is classified as a primary determinant of fetal growth (Lackman et al., 2001). This fetal condition of malnutrition impacts ultimately organogenesis and is associated with short- and long-term neurodevelopmental damage, cognitive dysfunctions and cardiovascular adverse outcomes (Batalle et al., 2014; Eixarch et al., 2016). The impaired placentation is commonly identified by serial ultrasound as abnormal uterine arteries or umbilical artery (UA) Doppler studies (Figueras and Gratacos, 2017). An abnormal UA Doppler pulsatility index reflects an increased restricted blood flow in the umbilical circulation and is an indicator of placental disease (Lees et al., 2022).

The terms early- and late-onset IUGR are used to subclassify two phenotypes of IUGR characterized by onset, fetoplacental Doppler, association with preeclampsia and severity, which are summarized in table 1. Early-onset IUGR represents 20-30% and late-onset 70-80% of all IUGR cases (Crovetto et al.,

2014). The optimal cut-off between early- and late onset IUGR was established at 32 gestational weeks discriminated by abnormal and normal UA Doppler (Gordijn et al., 2016; Savchev et al., 2014). The Early-onset form is highly associated with severe placental insufficiency and chronic fetal hypoxia with abnormal UA Doppler. Immature fetuses tend to have a higher tolerance to hypoxia and a better systemic cardiovascular adaptation than late-onset cases. However, the latency of severe deterioration can last for weeks, which is displayed in severe Doppler changes, leading to decompensated hypoxia and acidosis (Figueras and Gratacós, 2014; Turan et al., 2008). The decision of keeping the fetus in utero or dealing with complications of prematurity has to be carefully considered and remains an immense clinical challenge (Figueras and Gardosi, 2011; Figueras and Gratacós, 2014). Late-onset IUGR is linked with mild placental disease presented in normal UA Doppler, and it is rarely associated with preeclampsia. Despite normal UA Doppler, 25% of all late IUGR cases develop advanced brain vasodilation indicating chronic hypoxia, which has been detected by Middle Cerebral Artery Doppler (Oros et al., 2011). In late-onset IUGR, a progressive fetal deterioration with clear changes in UA Doppler is absent (Cruz-Martinez et al., 2011; Oros et al., 2011) and a 'natural history' to identify first signs of the disease is usually lacking, which makes the detection complicated. Before term, there is a high risk of acute hypoxic deterioration leading to severe injury, neonatal acidosis, or even fetal death (Kady and Gardosi, 2004). This may explain the lower tolerance to hypoxia in mature fetus compared to early-onset cases. Even though late-onset IUGR has a lower mortality in comparison to early-onset IUGR, it is responsible for several late stillbirths due to its high prevalence (Crovetto et al., 2014; Gardosi et al., 2005). The clinical challenge of IUGR in late gestation remains the diagnosis, however abnormalities of UA Doppler (absent or reversed end-diastolic velocities) have been demonstrated to be visible approximately one week before acute deterioration (Ferrazzi et al., 2002; Figueras and Gratacós, 2014). Fetus' with these Doppler abnormalities after 30 gestational weeks are at higher risk of mortality than at risk of prematurity (Cruz-Lemini et al., 2012; GRIT Study Group, 2003), and thus premature delivery is suggested (Figueras and Gratacós, 2014).

**Table 1.** Summary of the main differences between early- and late-onset IUGR. Adapted from (Figueras et al., 2018; Figueras and Gratacós, 2014).

| <b>Early-onset IUGR</b>   | <b>Late-onset IUGR</b>   |
|---|--|
| Incidence of all IUGR cases: 20-30%   | Incidence of all IUGR cases: 70-80%  |
| Challenge: management (gestational age at delivery)                                 | Challenge: detection and diagnosis   |
| Placental disease: severe (UA Doppler abnormal, high association with preeclampsia) | Placental disease: mild (UA Doppler normal, low association with preeclampsia) |
| Hypoxia +/+ : systemic cardiovascular adaptation                                    | Hypoxia +/- : central cardiovascular adaptation                                |



|   |   |
|---|---|
| Immature fetus = higher tolerance to hypoxia =<br>natural history | Mature fetus = lower tolerance to hypoxia =<br>(or very short) natural history                    |
| Higher mortality/morbidity; lower prevalence                      | Lower mortality/morbidity, but high prevalence<br>= large etiological fraction of adverse outcome |

Despite remarkable differences in the severity of early- and late-onset IUGR caused by placental diseases, both are associated with neurodevelopmental, cardiovascular and metabolic (e.g. insulin secretion) adverse outcomes (Crispi et al., 2010; Larroque et al., 2001; Van Vliet et al., 2012; Verkauskiene et al., 2008). Therefore, it is crucial to early diagnose, monitor and, hopefully, find a potential therapy that could mitigate or even prevent the long-lasting consequences of IUGR.

### 1.2.1 Neurodevelopmental damage induced by IUGR

Placental insufficiency induces a reduction of the quantity of nutrients that reach the fetus, as well as hypoxia, which can be followed in severe IUGR cases by fetal acidosis (Bernstein et al., 2000). IUGR babies have an increased risk of neurodevelopment impairment (Geva et al., 2006; Tolcos et al., 2017), as shown by follow-up studies where half of the cases exhibited neurological alterations (Fouron et al., 2001) with higher or lower severity depending on the IUGR grade and onset. For example the risk of developing cerebral palsy, correlates with the severity of IUGR of both early- and late-onset cases (Baschat, 2014; Blair and Nelson, 2015; Jacobsson et al., 2008; Miller et al., 2016). Early-onset IUGR cases tend to have the most severe cases and usually encompass serious neurodevelopmental disorders, with clinical manifestations such as neonatal encephalopathy related to hypoxia-ischemia (HIE), intraventricular hemorrhage (IVH) or periventricular leukomalacia (PVL) manifesting in cerebral palsy (Fleiss et al., 2021; Miller et al., 2016). In contrast, late IUGR commonly results in mild cases that are related to subtle neurodevelopmental insults. Alterations on attention, habituation, emotional state regulation or a reduced social competence have been reported within the neonatal period until 2 years of age (Eixarch et al., 2008; Figueras et al., 2009; Oros et al., 2010; Tolsa et al., 2004). However, long term effects have been described in early and late IUGR associated with memory disorders, learning difficulties, low academic performance, lack of attention and psychosocial alterations (O’Keeffe et al., 2003), plus a higher risk to develop attention deficit hyperactivity disorder (Heinonen et al., 2010). Indeed, IUGR is considered altogether with brain prematurity, as a condition that requires special education needs (Fischi-Gómez et al., 2015; Larroque et al., 2001; Mackay et al., 2013; Van Vliet et al., 2012).

Recent clinical studies have used advanced imaging (magnetic resonance imaging (MRI) or spectroscopy) to investigate the structural correlation among neurodevelopmental anomalies. These

studies in IUGR patients have unraveled changes in the formation of cortical sulcation (Egaña-Ugrinovic et al., 2013), cortex morphology, connectivity (Batalle et al., 2012) and brain metabolism (Sanz-Cortés et al., 2010). Studies confirmed that the connectivity in motor and cortico-striatal-thalamic networks of 1 and 6 aged kids is altered, which correlates with poor development of motor, cognitive and social behavior (Eixarch et al., 2016; Fisci-Gómez et al., 2015; Tolcos et al., 2017). The implications for learning and memory in IUGR children might be due to a reduced cortical GM and hippocampal volume (Lodygensky et al., 2008; Padilla et al., 2014; Tolsa et al., 2004). Certain neuronal populations such as hippocampal or cortex neurons are believed to be particularly susceptible to IUGR. In a rat model of IUGR, Gilchrist et al. (2018), revealed a reduced number of neurons and morphological alterations in the GM of the hippocampus (Gilchrist et al., 2018). This neuronal anomalies may be related to a synapsis alteration as well as density and morphology of the dendritic spines as seen in the hippocampus of growth restricted guinea pigs and rabbits, both in neonatal and long-term stage (Dieni and Rees, 2003; Illa et al., 2018; Piorkowska et al., 2014). In contrast to the poor neuronal outcome in the hippocampus, Pla et al. discovered a more advanced dendritic branching of neurons in the frontal cortex of IUGR rabbit brains (Pla et al., 2020). Another study using the same rabbit model, identified reduced fractional anisotropy in cortical brain regions of IUGR rabbits (Eixarch et al., 2012a), which is associated with an advanced dendritic arborization (McKinstry et al., 2002). In a follow-up study in adult rats, decreased dendritic branching was described after acute ischemic hypoxia, whereas shortly after the hypoxia event, dendritic branching increased, which may indicate a compensatory effect (Ruan et al., 2006).

Besides of GM alterations, IUGR is related to WM impairment, which has been described in several animal models (Eixarch et al., 2012b; Olivier et al., 2005; Reid et al., 2012; Rideau Batista Novais et al., 2016; Tolcos et al., 2011). MRI of IUGR babies born at term confirmed a reduced WM volume and delayed myelination (Ramenghi et al., 2011). In the situation of fetal hypoxia, newly generated pre-OLs often fail to myelinate despite a numerous presence of axon signals (Stephen A Back, 2017), because OPCs and pre-myelinating OLs present a lower level of antioxidant enzymes and are especially susceptible to oxidative stress compared to mature OLs (Back et al., 2002a). During brain development the population of these early staged OLs is particularly high, which in turn is associated with a high risk of OL impairment often resulting in diffuse white matter injury (WMI) (Stephen A Back, 2017). Hypoxic-ischemic or placental insufficiency resulting in WMI is still a leading cause of brain injury in premature babies and the principal feature of PVL and cerebral palsy (Back, 2001). However, OPCs continue to be produced throughout intra-uterine until postnatal life (Bergles and Richardson, 2016; Jakovcevski et al., 2009) and it is presumed that an endogenous pool of OPCs remains available to therapeutically support OL impairment (Tolcos et al., 2017).

Currently, there is no efficient treatment to avoid the described deleterious consequences related to IUGR, especially in the neurodevelopmental field. Therefore, the characterization of neurostructural changes in fetus with IUGR is essential to design therapeutic strategies directed to limit its adverse effects.

### 1.3 Models of IUGR induced neurodevelopmental effects

Reproducing human conditions of IUGR in a laboratory remains a scientific challenge and thus, animal models are crucial to improve our understanding about neurostructural and cellular changes related to IUGR. Several models mimicking placental insufficiency have been developed including rats (Delcour et al., 2012; Gilchrist et al., 2018; Reid et al., 2012), guinea pig (Dieni and Rees, 2003; Piorkowska et al., 2014; Tolcos et al., 2011), rabbits (Eixarch et al., 2009) and sheep (Miller et al., 2014). Even though efforts have arisen to develop IUGR models, there is a huge lack of reliable systems mimicking the spatiotemporal neurodevelopmental processes to characterize and better understand the mechanisms of IUGR induced brain alterations (reviewed by (Fleiss et al., 2019)). The pre- and perinatal neurodevelopment requires a perfect coordination of the basic processes of neurogenesis, such as proliferation, migration, differentiation and organization of neurons, formation of synapsis, myelination and finally, establishment of neuronal networks (Fritsche et al., 2018a; Stiles and Jernigan, 2010). In this thesis, we developed for the first time a novel *in vitro* rabbit neurosphere system to untangle the obscure processes of IUGR related brain injury and to improve neurological sequelae.

#### 1.3.1 Rabbit IUGR model

To have a human-relevant experimental model of neurodevelopmental damage induced by IUGR, the BCNatal research group developed an IUGR model in pregnant rabbits (Eixarch et al., 2009). The species rabbit was chosen due to its similarity to human placentation and perinatal brain development (Barenys et al., 2021; Drobyshevsky et al., 2014; Workman et al., 2013). The placenta of rabbits is discoid, villous, and hemochorial similar to humans (Carter, 2007). Besides, it was previously proven that rabbits reflect better the brain maturation observed in humans than other species (Workman et al., 2013). The degree of brain maturation at birth determined with the precocial score according to 271 neuronal events compared between 18 mammalian species accounts for 54% in rabbits, which is more similar to human (65%) than other species (45% in rats, 84% in guinea pig and 82% in sheep, Fig. 3) (Pla et al., 2020; Workman et al., 2013).

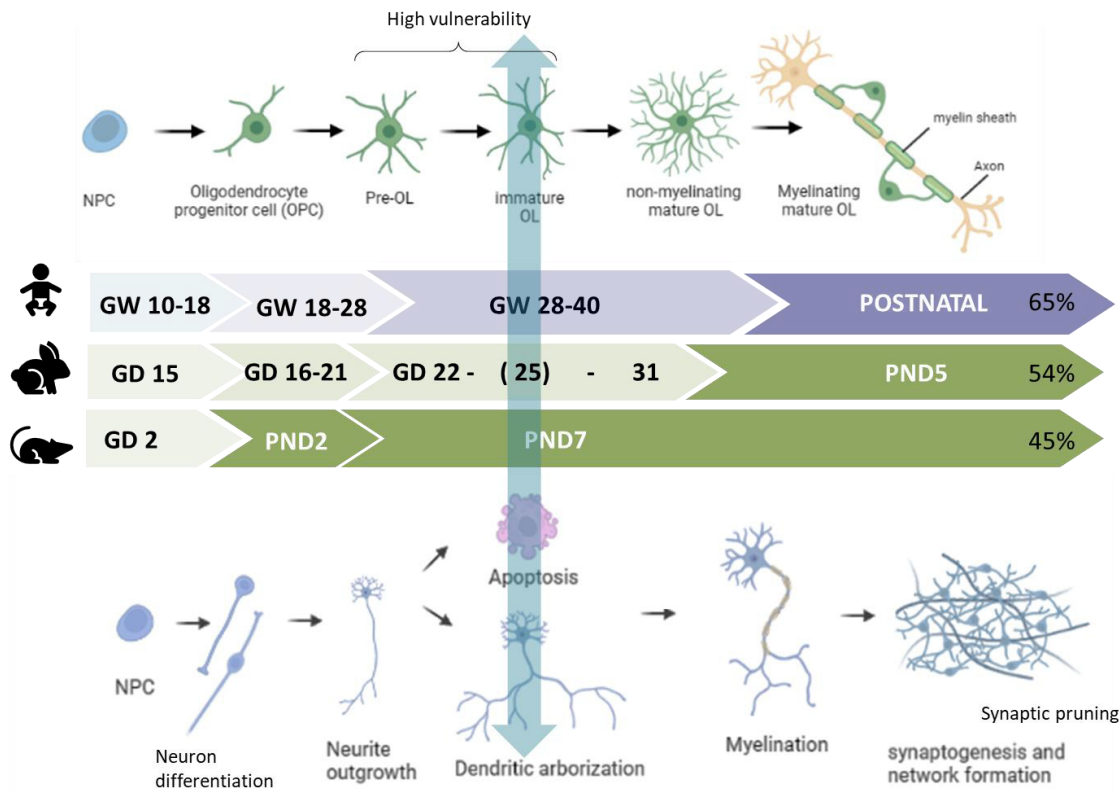


**Figure 3. Schematic representation of the timing and duration of brain development in humans, rabbits, and rats.** The blue arrow indicates that IUGR is induced on the 25<sup>th</sup> day of gestation (GD) in rabbits. Most cases of IUGR occur in humans with a late onset of 28-40 weeks' gestation (GW), a time when pre- and immature OLs are predominantly located in the brain and therefore premature white matter (WM) is particularly vulnerable. During rabbit brain development, pre-OLs predominate in the WM at GD22, followed by increasing density and OL lineage progression between GD24-25, while in rat the OL maturation occurs postnatally. Neurite outgrowth followed by neuronal arborization and apoptosis are the predominant neuronal stages at GD25 in rabbits, GW28-40 in humans, and after postnatal day (PND) 7 in rats. Perinatal development is characterized by massive growth of dendrites and axons, followed by myelination, synaptogenesis, and synaptic pruning, especially in the forebrain and cerebellum in humans (Silbereis et al., 2016) and rabbits. According to the precocial score, human brain is 65% developed at birth, more similar to rabbit (54%) than to rat (45%) (Workman et al., 2013). In human and rabbit, brain development occurs mainly perinatal and is therefore more similar than compared with the species rat, where the brain development happens mainly postnatally. OL= oligodendrocyte; Pre-OL: pre-oligodendrocyte; NPC = neural progenitor cell; GW= gestational week; GD = gestational day; PND = postnatal day. Created in Biorender.com adapted from (Back, 2001; Back et al., 2002a; Barateiro and Fernandes, 2014; Baud et al., 2004; Buser et al., 2010; Drobyshesky et al., 2014; Silbereis et al., 2016; Workman et al., 2013).

In the rabbit IUGR model, IUGR is surgically induced in pregnant New Zealand rabbits at gestational day (GD) 25, by ligation of 40-50% of uteroplacental vessels of each gestational sac of one uterine horn, whereas the contralateral horn remains as control, as described in detail in (Eixarch et al., 2009). Cesarean (C)-section is performed at GD30 (term 31 days) to obtain IUGR and control rabbit pups. On postnatal day (PND) 0, IUGR cases with a body weight lower than the 25<sup>th</sup> percentile (39.7 g, Table 1 in (Barenys et al., 2021)) and control animals with a body weight higher than the 25<sup>th</sup> percentile are included. To exclude spontaneous IUGR in control pups and controls in ligated animals, cases with a body weight higher than the 25<sup>th</sup> percentile were excluded. The timepoint of IUGR induction at GD25 was chosen because it correlates with 28-40 gestational weeks (GW) in human, when the onset of IUGR in the most cases occur, and the clinical detection and diagnostic remain difficult (Fig. 3, Table

1). To this time, pre- and immature OLs are predominantly in the brain and thus, white matter (WM) development is particularly vulnerable (Fig. 3). This model corresponds to a mild late-onset IUGR reproducing chronic placental insufficiency with hemodynamical changes in the blood flow, which results in the significant birth weight reduction (Eixarch et al., 2012b, 2009). The derived offspring presents neurodevelopmental manifestations of IUGR occurring in clinical cases, including neonatal and long-term functional and structural deficits. During the neonatal period (PND1), IUGR animals exhibit significant functional impairments in locomotion, lineal movements, reflexes, head turn during feeding and smelling response (Eixarch et al., 2011). In the long-term period (PND70), IUGR rabbits show large problems in learning, memory, and a higher level of anxiety (Illa et al., 2013). High-resolution magnetic resonance imaging (MRI) studies revealed that IUGR animals do not present any gross structural abnormality in anatomical sequences either at neonatal or long-term period. However, advanced diffusion MRI, a technique that measures the diffusion of water molecules in tissues and provides information about brain microstructure and the disposition of fiber tracts (Eixarch et al., 2012b), has detected subtle cerebral changes in mild chronic hypoxic conditions (Sanz-Cortés et al., 2010). Indeed, after IUGR induction, diffusion MRI revealed subtle changes in brain structures with an altered diffusivity in several brain areas including the frontal cortex and the corpus callosum (CC) indicating an abnormal brain maturation affecting both the GM and WM (Eixarch et al., 2012b; Illa et al., 2013; Pla et al., 2020). The decreased WM myelination and organization of WM tracts in IUGR animals was linked with neurobehavioral alterations, whereas the GM alterations of the hippocampus showed significant correlations with learning and memory (Eixarch et al., 2012b; Tolcos et al., 2017). Previous studies using this model have unraveled changes in cerebral connections in the IUGR affected rabbits (Batalle et al., 2014; Illa et al., 2013), which correlate very well with the clinical observation that IUGR-affected children also present cerebral connection alterations in connectomic-studies (Batalle et al., 2012). Linking this clinical adverse outcome with the neurodevelopmental alterations observed in rabbits gives evidence that the rabbit IUGR model is a good model to study IUGR-induced structural changes in humans (Barenys et al., 2021; Bassan et al., 2000; Eixarch et al., 2011, 2009).

### 1.3.2 In vitro neurosphere model

With the aim of characterizing and understanding the origin of brain damage caused by IUGR we established for the first time an *in vitro* model based on primary rabbit neuronal progenitor cells (NPCs) (Manuscript 4.2 (Barenys et al., 2021)). Because rabbits have a bicornuate uterus with two separate uterus horns, we were able to obtain control and IUGR NPCs always in parallel from a pregnant rabbit for direct comparison. NPCs were derived from whole brain of rabbit pups, which form spontaneously 3D cell the aggregates called neurospheres under proliferation conditions with the addition of growth

factors. NPCs plated on an extracellular matrix containing laminin and PDL and after withdrawal of growth factors migrate out of their sphere core and differentiate while migrating into neuronal target cells. Neurospheres, previously established with the species rat, mouse and human, are able to mimic essential key events (KEs) of fetal brain development such as NPC proliferation, migration, differentiation into the main effector cells of the brain, neurons ( $\beta$ III-Tubulin+ cells), OLs (O4+ cells), and astrocytes (GFAP+ cells), network formation and function (Barenys et al., 2017; Baumann et al., 2014; Breier et al., 2010; Gassmann et al., 2010; Moors et al., 2007, 2009; Schreiber et al., 2010). Therefore, the neurosphere model covers several endpoints of brain development imitating spatiotemporal neurodevelopmental processes that are essential to form a functional brain (Fritsche et al., 2018b, 2018a). The disturbance of at least one of these endpoints due to a decrease in oxygen/nutrition or chemical exposure can lead to severe adverse outcome (Fritsche et al., 2018a). Thus, the 'Neurosphere Assay' is a valuable system to perform developmental neurotoxicity (DNT) testing comprising the safety evaluation of drugs and chemicals in a concentration dependent manner. With the *in vitro* system we can test many concentrations of each compound simultaneously, not only saving time and money regarding *in vivo* studies, but also providing the essential information about the effective therapeutic concentration required for the extrapolation of the dose to the situation *in vivo*. The neurosphere model of human and rodent origin has already been applied for the investigation of the DNT potential of several compounds (Barenys et al., 2017; Dach et al., 2017; Klose et al., 2021b, 2022; Masjosthusmann et al., 2019). The novel rabbit 'Neurosphere Assay' allows us to study the pathophysiological mechanisms of IUGR during neurodevelopment by characterizing structural changes in the brain and discriminating cellular effects of compound exposure. Whereas the well characterized rat neurospheres model was suitable to perform toxicological potency rankings of chemicals, as the species rat has been previously used in several toxicological approaches (Barenys et al., 2017; Dach et al., 2017; Klose et al., 2021b, 2022; Masjosthusmann et al., 2019).

"Due to the multicellular nature of the neurosphere method and the possibility to study a variety of neurodevelopmental processes with it, neurospheres are a valuable test system for studying a plethora of cellular effects initiated by a variety of different modes-of-action" (Manuscript 4.2 (Barenys et al., 2021)). Which means in turn that neurospheres are well suited for characterizing so far unknown neurodevelopmental effects on the cellular level that are triggered by chemicals or IUGR. This new method opens the door to testing potential neuroprotective therapies for IUGR in a simple and cost-efficient manner. A schematic overview of the 'Neurosphere Assay' and endpoints is shown in Fig. 4.

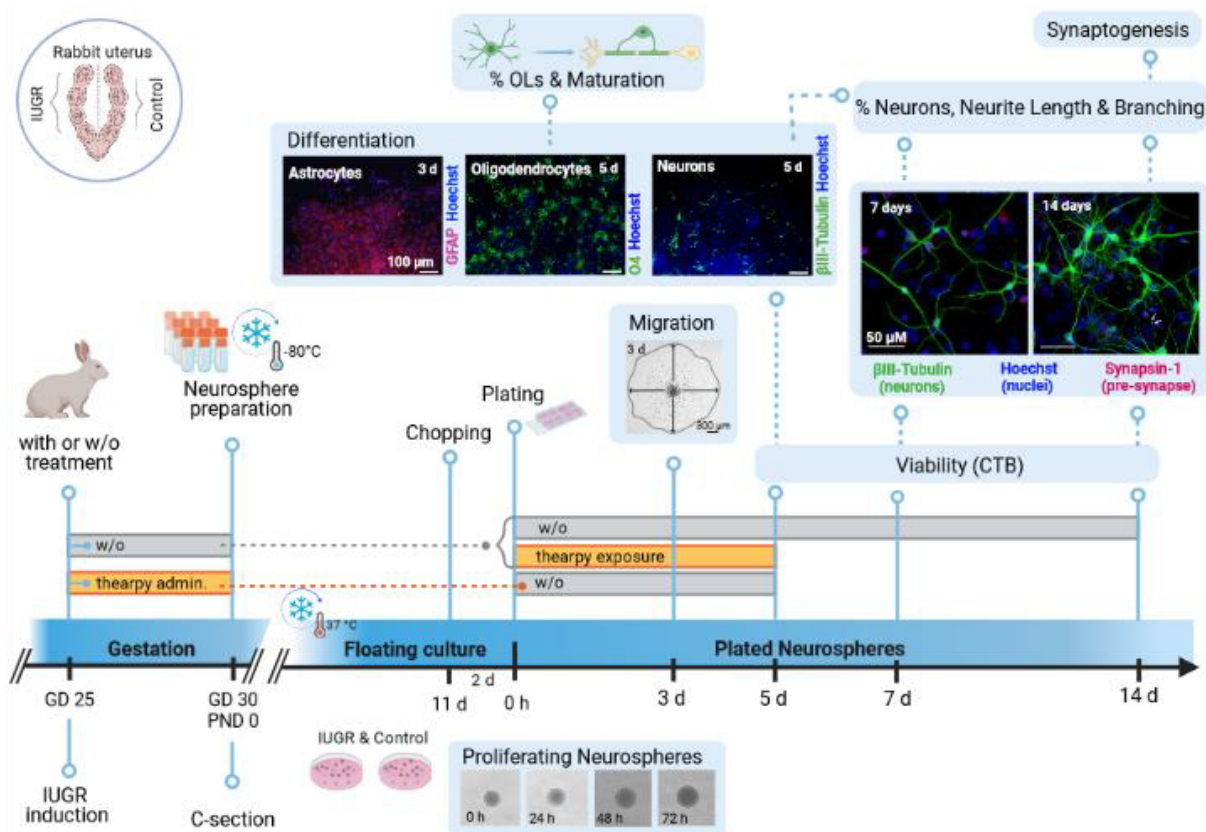


**Figure 4. Experimental setup.** On GD 25, IUGR was induced in pregnant New Zealand rabbits in one uterine horn, while the contralateral horn remained as a control. No treatment (w/o) or therapies were administrated orally for 5 consecutive days to the pregnant dam until C-section on GD 30. IUGR and control pups were obtained from every group on PND 0, neurospheres were prepared from pup's whole brain and frozen until used. Thawed neurospheres were cultivated for each group respectively in a floating culture for approx. 11 days and mechanically chopped. After 2 days, proliferating neurospheres reached a size of 0.3 mm. On experimental day 0, neurospheres were plated on a PDL/Laminin coated 8-chamber slide w/o or with exposure to increasing concentrations of therapies. After 3 days, the exposure was renewed, and migration assay performed. After 5 days, viability was measured, neurospheres were fixed and immunocytostained. Differentiation & OL maturation was analyzed. After 7 days % neurons, neurite length and branching was determined with subsequent analysis of synapses formation after 14 days. Rectangle bars = time of administration or exposure, blue circle = key events. w/o = without, GD = gestational day, PND = postnatal day, d = days, C-section = cesarean section, OL = oligodendrocyte, CTB = cell titer blue. Created with BioRender.com

## 1.4 Neuroprotective strategies

### 1.4.1 Current neuroprotective strategies

IUGR is one of the most common pregnancy complications and the only current prenatal treatment is preterm delivery, which requires a good management in timing of delivery including balancing the risk between adverse intrauterine environment and prematurity (Figueras and Gardosi, 2011). There is no standardized strategy proving to prevent or revert the neurodevelopmental alterations entailing IUGR. Several clinical and experimental appraisals give evidence that early postnatal approaches like breastfeeding (Rao et al., 2007), individualized newborn developmental care and assessment program

(Als et al., 2012), and environmental enrichment (Illa et al., 2018) can partially ameliorate the neurodevelopmental impairment caused by IUGR. However, all these strategies have been applied after birth, at a timepoint when adverse effects of IUGR on brain development have already been consolidated. A treatment applied during the prenatal period, the “critical window of opportunity” (Fig. 5) (Susan L Andersen, 2003), may have more likely a distinct effect. One of the most important challenges in medicine is to find a therapy to be applied during this time window preventing adverse effects of IUGR. Hence, the overall objective of this thesis is to find a promising therapy that can be applied during pregnancy bringing it to the pre-clinical stage in the future.

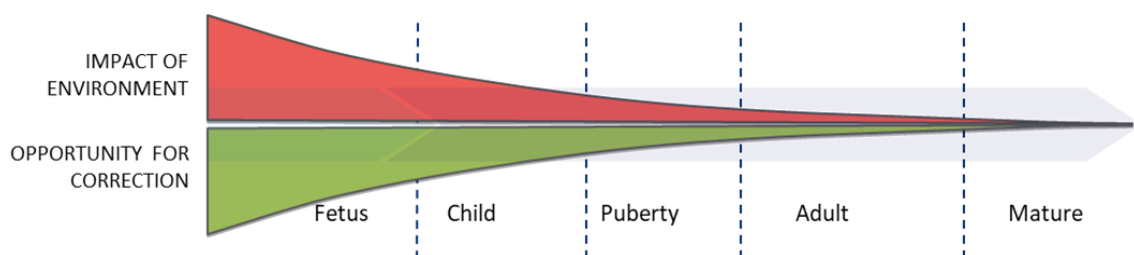


**Figure 5. Diagram displaying the tolerance to environmental impact and the opportunity for its correction.** The impact of the environment to the brain leading to neurodevelopmental insults is higher during the first years of life, especially during the prenatal life. However, the opportunity to correct adverse neurodevelopmental effects is likewise higher during the first stages of fetal development, what is known as the “critical window of opportunity”, due to brain plasticity, a process that involves adaptive structural and functional changes to the brain.

#### 1.4.2 Safety and efficacy testing

By aiming to bring potential therapies to the clinical field the balance between benefit and risk must always be considered. A potential therapy can elicit adverse effects by acting on the pharmacological target (on-target) or a known or unknown unintended target (off-target) causing mechanistic toxicity (Muller and Milton, 2012). Understanding the underlying toxicity is essential to make a safety related decision and to prioritize compounds for further preclinical studies. Toxicological risk assessment integrates hazard identification and exposure assessment to establish a safe product, while pharmacological assessment comprises the description of the drug’s efficacy and potency. A substantial part of early drug discovery and development is the characterization of the safety and efficacy of drug candidates to determine their margin of safety (MoS) (Muller and Milton, 2012). The therapeutic index (TI) calculates the MoS by the ratio between the highest exposure to a drug that does not exhibit toxicity to the exposure that produces the desired effect (effective concentration (EC); Fig. 6, (Muller and Milton, 2012)). The narrower the index, the more likely it is that the substance will have an adverse effect. The TI includes the assessment of various endpoints by taking quantitative *in vitro* and *in vivo* data into account and is crucial for early therapy development to report unfavorable characteristics or redirect researchers to find alternative candidates (Muller and Milton, 2012). Dose-



response curves in animal studies reveal no observed adverse effect level (NOAEL) and lowest observed adverse effect level (LOAEL), and the NOAEL serves as a reference safety endpoint in non-clinical studies (Baird et al., 2019; Dorato and Engelhardt, 2005). The NOAEL is defined as the concentration of a substance that causes no detectable adverse alterations within a respective safety experiment (Baird et al., 2019; Kerlin et al., 2016). *In vitro* safety and efficacy assays addressing diverse endpoints with concentration-response curves and allow the determination of e.g., half-maximal effective concentration (EC<sub>50</sub>) and half-maximal inhibitory concentration (IC<sub>50</sub>) values, or maximum tolerated concentration (MTC) and minimum/most EC (mEC). IC<sub>50</sub> quantitatively measures the drug's potency in inhibiting a biological process *in vitro* and EC<sub>50</sub> is the drug concentration required to obtain 50% of the maximum desired therapeutical effect (Aykul and Martinez-Hackert, 2016; Muller and Milton, 2012). The MTC is the highest concentration that will not produce a toxic effect on any of the tested endpoints and mEC is the concentration required to obtain the desired therapeutical effect *in vitro* (Kühne et al., 2022).

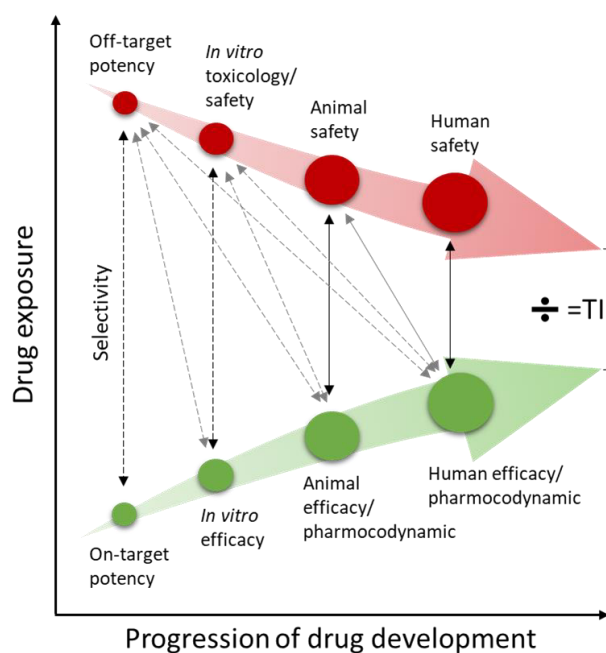


**Figure 6. Therapeutic index during progression of drug development.** With the progression of drug development, the extent of safety (red) and efficacy (green) data increases, as indicated by the size of the circles. Therapeutic index (TI) or safety margin is calculated by the ratio of the drug concentration by which the adverse effects occur to the drug concentration by which the therapeutic effects occur. Initially target selectivity is assessed by analyzing the off- and on-target potency *in vitro*. Black arrows: margins of data of equivalent types; grey arrows: margins including data of different types; solid arrows: margins of *in vivo* data; dashed arrows: margins restricted to concentration-based *in vitro* data compared to *in vitro* or *in vivo* data. Adapted from (Muller and Milton 2012).

Figure 6 adapted from Muller and Milton (2012) describes the TI during the progression of drug development and the increasing extent of availability of safety and efficacy data over time. The first phase involves the selectivity profile of a new drug, which is an important attribute for the optimization of pharmacotherapy defined by the division of its off-target IC<sub>50</sub> by the on-target IC<sub>50</sub> (Vlot et al., 2018), followed by *in vitro*, *in vivo* and human studies. Even if a drug has high target selectivity, it may have a challenging safety profile, and steps should be taken to minimize harm by describing all anticipated risks.

The International Conferences on Harmonization of Technical Requirements for Pharmaceuticals for Human Use (ICH) brings regulatory authorities and pharmaceutical industry together to develop safe, effective, and high-quality pharmaceuticals (<https://www.ich.org/>). The ICH provides quality (Q), safety (S), efficacy (E) and multidisciplinary (M) guidelines. ICH-S guidelines give assistance to uncover potential risk of a compound, whereas ICH-E guidelines recommend design, conduct, safety, and reporting of clinical development of a new drug. However, these guidelines are mainly based on animal experiments, which are time-, resource- and cost-intensive. Over the last decades there has been a continuous decline in productivity of pharmaceutical research and development that drives scientists to try to improve strategies identifying unsuitable therapeutic candidates in an earlier stage of drug development (Muller and Milton, 2012; Paul et al., 2010). According to the well-established concept of Russell and Burch 1959 describing replacement, refinement, and reduction of animals in research (the 3Rs) (Russell and Burch, 1959), an international workshop on pharmaceutical toxicology was convened to find strategies to reduce animals in non-clinical studies, while improving efficacy in drug development and human translation (Chapman et al., 2013). The consortium warned especially about the high need of animals in developmental and reproductive toxicity testing, which is based on the guidance document of the ICH S5(R3) (2020). The experts discussed the lack of regulatory acceptance of *in vitro* methods and explained that mechanistically based *in vitro* methods should be used at all stages of pharmaceutical and chemical development to reduce and inform *in vivo* studies (Chapman et al., 2013). In recent years, however, regulatory acceptance of *in vitro* methods has gained momentum, and novel *in vitro* methods are already supporting decision making in risk assessment (Firestone et al., 2010; Gibb, 2008; Krewski et al., 2009) and early drug development by providing valuable information about chemical induced mode of actions revealing their maximum efficacy and minimum toxicity of chemicals (Chapman et al., 2013; Whitebread et al., 2005).

#### 1.4.2.1 Developmental neurotoxicity (DNT)

DNT is defined as the disturbance of brain developmental processes by an external stimulus e.g. chemical agent, which might lead to an adverse neurological outcome (OECD, 2007). In the last decade neurospheres of rodent origin has widely been used for DNT testing (Baumann et al., 2014; Dach, 2015; Schmuck et al., 2014), even though the degree of brain maturation of rodents is less similar to human compared to other animal models (see 1.3.1). However, primary human neurospheres are very rare material and therefore the rat neurospheres assay has been considered as particularly suitable model for compound prioritization and ranking for further DNT testing. This applies especially to chemicals with unknown DNT potential to discover first indications of neurodevelopmental hazardous effects or underlying mode-of-actions. To overcome discrepancies between human and rodent brain development, neurospheres from both origins were comparably analyzed in several approaches

unraveling toxicodynamic species differences *in vitro* (Baumann et al., 2014; Masjosthusmann et al., 2019, 2018b). In this thesis, we have used the rat neurosphere model to rank epigallocatechin gallate (EGCG) synthetic analogs according to their potency to disturb the endpoint NPC migration (Manuscript 4.5 (Kühne et al., 2019)). Subsequently, we used the safest alternative compound for further analysis in the rabbit neurospheres model of IUGR (Manuscript 4.6 (Kühne et al., submitted)).

Exposure to chemicals during fetal development can cause moderate to severe brain injury at much lower doses than those disturbing adult brain function (Grandjean and Landrigan, 2006). Every stage of development can be a target for chemicals and there has been substantial concern that chemical exposure contributes to increasing incidence of neurodevelopmental diseases in infants (Fritsche et al., 2018a; Grandjean and Landrigan, 2014, 2006). Despite of this concern, a large number of chemical agents in the market have not been tested for their DNT potential, which can be traced back and explained due to the resource-intensive test guidelines (TGs) required 'EPA 870.6300' (EPA, 1998) and 'OECD 426' (OECD, 2007) demanding an abundant amount of time, money and animals (Crofton et al., 2012; Lein et al., 2005). The report 'Toxicity Testing in the 21st Century: A Revision and a Strategy' (Gibb, 2008) suggests a paradigm shift for toxicity testing away from the apical endpoint measurements in *in vivo* studies towards the use of alternative methods, including *in vitro* models or alternative model organisms (*Danio rerio* (zebrafish), *Caenorhabditis elegans*, or *Drosophila melanogaster*) in combination with computer based *in silico* models. Scientists from regulatory agencies, academia and industry reached a consensus that there is a high need for alternative test strategies permitting mode-of-action (MoA) based DNT assessment in a more time- and cost-efficient way as well as in a more human-relevant way (Bal-Price, 2018; EFSA, 2013; Fritsche et al., 2018c, 2017). On a workshop in 2016 organized by the Organization for Economic Co-operation and Development (OECD) and the European Food Safety Authority (EFSA), the consortium emphasized that the current approaches described in the mentioned guidelines are not sufficient to screen and characterize potentially hazardous compounds for DNT and highlighted the urgency to develop a standardized *in vitro* testing battery for regulatory purposes (Fritsche et al., 2017). In response, efforts have been made to develop a framework for the interpretation of *in vitro* DNT testing and the use of DNT *in vitro* battery (IVB) data in 'Integrated Approaches to Testing and Assessment' (IATA) based on case studies, presented by Crofton and Mundy 2021 (Crofton and Mundy, 2021). Just recently, in May 2022, a revised draft 'Guidance on Evaluation of Data from the DNT In-Vitro Testing Battery' has been published by the members of the OECD Expert Group on DNT IVB (OECD, 2022). IATA is a framework introduced by the OECD allowing to integrate all available hazard and exposure data, including *in vitro*, *in silico*, *in chemico*, *ex vivo*, *in vivo*, or read-across approaches for the use in regulatory assessments and decisions (OECD, 2022, 2017). The IATA concept follows an iterative approach by (1) gathering existing knowledge of mechanisms through which chemicals exert their toxicity and (2) weight of

evidence assessment answering if adequate information are available or if additional information are required for a decision-making, ultimately followed by a (3) regulatory conclusion (OECD, 2017; Sachana and Leinala, 2017; Sakuratani et al., 2018). A different kind of information organization named Adverse Outcome Pathway (AOP), defined as “a model that identifies the sequence of molecular and cellular events required to produce a toxic effect when an organism is exposed to a substance” (National Toxicology Program, 2022), can be used to inform and structure IATA in a regulatory decision context (OECD, 2017; Sachana and Leinala, 2017; Sakuratani et al., 2018).

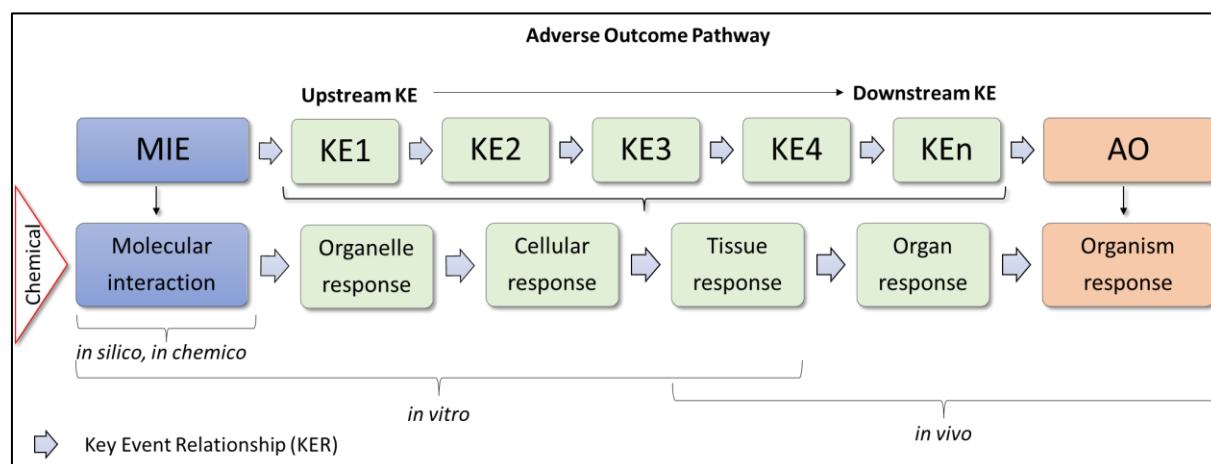


**Figure 7. Schematic illustration from an adverse outcome pathway (AOP).** Upper row: AOP, lower row: Level of biological organization. An AOP consists of key events (KEs) causally linked through key event relationships (KERs) at different levels of biological organization. The AOP begins with an initial interaction of a chemical which initiates a molecular event (molecular initiating event; MIE) followed by sequences of KEs on organelle, cellular, tissue and organ level leading to an adverse outcome (AO) at organism level. At a sufficient concentration and duration of chemical exposure, upstream KEs will trigger downstream KEs. The AOP allows mapping and integration of available information from *in silico/in chemico*, *in vitro* or *in vivo* data. Adapted from (Bal-Price and Meek, 2017; OECD, 2017)

An AOP is a logical sequence of biological events beginning with a molecular initiating event (MIE) triggered by chemical exposure leading to KEs at molecular, cellular, or organ level. These KEs are causally connected through key event relationships (KERs) leading to an adverse outcome (AO) on whole organism or population level (Ankley et al., 2010; OECD, 2017). A detailed illustration of the AOP framework is displayed Fig. 7. The biological plausibility of KERs depends on how good the mechanistic structural/functional relationships of a pathway is understood. Empirical data ought to support the relationship between KEs induced by a stressor and investigations of knock-out or blocking experiments can unravel if downstream KEs or the AO can be prevented (Bal-Price et al., 2017). AOPs are divided into 3 stages: putative, qualitative, and quantitative AOP (OECD, 2017; Villeneuve et al., 2014). The putative AOP assemble hypothesized KEs and KERs supported by biological plausibility and/or statistical interpretation. It can include incomplete linkage between MIE and AO due to known gaps or uncertainties. A qualitative or descriptive AOP is based on empirical evidence of exposure data

supporting the extrapolation or inference from upstream KEs to downstream KEs through KERs (Villeneuve et al., 2014). A quantitative AOP (qAOP) is based on information that defines a quantitative relationship between KEs including threshold, dose-response or time-course prediction factors (e.g. NOAEL, LOAEL; (OECD, 2017; Villeneuve et al., 2014)). While a descriptive AOP can be used for hazard assessment, a quantitative relationship from exposure assessment is more valuable for integrated testing strategies like IATA and is required for risk assessment (Zgheib et al., 2019).

### 1.4.3 Potential neuroprotective therapies

The neonatal and postnatal brain develops rapidly possessing a high degree of plasticity and is most vulnerable to insufficient nutrient and oxygen supply. Many important molecules are known to beneficially impact brain development, including omega-3 fatty acids, zinc, sialylated human milk glycoconjugates or hormones like melatonin or T3, suggested to act as neuroprotective agent for mental and motor development (De Souza et al., 2011; Szajewska, 2011; Wang, 2016). The selection of the following potential therapies to support impaired brain development caused by IUGR in this thesis was based on literature research, which provided promising information about fetal neuroprotective characteristics of the substances. Based on the results of this research, this thesis will subsequently try to find the most efficient and safe candidates in the context of IUGR.

#### 1.4.3.1 DHA

Docosahexaenoic acid (DHA) is an essential long-chain polyunsaturated fatty acid known as omega-3 fatty acid that has regulatory, anti-oxidative, anti-apoptotic, and anti-inflammatory effects in brain development, with the highest demand documented to be during the last trimester of pregnancy and first two postnatal years in human (Greenberg et al., 2008; Lauritzen et al., 2016; Swanson et al., 2012). The omega-3 fatty acid is delivered maternally via the placenta to the fetus, where it is a key component of brain membrane phospholipids (Gil-Sánchez et al., 2010; Lauritzen et al., 2016). DHA cannot be endogenous synthesized from the body and its fetal deposition rate depends ultimately on the maternal diet by placental transfer (Greenberg et al., 2008; Lauritzen et al., 2016). However the western population does not include an adequate amount of DHA to its daily food consumption, which raises concern about the development of the nervous system of infants (Greenberg et al., 2008; Judge et al., 2007). During the last trimester the fetus accumulates approximately 50-70 mg/day of DHA in the whole body, while its accumulation is significantly higher in the brain (Gil-Sánchez et al., 2010; Lauritzen et al., 2016). In the developing brain, DHA contributes to neuronal cell differentiation and neuronal signaling (Lauritzen et al., 2016). In addition, it promotes the expression of several brain derived neurotrophic factors, motivating the production of myelin as well as synaptogenesis, which

leads to a better maintenance of interneuronal networks (Crupi et al., 2013). Bernardo et al. (2017) found out that DHA promotes the maturation process of OPC to OLs by strengthening the anti-oxidative and anti-inflammatory mechanisms in a rat OPCs culture (Bernardo et al., 2017). Wurtman et al. (2009) reviewed that DHA increases the number of dendritic spines and synapse formation in hippocampal neurons during brain development (Wurtman et al., 2009). Preliminary findings from animal models confirm the involvement of DHA in ameliorating hypoxia-ischemia-induced brain damage (Zhang et al., 2010).

#### 1.4.3.2 Melatonin

Melatonin (MEL) is a hormone with powerful antioxidant properties through a direct regulation of certain genes related to cellular oxidative stress (Rodriguez et al., 2004). MEL is responsible for a regular maternal sleep/wake cycle, and it is secreted by the pineal gland in the brain at night. During pregnancy, endogenous MEL readily crosses the placenta and blood-brain barrier (BBB), but it is also directly produced in the placenta and ovary, where it works as a direct free radical scavenger and protects for cellular dysfunction arising from oxidative stress (Reiter et al., 2014a). MEL has therefore an essential function in placenta/uterine homeostasis and fetal maturation (Reiter et al., 2014a). Berbets et al., discovered that placental insufficiency caused a significantly declined MEL concentration in maternal blood accompanied with a reduced expression of MEL receptors in the placenta (Berbets, 2019; Berbets et al., 2021a). In a model of undernourished pregnant rats, maternal intake of MEL has shown to improve placental efficiency and birth weight by upregulating placental antioxidant enzymes (Richter et al., 2009). In an ovine model of IUGR, antenatal MEL treatment reduced fetoplacental oxidative stress resulting in an improvement of WM and GM injury (Castillo-Melendez et al., 2017; Miller et al., 2014) and prevented WM myelination defects by promoting the number of mature OLs in neonatal rats complicated with IUGR (Olivier et al., 2009). The increased OL maturation appears to positively depend on the MEL-receptor as reproduced *in vitro* (Olivier et al., 2009). Besides, antenatal MEL administration supported the maintenance of the BBB, brain homeostasis, and BBB integrity by protecting WM vascular endothelium in a sheep model of IUGR (Castillo-Melendez et al., 2017). Nowadays, there is only one pilot study of dietary supplementation of MEL to pregnant women with IUGR (Miller et al., 2014), and further analysis of the neuroprotective activity of MEL is needed.

#### 1.4.3.3 Zinc

Zinc is an essential dietary micronutrient and after iron the most abundant metal in the brain (Elitt et al., 2019). This metal is crucial for normal brain development because its absence induces alterations in the finely tuned processes of neurogenesis including NPC proliferation, neuronal migration,

differentiation and triggers apoptosis (Adamo and Oteiza, 2010; Ladd et al., 2010; N B Mathur and Agarwal, 2015; Nuttall and Oteiza, 2012). The zinc homeostasis in the brain is critical, since both, deficiency and excess of intracellular zinc can rapidly cause neuronal cell death via necrotic, apoptotic, or autophagic pathways (Elitt et al., 2019). There is less information about the impact of zinc on WM development, however zinc interacts with the proteins MBP and MAG stabilizing myelin membranes, which implies zinc as a component of major myelin proteins with an important functional role in myelin homeostasis (Elitt et al., 2019). In hyponutrition and IUGR animal models, its deficiency has been related to a decrease in neurogenesis and cell differentiation (Ladd et al., 2010; Zong et al., 2017), followed by an increase in apoptosis (Adamo and Oteiza, 2010). In contrast, an intracellular release of free zinc due to e.g. oxidative stress is described to initiate neuronal and OL death (Elitt et al., 2019; Mato et al., 2013; Zhang et al., 2007). However, in a randomized controlled trial, zinc supplementation in preterm neonates has been linked to an improvement in the alert state and attention (N. B. Mathur and Agarwal, 2015). The influence of zinc on brain development is controversially discussed and it appears to have a concentration dependent effect on neurogenesis. Therefore, it is important to assess the neurodevelopmental consequences of zinc in a model of IUGR.

#### 1.4.3.4 Lactoferrin and its main metabolite sialic acid

Lactoferrin (LF) is a sialic-acid rich, iron-binding milk glycoprotein, which possesses anti-inflammatory, immunomodulatory, antiviral, antibacterial, and antioxidant physiological functions as confirmed from several studies and reviewed by Sienkiewicz et al. (2021) and Wang (2016). The main source of LF includes human colostrum (>5 g/L) and milk (2-3 g/L) and has a blood concentration of 0.02-2 µg/mL in healthy human, while its concentration increases rapidly during inflammation, infection, or iron-excess (up to 200 µg/mL) (Sienkiewicz et al., 2021). LF with its iron-binding property is crucial for brain development as iron has a structural and functional role in improving cognitive and motor development. LF's main metabolite sialic acid (SA) is involved in the synthesis of brain gangliosides, which is enriched in cell membranes and neural cell adhesion molecules involved in cell-cell interaction, cell migration, neurite outgrowth and synaptic plasticity (Wang, 2016).

Wang (2016), summarize that a LF rich diet modifies the expression of genes related to brain maturation, producing for example increases in genes involved in neurite formation, outgrowth, organization of cytoskeleton or microtubule dynamics, while decreasing genes related to anxiety (Wang, 2016). Moreover, studies have stated that LF during lactation has neuroprotective effects on cerebral metabolism, and GW and WM recovery in ischemic processes (van de Looij et al., 2014). In a rat IUGR model, LF restored the impaired OPC marker NG2 (Van De Looij et al., 2019) and was able to revert IUGR-induced brain hippocampal changes (Somm et al., 2014). In this way, we aimed to improve

IUGR-related altered neurodevelopment by administering this therapy to our model improving brain metabolism and maturation.

#### 1.4.3.5 T3

Thyroid hormones (THs) are involved in the fine-tuned regulation of fetal growth and play a key role in the vulnerability of the developing brain (Baud and Berkane, 2019). In the first trimester, the fetus does not produce endogenous THs and depends on maternal THs crossing the placenta into the fetal circulation and brain (James et al., 2007; Landers and Richard, 2017). The transport from TH to the fetal brain requires an integral membrane transporter, particularly the membrane monocarboxylate transporter 8 (MCT8) expressed in the BBB and neural cells with affinity to the prohormone thyroxine (T4) and 3,3',5-triiodothyronine (T3) (Bernal, 2016, 2005; Landers and Richard, 2017). In humans, the majority of T4 is converted into the active form T3 by the enzyme type II iodothyronine deiodinase (DIO2), which is expressed in glial cells and astrocytes (Bernal, 2016). The level of fetal endogenous TH gradually rises from the second trimester until the neonatal period, and peaks on a stage of active myelination (LaFranchi, 2021; Lee and Petratos, 2016), where it is involved in the expression of major myelin proteins like MBP, MAG and PLP (Bernal, 2002; Schoonover et al., 2004). T3 carefully regulates fetal brain development by supporting especially the terminal differentiation of OPCs into myelinating OLs (Billon et al., 2002, 2001; Fernández et al., 2009). Kilby et al. (2000), discovered that the expression of thyroid hormone receptors (TRs) was significantly reduced in human fetal cerebral cortex and cerebellum in severe IUGR fetuses, which was associated with a reduced circulating TH concentration (Kilby et al., 2000). These clinical findings of reduced circulating TH levels in severe IUGR cases prompted further investigations of the potential therapeutic role of THs (LaFranchi, 2021). Already mild maternal hypothyroidism during pregnancy has been associated with neurodevelopmental impairment in children in later life (Ghassabian et al., 2011; Haddow et al., 1999; Pop et al., 1999; Williams et al., 2012). However, therapeutical alteration of the maternal TH level can cause possible complications and difficulties in the translation to the clinical field, which are controversially discussed (Fumarola et al., 2011; LaFranchi, 2021; LaFranchi and Austin, 2007).

#### 1.4.3.6 EGCG and derivatives

EGCG is the most abundant polyphenolic catechin in green tea and has been broadly described as neuroprotective agent due to its strong anti-oxidative and -inflammatory characteristics. It has been shown to have beneficial effects in obesity, cancer, diabetes and in several neurodegenerative diseases including anti-seizure strategy for temporal lobe epilepsy Alzheimer', Huntington' and Parkinson's disease (Cano et al., 2021, 2019, 2018; Pervin et al., 2018). EGCG has been suggested to suppress inflammatory processes inhibiting hyperproliferation or carcinogenesis by decreasing the expression



of genes involved in proliferation, migration, and survival (Mineva et al., 2013; Shankar et al., 2008; Singh et al., 2011; Suzuki and Isemura, 2001). During pregnancy, EGCG has been proposed as a therapy to diminish alterations of brain development due to Down's syndrome (Catuara-Solarz et al., 2016; Souchet et al., 2019; Stagni et al., 2021, 2016), and fetal alcoholic syndrome (Almeida-Toledano et al., 2021; Long et al., 2010; Tiwari et al., 2010). There are very few clinical studies attending the effect of EGCG on gestational complications as reviewed by (Sebastiani et al., 2022). To date, there is no single study testing the impact of EGCG on neurodevelopmental impairment induced by IUGR, only one study analyzed EGCG co-administrated with nifedipine on preeclampsia (Sebastiani et al., 2022; Shi et al., 2018). Due to the lack of studies and the likely health benefit of EGCG attributed to its antioxidative properties, it was decided to include EGCG in the selection of potential therapies.

Despite the alleged benefits, the safety of EGCG for brain development is unclear because herbal medicines are not required to undergo classical risk assessment and comprehensive data on subtle endpoints such as developmental neurotoxicity (DNT) are lacking (Abdel-Rahman et al., 2011; Barenys et al., 2016; Ekor, 2014). In a previous study using human and rat neurospheres, EGCG induced in a concentration-dependent manner adverse effects on neurodevelopmental KEs (Barenys et al., 2017). Barenys et al. (2017), discovered that EGCG binds to the ECM glycoprotein laminin, preventing its binding to the NPC adhesion molecule  $\beta$ 1-integrin (int- $\beta$ 1), which caused an altered glia alignment, disturbed migration, and fewer migrating young neurons (Barenys et al., 2017). This effect was confirmed by an independent research group, where EGCG inhibited the migration of neural crest cells (NCCs) *in vitro* (Nyffeler et al., 2017). Due to the evidence of EGCG induced DNT in a concentration dependent manner, we assessed besides from the efficacy the margin of safety to characterize the risk of chemical exposure on normal and IUGR brain development. Besides, we evaluated the safety of possible alternative agents derived from EGCG on basic processes of neurogenesis. The alternative compounds included EGCG PEGylated PLGA nanoparticles (Nano-EGCG) and 4 synthetic analogs: G37 (1,4-bis[(3,4,5-trihydroxybenzoyl)oxy]naphthalene), G56 (4,4'-bis[(3,4,5-trihydroxybenzoyl)oxy]-1,1'-biphenyl), M1 (4-hydroxy-2-naphthyl 3,4,5-trihydroxybenzoate) and M2 (3-hydroxy-1-naphthyl 3,4,5-trihydroxybenzoate).

## 2 Objectives of the thesis

Overall objective:

The overall objective of this thesis is to find a promising therapy against IUGR-induced neurodevelopmental alterations that can be applied prenatally.

Specific objectives:

1. To establish an *in vitro* neurosphere model derived from control and IUGR rabbit pup's whole brain.
2. To characterize differences in basic processes of neurogenesis induced by IUGR in an *in vitro* and *in vivo* model of IUGR.
3. To further characterize IUGR induced changes in neurodevelopment within the adverse outcome pathway (AOP) framework.
4. To evaluate *in vitro* the safety (Maximum Tolerated Concentrations; MTC) of the potential neuroprotective therapies: DHA, MEL, T3, Zinc, LF/SA, EGCG and derivatives.
5. To evaluate *in vitro* the efficacy (Effective Concentration; EC) of the potential neuroprotective therapies: DHA, MEL, T3, Zinc, LF/SA, EGCG and derivatives.
6. To confirm in the *in vitro* model the neuroprotective effects of the most effective therapies selected from objectives 3 and 4 after the *in vivo* prenatal administration in the IUGR rabbit model.

### 3 Material and methods

The section “material and methods” includes the methodological publication ‘Protocols for the evaluation of neurodevelopmental alterations in rabbit models *in vitro* and *in vivo*’ with a shared first authorship between L. Pla and B. A. Kühne. This publication consists of 14 protocols covering toxicologically relevant endpoints using the rabbit *in vivo* model during the neonatal and long-term postnatal period and the *in vitro* neurosphere assay. Although this publication includes a detailed explanation of most of the techniques used in this thesis, it doesn’t include them all. Therefore, a list of all techniques used has been prepared (Table 2) indicating in which manuscript/publication section 4 “manuscripts” is the methodology explained.

**Table 2.** Summary of manuscripts/publications including the methodology used in this thesis for the assessment of neurodevelopmental alterations. [1] Manuscript 3.1 (Pla et al., 2022), [2] Manuscript 4.1 (Pla et al., 2020), [3] Manuscript 4.2 (Barenys et al., 2021), [4] Manuscript 4.3 (Kühne et al., 2022), [5] Manuscript 4.4 (Kühne et al., to be submitted), [6] Manuscript 4.5 (Kühne et al., 2019), [7] Manuscript 4.6 (Kühne et al., submitted).

| METHODOLOGY   | MANUSCRIPT/PUBLICATION       |
|---|------------------------------|
| Rabbit <i>in vivo</i> model:<br>Including functional evaluation and histological procedures |                              |
| - Neonatal (PND1)   | [1], [2]                     |
| - Long-term postnatal (PND50-70)  | [1]                          |
| Rabbit IUGR Induction   | [2], [3], [4], [5],          |
| <i>In vivo</i> administration of potential therapies  | [4], [5]                     |
| <i>In vitro</i> Neurosphere preparation   |                              |
| - Rabbit  | [1], [3], [4], [5], [7]      |
| - Rat   | [6], [7]                     |
| <i>In vitro</i> exposure of potential therapies   | [4], [5], [6], [7]           |
| <i>In vitro</i> Neurosphere Assay:  |                              |
| - Migration Distance  | [1], [3], [4], [5], [6], [7] |
| - Migration Corona Formation  | [6], [7]                     |
| - OL Differentiation Assay  | [1], [3], [4], [7]           |

|  |                              |
|--|------------------------------|
| - OL Maturation Assay                          | [4]                          |
| - Neuronal Differentiation                     | [1], [3], [5], [6], [7]      |
| - Neurite Length, Branching, Network formation | [5], [7]                     |
| - Cell Viability by metabolic activity         | [1], [3], [4], [5], [6], [7] |
| qRT-PCR  | [4], [7]                     |
| Western blot                                   | [7]                          |
| AOP concept                                    | [7]                          |

### 3.1 Protocols for the evaluation of neurodevelopmental alterations in rabbit models in vitro and in vivo

Laura Pla <sup>\*,1</sup>, **Britta Anna Kühne** <sup>\*1,2</sup>, Laia Guardia-Escote <sup>2,3</sup>, Paula Vázquez-Aristizabal <sup>1,2</sup>, Carla Loreiro <sup>1</sup>, Burkhard Flick <sup>4</sup>, Eduard Gratacós <sup>1</sup>, Marta Barenys <sup>2</sup>, Miriam Illa <sup>1</sup>.

\*Both authors contributed equally to this manuscript

<sup>1</sup>. BCNatal-Barcelona Center for Maternal-Fetal and Neonatal Medicine (Hospital Clínic and Hospital Sant Joan de Déu), Fetal i+D Fetal Medicine Research Center, IDIBAPS, University of Barcelona, Center for Biomedical Research on Rare Diseases (CIBER-ER), Barcelona, Spain.

<sup>2</sup>. GRET, INSA-UB and Toxicology Unit, Pharmacology, Toxicology and Therapeutical Chemistry Department, Faculty of Pharmacy, University of Barcelona, Barcelona, Spain

<sup>3</sup>. Universitat Rovira i Virgili, Department of Psychology, Faculty of psychology, Tarragona, Spain.

<sup>4</sup>. Experimental Toxicology and Ecology, BASF SE, 67056 Ludwigshafen, Germany.

|                       |  |
|-----------------------|--|
| Journal               | Frontiers in Toxicology<br>Methods and Protocols in Neurotoxicology  |
| Impact Factor         | No Impact Factor. [OA]   |
| Type of authorship    | Shared first authorship  |
| Status of publication | Published: Front. Toxicol., 22 July 2022 Sec. Neurotoxicology<br><a href="https://doi.org/10.3389/ftox.2022.918520">https://doi.org/10.3389/ftox.2022.918520</a> |

## Summary

The rabbit model is gaining importance in the field of neurodevelopmental evaluation due to their higher similarity to humans in terms of brain development and maturation than rodents. In this publication we detail 14 protocols covering toxicological relevant endpoints for the assessment of neurodevelopmental adverse effects in the rabbit species. These protocols include both *in vitro* and *in vivo* techniques, which also cover different evaluation time-points, the neonatal period, and long-term examinations at postnatal day (PND) 50-70. Specifically, the protocols (P) included are: neurosphere preparation (GD30/PND0; P2) and neurosphere assay (P3), behavioral ontogeny (PND1; P4), brain obtaining and brain weight measurement at two different ages: PND1 (P5) and PND70 (P12), neurohistopathological evaluations after immersion fixation for neurons, astrocytes, oligodendrocytes and microglia (PND1; P6-9) or perfusion fixation (PND70; P12), motor activity (P11, open field), memory and sensory function (P11, object recognition test), learning (P10, Skinner box) and histological evaluation of plasticity (P13 and P14) by means of dendritic spines and perineuronal nets assessment. The expected control values and their variabilities are presented together with the information on how to face the most common troubles related with each protocol. To sum up, this publication offers a comprehensive compilation of reliable protocols adapted to the rabbit model for neurodevelopmental assessment in toxicology.



# Protocols for the Evaluation of Neurodevelopmental Alterations in Rabbit Models *In Vitro* and *In Vivo*

Laura Pla<sup>1†</sup>, Britta Anna Kühne<sup>1,2†</sup>, Laia Guardia-Escote<sup>2,3</sup>, Paula Vázquez-Aristizabal<sup>1,2</sup>, Carla Loreiro<sup>1</sup>, Burkhard Flick<sup>4</sup>, Eduard Gratacós<sup>1</sup>, Marta Barenys<sup>2</sup> and Miriam Illa<sup>1\*</sup>

<sup>1</sup>BCNatal-Barcelona Center for Maternal-Fetal and Neonatal Medicine (Hospital Clínic and Hospital Sant Joan de Déu), Fetal i+D Fetal Medicine Research Center, IDIBAPS, University of Barcelona, Center for Biomedical Research on Rare Diseases (CIBER-ER), Barcelona, Spain, <sup>2</sup>GRET, INSA-UB and Toxicology Unit, Pharmacology, Toxicology and Therapeutical Chemistry Department, Faculty of Pharmacy, University of Barcelona, Barcelona, Spain, <sup>3</sup>Department of Psychology, Faculty of Psychology, Universitat Rovira i Virgili, Tarragona, Spain, <sup>4</sup>Department of Toxicology, NUVISAN ICB GmbH, Berlin, Germany

## OPEN ACCESS

### Edited by:

Christoph van Thriel,  
Leibniz Research Centre for Working  
Environment and Human Factors  
(IfADo), Germany

### Reviewed by:

Mojmir Mach,  
Slovak Academy of Sciences (SAS),  
Slovakia  
David W Herr,  
United States Environmental  
Protection Agency (EPA),  
United States

### \*Correspondence:

Miriam Illa  
miriamil@clinic.cat

<sup>†</sup>These authors have contributed  
equally to this work

### Specialty section:

This article was submitted to  
Neurotoxicology,  
a section of the journal  
Frontiers in Toxicology

Received: 12 April 2022

Accepted: 09 June 2022

Published: 22 July 2022

### Citation:

Pla L, Kühne BA, Guardia-Escote L,  
Vázquez-Aristizabal P, Loreiro C,  
Flick B, Gratacós E, Barenys M and  
Illa M (2022) Protocols for the  
Evaluation of Neurodevelopmental  
Alterations in Rabbit Models *In Vitro*  
and *In Vivo*.  
Front. Toxicol. 4:918520.  
doi: 10.3389/ftox.2022.918520

The rabbit model is gaining importance in the field of neurodevelopmental evaluation due to its higher similarity to humans in terms of brain development and maturation than rodents. In this publication, we detailed 14 protocols covering toxicological relevant endpoints for the assessment of neurodevelopmental adverse effects in the rabbit species. These protocols include both *in vitro* and *in vivo* techniques, which also cover different evaluation time-points, the neonatal period, and long-term examinations at postnatal days (PNDs) 50–70. Specifically, the protocols (P) included are as follows: neurosphere preparation (GD30/PND0; P2) and neurosphere assay (P3), behavioral ontogeny (PND1; P4), brain obtaining and brain weight measurement at two different ages: PND1 (P5) and PND70 (P12), neurohistopathological evaluations after immersion fixation for neurons, astrocytes, oligodendrocytes and microglia (PND1; P6–9) or perfusion fixation (PND70; P12), motor activity (P11, open field), memory and sensory function (P11, object recognition test), learning (P10, Skinner box), and histological evaluation of plasticity (P13 and P14) through dendritic spines and perineuronal nets. The expected control values and their variabilities are presented together with the information on how to troubleshoot the most common issues related to each protocol. To sum up, this publication offers a comprehensive compilation of reliable protocols adapted to the rabbit model for neurodevelopmental assessment in toxicology.

**Keywords:** neurospheres, object recognition test, behavioral ontogeny, Skinner box, Golgi staining, open field, perineuronal nets, neurodevelopment

## INTRODUCTION

The rabbit model has become increasingly popular in neurodevelopmental studies within the translational medicine research field because it is a perinatal “brain developer”, similar to humans (Derrick et al., 2004; Eixarch et al., 2012; Workman et al., 2013). In the toxicology field, the most commonly used species is the rat. However rabbit is the preferred non-rodent species for prenatal developmental toxicity studies as detailed in OECD Test Guideline (TG) 414 (OECD, 2018). Besides that, in the OECD TG 426 (OECD, 2007) for testing the effects of chemicals on developmental neurotoxicity it is stated that developmental neurotoxicity studies can be conducted separately, or in addition to a prenatal developmental toxicity study (OECD TG 414 (OECD, 2018)). The OECD TG

426 indicates that the rat is the preferred test species to perform *in vivo* studies but states that other species can be used when appropriate (OECD, 2007). In that case, the use of other species should be justified based on toxicological, pharmacokinetic, or other data and should include the availability of species-specific postnatal neurobehavioral and neuropathological assessments.

The adaptation of protocols regularly used to evaluate developmental neurotoxicity in rats to rabbits could be useful in specific cases where the rabbit could mimic human conditions better than the rat, especially if it is taken into account that the OECD TG 426 indicates that if there is an earlier test raising concerns on developmental neurotoxicity the species/strain that raised this concern should be considered for the developmental neurotoxicity assay instead of the rat (OECD, 2007). From several review articles comparing the effects of test compounds in the OECD TG 414 performed in rats and rabbits, it has been demonstrated that there is an overlap of detectable effects in these species (Theunissen et al., 2016; Theunissen et al., 2017; Teixidó et al., 2018). However, there is a significant proportion of compounds with embryo-fetal developmental toxicity only detected in one of both species. The proportion of chemicals or drugs whose developmental toxic potential was only described in rabbits and not in rats was around 13% in several large-scale comparative studies (Theunissen et al., 2016; Theunissen et al., 2017; Teixidó et al., 2018). For all these reasons, it is plausible that the rabbit species becomes relevant for the evaluation of developmental neurotoxicity in particular cases. For this purpose, all developmental neurotoxicity protocols would need to be adapted to the new species, such as the moment of postnatal behavioral evaluation, behavioral equipment sizes, the inclusion of species-specific behaviors, scoring systems, antibodies used in histopathological analyses, incubation times, etc., and the reliability and sensitivity of the rabbit species to detect developmental neurotoxicity all would need to be documented.

The preparation of rabbit neurospheres from surplus control rabbit pups from OECD TG 426 (OECD, 2007) for later developmental neurotoxicity testing *in vitro* of other compounds or for mechanistic studies *in vitro* would help in the reduction of animal numbers used for neuropathological evaluations, although behavioral studies would still need to be tested *in vivo*.

The main advantages of using the rabbit species in developmental neurotoxicity studies are 1) a higher similarity to humans than rodent species regarding brain development and white matter maturation-timing, since they undergo perinatal brain development and begin myelination postnatally (Derrick et al., 2004; Eixarch et al., 2012; Workman et al., 2013), 2) a more complex brain structure than rodents with a higher ratio of other cells/neurons (Herculano-Houzel et al., 2011; Ferraris et al., 2018), and 3) a higher similarity to humans than rodents in terms of extraembryonic membranes, placenta development and circulatory changes during gestation (Foote and Carney, 2000; Carter, 2007; Eixarch et al., 2009). According to the inter-species comparison model developed by Clancy, Darlington, and Finlay 2001 and Workman et al., 2013 to predict the “precocial score” for neurodevelopment, rabbit species have a precocial score at birth

(0.537) more similar to humans (0.654) than rats (0.445) or mice (0.408). In addition to that and from a practical point of view, several tools are facilitating the use of this model for the evaluation of neurodevelopmental alterations: the availability of a rabbit brain atlas since 2013 (Muñoz-Moreno et al., 2013), and the availability of the *in vivo* reference database (ToxRefDB) including a public dataset on endpoints from guideline prenatal developmental toxicity studies in pregnant rabbits (Knudsen et al., 2009; Knudsen et al., 2013) (<http://actor.epa.gov/toxrefdb/faces/Home.jsp>).

However, performing developmental neurotoxicity studies in rabbits entails some difficulties compared to the commonly used rat species, since the time and cost of the experiments are increased due to a longer gestation period, a higher amount of test compound needed per animal, and to the much larger room space required, among others. If the study follows OECD TG 426, including 20 rabbit litters per group can be logistically limiting, especially considering that a very careful animal housing of reproducing does in individual cages where the nest area is in a separate section of the mother’s living environment is needed to avoid mismothering and to ensure proper development of the litter.

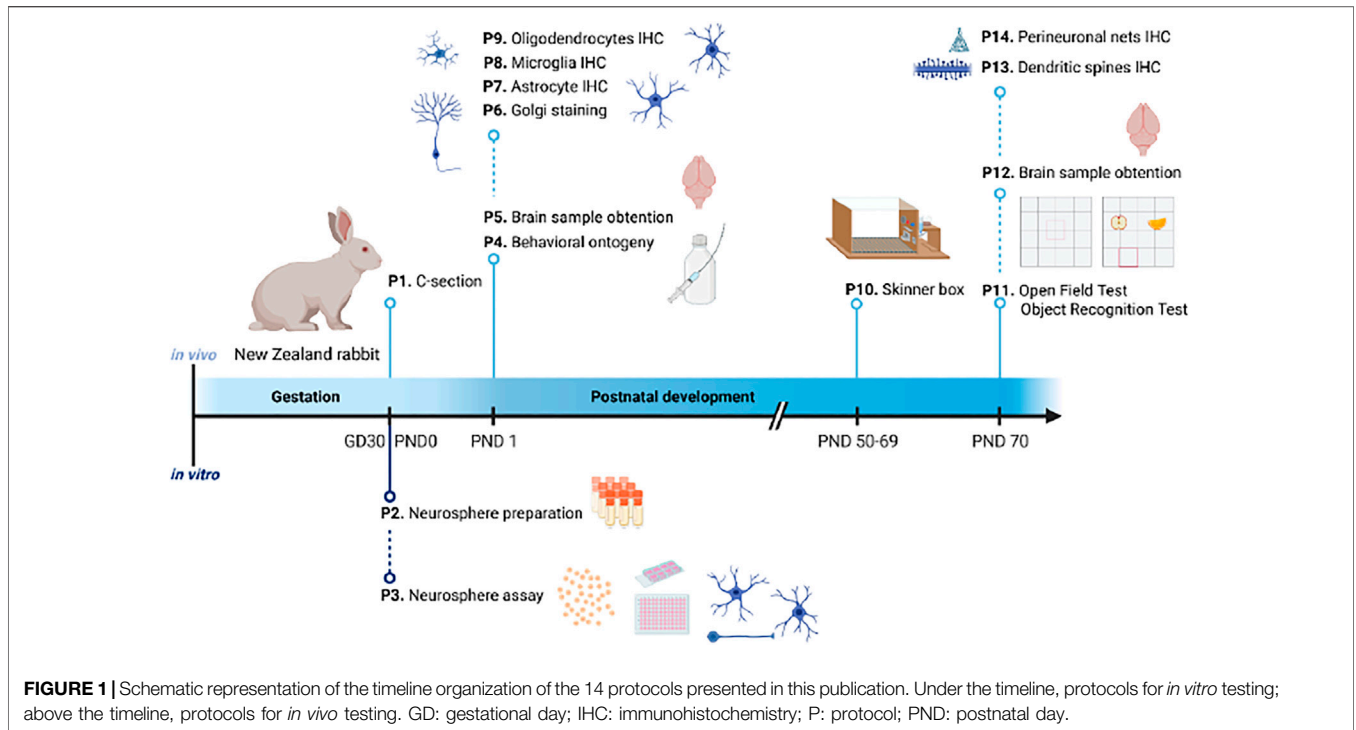
Taking all that into consideration, in this manuscript, we present a first comprehensive approach for the adaptation of protocols for the evaluation of neurodevelopmental adverse effects during the neonatal period and in the long-term period in the rabbit species including behavioral tests and neuropathological evaluations *in vivo* and *in vitro*. Critical steps in the protocols and limitations of the techniques are presented and discussed together with the expected control values and variabilities, as well as with orientation on data interpretation combining the different tests. The 14 protocols proposed allow the assignment of rabbit fetuses or pups to a combination of tests depending on the interest of the researchers and cover most of the endpoints currently required for developmental neurotoxicity in OECD TG 426 (OECD, 2007). Explanations on the exposure of the does during gestation and evaluation of maternal toxicity are not a matter of this protocol series, since they are already presented in detail in OECD TG 414 for prenatal developmental toxicity studies (OECD, 2018).

## PROTOCOLS

All procedures should comply with applicable governmental and institutional regulations for the use of laboratory animals in research.

An overview of the 14 protocols detailed in this work is presented in **Figure 1**. On GD30/PND0, New Zealand rabbit fetuses or pups are selected from the different study groups and are assigned for *in vivo* endpoint assessments. The *in vivo* protocols presented cover toxicological relevant endpoints in neurologic development required or optional in OECD TG 426 (OECD, 2007) ranging from basic behavior ontogeny to complex operant conditioning or sensory behavior, as well as neurohistopathological evaluation of different cell types and cell characteristics. Specifically, they include brain weight measurement at two different ages: PND1 (P5) and PND70





(P12), neurohistopathological evaluations after immersion fixation (PND1; P6-9) or perfusion fixation (PND70; P13 and 14), behavioral ontogeny (P4), motor activity (P11, open field), memory and sensory function (P11, object recognition test), learning (P10, Skinner box), and plasticity (P13 and P14). Protocols to evaluate relevant endpoints required in OECD TG 426 (OECD, 2007) which are not included in this first approach are neurohistopathological evaluation of peripheral nervous system (PNS) at PND70, global behavior assessment using a functional observational battery (FOB) or modified Irwin test, sexual maturation evaluation, and assessment of other developmental landmarks (optional in TG 426).

Offspring are randomly selected from within litters for the different neurotoxicity evaluations. Among the protocols included in the present approach, there are different possibilities to assign pups to these neonatal (PND1) and long-term examinations (PND50 to 70), but to avoid interferences among tests, the recommended assignment is as follows:

Neonatal examinations

- P4: 2 pups/sex/litter
- P5: 3 pups/litter
- P6: 1 pup/litter
- P7: 1 pup/litter
- P8: 1 pup/litter
- P9: 1 pup/litter

Long-term examinations

- P10: 1 pup/litter
- P11: 1 pup/litter
- P12: 2 pups/litter
- P13: 1 pup/litter
- P14: 1 pup/litter

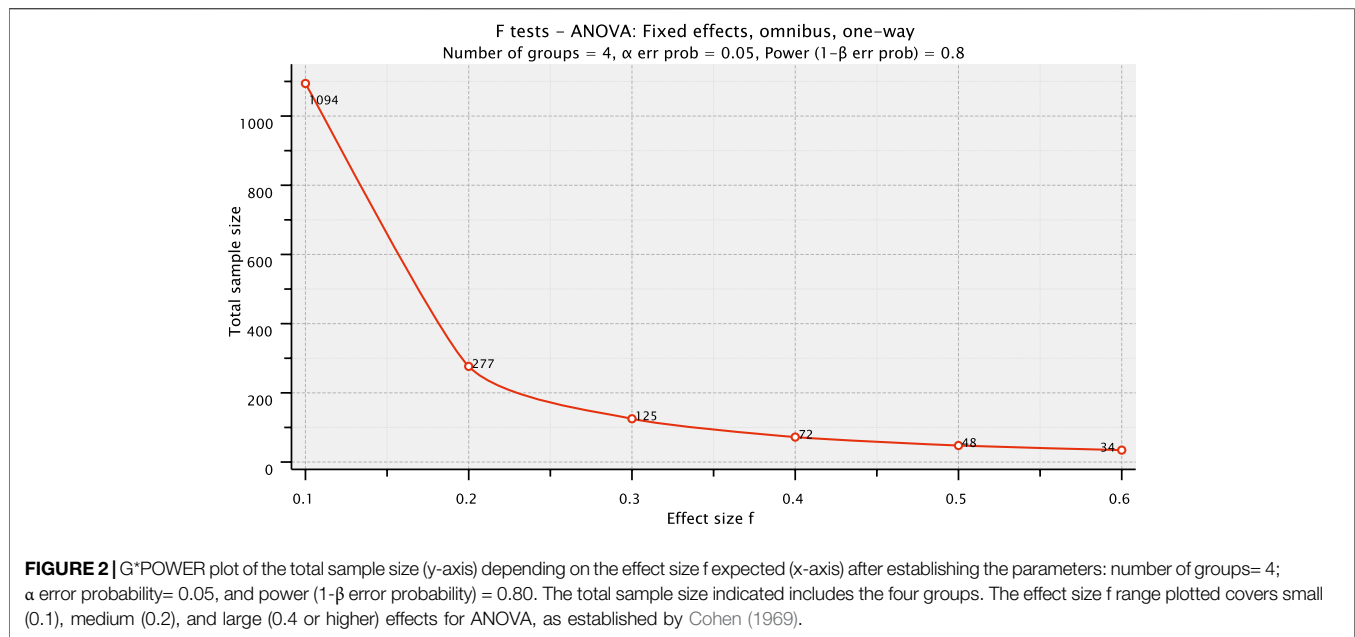
The number of litters to be assigned to each group depends on the aim of the study, the statistical power desired, and the effect size expected. Using the statistical power analysis tool G\*POWER (Faul

et al., 2007; Faul et al., 2009) and considering a typical assay with four groups (1 control and three treatment groups), whose results would be analyzed using a one-way ANOVA test and establishing an  $\alpha$  error probability of 0.05 ( $p \leq 0.05$ ; Type I error [false positive] less than 5%) and a power of 0.80 [ $1-\beta$  error probability; Type II error (false negative) less than 20%], if the expected effect size  $f$  is large (0.4), 19 litters per group would be recommended, similarly to the OECD TG 426 recommendation of 20 litters per group; but if a larger effect size  $f$  is expected (0.57) the requirements decrease to 9 litters per group. Therefore, pilot/screening studies with less than 10 litters per group would be sufficient to detect very large effects, while higher numbers of litters would be needed if a small effect size  $f$  is expected (0.1) as exemplified in **Figure 2**.

In addition to these considerations, litter size standardization (culling) prior to functional endpoints testing is accepted in OECD TG 426 (OECD, 2007); therefore, control pups not selected for *in vivo* evaluations can be assigned to Protocol 2 (neurosphere preparation) for the isolation of neural progenitor cells (NPC) which can be frozen for future *in vitro* testing in the neurosphere assay (Protocol 3).

### Protocol 1: Cesarean Section

There are two options to obtain the fetuses or pups for protocols from 2 to 14, by natural delivery and proceed with all the protocols at the PND indicated in **Figure 1** or to obtain them by cesarean section and proceed in the same way. This protocol describes the basic procedures to perform a cesarean section on GD30 in New Zealand rabbits. The protocol is not strictly necessary for toxicological studies, but it can be necessary in case a different condition needs to be induced during gestation in the two different uterus horns, such as intra-uterine growth restriction induced in one of the uterus horns by ligation of



uteroplacental vessels, and to allow the identification of the case and control pups. As the control values presented in the results section are from pups obtained by cesarean section, this protocol is also included in this collection. If the cesarean section step can be avoided, the number of animals needed will be reduced since after cesarean section pups need to be assigned to a nursing mother for further development.

## P1 Materials and Equipment

- Data collection sheets.
- Monitor for blood pressure, heart rate, and blood oxygen level.
- Gauzes.
- Scalpel blade number 24 and scalpel handle.
- Atraumatic forceps.
- Dissection scissors.
- 1 syringe (2.5 ml).
- Surgical table: bandage to hold the animal, soaker, surgical drape, and iodine.
- Venous catheter.
- Fixing paper for the catheter.
- Three-way catheter.
- Incubator.
- High-precision flow regulator.
- Medication for anesthetic induction based on ketamine and xylazine: (see **Supplementary File S1: Reagents and Solutions list**).
- Medication for anesthetic maintenance based on ketamine and xylazine: (see **Supplementary File S1: Reagents and Solutions list**).

## P1 Methods

### P1.1. Before the Surgery

- 1| Prepare all the medication before the cesarean section.
- 2| Anesthesia induction:

- a) Administer the anesthetic medication i.m.
- b) Bring the rabbit to the surgical table, fix the limbs and set the monitor for blood pressure, heart rate, and blood oxygen level.
- c) Place the catheter in the lateral vein of the ear, fix it, and place a three-way catheter. Administer a small volume of propofol to check the permeability of the catheter.
- d) Anesthesia maintenance:
  - i. Inhalation: place a mask in the airway, connected to the machine, and then start the administration of 2 L of O<sub>2</sub> and 1.5–2 ml of isoflurane.
  - ii. Intravenous: add 4 ml ketamine and 3 ml xylazine in 100 ml saline solution and connect the high-precision flow regulator adjusted to administer 30–40 ml/h (corresponds to the necessary dose for a 4–5 kg animal).

### P1.2. During the Surgery

- 1| Cover the skin with iodine, place a sterile surgical drape, and dissect planes until opening the abdominal cavity and identify both uterine horns. All the procedures must be carried out under aseptic conditions.
- 2| Fetus extraction:
  - a) Open the uterine cavity with dissection scissors, extract the fetuses (without ligation of the umbilical cord), and extract the placenta. Once all the fetuses have been removed, administer i. v. the first dose of pentobarbital 40 mg/kg, and afterward the second dose of 360 mg/kg for euthanization.
  - b) Identify each pup with holes in the ears.
  - c) Start cardiopulmonary resuscitation maneuvers in the incubator area and maintain body heat.

### P1.3. After the Surgery

- 1| Remove pups from the incubator (maintaining body heat); weigh each newborn and annotate the information. Put them with a nursing mother, all of them at the same time.

## Protocol 2: Rabbit Neurosphere Preparation

On GD30/PND0 control fetuses/pups which are not needed in any *in vivo* evaluation group can directly be assigned to the preparation of neurospheres. The aim of this protocol was to generate a cell suspension from rabbit GD30/PND0 brains and to freeze it in cryovials at  $-80^{\circ}\text{C}$  until its use in protocol 3. The cell suspension obtained in protocol 2 will be the starting material for the generation of neurospheres.

### P2 Materials and Equipment

- Heater and water bath ( $37^{\circ}\text{C}$ ).
- Binocular microscope.
- 15 and 50 ml centrifuge tubes.
- Petri dishes (60 and 90 mm  $\pm$  poly-HEMA).
- Pipettes (1000  $\mu\text{l}$ , 100  $\mu\text{l}$ , and 10  $\mu\text{l}$ ).
- Preparation cutlery: forceps and scissors.
- Centrifuge for 15 and 50 ml tubes.
- Syringes (20 ml).
- Syringe filters (sterile membranes with 0.22  $\mu\text{m}$  pore size).
- Cell strainer (sterile, 100  $\mu\text{m}$ ).
- Cryo-freezing container filled with isopropyl alcohol.
- Cryogenic storage vials.
- DMSO.
- Sterile PBS.
- MEM.
- DMEM.
- B27 proliferation medium.
- Tissue digestion solution (see **Supplementary File S1: Reagents and Solutions list**).
- Ovomuroid solution (see **Supplementary File S1: Reagents and Solutions list**).
- Papain.
- DNaseI (dilute 4 mg/ml in MEM).
- Trypsin inhibitor (dilute 1 mg/ml in DMEM).
- BSA (10% in PBS).
- Fetal bovine serum.
- Class II biological safety cabinet.
- Vial with Rabbit NPC (not older than 6 months).
- Human recombinant fibroblast growth factor (rhFGF).
- B27 proliferation medium (Supplement B27 (50x) serum-free).
- Freezing medium (see **Supplementary File S1: Reagents and Solutions list**).
- ROCK inhibitor Y-276322.
- Tissue chopper.
- Razor blade (5 cm) stored in 70% ethanol.

### P2 Methods

#### P2.1. NPC Isolation

- 1| Fill one tissue culture dish per two brains with sterile 1x PBS (prewarmed) and one dish per two brains with MEM (prewarmed).
- 2| Fill one 15 ml tube with 1 ml MEM for each half brain.
- 3| Transfer the pup's head into a PBS-filled tissue culture dish.
- 4| Remove skin and cartilage with forceps to uncover the brain. Transfer the brain from the skull base into a tissue culture dish filled with MEM.

- 5| Remove meninges and olfactory bulbs from the brain, cut the brain (sagittal) in two halves, and place each one in one of the tubes with 1 ml MEM (prepared in step 2).
- 6| Repeat steps three to five for all brains.
- 7| Prepare tissue digestion solution, for each half brain (calculate for two additional half brains).
- 8| Cut the brains into small pieces and add 1 ml tissue digestion solution to the tissue, shake the tube gently, and incubate at  $37^{\circ}\text{C}$ , 20 min.
- 9| Fill one 15 ml tube with 9 ml DMEM (prewarmed) for each half brain.
- 10| Prepare ovomuroid solution, for each half brain (calculate for two additional half brains).
- 11| Triturate the tissue gently with a 1000  $\mu\text{l}$  tip (until all cells are dispersed).
- 12| Add 1 ml ovomuroid solution to each brain-tube to stop the digestion and mix by pipetting.
- 13| Transfer each single-cell suspension of one brain into one tube with 9 ml DMEM (prepared in step 9).
- 14| Centrifuge for 10 min at 163 rcf.
- 15| Discard the supernatant by decanting and resuspending pellet in 1 ml B27 proliferation media (prewarmed).
- 16| Pool the two half brains of each brain while pouring or pipetting the cell suspension over a cell strainer (100  $\mu\text{m}$ ) fitted on a 50 ml tube. Rinse the cell strainer with another 1 ml of B27 media.
- 17| Centrifuge again the cell suspension for 10 min at 163 rcf.
- 18| Prepare the freezing medium.
- 19| Discard the supernatant and gently resuspend the pellet in 1 ml freezing medium.
- 20| Transfer cell solution to labeled cryovials and directly place it in a cryodevice into  $-80^{\circ}\text{C}$  for 24 h.
- 21| Remove vials from the cryodevice and store the vials not longer than 6 months at  $-80^{\circ}\text{C}$ .

#### P2.2. Thawing Rabbit NPC and Forming Neurospheres

Preparation for each vial to be thawed:

- Prewarm 2  $\times$  50 ml of B27 medium in a culture flask for 2 h at  $37^{\circ}\text{C}$ .
  - Prepare preconditioned B27 medium + 20 ng/ml rhFGF<sub>2</sub> + 10  $\mu\text{M}$  ROCK inhibitor Y-276322 (1:1000 from stock solution).
  - Fill six 6 cm poly-HEMA coated Petri dishes (6 ml) and one 15 ml centrifuge tube with prepared B27 medium (10 ml).
- 1| Thaw vials in warm water until the ice starts to melt.
  - 2| Quickly transfer the complete content of the vial to a 15 ml centrifuge tube previously filled with 10 ml of preconditioned B27.
  - 3| Centrifuge at 163 rcf for 10 min.
  - 4| Discard the supernatant.
  - 5| Resuspend spheres gently in 0.5 ml of preconditioned B27 medium and distribute it homogeneously (approx. 10  $\mu\text{l}$ ) to the previously prepared 6 cm poly-HEMA Petri dishes (with 6 ml B27).
  - 6| Incubate rabbit NPCs at  $37^{\circ}\text{C}$  and 5%  $\text{CO}_2$ .
  - 7| Change half of the medium with fresh B27 medium without the ROCK inhibitor every 2–3 days.

8| After approx. 11 days, spheres should be ready to be chopped for starting experiments.

### P2.3. Chopping Neurospheres

- 1| Chop rabbit NPCs 2–3 days to 0.2 mm always before starting an experiment.
- 2| Prewarm B27 proliferation medium (37°C); add 20 ng/ml rhFGF.
- 3| Label required Petri dishes (90 mm) previously coated with Poly-HEMA: animal code, P0: thawing date, P1: new passage number, date.
- 4| Pipette 20 ml of fresh prewarmed B27 into each Petri dish previously coated with Poly-HEMA.
- 5| Disinfect the tissue chopper with 70% ethanol. Make sure that no ethanol remains on the blade before placing the neurospheres under the chopping arm.
- 6| Pinch a coverlid of a small Petri dish (60 mm) on the intended position under the chopping arm.
- 7| Take the razor blade out of a centrifuge tube filled with ethanol. Use one side for a maximum of two times.
- 8| Screw the razor blade on the chopping arm, align its position, and fixate the blade. Run the chopper to test if the blade is in the right position; otherwise, adjust it again.
- 9| Set the chopper to 0.2 mm.
- 10| Gently swirl the Petri dish to bring all neurospheres in the middle, collect and place them on the lid (center) of a small Petri dish (60 mm) with as less medium as possible (If you want to chop neurospheres from the same animal from two or multiple dishes, transfer and pool them first in one Petri dish).
- 11| Remove the medium surrounding the spheres under the binocular microscope until the pink shimmer can no longer be recognized. This is to ensure that the spheres will be really cut and not just pushed aside by the blade in the liquid film.
- 12| Pinch the coverlid with spheres below the chopper arm and start (the arm of the blade must be positioned to the right of the neurospheres). After the first run, turn the lid of the Petri dish to 90° and chop again.
- 13| Place on top of the freshly chopped spheres ca. 500 µl B27 medium with rhFGF and separate them by repeated up and down pipetting using a 1000 µl pipette (avoid producing air bubbles).
- 14| Subsequently, distribute evenly the cell suspension on the prepared Petri dishes.
- 15| In case you want to chop several neurosphere cultures from different animals, clean the razor blade with ethanol before each subsequent chopping session.
- 16| Finally, clean the chopper with 70% ethanol and remove it from the bench.

## Protocol 3: Neurosphere Assay

This protocol includes all steps needed to perform the whole neurosphere assay with rabbit neurospheres. For a graphical summary of the timeline of the neurosphere assay, see **Figure 3**. The neurosphere assay allows the *in vitro* evaluation of developmental neurotoxic effects in several

endpoints in parallel: differentiation, migration, viability, and proliferation.

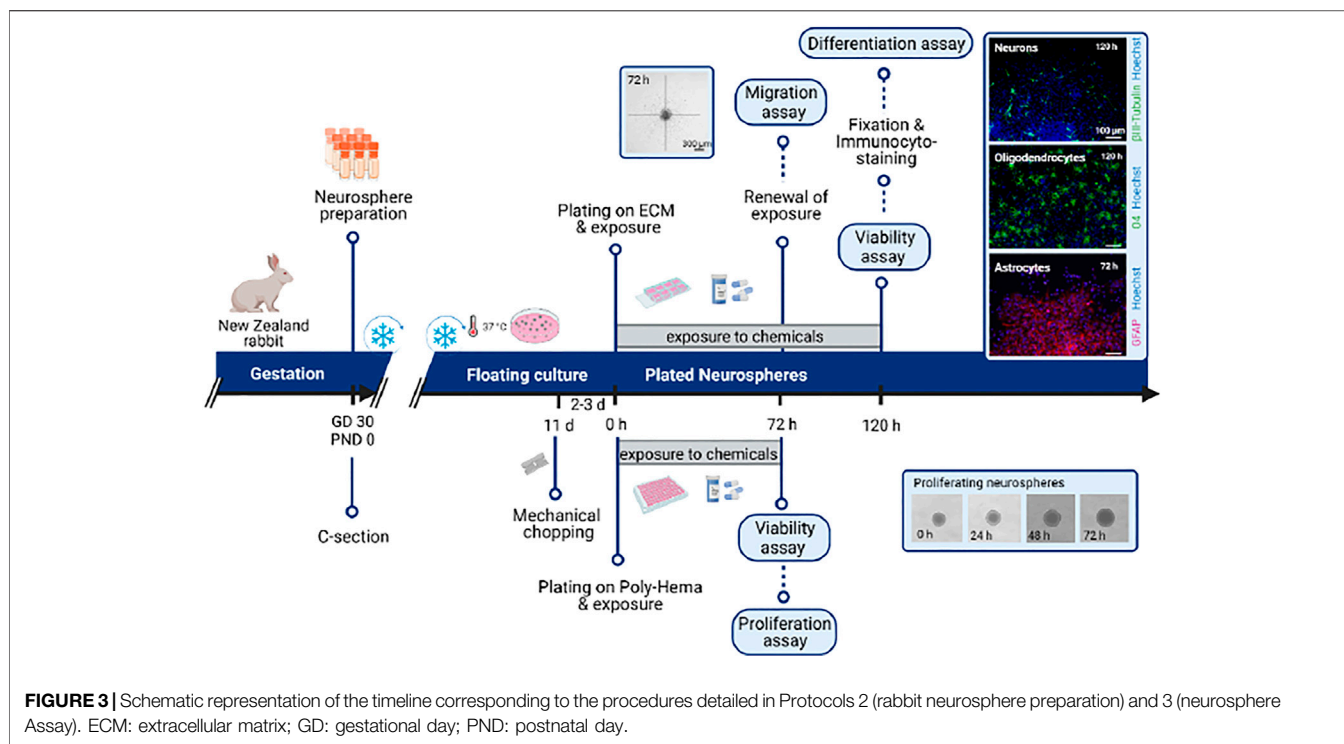
## P3 Materials and Equipment

- Class II biological safety cabinet.
- Cell culture incubator (37°C; 5% CO<sub>2</sub>).
- Laboratory heating oven (37°C).
- Binocular microscope.
- Poly-D-Lysin (PDL).
- PDL solution.
- Laminin.
- H<sub>2</sub>O, deionized and sterile.
- Sterile PBS.
- N2 media.
- 12% paraformaldehyde solution in PBS, pH 7.4.
- Eight-chambered cell culture slides.
- Unsterile PBS.
- PBST 0.5%.
- Mounting medium.
- Goat serum.
- Bovine serum albumin.
- Nucleic acid stain.
- O4 mouse monoclonal antibody IgM (R&D Systems #MAB1326).
- Anti-β-Tubulin III rabbit antibody IgG (Sigma #T2200).
- Anti-Glial Fibrillary Acidic Protein (GFAP) rabbit antibody IgG (Sigma #G9269).
- Goat anti-Mouse IgM Secondary Antibody.
- Goat anti-Rabbit IgG Secondary Antibody.
- Fluorescence plate reader.
- CellTiter-Blue cell viability assay kit.
- CellTiter-Blue reagent (protect from light).
- DMSO.
- B27 w/o (without growth factors) media.
- 96-well plate (clear, U-bottom).
- Poly-HEMA solution (see Poly-HEMA coating in **Supplementary File S1**: Reagents and Solutions list).
- Solutions to be used as positive controls in the neurosphere assay.

## P3 Methods

### P3.1. Neurosphere Differentiation Assay

- 1| Preparation for cell plating:
  - a) Chop neurospheres to a size of 0.2 mm 2–3 days prior to the experiment. Only rabbit neurospheres in passage 1 are used for the differentiation assay.
  - b) Prewarm N2 media at 37°C.
  - c) Prepare previously coated 8-chamber slides by removing PBS (for PDL-Laminin coating protocol, see **Supplementary File S1**: Reagents and Solutions list).
  - d) Prepare all treatments and control solutions and add 500 µl to each chamber of an 8-chamber slide.
  - e) Equilibrate the slide at 37°C and 5% CO<sub>2</sub> for 20 min.
- 2| Plating and cultivation of spheres:
  - a) Sort the desired amount of 0.3 mm sized spheres from a Petri dish into a new Petri dish (60 mm) with 5 ml of N2 media (37°C).



- b) From the presorted spheres transfer 5 spheres in 10  $\mu$ l media into one PDL/Laminin coated chamber of an 8-chamber slide. Place spheres in each well (except in the well of the background control) in the same position as the dots of dice in face 5.
  - c) Culture the spheres for 3 or 5 days depending on the endpoint at 37°C and 5% CO<sub>2</sub>:
    - i. 3 days: GFAP and  $\beta$ -Tubulin III staining
    - ii. 5 days: O4 and  $\beta$ -Tubulin III staining
  - d) After 3 days in culture, take brightfield pictures from the migration area from each sphere using the microscope and camera to analyze the migration distance (see 3.2. Migration of neurospheres).
  - e) For experiments ending on day 3 the viability assay “Cell Titer Blue (CTB) Assay” can be performed.
  - f) For experiments ending on day 5, after 3 days feed the spheres by removing half of the media (250  $\mu$ l) and carefully adding freshly prepared control/treatment solution (prewarmed to 37°C). Continue culturing the slide at 37°C and 5% CO<sub>2</sub> until day 5 and perform the viability assay “Cell Titer Blue (CTB) Assay”.
  - g) Add PFA (12%) in a 1:3 proportion to each chamber (final concentration 4%) and incubate 30 min at 37°C.
  - h) Carefully remove PFA.
  - i) Wash 3  $\times$  3 min by addition and removal of 500  $\mu$ l PBS.
  - j) Slides can be stored filled with 500  $\mu$ l PBS/chamber and sealed with Parafilm at 4°C for a maximum of 4 weeks until immunocytochemical staining is performed.
- 3| Immunocytochemical staining of neurospheres:
    - a) Fixation: see steps g) to j) of step 2 of this protocol.
    - b) Washing:
      - i. Carefully remove PBS and discard the PFA waste.
      - ii. Remove the chamber.
      - iii. 2  $\times$  5 min washing in PBS in a Coplin jar.
    - c) Staining:
      - i. Prepare first antibody solution.
      - ii. Add 30  $\mu$ l antibody solution to each well (see **Supplementary File S1**. Reagents and Solutions list).
      - iii. Incubation: 60 min at 37°C or overnight (o.n.) at 4°C (see **Supplementary File S1**. Reagents and Solutions list).
      - iv. 3  $\times$  5 min washing in PBS in a Coplin jar.
      - v. Prepare second antibody solution.
      - vi. Add 30  $\mu$ l antibody solution to each well.
      - vii. Incubation: 30 min at 37°C.
      - viii. 3  $\times$  5 min washing in PBS in a Coplin jar.
      - ix. Wash with dH<sub>2</sub>O in a Coplin jar.
      - x. Drop the mounting medium on each well and carefully cover the slide with a cover slide.
  - 4| Analysis of differentiation assay:
    - a) Acquire two images per neurosphere, from the upper and lower part of the migration area without capturing the sphere core, by using a fluorescence microscope.
    - b) Take a picture from exactly the same area of the nucleic acid staining (nuclei, blue) and O4 (oligodendrocytes, green),  $\beta$ -Tubulin III (neurons, green) or GFAP (astrocytes, red) staining, depending on the endpoint to measure.
    - c) Save images with the respective experiment number.
    - d) Install/open ImageJ.
    - e) Count nuclei in a single-color image in ImageJ by processing the “binary watershed” function which separates merged nuclei and “analyzing particles” function.

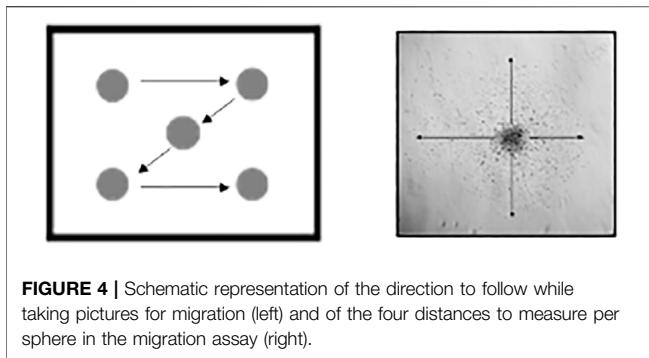


**FIGURE 4** | Schematic representation of the direction to follow while taking pictures for migration (left) and of the four distances to measure per sphere in the migration assay (right).

- f) Overlay fluorescence pictures in an 8-bit format by merging the nuclei channel with O4,  $\beta$ -Tubulin III, or GFAP channel and save merged images in the RGB format.
- g) Subsequently, count the quantity of O4+ and  $\beta$ -Tubulin III + cells manually and normalize them by the number of nuclei.

### P3.2. Migration of Neurospheres

- 1| Brightfield pictures of the migration area:
  - a) Take a brightfield image of each sphere on day 3 under differentiation conditions (see 3.1. Differentiation assay).
  - b) Take a picture of the chamber number and one of each sphere in it following a 'Z' direction (see **Figure 4**).
  - c) Save all pictures in a folder with the experiment identification number.
- 2| Analysis of cell migration in ImageJ:
  - a) Install/open ImageJ.
  - b) Open the images of the experiment to be analyzed.
  - c) Click "Analyze"—"Set Scale". Set scale from pixels to  $\mu\text{m}$  according to your microscope's camera.
  - d) Measure with the tool "straight line" the distance from the sphere core until the furthest migrated cell.
  - e) Measure this distance four times in right-angled directions of the migration area.
  - f) Calculate the mean of the four measurements.
  - g) For each condition calculate the mean of the five spheres.

### P3.3. Viability Assay (CellTiter Blue, CTB Assay)

For migration or differentiation assays:

- 1| Add DMSO to a final concentration of 10% 30 min before the addition of CTB-reagent to the lysis control well.
- 2| Mix CTB-reagent with N2 Media 1:3.
- 3| Discard 200  $\mu\text{l}$  medium from slide chambers so that 300  $\mu\text{l}$  medium remains.
- 4| Add the prepared CTB dilution 1:4 to each chamber (300  $\mu\text{l}$  media in chamber + 100  $\mu\text{l}$  dilution).
- 5| Incubate for 2 h at 37°C and 5%  $\text{CO}_2$ .
- 6| Pipette 2  $\times$  100  $\mu\text{l}$  out of the 8-chamber slide into a 96 well plate (two replicates for each chamber).
- 7| Fixation steps can be performed now (see 3.1. Differentiation assay)
- 8| Measure in a fluorescence plate reader at 540 Ex/590 Em.

For proliferation assay:

- 1| Add DMSO to a final concentration of 10% 45 min before the addition of CTB-reagent to the lysis control wells.
- 2| Dilute CTB reagent 1:3 in B27 (without growth factors) media.
- 3| Add 33  $\mu\text{l}$  to each well and incubate at 37°C and 5%  $\text{CO}_2$  for 2 h.

### P3.4. Proliferation Assay

- 1| Preparation for neurosphere plating:
  - a) Coat 96-well plates (clear, U-bottom) with 25  $\mu\text{l}$  Poly-HEMA.
  - b) 2–3 days earlier to the experimental plating day, chop rabbit neurospheres into 0.2-mm sized spheres.
  - c) Prewarm B27 media with and without growth factors at 37°C.
  - d) Prepare all desired treatment and control solutions and add 100  $\mu\text{l}$  to each well of a 96-well plate previously coated with Poly-HEMA.
  - e) Prepare solutions for four replicates per condition.
  - f) Fill the surrounding wells with 100  $\mu\text{l}$  sterile  $\text{dH}_2\text{O}$ .
- 2| Plating of spheres:
  - a) Sort the desired number of spheres (0.3 mm) and place them into a new Petri dish (60 mm) previously filled with 5 ml B27 media without growth factors (37°C).
  - b) From the sorted spheres, transfer one sphere in 1.5  $\mu\text{l}$  media into a well of a 96-well plate (U-bottom). Change the tip between different conditions.
  - c) Take a picture of every sphere under the brightfield microscope using the camera on day 0 and 7 consecutive days at the same hour of the day.
  - d) Incubate plate at 37°C, 5%  $\text{CO}_2$  for 7 days.
  - e) Feed every 2 or 3 days the spheres by removing half of the media (50  $\mu\text{l}$ ) and adding fresh treatment and control solutions (prewarmed to 37°C).
  - f) On day 7 a CellTiter Blue (CTB) assay for viability testing can be performed.
- 3| Analysis of the area increase in ImageJ.
  - a) Install/open ImageJ.
  - b) Open the images of the experiment to be analyzed.
  - c) Measure the two diameters of the sphere and calculate the mean.
  - d) Calculate the slope for the diameter increase and take the mean of 4 replicates per condition.

## Protocol 4. Behavioral Ontogeny

Alterations of behavior ontogeny are important neurodevelopmental adverse outcomes that can only be evaluated *in vivo*. In this protocol, the procedures needed to evaluate early behaviors of New Zealand rabbits at PND1 are presented together with the scoring system established to measure them. These procedures are based on the previous methodology described by Derrick et al. (2004).

### P4 Materials and Equipment

- Data collection sheet (see **Supplementary File S2**).
- Prepare the observation area: put on a table the heating bed/electric blanket (50  $\times$  50 cm approximately), switch it on at the lowest level, and cover it with an underpad. Draw a 15 cm line on the center of the underpad.
- Timer.

**TABLE 1** | Scoring system for behavioral ontogeny tests.

| Endpoint               | Score   |
|------------------------|---|
| Posture                | 0: lays supine<br>1: lays on the side<br>2: cannot maintain prone position, wobbly<br>3: prone position with legs coiled  |
| Righting reflex        | Number of times the animal turns  |
| Tone                   | 0: no increase in tone<br>1: slight increase in tone when the limb is moved<br>2: marked increase in tone but the limb is easily flexed<br>3: increase in tone, passive movement difficult<br>4: limb rigid in flexion or extension |
| Circular motion        | 0: no movement<br>1: slight movement; slight jump<br>2: good range of motion; maintains for 1 or 2 steps; occasional jump<br>3: entire range of motion; at least 3 steps; rapid jumps   |
| Hind limb locomotion   | 0: no movement<br>1: slight movement<br>2: distinct movement<br>3: rapid movement   |
| Intensity              | 0: no movement<br>1: slight activity<br>2: distinct forceful movements<br>3: rapid forceful movements   |
| Duration               | 0: no movement<br>1: activity <20 s<br>2: activity 20–40 s<br>3: activity >40 s   |
| Lineal movement        | Number of times crosses the perpendicular line  |
| Fore-hind paw distance | Measurement (cm)  |
| Sucking and swallowing | 0: no movement of jaw; all milk dribbles out<br>1: some movement of jaw; most of milk dribbles out<br>2: definite suck and swallow; some milk in nose<br>3: good suck and swallow; no milk in nose                                  |
| Head turning           | 0: no movement<br>1: slight occasional movement of the head<br>2: distinct movement of the head<br>3: rapid forceful movement of the head and body  |
| Olfaction              | 0: no<br>1: subtle<br>2: low response<br>3: correct   |
| Olfaction time         | Latency time (seconds)  |

General motor skills, tone, reflexes, and olfactory sensitivity scores grading, following previous methodology described by Derrick et al. (2004).

- Plastic Pasteur pipette loaded with warm puppy milk replacement formula (enriched with colostrum and omega 3).
- Ethanol-soaked gauze. Soak it again before each test.
- Optional: Recording setting (tripod and camera).

## P4 Methods

This method can be evaluated in real-time if it is performed by two experimenters. In case only one experimenter is performing it, it needs to be recorded and evaluated afterward. The protocol consists of 12 tests scored with a scale from 0 to 3 or 0 to 4 (0: worst—3 or 4: best; see **Table 1** for the detailed scoring system). In case the whole protocol is recorded, each animal should be

recorded for 1 min. This one 1 min observation includes the evaluation of:

- 1| Place a PND1 New Zealand rabbit at the center of the observation area (optional: start video recording) and start the animal observation.

Test 1. Posture: place the animal in the observation area and evaluate the posture.

Test 2. Righting reflex: the pup will be forced to lay in supine position, and the number of times it manages to adopt the prone position in 10 trials will be recorded. Write down if it is an early or a late response since the expected behavior in controls is an immediate response.

Test 3. Tone: evaluate the muscle tone of the fore and hind limbs (right and left) by evaluating the resistance degree of the limb to passive flexo-extension. The less resistance the better score.

Test 4. Circular movement: it is the main movement performed by newborns (stronger forelimbs than hind limbs). Count the number of complete circular movements the pups perform. Simultaneously evaluate the jumps/hops associated with those circular movements (the faster and more frequent the better) for 1 min.

Test 5. Hind limbs locomotion: analyze the quantity and quality of the spontaneous head and limb movements associated with wandering.

Test 6. Intensity of the movements: non-spontaneous as well as almost spasmodic or very fast and energetic movements.

Test 7. Duration of movements: duration of continuous activity - not resting (within a min).

Test 8. Lineal movement. Place the animal perpendicular and 15 cm far from the line. Evaluate the number of times the pups cross the perpendicular line while walking a straight distance of 15 cm within a min.

Test 9. Shortest distance between fore and hind limbs: five measurements (in cm) of the distance between hind limbs and forelimbs. Consider only when walking straight. Write the mean down.

2| After this minute of evaluation, the following three tests are performed:

Test 10. Sucking and swallowing: place the plastic Pasteur pipette loaded with milk in the mouth of the pup. Evaluate the sucking reflex, milk spill, presence of milk in the nasal orifices as well as the overall head and body movement.

Test 11. Head movements: evaluate the head movements associated with the suction reflex when administering the milk in test 10.

Test 12. Olfactory test: soak a gauze in medical degree ethanol and bring it close to the nose of the pup without touching it. The Control group should have a quick aversive response such as moving the head away from the ethanol. Evaluate a null, mild, moderate or intense response, as well as the latency time in seconds.

3| Optional: Off-line analysis of the evaluation.

4| Fill in the data collection sheets.

## Protocol 5. Brain Sample Collection

This protocol describes the obtaining of brain samples at PND1 to be further processed in protocols 7, 8, and 9. For obtaining brain samples for protocol 6, please see protocol 6. For obtaining brain samples for protocols 13 and 14, please see protocol 12.

### P5 Materials and Equipment

- 0.9% saline solution.
- 10% formalin.
- Sucrose 30% (see **Supplementary File S1**. Reagents and Solutions list).
- Plastic bags for freezing previously labeled with a different number for each brain.
- Dry ice.

- Scissors.
- Tweezers.
- Scale.

### P5 Methods

- 1| Obtain the brain and record the weight.
- 2| Wash the brain with saline solution.
- 3| Fix the brain in 10% formalin for 24 h.
- 4| Immerse the whole brain in sucrose 30% for 48 h.
- 5| Collect the brain and place it in a labeled hermetic plastic bag for freezing.
- 6| Store samples at  $-80^{\circ}\text{C}$ .

## Protocol 6. Golgi Staining Protocol

Protocols 6, 7, 8, and 9 describe the steps to perform neuropathological evaluations through Immuno-/stainings in brain slices of PND1 animals to evaluate adverse effects in neurons, astrocytes, microglia, and oligodendrocytes, respectively.

### P6 Materials and Equipment

- FD Rapid GolgiStain kit (FD Neurotechnologies Inc.).
- Sterile 50 ml tubes.
- Double  $\text{d}_2\text{H}_2\text{O}$ .
- Paintbrush.
- Slides.
- Vibratome.
- Epifluorescence microscope.

### P6 Methods

#### *P6.1. Obtaining Brain Tissue and Golgi Solution Incubations*

- 1| Sacrifice the neonate by decapitation at PND1.
- 2| Obtain the brain and cut it into three different parts:
  - a) Right hemisphere
  - b) Left hemisphere
  - c) Cerebellum and medulla
- 3| Wash the tissue with double  $\text{d}_2\text{H}_2\text{O}$  to remove the blood.
- 4| Immerse the tissue in the supernatant A + B Solution (It is important to use the top part of the solution that is free of precipitate).
- 5| After 24 h renew solution A + B.
- 6| Incubate in A + B solution for 2 weeks at RT and in darkness. Gently swirl side to side for a few seconds twice a week.
- 7| After 2 weeks, transfer the tissue into solution C and store at RT in darkness for 3–7 days (ideally 5 days).
- 8| Replace the solution C once after 24 h (on the next day of the replacement).
- 9| Cut 100  $\mu\text{m}$  sections with a vibratome (speed 5, amplitude 5), using Solution C or PBS as the medium.
- 10| Collect the sections with a paintbrush and mount them on adhesion or gelatin-coated slides.
- 11| Dry at RT in darkness, 2–3 days (max.).

Note: use at least 5 ml of the impregnation solution (solutions A, B, or C) for each cubic cm of tissue processed. It should be noted that using a lower volume of impregnation solution may decrease the sensitivity and reliability of staining.



## P6.2. Staining Protocol

- 1| Rinse sections in double  $d_4H_2O$  for 4 min (2 times).
- 2| Incubate with the stock solution for 10 min (prepare just before use as follows):
  - a) 1 part of Solution D.
  - b) 1 part of Solution E.
  - c) 2 parts of double  $d_4H_2O$ .
- 3| Rinse with double  $d_4H_2O$  for 5 min (4 times).
- 4| Contrast: incubate for 6 min with Cresyl violet
- 5| Dehydration:
  - a) 4 min, 50% ethanol.
  - b) 4 min, 75% ethanol.
  - c) 4 min, 95% ethanol.
  - d) 4 min, ethanol absolute (4 times).
- 6| Xylene for 4 min (3 times).
- 7| Cover slip with Permount and dry at RT protected from light o.n.
- 8| Acquire images under 40x objective magnification in an AF6000 epifluorescence microscope.
- 9| Analysis of the images. Here we present an example evaluating pyramidal neurons; however, other neuronal types can be included depending on the interest of the study. Five pyramidal neurons from the area of interest from each brain hemisphere (10 neurons per animal) that fulfill the inclusion criteria are randomly selected.

Inclusion criteria: pyramidal neurons within layers II and III, and complete filling of the dendritic tree, especially for the basal dendrites, as evidenced by well-defined endings.

- 10| Measure the following parameters from each neuron using ImageJ software:
  - a) Area of the soma (obtained by manual delineation of the shape of the neuronal soma in a 2D image).
  - b) Number of basal dendrites (obtained by manual counting).
  - c) Total basal dendritic length (obtained after performing manual delineation of the length of each basal dendrite and then calculating the addition of all lengths from all basal dendritic branches).
  - d) Basal dendritic complexity, which includes the evaluation of the number of basal dendritic intersections and the number of each basal dendritic branches. The basal dendritic complexity is evaluated by using the Sholl technique, as previously described (Sholl, 1953). Sholl rings are placed concentrically in 10  $\mu m$  increasing intervals centered on the soma. For the basal dendritic intersections, the number of intersections that dendritic branches have per each Sholl ring and the addition of all of them are recorded. For the number of each basal dendritic branch, each basal dendritic branch is divided into primary, secondary, tertiary, quaternary, quinary, and senary dendrites. Primary dendrites are considered those dendrites that are originated from the soma; secondary dendrites those that are derived from the primary dendrites, and so on, up to the senary dendrites, corresponding to those derived from the quinary dendrites.

## Protocol 7. Astrocyte IHC

### P7 Materials and equipment

- Anti-GFAP (GA-5): NBP2-29415- 20  $\mu g$  (Bio-Techne).
- Goat anti-Mouse IgG secondary antibody.
- PBS.
- PBST 0.3%.
- Citrate buffer (pH 6).
- IHC blocking solution (see **Supplementary File S1**. Reagents and Solutions list).
- Mounting media.
- Humid chamber.
- Slides.
- Hydrophobic pen.
- Paintbrush.
- Confocal scanning laser microscope.

### P7 Methods

- 1| Obtain and store PND1 brains, as detailed in PROTOCOL 5.
- 2| Acquire consecutive 40  $\mu m$  sections by cryotomy.
- 3| Select the sections containing the area of interest with the help of a rabbit brain atlas (Muñoz-Moreno et al., 2013).
- 4| Use a slide per animal with three consecutive cuts in each slide and delimit them with a hydrophobic pen.
- 5| Process the slides for heat-induced-epitope-retrieval (HIER) in citrate buffer (pH 6) for 3 min (at 90°C in a Coplin jar inside a double-boiler).
- 6| Permeabilize tissue with Triton X-100 0.3% in PBS for 30 min at RT in a humid chamber.
- 7| Block the samples by incubating slides with 1% BSA and 5% goat serum for 1 h at RT.
- 8| Incubate tissue sections with 1:400 anti-GFAP at 4°C o.n.
- 9| Wash 3 times with Triton X-100 0.3% in PBS for 5 min.
- 10| Incubate with goat anti-mouse IgG and 1:1000 nucleic acid stain for 1 h at RT.
- 11| Wash once with Triton X-100 0.3% in PBS for 5 min at RT.
- 12| Wash twice with PBS for 5 min at RT.
- 13| Rinse in  $d_4H_2O$ .
- 14| Add mounting media and store at 4°C o.n.
- 15| Seal with nail polish and store at -20°C.
- 16| When slides are dry, observe them with confocal scanning laser microscopy.
- 17| Acquire images with a 63x/1.40 oil immersion differential interference contrast (DIC) objective. Quantify images by counting GFAP + cells/ $mm^2$ .

## Protocol 8. Microglia IHC

### P8 Materials and Equipment.

- Primary antibody: biotinylated *Lycopersicon esculentum* tomato lectin (VectorLabs #B-1175).
- Cy3-conjugated streptavidin.
- PBS.
- PBST 0.3%.
- Nucleic acid stain.
- IHC blocking solution (see **Supplementary File S1**. Reagents and Solutions list).

- Slides.
- Cryomicrotome.
- Paintbrush.
- Mounting media.
- Hydrophobic pen.
- Nail polish.
- Confocal scanning laser microscope.

## P8 Methods

- 1| Obtain and store PND1 brains, as detailed in PROTOCOL 5.
- 2| Obtain with the cryomicrotome 40  $\mu\text{m}$  cuts covered with poli-L-lysine.
- 3| Select the sections containing the area of interest with the help of a rabbit brain atlas (Muñoz-Moreno et al., 2013).
- 4| Use a slide per animal with three consecutive cuts in each slide.

In all steps, add 50–100  $\mu\text{l}$ /cut, except for the antibody incubation steps, where 50  $\mu\text{l}$ /cut has to be added but the excess solution has to be removed with the vacuum.

- 5| Thaw the slides with the samples and leave them at RT to dry for 10 min.
- 6| Delimit the slide using a hydrophobic pen and wait until it is completely dry.
- 7| Permeabilize with PBST 0.3% with 0.5% BSA at RT for 1 h.
- 8| Incubate with the primary antibody biotinylated *Lycopersicon esculentum* tomato lectin at RT for 60 min.
- 9| Wash the samples with PBST 0.3%.
- 10| Incubate with conjugated Cy3-conjugated Streptavidin for 30 min at RT with 1% nucleic acid stain.
- 11| Wash the samples with PBST for 5 min at RT.
- 12| Wash the samples two times with PBS for 5 min at RT.
- 13| Immerse the samples in  $\text{dH}_2\text{O}$  one time.
- 14| Add mounting media (80  $\mu\text{l}$ /slide) and remove the excess.
- 15| Keep in the fridge until the next day.
- 16| Then, 24 h later, seal with nail polish and store at  $-20^\circ\text{C}$ .
- 17| Observe with confocal scanning laser microscopy.
- 18| Images are taken under 40x objective magnification with 10 steps of 1  $\mu\text{m}$  in the Z-stack. The total number of stained cell nuclei and the number of cells with positive fluorescent staining around the nucleus are counted using ImageJ software. The number of positive cells/ $\text{mm}^2$  is then calculated.

## Protocol 9. Oligodendrocyte IHC

### P9 Materials and equipment.

- Slides.
- Paintbrush.
- PBS.
- PBST 0.3%.
- Nucleic acid stain.
- IHC blocking solution (see **Supplementary File S1**. Reagents and Solutions list).

- Primary antibody Mouse IgM anti-O4 (Merck Millipore #MAB345).
- Secondary antibody goat anti-mouse IgM.
- $\text{dH}_2\text{O}$ .
- Mounting media.
- Nail polish.
- Cryostat.
- Hydrophobic pen.
- Confocal scanning laser microscope.

## P9 Methods

- 1| Obtain and store PND1 brains, as detailed in PROTOCOL 5.
- 2| Obtain with the cryostat 40  $\mu\text{m}$  cuts. Use a slide per animal with three consecutive cuts in each of them.

In all steps, add 50–100  $\mu\text{l}$ /cut, except for the antibody incubation steps, where 50  $\mu\text{l}$ /cut has to be added but the excess solution has to be removed with the vacuum.

- 3| Thaw the slides with the samples and leave them at RT to dry for 10 min.
- 4| Delimit the slide using a hydrophobic pen and wait until it is completely dry.
- 5| Wash the samples two times with PBS for 5 min at RT.
- 6| Permeabilize with PBST 0.3% at RT for 20 min.
- 7| Incubate with the IHC blocking solution in a humidity chamber at RT for 1 h.
- 8| Incubate with the primary antibody Mouse IgM anti-O4 (#MAB345) o.n. at  $4^\circ\text{C}$  (ensure more than 14 h incubation).
- 9| Leave the sample at RT for 60 min.
- 10| Wash the samples three times with PBST 0.3% for 5 min at RT.
- 11| Incubate for 1 h with the secondary antibody goat anti-mouse IgM at RT with 1% nucleic acid stain.
- 12| Wash the samples with PBST 0.3% for 5 min at RT.
- 13| Wash the samples with PBS for 5 min at RT.
- 14| Immerse the samples in  $\text{dH}_2\text{O}$  one time.
- 15| Add mounting media (80  $\mu\text{l}$ /slide) and remove the excess.
- 16| Keep in the fridge until the next day.
- 17| 24 h later, seal with nail polish and store at  $-20^\circ\text{C}$ .
- 18| Observe with a confocal scanning laser microscope.
- 19| Images are taken under 40x objective magnification with 10 steps of 1  $\mu\text{m}$  in the Z-stack. The total number of stained cell nuclei and the number of cells with positive fluorescent staining around the nucleus are counted using ImageJ software. The number of positive cells/ $\text{mm}^2$  is then calculated.

## Protocol 10. Skinner Box

Operant conditioning behavior can be studied using a Skinner box adapted to rabbit. In this test, the response of the animals to the environment when they receive food reinforcements is evaluated and can be used as a measure of learning. According to OECD TG 426, learning and memory tests should be performed in adolescents as well as in young adult animals. Here, we present a protocol for performing the Skinner box

test in young adults on PND70, which is adapted from Zworykina et al. (1997). Further evaluations are needed to establish if this protocol can directly be used during the adolescence period, if the protocol needs adaptations, or if another learning test should be used at that age since the TG allows the use of the same or different tests at these two stages of development.

## P10 Materials and Equipment

- Data collection sheets.
- Neurological observation area: Skinner box for rabbits constructed as detailed in Leal-Campanario et al., (box for operant conditioning and instrumental learning for rabbits, 2012. Inscription number in Spain: P2001231369). Briefly, the operant box (780 × 595 × 985 mm) has three aluminum lateral walls and the central lateral wall is made of methacrylate. The floor is a 590 × 815 mm multi-perforated PVC plate that allows the free movement of the animal. It also includes a tray with sawdust bedding to collect the feces. The lever (130 × 100 mm), made of aluminum, is located on one of the side walls, 30 mm above the floor level, and protrudes 67.5 mm toward the inside of the box. In addition, it has a recovery mechanism to return to its starting position. The lever is connected to a control panel. The food dispenser is located outside of the box and connected to the feeder. The food dispenser is connected to the control panel and receives a signal when the lever has been hit, allowing a pellet to fall into the feeder. The diameter of the feeder is 60 mm and it is located 10 mm above the floor level.

## P10 Methods

### P10.1. Reduction of Food Intake and Body Weight Control

- 1| Weighing the animals daily. The goal is to achieve a 15% reduction of the initial weight before starting the test.
- 2| Proceed with the intake reduction protocol:
  - a) Monday to Tuesday of the week prior to the start of the test: 80 g of food/day + hay.
  - b) Afterward and during the Skinner test: 20 g/day + hay.
  - c) On weekends: 20 g/day + hay.

### P10.2. Skinner Box Test

Drive the animals to the experimental room 30 min before the test. The experimental room has to be dimly lit and present standard conditions. Clean the apparatus with 70% ethanol.

- 1| During the first week (PND50-59): habituation and training.
  - a) First day of exploration: habituation for 10 min. Record global animal behavior (freezing, defecation and urination, exploration, approach to the feeder and lever, rearing and grooming).
  - b) Second day of exploration (training 1): 10 min.
    - i. Reinforce the feeder. Put food in the feeder whenever the animal explores the feeder, after exploring the rest of the box.

- ii. Register the number of reinforcements administered in the first 5 min and the last 5 min.
    - iii. Register in observations the global animal behavior.
  - c) Third day of exploration (training 2): 10 min.
    - i. Reinforce the feeder and the lever. Put food in the feeder and the lever whenever the animal explores the feeder and the lever, after exploring the rest of the box.
    - ii. Register the number of reinforcements administered in the first 5 min and the last 5 min.
    - iii. Register in observations the global animal behavior.
  - c) Fourth day of exploration (training 3): 10 min.
    - i. Reinforce the lever. During the first 5 min: feed the lever and then reward the animal with food in the feeder. During the last 5 min: reinforce the lever with only smell and then reward the animal with food in the feeder.
    - ii. Register the number of reinforcements administered in the first 5 min and the last 5 min.
    - iii. Register in observations: global animal behavior and whether or not it takes a long time to search for food from the feeder.
  - c) Fifth day of exploration (training 4): 10 min.
    - i. Reinforce the lever with smell and then reward the animal with food in the feeder (the first stimulus can be putting food in the lever).
    - ii. Register the number of reinforcements administered in the lever in the first 5 min and the last 5 min.
    - iii. Register in observations: global animal behavior and whether it takes a long time to search for food from the feeder.
- 2| During the second week (PND60-69): fixed reason 1 (FR1: one lever—one piece of food).
- a) First-day session FR1: 10 min.
    - i. Only administer food when the animal presses the lever.
    - ii. At the beginning of the session you can administer a reinforcement in the lever. If the animal does not remember, you can give other level reinforcements throughout the examination (maximum 2-3).
    - iii. Register the number of levers hit correctly during the first 5 min and the 5 last min.
    - iv. Register in observations: global animal behavior and whether it takes a long time to search for food from the feeder once it has hit the lever.
  - b) Second-day session FR1: 10 min.
  - c) Third-day session FR1: 10 min.
  - d) Fourth-day session FR1: 10 min.
    - i. Only administer food when the animal presses the lever.
    - ii. At the beginning of the session you can administer reinforcement in the lever. You should not give any more reinforcements.
    - iii. Register the number of levers hit correctly during the first 5 min and the 5 last min.
    - iv. Register in observations: global animal behavior and whether it takes a long time to search for food from the feeder once it has hit the lever.
  - e) Fifth-day session FR1: 10 min.
    - i. Only administer food when the animal presses the lever.
    - ii. You should not give reinforcements.

- iii. Register the number of levers hit correctly during the first 5 min and the 5 last min.
  - iv. Register in observations: global animal behavior and whether it takes a long time to search for food from the feeder once it has hit the lever.
- 3| Complete the data collection sheets.
  - 4| Weigh animals and offer food *ad libitum*.

## Protocol 11. Open-Field Test and Object Recognition Test

These two common behavioral assays are used to evaluate motor activity in the open field test, and learning and memory, combined with sensory function (olfactory) in the object recognition test. This protocol is established to perform the open field behavioral test, and the phase A of the object recognition test one after the other with the same animal on PND70. Once all animals have performed both tests, phase B of the object recognition test starts following the same animal order. OECD TG 426 requires motor and sensory functions to be examined in detail at least once for the adolescent period and once during the young adult period. The open-field test can probably be also used during the adolescence period, but further studies checking the adjustments needed for this developmental stage are required.

### P11 Materials and Equipment

- Data collection sheets.
  - Two apples and one orange.
  - Self-made open field box (140 × 140 cm; surrounded by a 40 cm height wall).
- i. Preparation of the open field box: avoid light reflection on the floor by keeping the room dimly lit.
  - ii. Preparation for the object recognition test: two specimen collection containers with two identical fruits (familiar object) and a third specimen collection container with a different fruit (novel object). In this case, two apples as familiar objects and one orange as novel objects were used. They were sliced and put in the container. The lids must have some holes to release the smells.
- Video Tracking Software.
  - Ethanol-soaked gauze. Soak it again before each test.
  - Recording setting (tripod and camera).

### P11 Methods

#### P11.1. Open-Field Test

Drive the animals to the experimental room 30 min before the test. The experimental room has to be dimly lit and present standard conditions. Clean the open field box with 70% ethanol.

- 1| Open the video tracking software and start a new experiment.
- 2| Identify the animal and name the file (use the same naming once the acquisition is finished).
- 3| Define acquisition settings and save them as a default:
  - a) Define the observation area: adjust the acquisition limits setting them to 140 × 140 cm.

- b) Adjust brightness and contrast if necessary.
- 4| Start the test: start recording:
  - a) Put the cloth inside the open field and start filming (consider if the video tracking software needs some recording of the open field without the animal).
  - b) Immediately after, pick the subject, cover it with a cloth, place the animal in the starting point and remove the covering cloth. The starting point is defined as a limited field of about 1/5 of the whole observation area, preferably the opposite site to the corridor where the camera is set.
  - c) The observer must leave the room.
  - d) After 10 min of recording, the observer enters the room and picks the subject up. Then, and not before, the recording is stopped. Save the file using the same naming.

#### P11.2. Object Recognition Test: Phase A or B

- 1| Open the video tracking software and start a new experiment.
- 2| Identify the animal and name the file (use the same naming once the acquisition is finished. Indicate whether it is phase A or B).
- 3| Define acquisition settings and save them as a default
  - a) Define the observation area: adjust the acquisition limits setting them to 140 × 140 cm.
  - b) Adjust brightness and contrast if necessary.
- 4| Start the test: start recording
  - a) Two separated familiar objects are placed in the center of the observation area.
    - i. Phase A evaluation: two identical familiar objects are placed in the area.
    - ii. The familiar object is a specimen collection container that has a drilled lid to enable recognition and is filled with apple slices.
    - iii. Leave an inter-trial time of 30 min between phase A and phase B
    - iv. Phase B: a familiar object is replaced by a novel one. In this case, a new drilled-lid specimen container is filled with orange slices.
    - v. There is no need to wash the fruit rigorously or control the size of the slices.
  - b) The recording must start at least 1 s before bringing the subject in.
  - c) Immediately after the animal is placed at the starting point, the observer must leave the room during the 5-min recording.
  - d) After 5 min recording, the observer enters the room and picks the subject up. Then, and not before, the recording is stopped. Save the file using the same naming.

Every subject is studied individually to avoid unwanted smell recognition.

- 5| Fill in the data collection sheets.

## Protocol 12. Brain Sample Collection

This protocol describes the obtaining of brain samples at PND70 to be further processed in protocols 13 and 14. For obtaining brain samples for protocol 6, please see protocol 6. For the obtaining of brain samples for protocols 7, 8 and 9, please see protocol 5.

## P12 Materials and Equipment

- 0.9% saline solution.
- Paraformaldehyde 4%.
- Sucrose 30% (see **Supplementary File S1**. Reagents and Solutions list).
- Plastic bags for freezing labeled with a different number for each brain.
- Dry ice.
- A 100 ml beaker filled with 2-methyl butane (cold).
- Guillotine.
- Scissors.
- Tweezers.
- Infusion pump.
- Needle 18G.
- Scale.

## P12 Methods

- 1| Perfuse the animal with 0.9% saline and paraformaldehyde 4%.
- 2| Obtain the brain and record the weight.
- 3| Immerse the whole brain for 24 h in paraformaldehyde 4%.
- 4| Immerse the whole brain in sucrose 30% for 48 h.
- 5| Cut the brain as needed depending on the area of interest (it is recommended to cut it at least in three parts to ease the cutting step with the cryotome).
- 6| Incubate the brain samples in 2-methyl butane (placed in dry ice) for 1 min.
- 7| Collect the brain samples and place them in a labeled hermetic plastic bag for freezing.
- 8| Store samples at  $-80^{\circ}\text{C}$ .

## Protocol 13. Dendritic Spines IHC

Protocols 13 and 14 describe the steps to perform neuropathological evaluations through Immuno-/stainings in brain slices of PND70 animals to evaluate adverse effects in dendritic spines or perineuronal nets, respectively.

## P13 Materials and Equipment

- Gene Gun System.
- Tubing for the Gene Gun System.
- Dil Stain.
- Cryomicrotome.
- Methylene chloride.
- Tungsten particles (1.7 mm diameter).
- Slides.
- $\text{d}_2\text{H}_2\text{O}$ .
- Nitrogen flow gas.
- Membrane filter of 3  $\mu\text{m}$  pore size and  $8 \times 10$  pores/ $\text{cm}^2$ .
- PBS.
- DAPI.
- Mounting media.
- Confocal microscope with a 63x oil-immersion objective.

## P13 Methods

- 1| Obtain the brain at PND70, as detailed in PROTOCOL 12.
- 2| Acquire 150  $\mu\text{m}$  coronal sections by cryotomy.

- 3| Prepare a suspension containing 3 mg of Dil dissolved in 100  $\mu\text{l}$  of methylene chloride mixed with 50 mg of tungsten particles.
- 4| Spread the suspension on a slide to air-dry.
- 5| Resuspend the mixture in 3.5 ml  $\text{d}_2\text{H}_2\text{O}$  and sonicate it.
- 6| Drawn the mixture into a Tefzel tubing and remove it to allow the tube to dry under nitrogen flow gas for 5 min.
- 7| Cut the tube into 13 mm pieces to be used as gene gun cartridges.
- 8| Deliver particles to the area of interest using a modification of the gun to enhance accuracy by restricting the target area.
- 9| Deliver Dil-coated particles in the area of interest shooting over 150  $\mu\text{m}$  coronal sections at 80  $\psi$  through a membrane filter of 3  $\mu\text{m}$  pore size and  $8 \times 10$  pores/ $\text{cm}^2$ .
- 10| Store sections in PBS at RT for 3 h protected from light.
- 11| Incubate with DAPI and use mounting media to be analyzed.
- 12| Image Dil-labeled pyramidal neurons from the area of interest using a confocal microscope with a 63x oil-immersion objective.
  - a) Held constant throughout the study the pinhole size (1 AU) and frame averaging (four frames per z-step).
  - b) Take confocal z-stacks with a digital zoom of 5, a z-step of 0.5  $\mu\text{m}$ , and at  $1,024 \times 1,024$  pixel resolution, yielding an image with pixel dimensions of  $49.25 \times 49.25 \mu\text{m}$ .
- 13| Select two or three basal dendrites of various neurons for the analysis of spine density.
  - a) Select segments with no overlap with other branches that would block visualization of spines.
  - b) Select segments either “parallel” to or “at acute angles” relative to the coronal surface of the section to avoid ambiguous identification of spines.
  - c) Select spines arising from the lateral surfaces of the dendrites and dendritic segments of basal dendrites 45  $\mu\text{m}$  away from the cell body.

## Protocol 14. Perineuronal Nets IHC

### P14 Materials and equipment.

- PBS.
- PBST 0.3%.
- Nucleic acid stain.
- Cryomicrotome.
- IHC blocking solution (see **Supplementary File S1**. Reagents and Solutions list).
- Primary antibody: lectin from *Wisteria floribunda* (Sigma #L1516; 1:20).
- Secondary antibody: streptavidin, Alexa Fluor 488 conjugate (1:2000).
- Slides.
- Paintbrush.
- Hydrophobic pen.
- Mounting medium.
- Confocal scanning laser microscope.

## P14 Methods

- 1| Obtain the brain at PND70 as detailed in PROTOCOL 12.
- 2| Acquire 20  $\mu\text{m}$  sections by cryotomy and include three sections per slide.
- 3| Dry sections at  $37^{\circ}\text{C}$  for 10 min and store at  $-20^{\circ}\text{C}$ .

**TABLE 2** | General summary of critical parameters and troubleshooting.

| Protocol | Problem   | Possible reason   | Solution   |
|----------|---|---|--|
| 2        | Rabbit neurospheres do not form/proliferate   | Rabbit NPC need to be cultured in a relatively high density to form neurospheres    | After thawing neurospheres, use small 60 mm Petri dishes. As soon as they have a certain size (ca. 11 days in proliferation media) chop or transfer the neurospheres to a 90 mm Petri dish |
| 3        | Too low oligodendrocyte differentiation   | Neurospheres are kept too long out of the incubator                                 | Do not plate longer than 30 min one 8-chamber slide  |
| 3        | The migration area of different spheres overlaps or is too close to the chamber edges | Neurospheres were plated too close to the chamber edge or too close to each other   | Place neurospheres like the dots of a dice in face number 5  |
| 3        | The lysis of the neurospheres is not completed  | Proliferating neurospheres need more time to lyse than differentiating neurospheres | Incubate proliferating neurospheres for 45 min and differentiated ones for 30 min in lysis control (10% DMSO)  |
| 3        | Spheres easily detach from the slide surface  | The fixation is not correct   | Do not thaw PFA more than once   |
| 3        | Neurospheres detach from the slide surface during the staining                        | Problems with pipetting during washing steps  | Pipette gently and carefully during the washing steps  |
| 3        | High background signal  | Less washing steps than indicated   | Wash as indicated  |
| 4        | Some of the pups are very weak  | —   | Make sure the bed is warm and the milk preparation is warm   |
| 4        | Difficulties with the simultaneous evaluation of the parameters                       | —   | Conduct the test in pairs. If not, record the whole process  |
| 4        | The animal gets out of the observation area   | —   | Get it back and continue the observation   |
| 6        | Difficulties in finding neurons with well-defined endings                             | Brain sectioning problems   | Manipulate carefully the tissue slices when performing the 100 $\mu\text{m}$ cut sections with the vibratome   |
| 6        | It takes a long time for image evaluation   | A lot of parameters to be evaluated in the same neuron                              | Try to analyze one neuron for each experimental group each day you perform the analysis  |
| 7        | Difficulties in the cryosectioning of samples   | Temperature difference between the sample and the cryomicrotome                     | Put the samples stored at $-80^{\circ}\text{C}$ in the freezer ( $-20^{\circ}\text{C}$ ) o.n. to facilitate cryosectioning   |
| 7        | Weak or absent fluorescence   | Anti-GFAP antibodies do not reach the protein                                       | Perform HIER (heat-induced epitope retrieval)  |
| 7        | Detachment of the tissue slices   | Incorrect manipulation of the tissue slices.<br>Inappropriate coating of the slide  | Manipulate carefully the tissue slices and liquids. Select slides for cryosectioning   |
| 7        | Unspecific fluorescence in the IHC  | Incorrect blocking step   | Always include a negative control of each subject to define unspecific fluorescence  |
| 10       | Stressed/hungry animals   | Intake reduction  | Try to perform the evaluation early in the morning and afterward give them the food indicated by the protocol  |
| 10       | Some animals do not move inside of the Skinner box                                    | They are scared   | In the habituation and training week, try to stimulate them by doing noise in the lever and the feeder   |
| 11       | Anomalous initial response in the open-field test and object recognition test         | The animal is stressed  | Manipulate the animal with kindness and try to stay silent while the test is running   |

- 4| Thaw sections and dry at  $37^{\circ}\text{C}$ .
- 5| Delimit the slide using a hydrophobic pen and wait until it is completely dry.
- 6| Hydrate with PBS for 10 min.
- 7| Permeabilize with PBST 0.3%.
- 8| Block the samples with IHC blocking solution at RT for 60 min.
- 9| Incubate o.n. with the primary antibody at  $4^{\circ}\text{C}$  (400  $\mu\text{l}$ /slide).
- 10| Leave samples at RT for 1 h.
- 11| Wash the samples two times with PBST 0.3% (from now on, protect the samples from light).
- 12| Incubate with the secondary antibody at RT (400  $\mu\text{l}$ /slide) for 90 min.
- 13| Wash the samples four times with PBST 0.3%.
- 14| Wash the samples with PBS for 10 min.
- 15| Incubate with nucleic acid stain 1/1000 with PBS for 20 min.
- 16| Wash the samples with PBS for 10 min.
- 17| Wash the samples with PBS for 10 min.
- 18| Dry the samples and add mounting medium, with 60  $\mu\text{l}$ /slide covering the tissue.
- 19| Observe with a confocal scanning laser microscope

- 20| Images are taken under 40x objective magnification with 20 steps of 1  $\mu\text{m}$  in the Z-stack.
- 21| Analyze perineuronal nets by quantifying the average density of immunolabeling (contacts/ $\mu\text{m}^2$ ) in the region of interest.

A summary of critical parameters and troubleshooting of protocols described in this section is presented in **Table 2**.

## RESULTS

The results summarized in this section include the control values obtained in several studies evaluating the adverse effects of a mild and chronic hypoxia-ischemia insult during gestation in one of the uterus horns by ligation of 40–50% of uteroplacental vessels on day 25 of pregnancy (Illa et al., 2013; Illa et al., 2017; Illa et al., 2018; Pla et al., 2021). The control values presented here are from GD30 fetuses in the contralateral control horn and are therefore obtained from control fetuses after a cesarean section and not by natural delivery.

*In vitro* results are presented as the mean of independent experiments ( $n = 5–25$ ) with standard deviation (SD) and include at least five neurospheres per condition in each independent

**TABLE 3** | Results of PROTOCOL 3

| Endpoint  | Solvent control<br>mean $\pm$ SD (n) | Positive control<br>mean $\pm$ SD (n) |
|---|--------------------------------------|---------------------------------------|
| Oligodendrocyte differentiation (%)               | 6.2 $\pm$ 0.4 (24)                   | 0.6 $\pm$ 0.1 (15)                    |
| Neuronal differentiation (%)                      | 2.4 $\pm$ 0.4 (14)                   | 0.4 $\pm$ 0.2 (8)                     |
| Migration distance ( $\mu$ m)                     | 803.5 $\pm$ 46.4 (22)                | 238.5 $\pm$ 40.2 (8)                  |
| Proliferation ( $\mu$ m of diameter increase/day) | 15.7 $\pm$ 3.6 (5)                   | -3.6 $\pm$ 1.2 (5)                    |
| Viability (RFU)                                   | 22406.0 $\pm$ 1670.2 (25)            | 2005 $\pm$ 299.4 (22)                 |

**TABLE 4** | Threshold PROTOCOL 3

| Endpoint                        | Endpoint-specific<br>Positive control | Exclusion criteria in<br>experiments with rabbit<br>neurospheres             |
|---------------------------------|---------------------------------------|--|
| Oligodendrocyte differentiation | 100 ng/ml BMP7                        | 5 days diff: < 1.5% in solvent control                                       |
| Neuron differentiation          | 10 ng/ml EGF                          | 5 days diff: < 1.5% in solvent control; 3 days diff: < 1% in solvent control |
| Migration distance              | 10 $\mu$ M PP2                        | <250 $\mu$ m in solvent control  |
| Viability                       | 10% DMSO                              | <5700 RFU  |
| Proliferation                   | B27 media without growth factors      | <10 $\mu$ m of diameter increase/day   |

experiment. *In vivo* results are presented as mean values of controls with SD, but the mean is calculated in two different ways, considering the litter or the pup/hemisphere/cell as a statistical unit for later comparison.

*In vitro* results of the neurosphere assay (Protocol 3) are summarized in **Table 3**, where both solvent control values and specific positive control values for each endpoint are presented. Details on which positive control was used for each endpoint are given in **Table 4**. These results show the ability of rabbit neurospheres to perform several processes of neurogenesis and demonstrate that the different endpoints can be affected by exposure to known disturbing substances (positive controls) as described before (Barenys et al., 2021). Previous work has also provided evidence that the technique can detect alterations after exposure to a known developmental neurotoxicant like methylmercury chloride, while no significant alterations are observed after exposure to a negative control like saccharine (Barenys et al., 2021). From the experience generated, a quality threshold has been established for each endpoint, which is summarized in **Table 4**. If control results do not reach the minimum values indicated in this table, the experiment should be discarded, otherwise, the effects of the compounds could be overestimated.

*In vivo* results for protocols performed on PND1 are presented in **Table 5**: Behavioral ontogeny, **Table 6**: Golgi staining, and **Table 7**: Astrocytes, microglia and oligodendrocytes IHC. Afterward, results of protocols performed from PND50 are presented in **Table 8** for Skinner box test, open field and object recognition test, and **Table 9** for dendritic spines and perineuronal nets evaluation. In all these tables, the symbol # indicates results where variability is equal to or higher than the mean of controls for that particular way of calculation. This has been highlighted to allow the detection of measured endpoints with high variability in relation to the mean value, which in fact can render the endpoint as not useful to discriminate adverse effects.

In the behavioral ontogeny evaluation (**Table 5**) the expected scores for control pups are, in general, the maximum possible scores of the scale, with few exceptions of pups receiving the next maximum score possible. This results in very high scores for almost all endpoints and relatively low standard deviations in the control group. There is only one endpoint showing a deviation bigger than the mean value itself, the endpoint “Fore-hind paw distance,” but this is an endpoint in which the treatment effect is expected to probably increase the mean value and not decrease it as in all other endpoints evaluated with a score. Due to this difference in the dynamic range of the endpoint, it is still considered a valuable and informative endpoint of the battery, worth being included in it, despite the variation in the controls.

Neuronal evaluation with Golgi staining was performed in the frontal cortex of PND1 rabbits, as detailed by Pla et al. (2021). Neurons presented mainly principal and secondary branches in a similar proportion, while tertiary branches were less than half of the previous ones. At this developing time and in this area of analysis, there were almost no quaternary, quinary and senary branches. In fact, the number of the three latest ones was so low that small variations resulted in a high relative variability compared to the mean value. Because of that, if reductions in the number of branches are expected, it is suggested to evaluate the number of branches above tertiary altogether to improve the sensitivity and the dynamic range of the endpoint, since these measurements are not difficult to be performed and can still be informative.

IHCs of astrocytes, microglia, and oligodendrocytes were evaluated in the corpus callosum genu area and the results expressed as GFAP + cells/mm<sup>2</sup>, tomato lectin positive cells/mm<sup>2</sup> and O4+ cells/mm<sup>2</sup>. The most abundant cells in this area were oligodendrocytes but the density of cells in these three endpoints was enough to allow a positive and negative dynamic range in them. Their variabilities were low in all cases except for microglial density when the statistical unit was the pup. In this

case, variability was higher than 50% of the mean control value but still lower than the mean.

In the Skinner box, the learning criterion was considered to be met when the animal pressed the lever and went directly toward the food dispenser to obtain the reward at least three times in one session. 86% of controls (statistical unit = litter) reached this learning criterion and they did it in approximately 6 days. The rate of acquisition (mean increase in lever hits between sessions) was  $1.4 \pm 0.3$ . As no other studies reporting control values for Skinner box in rabbits could be found for comparison, we compared to control values reported in rats. In Wistar rats 79% of the tested animals achieved the learning criterion at a maximum of 7 days (Gallo et al., 1995), being the criterion 10 lever pressings with correct response in one session of 15 min. Another study in Wistar rats with a more demanding

learning criterion (20 lever pressings with correct response in 15 min), described that controls needed approximately four sessions to reach it (Reyes-Castro et al., 2012). The heterogeneity of Skinner-box protocols must be taken into account when comparing results, and for example, the learning criterion has to be adapted to the species of work. In our protocol, if a learning criterion of 10 lever presses with correct response in one session would have been established, only 35% of the animals would have achieved it (again taking the litter as a statistical unit). Differences, not only in the learning criterion but also in the reward offered make it difficult, in general, to compare between studies.

On the contrary, the open-field test has been applied to rabbits in several other studies from different groups. In our case, latency time (calculated as the time in seconds the animal needs to leave

**TABLE 5 |** Results of PROTOCOL 4.

| Endpoint (units)               | Statistical unit: pup (n = 11)<br>Median (IQR) or mean ± SD | Statistical unit: litter (n = 4)<br>Median (IQR) or mean ± SD |
|--------------------------------|---|---|
| Posture (score)                | Mdn: 3.0 (0.0)  | Mdn: 3.0 (0.0)  |
| Righting reflex (n. of times)  | M: 9.3 ± 1.4  | M: 9.5 ± 0.8  |
| Tone (score)                   | Mdn: 4.0 (0.0)  | Mdn: 4.0 (0.0)  |
| Circular motion (score)        | Mdn: 3.0 (1.0)  | Mdn: 2.8 (0.6)  |
| Hind limb locomotion (score)   | Mdn: 3.0 (1.0)  | Mdn: 3.0 (0.4)  |
| Intensity (score)              | Mdn: 3.0 (0.0)  | Mdn: 3.0 (0.0)  |
| Duration (score)               | Mdn: 3.0 (0.0)  | Mdn: 3.0 (0.0)  |
| Lineal movement (n. of times)  | M: 2.9 ± 1.7  | M: 2.9 ± 1.1  |
| Fore-hind paw distance (cm)    | M: 0.5 ± 1.2 <sup>#</sup>                                   | M: 0.6 ± 0.8 <sup>#</sup>                                     |
| Sucking and swallowing (score) | Mdn: 3.0 (0.5)  | Mdn: 3.0 (0.6)  |
| Head turning (score)           | Mdn: 3.0 (0.0)  | Mdn: 3.0 (0.1)  |
| Olfaction (score)              | Mdn: 3.0 (1.0)  | Mdn: 2.3 (0.6)  |
| Olfaction time (seconds)       | M: 3.4 ± 2.6  | M: 3.0 ± 1.6  |

The mean (M) ± SD is presented for righting reflex, lineal movement, fore-hind paw distance, and olfaction time; the median (Mdn) and (Interquartile Range (IQR)) are presented for the rest of the endpoints.

**TABLE 6 |** Results of PROTOCOL 6

| Endpoint   | Statistical unit: neuron<br>mean ± SD (n = 40) | Statistical unit: litter<br>mean ± SD (n = 3) |
|--|--|---|
| Total length (µm)                                  | 676.2 ± 289.3                                  | 681.0 ± 94.2                                  |
| Number of principal branches                       | 7.2 ± 2.1                                      | 7.3 ± 0.6                                     |
| Number of secondary branches                       | 8.3 ± 3.2                                      | 8.2 ± 0.8                                     |
| Number of tertiary branches                        | 3.5 ± 2.6                                      | 3.3 ± 1.1                                     |
| Number of quaternary branches                      | 1.1 ± 1.5 <sup>#</sup>                         | 0.9 ± 0.6                                     |
| Number of quinary branches                         | 0.2 ± 0.6 <sup>#</sup>                         | 0.2 ± 0.2 <sup>#</sup>                        |
| Number of senary branches                          | 0.1 ± 0.6 <sup>#</sup>                         | 0.1 ± 0.1 <sup>#</sup>                        |
| Number of quaternary, quinary, and senary branches | 1.4 ± 2.2 <sup>#</sup>                         | 1.2 ± 0.9                                     |
| Total branches                                     | 20.5 ± 7.6                                     | 20.0 ± 2.9                                    |
| Area soma (µm <sup>2</sup> )                       | 337.5 ± 79.5                                   | 322.9 ± 51.2                                  |

**TABLE 7 |** Results of PROTOCOLS 7, 8, and 9

| Endpoint  | Statistical unit: pup<br>mean ± SD (n) | Statistical unit: litter<br>mean ± SD (n) |
|---|--|---|
| Astrocyte IHC (from protocol 7) (GFAP+ cells/mm <sup>2</sup> )                  | 7.6 ± 3.0 (7)                          | 8.7 ± 2.2 (4)                             |
| Microglia IHC (from protocol 8) (tomato lectin positive cells/mm <sup>2</sup> ) | 13.8 ± 8.1 (8)                         | 12.4 ± 6.0 (4)                            |
| Oligodendrocyte IHC (from protocol 9) (O4+ cells/mm <sup>2</sup> )              | 50.4 ± 16.7 (8)                        | 48.7 ± 12.4 (4)                           |



**TABLE 8** | Results of PROTOCOLS 10 and 11.

| Endpoint   | Statistical unit: pup<br>mean ± SD (n) | Statistical unit: litter<br>mean ± SD (n) |
|--|--|---|
| Learning criteria (% of animals meeting the learning criterion)    | 77 ± 44 (13)                           | 86 ± 22 (6)                               |
| Rate of acquisition (mean increase in lever hits between sessions) | 1.4 ± 0.3 (13)                         | 1.4 ± 0.3 (6)                             |
| Learning day   | 6.5 ± 2.5 (13)                         | 6.4 ± 2.7 (6)                             |
| Of latency time (s)  | 122.0 ± 71.5 (13)                      | 125.4 ± 83.6 (6)                          |
| Of total distance (cm)   | 3566.3 ± 2749.2 (13)                   | 2575.0 ± 2840.7# (6)                      |
| Of time center (s)   | 31.2 ± 20.4 (13)                       | 30.9 ± 15.6 (6)                           |
| Of time periphery (s)  | 490.3 ± 114.5 (13)                     | 479.5 ± 126.8 (6)                         |
| ORT Discrimination Index (DI)                                      | 0.1 ± 0.3 (17)                         | 0.1 ± 0.3 (8)                             |

**TABLE 9** | Results of PROTOCOLS 13 and 14.

| Endpoint   | Statistical unit: hemisphere<br>mean ± SD (n) | Statistical unit: litter<br>mean ± SD (n) |
|--|---|---|
| Density of dendritic spines (number of spines/μm) from protocol 13 | 1.8 ± 0.2 (6)                                 | 1.8 ± 0.2 (4)                             |
| Perineuronal nets (contacts/μm <sup>2</sup> ) from protocol 14     | 0.24 ± 0.05 (6)                               | 0.25 ± 0.05 (4)                           |

the familiar starting point and start exploring the open field) was above 100 s while in many other studies it was less than 50 s (Gümüş et al., 2018; Van der Veecken et al., 2019, 2020). This is probably related to the fact that our protocol does not include a habituation session before the performance of the test. Total distance was very high compared to Van der Veecken et al. (2020) (ca. 1,600 cm), Van der Veecken et al. (2019) (ca. 1,400 cm) or Gümüş et al. (2018) (ca. 800 cm), but the mean time spent in the central area was similar to the one reported in (Van der Veecken et al., 2019) and was in accordance to the observed range in (Gümüş et al., 2018). The object recognition task has also been performed in rabbits by different groups but some of them perform it using visual objects (Hoffman et al., 2010; Hoffman and Basurto, 2013). This testing modality is also considered valid for assessing object recognition (Gümüş et al., 2018). However, some studies report that rabbits may be able to distinguish a novel visual object after a 5 min inter-trial interval, but not after 20, 180, or 360 min (Hoffman et al., 2010; Hoffman and Basurto, 2013), whereas in our studies discrimination with olfactory stimuli is present after a 30 min inter-trial interval (Illa et al., 2013) and this result could be replicated by another group (Gümüş et al., 2018).

The evaluation of plasticity-related endpoints on PND70 was performed in the hippocampus: the density of dendritic spines was measured in the hippocampal CA1 area, while the CA3 area was preferred for the analysis of perineuronal nets since a greater amount of *Wisteria floribunda* staining was observed in comparison to the CA1 (Illa et al., 2018), in agreement with previous works (Brückner et al., 2003; Hylín et al., 2013). The mean number of dendritic spines/μm obtained in the controls (1.8; **Table 9**) was very similar to the one previously reported by another research group in newborn rabbits (1.4, calculated from 67.8 spines in 50 μm in Balakrishnan et al., 2013). The number of contacts/μm<sup>2</sup> of the extracellular matrix surrounding neurons, also referred to as perineuronal nets could not be compared to

previous works, since, to the best of our knowledge, this endpoint was not evaluated before in rabbits.

In general, the evaluation of the results taking the litter as a statistical unit brings very similar results to those obtained taking the pup as a statistical unit in the controls. The standard deviations calculated for results obtained on PND1 were in all cases equal or smaller in case the litter was used as a statistical unit, but this was not the case for results obtained from PND50 on. However, in developmental neurotoxicity studies, to avoid previously described effects of serious exaggeration of significant effects in treated groups (Haseman and Hogan, 1975), the statistical unit of measure should be the litter and not the pup as also recommended in OECD TG 426 (OECD, 2007). For further discussion about this, the authors are referred to Harry et al. (2022), and articles included in this special issue.

## DISCUSSION

Here, we present for the first time a comprehensive compilation of detailed protocols for the evaluation of neurodevelopmental alterations in the rabbit species. The protocols included covering relevant endpoints for developmental neurotoxicity assessment included in OECD TG 426 (OECD, 2007), which consists of “observations to detect gross neurologic and behavioral abnormalities, including the assessment of physical development, behavioral ontogeny, motor activity, motor and sensory function, and learning and memory; and the evaluation of brain weights and neuropathology during postnatal development and adulthood”. In addition, *in vitro* procedures to test developmental neurotoxicity effects in the rabbit species and to investigate their mechanism/mode of action have also been proposed in a way that the sample obtained for these procedures does not alter the integrity of the *in vivo* procedures.

Comparing the protocols included here with the tests requested in OECD TG 426 (OECD, 2007), the behavioral ontogeny evaluation proposed (Protocol 4) is much more comprehensive than the required one in OECD TG 426 (OECD, 2007), which only includes righting reflex, negative geotaxis, and motor activity. We include, as requested in the TG, protocols to evaluate neurologic adverse effects at different developmental time points, in our case one at the early postnatal period (PND 1) and one for young adults (around PND 70). In addition, the protocols presented allow, as recommended, the evaluation of relationships, in case they are present, between neuropathological and behavioral alterations at these different time points. However, in our battery we do not include a protocol to evaluate neuropathology in the PNS at a young adult stage, general neurobehavior assessment (FOB/Irwin test), or sexual maturation, and these assessments are required in OECD TG 426 (OECD, 2007). For articles describing the right endpoints and timings for sexual maturation evaluation in rabbits, the reader is referred to the work of Laffan et al. (2018) for female evaluation and the work of García-Tomás et al. (2009) for male evaluation. Also, in case more complex learning and memory tasks need to be evaluated, the reader is referred to previous descriptions of fear conditioning testing in rabbits (Chisholm and Moore, 1970; Supple et al., 1993). Concerning the analysis and interpretation of the results of the protocols, we have presented results analyzed in two different ways, one considering the litter and another one considering the pup/hemisphere/neuron as a statistical unit. In the present study, these two ways of analyzing the data have had minimal differences in the mean values of control animals and the standard deviations we obtained from these calculations were, in general, smaller when the litter was considered as the statistical unit (except for some of the Skinner test and open field results). However, when testing for developmental neurotoxicity, as indicated in the OECD TG 246 (OECD, 2007), littermates should not be treated as independent observations. This is because litter effects have been shown to exist and they can have a high impact in a toxicological study if the pup is taken as a statistical unit. Therefore, to avoid false-positive results, the statistical unit of measure should be the litter and not the pup (Abbey and Howard, 1973; Haseman and Hogan, 1975; Nelson et al., 1985; Holson and Pearce, 1992).

All tests presented in this collection have been used to evaluate the neurodevelopmental alterations induced by mild-hypoxic conditions during the prenatal period and some of them have been used by other authors to study the neurodevelopmental effects of caffeine exposure or maternal endotoxin exposure (Balakrishnan et al., 2013; Van der Veecken et al., 2020). The whole battery of tests has not been used to assess known neurotoxic compounds so far, but a broad definition of teratogen includes “any infection, physical, chemical, or environmental agent that can disrupt or disturb the development of a fetus or embryo (Adam, 2012)”, and in fact, hypoxia is accepted as a teratogen agent (Adam et al., 2021). Hypoxia, or low oxygen levels, is a neurodevelopmental key event that can be triggered by multiple causes, including a reduction or lack of blood flow (as presented here), low oxygen levels in the

blood, low levels of red blood cells and/or hemoglobin, but also by the inability of the tissues to utilize oxygen due to, for example, carbon monoxide poisoning (Adam et al., 2021). Therefore, as an illustrative case study, the results of this battery of tests after chronic hypoxia-ischemia insult during gestation induced in one of the uterus horns by ligation of 40–50% of uteroplacental vessels on day 25 of pregnancy are discussed here, to show the potential of the combination of the different tests described in these protocols.

According to Nalivaeva et al. (2018), prenatal hypoxia in critical periods of neurodevelopment induces significant changes in cognitive functions at different postnatal stages which correlate with morphological changes in brain structures involved in learning and memory. The use of the battery of protocols proposed here allowed to detect learning and memory alterations in rabbits, since Skinner test results showed a lower proportion of cases reaching the learning criteria when compared with their controls (30 vs. 77%,  $p = 0.03$ , cases vs. controls, respectively; Illa et al., 2017) and a decreased discrimination index was observed in cases compared to controls when ORT was assessed (Illa et al., 2013; Illa et al., 2017). Morphological changes correlating with these findings were that cases presented a significant decrease in dendritic spines density and perineuronal nets immunoreactivity in the hippocampus when compared to controls (Illa et al., 2018). Even though the histological analysis presented here can be adapted to the region of interest for each study, in the results section we present the outcomes from the experimental design used to evaluate the effects of a chronic hypoxia-ischemia insult (Illa et al., 2018; Pla et al., 2021), which was selected in accordance to the degree of maturation and the susceptibility to hypoxic-ischemic events. The selected regions in the brain in the rabbit model are consistent with the ones chosen in other models such as rats (Back et al., 2002; Ruff et al., 2017), as detailed in each results section. However, the OECD TG 426 (OECD, 2007) indicates that tissue samples for the neuropathological examination should be representative of all major brain regions at PND 22 or earlier (as also recommended by Rao et al. (2011)), and also include samples from the spinal cord and PNS at study termination.

Additional information obtained at the functional level was that cases showed poorer results than controls in several of the endpoints assessed in the behavior ontogeny test at PND 1, including righting reflex, circular motion, intensity, sucking and swallowing, and head-turning (Pla et al., 2021). These findings were in accordance with decreased oligodendrogenesis observed in brain samples (Pla et al., 2021) as well as in neurospheres generated from these animals (Barenys et al., 2021), which could be related to this delay in the behavior ontogeny. The good correlation of the *in vivo* and *in vitro* findings indicates the added value of including protocols 2 and 3 in the battery.

Other functional deficits were also present at later time-points when cases presented a significantly increased latency of leaving the familiar starting point and a reduced number of external and internal boxes explored in the open field test at PND 70 (Illa et al., 2013; Illa et al., 2017). This result indicated that no motor

problem was present in these animals, but they presented a higher degree of anxiety.

Considering all these results, we can distinguish a pattern of mild short-term impairments in motor, reflex and sensitivity and a long-term group of moderate alterations in learning, memory, and anxiety.

With all the information obtained, the theoretical benefits already mentioned in the introduction of having a rabbit developmental neurotoxicity model can also be discussed. The protocols included here take into account the higher similarity of rabbits to humans than rodent species regarding white matter maturation-timing and include endpoints that can measure alterations on it (such as astrocytes or oligodendrocyte IHC in Protocols 7 and 9 or reflex ontogeny in Protocol 4). Moreover, we have shown that the model can reflect neurodevelopmental alterations related to circulatory alterations, another aspect in which rabbits are more similar to humans than rodents (Foote and Carney, 2000; Carter, 2007; Eixarch et al., 2009). Considering these points, it is reasonable to think that for certain compounds or compound classes expected to cause neurodevelopmental alterations related to white matter alterations, or related to circulatory changes, the rabbit model could be useful for screening purposes, since it would be expected to better predict the human response. Other possible application scenarios would be in cases where the metabolism in rabbits is more similar to humans than in rodents, or in situations where a previous rabbit study raised concerns about neurotoxic effects (for example an OECD TG 414 study where the rabbit is the preferred non-rodent species). In this case, the recommendation of the OECD TG 426 is that the study is conducted in the species increasing the concern, but so far this could not be completely carried out if the concern was raised in rabbits because there were no protocols available. Some specific examples of compounds displaying structural-developmental neurotoxicity in rabbits and not in rats have already been identified (Theunissen et al., 2016; Teixidó et al., 2018). Unfortunately, one of the studies is based on a coded dataset that did not reveal the identity of the compounds showing species differences, but the identified substances (and the adverse neurodevelopmental effect) were: 10224 (small or absent cerebrum), 10330 (enlarged cerebral ventricle), and tafluprost (cranial and spinal malformations). Among the limitations of the protocols described here, we have to mention that the relevance of *in vitro* results in Protocol 3 to *in vivo* complex alterations such as learning or memory changes needs further assessment. Another limitation is that with the microglial protocol (Protocol 8) one can evaluate the density of microglia in a selected area, but it is not possible to evaluate the morphology of the cells. Similarly, for the evaluation of the perineuronal nets (Protocol 14), other studies include more comprehensive evaluations of structural alterations of perineuronal nets such as the number of perineuronal nets units, area, mean intensity of perineuronal nets marker expression, and shape parameters of perineuronal nets (Kaushik et al., 2021). Another limitation is the very high variability in the results of the total distance in the open field test, but other studies have reported high variabilities

in this endpoint as well (Van der Veecken et al., 2020), which might indicate that other assessments within this assay, such as latency time or percentage of time spent in the central area, might be more useful to distinguish alterations in this test in rabbits.

However, should the proposed protocols be used under OECD TG 426 in the future, other important needs have to be addressed before regulatory acceptance: some required endpoints are not included in the approach: the minimum number of animals to be assigned to each group has to be clarified, the methods need to be validated and a higher number of studies should be evaluated to obtain more robust historical control values in this species.

As a final remark, the predictivity and sensitivity of this battery of tests for the assessment of developmental neurotoxicity in the rabbit species still need to be clarified, but this first approach of protocols adaptation is already a valuable tool for all research groups in need to study neurodevelopment in the rabbit species in toxicology and the first step to a possible future application under OECD TG 426.

## DATA AVAILABILITY STATEMENT

The original contributions presented in the study are included in the article/**Supplementary Material**; further inquiries can be directed to the corresponding author.

## ETHICS STATEMENT

The animal study was reviewed and approved by the Animal Experimental Ethics Committee (CEEAA) of the University of Barcelona. Study approved with license number 03/17.

## AUTHOR CONTRIBUTIONS

Conceptualization: MB and MI. Methodology: BK, CL, LP, MB, MI, and PV-A. Validation: BK, LP, MB, and MI. Formal analysis: BK, LG-E, LP, MB, and MI. Investigation: BK, CL, LP, MB, MI, and PV-A. Writing—original draft: BK, LG-E, LP, MB, MI, and PV-A. Writing—review and editing: BF and EG. Visualization: BK, BF, LG-E, and MB. Supervision: EG, MB, and MI. Project administration: MB and MI. Funding acquisition: MI and MB.

## FUNDING

This study has been funded by Instituto de Salud Carlos III through projects PI08/0230, PI12/00851, and PI18/01763 and co-funded by the European Union, from “LaCaixa” Foundation under grant agreements LCF/PR/GN14/10270005 and LCF/PR/GN18/10310003 and from AGAUR under grant 2017 SGR number 1531. BK received a scholarship from Fundació Bosch i Gimpera (project number: 300155), and CL received the support of the Health Department of the Catalan Government (grant

number SLT006/17/00325). MI was supported by Rio Hortega grant (CM11/00032) and Emili Letang fellowship by Hospital Clinic. LG-E was supported by the Margarita Salas program funded by the European Union—NextGenerationEU. **Figure 1** and **Figure 2** were created with BioRender.com.

## REFERENCES

- Abbey, H., and Howard, E. (1973). Statistical Procedure in Developmental Studies on Species with Multiple Offspring. *Dev. Psychobiol.* 6, 329–335. doi:10.1002/dev.420060406
- Adam, A. P., Payton, K. S. E., Sanchez-Lara, P. A., Adam, M. P., and Mirzaa, G. M. (2021). Hypoxia: A Teratogen Underlying a Range of Congenital Disruptions, Dysplasias, and Malformations. *Am. J. Med. Genet.* 185, 2801–2808. doi:10.1002/ajmg.a.62235
- Adam, M. P. (2012). The All-Or-None Phenomenon Revisited. *Birth Defects Res. Part A Clin. Mol. Teratol.* 94, 664–669. doi:10.1002/bdra.23029
- Back, S. A., Han, B. H., Luo, N. L., Chrifton, C. A., Xanthoudakis, S., Tam, J., et al. (2002). Selective Vulnerability of Late Oligodendrocyte Progenitors to Hypoxia-Ischemia. *J. Neurosci.* 22, 455–463. doi:10.1523/jneurosci.22-02-00455.2002
- Balakrishnan, B., Dai, H., Janisse, J., Romero, R., and Kannan, S. (2013). Maternal Endotoxin Exposure Results in Abnormal Neuronal Architecture in the Newborn Rabbit. *Dev. Neurosci.* 35, 396–405. doi:10.1159/000353156
- Barenys, M., Illa, M., Hofrichter, M., Loreiro, C., Pla, L., Klose, J., et al. (2021). Rabbit Neurospheres as a Novel *In Vitro* Tool for Studying Neurodevelopmental Effects Induced by Intrauterine Growth Restriction. *Stem Cells Transl. Med.* 10, 209–221. doi:10.1002/sctm.20-0223
- Brückner, G., Grosche, J., Hartlage-Rübsamen, M., Schmidt, S., and Schachner, M. (2003). Region and Lamina-specific Distribution of Extracellular Matrix Proteoglycans, Hyaluronan and Tenascin-R in the Mouse Hippocampal Formation. *J. Chem. Neuroanat.* 26, 37–50. doi:10.1016/S0891-0618(03)00036-X
- Carter, A. M. (2007). Animal Models of Human Placentation - A Review. *Placenta* 28, S41–S47. doi:10.1016/j.placenta.2006.11.002
- Chisholm, D. C., and Moore, J. W. (1970). Effects of Chlordiazepoxide on Discriminative Fear Conditioning and Shuttle Avoidance Performance in the Rabbit. *Psychopharmacologia* 18, 162–171. doi:10.1007/BF00401498
- Clancy, B., Darlington, R. B., and Finlay, B. L. (2001). Translating Developmental Time across Mammalian Species. *Neuroscience* 105, 7–17. doi:10.1016/S0306-4522(01)00171-3
- Cohen, J. (1969). *Statistical Power Analysis for the Behavioral Sciences*. Routledge. doi:10.4324/9780203771587
- Derrick, M., Luo, N. L., Bregman, J. C., Jilling, T., Ji, X., Fisher, K., et al. (2004). Preterm Fetal Hypoxia-Ischemia Causes Hypertonia and Motor Deficits in the Neonatal Rabbit: A Model for Human Cerebral Palsy? *J. Neurosci.* 24, 24–34. doi:10.1523/jneurosci.2816-03.2004
- Eixarch, E., Batalle, D., Illa, M., Muñoz-Moreno, E., Arbat-Plana, A., Amat-Roldan, I., et al. (2012). Neonatal Neurobehavior and Diffusion MRI Changes in Brain Reorganization Due to Intrauterine Growth Restriction in a Rabbit Model. *PLoS One* 7, e31497–12. doi:10.1371/journal.pone.0031497
- Eixarch, E., Figueras, F., Hernández-Andrade, E., Crispí, F., Nadal, A., Torre, I., et al. (2009). An Experimental Model of Fetal Growth Restriction Based on Selective Ligation of Uteroplacental Vessels in the Pregnant Rabbit. *Fetal Diagn. Ther.* 26, 203–211. doi:10.1159/000264063
- Faul, F., Erdfelder, E., Buchner, A., and Lang, A.-G. (2009). Statistical Power Analyses Using G\*Power 3.1: Tests for Correlation and Regression Analyses. *Behav. Res. Methods* 41, 1149–1160. doi:10.3758/BRM.41.4.1149
- Faul, F., Erdfelder, E., Lang, A.-G., and Buchner, A. (2007). G\*Power 3: a Flexible Statistical Power Analysis Program for the Social, Behavioral, and Biomedical Sciences. *Behav. Res. Methods* 39, 175–191. doi:10.3758/bf03193146
- Ferraris, S., van der Merwe, J., Van Der Veecken, L., Prados, F., Iglesias, J.-E., Melbourne, A., et al. (2018). A Magnetic Resonance Multi-Atlas for the Neonatal Rabbit Brain. *Neuroimage* 179, 187–198. doi:10.1016/j.neuroimage.2018.06.029
- Foote, R. H., and Carney, E. W. (2000). The Rabbit as a Model for Reproductive and Developmental Toxicity Studies. *Reprod. Toxicol.* 14, 477–493. doi:10.1016/S0890-6238(00)00101-5
- Gallo, A., Duchatelle, E., Elkhessaimi, A., Pape, G. L., and Desportes, J.-P. (1995). Topographic Analysis of the Rat's Bar Behaviour in the Skinner Box. *Behav. Process.* 33, 319–327. doi:10.1016/0376-6357(94)00032-C
- García-Tomás, M., Sánchez, J., and Piles, M. (2009). Postnatal Sexual Development of Testis and Epididymis in the Rabbit: Growth and Maturity Patterns of Macroscopic and Microscopic Markers. *Theriogenology* 71, 292–301. doi:10.1016/j.theriogenology.2008.07.021
- Gümüş, H. G., Agyemang, A. A., Romantsik, O., Sandgren, R., Karlsson, H., Gram, M., et al. (2018). Behavioral Testing and Litter Effects in the Rabbit. *Behav. Brain Res.* 353, 236–241. doi:10.1016/j.bbr.2018.02.032
- Harry, G. J., McBride, S., Witchev, S. K., Mhaouty-Kodja, S., Trembleau, A., Bridge, M., et al. (2022). Roadbumps at the Crossroads of Integrating Behavioral and *In Vitro* Approaches for Neurotoxicity Assessment. *Front. Toxicol.* 4, 1–29. doi:10.3389/ftox.2022.812863
- Haseman, J. K., and Hogan, M. D. (1975). Selection of the Experimental Unit in Teratology Studies. *Teratology* 12, 165–171. doi:10.1002/tera.1420120209
- Herculano-Houzel, S., Ribeiro, P., Campos, L., Valotta da Silva, A., Torres, L. B., Catania, K. C., et al. (2011). Updated Neuronal Scaling Rules for the Brains of Glires (Rodents/lagomorphs). *Brain. Behav. Evol.* 78, 302–314. doi:10.1159/000330825
- Hoffman, K. L., and Basurto, E. (2013). One-trial Object Recognition Memory in the Domestic Rabbit (*Oryctolagus cuniculus*) Is Disrupted by NMDA Receptor Antagonists. *Behav. Brain Res.* 250, 62–73. doi:10.1016/j.bbr.2013.04.049
- Hoffman, K. L., Hernández Decasa, D. M., Beyer Ruiz, M. E., and González-Mariscal, G. (2010). Scent Marking by the Male Domestic Rabbit (*Oryctolagus cuniculus*) Is Stimulated by an Object's Novelty and its Specific Visual or Tactile Characteristics. *Behav. Brain Res.* 207, 360–367. doi:10.1016/j.bbr.2009.10.021
- Holson, R. R., and Pearce, B. (1992). Principles and Pitfalls in the Analysis of Prenatal Treatment Effects in Multiparous Species. *Neurotoxicology Teratol.* 14, 221–228. doi:10.1016/0892-0362(92)90020-B
- Hylin, M. J., Orsi, S. A., Moore, A. N., and Dash, P. K. (2013). Disruption of the Perineuronal Net in the hippocampus or Medial Prefrontal Cortex Impairs Fear Conditioning. *Learn. Mem.* 20, 267–273. doi:10.1101/lm.030197.112
- Illa, M., Brito, V., Pla, L., Eixarch, E., Arbat-Plana, A., Batallé, D., et al. (2018). Early Environmental Enrichment Enhances Abnormal Brain Connectivity in a Rabbit Model of Intrauterine Growth Restriction. *Fetal Diagn. Ther.* 44, 184–193. doi:10.1159/000481171
- Illa, M., Eixarch, E., Batalle, D., Arbat-Plana, A., Muñoz-Moreno, E., Figueras, F., et al. (2013). Long-Term Functional Outcomes and Correlation with Regional Brain Connectivity by MRI Diffusion Tractography Metrics in a Near-Term Rabbit Model of Intrauterine Growth Restriction. *PLoS One* 8, e76453. doi:10.1371/journal.pone.0076453
- Illa, M., Eixarch, E., Muñoz-Moreno, E., Batalle, D., Leal-Campanario, R., Gruart, A., et al. (2017). Neurodevelopmental Effects of Undernutrition and Placental Underperfusion in Fetal Growth Restriction Rabbit Models. *Fetal Diagn. Ther.* 42, 189–197. doi:10.1159/000454859
- Kaushik, R., Lipachev, N., Matuszko, G., Kochneva, A., Dvoeglazova, A., Becker, A., et al. (2021). Fine Structure Analysis of Perineuronal Nets in the Ketamine Model of Schizophrenia. *Eur. J. Neurosci.* 53, 3988–4004. doi:10.1111/ejn.14853
- Knudsen, T. B., Martin, M. T., Kavlock, R. J., Judson, R. S., Dix, D. J., and Singh, A. V. (2009). Profiling the Activity of Environmental Chemicals in Prenatal Developmental Toxicity Studies Using the U.S. EPA's ToxRefDB. *Reprod. Toxicol.* 28, 209–219. doi:10.1016/j.reprotox.2009.03.016
- Knudsen, T., Martin, M., Chandler, K., Kleinstreuer, N., Judson, R., and Sipes, N. (2013). *Predictive Models and Computational Toxicology*. Totowa, NJ: Humana Press Incorporated, 343–374. doi:10.1007/978-1-62703-131-8\_26
- Laffan, S. B., Posobiec, L. M., Uhl, J. E., and Vidal, J. D. (2018). Species Comparison of Postnatal Development of the Female Reproductive System. *Birth Defects Res.* 110, 163–189. doi:10.1002/bdr2.1132

## SUPPLEMENTARY MATERIAL

The Supplementary Material for this article can be found online at: <https://www.frontiersin.org/articles/10.3389/ftox.2022.918520/full#supplementary-material>

- Muñoz-Moreno, E., Arbat-Plana, A., Batalle, D., Soria, G., Illa, M., Prats-Galino, A., et al. (2013). A Magnetic Resonance Image Based Atlas of the Rabbit Brain for Automatic Parcellation. *PLoS One* 8, e67418. doi:10.1371/journal.pone.0067418
- Nalivaeva, N. N., Turner, A. J., and Zhuravin, I. A. (2018). Role of Prenatal Hypoxia in Brain Development, Cognitive Functions, and Neurodegeneration. *Front. Neurosci.* 12, 1–21. doi:10.3389/fnins.2018.00825
- Nelson, C. J., Felton, R. P., Kimmel, C. A., Buelke-Sam, J., and Adams, J. (1985). Collaborative Behavioral Teratology Study: Statistical Approach. *Neurobehav. Toxicol. Teratol.* 7, 587–590.
- OECD (2018). *Test No. 414: Prenatal Developmental Toxicity Study*. OECD. doi:10.1787/9789264070820-en
- OECD (2007). *Test No. 426: Developmental Neurotoxicity Study*. OECD. doi:10.1787/9789264067394-en
- Pla, L., Illa, M., Loreiro, C., Lopez, M. C., Vázquez-Aristizabal, P., Kühne, B. A., et al. (2021). Structural Brain Changes during the Neonatal Period in a Rabbit Model of Intrauterine Growth Restriction. *Dev. Neurosci.* 42, 217–229. doi:10.1159/000512948
- Rao, D. B., Little, P. B., Malarkey, D. E., Herbert, R. A., and Sills, R. C. (2011). Histopathological Evaluation of the Nervous System in National Toxicology Program Rodent Studies: A Modified Approach. *Toxicol. Pathol.* 39, 463–470. doi:10.1177/0192623311401044
- Reyes-Castro, L. A., Rodriguez, J. S., Charco, R., Bautista, C. J., Larrea, F., Nathanielsz, P. W., et al. (2012). Maternal Protein Restriction in the Rat during Pregnancy And/or Lactation Alters Cognitive and Anxiety Behaviors of Female Offspring. *Int. J. Dev. Neurosci.* 30, 39–45. doi:10.1016/j.ijdevneu.2011.10.002
- Ruff, C. A., Faulkner, S. D., Rumajogee, P., Beldick, S., Foltz, W., Corrigan, J., et al. (2017). The Extent of Intrauterine Growth Restriction Determines the Severity of Cerebral Injury and Neurobehavioural Deficits in Rodents. *PLoS One* 12, e0184653–22. doi:10.1371/journal.pone.0184653
- Sholl, D. A., and Uttley, A. M. (1953). Pattern Discrimination and the Visual Cortex. *Nature* 171, 387–388. doi:10.1038/171387a0
- Supple, W. F., Sebastiani, L., and Kapp, B. S. (1993). Purkinje Cell Responses in the Anterior Cerebellar Vermis during Pavlovian Fear Conditioning in the Rabbit. *Neuroreport* 4, 975–978. doi:10.1097/00001756-199307000-00035
- Teixidó, E., Krupp, E., Amberg, A., Czich, A., and Scholz, S. (2018). Species-specific Developmental Toxicity in Rats and Rabbits: Generation of a Reference Compound List for Development of Alternative Testing Approaches. *Reprod. Toxicol.* 76, 93–102. doi:10.1016/j.reprotox.2018.01.005
- Theunissen, P. T., Beken, S., Beyer, B., Breslin, W. J., Cappon, G. D., Chen, C. L., et al. (2017). Comparing Rat and Rabbit Embryo-Fetal Developmental Toxicity Data for 379 Pharmaceuticals: on Systemic Dose and Developmental Effects. *Crit. Rev. Toxicol.* 47, 409–421. doi:10.1080/10408444.2016.1224808
- Theunissen, P. T., Beken, S., Beyer, B. K., Breslin, W. J., Cappon, G. D., Chen, C. L., et al. (2016). Comparison of Rat and Rabbit Embryo-Fetal Developmental Toxicity Data for 379 Pharmaceuticals: on the Nature and Severity of Developmental Effects. *Crit. Rev. Toxicol.* 46, 900–910. doi:10.1080/10408444.2016.1224807
- Van der Veeken, L., Grönlund, S., Gerdtsen, E., Holmqvist, B., Deprest, J., Ley, D., et al. (2020). Long-term Neurological Effects of Neonatal Caffeine Treatment in a Rabbit Model of Preterm Birth. *Pediatr. Res.* 87, 1011–1018. doi:10.1038/s41390-019-0718-8
- Van der Veeken, L., Van der Merwe, J., Devroe, S., Inversetti, A., Galgano, A., Bleeser, T., et al. (2019). Maternal Surgery during Pregnancy Has a Transient Adverse Effect on the Developing Fetal Rabbit Brain. *Am. J. Obstetrics Gynecol.* 221, 355.e1–355.e19. doi:10.1016/j.ajog.2019.07.029
- Workman, A. D., Charvet, C. J., Clancy, B., Darlington, R. B., and Finlay, B. L. (2013). Modeling Transformations of Neurodevelopmental Sequences across Mammalian Species. *J. Neurosci.* 33, 7368–7383. doi:10.1523/jneurosci.5746-12.2013
- Zworykina, S. V., Budaev, S. V., and Zworykin, D. D. (1997). Consistency of Skinner Box Activity Measures in the Domestic Rabbit (*Oryctolagus Cuniculus*). *Int. J. Comp. Psychol.* 10, 159–166.

**Conflict of Interest:** The authors declare that the research was conducted in the absence of any commercial or financial relationships that could be construed as a potential conflict of interest.

**Publisher's Note:** All claims expressed in this article are solely those of the authors and do not necessarily represent those of their affiliated organizations, or those of the publisher, the editors, and the reviewers. Any product that may be evaluated in this article, or claim that may be made by its manufacturer, is not guaranteed or endorsed by the publisher.

Copyright © 2022 Pla, Kühne, Guardia-Escote, Vázquez-Aristizabal, Loreiro, Flick, Gratacós, Barenys and Illa. This is an open-access article distributed under the terms of the Creative Commons Attribution License (CC BY). The use, distribution or reproduction in other forums is permitted, provided the original author(s) and the copyright owner(s) are credited and that the original publication in this journal is cited, in accordance with accepted academic practice. No use, distribution or reproduction is permitted which does not comply with these terms.

## GLOSSARY

|   |  |
|---|--|
| <b>AU</b> airy unit                                     | <b>GFAP</b> glial fibrillary acidic protein                        |
| <b>BMP7</b> bone morphogenetic protein 7                | <b>HIER</b> heat-induced epitope retrieval                         |
| <b>BSA:</b> bovine serum albumin                        | <b>IHC</b> immunohistochemistry                                    |
| <b>CTB:</b> CellTiter Blue                              | <b>MEM</b> minimum essential medium                                |
| <b>DAPI:</b> 4',6-diamidino-2-phenylindole              | <b>NPC</b> neural progenitor cells                                 |
| <b>dH<sub>2</sub>O</b> distilled water                  | <b>OECD</b> Organisation for Economic Co-operation and Development |
| <b>DIC</b> differential interference contrast           | <b>o.n.</b> overnight  |
| <b>DMEM</b> Dulbecco's modified Eagle's medium          | <b>PBS</b> phosphate-buffered saline                               |
| <b>DMSO</b> dimethyl sulfoxide                          | <b>PBST</b> PBS-triton X-100                                       |
| <b>DNT</b> developmental neurotoxicity                  | <b>PDL</b> poly-D-lysine   |
| <b>ECM</b> extracellular matrix                         | <b>PFA</b> paraformaldehyde  |
| <b>EGF</b> epidermal growth factor                      | <b>PND</b> postnatal day   |
| <b>FBS</b> fetal bovine serum                           | <b>PNS</b> peripheral nervous system                               |
| <b>rhFGF</b> human recombinant fibroblast growth factor | <b>Poly-HEMA</b> Poly(2-hydroxyethyl methacrylate)                 |
| <b>FR</b> fixed ratio                                   | <b>rcf</b> relative centrifugal force                              |
| <b>GD</b> gestational day                               | <b>RT</b> room temperature   |

## 4 Results

### 4.1 Structural Brain Changes during the Neonatal Period in a Rabbit Model of Intrauterine Growth Restriction.

Laura Pla <sup>1</sup>, Miriam Illa <sup>2,3</sup>, Carla Loreiro <sup>1,4</sup>, Mari Carmen Lopez <sup>1</sup>, Paula Vázquez-Aristizabal <sup>1</sup>,  
**Britta Anna Kühne** <sup>1,5</sup>, Marta Barenys <sup>5</sup>, Elisenda Eixarch <sup>1,4,6</sup>, Eduard Gratacós <sup>1,7,4,6</sup>

<sup>1</sup> BCNatal | Fetal Medicine Research Center (Hospital Clínic and Hospital Sant Joan de Déu),  
Universitat de Barcelona, Barcelona, Spain.

<sup>2</sup> BCNatal | Fetal Medicine Research Center (Hospital Clínic and Hospital Sant Joan de Déu),  
Universitat de Barcelona, Barcelona, Spain, MIRIAMIL@clinic.cat.

<sup>3</sup> Institut de Recerca Sant Joan de Déu, Esplugues de Llobregat, Spain, MIRIAMIL@clinic.cat.

<sup>4</sup> Institut d'Investigacions Biomèdiques August Pi i Sunyer (IDIBAPS), Barcelona, Spain.

<sup>5</sup> GRET, INSA-UB and Toxicology Unit, Pharmacology, Toxicology and Therapeutical Chemistry  
Department, Faculty of Pharmacy, University of Barcelona, Barcelona, Spain.

<sup>6</sup> Center for Biomedical Research on Rare Diseases (CIBER-ER), Barcelona, Spain.

<sup>7</sup> Institut de Recerca Sant Joan de Déu, Esplugues de Llobregat, Spain.

|                       |   |
|-----------------------|---|
| Journal               | Developmental Neuroscience  |
| Impact Factor 2020    | 2.984   |
| Quartile              | Q2 in Developmental biology   |
| Type of authorship    | Co-author   |
| Status of publication | Published: Dev Neurosci 42 (2020) 217-229<br>DOI: 10.1159/000512948 |

## Summary

**Background:** Intrauterine growth restriction (IUGR) is associated with abnormal neurodevelopment, but the associated structural brain changes are poorly documented. The aim of this study was to describe in an animal model the brain changes at the cellular level in the gray and white matter induced by IUGR during the neonatal period.

**Methods:** The IUGR model was surgically induced in pregnant rabbits by ligating 40-50% of the uteroplacental vessels in 1 horn, whereas the uteroplacental vessels of the contralateral horn were not ligated. After 5 days, IUGR animals from the ligated horn and controls from the nonligated were delivered. On the day of delivery, perinatal data and placentas were collected. On postnatal day 1, functional changes were first evaluated, and thereafter, neuronal arborization in the frontal cortex and density of pre-oligodendrocytes, astrocytes, and microglia in the corpus callosum were evaluated.

**Results:** Higher stillbirth in IUGR fetuses together with a reduced birth weight as compared to controls was evidenced. IUGR animals showed poorer functional results, an altered neuronal arborization pattern, and a decrease in the pre-oligodendrocytes, with no differences in microglia and astrocyte densities.

**Conclusions:** Overall, in the rabbit model used, IUGR is related to functional and brain changes evidenced already at birth, including changes in the neuronal arborization and abnormal oligodendrocyte maturation.

**Keywords:** Animal model; Intrauterine growth restriction; Neurodevelopment; Neuronal arborization; Oligodendrocyte.



# Structural Brain Changes during the Neonatal Period in a Rabbit Model of Intrauterine Growth Restriction

Laura Pla<sup>a</sup> Miriam Illa<sup>a, b</sup> Carla Loreiro<sup>a, c</sup> Mari Carmen Lopez<sup>a</sup>  
Paula Vázquez-Aristizabal<sup>a</sup> Britta Anna Kühne<sup>a, d</sup> Marta Barenys<sup>d</sup>  
Elisenda Eixarch<sup>a, c, e</sup> Eduard Gratacós<sup>a, b, c, e</sup>

<sup>a</sup>BCNatal | Fetal Medicine Research Center (Hospital Clínic and Hospital Sant Joan de Déu), Universitat de Barcelona, Barcelona, Spain; <sup>b</sup>Institut de Recerca Sant Joan de Déu, Esplugues de Llobregat, Spain; <sup>c</sup>Institut d'Investigacions Biomèdiques August Pi i Sunyer (IDIBAPS), Barcelona, Spain; <sup>d</sup>GRET, INSA-UB and Toxicology Unit, Pharmacology, Toxicology and Therapeutical Chemistry Department, Faculty of Pharmacy, University of Barcelona, Barcelona, Spain; <sup>e</sup>Center for Biomedical Research on Rare Diseases (CIBER-ER), Barcelona, Spain

## Keywords

Animal model · Intrauterine growth restriction · Neurodevelopment · Neuronal arborization · Oligodendrocyte

## Abstract

**Background:** Intrauterine growth restriction (IUGR) is associated with abnormal neurodevelopment, but the associated structural brain changes are poorly documented. The aim of this study was to describe in an animal model the brain changes at the cellular level in the gray and white matter induced by IUGR during the neonatal period. **Methods:** The IUGR model was surgically induced in pregnant rabbits by ligating 40–50% of the uteroplacental vessels in 1 horn, whereas the uteroplacental vessels of the contralateral horn were not ligated. After 5 days, IUGR animals from the ligated horn and controls from the nonligated were delivered. On the day of delivery, perinatal data and placentas were collected. On postnatal day 1, functional changes were first

evaluated, and thereafter, neuronal arborization in the frontal cortex and density of pre-oligodendrocytes, astrocytes, and microglia in the corpus callosum were evaluated. **Results:** Higher stillbirth in IUGR fetuses together with a reduced birth weight as compared to controls was evidenced. IUGR animals showed poorer functional results, an altered neuronal arborization pattern, and a decrease in the pre-oligodendrocytes, with no differences in microglia and astrocyte densities. **Conclusions:** Overall, in the rabbit model used, IUGR is related to functional and brain changes evidenced already at birth, including changes in the neuronal arborization and abnormal oligodendrocyte maturation.

© 2021 S. Karger AG, Basel

## Introduction

Intrauterine growth restriction (IUGR) is a well-recognized cause of abnormal brain development, placental insufficiency being one of its major causes. The com-

promised placenta results in a sustained hypoxemia and undernutrition of the developing fetus [1], having a special impact on the developing brain [2, 3]. During the neonatal period, neurofunctional impairments have been described [4, 5], which also persist in later stages of life [6, 7]. Regarding the structural correspondence underlying these functional impairments, contrary to acute and severe prenatal hypoxia-ischemia events in which evident structural changes are widely described, including hypoxic-ischemic encephalopathy, intraventricular hemorrhage, and periventricular leukomalacia, the IUGR effect on the fetal brain seems to be subtle and more related to disruption of normal brain development, rather than gross tissue destruction [8]. Going in this line, clinical imaging studies described changes in gray matter (GM) and white matter (WM) volumes [9, 10], altered complexity of WM [11], and altered cortical maturation [12] in IUGR infants. Despite all these evidence, the structural brain correspondence at the cellular level remains poorly documented. Since the IUGR effect on the fetal brain is subtle, its identification and characterization are challenging, requiring the use of advanced histological modalities. The description of the cellular changes underlying IUGR is essential in order to select effective strategies to act upon these specific targets.

Animal models are still required in order to evaluate structural brain changes in brain tissue specimens. Different animal models mimicking the human IUGR condition have been previously used, giving us preliminary evidence on the structural brain changes secondary to IUGR. Chronic hypoxia-ischemia in pregnant sheep and guinea pig models has described abnormal neuronal connectivity, including abnormal axonal and dendritic development in the cerebellar cortex and in the hippocampal neurons [13–15]. However, neuronal connectivity abnormalities in the frontal cortex have not yet been evaluated in IUGR. The evaluation of such changes in the cortical area would be relevant as it has been described to be a vulnerable area related to IUGR in previous human [4, 16, 17] and animal studies [18, 19]. At the WM level, transient delay of WM myelination during the postnatal period has been described in mild and chronic guinea pig IUGR models [20]. This transient delay during the postnatal period seemed to be secondary to a disruption in the oligodendrocyte lineage maturation, especially affecting the late oligodendrocyte progenitor cells and the pre-oligodendrocyte cells (pre-OLs) in the corpus callosum (CC) [21–23], parietal WM [24], and corona radiata [22]. Additionally, WM damage in some IUGR models has

been associated with an increase in the number of microglia and astrocytes [25–29].

Despite the value of all of the above evidence, one of the major limitations of animal experimentation is the transferability of these data to humans. In this sense, an animal species in which the pattern of brain maturation and especially the degree of maturation at the time of presentation of the IUGR are as similar as possible to what occurs in humans [3] should be selected. Workman et al. [30] developed a model to predict the degree of brain maturation at birth (precocial score) for 18 mammalian species with empirical data of 271 neuronal events. Derived of their work, the rabbit species presented a precocial score (54%) that was more similar to humans (65%) than other species (45% in rats, 84% in guinea pig, and 82% in sheep). Furthermore, surgical IUGR induction in pregnant rabbits demonstrated to reproduce clinical features of human IUGR [31–35]. Advanced MRI studies by using this model confirmed subtle structural changes underlying IUGR with an altered diffusivity in several brain areas, including the frontal cortex and the CC, suggesting an abnormal brain maturation affecting both the GM and WM [33]. Understanding the histological substrate of this brain injury seen on MRI of this animal model would provide further insights into the mechanisms of injury during brain development.

The current study aims to describe structural changes during the neonatal period in a well-characterized animal model of IUGR in rabbits [31–33]. We hypothesize that IUGR was related to a reduction in the oligodendrocytes along with changes in dendritic arborization. For that purpose, IUGR animals were functional and structurally evaluated during the neonatal period (postnatal day 1: +1P). Structural brain changes were evaluated in the GM at the frontal cortex and the WM at the CC. As noted above, the frontal cortex was selected due to its susceptibility secondary to IUGR [4, 16–19]. Taking into consideration the degree of neuronal maturation at the time of birth in rabbits, neuronal arborization as a surrogate marker of neuronal connectivity was evaluated in this brain area, instead of other brain connectivity parameters like dendritic spines that are still in formation (personal observation). Similarly, the CC was the selected WM brain area considering its susceptibility to IUGR in human [36] and animal models [20, 21, 37]. In this brain area, changes in the pre-OLs, microglia, and astrocyte densities were assessed. The selection of the pre-OL was done taking into consideration previous evidence in human and experimental models describing its special vulnerability to perinatal hypoxia in comparison to other

maturational stages of oligodendrocytes [21–24, 38, 39]. Likewise, as a novelty in our study, we evaluated the vulnerability in this type of oligodendrocytes secondary to IUGR by using an animal species in which the predominant cell at the time of IUGR induction is the pre-OL, like rabbit species [40]. Additionally, we also evaluate histological changes in the placenta in order to characterize the degree of placental insufficiency recreated by the model. We hypothesized that significant changes would be detected in ligated placentas in comparison to nonligated placentas, especially in the degree of ischemia.

## Materials and Methods

### *Ethics Statement, Experimental Groups, and IUGR Induction*

All procedures were performed following all applicable regulations and guidelines of the Animal Experimental Ethics Committee (CEEAA) of the University of Barcelona and were approved with the license number 03/17. Also, animal work has been conducted fulfilling ARRIVE's guidelines and reported accordingly [41]. A total of 6 pregnant rabbits were included in the IUGR induction protocol for 25 days of gestation. The selection of 6 pregnant rabbits was done following previous experience from the group [31, 35, 42]. Considering fetal mortality related to the IUGR model, 12 IUGR models and 18 controls were theoretically obtained at the time of delivery. This sample size would allow us to include the required number of animals for each analyses of the study. Sample size estimation for each main variable of the study has been performed following previous evidence (see the following paragraphs for detailed information). The IUGR induction protocol was performed as previously described [31]: after a midline laparotomy, 40–50% of the uteroplacental vessels of each gestational sac from 1 horn were ligated obtaining IUGP animals, whereas nonligated gestational sacs from the contralateral horn provided normally grown animals (controls). Postoperative analgesia with buprenorphine 0.05 mg/kg was administered subcutaneously, and animals were again housed with free access to water and standard chow ad libitum and were monitored daily for general health. At 30 days of pregnancy (term at 31 days), a cesarean section was performed obtaining living and stillborn animals and their placentas. All living newborns and their placentas were weighed. A total of 18 living IUGR animals and 20 controls were obtained and included in each experimental group. None of them presented any of the following exclusion criteria: control's birth weight below 40 g or IUGR model's birth weight above 60 g. The study design is shown in Figure 1.

### *Functional Evaluation*

On +1P, general motor skills, tone, reflexes, and olfactory sensitivity were evaluated in 12 animals per group selected randomly (IUGR  $n = 12$ ; control  $n = 12$ ), following previously described methodology [43]. For each animal, testing was videotaped and variables were scored on a scale of 0–3 (0 = worst and 3 = best), except for tone that was scored (0–4) according to Ashworth scale [44], by 2 blinded observers (M.I. and L.P.). A detailed explanation of how each variable was assessed is given below.

The first part of evaluation lasted 1 min and included the evaluation of (i) posture, (ii) righting reflex (number of times the animal turned prone from supine position in 10 tries), (iii) tone (assessed by an active flexion and extension of the forelimbs and hind limbs), (iv) circular motion (evaluation of the range of movements and jumpings), (v) hind limb locomotion (spontaneous movement of the hind limbs), (vi) intensity of the movements, (vii) duration of the movement, (viii) lineal movement (number of times the animal crossed a perpendicular line of 15 cm when walking straight), and (ix) mean of the shortest fore-hind paw distance. After this first minute of evaluation, suck and swallow, head turning, and olfaction were evaluated as follows: (i) suck and swallow (assessed by the introduction of formula [Lactadiet with omega 3; Royal Animal, S.C.P.] into the rabbit's mouth with a plastic pipette), (ii) head turning (assessed by observing the head-body movements corresponding to the suction reflex), and (iii) olfaction (counting the time in seconds when the animal moves its nose away from a cotton swab soaked with pure ethanol when placed close to its nose). The score grading used for each variable is detailed in online suppl. material (see online suppl. Table 1; for all online suppl. material, see [www.karger.com/doi/10.1159/000512948](http://www.karger.com/doi/10.1159/000512948)).

### *Sample Collection*

After the cesarean section, placentas were obtained, carefully washed with saline solution, weighed, and fixed for 24 h by immersion in 10% formalin. Regarding neonates, after functional evaluation, newborns were weighed and sacrificed by decapitation after administration of ketamine 35 mg/kg and xylazine (5 mg/kg) intramuscularly. All their brains were carefully dissected and weighed. In total, 16 brains (8 controls and 8 IUGR brains) were selected randomly, fixed for 24 h in 10% formalin, dehydrated for 48 h with sucrose 30%, and finally frozen at  $-80^{\circ}\text{C}$ . All other fresh brains (4 controls and 4 IUGR brains) were processed according to the Golgi-Cox staining protocol (see section Neuronal Arborization Analyses in Frontal Cortex).

### *Histological Procedures*

#### *Placenta*

After fixation, paraffin blocks were obtained, and 4- $\mu\text{m}$  transversal cuts with a microtome were then performed in 5 placentas randomly selected from each group. The sample size was defined following previous literature and considering ischemia as the main variable of these analyses [45]. Hematoxylin and eosin staining were performed in 2 consecutive slices from each placenta. Analysis was performed using a bright-field microscope by a trained pathologist who was blinded to the experimental groups following previous assessments performed in pregnant rabbits [46]. A semi-quantitative grading system of the histological findings was performed with lesions graded from 0 to 5: 0, unremarkable; 1, minimal; 2, mild; 3, moderate; 4, marked; and 5, severe. Necrosis was expressed as percentage of necrotic area. The analyses were attempted in the 2 zones of the placenta: the decidua basalis (maternal part) and the labyrinth zone (fetal part).

#### *Neuronal Arborization Analyses in Frontal Cortex*

Four animals per group were included in this analysis, similar to previous evidence [47]. A vibratome was used to obtain 100- $\mu\text{m}$  serial and coronal sections from whole fresh brains. Afterward, sections were processed for Golgi-Cox impregnation with an FD Rapid GolgiStain kit (FD Neurotechnologies Inc.). Coronal slices

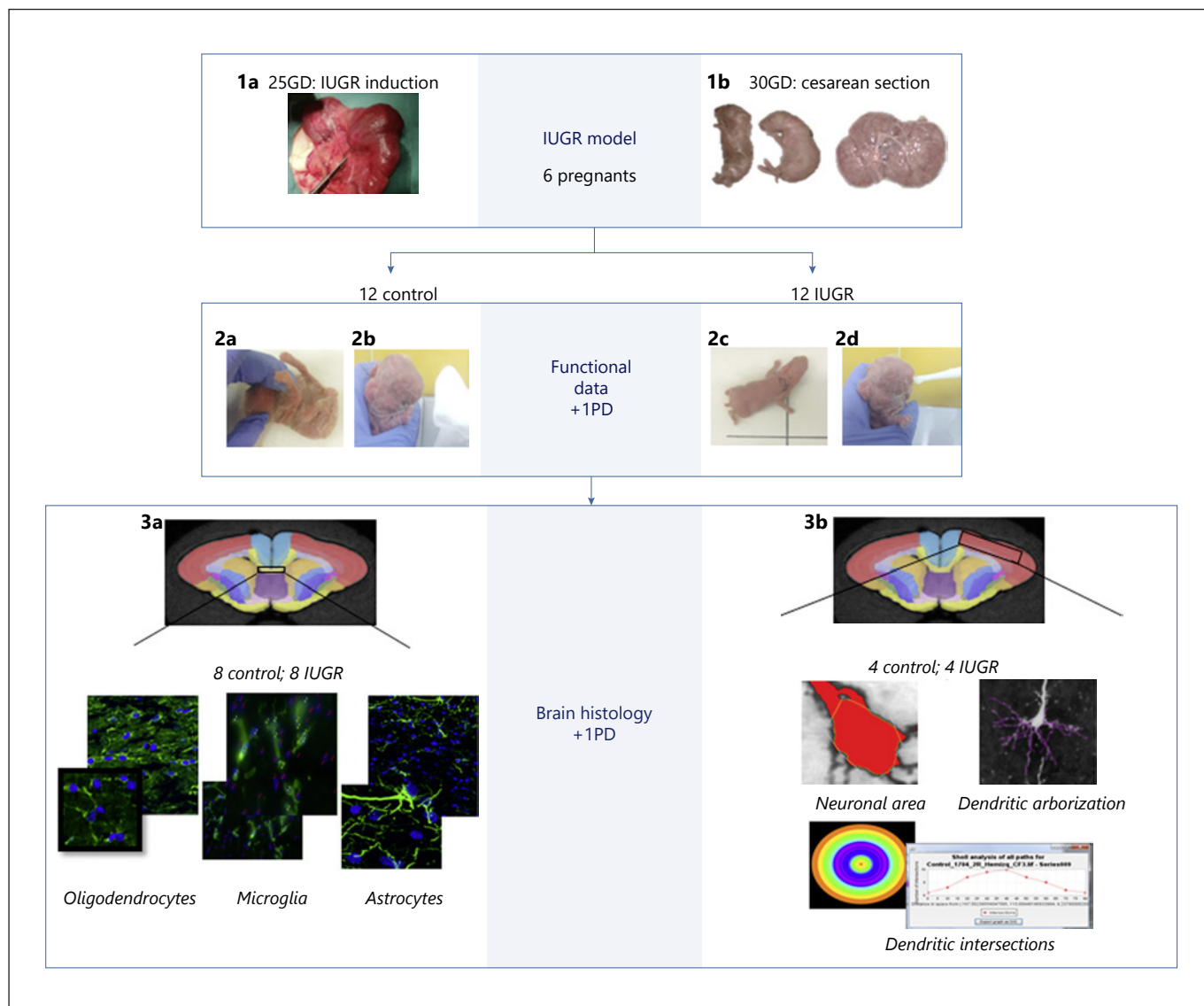


**Fig. 1.** Graphical representation of the study design and methods. Summary of the study design. Illustrative image of unilateral ligation of 40–50% of uteroplacental vessels on day 25 of pregnancy (**1a**); illustrative images of living newborns and placenta on day 30 of pregnancy, day of the caesarean section (**1b**); illustrative images of the neurobehavioral evaluation of righting reflex (**2a**), smelling

test (**2b**), locomotion (**2c**), and sucking and swallowing (**2d**), performed on +1P; illustrative images of the neuronal arborization analyses in the frontal cortex (**3b**). IUGR, intrauterine growth restriction; CC, corpus callosum.

with reference to the bregma were observed under  $\times 40$  objective magnification in an AF6000 epifluorescence microscope. Five pyramidal neurons from the frontal cortex from each brain hemisphere (10 neurons per animal) that fulfilled the inclusion criterion were randomly selected, and 1 image per neuron was obtained. In order to obtain the dendritic tree of each neuron, different Z-stacks per each image were needed. The inclusion criterion was pyramidal neurons within layers II and III, and complete filling of the dendritic tree, especially for the basal dendrites, as evidenced by well-defined endings.

Dendrites that emerged from the soma and that were in the opposite side of the thick and long apical dendrite (basal dendrites) [48] were selected for these analyses. Blinded to the experimental groups (M.C.L. and L.P.), several parameters from each neuron were collected by using ImageJ software, including (i) the area of the soma (obtained by manual delineation of the shape of the neuronal soma in a 2D image); (ii) the number of basal dendrites (obtained by manual counting); (iii) the total basal dendritic length (obtained after performing manual delineation of the length of each basal dendrite and then calculating the sum of all lengths from all

basal dendritic branches); and (iv) basal dendritic complexity, which included the evaluation of the number of basal dendritic intersections and the number of each basal dendritic branches. The basal dendritic complexity was evaluated by using the Sholl technique, as previously described [49]. Sholl rings were placed concentrically in 10- $\mu$ m increasing intervals centered on the soma. For the basal dendritic intersections, the number of intersections that dendritic branches made per each Sholl ring and the summation of all of them were recorded. For the number of each basal dendritic branch, each basal dendritic branch was divided into primary, secondary, tertiary, quaternary, quinary, and senary dendrites. Primary dendrites were considered those dendrites that were originated from the soma; secondary dendrites those that were derived from the primary dendrites, and so on, up to the senary dendrites, corresponding to those derived from the quinary dendrites.

#### WM Evaluation in CC: pre-OLs, Microglia, and Astrocytes

Following previous studies with the same animal model, 4 brains per experimental group would be required for the assessment of oligodendrocytes [42]. However, due to differences in the methodology used (in vitro vs. ex vivo), 8 brains per experimental group were finally included. The same 8 brains were used for microglia and astrocyte evaluation, following similar sample sizes as given in previous literature [26–28]. All WM evaluations were analyzed blinded per experimental group (L.P. for O4-OL and P.V.-A. for microglia and astrocyte evaluation). Formalin-fixed brains were cut with a cryostat obtaining 40- $\mu$ m-thick coronal sections. For pre-OL evaluation, 3 representative serial sections at the level of the genu CC were blocked with 10% fetal bovine serum for 1 h, followed by overnight incubation at 4°C with an anti-oligodendrocyte marker O4 (1:50, Chemicon). Specifically, the O4 marker stains latter stages of oligodendrocyte maturation (O4-OL), including pre-OLs, pre-myelinating OL, and myelinating OL (Sarah Kuhn 2019). After PBS 0.3% Triton X-100 washes, 60-min incubation with 1% Hoechst 33258 (1:1,000, Thermo Fischer) for the visualization of the total cellular nucleus was done. Afterward, the specific secondary antibody conjugated to 488 Alexa Fluor (1:400, MoBitec) was added. Immunoreactive sites were revealed and observed under  $\times 40$  objective magnification by using a confocal microscope. Images were taken with 10 steps in the Z-stack. The total number of cell nuclei (stained with Hoechst) and the number of cells with positive O4 fluorescent staining around the nucleus (O4-OL) were counted using ImageJ software. O4-OL density (O4+ cells/mm<sup>2</sup>) was then calculated.

For microglia evaluation, similar to O4-OL evaluation, 3 representative serial sections at the level of the genu CC were blocked with 0.5% of bovine serum albumin for 1 h, followed by 1-h incubation at 37°C with the first antibody biotinylated *Lycopersicon esculentum* (tomato) lectin (1:100, vector). After PBS 0.3% Triton X-100 washes, 30-min incubation with the secondary antibody (streptavidin-cyanine CyTM3-conjugated, Jackson Immunoresearch) and 1% Hoechst 33258 (1:1000, Thermofischer) was done for the visualization of the total cell nuclei. Immunoreactive sites were revealed and observed under  $\times 40$  objective magnification by using a confocal microscope. Images were then taken and analyzed using the same methodology described for the O4-OL evaluation, obtaining the microglial cell density (tomato lectin + cells/mm<sup>2</sup>). It is worth to mention that *Lycopersicon esculentum* (tomato) lectin antibody presents specific affinity for poly-N-acetyl lactosamine sugar residues found in the cytoplasm of microglia. In this regard, activated microglia apart from the changes in morphology

**Table 1.** Functional results

| Variable                                   | Control, n = 12 | IUGR, n = 12 | p value |
|--|-----------------|--------------|---------|
| Posture, score <sup>#</sup>                | 3 (0)           | 3 (0)        | 1.00    |
| Righting reflex, number of turns           | 10 (1)          | 8 (5)        | 0.03*   |
| Tone, score <sup>#</sup>                   | 4 (0)           | 4 (0)        | 1.00    |
| Circular motion, score <sup>#</sup>        | 3 (1)           | 1 (2)        | 0.03*   |
| Hind limb locomotion, score <sup>#</sup>   | 3 (1)           | 2 (2)        | 0.09    |
| Intensity, score <sup>#</sup>              | 3 (0)           | 2 (1)        | 0.03*   |
| Duration, score <sup>#</sup>               | 3 (0)           | 3 (0)        | 0.54    |
| Lineal movement                            | 3 (2)           | 2 (2)        | 0.11    |
| Fore-hind paw distance, mm                 | 0 (0)           | 0 (3)        | 0.21    |
| Sucking and swallowing, score <sup>#</sup> | 3 (1)           | 1 (2)        | 0.02*   |
| Head turning, score <sup>#</sup>           | 3 (0)           | 2 (2)        | 0.02*   |
| Olfaction, score <sup>#</sup>              | 3 (1)           | 3 (1)        | 0.47    |
| Olfaction time, s                          | 2 (4)           | 3 (5)        | 0.13    |

Functional results are expressed as median and IQR, except the variable “lineal movement,” which is expressed as mean and SD. IUGR, intrauterine growth restriction; SD, standard deviation; IQR, interquartile range. <sup>#</sup>Statistical comparisons between control and IUGR groups were performed by ordered logistic regression for each ordinal variable and multiple linear regression for continuous variables. \*Statistical significance was declared when  $p < 0.05$ .

also increase the expression of N-acetyl lactosamine residues. Therefore, the antibody used, tomato lectin, could easily demonstrate the reactive changes of this cell population [50].

Regarding astrocyte evaluation, although 8 animals were to be included for each experimental group, only 7 animals per group were finally included in the astrocyte evaluation due to technical problems with tissue processing. Three representative serial sections at the level of the genu CC were put through heat-induced epitope retrieval and later washed with PBS 0.3% Triton X-100 for 30 min. After blocking the sections with 1% bovine serum albumin and 5% goat serum for 1 h, they were incubated with the antibody GFAP (1:400, Biotechne), a marker of astrogliosis [51], at 4 °C overnight. Following PBS 0.3% Triton X-100 washes, 1-h incubation with the secondary Ab conjugated to 488 Alexa Fluor (1:400, Life Technologies) and 1% Hoechst 33258 (1:1,000, Thermofisher) was performed for the visualization of the total cell nuclei. Immunoreactive sites were revealed and observed under  $\times 63$  objective magnification by using a confocal microscope. Images were taken and analyzed using the same methodology as previously described, obtaining astrocyte density (GFAP + cells/mm<sup>2</sup>).

#### Statistical Analyses

The software packages STATA14.0 and GraphPad 5 were used for the statistical analyses or graphical representation. For quantitative variables, normality was assessed by using the Shapiro-Wilk test, and the homoscedasticity was determined by using Levene’s Test, except if variables were  $>30$  (Golgi-Cox variables), normal distribution was already assumed. For ordinal variables, nonnormal distribution was assumed.

**Table 2.** Placenta histological results

| Study group | Decidua basalis |                |                     |                     |
|-------------|-----------------|----------------|---------------------|---------------------|
|             | ischemia, %     | necrosis, %    | fibrin, %           | calcification (0–4) |
| Control     | 92.5            | 90             | 3.5                 | 2                   |
| IUGR        | 100*            | 97.5           | 4.5                 | 3                   |
| Study group | Labyrinth zone  |                |                     |                     |
|             | ischemia, %     | collapse (0–4) | calcification (0–4) |                     |
| Control     | 20              | 0              | 0.5                 |                     |
| IUGR        | 95*             | 2.5            | 2.7                 |                     |

Results are expressed as percentages or as a semiquantitative grading system of the histological findings from the decidua basalis and the labyrinth zone. IUGR, intrauterine growth restriction. \* Statistical significance was declared when  $p < 0.05$ .

Descriptive variables were expressed as mean and standard deviation for normal distributions, whereas median and interquartile range were used for nonnormal distributions or ordinal variables. For nonnormal variables and when the null hypothesis from Levene's test was rejected, log-transformation was performed prior to the statistical analysis. Multiple, logistic, or ordered logistic regressions when needed were performed in all quantitative, qualitative or ordinal variables. Also, the association of O4-OL, microglia, and astrocytes with birth weight was analyzed by means of Pearson correlation analysis. Statistical significance was declared at  $p < 0.05$  in all variables evaluated.

## Results

### Perinatal Data

In comparison to normally grown animals (controls), IUGR animals presented a significantly reduced birth weight (IUGR vs. controls:  $38.65 \pm 9.84$  vs.  $48.48 \pm 7.34$  g,  $p = 0.001$ ) and an increased stillbirth rate (IUGR vs. controls: 42.42 vs. 11.11%,  $p = 0.01$ ). In the same line, the brain weight was significantly reduced in the IUGR group in comparison to control animals (IUGR vs. controls:  $1.12 \pm 0.12$  g vs.  $1.24 \pm 0.07$  g,  $p = 0.03$ ). However, when the brain weight/birth weight ratio was calculated, the IUGR group presented a significant increase in the brain weight ratio in comparison to controls (IUGR vs. controls:  $0.033 \pm 0.007$  vs.  $0.026 \pm 0.003$ ,  $p = 0.030$ ).

### Functional Results

IUGR rabbits showed poorer functional results than controls in several of the variables assessed, including righting reflex, circular motion, intensity, sucking and swallowing, and head turning (Table 1). No differences

were observed in posture, tone, hind limb locomotion, duration, lineal movement, fore/hind paw distance, olfaction score, and time.

### Placenta Analyses

The placental weight was lower in the IUGR group than the control group without reaching statistical significance (IUGR vs. controls:  $5.23 \pm 1.72$  g vs.  $6.11 \pm 1.46$  g,  $p = 0.08$ ). Macroscopic assessment of the placentas did not show any visible differences between the groups. However, histological examination of the placenta showed a higher proportion of ischemia, with trends in necrosis, fibrin deposition, and calcifications in the IUGR group, especially in the labyrinth zone. Also, trends presenting a higher degree of vascular collapse in IUGR groups were observed with no signs of these findings in the control group (Table 2). Representative images and the semiquantitative grading systems of the histological findings from the decidua basalis and labyrinth zone are shown in Figure 2.

### Neuronal Arborization Analyses in the Frontal Cortex

IUGR animals showed a trend to present decreased primary and secondary dendrites with a significant increase in the number of the more distal dendrites (tertiary, quaternary, and quinary dendrites) in comparison to controls (shown in Fig. 3). No statistical differences between groups were observed in the rest of variables (dendritic length, number of basal dendrites, area of the soma, number of total intersections, and number of intersections per each Sholl ring) (shown in online suppl. Table 2; online suppl. Fig. 1).

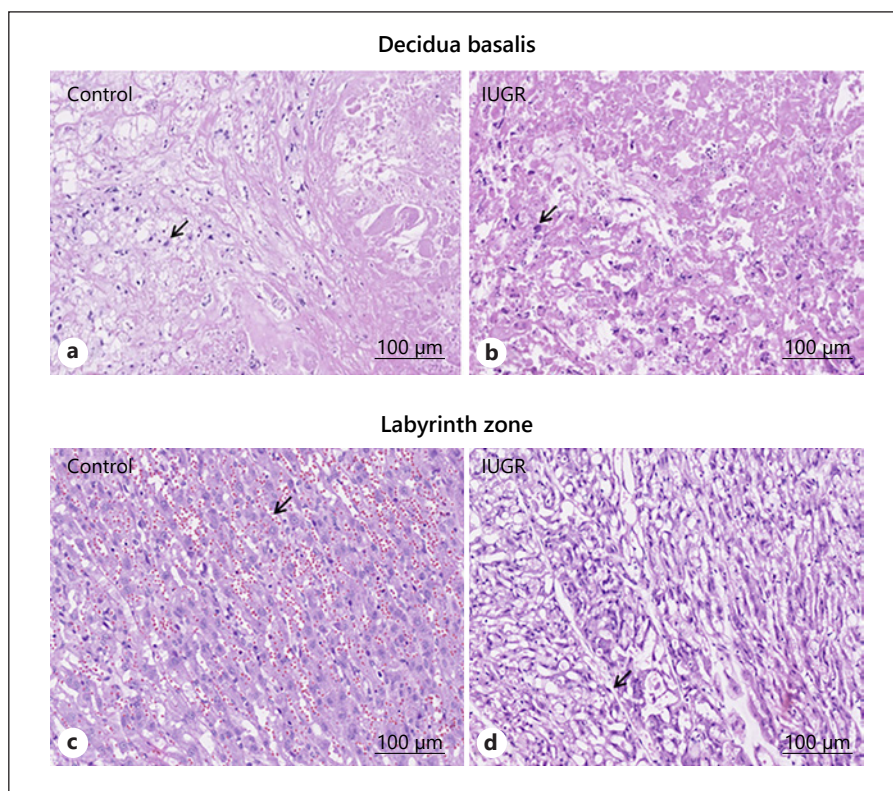


**Fig. 2.** Placenta histological findings. **a, b** Representative images of necrosis from the decidua basalis in the study groups. Necrosis is observed as a disintegrated nucleus (arrow). **c, d** Representative images of vascular channels (arrow in control) or vascular collapse (arrow in IUGR) from the labyrinth zone in the study groups. IUGR, intrauterine growth restriction.

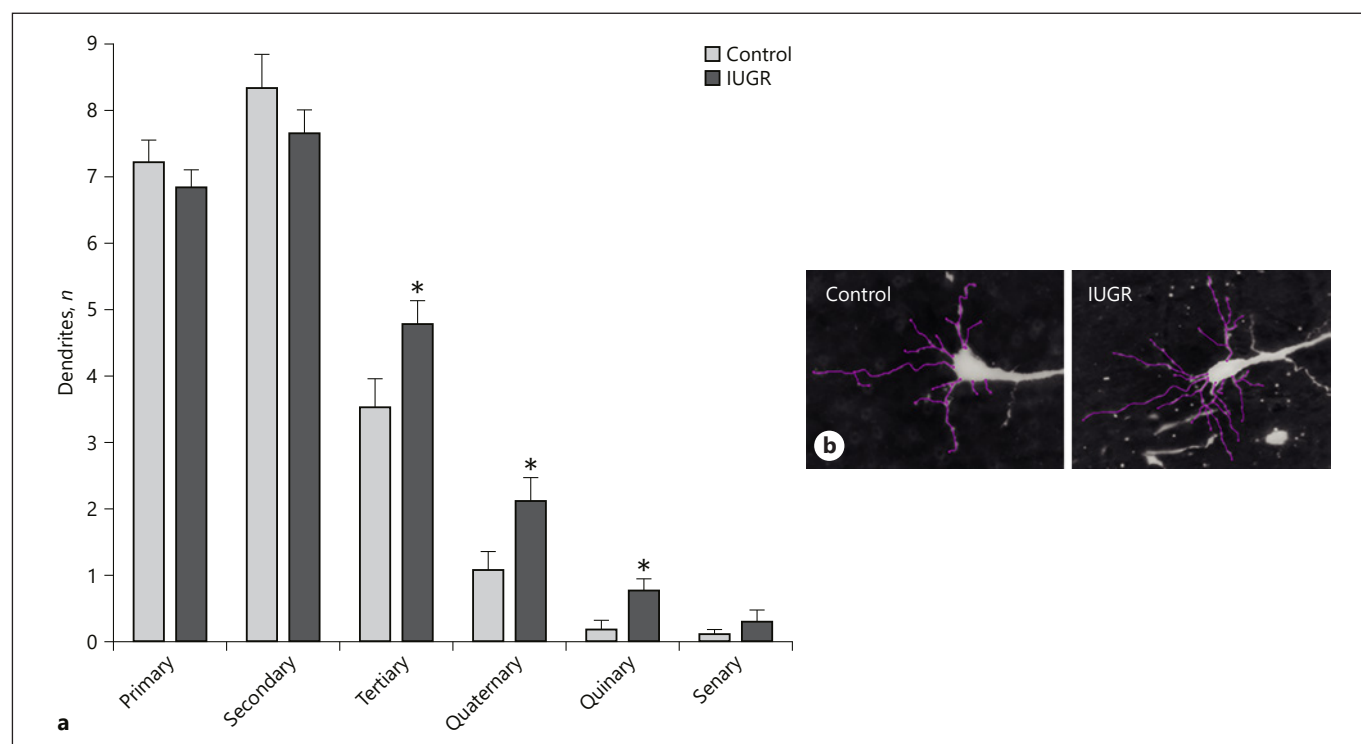


**Fig. 3.** Number of each basal dendritic branch. **a** Number of each basal dendritic branch (primary, secondary, tertiary, quaternary, quinary, and senary) in the frontal cortex in control and IUGR groups. Statistical significance was declared when  $p < 0.05$  between control and IUGR (\*). **b** Illustrative images of basal dendritic ramification in control and IUGR groups. IUGR, intrauterine growth restriction.

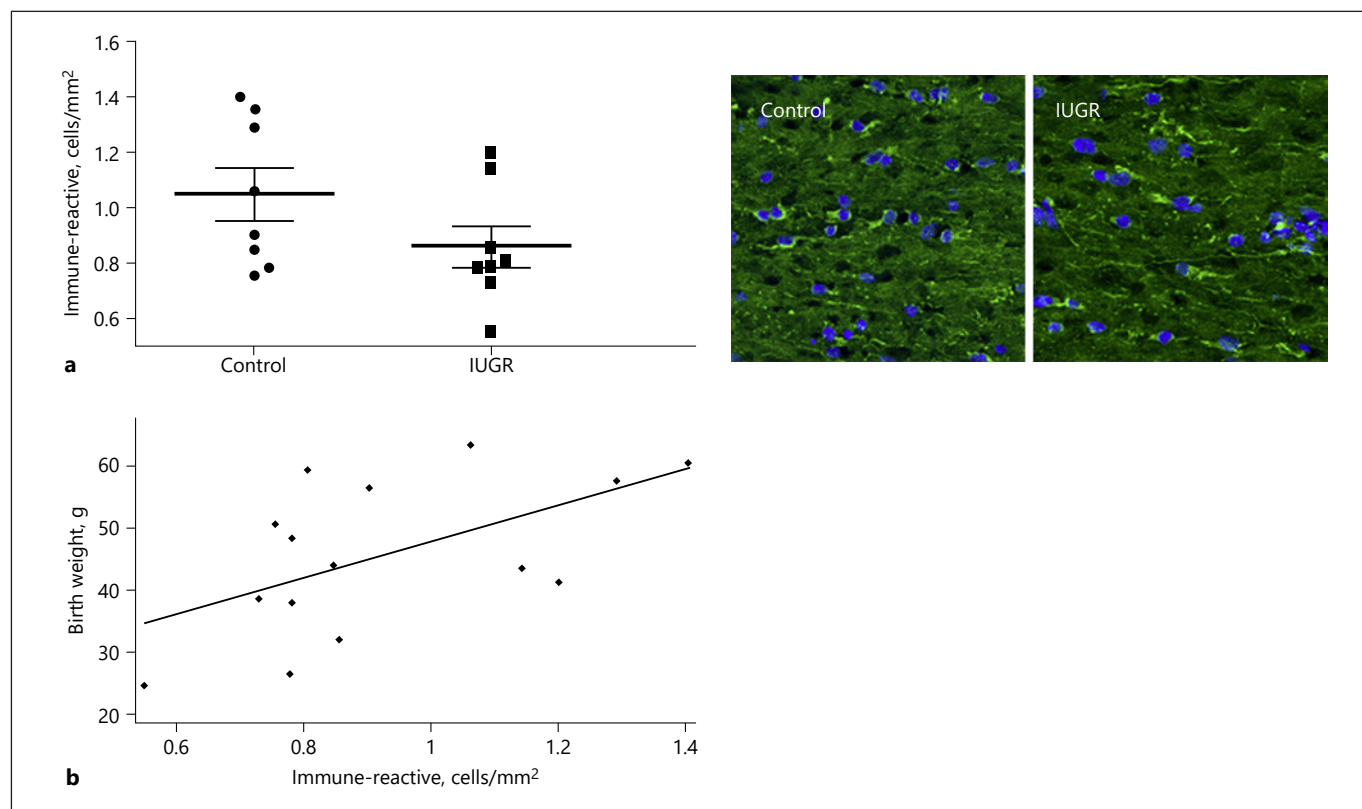


**Fig. 4.** O4-OL analyses. **a** O4-OL (immunoreactive cells/mm<sup>2</sup>) in the CC in control and IUGR groups. Statistical significance was declared when  $p < 0.05$  between control and IUGR (\*); and illustrative images of the immunolabeling of O4-OL in control and IUGR groups. **b** Association between O4-OL density with birth weight results performed by means of Pearson correlation. IUGR, intrauterine growth restriction; CC, corpus callosum.

#### WM Evaluation in CC: O4-OL, Microglia, and Astrocytes

Density of O4-OL (O4+ cells/mm<sup>2</sup>) was significantly correlated with birth weight ( $R^2 = 0.32$  and  $p = 0.03$ ), with trends to present a decrease in the IUGR's O4-OL density when compared with controls (IUGR vs. controls:  $0.86 \pm 0.21$  cells/mm<sup>2</sup> vs.  $1.05 \pm 0.27$  cells/mm<sup>2</sup>,  $p = 0.13$ ) (shown in Fig. 4). No differences were observed in microglia and astrocyte density (microglia density = IUGR vs. controls:  $0.29 \pm 0.06$  cells/mm<sup>2</sup> vs.  $0.28 \pm 0.06$  cells/mm<sup>2</sup>,  $p = 0.570$ ; astrocytes density = IUGR vs. controls:  $0.95 \pm 0.28$  cells/mm<sup>2</sup> vs.  $1.13 \pm 0.30$  cells/mm<sup>2</sup>,  $p = 0.89$ ).

#### Discussion

The present study described the structural brain changes affecting both the GM and WM during the neonatal period secondary to placental insufficiency in a rab-

bit model of IUGR animals. Overall, abnormal neuronal arborization and an altered WM maturation were observed in the IUGR animals. These findings give us insights into the correspondence at the cellular level of the structural brain changes underlying neurodevelopmental impairments secondary to IUGR during the neonatal period.

The reduced survival and birth weight together with the poorer functional outcomes of the IUGR neonates are in good agreement with previous data [4, 33, 35]. Clinical studies have linked IUGR with an increased risk of perinatal mortality [52], and among survivors, IUGR neonates are at great risk for neurodevelopmental dysfunction, attention, habituation, regulation of state, motor activity, and social interactive clusters being the most affected during the neonatal period [4]. In the experimental setting, previous articles using the same animal model described similar results to those reported in this work, with weakened motor activity, and sucking and swallow-



ing function [33, 35]. As expected, these functional impairments were less marked than impairments reported in models with acute and severe prenatal insults that are related to hypertonia and locomotion deficits, mimicking human cerebral palsy [40, 53]. Additionally, we observed a significant brain weight reduction in the IUGR animals in comparison to controls. This observation is in accordance with previous data from clinical [54–56] and experimental studies [18, 33, 57, 58]. The relative increase in the proportion of brain weight compared to fetal weight is probably related to the “brain-sparing effect” documented in previous literature [59].

Regarding placental evaluation, both labyrinth and decidua parts of the placenta presented structural changes in IUGR animals. The most relevant change was the ischemia, also with an increase in the fibrin and calcification deposition, reflecting the effect of uteroplacental vessel ligation on the placenta. This finding is also in accordance with previous clinical [60, 61] and experimental data [45, 46, 62] where placental histology assessment evidenced higher levels of fibrin deposition, placenta infarction, and calcifications in IUGR.

Regarding the neuronal arborization analyses in the frontal cortex, abnormal neuronal arborization was detected in cortical neurons from the frontal cortex. We observed lower primary and secondary dendrites with an increase in the number of tertiary to quinary dendrites in IUGR in comparison to controls. It is worth noting that changes in the pattern of dendritic branching or dendritic arborization area are key features of several human neurodevelopmental disorders, including Down and Rett syndromes [63]. In the experimental field, abnormal dendritic branching has also been reported after intrauterine inflammatory insults [64], protein malnutrition [65], and hypoxic-ischemic events [13, 14, 47, 66]. Decreased dendritic arborization in pyramidal neurons of the hippocampus, and frontal and cerebellar cortices was observed in guinea pig and sheep models after either acute [47, 66] or chronic hypoxic-ischemic events [13, 14]. These previous data are in line with our observations, although our results are less pronounced and only for the primary and secondary dendrites, which could be explained by several factors. One of the most important factors to consider is the maturational stage of the brain at the moment of insult presentation. Differences in the state of arbor development at the time of insult presentation might result in different patterns of dendritic arborization changes [3, 67]. This issue is especially relevant when data are extrapolated within species, since the pattern of brain development and maturation varies considerably across species.

At birth, the precocial score in rabbits has been estimated to be around 54%, which is more similar to humans (65%) than that in other species, including rats (45%), guinea pig (84%), and sheep (82%) [30]. Another factor to consider is the difference in the degree of the insult [68]. The IUGR model reported in this study induces a mild and chronic hypoxia-ischemia, and in consequence, the neurological alterations might be less marked than in other models with a more severe hypoxia-ischemia IUGR induction [13, 14]. Finally, differences in the brain area evaluated might also explain these different results. The present study is the first to evaluate the neuronal arborization parameters in the frontal cortex in mild and chronic models of IUGR. Regarding the increase in distal dendrites found in our study, it is worth mentioning that dendritic arbors are highly dynamic structures, especially in the latter half of gestation [69]. Follow-up studies in adult rats demonstrated that shortly after an acute ischemic event, dendritic arborization was reduced, whereas 24 h after the insult, dendritic arbors increased [70]. It has been hypothesized that the reduction in dendritic branches shortly after hypoxic/ischemic insult may reflect the neuronal damage, while the increase in dendritic arborization after the insult probably represents a later compensatory effect [70]. Since the neuronal arborization is a surrogate marker of neuronal synapses, the increase in the distal dendrites reported in our study probably reflects the compensatory mechanisms of the brain to overcome the abnormal neuronal connectivity caused by the insult. In this context, diffusion tensor imaging studies using the same animal model discovered decreased fractional anisotropy (FA) in the frontal cortex in IUGR young rabbits [33]. The decrease in FA in the cortex has been described during the maturation process and related to the increase in the expansion of dendritic trees and ramification in neurons [71]. Therefore, the distal dendrite increase in the cortical neurons from IUGR young rabbits might be considered as part of the structural correspondence for the decreased cortical FA previously reported in studies from the group [33].

In WM evaluation, we observed a significant correlation between O4-OL and birth weight. This result goes in line with previous evidences in which positive correlation between O4-OL in the CC and birth weight were also found on postnatal day 7 in a moderate IUGR rat model [28]. Going in the same line, a recent article from our group has demonstrated impairments in the O4-OL differentiation after 5 days of incubation in a novel neurosphere culture obtained from our animal model [42]. Disruption in the oligodendrocyte maturation process dur-

ing neurodevelopment is of relevance as it has been linked with neurodevelopmental impairments later on [15, 20, 29, 38, 72]. While in severe animal models of IUGR, deficits in myelin persisted up to a long-term period [29], in less severe phenotypes of IUGR, after a transient delay in myelination during the perinatal period, the myelin content was restored during the long-term period [20, 22, 37, 73]. However, despite this apparent recovery of the myelination, mild motor deficits have been described during the long-term period in an IUGR model in pregnant rats [73]. Although we did not conduct a prospective study evaluating consequences of this altered oligodendrocyte maturation in our animal model, previous diffusion MRI studies in the same animal model showed structural changes affecting the WM during the neonatal period [33] that also persisted on postnatal day 70 [32, 35, 74]. On +1P, we observed a decreased FA in the CC [33], suggesting diffuse oligodendrocyte injury [75, 76]. On postnatal day 70, IUGR rabbits presented a decrease in FA in the hippocampus and in the subventricular WM [32] and an altered brain network [35, 74], which correlated again with functional disturbances. These results confirm the persistence of WM brain reorganization in the IUGR during the long-term period with less organized and mature fiber tracts [77] that might be secondary to the disruption of the oligodendrocyte maturation during the prenatal period reported in this study. The disruption of the oligodendrocyte maturation may especially affect the pre-OL population since in rabbits, the predominant WM cell is the pre-OL late during pregnancy [40].

Additionally, microglia and astrocyte densities were evaluated in this study during the neonatal period, since they have been implied in the pathogenesis of WM injury in the developing brain. Prenatal insults might facilitate the activation of microglia and astrocytes through a neuro-inflammatory mechanism [28, 72, 78–80]. Different rodent models of IUGR based on hypoxia, uterine artery ligation, or protein reduction demonstrated delayed oligodendrocyte maturation along with microgliosis [28, 29, 78] and astrogliosis [28, 29, 73]. In the present IUGR model, disrupted maturation occurred with no differences in the density of activated microglia and astrocytes between groups. Regarding the microglia, we must take into consideration that previous literature has demonstrated no differences in tomato lectin-positive microglial cells in the cingulate WM of an IUGR rat model, but at the same time, the expression of genes related to microglial activation were increased in the IUGR group [78]. Further investigation in this regard should be done.

Our study has some strengths and limitations that need to be mentioned. One of the major strengths of this research is the animal model used to characterize mild and chronic effects of IUGR in brain development. Functional impairments described in this work are consistent with previous literature in the IUGR rabbit model [33, 35] and also in human studies of IUGR [4, 81]. In addition, the similarity of brain maturation of rabbit species with humans makes the rabbit species a reliable model for translational data to humans [30].

Regarding the limitations of the study, we acknowledge our study to be underpowered for some of the variables assessed. Since we aimed to evaluate structural brain changes secondary to mild and chronic prenatal insults, the histological alterations detected were indeed subtle, and some of the variables were underpowered for the sample size used (shown in online suppl. Table 3). As an example, in order to have at least 80% of statistical power to detect differences between the groups, we have worked on a sample size of around 30 animals per group in the pre-OL evaluation, making it a very ambitious goal. Alternatively, *in vitro* studies allow us to bypass the sample size limitation observed in *in vivo* models. In comparison to *in vivo* studies, the *in vitro* experimental setting is even more controlled allowing to obtain significant differences even with a smaller number of animals. In fact, a recent study from our group working on the same IUGR rabbit model but performing histological analyses in *in vitro* conditions has demonstrated impairments in the O4-OL using 4 animals from each group [42]. Another limitation of our study is that we did not explore if the results reported here could be extrapolated to other brain regions and in different time points. In this regard, future studies evaluating WM sequels at different postnatal time points would be required to further characterize the long-term consequences of abnormal oligodendrocyte maturation occurred during the fetal period in our animal model. Finally, the evaluation of the molecular pathways underlying the GM and WM alterations, such as the evaluation of glutamate [82, 83], bone-derived neurotrophic factor [84, 85], and morphogenetic protein family 4 [73], would help corroborate the structural brain changes detected in this work at molecular level.

In summary, this study provides experimental evidence that mild and chronic insults during prenatal life disrupt normal patterns of neurodevelopment, interfering with both WM and GM development. The most remarkable changes are detected in neuronal branching and maturational pattern of oligodendrocytes. These

findings enable us to propose this model as a suitable model to further characterize structural brain changes underlying the neurodevelopmental impairments due to IUGR and evaluate potential therapeutic agents aiming to mitigate these deleterious consequences on neurodevelopment.

### Acknowledgements

We thank the animal facility of Hospital Sant Joan de Déu for their help in maintaining the animal welfare. We also thank Ms. Maria Calvo, Ms. Anna Bosch, and Ms. Elisenda Coll from Centres Científics i Tecnològics – Universitat de Barcelona for their technical support in using the confocal microscope.

### Statement of Ethics

All experimental procedures conducted during the animal experiments were performed following all applicable regulations and guidelines of the Animal Experimental Ethics Committee (CEEA) of the University of Barcelona and were approved by them (license number 03/17).

### References

- Meschia G. *Reasy and resnik's maternal-fetal medicine: principles and practice, placenta respiratory gas exchange and fetal oxygenation*: Elsevier Health Sciences; 2008. Vol. 14; p. 181–91.
- Baschat AA, Hecher K. Fetal growth restriction due to placental disease. *Semin Perinatol*. 2004;28(1):67–80.
- Rees S, Harding R, Walker D. An adverse intrauterine environment: implications for injury and altered development of the brain. *Int J Dev Neurosci*. 2008;26(1):3–11.
- Figueras F, Oros D, Cruz-Martínez R, Padilla N, Hernandez-Andrade E, Botet F, et al. Neurobehavior in term, small-for-gestational age infants with normal placental function. *Pediatrics*. 2009;124(5):e934–41.
- Feldman R, Eidelman AI. Neonatal State Organization, neuromaturation, mother-infant interaction, and cognitive development in small-for-gestational-age premature infants. *Pediatrics*. 2006;118(3):e869–78.
- Leitner Y, Fattal-Valevski A, Geva R, Eshel R, Toledano-Alhadeif H, Rotstein M, et al. Neurodevelopmental outcome of children with intrauterine growth retardation: a longitudinal, 10-year prospective study. *J Child Neurol*. 2007;22(5):580–7.
- Tideman E, Marsál K, Ley D. Cognitive function in young adults following intrauterine growth restriction with abnormal fetal aortic blood flow. *Ultrasound Obstet Gynecol*. 2007;29(6):614–8.
- Rees S, Harding R, Walker D. The biological basis of injury and neuroprotection in the fetal and neonatal brain. *Int J Dev Neurosci*. 2011;29(6):551–63.
- Esteban FJ, Padilla N, Sanz-Cortés M, de Miras JR, Bargalló N, Villoslada P, et al. Fractal-dimension analysis detects cerebral changes in preterm infants with and without intrauterine growth restriction. *Neuroimage*. 2010;53(4):1225–32.
- Padilla N, Falcón C, Sanz-Cortés M, Figueras F, Bargallo N, Crispi F, et al. Differential effects of intrauterine growth restriction on brain structure and development in preterm infants: a magnetic resonance imaging study. *Brain Res*. 2011;1382:98–108.
- Batalle D, Eixarch E, Figueras F, Muñoz-Moreno E, Bargallo N, Illa M, et al. Altered small-world topology of structural brain networks in infants with intrauterine growth restriction and its association with later neurodevelopmental outcome. *Neuroimage*. 2012;60(2):1352–66.
- Dubois J, Benders M, Borradori-Tolsa C, Cachia A, Lazeyras F, Ha-Vinh Leuchter R, et al. Primary cortical folding in the human newborn: an early marker of later functional development. *Brain*. 2008;131(Pt 8):2028–41.
- Dieni S, Rees S. Dendritic morphology is altered in hippocampal neurons following prenatal compromise. *J Neurobiol*. 2003;55(1):41–52.
- Rees S, Harding R. The effects of intrauterine growth retardation on the development of the Purkinje cell dendritic tree in the cerebellar cortex of fetal sheep: a note on the ontogeny of the Purkinje cell. *Int J Dev Neurosci*. 1988;6(5):461–9.
- Piorkowska K, Thompson J, Nygard K, Matushewski B, Hammond R, Richardson B. Synaptic development and neuronal myelination are altered with growth restriction in fetal guinea pigs. *Dev Neurosci*. 2014;36(6):465–76.
- Geva R, Eshel R, Leitner Y, Valevski AF, Harel S. Neuropsychological outcome of children with intrauterine growth restriction: a 9-year prospective study. *Pediatrics*. 2006;118(1):91–100.
- Simões RV, Muñoz-Moreno E, Cruz-Lemini M, Eixarch E, Bargallo N, Sanz-Cortés M, et al. Brain metabolite alterations in infants born preterm with intrauterine growth restriction: association with structural changes and neurodevelopmental outcome. *Am J Obstet Gynecol*. 2017;216(1):62–e14.
- Simões RV, Muñoz-Moreno E, Carbajo RJ, González-Tendero A, Illa M, Sanz-Cortés M, et al. In vivo detection of perinatal brain metabolite changes in a rabbit model of intrauterine growth restriction (IUGR). *PLoS One*. 2015;10(7):e0131310.
- Xie L, Antonow-Schlörke I, Schwab M, McDonald TJ, Nathanielsz PW, CLC. The frontal cortex IGF system is down regulated in the term, intrauterine growth restricted fetal baboon. *Growth Horm IGF Res*. 2013;23(5):187–92.

### Conflict of Interest Statement

The authors have no conflicts of interest to declare.

### Funding Sources

This work was supported by “la Caixa” Foundation [LCF/PR/GN14/10270005 and LCF/PR/GN18/10310003], the Instituto de Salud Carlos III [PIE15/00027, PI15/00130, and PI18/01763] within the Plan Nacional de I + D + I and cofinanced by ISCIII-Subdirección General de Evaluación together with the Fondo Europeo de Desarrollo Regional (FEDER) “Una manera de hacer Europa,” AGAUR (grant 2017 SGR no. 1531), and Cellex Foundation. E. Eixarch and C. Loreiro have received funding from the Departament de Salut [SLT008/18/00156 and SLT006/17/00325].

### Author Contributions

L. Pla, C. Loreiro, P. Vázquez-Aristizabal, and M.C. Lopez participated in the animal care, animal study, and immunohistochemistry study; L. Pla and M. Illa participated in the analyses, interpretation of the data, and the writing of the original draft; B.A. Kühnea and M. Barenys participated in the reviewing and editing of the original draft; M. Illa, E. Eixarch, and E. Gratacós participated in the conceptualization and supervision.

- 20 Li M, Bateman E, O'Dowd R, Markwick R, Vrijzen K, Rehn A, et al. Intrauterine growth restriction affects the maturation of myelin. *Exp Neurol*. 2011;232(1):53–65.
- 21 Back SA, Han BH, Luo NL, Chricton CA, Xanthoudakis S, Tam J, et al. Selective vulnerability of late oligodendrocyte progenitors to hypoxia-ischemia. *J Neurosci*. 2002;22(2):455–63.
- 22 Buser JR, Segovia KN, Dean JM, Nelson K, Beardsley D, Gong X, et al. Timing of appearance of late oligodendrocyte progenitors coincides with enhanced susceptibility of preterm rabbit cerebral white matter to hypoxia-ischemia. *J Cereb Blood Flow Metab*. 2010;30(5):1053–65.
- 23 Segovia KN, McClure M, Moravec M, Luo NL, Wan Y, Gong X, et al. Arrested oligodendrocyte lineage maturation in chronic perinatal white matter injury. *Ann Neurol*. 2008;63(4):520–30.
- 24 Back SA, Luo NL, Borenstein NS, Levine JM, Volpe JJ, Kinney HC. Late oligodendrocyte progenitors coincide with the developmental window of vulnerability for human perinatal white matter injury. *J Neurosci*. 2001;21(4):1302–12.
- 25 Campbell LR, Pang Y, Ojeda NB, Zheng B, Rhodes PG, Alexander BT. Intracerebral lipopolysaccharide induces neuroinflammatory change and augmented brain injury in growth-restricted neonatal rats. *Pediatr Res*. 2012;71(6):645–52.
- 26 Pham H, Duy AP, Pansiot J, Bollen B, Gallego J, Charriaut-Marlangue C, et al. Impact of inhaled nitric oxide on white matter damage in growth-restricted neonatal rats. *Pediatr Res*. 2015;77(4):563–9.
- 27 Wixey JA, Lee KM, Miller SM, Goasdoue K, Colditz PB, Tracey Bjorkman S, et al. Neuro-pathology in intrauterine growth restricted newborn piglets is associated with glial activation and proinflammatory status in the brain. *J Neuroinflammation*. 2019;16(1):5.
- 28 Olivier P, Baud O, Bouslama M, Evrard P, Gressens P, Verney C. Moderate growth restriction: deleterious and protective effects on white matter damage. *Neurobiol Dis*. 2007;26(1):253–63.
- 29 Olivier P, Baud O, Evrard P, Gressens P, Verney C. Prenatal ischemia and white matter damage in rats. *J Neuropathol Exp Neurol*. 2005;64(11):998–1006.
- 30 Workman AD, Charvet CJ, Clancy B, Darlington RB, Finlay BL. Modeling transformations of neurodevelopmental sequences across mammalian species. *J Neurosci*. 2013;33(17):7368–83.
- 31 Eixarch E, Figueras F, Hernández-Andrade E, Crispi F, Nadal A, Torre I, et al. An experimental model of fetal growth restriction based on selective ligation of uteroplacental vessels in the pregnant rabbit. *Fetal Diagn Ther*. 2009;26(4):203–11.
- 32 Illa M, Eixarch E, Batalle D, Arbat-Plana A, Muñoz-Moreno E, Figueras F, et al. Long-term functional outcomes and correlation with regional brain connectivity by MRI diffusion tractography metrics in a near-term rabbit model of intrauterine growth restriction. *PLoS One*. 2013;8(10):e76453.
- 33 Eixarch E, Batalle D, Illa M, Muñoz-Moreno E, Arbat-Plana A, Amat-Roldan I, et al. Neonatal neurobehavior and diffusion MRI changes in brain reorganization due to intrauterine growth restriction in a rabbit model. *PLoS One*. 2012;7(2):e31497.
- 34 Eixarch E, Hernandez-Andrade E, Crispi F, Illa M, Torre I, Figueras F, et al. Impact on fetal mortality and cardiovascular Doppler of selective ligation of uteroplacental vessels compared with undernutrition in a rabbit model of intrauterine growth restriction. *Placenta*. 2011;32(4):304–9.
- 35 Illa Armengol M, Eixarch E, Muñoz-Moreno E, Batalle D, Leal-Campanario R, Gruart A, et al. Neurodevelopmental effects of undernutrition and placental underperfusion in fetal growth restriction rabbit models. *Fetal Diagn Ther*. 2017;42(3):189–97.
- 36 Padilla N, Junqué C, Figueras F, Sanz-Cortes M, Bargalló N, Arranz A, et al. Differential vulnerability of gray matter and white matter to intrauterine growth restriction in preterm infants at 12 months corrected age. *Brain Res*. 2014;1545:1–11.
- 37 Drobyshevsky A, Song SK, Gamkrelidze G, Wyrwicz AM, Derrick M, Meng F, et al. Developmental changes in diffusion anisotropy coincide with immature oligodendrocyte progression and maturation of compound action potential. *J Neurosci*. 2005;25(25):5988–97.
- 38 Baud O, Greene AE, Li J, Wang H, Volpe JJ, Rosenberg PA. Glutathione peroxidase-catalase cooperativity is required for resistance to hydrogen peroxide by mature rat oligodendrocytes. *J Neurosci*. 2004;24(7):1531–40.
- 39 Fern R, Möller T. Rapid ischemic cell death in immature oligodendrocytes: a fatal glutamate release feedback loop. *J Neurosci*. 2000;20(1):34–42.
- 40 Saadani-makki F, Kannan S, Lu X, Janisse J, Dawe E, Edwin S, et al. Intrauterine administration of endotoxin leads to motor deficits in a rabbit model: a link between prenatal infection and cerebral palsy. *Am J Obstet Gynecol*. 2008;199(6):651–7.
- 41 Percie Du Sert N, Hurst V, Ahluwalia A, Alam S, Avey MT, Baker M, et al. The ARRIVE guidelines 2.0: updated guidelines for reporting animal research. *BMC Vet Res*. 2020;16(1):242–7.
- 42 Barenys M, Illa M, Hofrichter M, Loreiro C, Pla L, Klose J, et al. Rabbit neurospheres as a novel in vitro tool for studying neurodevelopmental effects induced by intrauterine growth restriction (IUGR). *Stem Cells Transl Med*. 2021 Feb;10(2):209–21.
- 43 Derrick M, Luo NL, Bregman JC, Jilling T, Ji X, Fisher K, et al. Preterm fetal hypoxia-ischemia causes hypertonia and motor deficits in the neonatal rabbit: a model for human cerebral palsy? *J Neurosci*. 2004;24(1):24–34.
- 44 Damiano DL, Quinlivan JM, Owen BF, Payne P, Nelson KC, Abel MF. What does the Ashworth scale really measure and are instrumented measures more valid and precise? *Dev Med Child Neurol*. 2002;44(2):112–8.
- 45 Qi L, Jiang J, Zhang J, Zhang L, Wang T. Maternal curcumin supplementation ameliorates placental function and fetal growth in mice with intrauterine growth retardation†. *Biol Reprod*. 2020;102(5):1090–101.
- 46 López-Tello J, Arias-Álvarez M, Jiménez-Martínez MÁ, Barbero-Fernández A, García-García RM, Rodríguez M, et al. The effects of sildenafil citrate on foeto-placental development and haemodynamics in a rabbit model of intrauterine growth restriction. *Reprod Fertil Dev*. 2016;29(6):1239–48.
- 47 Dean JM, McClendon E, Hansen K, Azimi-Zonooz A, Chen K, Riddle A, et al. Prenatal cerebral ischemia disrupts MRI-defined cortical microstructure through disturbances in neuronal arborization. *Sci Transl Med*. 2013;5(168):168ra7.
- 48 DeFelipe J, Fariñas I. The pyramidal neuron of the cerebral cortex: Morphological and chemical characteristics of the synaptic inputs. *Prog Neurobiol*. 1992;39(6):563–607.
- 49 Sholl DA. Dendritic organization in the neurons of the visual and motor cortices of the cat. *J Anat*. 1953;87(4):387–406.
- 50 Villacampa N, Almolda B, González B, Castellano B. Microglia. Methods and protocols. *Methods Mol Biol*. 2013;1041:261–79.
- 51 Eng LF, Ghirnikar RS. GFAP and astrogliosis. *Brain Pathol*. 1994;4(3):229–37.
- 52 Kady SM, Gardosi J. Perinatal mortality and fetal growth restriction. *Best Pract Res Clin Obstet Gynaecol*. 2004;18(3):397–410.
- 53 Tan S, Drobyshevsky A, Jilling T, Ji X, Ullman LM, Englof I, et al. Model of cerebral palsy in the perinatal rabbit. *J Child Neurol*. 2005;20(12):972–9.
- 54 Parikh NA, Lasky RE, Kennedy KA, McDavid G, Tyson JE. Perinatal factors and regional brain volume abnormalities at term in a cohort of extremely low birth weight infants. *PLoS One*. 2013;8(5):e62804.
- 55 Tolsa CB, Zimine S, Warfield SK, Freschi M, Sancho Rossignol A, Lazeyras F, et al. Early alteration of structural and functional brain development in premature infants born with intrauterine growth restriction. *Pediatr Res*. 2004;56(1):132–8.
- 56 Benavides-Serralde A, Hernández-Andrade E, Fernández-Delgado J, Plasencia W, Scheier M, Crispi F, et al. Three-dimensional sonographic calculation of the volume of intracranial structures in growth-restricted and appropriate-for-gestational age fetuses. *Ultrasound Obstet Gynecol*. 2009;33(5):530–7.
- 57 Ohshima M, Coq JO, Otani K, Hattori Y, Ogawa Y, Sato Y, et al. Mild intrauterine hypoperfusion reproduces neurodevelopmental disorders observed in prematurity. *Sci Rep*. 2016;6:39377.

- 58 Ruff CA, Faulkner SD, Rumajogee P, Beldick S, Foltz W, Corrigan J, et al. The extent of intrauterine growth restriction determines the severity of cerebral injury and neurobehavioral deficits in rodents. *PLoS One*. 2017;12(9):e0184653.
- 59 Giussani DA. The vulnerable developing brain. *Proc Natl Acad Sci U S A*. 2011;108(7):2641–2.
- 60 Khajuria R, Sharma M. Histopathology of placenta in intrauterine growth restriction (IUGR). *Int J Res Med Sci*. 2019;7(3):889–92.
- 61 Günyeli I, Erdemoglu E, Ceylaner S, Zergeroglu S, Mungan T. Histopathological analysis of the placental lesions in pregnancies complicated with IUGR and stillbirths in comparison with noncomplicated pregnancies. *J Turk Ger Gynecol Assoc*. 2011;12(2):75–9.
- 62 Lopez-Tello J, Arias-Alvarez M, Jimenez-Martinez MA, Garcia-Garcia RM, Rodriguez M, Lorenzo Gonzalez PL, et al. Competition for maternal-fetal resource partitioning in a rabbit model of undernourished pregnancy. *PLoS One*. 2017;12(1):e0169194.
- 63 Kulkarni VA, Firestein BL. The dendritic tree and brain disorders. *Mol Cell Neurosci*. 2012;50(1):10–20.
- 64 Balakrishnan B, Dai H, Janisse J, Romero R, Kannan S. Maternal endotoxin exposure results in abnormal neuronal architecture in the newborn rabbit. *Dev Neurosci*. 2013;35(5):396–405.
- 65 Cintra L, Aguilar A, Granados L, Galván A, Kemper T, DeBassio W, et al. Effects of prenatal protein malnutrition on hippocampal CA1 pyramidal cells in rats of four age groups. *Hippocampus*. 1997;7(2):192–203.
- 66 McClendon E, Chen K, Gong X, Sharifnia E, Hagen M, Cai V, et al. Prenatal cerebral ischemia triggers dysmaturation of caudate projection neurons. *Ann Neurol*. 2014;75(4):508–24.
- 67 Baschat AA. Neurodevelopment following fetal growth restriction and its relationship with antepartum parameters of placental dysfunction. *Ultrasound Obstet Gynecol*. 2011;37(5):501–14.
- 68 Rees S, Harding R. Brain development during fetal life: influences of the intra-uterine environment. *Neurosci Lett*. 2004;361(1–3):111–4.
- 69 de Graaf-Peters VB, Hadders-Algra M. Ontogeny of the human central nervous system: what is happening when? *Early Hum Dev*. 2006;82(4):257–66.
- 70 Ruan YW, Zou B, Fan Y, Li Y, Lin N, Zeng YS, et al. Dendritic plasticity of CA1 pyramidal neurons after transient global ischemia. *Neuroscience*. 2006;140(1):191–201.
- 71 McKinstry RC, Mathur A, Miller JH, Ozcan A, Snyder AZ, Scheff GL, et al. Radial organization of developing preterm human cerebral cortex revealed by non-invasive water diffusion anisotropy MRI. *Cereb Cortex*. 2002;12(12):1237–43.
- 72 Nitsos I, Rees S. The effects of intrauterine growth retardation on the development of neuroglia in fetal guinea pigs. An immunohistochemical and an ultrastructural study. *Int J Dev Neurosci*. 1990;8(3):233–44.
- 73 Reid MV, Murray KA, Marsh ED, Golden JA, Simmons RA, Grinspan JB. Delayed myelination in an intrauterine growth retardation model is mediated by oxidative stress upregulating bone morphogenetic protein 4. *J Neuropathol Exp Neurol*. 2012;71(7):640–53.
- 74 Illa M, Brito V, Pla L, Eixarch E, Arbat-Plana A, Batallé D, et al. Early environmental enrichment enhances abnormal brain connectivity in a rabbit model of intrauterine growth restriction. *Fetal Diagn Ther*. 2018;44(3):184–93.
- 75 Van De Looij Y, Lodygensky GA, Dean J, Lazeyras F, Hagberg H, Kjellmer I, et al. High-field diffusion tensor imaging characterization of cerebral white matter injury in lipopolysaccharide-exposed fetal sheep. *Pediatr Res*. 2012;72(3):285–92.
- 76 Drobyshevsky A, Derrick M, Wyrwicz AM, Ji X, Englof I, Ullman LM, et al. White matter injury correlates with hypertonia in an animal model of cerebral palsy. *J Cereb Blood Flow Metab*. 2007;27(2):270–81.
- 77 Sen PN, Basser PJ. A model for diffusion in white matter in the brain. *Biophys J*. 2005;89(5):2927–38.
- 78 Rideau Batista Novais A, Pham H, Van de Looij Y, Bernal M, Mairesse J, Zana-Taieb E, et al. Transcriptomic regulations in oligodendroglial and microglial cells related to brain damage following fetal growth restriction. *Glia*. 2016;64(12):2306–20.
- 79 Hagberg H, Mallard C, Ferriero DM, Vanucci SJ, Levison SW, Vexler ZS, et al. The role of inflammation in perinatal brain injury. *Nat Rev Neurol*. 2015;11(4):192–208.
- 80 Haynes RL, Folkert RD, Keefe RJ, Sung I, Swzeda LI, Rosenberg PA, et al. Nitrosative and oxidative injury to premyelinating oligodendrocytes in periventricular leukomalacia. *J Neuropathol Exp Neurol*. 2003;62(5):441–50.
- 81 Fouron JC, Gosselin J, Amiel-Tison C, Infante-Rivard C, Fouron C, Skoll A, et al. Correlation between prenatal velocity waveforms in the aortic isthmus and neurodevelopmental outcome between the ages of 2 and 4 years. *Am J Obstet Gynecol*. 2001;184(4):630–6.
- 82 Nuijtinck RR, Baker RE, Ter Gast E, Struik ML, Mud MT. Glutamate dependent dendritic outgrowth in developing neuronal networks of rat hippocampal cells in vitro. *Int J Dev Neurosci*. 1997;15(1):55–60.
- 83 Nishizawa Y. Glutamate release and neuronal damage in ischemia. *Life Sci*. 2001;69(4):369–81.
- 84 Kokaia Z, Nawa H, Uchino H, Elmér E, Kokaia M, Carnahan J, et al. Regional brain-derived neurotrophic factor mRNA and protein levels following transient forebrain ischemia in the rat. *Brain Res Mol Brain Res*. 1996;38(1):139–44.
- 85 Lindvall O, Ernfors P, Bengzon J, Kokaia Z, Smith ML, Siesjö BK, et al. Differential regulation of mRNAs for nerve growth factor, brain-derived neurotrophic factor, and neurotrophin 3 in the adult rat brain following cerebral ischemia and hypoglycemic coma. *Proc Natl Acad Sci U S A*. 1992;89(2):648–52.

## 4.2 Rabbit neurospheres as a novel in vitro tool for studying neurodevelopmental effects induced by intrauterine growth restriction

Marta Barenys <sup>1,2</sup>, Miriam Illa <sup>3</sup>, Maxi Hofrichter <sup>1</sup>, Carla Loreiro <sup>3</sup>, Laura Pla <sup>3</sup>, Jördis Klose <sup>1</sup>, **Britta Anna Kühne** <sup>2,3</sup>, Jesús Gómez-Catalán <sup>2</sup>, Jan Matthias Braun <sup>1</sup>, Fatima Crispi <sup>3</sup>, Eduard Gratacós <sup>3</sup>, Ellen Fritsche <sup>1</sup>

<sup>1</sup>IUF—Leibniz Research Institute for Environmental Medicine, Düsseldorf, Germany

<sup>2</sup>GRET, INSA-UB and Toxicology Unit, Pharmacology, Toxicology and Therapeutical Chemistry Department, Faculty of Pharmacy, University of Barcelona, Barcelona, Spain

<sup>3</sup>BCNatal-Barcelona Center for Maternal-Fetal and Neonatal Medicine (Hospital Clínic and Hospital Sant Joan de Déu), Fetal i+D Fetal Medicine Research Center, IDIBAPS, University of Barcelona, Center for Biomedical Research on Rare Diseases (CIBER-ER), Barcelona, Spain

|                       |   |
|-----------------------|---|
| Journal               | Stem Cell Translational Medicine  |
| Impact Factor 2020    | 6.940 [OA]  |
| Quartile              | Q1 in Cell and tissue engineering   |
| Type of authorship    | Co-author   |
| Status of publication | Published: Stem Cells Transl Med 10 (2021 Feb) 209-221.<br>DOI: 10.1002/sctm.20-0223. |

## Summary

The aim of this study was to develop a rabbit neurosphere culture to characterize differences in basic processes of neurogenesis induced by intrauterine growth restriction (IUGR). A novel *in vitro* neurosphere culture has been established using fresh or frozen neural progenitor cells from newborn (PND0) rabbit brains. After surgical IUGR induction in pregnant rabbits and cesarean section 5 days later, neural progenitor cells from both control and IUGR groups were isolated and directly cultured or frozen at  $-80^{\circ}\text{C}$ . These neural progenitor cells spontaneously formed neurospheres after 7 days in culture. The ability of control and IUGR neurospheres to migrate, proliferate, differentiate to neurons, astrocytes, or oligodendrocytes was compared and the possibility to modulate their responses was tested by exposure to several positive and negative controls. Neurospheres obtained from IUGR brains have a significant impairment in oligodendrocyte differentiation, whereas no significant differences are observed in other basic processes of neurogenesis. This impairment can be reverted by *in vitro* exposure of IUGR neurospheres to thyroid hormone, which is known to play an essential role in white matter maturation *in vivo*. Our new rabbit neurosphere model and the results of this study open the possibility to test several substances *in vitro* as neuroprotective candidates against IUGR induced neurodevelopmental damage while decreasing the number of animals and resources and allowing a more mechanistic approach at a cellular functional level.



# Rabbit neurospheres as a novel in vitro tool for studying neurodevelopmental effects induced by intrauterine growth restriction

Marta Barenys<sup>1,2</sup> | Miriam Illa<sup>3</sup> | Maxi Hofrichter<sup>1</sup> | Carla Loreiro<sup>3</sup> |  
Laura Pla<sup>3</sup> | Jördis Klose<sup>1</sup> | Britta Anna Kühne<sup>2,3</sup> | Jesús Gómez-Catalán<sup>2</sup> |  
Jan Matthias Braun<sup>1</sup> | Fatima Crispi<sup>3</sup> | Eduard Gratacós<sup>3</sup> | Ellen Fritsche<sup>1</sup>

<sup>1</sup>IUF—Leibniz Research Institute for Environmental Medicine, Düsseldorf, Germany

<sup>2</sup>GRET, INSA-UB and Toxicology Unit, Pharmacology, Toxicology and Therapeutical Chemistry Department, Faculty of Pharmacy, University of Barcelona, Barcelona, Spain

<sup>3</sup>BCNatal-Barcelona Center for Maternal-Fetal and Neonatal Medicine (Hospital Clínic and Hospital Sant Joan de Déu), Fetal i+D Fetal Medicine Research Center, IDIBAPS, University of Barcelona, Center for Biomedical Research on Rare Diseases (CIBER-ER), Barcelona, Spain

## Correspondence

Marta Barenys, PhD, GRET, INSA-UB and Toxicology Unit, Pharmacology, Toxicology and Therapeutical Chemistry Department, Faculty of Pharmacy, University of Barcelona, Av. Joan XXIII, 27-31, 08028 Barcelona, Spain. Email: mbarneys@ub.edu

## Funding information

Health Department of the Catalan Government, Grant/Award Number: SLT006/17/00325; Fundació Bosch i Gimpera, Grant/Award Number: 300155; AGAUR, Grant/Award Number: 2017 SGR n° 1531; "LaCaixa" Foundation, Grant/Award Numbers: LCF/PR/GN18/10310003, LCF/PR/GN14/10270005; European Regional Development Fund/European Social Fund; Instituto de Salud Carlos III, Grant/Award Number: PI18/01763

## Abstract

The aim of this study was to develop a rabbit neurosphere culture to characterize differences in basic processes of neurogenesis induced by intrauterine growth restriction (IUGR). A novel in vitro neurosphere culture has been established using fresh or frozen neural progenitor cells from newborn (PND0) rabbit brains. After surgical IUGR induction in pregnant rabbits and cesarean section 5 days later, neural progenitor cells from both control and IUGR groups were isolated and directly cultured or frozen at  $-80^{\circ}\text{C}$ . These neural progenitor cells spontaneously formed neurospheres after 7 days in culture. The ability of control and IUGR neurospheres to migrate, proliferate, differentiate to neurons, astrocytes, or oligodendrocytes was compared and the possibility to modulate their responses was tested by exposure to several positive and negative controls. Neurospheres obtained from IUGR brains have a significant impairment in oligodendrocyte differentiation, whereas no significant differences are observed in other basic processes of neurogenesis. This impairment can be reverted by in vitro exposure of IUGR neurospheres to thyroid hormone, which is known to play an essential role in white matter maturation in vivo. Our new rabbit neurosphere model and the results of this study open the possibility to test several substances in vitro as neuroprotective candidates against IUGR induced neurodevelopmental damage while decreasing the number of animals and resources and allowing a more mechanistic approach at a cellular functional level.

## KEYWORDS

cell culture, differentiation, experimental models, growth inhibition, nervous system, oligodendrocytes, progenitor cells

This is an open access article under the terms of the Creative Commons Attribution-NonCommercial License, which permits use, distribution and reproduction in any medium, provided the original work is properly cited and is not used for commercial purposes.

© 2020 The Authors. STEM CELLS TRANSLATIONAL MEDICINE published by Wiley Periodicals LLC on behalf of AlphaMed Press.



## 1 | INTRODUCTION

Intrauterine growth restriction (IUGR) is defined as a significant reduction of the fetal growth rate leading to a birth weight below the 10th centile for the corresponding gestational age.<sup>1</sup> The prevalence in developing countries accounts for 5% to 10% of all pregnancies, being a global health issue that is associated to short- and long-term neurodevelopmental damage, cognitive dysfunctions and cardiovascular adverse outcomes.<sup>2,3</sup> Placental insufficiency, the primary cause of IUGR, reduces the quantity of nutrients reaching the fetus and leads to fetal development under chronic hypoxia followed by fetal acidosis. Placental insufficiency affects up to 7% of all gestations<sup>4,5</sup> and in approximately 50% of these cases it derives in clinically evident middle and long-term neurological consequences defined as subtle cognitive and behavioral disabilities.<sup>6-9</sup> Different animal models and advanced imaging techniques have been used to better understand the mechanisms underlying neuronal impairments and perinatal brain maturation alterations induced by IUGR.<sup>10</sup> However, there is still a large knowledge gap on the mechanisms underlying these alterations<sup>2</sup> and a lack of research models to better characterize the IUGR-associated brain injury (reviewed by Fleiss et al. 2019<sup>11</sup>).

In order to have a human-relevant experimental model of neurodevelopmental damage induced by IUGR, the BCNatal research group developed an IUGR model in pregnant rabbits.<sup>12</sup> This animal model reproduces the neurodevelopmental manifestations of IUGR occurring in clinical cases, including postnatal functional and structural deficits.<sup>12,13</sup> The selection of the rabbit species was based on the higher similarity to humans in terms of placentation and gestational circulatory changes,<sup>12,14</sup> as well as the resemblance regarding white matter maturation, which in both species happens during the postnatal period.<sup>13,15,16</sup> According to the model developed by Workman et al.,<sup>16</sup> to predict the “precocial score” for neurodevelopment, rabbit species presents a precocial score at birth (0.537) more similar to humans (0.654) than other species, including rats (0.445) or mice (0.408). Likewise, at the neonatal period, diffusion MRI in whole organ preparations from a rabbit model showed differences on diffusion related parameters either at gray and white matter, revealing a pattern of microstructural brain changes produced by IUGR already at birth.<sup>13</sup> Interestingly, decreased fractional anisotropy in white matter structures has been suggested to reflect oligodendrocyte injury,<sup>17,18</sup> whereas in the gray matter areas it seems to reflect changes in neuronal arborisation.<sup>19</sup> Furthermore, follow-up studies of IUGR rabbits have unraveled changes in their cerebral connections,<sup>3,20</sup> which correlate very well with the clinical observation that IUGR-affected children also present cerebral connection alterations in connectomic-studies.<sup>21</sup> Linking this clinical adverse outcome with the neurodevelopmental alterations observed in rabbits gives evidence that the rabbit IUGR model is a good model to study IUGR-induced structural changes in humans.<sup>12,22,23</sup>

However, in this *in vivo* model, it is difficult to identify the origin of the functional and structural deficits induced by IUGR, and so far, it was not possible to understand which basic cellular processes are altered during brain development under IUGR. To solve this limitation, we established an *in vitro* model based on primary rabbit neuronal progenitor cells (NPCs) allowing the investigation of the basic

### Significance statement

Our research describes for the first time a valuable method for generation of 3D rabbit neurospheres that can be differentiated to neurons, astrocytes and oligodendrocytes. Such method is applied for modeling the neurodevelopmental effects of intrauterine growth restriction (IUGR), for toxicity testing and for efficacy testing of possible new pharmaceuticals. We have found differences in basic processes of neurogenesis induced by IUGR, we have shown that neurospheres obtained from IUGR brains have a significant impairment in oligodendrocyte differentiation and we have demonstrated that this impairment can be reverted by *in vitro* exposure of IUGR neurospheres to thyroid hormone.

neurodevelopmental processes affected by IUGR. In this model, rabbit NPCs obtained from control and IUGR pups are cultured as three-dimensional (3D) cell aggregates called neurospheres. Neurosphere cultures from other species have previously been established and have been utilized for mimicking basic processes of fetal brain development like NPC proliferation, migration and differentiation into neurons, oligodendrocytes and astrocytes.<sup>24-29</sup> In this study, for the very first time, a rabbit neurosphere culture was developed and characterized. In addition, we successfully developed a freezing and thawing protocol, which allows storing and prolonging the use of rabbit NPCs obtained from one litter and enables interlaboratory transfer of material. The ability to freeze and thaw rabbit neurospheres reduces the number of animals used and is thus much more time- and cost-efficient. Due to the multicellular nature of the neurosphere method and the possibility to study a variety of neurodevelopmental processes with it, neurospheres are a valuable test system for studying a plethora of cellular effects initiated by a variety of different modulators.<sup>24,28,30-33</sup> Therefore, they seemed well suited for characterizing so far unknown neurodevelopmental effects on the cellular level induced by IUGR. With this method, we identified that rabbit NPCs derived from IUGR pups have a significant impairment in oligodendrocyte differentiation. Moreover, we discovered that exposure to thyroid hormone L-triiodothyronine (T3) can revert this significant impairment unraveling a possible future therapeutic strategy. This new method thus opens the door to easy and cost-efficient testing of possible neuroprotective therapies for IUGR.

## 2 | MATERIAL AND METHODS

### 2.1 | Rabbit neurospheres generation

Rabbit tissue obtention for this study was approved by the Ethic Committee for Animal Experimentation of the University of Barcelona. Protocols were accepted with the license number: OB 392/19 SJD. Rabbit neural progenitor cells were isolated from nine newborn

postnatal day (PND) 0 or 1 New Zealand rabbits whole brains by dissection, mechanical dissociation, digestion (20 minutes incubation with papain 20 U/mL at 37°C), mechanical homogenization into a cell suspension, and centrifugation (5 minutes at 800 rpm). The cell pellet obtained was cultured as a cell suspension for 1 week at 37°C and 7.5% CO<sub>2</sub> in polyhydroxyethylmethacrylate (Poly-HEMA) coated dishes with “proliferation medium” [consisting in DMEM and Hams F12 3:1 supplemented with 2% B27, and 20 ng/mL epidermal growth factor (EGF) and recombinant human fibroblast growth factor (FGF), 100 U/mL penicillin and 100 µg/mL streptomycin], half volume of which was exchanged every 2 to 3 days.

## 2.2 | Neurospheres freezing and thawing protocol

During the neural progenitor cells isolation from 8 out of the 9 whole rabbit pup brains described above, half of the volume of the cell suspension obtained after resuspension in proliferation medium was centrifuged again (5 minutes at 800 rpm), the supernatant discarded and the pellet gently resuspended in freezing media instead (1:1; volume of pellet: volume of “freezing medium” [consisting in 70% (v/v) proliferation medium, 20% (v/v) fetal calf serum, and 10% (v/v) dimethyl sulfoxide (DMSO)]). Cell suspension in freezing medium was distributed in 1 mL per cryo-vial and immediately placed in a cryo-device filled with propanol to ensure a freezing rate of  $-1^{\circ}\text{C}/\text{min}$ , and stored at  $-80^{\circ}\text{C}$ .

Each cryo-vial was thawed approximately 1 month after freezing by brief immersion in a 37°C water bath, transference of cells to 15 mL of “proliferation medium” preconditioned at 37°C and 7.5% CO<sub>2</sub> for 2 hours, and gentle resuspension. Cell suspension was centrifuged (5 minutes, 800 rpm), supernatant discarded and cells transferred to Poly-HEMA coated dishes filled with “proliferation medium” supplemented with Rho kinase (ROCK) inhibitor Y-276322 at a final concentration of 10 µM, to enhance recovery and growth of cryopreserved cells.<sup>34</sup> Half of the volume of “proliferation medium” per petri dish was exchanged every 2 to 3 days by “proliferation medium” without ROCK inhibitor.

## 2.3 | Rabbit “Neurosphere Assay”

Fresh or thawed neurospheres formed in the “proliferation medium” culture, were mechanically passaged before starting experiments with a chopper to 0.2 mm<sup>2</sup> squares to ensure homogeneous neurosphere size, and allowed to recover spherical shape in “proliferation medium” in Poly-HEMA coated dishes. On the experiment plating day (considered experiment day 0), 0.3 mm diameter neurospheres were selected and plated in one of the following conditions depending on the assay to perform.

### 2.3.1 | Proliferation assay

One neurosphere per well was plated in 96 well-round bottom-plates coated with Poly-HEMA and filled with 100 µL of “proliferation

medium.” Plate was cultured at 37°C and 7.5% CO<sub>2</sub> for 7 days. One bright-field picture per neurosphere was taken on days 0, 2, 4, 6, and 7. Every 2 days, 50 µL of “proliferation medium” per well were renewed. Neurosphere diameter was measured in each picture with ImageJ.

### 2.3.2 | Migration assays

Five neurospheres per chamber were plated in PDL/Laminin coated 8-chamber slides filled with 500 µL of “differentiation medium” [consisting in DMEM and Hams F12 3:1 supplemented with N2 (Invitrogen), penicillin and streptomycin (100 U/mL and 100 µg/mL)]. After 1 and 3 days of culture, bright-field pictures were taken to monitor migration progression by measuring the distance from the neurosphere core to the furthest migrated cells in four points per neurosphere using ImageJ.

### 2.3.3 | Neuronal differentiation assay

At day 3, after taking pictures for migration, neurospheres were fixed with paraformaldehyde (PFA) 4% (1 hour, 37°C), washed twice with phosphate-buffered saline (PBS) and stored in PBS until immunostained. For immunostaining, slides were incubated at room temperature with a blocking solution with 10% goat serum in PBS-T (PBS containing 0.1% Triton X-100) for 5 minutes. Neurospheres were incubated with a primary antibody solution containing 10% goat serum and 1:100 rabbit IgG anti-βIII-tubulin antibody in PBS-T for 1 hour at 37°C. After three washing steps with PBS, slides were incubated with secondary antibody solution containing 2% goat serum, 1:100 Hoechst 33258 and 1:200 Alexa 546 anti-rabbit IgG in PBS for 30 minutes at 37°C. After three washing steps with PBS and one with distilled water, slides were mounted with Acqua Poly/Mount (Polysciences, Inc.) and stored at 4°C until image acquisition. After immunostaining, 200× fluorescent images of two extracts of the migration area were taken per sphere in five spheres per condition in at least three independent experiments. The percentage of βIII-tubulin positive cells was quantified manually using ImageJ software<sup>34</sup> cell count tool.

### 2.3.4 | Astrocyte immunostaining

To immunostain astrocytes, the same protocol used to immunostain neurons was applied but the primary antibody solution contained 10% goat serum and 1:100 rabbit IgG anti GFAP antibody in PBS and the secondary antibody solution contained 2% goat serum, 1:100 Hoechst 33258, and 1:200 Alexa 546 anti-rabbit IgG in PBS 1:200.

### 2.3.5 | Oligodendrocyte differentiation assay

Five neurospheres per chamber were plated following the same procedure described for the migration assay. After 5 days of culture,

neurospheres were fixed (4% PFA, 1 hour, 37°C) washed twice with PBS and stored in PBS until immunostained. Slides were incubated with a primary antibody solution containing 10% goat serum, 1:200 mouse IgM anti-O4 antibody in PBS for 1 hour at 37°C. After three washing steps with PBS, slides were incubated with secondary antibody solution containing 2% goat serum, 1:100 Hoechst 33258, and 1:200 Alexa 488 anti-mouse IgM in PBS for 30 minutes at 37°C. After three washing steps with PBS and one with distilled water, slides were mounted with Acqua Poly/Mount (Polysciences, Inc.) and stored at 4°C until image acquisition. After immunostaining, 200× fluorescent images of two extracts of the migration area were taken per sphere in five spheres per condition in at least three independent experiments. The percentage of O4 positive cells was quantified manually using ImageJ software<sup>35</sup> cell count tool.

### 2.3.6 | Viability assay

At the end of migration/neuronal differentiation and oligodendrocyte differentiation assays (on days 3 and 5, respectively), and prior to fixation, a viability assay was performed by removing 200  $\mu$ L medium per chamber, adding 100  $\mu$ L of CellTiter-Blue Reagent (Promega) diluted 1:3 (v/v) in "differentiation medium" per chamber and incubating for 2 hours at 37°C and 7.5% CO<sub>2</sub> to measure the metabolic activity of the culture. Fluorescence of the supernatant was measured at 544/590 nm in two replicates of 100  $\mu$ L per chamber transferred to two wells of a 96 well-plate and expressed as relative fluorescence units.

## 2.4 | IUGR induction in rabbits

Animal experimentation of this study was approved by the Ethic Committee for Animal Experimentation of the University of Barcelona. Protocols were accepted by the Department of Environment and Housing of the Generalitat de Catalunya with the license number: 03/17. New Zealand pregnant rabbits provided by a certified breeder were housed in separate cages with a 12/12 hours light/dark cycle, with free access to water and standard chow.

After at least 72 hours of acclimatization, IUGR was surgically induced following a previously described technique in four pregnant rabbits at 25 days of gestation.<sup>12</sup> Briefly, 40% to 50% of uteroplacental vessels that irrigate each gestational sac of one uterine horn (left or right randomly selected) were ligated obtaining the IUGR fetuses, while non-ligated gestational sacs from the contralateral horn provided normally-grown fetuses (controls). Postoperative analgesia with Buprenorphine 0.05 mg/kg was administered subcutaneously and animals were again housed with free access to water and standard chow ad libitum and were monitored daily for general health. Cesarean section was performed at 30 days of gestation. All living PND0 pups were identified and classified in control or IUGR groups depending on the uterine horn, weighted and sacrificed. Brains were immediately dissected and neural progenitor cells obtained as described in the "rabbit neurosphere generation" section.

All neural progenitor cells obtained from control and IUGR siblings were frozen at  $-80^{\circ}\text{C}$  and thawed in parallel before performing any Neurosphere Assay.

## 2.5 | Inclusion criteria of IUGR PND0 rabbit pups

Strong IUGR cases are defined by a body weight lower than the 10th percentile (32.7 g; Table 1). To cover a broad range of IUGR cases, neurospheres were prepared from mild and strong IUGR pups. In this study, IUGR rabbit pups were included for neurosphere preparation if their body weight was lower than the 90th percentile (57.8 g).

## 2.6 | Statistics

Statistical analysis was performed using GraphPad Prism v6 and v7 (GraphPad Software, La Jolla, California). Concentration-dependent effects were assessed performing a one-way ANOVA analysis followed by Bonferroni post hoc test for multiple comparisons. Comparisons of two groups were performed with two-tailed *t* test. Significance threshold was established at  $P < .05$ .

# 3 | RESULTS

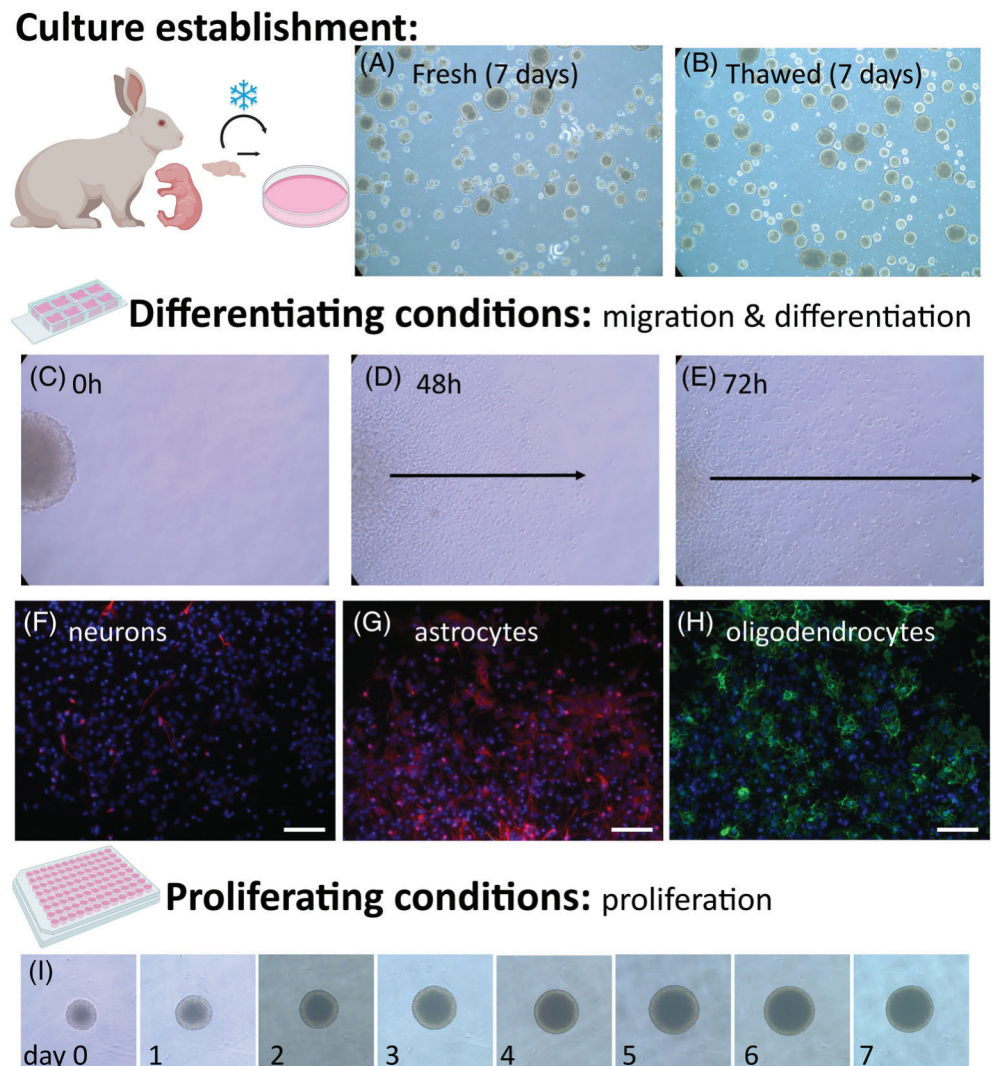
## 3.1 | Establishment of a rabbit neurosphere model

To establish a rabbit developmental neurosphere model, we first started isolating NPCs from control rabbit PND0 or PND1 brains, testing their ability to spontaneously form neurospheres and evaluating the competence of these freshly formed neurospheres to perform basic processes of neurogenesis like proliferation, migration, and differentiation. Freshly isolated rabbit NPCs spontaneously formed recognizable floating neurospheres after 4 days in culture, kept proliferating further and were big enough to be mechanically passaged (chopped) after 7 days in culture (Figure 1). Chopped neurospheres were used to start the "Neurosphere Assay" in control conditions, always compared to a positive control condition which was specific for each endpoint tested (endpoint-specific control known to alter the measured variable): the src-kinase inhibitor PP2 for migration, Epidermal Growth Factor (EGF) for neuronal differentiation and viability, bone morphogenic protein 7 (BMP7) for oligodendrocyte differentiation and withdrawal of all growth factors for proliferation. Freshly prepared rabbit NPCs growing as neurospheres migrated (mean  $\pm$  SEM =  $806 \pm 29 \mu\text{m}$ , Figure 2) and proliferated (mean  $\pm$  SEM =  $18 \pm 2 \mu\text{m}/\text{day}$ , Figure 2) in culture. Among cells in the migration area, we identified cells differentiating to astrocytes (GFAP<sup>+</sup> cells), to oligodendrocytes (O4<sup>+</sup> cells) and to neurons ( $\beta$ III-tubulin<sup>+</sup> cells) (Figure 1). We also quantified the percentage of migrating cells differentiating to O4<sup>+</sup> cells after 5 days (mean  $\pm$  SEM =  $12 \pm 1\%$ , Figure 2) and to  $\beta$ III-tubulin<sup>+</sup> cells after 3 days (mean  $\pm$  SEM =  $3 \pm 1$ , Figure 2). For all endpoints, results

**TABLE 1** Percentile and body weight of rabbit pups on day PND0

| Percentile           | 5    | 10   | 25   | 50   | 75   | 90   | 95   |
|----------------------|------|------|------|------|------|------|------|
| PND0 body weight (g) | 29.5 | 32.7 | 39.7 | 46.3 | 52.2 | 57.8 | 62.1 |

**FIGURE 1** Graphical summary of the rabbit “Neurosphere Assay.” Culture establishment: PND0 rabbit brains are dissected and either frozen or directly cultured until neurosphere formation (A, 7 days in culture after dissection; B, 7 days in culture after thawing). “Neurosphere Assay” starts when neurospheres of a diameter of 300  $\mu\text{m}$  are plated in 8-chamber slides and maintained under differentiating conditions to evaluate migration (C, 0 hours; D, 48 hours; E, 72 hours after plating) and differentiation into neurons (F, 72 hours after plating,  $\beta$ III-tubulin in red and Hoechst 33258 in blue), into astrocytes (G, 72 hours after plating, GFAP in red and Hoechst 33258 in blue) or into oligodendrocytes (H, 120 hours after plating, O4 in green and Hoechst 33258 in blue). Scale bars = 100  $\mu\text{m}$ . Neurospheres were also plated in 96-well plates under proliferating conditions and evaluated for diameter increase up to 7 days (I, representative image of a proliferating neurosphere from day 0 to day 7)



obtained with rabbit neurospheres allowed to observe alterations of the endpoint in both directions, positive and negative as recommended for the development of new alternative methods.<sup>36</sup> Besides, all positive controls included to each endpoint and tested in parallel to control, proved to be able to significantly modify the response obtained similar to human NPCs, indicating that the system is dynamic and can be influenced by known substances interfering with neurogenic processes. However, neuronal differentiation was relatively low compared to the values established for other species (human neurospheres = 5%<sup>37</sup>). Therefore, other culture conditions were tested, mainly the addition of fetal calf serum (FCS) either in differentiation medium or in both proliferation and differentiation medium (Figure 2). Both conditions led to an increased percentage of cells differentiating into neurons and exceeding 5% of differentiation. The longer the cells were exposed to FCS, the higher the percentage of neurons was (Figure 2).

After establishing all endpoints of the “Neurosphere Assay” for fresh neurospheres, a freezing protocol was tested, either after first passaging of neurospheres (passage 1) or directly after isolation of neural progenitor cells from rabbit brain (passage 0).

When the freezing protocol was applied after the first passaging of neurospheres (passage 1), NPCs lost their capabilities to develop in all endpoints of the “Neurosphere Assay” (mainly due to too low neuronal differentiation and too low proliferation; see Supporting Information Figure S1), and therefore, this option was directly discarded. Nevertheless, the application of the freezing protocol on freshly isolated NPCs, before the formation of neurospheres (passage 0), led to results in the “Neurosphere Assay” comparable to fresh neurospheres (see Material and methods section for more details about freezing and thawing protocol). Thawed NPCs spontaneously formed recognizable neurospheres after 4 days in vitro and were big enough to be chopped after 7 days in vitro (Figure 1). Results of proliferation, migration and

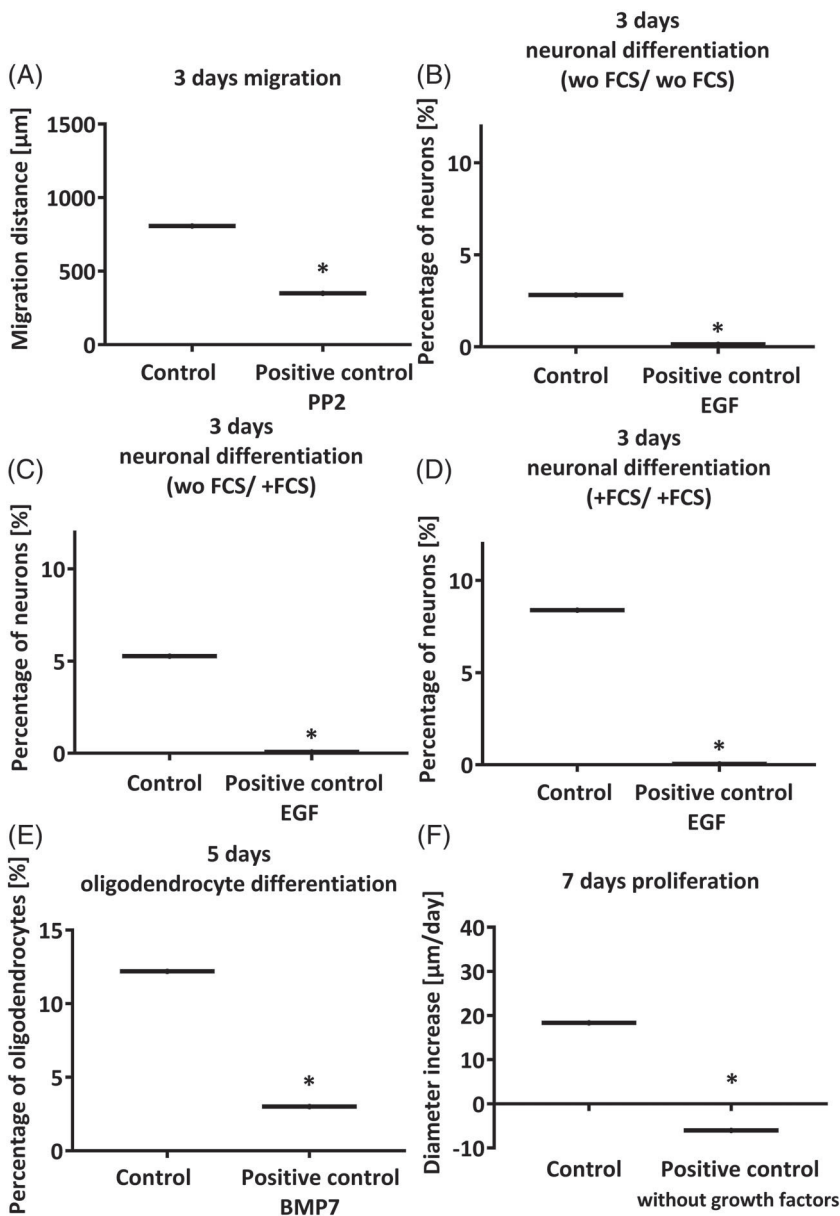


**FIGURE 2** Results of the “Neurosphere Assay” establishment with freshly prepared rabbit neurospheres. Rabbit neurospheres were cultured for 3, 5, or 7 days under control or specific positive control conditions for each endpoint tested (PP2 10  $\mu\text{M}$ ; EGF 10 ng/mL; BMP7 100 ng/mL). A, 3 days migration; B, 3 days neuronal differentiation without supplementary FCS in the medium (wo FCS/wo FCS); C, 3 days neuronal differentiation with addition of 1% FCS in the differentiation medium (wo FCS/+FCS); D, 3 days neuronal differentiation with addition of 1% FCS in the proliferation and differentiation medium (+FCS/+FCS); E, 5 days oligodendrocyte differentiation; F, 7 days proliferation. All endpoints were evaluated in five neurospheres/condition in at least three independent experiments. Results presented as boxes and whiskers according to Tukey method. \* $P < .05$  vs control

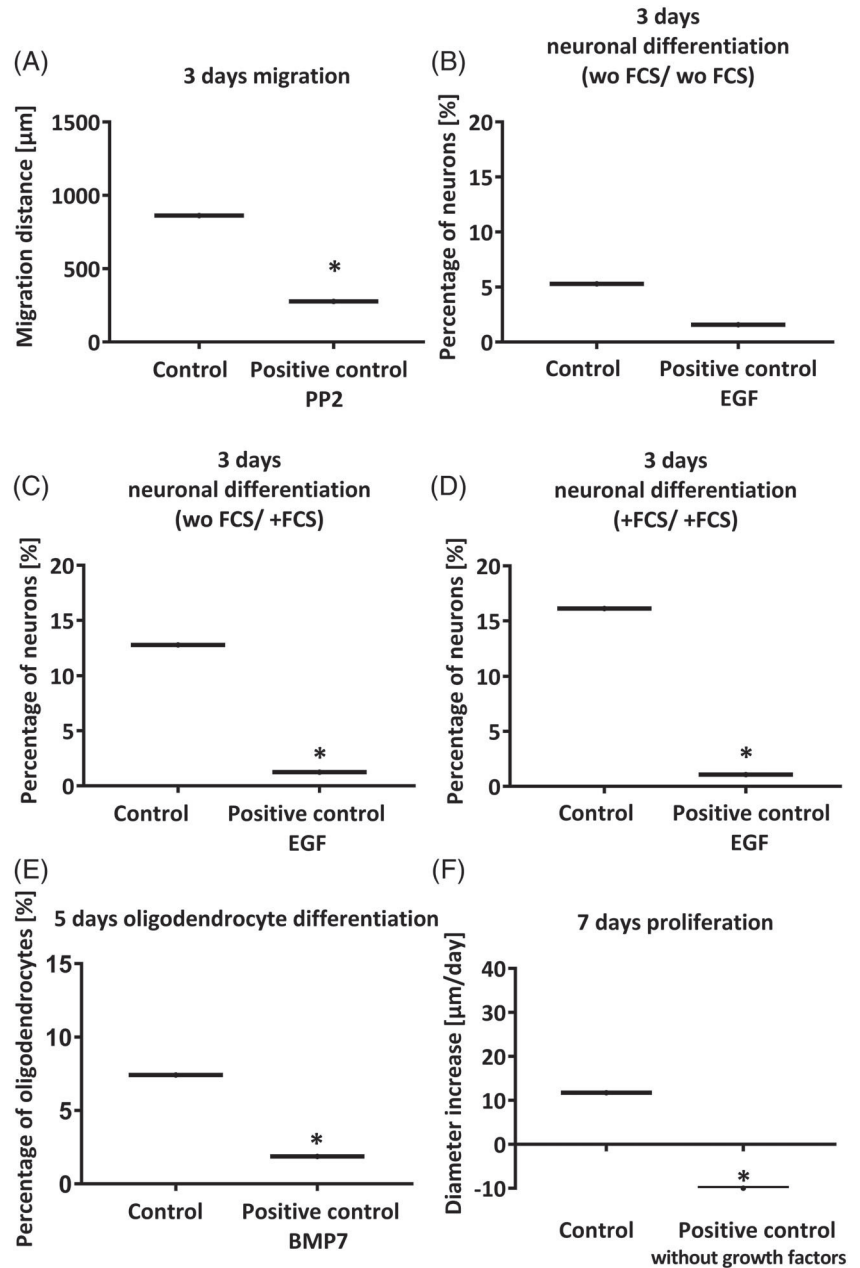
differentiation assays met quality criteria as shown in Figure 3. Interestingly, thawed neurospheres also achieved a 5% mean differentiation to neurons without adding any FCS to the differentiation or proliferation medium, probably because the freezing medium already contained FCS. Even so, as previously assayed with fresh spheres, FCS addition to differentiation and/or proliferating medium was also tested. In this case, FCS addition also induced an increase in neuronal differentiation, and as previously observed for fresh neurospheres, the longer the cells were exposed to FCS, the higher the percentage of neurons was. However, in this case, the percentage of neurons was so high in some wells (Figure 3; mean > 15%) that neurons were growing in clumps and overlapping one another making it very difficult to correctly quantify them. As thawed neurospheres without FCS addition in culture produced a percentage of neurons that could be precisely quantified, and also with the aim to not introduce more factors to the medium which could mask adverse effects induced by

physical or chemical agents in future tests, this culture condition (without FCS) was chosen for further experiments.

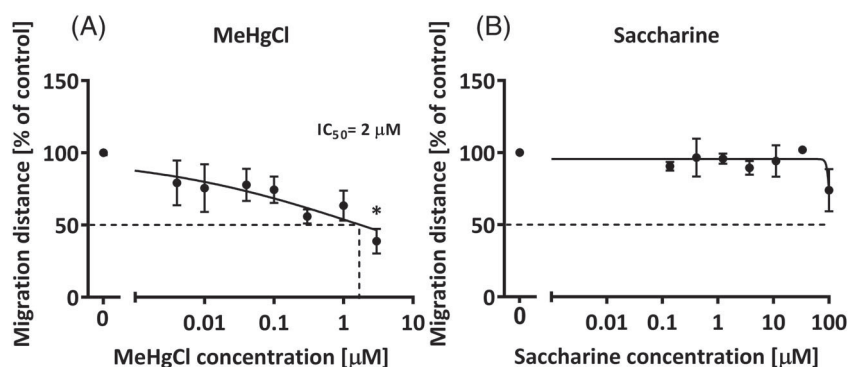
Thawed neurospheres were also tested in parallel in control and positive control conditions, using the same compounds than for fresh neurospheres. In all cases, positive controls decreased the result obtained in control conditions. In view of these results, all further experiments were performed with neurospheres submitted to the freezing protocol at passage 0.

To prove that rabbit neurospheres are able to detect alterations induced during the course of neurodevelopment without being oversensitive, we exposed them to two compounds in a concentration-range mode, a positive and a negative control, following the recommendations of Crofton et al.<sup>36</sup> One is a known neurodevelopmental toxicant in humans and animals, methylmercury chloride (MeHgCl; positive control) and the other one a compound known to have no effects on neurodevelopment in humans and animals, saccharine

**FIGURE 3** Results of the “Neurosphere Assay” establishment with thawed rabbit neurospheres. Thawed rabbit neurospheres were cultured for 3, 5, or 7 days under control conditions or exposed to specific positive controls for each endpoint tested (PP2 10  $\mu$ M; EGF 10 ng/mL; BMP7 100 ng/mL). A, 3 days migration; B, 3 days neuronal differentiation without supplementary FCS in the medium (wo FCS/wo FCS); C, 3 days neuronal differentiation with addition of 1% FCS in the differentiation medium (wo FCS/+FCS); D, 3 days neuronal differentiation with addition of 1% FCS in the proliferation and differentiation medium (+FCS/+FCS); E, 5 days oligodendrocyte differentiation; F, 7 days proliferation. All endpoints were evaluated in five neurospheres/condition in at least three independent experiments. Results presented as boxes and whiskers according to Tukey method. \* $P < .05$  vs control



**FIGURE 4** Rabbit neurospheres sensitivity and specificity evaluation. Thawed rabbit neurospheres were cultured for 1 day with increasing concentrations of the known neurodevelopmental toxicant: MeHgCl, A, or a compound known to have no neurodevelopmental adverse effects: Saccharine, B. Results presented as mean  $\pm$  SEM of at least three independent experiments including five neurospheres/concentration and analyzed by ANOVA and Bonferroni post hoc test. \* $P < .05$  vs control



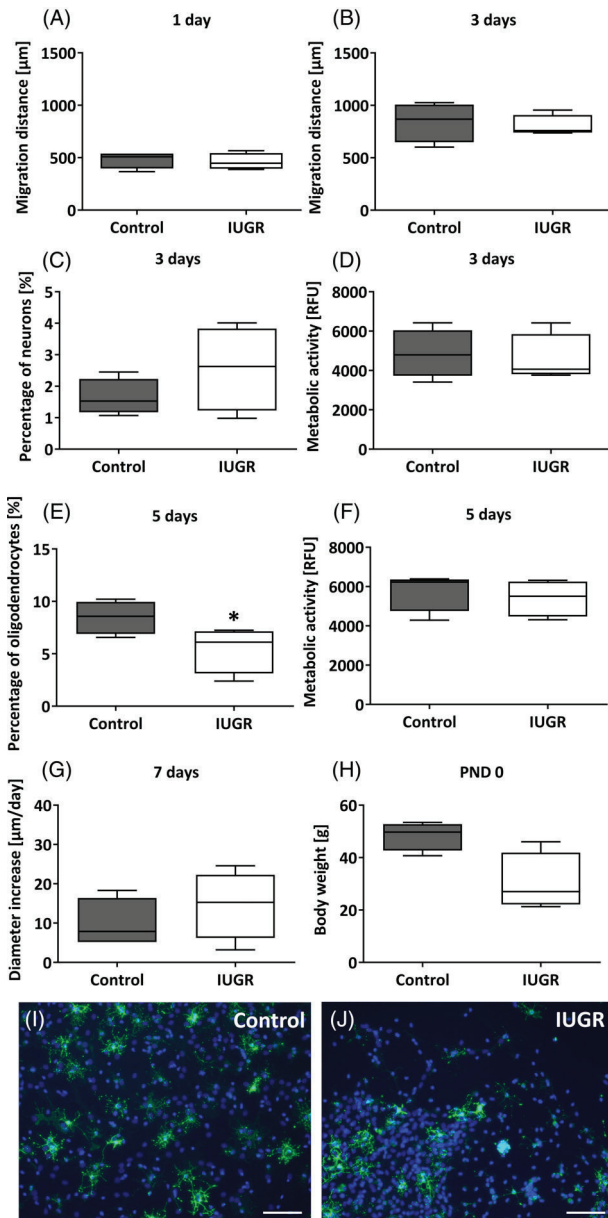


**FIGURE 5** Comparison of control and IUGR neurospheres on basic processes of neurogenesis. Thawed rabbit neurospheres obtained from control and IUGR animals were cultured for 3, 5, or 7 days and comparatively tested for each endpoint of the “Neurosphere Assay.” A, Migration distance after 1 day; or B, 3 days; C, neuronal differentiation after 3 days; D, metabolic activity after 3 days; E, oligodendrocyte differentiation after 5 days; F, metabolic activity after 5 days; G, diameter increase after 7 days; H, body weight of control and IUGR pups on PND0; I and J, representative pictures of oligodendrocyte differentiation in control and IUGR neurospheres, respectively. Scale bars = 100  $\mu\text{m}$ . All endpoints (except body weight, H) were evaluated in five neurospheres/condition in at least three independent experiments. Results presented as boxes and whiskers according to Tukey method. \* $P < .05$  IUGR vs control

(negative control; reviewed by Aschner et al.<sup>38</sup>). MeHgCl induced a significant and concentration-dependent decrease in neural progenitor cell migration, with an  $\text{IC}_{50}$  of 2  $\mu\text{M}$  (Figure 4), while saccharine did

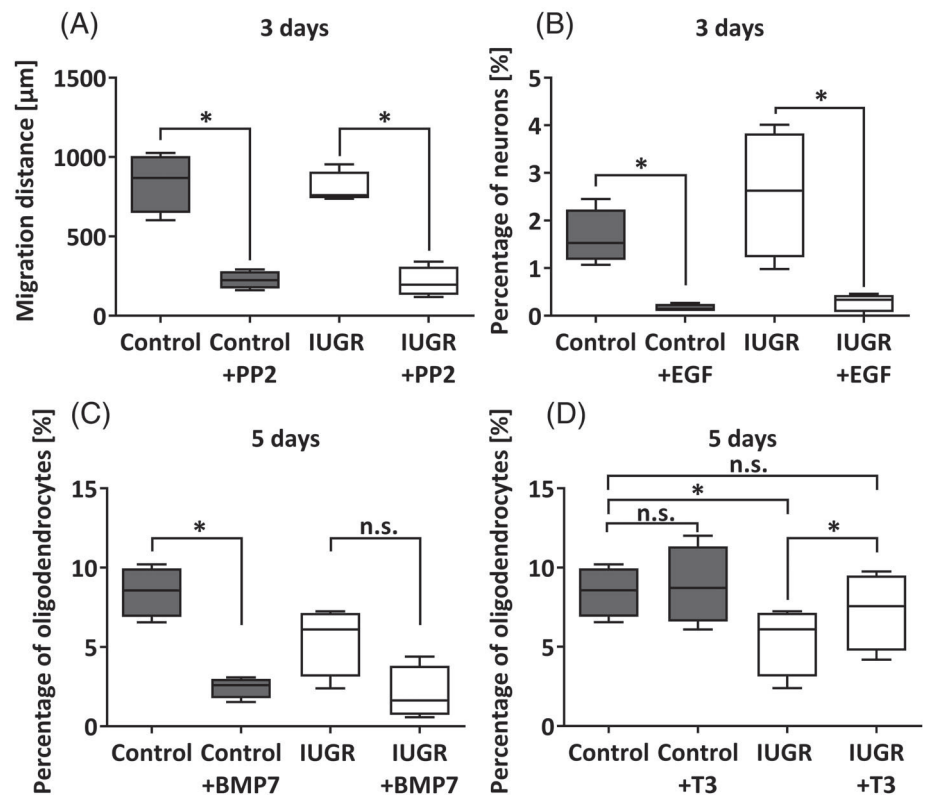
not significantly decrease migration at any concentration tested (maximum concentration tested = 100  $\mu\text{M}$ ).

### 3.2 | Evaluation of the effects of IUGR in neurodevelopmental processes

The aim of establishing a rabbit neurosphere culture was to develop a model to study the effects of IUGR on brain development in a more time- and cost-efficient way with using fewer numbers of animals. Therefore, we used the rabbit “Neurosphere Assay” to investigate the specific consequences of IUGR induction by ligation of 40% to 50% of uteroplacental vessels irrigating the gestational sac between GD25 and GD30. Neurospheres from four control and four IUGR pups with mean birth weight  $\pm$  SEM = 48.4  $\pm$  1.4 g and 30.3  $\pm$  2.7 g respectively ( $P = .06$ ; Figure 5), and belonging to three different litters were frozen and thawed in pairs and submitted to exactly the same conditions in vitro. The neurospheres of these four pups per experimental group were used to perform all following experiments. Neurospheres from IUGR animals did not present any significant difference in NPC proliferation after 7 days in culture or in migration after 1 or 3 days in culture (Figure 5). A non-significant increase in neuronal differentiation was observed in IUGR neurospheres (Figures 5), while oligodendrocyte differentiation was significantly decreased in IUGR neurospheres compared to control spheres (Figures 5). Viability of these NPCs, measured by their metabolic activity, was not altered in any of these cases (3 or 5 days in culture; Figure 5), indicating that the decreased number of differentiated oligodendrocytes is a specific effect not induced by general cytotoxicity. By contrast, there were no differences between control and IUGR neurospheres proliferating capabilities (Figure 5). In summary, the results of the “Neurosphere Assay” indicated that IUGR impairs NPCs’ differentiation ability into oligodendrocytes, while their proliferation and migration potential is not affected. To contextualize these in vitro results, it is important to remark that both, mild and strong IUGR cases were included (Figure 5) in the preparation of neurospheres for these tests and therefore, the total body weight of IUGR pups was not significantly reduced compared to the controls ( $P = .06$ ). This approach was chosen to cover the broad range of cases that IUGR can display, and to exclude the possibility of detecting effects that are only present in the most severe IUGR cases.

Furthermore, the response of control and IUGR neurospheres to positive controls known to modulate the response of each endpoint was also compared (Figure 6). As previously shown in Figure 3, positive controls significantly reduce the respective readouts of all endpoints in control spheres. However, in IUGR spheres, the exposure to BMP7 did not significantly reduce oligodendrocyte differentiation, probably because in IUGR neurospheres oligodendrocyte differentiation was already reduced per se (Figure 6). Even if the effect of BMP7 was not significant, it reduced the mean oligodendrocyte differentiation in IUGR neurospheres. These data show that the process is also dynamic in IUGR neurospheres as compounds in vitro can still modulate the impairment of oligodendrocyte differentiation. In the next step, we tested if this decreased differentiation can also be modulated

**FIGURE 6** Comparison of the response of IUGR and control neurospheres to known modulators of basic neurogenesis processes. Thawed rabbit neurospheres obtained from control and IUGR animals were cultured for 3 or 5 days and comparatively tested for each endpoint. Neuronal differentiation was analyzed after 3 days under control conditions or exposed to either PP2 10  $\mu$ M, A, or EGF 20 ng/mL, B, oligodendrocyte differentiation was analyzed after 5 days under control conditions or exposed to either BMP7 100 ng/mL, C, or T3 3 nM, D. All endpoints were evaluated in five neurospheres/condition in at least three independent experiments. Results presented as boxes and whiskers according to Tukey method. \* $P < .05$  vs control condition; n.s.: not significant



in the opposite direction to increase the percentage of oligodendrocytes and revert the observed adverse effect. Thyroid hormone (TH) plays an essential role in white matter maturation and myelin formation.<sup>39-42</sup> For this reason, we exposed control and IUGR neurospheres to L-triiodothyronine (T3; CAS: 55-06-1; Sigma-Aldrich), the active form of TH, at a concentration similar to the total T3 concentration in human serum, 3 nM.<sup>43-46</sup> T3 exposure significantly induced the percentage of oligodendrocyte differentiation of IUGR neurospheres to control levels, while it did not affect the percentage of differentiation in control neurospheres (Figure 6). Hence, although the cellular damage was set while cells were still in the in vivo context, in vitro exposure of ex vivo NPCs to T3 can revert the deleterious effect of IUGR in oligodendrocyte differentiation.

## 4 | DISCUSSION

The neurosphere model based on NPCs is a valuable tool to study the progress of basic neurodevelopmental processes.<sup>47</sup> Therefore, we have previously established “Neurosphere Assays” based on rat, mouse or human NPCs as methods to evaluate the adverse effects of chemical or physical agents on neurodevelopment.<sup>24-28,30,37,48</sup> Due to its nature as a primary cell culture, the neurosphere model retains the original characteristics of the neuro- and gliogenic populations of the brain, and reflects their physiological and pathophysiological characteristics. To evaluate the effects of IUGR in neurodevelopment, the ideal situation would be to use a human NPC based “Neurosphere Assay” to avoid species translation limitations.<sup>49</sup> Yet commercially

available hNPCs are derived from healthy individuals, and hNPCs from IUGR individuals are such an extremely scarce material that they are unviable to establish a permanent research model for mechanistic investigations. Therefore, and considering that the rabbit in vivo model previously developed in BCNatal mimics the neurodevelopmental features of human IUGR individuals better than other rat in vivo models, and that rabbits are perinatal brain developers<sup>50</sup> similar to humans and unlike rodents,<sup>51</sup> we decided to establish a rabbit neurosphere culture for the first time. The combination of a 3D in vitro neurodevelopmental testing strategy, with the clinically relevant IUGR experimental animal model allowed us to study IUGR neurodevelopmental consequences by decomposing them into basic neurodevelopmental processes, which are evaluated separately. This methodology offers a research approach that allows studying a complex clinical problem on the cellular, and eventually also molecular level. By employing this newly established in vitro model we identified that rabbit NPCs from IUGR individuals have a significantly reduced ability to form oligodendrocytes. Moreover, we were able to revert this damage by T3 in vitro exposure.

In the present study, we established the in vitro rabbit neurosphere model with cells obtained from freshly dissected rabbit brains (Figure 2) and we tested different freezing protocols, choosing the best one (based on P0 cells) for the use of NPCs in the “Neurosphere Assay” (Figure 3). Neurospheres obtained from both protocols (from fresh and frozen cells) spontaneously formed after 7 days in culture and were able to perform all basic neurodevelopmental processes (proliferation, migration, and differentiation) similar to neurospheres from other species, for example, rats, mice and humans.<sup>24-28,30,37,48</sup> Among the



differentiated cells, glial cells outnumbered neuronal cells, according to the situation described *in vivo* for other species indicating that a massive number of glial cells is generated during postnatal neurodevelopment.<sup>52</sup> Specific data *in vivo* for rabbits during the postnatal period could not be found, but the glia neuron ratio described in adult rabbits also shows that in all brain areas except in the cerebellum, glial cells outnumber neurons.<sup>53</sup> According to the 3R principle of Russel and Burch (1959) for the reduction, replacement and refinement of animal experimentation the established freezing and thawing protocol for rabbit NPCs constitutes a durable technique to reduce and refine the use of animals. Neurospheres obtained from both protocols are dynamic systems since their ability to proliferate, migrate or differentiate was modified by exposure to known positive control compounds (PP2, EGF, BMP7, or growth factor removal in Figures 2 and 3). With respect to the modulation of the performance of these neurospheres, we also proved that a known developmental neurotoxic compound, MeHgCl, induces a significant decrease in cell migration (Figure 4), showing that this rabbit neurosphere model is sensitive to known noxious agents. The IC<sub>50</sub> concentration detected by the model is in line with previously detected IC<sub>50</sub> concentrations in human primary or human iPSC-derived neurosphere models for migration disturbance<sup>26,30,54</sup> and correlates well with concentrations achieved *in vivo* after the administration of MeHgCl doses affecting neurodevelopment.<sup>55</sup> Understanding the sensitivity of a model is a key step for its establishment, that is, it is also essential to ensure that the system is not over-reactive to any stimulus, which means that known innocuous compounds for neurodevelopment should not alter the response of neurospheres in the assay. For this purpose, saccharine was chosen as negative control, because it was already selected as a harmless compound for neurodevelopment by a panel of experts.<sup>38</sup> When saccharine was added to the neurosphere culture in concentrations up to 100  $\mu$ M no adverse effect in migration was observed, indicating the specificity of the assay. This tiered approach for the establishment of the rabbit neurosphere culture, besides being a necessary preliminary group of steps for our subsequent study of IUGR effects, is an essential procedure for the establishment of the method as an alternative model for developmental neurotoxicity detection and the screening and prioritization of chemicals (following the recommendations from Crofton et al.<sup>36</sup>). Current neurodevelopmental studies on the effects of exposure to substances during the pre- and early postnatal period are based on the *in vivo* OECD guidelines 426 (OECD, 2007), 414 (OECD, 2018), and FDA guideline S5 (R3) (FDA 2017) which define rat as the preferred rodent and rabbit as the preferred nonrodent animal. A rat neurosphere model for compound evaluation has already been available since 2014,<sup>37</sup> and now the addition of the neurosphere model of the preferred nonrodent animal opens the door to combine these two models for *in vitro* DNT evaluation in case the use of human material is not possible or for understanding species differences in response to exogenous insults.

After performing all establishment steps with control neurospheres: establishment of the (a) fresh culture, (b) freezing and thawing protocol, and analyzing the system's, (c) dynamism, (d) sensitivity, and (e) specificity, we compared the performance of control and IUGR NPCs in the "Neurosphere Assay." Here, we identified a significant reduction in oligodendrocyte formation in IUGR

NPCs. This observation *in vitro* leads to the possible correlation with a poor myelination *in vivo* as a cause of neurological damage secondary to IUGR. Our finding is in line with previous studies *in vivo* reporting that IUGR leads to white matter injury with a deficiency of mature oligodendrocytes<sup>56,57</sup> and adversely affected myelination processes in brain histology studies.<sup>13</sup> It is important to remark that the adverse effect on oligodendrogenesis in this study was detected in neurospheres obtained both from severe and mild IUGR cases, and therefore the effect was not only observed in the most severe IUGR cases. These findings are in line with clinical and neuroimaging data supporting the existence of fetal abnormal neurodevelopment across all stages of severity in IUGR. In comparison of control and IUGR neurospheres, we also observed an increase in neuronal differentiation after 3 days in culture but this effect was not significant. Future investigations should focus on the prolongation of the period in culture to obtain more stable results (decrease deviation of IUGR results) and to clarify if this incipient increase is significant after 5, 7, 14, or more days in culture and it is consequently another alteration underlying IUGR neural damage. Besides, after a longer culture period, further neurodevelopmental endpoints could also be added to the assay, like neurite outgrowth, neurite branching, synaptogenesis and probably neuronal network activity. In future work it would also be of high interest to assess alterations in astrocyte differentiation, using the protocol established here.

We finally tested a possible future neurotherapy for IUGR: *in vitro* exposure to 3 nM of T3 completely reverted the damage induced by IUGR by inducing oligodendrocyte differentiation, while it did not increase the percentage of oligodendrocytes in control neurospheres (Figure 6). This TH effect in rabbit control NPCs is similar to the one observed in human neurospheres *in vitro*, where 3 nM T3 exposure does not induce an increase in the percentage of oligodendrocytes in control neurospheres, but induces oligodendrocyte maturation.<sup>32</sup> If T3 also induces rabbit oligodendrocyte maturation *in vitro* will be subject to future studies. The transferability of this possible therapy to the clinical field, needs to be carefully assessed for this particular condition, but in support of its transferability it is important to mention that preclinical studies and clinical studies using Tetrac, the TH analog 3,5,3',5'-tetraiodothyroacetic acid, have already been conducted or are conducted at the moment with the goal of supplementing hypothyroid developing brains with TH (ClinicalTrials.gov identifier: NCT04143295). Preclinical studies in mice show that postnatal administration of this potent TH receptor agonist offers the opportunity to reduce the neurological damage associated to the lack of MCT8, a transporter playing a critical role in the uptake of thyroid hormones.<sup>58</sup> The results of the clinical trials conducted in MCT8 deficiency patients (also known as Allan-Herndon-Dudley syndrome) will be of high importance to evaluate the future transferability of the proposed therapeutic strategy in IUGR cases.

In summary, we established an *in vitro* model for the study of IUGR-induced neural damage which is faster, more economic and more ethical than the current *in vivo* approaches in rabbits. Using our new model we detected that oligodendrogenesis is reduced in IUGR brains and that this effect is reversed by exposure to T3. This work

opens the door to the use of the rabbit “Neurosphere Assay” (a) for testing developmental neurotoxic compounds as a complementary method to the rat “Neurosphere Assay,” (b) for studying IUGR-induced neural damage on the cellular and molecular level, (c) for a future identification of possible disease biomarkers, and (d) for the evaluation and selection of specific neuroprotective therapies.

## ACKNOWLEDGMENTS

We thank Dr. Catrin Albrecht for her logistical support and valuable advice. Graphical abstract and Figure 1 were created with BioRender.com. This study has been funded by Instituto de Salud Carlos III through the project “PI18/01763” (co-funded by European Regional Development Fund/European Social Fund, “Investing in your future”), from “LaCaixa” Foundation under grant agreements LCF/PR/GN14/10270005 and LCF/PR/GN18/10310003, and from AGAUR under grant 2017 SGR n° 1531. B.A.K. received a scholarship from Fundació Bosch i Gimpera (project number: 300155) and C.L. received the support the Health Department of the Catalan Government (grant n° SLT006/17/00325).

## CONFLICT OF INTEREST

The authors declared no potential conflicts of interest.

## AUTHOR CONTRIBUTIONS

M.B.: conception and design, collection and assembly of data, data analysis and interpretation, manuscript writing; M.I.: conception and design, provision of study material, data analysis and interpretation, manuscript critical revision; M.H.: collection and assembly of data, data analysis and interpretation; C.L.: collection and assembly of data; L.P.: collection and assembly of data; J.K.: collection and assembly of data; B.A.K.: data analysis and interpretation, manuscript writing; J.G.-C.: provision of study material, manuscript critical revision; J.M.B.: administrative support, provision of study material; F.C.: conception and design, data analysis and interpretation, financial support; E.G.: conception and design, financial support, manuscript critical revision; E.F.: conception and design, data analysis and interpretation, manuscript critical revision. All authors have read and approved the final manuscript.

## DATA AVAILABILITY STATEMENT

The data that support the findings of this study are available from the corresponding author upon reasonable request.

## ORCID

Marta Barenys  <https://orcid.org/0000-0001-5046-9796>

## REFERENCES

- Sharma D, Shastri S, Sharma P. Intrauterine growth restriction: antenatal and postnatal aspects. *Clin Med Insights Pediatr.* 2016;10: CMPed.S40070. <https://doi.org/10.4137/CMPed.S40070>.
- Eixarch E, Muñoz-Moreno E, Bargallo N, Batalle D, Gratacos E. Motor and cortico-striatal-thalamic connectivity alterations in intrauterine growth restriction. *Am J Obstet Gynecol.* 2016;214(6):725.e1-725.e9. <https://doi.org/10.1016/j.ajog.2015.12.028>.
- Batalle D, Muñoz-Moreno E, Arbat-Plana A, et al. Long-term reorganization of structural brain networks in a rabbit model of intrauterine growth restriction. *Neuroimage.* 2014;100:24-38. <https://doi.org/10.1016/j.neuroimage.2014.05.065>.
- Kady SM, Gardosi J. Perinatal mortality and fetal growth restriction. *Best Pract Res Clin Obstet Gynaecol.* 2004;18(3):397-410. <https://doi.org/10.1016/j.bpobgyn.2004.02.009>.
- Marsal K. Intrauterine growth restriction. *Curr Opin Obstet Gynecol.* 2002;14(2):127-135.
- Geva R, Eshel R, Leitner Y, Valevski AF, Harel S. Neuropsychological outcome of children with intrauterine growth restriction: a 9-year prospective study. *Pediatrics.* 2006;118(1):91-100. <https://doi.org/10.1542/peds.2005-2343>.
- Morsing E, Åsard M, Ley D, Stjernqvist K, Maršál K. Cognitive function after intrauterine growth restriction and very preterm birth. *Pediatrics.* 2011;127(4):e874-e882. <https://doi.org/10.1542/peds.2010-1821>.
- Tideman E, Maršál K, Ley D. Cognitive function in young adults following intrauterine growth restriction with abnormal fetal aortic blood flow. *Ultrasound Obstet Gynecol.* 2007;29(6):614-618. <https://doi.org/10.1002/uog.4042>.
- Geva R, Eshel R, Leitner Y, Fattal-Valevski A, Harel S. Memory functions of children born with asymmetric intrauterine growth restriction. *Brain Res.* 2006;1117(1):186-194. <https://doi.org/10.1016/j.brainres.2006.08.004>.
- Rees S, Harding R, Walker D. The biological basis of injury and neuroprotection in the fetal and neonatal brain. *Int J Dev Neurosci.* 2011;29(6):551-563. <https://doi.org/10.1016/j.ijdevneu.2011.04.004>.
- Fleiss B, Wong F, Brownfoot F, et al. Knowledge gaps and emerging research areas in intrauterine growth restriction-associated brain injury. *Front Endocrinol (Lausanne).* 2019;10:1-24. <https://doi.org/10.3389/fendo.2019.00188>.
- Eixarch E, Figueras F, Hernández-Andrade E, et al. An experimental model of fetal growth restriction based on selective ligation of uteroplacental vessels in the pregnant rabbit. *Fetal Diagn Ther.* 2009;26(4):203-211. <https://doi.org/10.1159/000264063>.
- Eixarch E, Batalle D, Illa M, et al. Neonatal neurobehavior and diffusion MRI changes in brain reorganization due to intrauterine growth restriction in a rabbit model. *PLoS One.* 2012;7(2):1-12. <https://doi.org/10.1371/journal.pone.0031497>.
- Carter AM. Animal models of human placentation—a review. *Placenta.* 2007;28(Suppl):S41-S47. <https://doi.org/10.1016/j.placenta.2006.11.002>.
- Derrick M, Luo NL, Bregman JC, et al. Preterm fetal hypoxia-ischemia causes hypertonia and motor deficits in the neonatal rabbit: a model for human cerebral palsy? *J Neurosci.* 2004;24(1):24-34. <https://doi.org/10.1523/JNEUROSCI.2816-03.2004>.
- Workman AD, Charvet CJ, Clancy B, Darlington RB, Finlay BL. Modeling transformations of neurodevelopmental sequences across mammalian species. *J Neurosci.* 2013;33(17):7368-7383. <https://doi.org/10.1523/JNEUROSCI.5746-12.2013>.
- Drobyshevsky A, Derrick M, Wyrwicz AM, et al. White matter injury correlates with hypertonia in an animal model of cerebral palsy. *J Cereb Blood Flow Metab.* 2007;27:270-281. <https://doi.org/10.1038/sj.jcbfm.9600333>.
- van de Looij Y, Lodygensky GA, Dean J, et al. High-field diffusion tensor imaging characterization of cerebral white matter injury in lipopolysaccharide-exposed fetal sheep. *Pediatr Res.* 2012;72(3):285-292. <https://doi.org/10.1038/pr.2012.72>.
- McKinstry RC, Mathur A, Miller JH, et al. Radial organization of developing preterm human cerebral cortex revealed by non-invasive water diffusion anisotropy MRI. *Cereb Cortex.* 2002;12(12):1237-1243. <https://doi.org/10.1093/cercor/12.12.1237>.

20. Illa M, Eixarch E, Batalle D, et al. Long-term functional outcomes and correlation with regional brain connectivity by MRI diffusion tractography metrics in a near-term rabbit model of intrauterine growth restriction. *PLoS One*. 2013;8(10):e76453. <https://doi.org/10.1371/journal.pone.0076453>.
21. Batalle D, Eixarch E, Figueras F, et al. Altered small-world topology of structural brain networks in infants with intrauterine growth restriction and its association with later neurodevelopmental outcome. *Neuroimage*. 2012;60(2):1352-1366. <https://doi.org/10.1016/j.neuroimage.2012.01.059>.
22. Bassan H, Leider Trejo L, Kariv N, et al. Experimental intrauterine growth retardation alters renal development. *Pediatr Nephrol*. 2000;15(3-4):192-195. <https://doi.org/10.1007/s004670000457>.
23. Eixarch E, Hernandez-Andrade E, Crispi F, et al. Impact on fetal mortality and cardiovascular Doppler of selective ligation of uteroplacental vessels compared with undernutrition in a rabbit model of intrauterine growth restriction. *Placenta*. 2011;32(4):304-309. <https://doi.org/10.1016/j.placenta.2011.01.014>.
24. Barenys M, Gassmann K, Baksmeier C, et al. Epigallocatechin gallate (EGCG) inhibits adhesion and migration of neural progenitor cells in vitro. *Arch Toxicol*. 2017;91:827-837. <https://doi.org/10.1007/s00204-016-1709-8>.
25. Moors M, Cline JE, Abel J, Fritsche E. ERK-dependent and -independent pathways trigger human neural progenitor cell migration. *Toxicol Appl Pharmacol*. 2007;221(1):57-67. <https://doi.org/10.1016/j.taap.2007.02.018>.
26. Moors M, Rockel TD, Abel J, et al. Human neurospheres as three-dimensional cellular systems for developmental neurotoxicity testing. *Environ Health Perspect*. 2009;117(7):1131-1138. <https://doi.org/10.1289/ehp.0800207>.
27. Breier JM, Gassmann K, Kayser R, et al. Neural progenitor cells as models for high-throughput screens of developmental neurotoxicity: state of the science. *Neurotoxicol Teratol*. 2010;32(1):4-15. <https://doi.org/10.1016/j.ntt.2009.06.005>.
28. Gassmann K, Abel J, Bothe H, et al. Species-specific differential AhR expression protects human neural progenitor cells against developmental neurotoxicity of PAHs. *Environ Health Perspect*. 2010;118(11):1571-1577.
29. Schreiber T, Gassmann K, Götz C, et al. Polybrominated diphenyl ethers induce developmental neurotoxicity in a human in vitro model: evidence for endocrine disruption. *Environ Health Perspect*. 2010;118(4):572-578. <https://doi.org/10.1289/ehp.0901435>.
30. Baumann J, Gassmann K, Masjosthusmann S, et al. Comparative human and rat neurospheres reveal species differences in chemical effects on neurodevelopmental key events. *Arch Toxicol*. 2016;90(6):1415-1427. <https://doi.org/10.1007/s00204-015-1568-8>.
31. Gassmann K, Schreiber T, Dingemans MML, et al. BDE-47 and 6-OH-BDE-47 modulate calcium homeostasis in primary fetal human neural progenitor cells via ryanodine receptor-independent mechanisms. *Arch Toxicol*. 2014;88(8):1537-1548. <https://doi.org/10.1007/s00204-014-1217-7>.
32. Dach K, Bendt F, Huebenthal U, et al. BDE-99 impairs differentiation of human and mouse NPCs into the oligodendroglial lineage by species-specific modes of action. *Sci Rep*. 2017;7(March):1-11. <https://doi.org/10.1038/srep44861>.
33. Masjosthusmann S, Siebert C, Huebenthal U, Bendt F, Baumann J, Fritsche E. Arsenite interrupts neurodevelopmental processes of human and rat neural progenitor cells: the role of reactive oxygen species and species-specific antioxidative defense. *Chemosphere*. 2019;235:447-456. <https://doi.org/10.1016/j.chemosphere.2019.06.123>.
34. Claassen DA, Desler MM, Rizzino A. ROCK inhibition enhances the recovery and growth of cryopreserved human embryonic stem cells and human induced pluripotent stem cells. *Mol Reprod Dev*. 2009;76(8):722-732. <https://doi.org/10.1002/mrd.21021>.
35. Schneider CA, Rasband WS, Eliceiri KW. NIH Image to ImageJ: 25 years of image analysis. *Nat Methods*. 2012;9(7):671-675. <https://doi.org/10.1038/nmeth.2089>.
36. Crofton KM, Mundy WR, Lein PJ, et al. Developmental neurotoxicity testing: recommendations for developing alternative methods for the screening and prioritization of chemicals. *ALTEX*. 2011;28(1):9-15. <https://doi.org/10.14573/altex.2011.1.009>.
37. Baumann J, Barenys M, Gassmann K, Fritsche E. Comparative human and rat "neurosphere assay" for developmental neurotoxicity testing. *Curr Protoc Toxicol*. 2014;1(SUPPL.59):1-24. <https://doi.org/10.1002/0471140856.tx1221s59>.
38. Aschner M, Ceccatelli S, Daneshian M, et al. Reference compounds for alternative test methods to indicate developmental neurotoxicity (DNT) potential of chemicals: example lists and criteria for their selection and use. *ALTEX*. 2017;34(1):49-74. <https://doi.org/10.14573/altex.1604201>.
39. Namba N, Etani Y, Kitaoka T, et al. Clinical phenotype and endocrinological investigations in a patient with a mutation in the MCT8 thyroid hormone transporter. *Eur J Pediatr*. 2008;167(7):785-791. <https://doi.org/10.1007/s00431-007-0589-6>.
40. Rodrigues F, Grenha J, Ortez C, et al. Hypotonic male infant and MCT8 deficiency—a diagnosis to think about. *BMC Pediatr*. 2014;14(38 cm):252. <https://doi.org/10.1186/1471-2431-14-252>.
41. Marta CB, Adamo AM, Soto EF, Pasquini JM. Sustained neonatal hyperthyroidism in the rat affects myelination in the central nervous system. *J Neurosci Res*. 1998;53(2):251-259. [https://doi.org/10.1002/\(SICI\)1097-4547\(19980715\)53:2<251::AID-JNR14>3.0.CO;2-9](https://doi.org/10.1002/(SICI)1097-4547(19980715)53:2<251::AID-JNR14>3.0.CO;2-9).
42. Rodriguez-Pena A, Ibarrola N, Iniguez MA, Munoz A, Bernal J. Neonatal hypothyroidism affects the timely expression of myelin-associated glycoprotein in the rat brain. *J Clin Invest*. 1993;91(3):812-818. <https://doi.org/10.1172/JCI116301>.
43. Anckarsäter R, Zetterberg H, Blennow K, Anckarsäter H. Association between thyroid hormone levels and monoaminergic neurotransmission during surgery. *Psychoneuroendocrinology*. 2007;32(8-10):1138-1143. <https://doi.org/10.1016/j.psyneuen.2007.07.007>.
44. Johansson P, Almqvist EG, Johansson J-O, et al. Reduced cerebrospinal fluid level of thyroxine in patients with Alzheimer's disease. *Psychoneuroendocrinology*. 2013;38(7):1058-1066. <https://doi.org/10.1016/j.psyneuen.2012.10.012>.
45. Hagen GA, Elliott WJ. Transport of thyroid hormones in serum and cerebrospinal fluid. *J Clin Endocrinol Metab*. 1973;37(3):415-422. <https://doi.org/10.1210/jcem-37-3-415>.
46. Nishikawa M, Inada M, Naito K, et al. 3,3',5'-Triiodothyronine (reverse T3) in human cerebrospinal fluid. *J Clin Endocrinol Metab*. 1981;53(5):1030-1035. <https://doi.org/10.1210/jcem-53-5-1030>.
47. Svendsen CN, ter Borg MG, Armstrong RJ, et al. A new method for the rapid and long term growth of human neural precursor cells. *J Neurosci Methods*. 1998;85(2):141-152. [https://doi.org/10.1016/S0165-0270\(98\)00126-5](https://doi.org/10.1016/S0165-0270(98)00126-5).
48. Fritsche E, Cline JE, Nguyen N-H, Scanlan TS, Abel J. Polychlorinated biphenyls disturb differentiation of normal human neural progenitor cells: clue for involvement of thyroid hormone receptors. *Environ Health Perspect*. 2005;113(7):871-876.
49. Leist M, Hartung T. Inflammatory findings on species extrapolations: humans are definitely no 70-kg mice. *Arch Toxicol*. 2013;87(4):563-567.
50. Harel S, Shapira Y, Tomer A, Donahue MJ, Quilligan E. Vascular-induced intrauterine growth retardation: relations between birth weight and the development of biochemical parameters in young rabbits. *Isr J Med Sci*. 1985;21(10):829-832.
51. Drobyshevsky A, Jiang R, Derrick M, Luo K, Tan S. Functional correlates of central white matter maturation in perinatal period in rabbits. *Exp Neurol*. 2014;261:76-86. <https://doi.org/10.1016/j.expneurol.2014.06.021>.

52. Herculano-Houzel S. The glia/neuron ratio: how it varies uniformly across brain structures and species and what that means for brain physiology and evolution. *Glia*. 2014;62(9):1377-1391. <https://doi.org/10.1002/glia.22683>.
53. Herculano-Houzel S, Ribeiro P, Campos L, et al. Updated neuronal scaling rules for the brains of Glires (rodents/lagomorphs). *Brain Behav Evol*. 2011;78(4):302-314. <https://doi.org/10.1159/000330825>.
54. Hofrichter M, Nimtz L, Tigges J, et al. Comparative performance analysis of human iPSC-derived and primary neural progenitor cells (NPC) grown as neurospheres in vitro. *Stem Cell Res*. 2017;25:72-82. <https://doi.org/10.1016/j.scr.2017.10.013>.
55. Lewandowski TA, Ponce RA, Charleston JS, Hong S, Faustman EM. Effect of methylmercury on midbrain cell proliferation during organogenesis: potential cross-species differences and implications for risk assessment. *Toxicol Sci*. 2003;75(1):124-133.
56. Tolcos M, Petratos S, Hirst JJ, et al. Blocked, delayed, or obstructed: what causes poor white matter development in intrauterine growth restricted infants? *Prog Neurobiol*. 2017;154:62-77. <https://doi.org/10.1016/j.pneurobio.2017.03.009>.
57. Reid MV, Murray KA, Marsh ED, Golden JA, Simmons RA, Grinspan JB. Delayed myelination in an intrauterine growth retardation model is mediated by oxidative stress upregulating bone morphogenetic protein 4. *J Neuropathol Exp Neurol*. 2012;71(7):640-653. <https://doi.org/10.1097/NEN.0b013e31825cfa81>.
58. Horn S, Kersseboom S, Mayerl S, et al. Tetrac can replace thyroid hormone during brain development in mouse mutants deficient in the thyroid hormone transporter Mct8. *Endocrinology*. 2013;154(2):968-979. <https://doi.org/10.1210/en.2012-1628>.

## SUPPORTING INFORMATION

Additional supporting information may be found online in the Supporting Information section at the end of this article.

**How to cite this article:** Barenys M, Illa M, Hofrichter M, et al. Rabbit neurospheres as a novel in vitro tool for studying neurodevelopmental effects induced by intrauterine growth restriction. *STEM CELLS Transl Med*. 2020;1-13. <https://doi.org/10.1002/sctm.20-0223>

### 4.3 Docosahexaenoic Acid and Melatonin Prevent Impaired Oligodendrogenesis Induced by Intrauterine Growth Restriction (IUGR)

**Britta Anna Kühne**<sup>1,2</sup>, Paula Vázquez-Aristizabal<sup>1,2</sup>, Mercè Fuentes-Amell<sup>1,2</sup>, Laura Pla<sup>2</sup>, Carla Loreiro<sup>2,3</sup>, Jesús Gómez-Catalán<sup>1</sup>, Eduard Gratacós<sup>2,3,4</sup>, Miriam Illa<sup>2,5,†</sup> and Marta Barenys<sup>1,\*,†</sup>

<sup>1</sup> Grup de Recerca en Toxicologia (GRET), INSA-UB and Toxicology Unit, Pharmacology, Toxicology and Therapeutical Chemistry Department, Faculty of Pharmacy, University of Barcelona, 08028 Barcelona, Spain

<sup>2</sup> BCNatal | Fetal Medicine Research Center (Hospital Clínic and Hospital Sant Joan de Déu), Universitat de Barcelona, 08028 Barcelona, Spain

<sup>3</sup> Institut d'Investigacions Biomèdiques August Pi i Sunyer (IDIBAPS), 08036 Barcelona, Spain

<sup>4</sup> Center for Biomedical Research on Rare Diseases (CIBER-ER), 08036 Barcelona, Spain

<sup>5</sup> Institut de Recerca Sant Joan de Déu, 08950 Esplugues de Llobregat, Spain

\* Author to whom correspondence should be addressed.

† These authors contributed equally to this work.

|                       |  |
|-----------------------|--|
| Journal               | MPDI Biomedicine   |
| Impact Factor 2020    | 6.081 [OA]   |
| Quartile              | Q1 in Pharmacology and pharmacy  |
| Type of authorship    | First author   |
| Status of publication | Published: Biomedicines 23 (2022 May) 1205<br>DOI: 10.3390/biomedicines10051205. |

## Summary

In this study, our aims were to characterize oligodendrogenesis alterations in fetuses with intrauterine growth restriction (IUGR) and to find therapeutic strategies to prevent/treat them using a novel rabbit in vitro neurosphere culture. IUGR was surgically induced in one uterine horn of pregnant rabbits, while the contralateral horn served as a control. Neural progenitor cells (NPCs) were obtained from pup's whole brain and cultured as neurospheres mimicking the basic processes of brain development including migration and cell differentiation. Five substances, chosen based on evidence provided in the literature, were screened in vitro in neurospheres from untreated rabbits: Docosahexaenoic acid (DHA), melatonin (MEL), zinc, 3,3',5-Triiodo-L-thyronine (T3), and lactoferrin (LF) or its metabolite sialic acid (SA). DHA, MEL and LF were further selected for in vivo administration and subsequent evaluation in the Neurosphere Assay. In the IUGR culture, we observed a significantly reduced percentage of oligodendrocytes (OLs) which correlated with clinical findings indicating white matter injury in IUGR infants. We identified DHA and MEL as the most effective therapies. In all cases, our in vitro rabbit neurosphere assay predicted the outcome of the in vivo administration of the therapies and confirmed the reliability of the model, making it a powerful and consistent tool to select new neuroprotective therapies.



## Article

# Docosahexaenoic Acid and Melatonin Prevent Impaired Oligodendrogenesis Induced by Intrauterine Growth Restriction (IUGR)

Britta Anna Kühne <sup>1,2</sup>, Paula Vázquez-Aristizabal <sup>1,2</sup>, Mercè Fuentes-Amell <sup>1,2</sup>, Laura Pla <sup>2</sup>, Carla Loreiro <sup>2,3</sup>, Jesús Gómez-Catalán <sup>1</sup>, Eduard Gratacós <sup>2,3,4</sup>, Miriam Illa <sup>2,5,†</sup> and Marta Barenys <sup>1,\*,†</sup>

<sup>1</sup> Grup de Recerca en Toxicologia (GRET), INSA-UB and Toxicology Unit, Pharmacology, Toxicology and Therapeutical Chemistry Department, Faculty of Pharmacy, University of Barcelona, 08028 Barcelona, Spain; brkuhnek24@alumnes.ub.edu (B.A.K.); vazquezaristizabal@gmail.com (P.V.-A.); mfuentam7@alumnes.ub.edu (M.F.-A.); jesusgomez@ub.edu (J.G.-C.)

<sup>2</sup> BCNatal | Fetal Medicine Research Center (Hospital Clínic and Hospital Sant Joan de Déu), Universitat de Barcelona, 08028 Barcelona, Spain; laura.pla.codina@gmail.com (L.P.); carla.lr2@gmail.com (C.L.); egratacos@ub.edu (E.G.); miriamil@clinic.cat (M.I.)

<sup>3</sup> Institut d'Investigacions Biomèdiques August Pi i Sunyer (IDIBAPS), 08036 Barcelona, Spain

<sup>4</sup> Center for Biomedical Research on Rare Diseases (CIBER-ER), 08036 Barcelona, Spain

<sup>5</sup> Institut de Recerca Sant Joan de Déu, 08950 Esplugues de Llobregat, Spain

\* Correspondence: mbareny@ub.edu; Tel.: +34-678456700

† These authors contributed equally to this work.

**Citation:** Kühne, B.A.; Vázquez-Aristizabal, P.; Fuentes-Amell, M.; Pla, L.; Loreiro, C.; Gómez-Catalán, J.; Gratacós, E.; Illa, M.; Barenys, M. Docosahexaenoic Acid and Melatonin Prevent Impaired Oligodendrogenesis Induced by Intrauterine Growth Restriction (IUGR). *Biomedicines* **2022**, *10*, 1205. <https://doi.org/10.3390/biomedicines10051205>

Academic Editor: Sónia Catarina Correia

Received: 26 April 2022

Accepted: 18 May 2022

Published: 23 May 2022

**Publisher's Note:** MDPI stays neutral with regard to jurisdictional claims in published maps and institutional affiliations.



**Copyright:** © 2022 by the authors. Licensee MDPI, Basel, Switzerland. This article is an open access article distributed under the terms and conditions of the Creative Commons Attribution (CC BY) license (<https://creativecommons.org/licenses/by/4.0/>).

**Abstract:** In this study, our aims were to characterize oligodendrogenesis alterations in fetuses with intrauterine growth restriction (IUGR) and to find therapeutic strategies to prevent/treat them using a novel rabbit in vitro neurosphere culture. IUGR was surgically induced in one uterine horn of pregnant rabbits, while the contralateral horn served as a control. Neural progenitor cells (NPCs) were obtained from pup's whole brain and cultured as neurospheres mimicking the basic processes of brain development including migration and cell differentiation. Five substances, chosen based on evidence provided in the literature, were screened in vitro in neurospheres from untreated rabbits: Docosahexaenoic acid (DHA), melatonin (MEL), zinc, 3,3',5-Triiodo-L-thyronine (T3), and lactoferrin (LF) or its metabolite sialic acid (SA). DHA, MEL and LF were further selected for in vivo administration and subsequent evaluation in the Neurosphere Assay. In the IUGR culture, we observed a significantly reduced percentage of oligodendrocytes (OLs) which correlated with clinical findings indicating white matter injury in IUGR infants. We identified DHA and MEL as the most effective therapies. In all cases, our in vitro rabbit neurosphere assay predicted the outcome of the in vivo administration of the therapies and confirmed the reliability of the model, making it a powerful and consistent tool to select new neuroprotective therapies.

**Keywords:** progenitor cells; cell culture; differentiation; oligodendrocytes; nervous system development; neurogenesis; fetal growth restriction

## 1. Introduction

Brain development is one of the most sensitive and vulnerable processes during pregnancy. Its disturbance can manifest in neurobehavioral disorders throughout life [1]. Intrauterine growth restriction (IUGR) is defined as a pathological fetal condition where the fetus has not attained its biologically determined growth potential and estimated fetal weight is below the 10th percentile for gestational age. IUGR is among the most frequent disorders, affecting 5–10% of all pregnancies [2]. Most commonly, IUGR occurs due to abnormal placental function, which reduces placental blood flow, leading to fetal development under chronic hypoxia. Restricted oxygen and nutrition supply can have serious

consequences for the developing brain, disrupting the normal patterns of gray and white matter development [3,4]. White matter injury occurs due to impaired myelination and oligodendrocyte maturation, which lead to adverse neurodevelopmental sequelae [5–8]. In the long run, IUGR-infants are prone to develop neurocognitive disorders, learning disabilities, attention deficit hyperactivity disorder, or autism spectrum disorder [1,9–11]. However, there is currently no therapy to prevent or revert, even at the prenatal period, the neurological insults that arise from IUGR [12,13].

With the aim of testing potential therapies applicable during the prenatal period to prevent IUGR-induced neurological disorders, we recently established an *in vitro* rabbit neurosphere model reproducing brain development under chronic and mild IUGR conditions [14]. In this model, neurospheres are prepared from a rabbit *in vivo* model mimicking placental insufficiency by selective ligation of uteroplacental vessels in late pregnancy. The rabbit *in vivo* model has already been shown to present cardiovascular Doppler changes similar to human IUGR, reduced birth weight and a higher brain to birth weight ratios [4,15,16]. The neurosphere model, prepared from IUGR and control postnatal day 0 (PND0) pups' whole brains, simulates the basic functions of brain development including cell proliferation, migration and differentiation to neurons, astrocytes, and oligodendrocytes (OLs) [14,17,18]. This 3D *in vitro* culture is an efficient choice because several potential therapies can be tested cost-effectively and more ethically than in *in vivo* experiments. In this technique, a wide concentration range of each potential therapy can be tested to select the *in vivo* concentration range of interest. Afterwards, it is also possible to prepare neurospheres from pups' brains exposed to the therapies *in vivo* during gestation to test the efficacy and safety of the treatment within the previously selected concentration range.

By using the neurosphere model, it is also possible to study the effects of nervous system diseases like Alzheimer's disease or glioma [19] as well as the mode of action of compounds [20,21]. This culture can be used to characterize the effects at a cellular level to fill the gaps in translational approaches going from *in vitro* functional alterations to *in vivo*, known adverse outcomes. With the rabbit neurosphere model, we previously discovered that IUGR has a severe impact on OL formation, reducing its differentiation significantly [14] and confirming previous results of impaired OL formation after IUGR *in vivo* [4,8]. In the present study, we included a time-course evaluation and a molecular characterization of this impact produced by IUGR in OLs. We analyzed the maturational stages over time and the expression of two major genes involved in myelination: Myelin basic protein (*Mbp*) and myelin oligodendrocyte glycoprotein (*Mog*). In parallel, the neurosphere assay included measurements of radial glial migration and cell viability.

Aiming to correct the identified adverse effect of IUGR in OLs, we further tested five potential therapies: docosahexaenoic acid (DHA), melatonin (MEL), zinc, L-triiodothyronine (T3), lactoferrin (LF), and its main metabolite sialic acid (SA). All therapies were selected based on literature research which indicated promising results to overcome fetal neurological disorders (Table S1). DHA, a long-chain polyunsaturated fatty acid, is essential for fetal brain development due to its contribution to myelin formation, neurotransmitter metabolism, and synaptogenesis leading to better maintenance of neuronal networks [22–24]. The hormone MEL reportedly reduces fetoplacental oxidative stress and is effective at reducing cerebral white and gray matter injury arising from placental insufficiency and IUGR *in vivo* in sheep [25]. Zinc is crucial for normal brain development because its deficit harms neuronal migration and differentiation and triggers apoptosis [26–29]. Thyroid hormones regulate the growth of the fetus and its brain development by supporting especially OL maturation [30–32]. LF is a sialic acid-rich glycoprotein that restores IUGR-induced impaired oligodendrocyte precursor cell marker NG2 [33] and supports neuronal outgrowth and synaptic connectivity during fetal brain development [34].

From the five potential therapies tested *in vitro*, three of them were selected to be administered *in vivo* during pregnancy after IUGR induction to find the most promising candidates to prevent/revert OL damage associated with IUGR.



## 2. Materials and Methods

### 2.1. In Vivo Procedures: IUGR Induction and Administration of Therapies

All animal experimentation procedures were approved by the Ethics Committee for Animal Experimentation (CEEA) of the University of Barcelona. All protocols were accepted by the Department of Environment and Housing of the Generalitat de Catalunya with the license number: 11126, date of approval 24 May 2021, and the procedure CEEA number OB 340/19 SJD. The procedure for the IUGR induction was previously described in Eixarch et al., 2009 [15]. Briefly, IUGR was induced at 25th gestational day (GD 25) of pregnant New Zealand rabbits by surgical ligation of 40–50% of the uteroplacental vessels of each gestational sac of one uterine horn (IUGR group), the contralateral horn was left for normal growth (control group). At the time of IUGR induction, pregnant rabbits were randomly assigned to 4 groups: without treatment (w/o), treatment with DHA, MEL or LF (Table 1, Figure 1). The therapies were administered orally to pregnant rabbits on the day of IUGR induction (GD 25) until Caesarean (C-) section was carried out at GD 30 followed by body weight measurement. For all groups, the inclusion criteria of IUGR PND0 rabbit pups was a birth weight lower and for control pups higher than the 25th percentile (39.7 g, Table 1 in Barenys et al., 2021 [14]). The in vitro neurosphere culture was generated by decapitation and whole-brain dissection at PND0 from control and IUGR pups. The administered dose, number, and birth weight of PND0 rabbit pups are listed in Table 1. Information about in vivo treatment calculations and supplier is presented in Supplemental Material 1 (SM1).

**Table 1.** Number and birth weight of PND0 rabbit pups included in the study.

| Treatment | Dose<br>(mg/kg bw/day) | Number of<br>Control Pups | Birth Weight [g] ±<br>SEM | Number of<br>IUGR Pups | Birth Weight [g] ±<br>SEM |
|-----------|------------------------|---------------------------|---------------------------|------------------------|---------------------------|
|           | Rabbit Doe             | Control Pups              |                           | IUGR Pups              |                           |
| w/o       | -                      | 12                        | 48.52 ± 1.93              | 10                     | 31.72 ± 2.17 *            |
| DHA       | 37                     | 2                         | 57.05 ± 3.90              | 2                      | 34.76 ± 5.20 *            |
| MEL       | 10                     | 2                         | 52.01 ± 9.38              | 2                      | 27.94 ± 2.52 *            |
| LF        | 166                    | 2                         | 59.72 ± 1.57              | 2                      | 37.86 ± 3.71 *            |

From one rabbit pup's whole brain, at least four independent experiments were performed. The rabbit pup's sex is not visible at PND0 and was not determined. The dose administered to the pregnant rabbit is indicated, w/o: without treatment, bw: bodyweight, \*:  $p < 0.05$  vs. corresponding control birth weight.

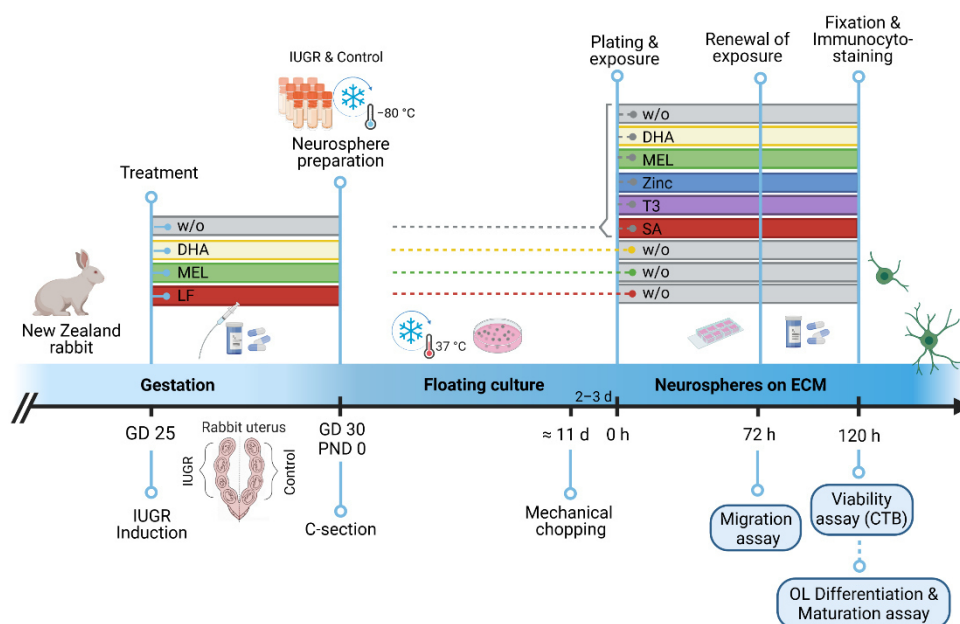


**Figure 1.** Experimental setup. IUGR was induced in one uterine horn of pregnant rabbits on gestational day (GD) 25, whereas the contralateral horn remained as control. No treatment (w/o) or therapies were administered to the pregnant rabbit until C-section (GD 30). On PND 0, IUGR and control pups were obtained from every group and neurospheres prepared from pup's whole brain. Neurospheres were cultivated in a floating culture for approx. 11 days and mechanically chopped 2–3 days before plating. On the experimental day (0 h), neurospheres (0.3 mm) were plated on a PDL/Laminin coated eight-chamber slide w/o or with exposure to therapies. After 72 h migration distanced was measured and after 120 h viability, oligodendrocyte (OL) differentiation & maturation assessed. Rectangle bars = time of administration or exposure, blue circle = endpoints. w/o = without, GD = gestational day, PND = postnatal day, ECM = extracellular matrix, OL = oligodendrocyte, CTB = cell titer blue. Created with BioRender.com (accessed on 20 May 2022).

## 2.2. Neurosphere Preparation

Rabbit neural progenitor cells (NPCs) were isolated from rabbits' whole brains. Meninges and olfactory bulbs were discarded followed by mechanical chopping, enzymatic digestion (20 min incubation with papain 20 U/mL at 37 °C), mechanical homogenization into a cell suspension, and centrifugation (10 min at 1200 rpm). The cell pellet obtained was resuspended in 1 mL freezing medium (1:1; volume of pellet: volume of freezing medium [consisting in 70% (*v/v*) proliferation medium, 20% (*v/v*) fetal calf serum and 10% (*v/v*) DMSO]) and immediately stored at –80 °C.

After thawing, the freezing medium was replaced by proliferation medium [consisting of DMEM and Hams F12 3:1 supplemented with 2% B27 (Invitrogen, Madrid, Spain), and 20 ng/mL epidermal growth factor (EGF) including recombinant human fibroblast growth factor (FGF2), 100 U/mL penicillin, and 100 µg/mL streptomycin] supplemented with Rho kinase (ROCK) inhibitor Y-276322 at a final concentration of 10 µM. NPCs were cultured for 11 days on Petri dishes coated with poly-HEMA. Half of the medium was replaced every 2–3 days.

### 2.3. The Neurosphere Assay

Two days before starting the neurosphere assay, neurospheres were mechanically chopped to a size of 0.2 mm (McIlwain tissue chopper) to ensure homogeneous size and spherical shape. On the experimental plating day, neurospheres of 0.3 mm in diameter were selected and transferred to PDL/laminin-coated, eight-chamber slides (Falcon, Madrid, Spain) containing 500  $\mu$ L differentiation medium [consisting of DMEM and Hams F12 3:1 supplemented with N2 (Invitrogen, Madrid, Spain), penicillin, and streptomycin (100 U/mL and 100  $\mu$ g/mL)] to assess migration, differentiation, and viability. Five neurospheres were plated in each chamber representing intra-experiment replicates. Subsequently, at least three independent experiments were performed for every endpoint and exposure (Figure 1).

#### 2.3.1. In Vitro Testing of Potential Therapies

Therapies were dissolved in their corresponding solvent depending on their maximum solubility (Table 2), and subsequently, in differentiation medium. Under differentiation conditions, NPCs were exposed for 5 days to the therapies and the exposure medium was renewed every 2–3 days. These 5 days of exposure were chosen because at this time-point, a significant difference of OL differentiation between control and IUGR cultures was previously detected [14], and because it is a time-point that makes it possible to observe all maturation stages of O4+ cells. Basic processes of neurogenesis were assessed to determine the maximum tolerated concentration (MTC) and most effective concentration (EC). The criteria to define the MTC was a viability >70% of solvent control (SC) values, a not significantly reduced migration distance, or a not significantly reduced OL percentage compared to the SC.

**Table 2.** In vitro testing concentrations of potential therapies.

| Compound (Synonym) | CAS Number  | Solubility                     | Concentration In Vitro         | MTC         |
|--------------------|-------------|--------------------------------|--------------------------------|-------------|
| <b>DHA</b>         | 6217-54-5   | 300 $\mu$ M (DMSO)             | 300–100–30–10–3–1–0.3 $\mu$ M  | 10 $\mu$ M  |
| <b>MEL</b>         | 73-31-4     | 100 $\mu$ M (DMSO)             | 100–30–10–3–1–0.3–0.1 $\mu$ M  | 3 $\mu$ M   |
| <b>T3</b>          | 55-06-1     | 30 nM (HCl/EtOH)               | 30–10–3–1–0.3–0.1–0.03 nM      | 30 nM       |
| <b>Zinc</b>        | 7440-66-6   | 300 $\mu$ M (H <sub>2</sub> O) | 300–100–30–10–3–1–0.3 $\mu$ M  | 100 $\mu$ M |
| <b>LF</b>          | 339615-76-8 | 10 mg/mL (H <sub>2</sub> O)    | 30–10–3–1–0.3–0.1–0.03 $\mu$ M | 30 $\mu$ M  |
| <b>SA</b>          | 131-48-6    | 30 $\mu$ M (DMSO)              | 30–10–3–1–0.3–0.1–0.03 $\mu$ M | 30 $\mu$ M  |

The tested compounds, the concentration range used in vitro based on their solubility and the resulting maximum tolerated concentration (MTC) is described. The maximum solvent percentage submitted was 0.1% (*v/v*).

#### 2.3.2. Migration Assay

Five neurospheres per chamber were plated in PDL/laminin-coated eight-chamber slides filled with 500  $\mu$ L differentiation medium. After 48 or 72 h under differentiation conditions, bright-field pictures were taken to monitor migration progression [EX-H30 camera (Casio, Japan)]. Migration distances were determined by measuring the distance from the sphere core to the furthest migrated cell at four pre-defined positions per neurosphere using ImageJ 1.53a software. For the time-course-assay, migration distance was measured every 24 h over 5 consecutive days. The src kinase inhibitor PP2 at 10  $\mu$ M served as endpoint-specific positive control in every experiment.

#### 2.3.3. OL Differentiation and Maturation Assay

After 5 days under differentiation conditions, neurospheres were fixed with 4% PFA for 30 min at 37  $^{\circ}$ C, washed and stored in PBS until immunostaining. Slides were washed with PBS and incubated with 1:200 mouse IgM anti-O4 antibody (R&D Systems, Madrid,

Spain) in PBS with 10% goat serum overnight at 4 °C. After washing with PBS, slides were incubated with secondary antibody (anti-mouse IgG Alexa Fluor® 488; Invitrogen, Madrid, Spain) 1:200, 2% goat serum and 1% Hoechst 33258 (Sigma Aldrich, Madrid, Spain) for nuclei counterstaining in PBS for 30 min at 37 °C. After washing with PBS, slides were mounted with Fluoromount-G™ Mounting Medium (Invitrogen, Madrid, Spain) and stored at 4 °C until image acquisition. Two images per neurosphere were taken with a BX61 microscope (Olympus, Tokyo, Japan) and analyzed with ImageJ 1.53a. The number of O4+ cells was manually counted and normalized by the number of nuclei. For the time-course assay OL differentiation was analyzed every 24 h over 5 consecutive days. Additionally, a maturation evaluation was performed using the same images: OLs were classified in different maturation stages according to their morphological appearance: immature, bipolar, mature, and myelinating (Figure 2D). The cell number of each maturation stage was normalized by the total number of O4+ cells. At least three independent experiments were performed for each endpoint. BMP7 [100 ng/mL] was used as positive control in every experiment.

#### 2.3.4. Cell Viability

Cell viability was assessed by using CellTiter-Blue® cell viability assay (Promega, Madrid, Spain). This assay is based on the measurement of mitochondrial reductase activity of living cells by conversion of resazurin to the fluorescent product resorufin. After 2 h of incubation with the reagent (1:3 *v/v*), the medium was placed in a 96-well plate and read with FLUOstar Optima microplate reader. Cell viability was determined after 5 days of differentiation and for the time-course-assay every 24 h over 5 consecutive days. Neurospheres exposed to 10% DMSO (2 h) were used as lysis control in every experiment.

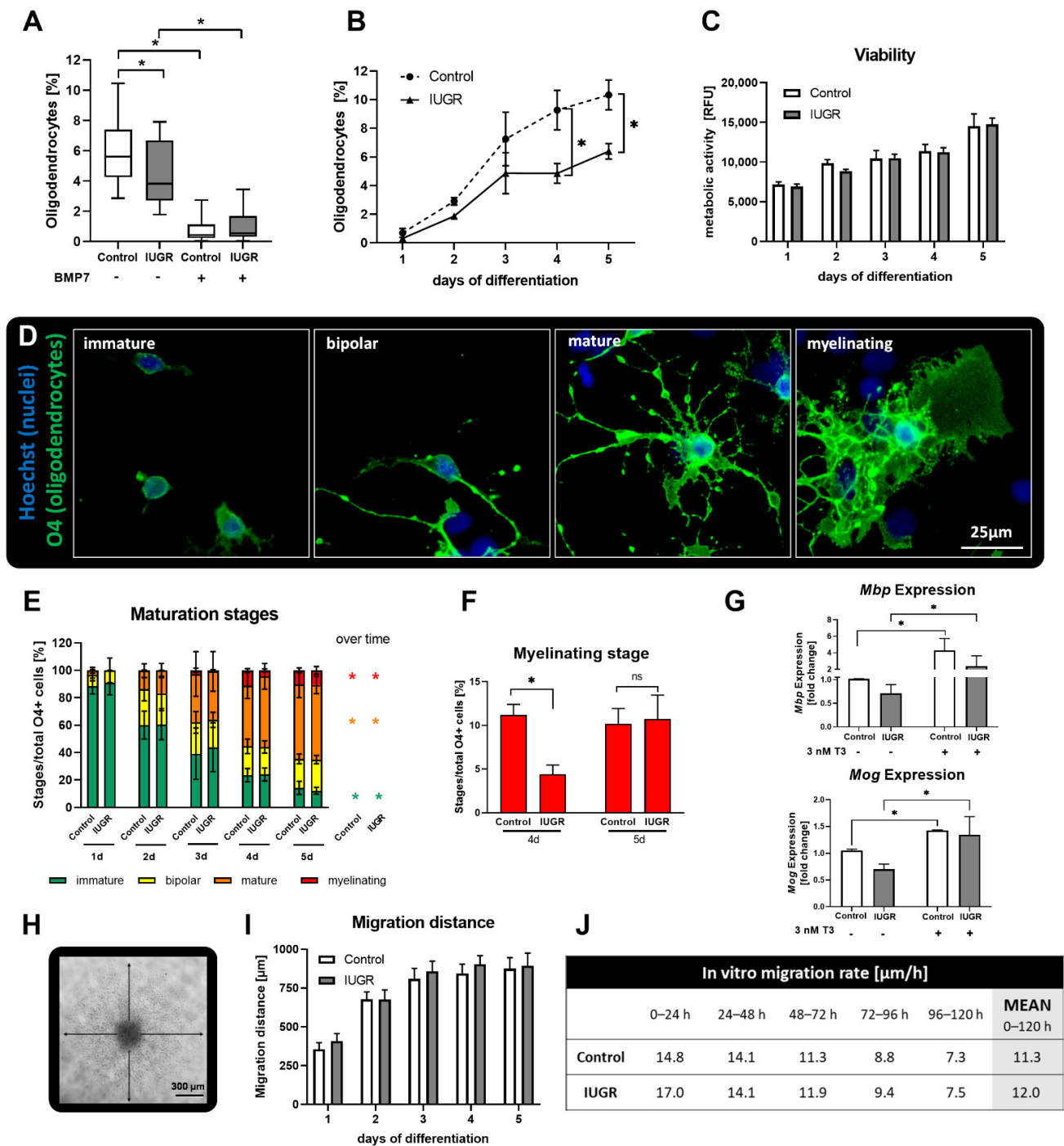


**Figure 2.** Oligodendrogenesis. Rabbit neurospheres obtained from control and IUGR pups were comparatively analyzed for each endpoint of the ‘Neurosphere Assay’. (A) Oligodendrocyte differentiation after 5 days with and without exposure to the positive control BMP7 [100 μM], (B) oligodendrocyte differentiation over five consecutive days, (C) cell viability determined by metabolic activity, (D) representative pictures of maturation stages in control neurospheres, from left to right: immature, bipolar, mature, myelinating with oligodendrocyte marker O4 (green) and nuclei marker Hoechst 33,258 (blue), scale bar = 25 μm. (E) Maturation stages of oligodendrocytes (O4+ cells) evaluated by morphological appearance over five days, (F) myelinating stage after 4 and 5 days, (G) qRT-PCR from *Mbp* and *Mog* expression in control and IUGR neurospheres, with and without exposure to the positive control 3 nM T3. (H) Representative picture of migrated NPCs after 3 days, (I) migration distance [μm] and (J) Migration rate [μm/h]. Mean ± SEM; ns: not significant, \*:  $p < 0.05$ .

### 2.3.5. qRT-PCR

After 5 days of differentiation, RNA was isolated, cDNA synthesized, and qRT-PCR performed. A detailed description of the method and primer sequences are given in SM2 and Table S2.

### 2.4. Statistics

Statistical analyses were performed using GraphPad Prism v9. Comparisons of two groups and time-course experiments were performed with a two-way ANOVA analysis. Significance over time was assessed by one-way ANOVA. Concentration-dependent effects were assessed by performing a one-way ANOVA. Post-hoc test Bonferroni's multiple comparison test followed ANOVA analysis. The difference between SC and one sample was calculated with a two-tailed student's *t*-test. The significance threshold was established at  $p < 0.05$ .

## 3. Results

### 3.1. IUGR Decreases OL Differentiation

Our previous study on the effects of IUGR in rabbit neurospheres already detected a significantly lower percentage of O4+ cells after 5 days in vitro [14]. This result was reproduced in the present study (Figures 2A and S1) and further investigated to distinguish if this significantly lower percentage at 5 days in vitro was due to a decrease in differentiation or to an increase in cell death.

Neurospheres were obtained from 12 control and 10 IUGR PND0 pups with a significantly reduced birth weight compared to control (Control:  $48.52 \pm 1.93$  g, IUGR:  $31.72 \pm 2.17$  g, Table 1). In a time-course assay over 5 days (Figure 2B) in both, the control and IUGR groups, the percentage of O4+ cells increased significantly over time (Control  $p = 0.0006$ ; IUGR  $p = 0.0013$ ). However, there was no increase in % O4+ cells in the IUGR culture between days 3 and 4, and on days 4 and 5 the percentages were significantly lower in IUGR than in control neurospheres. The time-course experiment revealed that the differentiation rate in IUGR neurospheres is slower than in control (Figure 2B). This effect was not derived from cytotoxicity since cell viability remained comparable between groups at all time points (Figure 2C). There was also no decline in the % of O4+ cells in IUGR neurospheres over time indicating no specific death of this cell type (Figure 2B). During the 5 days of study, OLs underwent several maturation stages with increasing morphological complexity from immature appearance over bipolar and mature until they reached their myelinating postmitotic stage (Figure 2D,E). Over time, the immature stage decreased significantly while mature and myelinating stages increased significantly (Figure 2E). On the first day of differentiation, in control and IUGR cultures, the OL population was composed of 88–91% immature OLs (green) while on day 2 more OLs developed a bipolar (yellow, control 26.20%; IUGR 22.37%) or mature morphology (orange, control 13.41%; IUGR 16.87%). The number of mature OLs increased on day three and remained as the main OL population until day five (orange, control 54.42%; IUGR 54.38%). In the IUGR group, the myelinating stage was significantly lower on day four (red, control 11.17%; IUGR 4.40%;  $p = 0.0183$ ) but increased on day five to reach a value comparable to control (red, control 10.16%; IUGR 10.74%) suggesting a delayed ability to mature (Figure 2E,F).

Besides the morphological appearance, the gene expression of the OL lineage maturation markers *Mbp* and *Mog* was analyzed on day 5 in control and IUGR neurospheres without exposure or after exposure to T3 [3 nM] as a positive control (Figure 2G), since T3 is known to increase the OL maturation in human and rat neurospheres [21]. The OL marker *Mbp* is expressed in mature and myelinating OLs, while *Mog* is expressed in the postmitotic state of myelinating OLs [35]. IUGR showed a mild downregulation of *Mbp* (0.71-fold) as well as *Mog* (0.70-fold) expression relative to the control. T3 significantly

enhanced the expression of *Mbp* (control: 4.3-fold; IUGR: 2.4-fold) and *Mog* (control: 1.4-fold; IUGR: 1.3-fold) in control and IUGR neurospheres, as expected.

During the 5 days in differentiation culture, neural progenitor cells migrated out from the neurosphere core and differentiated while migrating (Figure 2H). In both the control and IUGR groups, the migration distance increased over the first three days and remained almost constant until day 5 (Figure 2I). Accordingly, the migration rate decreased over time and exhibited analogue dynamics between IUGR and control neurospheres over the 5 days (average migration rate: 11.3  $\mu\text{m}/\text{h}$  (control); 12.0  $\mu\text{m}/\text{h}$  (IUGR); Figure 2J).

With this first evaluation, we proved that IUGR significantly impairs OL differentiation in rabbit neurospheres and that IUGR neurospheres present a slower differentiation rate compared to controls, while migration rate and cell viability remain unaffected. A morphology and gene expression analysis indicated a mild delayed OL myelination due to IUGR.

### 3.2. In Vitro Testing of Potential Therapies

Intending to foster the OL population under IUGR conditions, we tested five potential therapies in the neurosphere assay. The therapies were selected based on literature with preliminary evidence to prevent or revert the perinatal adverse results and neurological damage associated with IUGR: DHA, MEL, T3, zinc and LF as well as its main metabolite SA. LF, as a lactic compound, was not soluble in the medium (Figure S2), and thus SA was considered as a replacement candidate for in vitro experiments [34]. In a first approach, we determined the maximum tolerated concentration (MTC) of all potential therapies in control neurospheres (Figure 3). The criteria to set the MTC was viability higher than 70% of SC and no significant adverse effect in migration distance or OL differentiation.

The migration distance and OL differentiation were not specifically disturbed by any of the tested compounds in control neurospheres. A significant effect was only observed because of general cytotoxicity at high concentrations of DHA and zinc (100 and 300  $\mu\text{M}$  DHA and 300  $\mu\text{M}$  zinc; Figure 3A,B). DHA at 30  $\mu\text{M}$  reduced the viability to  $67.5 \pm 38.4\%$ , which was already below the acceptance limit. OL differentiation and migration were not significantly altered at concentrations below 30  $\mu\text{M}$  (Figure 3C). Taking all three endpoints into account, MTC for DHA was established at 10  $\mu\text{M}$ . MEL at 10  $\mu\text{M}$  displayed reduced viability to  $64.7 \pm 6.8\%$  of control value and no reduced OL differentiation or migration distance. In consequence, the MTC for MEL was set to 3  $\mu\text{M}$ . The MTC of T3 was established to the highest tested concentration (30 nM) since viability, migration and OL differentiation was not significantly reduced at any tested concentration. 300  $\mu\text{M}$  zinc significantly reduced the metabolic activity, and therefore the MTC was set to 100  $\mu\text{M}$ . Here, in control neurospheres 100  $\mu\text{M}$  zinc significantly increased the percentage of OL compared to SC (SC: 4.21%; 100  $\mu\text{M}$  zinc 10.98%;  $p=0.0238$ ). SA did not reduce viability, migration, or OL differentiation, thus its MTC was established at the highest tested concentration (30  $\mu\text{M}$ ).

The main interest was to find a concentration of the tested therapies which enhanced the OL differentiation of IUGR neurospheres to control neurosphere levels. Migration distance and viability assays were simultaneously performed to overcome the adverse effects of the therapies in these endpoints (Figure S3). Rabbit neurospheres from IUGR pups were exposed to the potential therapies with increasing concentrations up to their respective MTC (Figure 4A).

None of the potential therapies produced a significant concentration-dependent monotonic response in IUGR neurospheres. However, some of them induced non-monotonic responses with high increases in oligodendrocyte differentiation at specific concentrations. Exposure to 1  $\mu\text{M}$  DHA increased the OL differentiation to its maximum ( $9.7 \pm 5.4\%$ ) and showed a significant increase by comparison to the SC. Therefore, 1  $\mu\text{M}$  DHA was considered as its most effective concentration in vitro (Figure 4A).

### Control Neurospheres

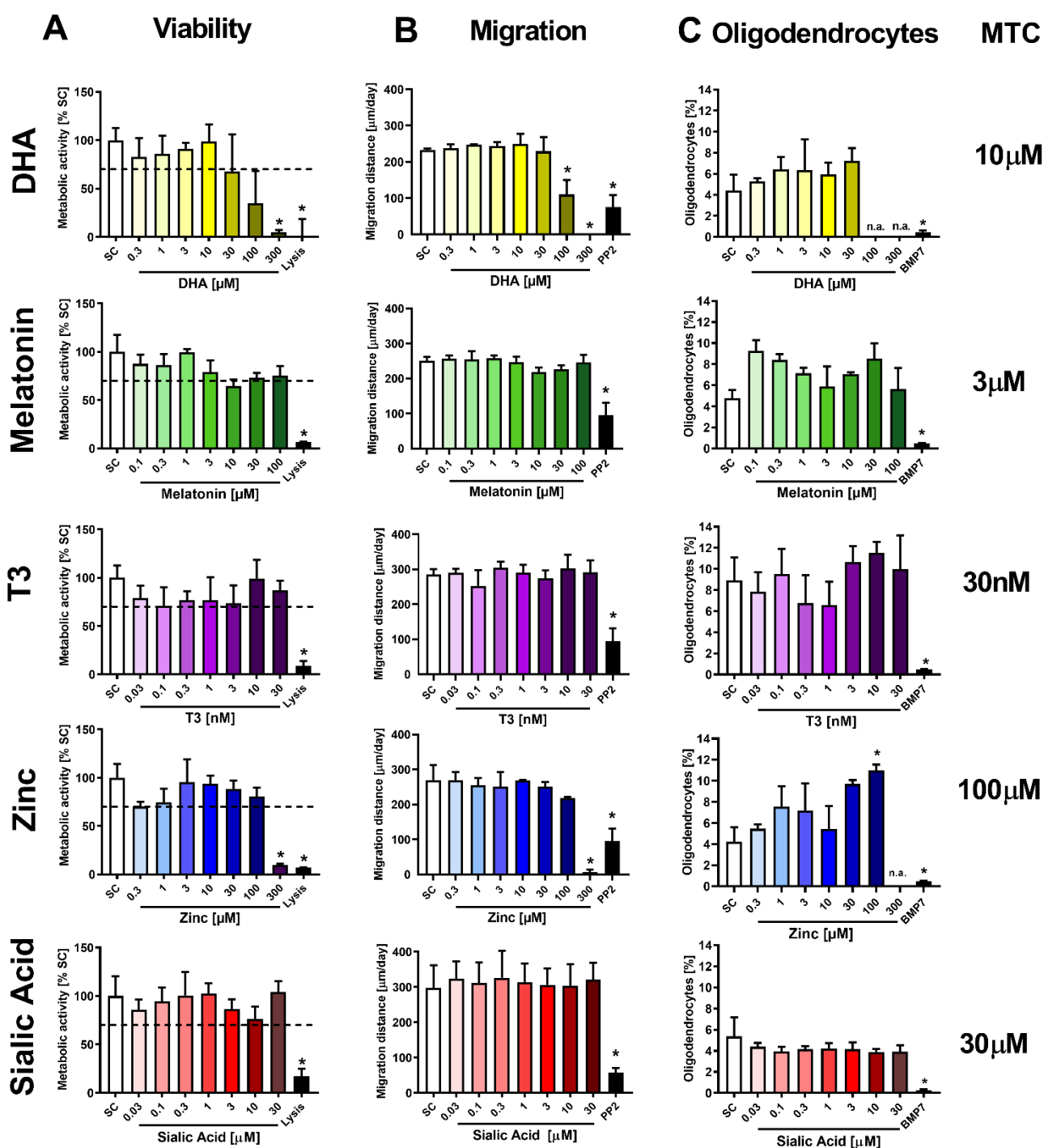


**Figure 3.** Maximum tolerated concentrations (MTCs) of potential therapies in control neurospheres. Rabbit neurospheres obtained from control pups were cultured for 3 or 5 days and tested for each endpoint with increasing concentrations of DHA, SA, MEL, zinc, T3, and an endpoint specific positive control. (A) Viability determined by metabolic activity after 5 days, positive control: lysis (10% DMSO), dotted line: 70 % of SC, (B) migration distance per day (mean ± SEM), positive control: PP2, (C) oligodendrocyte differentiation after 5 days (mean ± SEM), positive control: BMP7 [100 µM]. MTC: maximum tolerated concentration of each compound. All endpoints were evaluated in 5 neurospheres/condition in at least 3 independent experiments. n.a.: not analyzed. \*:  $p < 0.05$  vs. solvent control (SC).



## IUGR Neurospheres

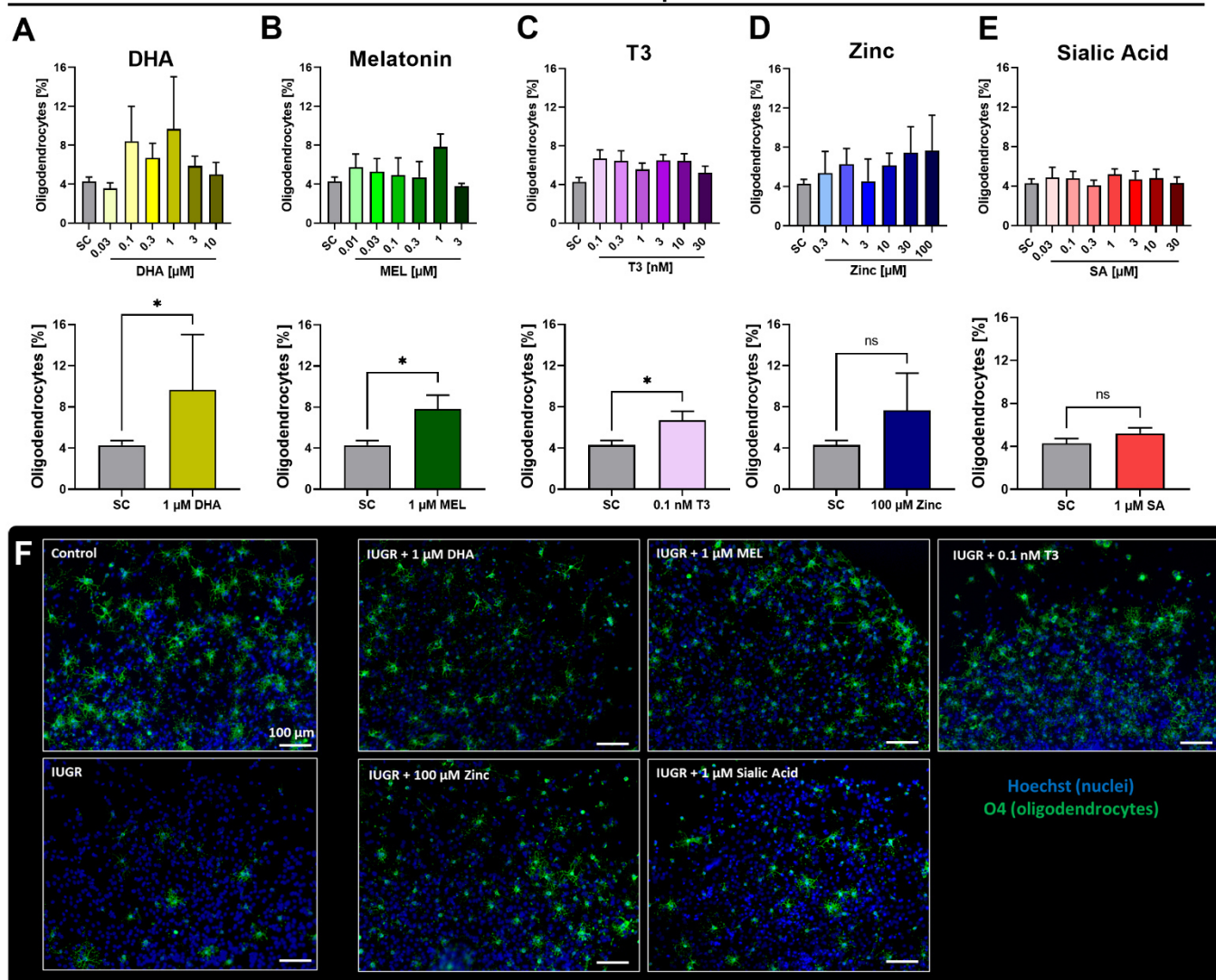


**Figure 4.** Effective concentrations of potential therapies in IUGR neurospheres. Rabbit neurospheres obtained from IUGR pups were cultured for 5 days and tested for oligodendrocyte percentage (mean  $\pm$  SEM) with increasing concentrations (upper row) or the most effective concentration (lower row) of (A) DHA, (B) MEL, (C) zinc, (D) T3 and (E) SA. (F) Representative pictures of control and IUGR neurospheres; and of IUGR neurospheres exposed to the most effective concentration of DHA, MEL, T3, zinc and SA. Oligodendrocyte marker O4 (green) and Hoechst 33258 (blue), Scale bar = 100  $\mu$ m. Analysis was evaluated in 5 neurospheres/condition in at least 3 independent experiments. ns: not significant, \*:  $p < 0.05$  vs. solvent control (SC).

Notably, 1  $\mu$ M MEL significantly increased the OL differentiation of NPCs obtained from IUGR pups ( $7.8 \pm 1.3\%$ ) and was set as its most effective concentration (Figure 4B). T3 showed a significant increase of the OL population in IUGR neurospheres with the lowest tested concentration (0.1 nM,  $6.7 \pm 0.9\%$ ). Thus, 0.1 nM T3 was determined as the most effective concentration (Figure 4C). Conversely, none of the tested zinc concentrations (not even the maximum tested concentration of zinc: 100  $\mu$ M,  $7.7 \pm 3.6\%$ ) significantly increased the percentage of O4+ cells compared to the differentiation in IUGR neurospheres. Consequently, we did not consider zinc as a promising therapy to reduce adverse outcomes induced by IUGR (Figure 4D). Additionally, SA did not increase the OL population in IUGR neurospheres at any tested concentration. Figure 4F displays representative pictures of control and IUGR neurospheres, as well as IUGR neurospheres exposed

to the most effective/best concentration of DHA, MEL, T3, zinc and SA. Based on these results, we can conclude that the compounds DHA, MEL and T3 are the most promising ones due to their stimulating effect in OL differentiation.

### 3.3. In Vivo Administration of Selected Therapies

To confirm the in vivo relevance of these results, we selected DHA, MEL and LF for daily administration during pregnancy after IUGR induction until C-section. In this study, T3 was not prioritized due to the higher difficulties this therapy would present in the future when transferred to the clinical field [36]. Although SA, the main metabolite of LF, was not effective in vitro (see Section 3.2), LF was still selected for in vivo administration, because a negative effect of the metabolite in vitro does not exclude a positive effect of the parent compound in vivo. The birth weight of IUGR pups from all treatment groups was significantly reduced compared to control pups in the untreated groups (Table 1), implying that the therapies did not interfere with the birth weight. This means that if a protective effect were detected in one therapy, it could not be assigned to a mere change in growth. Indeed, neurospheres from IUGR pups delivered from rabbits dosed with DHA presented a significantly increased percentage of OLs up to the control value (Figure 5). Whereas the OL population in control neurospheres after dosing with DHA remained on the control level. The cellular metabolic activity and migration were not diminished after DHA treatment (Figure S4). Moreover, the prenatal administration of MEL also significantly promoted the OL differentiation and increased the number of O4+ cells in IUGR cases to the control value (Figure 5). Besides, the viability did not differ significantly from the controls (Figure S4). Finally, our results showed that LF administered to the rabbit carrying control and IUGR pups could not revert the reduced OL population in IUGR cases (Figure 5). In this case, cell viability and migration were also not disturbed (Figure S4). From these results, DHA and MEL were identified as the best therapies among the tested ones, but no difference between them could be detected. The lack of adverse effects of these therapies in migration or viability is a preliminary information on the safety of these potential therapies during neurodevelopment.

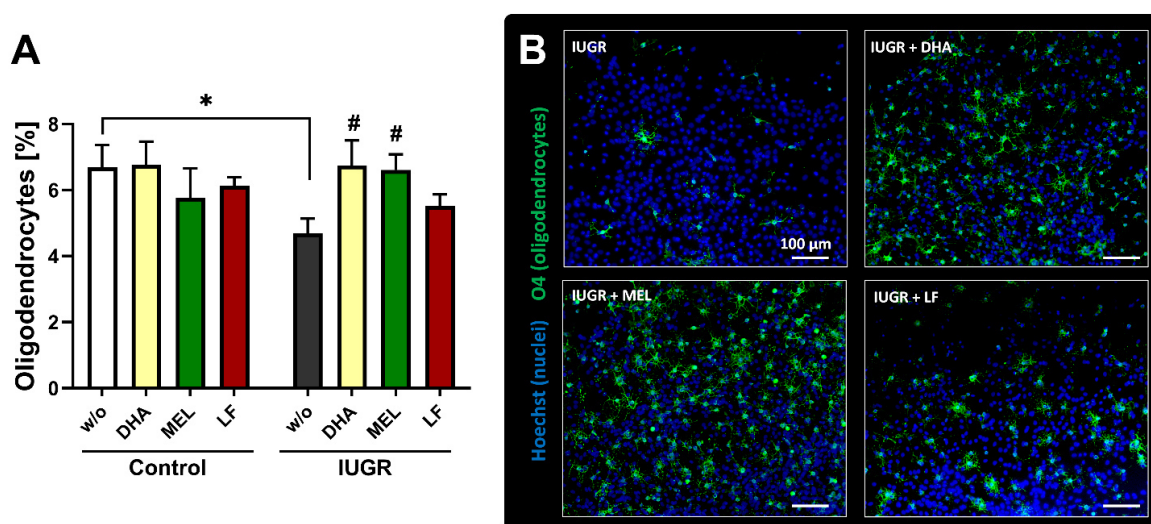


**Figure 5.** In vivo administration of selected therapies. Oligodendrocyte differentiation. Pregnant rabbits were administered to either MEL (10 mg/kg BW/day), DHA (37 mg/kg BW/day) or LF (166 mg/kg BW/day) at the day of IUGR induction until caesarean section. w/o = rabbit does without administered therapy. (A) Neurospheres obtained from control and IUGR pups were tested for % oligodendrocyte differentiation. (B) Representative pictures of IUGR neurospheres w/o and with administered therapies; Oligodendrocyte marker O4 (green) and Hoechst 33258 (blue), Scale bars = 100  $\mu$ m. Analysis was evaluated in 5 neurospheres/condition in at least 3 independent experiments. Mean  $\pm$  SEM; \*  $p < 0.05$  vs. w/o control, #  $p < 0.05$  vs. w/o IUGR.

#### 4. Discussion

In this study, we identified DHA and MEL as the most effective neuroprotective therapies for IUGR-induced oligodendrogenesis alterations. These two therapies were selected among five candidates using an *in vitro* approach, the rabbit neurosphere assay, and confirmed in this model after *in vivo* treatment.

Neurospheres have been used for many years as a model to study central nervous disorders including Alzheimer's, Parkinson's, demyelinating diseases, epilepsy and glioma [19], but it was not until recently that a rabbit and a rabbit IUGR neurosphere model were established [14], opening the door for investigations of the effects of IUGR on cell functions which are characteristic of the developing brain, and to test potential neuroprotective therapies in a more time- and cost-efficient way than traditional *in vivo* studies. The rabbit species was chosen because its brain development occurs largely perinatally, like in humans [14,37,38], whereas the rodent brain develops mainly during the prenatal phase [39]. In our previous studies with the rabbit neurosphere assay, we proved the ability of the model to identify the developmental neurotoxicity of known neurotoxicants like MeHgCl, and by using the IUGR rabbit neurospheres, we identified an adverse impact of IUGR on oligodendrogenesis. In the present study, we further characterized this oligodendrogenesis impairment and have applied the IUGR neurosphere model for drug screening for the first time.

The already identified oligodendrogenesis impairment consisted of a lower percentage of oligodendrocytes after 5 days *in vitro*. As such, we have determined that the main insult emerges already in pre-myelinating O4+ OLs. Our results reveal a significantly lower percentage of O4+ cells at day 4 in culture and a slower OL differentiation rate in IUGR neurospheres compared to control without an increase in specific cell death. Regarding myelination, our findings indicate that only at day 4 is myelination significantly reduced in IUGR neurospheres; however, this difference is only present for a short time in the culture, since 24 h later, the percentage of myelinating OL increases to the control level. This 24 h delay in myelination is in accordance with other studies of induced perinatal hypoxia-ischemia in rodents, indicating a failure of maturation rate in oligodendrocyte progenitor cells (OPC) or pre-myelinating OLs [40–42]. At the final time-point (day 5), maturation was assessed in two ways, *i.e.*, OL morphological analysis and gene expression analysis of *Mbp* and *Mog*. Both methods delivered the same result, with no significant differences in myelination between control and IUGR. Therefore, in this case, these are comparable alternatives with different advantages, *i.e.*, morphological evaluations with no extra cost but increased duration, and gene expression analyses with extra cost but reduced duration. The oligodendrogenesis alterations we found correlate very well with clinical findings indicating that brain damage in IUGR infants is related to white matter injury in its diffuse form, as this injury is associated with a selective vulnerability of the OL lineage [40,43]. Back et al. described it as a differentiation failure of newly generated pre-OLs, because these are especially susceptible to free radicals while later OL stages appear to be more resistant [40]. Other studies in primary rat OPC cultures with induced oxidative stress found that the expression of genes stimulating OL differentiation was downregulated, while the expression of genes inhibiting OL differentiation was upregulated [43]. Based on our results, potential neuroprotective therapies were devised to prevent this selective OL lower differentiation and not focus on increasing the OL myelination status, since this effect disappeared spontaneously after 24 h in our culture.

Potential neuroprotective therapies are required to be effective after a short treatment period, since late-onset IUGR is the most frequent IUGR-type, with an incidence of 70–80% of IUGR cases [44]. In these cases, there is often only a small time window between identification of the risk and intervention leading to a reduced opportunity for prevention/correction [45]. Nowadays the common clinical approach is induced delivery because no effective therapy for IUGR has been established to date [45,46]. Our neurosphere model reflects an IUGR condition induced at a late stage of pregnancy [14,15], and therefore, is a useful preclinical technique for the screening of new antenatal neuroprotective therapies.

Based on literature research, we selected five potential therapies to overcome IUGR-induced brain insult (DHA, MEL, T3, Zinc, and LF), and for all of them, we characterized the MTC in rabbit neurospheres in vitro. Among these five potential therapies, DHA (1  $\mu$ M) and MEL (1  $\mu$ M) could revert the reduced level of O4+ cells in vitro and were able to prevent pathological effects secondary to IUGR by administration during rabbit's pregnancy (37 mg/kg BW/day and 10 mg/kg BW/day, respectively).

DHA, an omega-3 fatty acid, is delivered maternally through uteroplacental circulation and is a key component of brain membrane phospholipids [23,24]. It is critical to fetal central nervous system growth and development; however, the majority of pregnant women do not consume an adequate amount of omega-3 fatty acids on a regular basis [22]. Maternal DHA supplementation in a rat model prevented neonatal brain injury by reducing oxidative stress and apoptotic neuronal death [47]. Other studies support the hypothesis that DHA enhances the differentiation of OL progenitors into mature OL in demyelinating diseases [48]. Several clinical studies have already been performed administering DHA in different forms to pregnant women, aiming to prevent other disorders, e.g., infant cardiac outcomes or depressive symptoms during pregnancy or postpartum, with positive and negative outcomes being reported [49,50]. In either case, no general safety concerns have been identified. Our results, together with this evidence, strongly support the proposal of a clinical trial of DHA administration to pregnant women carrying fetuses with IUGR to prevent white matter IUGR-induced alterations.

MEL is produced in the placenta and ovary, where it works as a free radical scavenger and potent antioxidant and has an essential function in placental homeostasis and fetal maturation [51]. Studies about pregnancies complicated with placental insufficiency revealed a significantly reduced MEL level in maternal blood [52] and significantly reduced expression of MEL receptors in the placenta [53]. In animal studies, MEL improved neurological outcomes in an ovine model [25,54] and a rat model of white matter damage [55,56]. To date, only one pilot clinical trial has been undertaken of oral MEL administration to women with IUGR [25]. Our results reinforce the evidence that MEL is a promising antenatal neuroprotective therapy due to its promoting effect in fetal pre-OL differentiation.

In our study, an in vitro exposure to T3 significantly increased the OL differentiation and the expression of the myelination marker *Mbp* and *Mog* in IUGR neurospheres. This effect is in accordance with increased O4+ cells and myelination in rodent and human neurospheres after T3 exposure [21,57]. However, due to the good results obtained with DHA and MEL, T3 was not prioritized in our study for in vivo maternal administration due to possible complications altering the maternal T3 level, and thus, to expected difficulties in the translation to the clinical field [36,58]. Clinical findings of reduced circulating thyroid hormone concentrations in severe IUGR fetuses prompted further investigations of the potential therapeutic role of peripartum thyroid hormone treatment; however, the reader is referred to the recent review of LaFranchi (2021) [59], which summarizes the mixed results of clinical trials and comments on unresolved questions and the main current areas of controversy surrounding this treatment. Surprisingly, exposure to zinc did not significantly increase the percentage of O4+ cells in IUGR neurospheres (Figure 3). This treatment was discarded for further investigations in the IUGR model, but these results could be useful for other researchers aiming to increase the percentage of O4+ cells in other disease models. Sialic acid, the main metabolite of LF, did not alter OL differentiation in vitro, nor did LF (166 mg/kg BW/day) after maternal treatment in vivo in our study. LF, an iron-binding glycoprotein with antioxidant and anti-inflammatory properties, reportedly supports the growth of neurons, maintains neuronal integrity, and increases neuronal density during brain development [34]. Administered postnatally to rat pups with cerebral hypoxic-ischemic injury, it shows neuroprotective effects on brain metabolism, and cerebral gray and white matter recovery [60]. This notwithstanding, in our model, no protective effect was observed after in vitro or in vivo treatment, perhaps due

to the shorter treatment period, to the earlier evaluation time-point or the different end-points measured.

Overall, it is remarkable that the *in vitro* rabbit neurosphere assay recently established by our group [14] predicted, in all of the studied endpoints, the *in vivo* outcome of the tested potential neuroprotective candidates, for both positive and negative effects. The good agreement of the *in vitro* and *in vivo* treatments increases the reliability of the model and supports its use for further drug screening. In future studies, it will be important to measure the impact and safety of the tested therapies not only in oligodendrogenesis, but also on neuronal differentiation in IUGR and control neurospheres, as well as their safety in terms of general developmental parameters.

## 5. Conclusions

Using the rabbit IUGR neurosphere model, we demonstrated an adverse impact of IUGR on the differentiation rate of pre-myelinating O4+ OL and identified two therapies, *i.e.*, DHA, and MEL, which are able to revert the reduced OL percentage in rabbits *in vitro* and prevent the impairment *in vivo* by maternal administration during pregnancy.

**Supplementary Materials:** The following supporting information can be downloaded at: <https://www.mdpi.com/article/10.3390/biomedicines10051205/s1>, [61–65]. Figure S1: Viability of control and IUGR neurospheres; Figure S2: Maximum tolerated concentrations of lactoferrin; Figure S3: Viability and migration of IUGR neurospheres; Figure S4: *In vivo* administration of selected therapies. Viability and Migration distance; Table S1: Summary of the literature supporting the selection of the five potential therapies; Table S2: Primer sequences 5'–3' designed with NCBI Blast Primer design; SM1: *In vivo* treatment calculations and supplier; SM2: qRT-PCR.

**Author Contributions:** Conceptualization, B.A.K., E.G., M.I. and M.B.; methodology, B.A.K., L.P., M.I. and M.B.; validation, B.A.K., P.V.-A. and M.F.-A.; formal analysis, B.A.K., P.V.-A., M.F.-A. and M.B.; investigation, B.A.K., P.V.-A. and M.F.-A.; resources, J.G.-C., E.G., M.I. and M.B.; data curation, B.A.K., P.V.-A., M.F.-A., L.P. and C.L.; writing—original draft preparation, B.A.K. and M.B.; writing—review and editing, B.A.K., P.V.-A., M.F.-A., L.P., J.G.-C., E.G., M.I. and M.B.; visualization, B.A.K., M.I. and M.B.; supervision, M.I. and M.B.; project administration, B.A.K., M.I. and M.B.; funding acquisition, E.G. and M.I. All authors have read and agreed to the published version of the manuscript.

**Funding:** This study has been funded by Instituto de Salud Carlos III through the project “PI18/01763” (Co-funded by European Regional Development Fund/European Social Fund “A way to make Europe”), from “LaCaixa” Foundation under grant agreements LCF/PR/GN14/10270005 and LCF/PR/GN18/10310003, and from AGAUR under grant 2017 SGR n° 1531. B.A.K. received a scholarship from Fundació Bosch i Gimpera (project number: 300155).

**Institutional Review Board Statement:** All animal experimentation procedures were approved by the Ethics Committee for Animal Experimentation (CEEAA) of the University of Barcelona. All protocols were accepted by the Department of Environment and Housing of the Generalitat de Catalunya with the license number: 11126, date of approval 24 May 2021, and the procedure CEEA number OB 340/19 SJD.

**Informed Consent Statement:** Not applicable.

**Data Availability Statement:** The data that support the findings of this study are available from the corresponding author upon reasonable request.

**Acknowledgments:** Graphical abstract and Figure 1 were created with BioRender.com (accessed on 20 May 2022, license number: SZ23XTEBMR). C.L. received the support the Health Department of the Catalan Government (grant n° SLT006/17/00325).

**Conflicts of Interest:** The authors declare no conflict of interest.

## References

1. Mwaniki, M.K.; Atieno, M.; Lawn, J.E.; Newton, C.R. Long-term neurodevelopmental outcomes after intrauterine and neonatal insults: A systematic review. *Lancet* **2012**, *379*, 445–452. [https://doi.org/10.1016/s0140-6736\(11\)61577-8](https://doi.org/10.1016/s0140-6736(11)61577-8).
2. Kady, S.M.; Gardosi, J. Perinatal mortality and fetal growth restriction. *Best Pract. Res. Clin. Obstet. Gynaecol.* **2004**, *18*, 397–410. <https://doi.org/10.1016/j.bpobgyn.2004.02.009>.
3. Esteban, F.J.; Padilla, N.; Sanz-Cortes, M.; de Miras, J.R.; Bargallo, N.; Villoslada, P.; Gratacos, E. Fractal-dimension analysis detects cerebral changes in preterm infants with and without intrauterine growth restriction. *NeuroImage* **2010**, *53*, 1225–1232. <https://doi.org/10.1016/j.neuroimage.2010.07.019>.
4. Pla, L.; Illa, M.; Loreiro, C.; Lopez, M.C.; Vázquez-Aristizabal, P.; Kühne, B.A.; Barenys, M.; Eixarch, E.; Gratacós, E. Structural Brain Changes during the Neonatal Period in a Rabbit Model of Intrauterine Growth Restriction. *Dev. Neurosci.* **2020**, *42*, 217–229. <https://doi.org/10.1159/000512948>.
5. Reid, M.V.; Murray, K.A.; Marsh, E.D.; Golden, J.A.; Simmons, R.A.; Grinspan, J.B. Delayed Myelination in an Intrauterine Growth Retardation Model Is Mediated by Oxidative Stress Upregulating Bone Morphogenetic Protein 4. *J. Neuropathol. Exp. Neurol.* **2012**, *71*, 640–653. <https://doi.org/10.1097/nen.0b013e31825cfa81>.
6. Novais, A.R.B.; Pham, H.; van de Looij, Y.; Bernal, M.; Mairesse, J.; Zana-Taieb, E.; Colella, M.; Jarreau, P.-H.; Pansiot, J.; Dumont, F.; et al. Transcriptomic regulations in oligodendroglial and microglial cells related to brain damage following fetal growth restriction. *Glia* **2016**, *64*, 2306–2320. <https://doi.org/10.1002/glia.23079>.
7. Eixarch, E.; Bataille, D.; Illa, M.; Muñoz-Moreno, E.; Arbat-Plana, A.; Amat-Roldan, I.; Figueras, F.; Gratacos, E. Neonatal Neurobehavior and Diffusion MRI Changes in Brain Reorganization Due to Intrauterine Growth Restriction in a Rabbit Model. *PLoS ONE* **2012**, *7*, e31497. <https://doi.org/10.1371/journal.pone.0031497>.
8. Tolcos, M.; Bateman, E.; O'Dowd, R.; Markwick, R.; Vrijzen, K.; Rehn, A.; Rees, S. Intrauterine growth restriction affects the maturation of myelin. *Exp. Neurol.* **2011**, *232*, 53–65. <https://doi.org/10.1016/j.expneurol.2011.08.002>.
9. Abel, K.M.; Dalman, C.; Svensson, A.C.; Susser, E.; Dal, H.; Idring, S.; Webb, R.T.; Rai, D.; Magnusson, C. Deviance in Fetal Growth and Risk of Autism Spectrum Disorder. *Am. J. Psychiatry* **2013**, *170*, 391–398. <https://doi.org/10.1176/appi.ajp.2012.12040543>.
10. Leitner, Y.; Fattal-Valevski, A.; Geva, R.; Eshel, R.; Toledano-Alhadeef, H.; Rotstein, M.; Bassan, H.; Radianu, B.; Bitchonsky, O.; Jaffa, A.J.; et al. Neurodevelopmental Outcome of Children with Intrauterine Growth Retardation: A Longitudinal, 10-Year Prospective Study. *J. Child Neurol.* **2007**, *22*, 580–587. <https://doi.org/10.1177/0883073807302605>.
11. Illa, M.; Eixarch, E.; Bataille, D.; Arbat-Plana, A.; Muñoz-Moreno, E.; Figueras, F.; Gratacos, E. Long-Term Functional Outcomes and Correlation with Regional Brain Connectivity by MRI Diffusion Tractography Metrics in a Near-Term Rabbit Model of Intrauterine Growth Restriction. *PLoS ONE* **2013**, *8*, e76453. <https://doi.org/10.1371/journal.pone.0076453>.
12. Fleiss, B.; Wong, F.; Brownfoot, F.; Shearer, I.K.; Baud, O.; Walker, D.W.; Gressens, P.; Tolcos, M. Knowledge Gaps and Emerging Research Areas in Intrauterine Growth Restriction-Associated Brain Injury. *Front. Endocrinol.* **2019**, *10*, 188. <https://doi.org/10.3389/fendo.2019.00188>.
13. Tolcos, M.; Petratos, S.; Hirst, J.J.; Wong, F.; Spencer, S.J.; Azhan, A.; Emery, B.; Walker, D.W. Blocked, delayed, or obstructed: What causes poor white matter development in intrauterine growth restricted infants? *Prog. Neurobiol.* **2017**, *154*, 62–77. <https://doi.org/10.1016/j.pneurobio.2017.03.009>.
14. Barenys, M.; Illa, M.; Hofrichter, M.; Loreiro, C.; Pla, L.; Klose, J.; Kühne, B.A.; Gómez-Catalán, J.; Braun, J.M.; Crispi, F.; et al. Rabbit neurospheres as a novel in vitro tool for studying neurodevelopmental effects induced by intrauterine growth restriction. *STEM CELLS Transl. Med.* **2021**, *10*, 209–221. <https://doi.org/10.1002/sctm.20-0223>.
15. Eixarch, E.; Figueras, F.; Hernández-Andrade, E.; Crispi, F.; Nadal, A.; Torre, I.; Oliveira, S.; Gratacos, E. An Experimental Model of Fetal Growth Restriction Based on Selective Ligation of Uteroplacental Vessels in the Pregnant Rabbit. *Fetal Diagn. Ther.* **2009**, *26*, 203–211. <https://doi.org/10.1159/000264063>.
16. Eixarch, E.; Hernandez-Andrade, E.; Crispi, F.; Illa, M.; Torre, I.; Figueras, F.; Gratacos, E. Impact on fetal mortality and cardiovascular Doppler of selective ligation of uteroplacental vessels compared with undernutrition in a rabbit model of intrauterine growth restriction. *Placenta* **2011**, *32*, 304–309. <https://doi.org/10.1016/j.placenta.2011.01.014>.
17. Baumann, J.; Barenys, M.; Gassmann, K.; Fritsche, E. Comparative Human and Rat “Neurosphere Assay” for Developmental Neurotoxicity Testing. *Curr. Protoc. Toxicol.* **2014**, *59*, 12–21.
18. Moors, M.; Rockel, T.D.; Abel, J.; Cline, J.E.; Gassmann, K.; Schreiber, T.; Schuwald, J.; Weinmann, N.; Fritsche, E. Human Neurospheres as Three-Dimensional Cellular Systems for Developmental Neurotoxicity Testing. *Environ. Health Perspect.* **2009**, *117*, 1131–1138. <https://doi.org/10.1289/ehp.0800207>.
19. Siqueira, L.D.S.; Majolo, F.; da Silva, A.P.B.; da Costa, J.C.; Marinowic, D.R. Neurospheres: A potential in vitro model for the study of central nervous system disorders. *Mol. Biol. Rep.* **2021**, *48*, 3649–3663. <https://doi.org/10.1007/s11033-021-06301-4>.
20. Masjosthusmann, S.; Siebert, C.; Hübenthal, U.; Bendt, F.; Baumann, J.; Fritsche, E. Arsenite interrupts neurodevelopmental processes of human and rat neural progenitor cells: The role of reactive oxygen species and species-specific antioxidative defense. *Chemosphere* **2019**, *235*, 447–456. <https://doi.org/10.1016/j.chemosphere.2019.06.123>.

21. Dach, K.; Bendt, F.; Huebenthal, U.; Giersiefer, S.; Lein, P.; Heuer, H.; Fritsche, E. BDE-99 impairs differentiation of human and mouse NPCs into the oligodendroglial lineage by species-specific modes of action. *Sci. Rep.* **2017**, *7*, srep44861. <https://doi.org/10.1038/srep44861>.
22. Greenberg, J.A.; Bell, S.J.; Ausdal, W. Van Omega-3 Fatty Acid Supplementation during Pregnancy. *Rev. Obstet. Gynecol.* **2008**, *1*, 162–169.
23. Gil-Sánchez, A.; Larqué, E.; Demmelmair, H.; Acien, M.I.; Faber, F.L.; Parrilla, J.J.; Koletzko, B. Maternal-fetal in vivo transfer of [<sup>13</sup>C]docosahexaenoic and other fatty acids across the human placenta 12 h after maternal oral intake. *Am. J. Clin. Nutr.* **2010**, *92*, 115–122. <https://doi.org/10.3945/ajcn.2010.29589>.
24. Lauritzen, L.; Brambilla, P.; Mazzocchi, A.; Harsløf, L.B.S.; Ciappolino, V.; Agostoni, C. DHA Effects in Brain Development and Function. *Nutrients* **2016**, *8*, 6. <https://doi.org/10.3390/nu8010006>.
25. Miller, S.L.; Yawno, T.; Alers, N.O.; Castillo-Melendez, M.; Supramaniam, V.G.; Vanzyl, N.; Sabaretnam, T.; Loose, J.M.; Drummond, G.R.; Walker, D.W.; et al. Antenatal antioxidant treatment with melatonin to decrease newborn neurodevelopmental deficits and brain injury caused by fetal growth restriction. *J. Pineal Res.* **2014**, *56*, 283–294. <https://doi.org/10.1111/jpi.12121>.
26. Nuttall, J.R.; Oteiza, P.I. Zinc and the ERK Kinases in the Developing Brain. *Neurotox. Res.* **2012**, *21*, 128–141. <https://doi.org/10.1007/s12640-011-9291-6>.
27. Adamo, A.M.; Oteiza, P.I. Zinc deficiency and neurodevelopment: The case of neurons. *BioFactors* **2010**, *36*, 117–124. <https://doi.org/10.1002/biof.91>.
28. Ladd, F.V.L.; Ladd, A.A.B.L.; Ribeiro, A.A.C.M.; Costa, S.B.C.; Coutinho, B.P.; Feitosa, G.A.S.; de Andrade, G.M.; de Castro-Costa, C.M.; Magalhães, C.E.C.; Castro, I.C.; et al. Zinc and glutamine improve brain development in suckling mice subjected to early postnatal malnutrition. *Nutrition* **2010**, *26*, 662–670. <https://doi.org/10.1016/j.nut.2009.11.020>.
29. Mathur, N.B.; Agarwal, D.K. Zinc supplementation in preterm neonates and neurological development: A randomized controlled trial. *Indian Pediatr.* **2015**, *52*, 951–955. <https://doi.org/10.1007/s13312-015-0751-6>.
30. Fernández, M.; Paradisi, M.; Del Vecchio, G.; Giardino, L.; Calzà, L. Thyroid hormone induces glial lineage of primary neurospheres derived from non-pathological and pathological rat brain: Implications for remyelination-enhancing therapies. *Int. J. Dev. Neurosci.* **2009**, *27*, 769–778. <https://doi.org/10.1016/j.ijdevneu.2009.08.011>.
31. Baud, O.; Berkane, N. Hormonal Changes Associated with Intra-Uterine Growth Restriction: Impact on the Developing Brain and Future Neurodevelopment. *Front. Endocrinol.* **2019**, *10*, 179. <https://doi.org/10.3389/fendo.2019.00179>.
32. Bernal, J. Thyroid Hormones and Brain Development. *Vitam. Horm.* **2005**, *71*, 95–122. [https://doi.org/10.1016/s0083-6729\(05\)71004-9](https://doi.org/10.1016/s0083-6729(05)71004-9).
33. van de Looij, Y.; Larpin, C.; Cabungcal, J.-H.; Sanches, E.F.; Toulotte, A.; Do, K.Q.; Sizonenko, S.V. Nutritional Intervention for Developmental Brain Damage: Effects of Lactoferrin Supplementation in Hypocaloric Induced Intrauterine Growth Restriction Rat Pups. *Front. Endocrinol.* **2019**, *10*, 46. <https://doi.org/10.3389/fendo.2019.00046>.
34. Wang, B. Molecular Determinants of Milk Lactoferrin as a Bioactive Compound in Early Neurodevelopment and Cognition. *J. Pediatr.* **2016**, *173*, S29–S36. <https://doi.org/10.1016/j.jpeds.2016.02.073>.
35. Baumann, N.; Pham-Dinh, D. Biology of Oligodendrocyte and Myelin in the Mammalian Central Nervous System. *Physiol. Rev.* **2001**, *81*, 871–927. <https://doi.org/10.1152/physrev.2001.81.2.871>.
36. Fumarola, A.; Di Fiore, A.; Dainelli, M.; Grani, G.; Carbotta, G.; Calvanese, A. Therapy of Hyperthyroidism in Pregnancy and Breastfeeding. *Obstet. Gynecol. Surv.* **2011**, *66*, 378–385. <https://doi.org/10.1097/ogx.0b013e31822c6388>.
37. Drobyshevsky, A.; Jiang, R.; Derrick, M.; Luo, K.; Tan, S. Functional correlates of central white matter maturation in perinatal period in rabbits. *Exp. Neurol.* **2014**, *261*, 76–86. <https://doi.org/10.1016/j.expneurol.2014.06.021>.
38. Workman, A.D.; Charvet, C.J.; Clancy, B.; Darlington, R.B.; Finlay, B.L. Modeling Transformations of Neurodevelopmental Sequences across Mammalian Species. *J. Neurosci.* **2013**, *33*, 7368–7383. <https://doi.org/10.1523/jneurosci.5746-12.2013>.
39. Chini, M.; Hanganu-Opatz, I.L. Prefrontal Cortex Development in Health and Disease: Lessons from Rodents and Humans. *Trends Neurosci.* **2021**, *44*, 227–240. <https://doi.org/10.1016/j.tins.2020.10.017>.
40. Back, S.A. White matter injury in the preterm infant: Pathology and mechanisms. *Acta Neuropathol.* **2017**, *134*, 331–349. <https://doi.org/10.1007/s00401-017-1718-6>.
41. Back, S.A.; Luo, N.L.; Borenstein, N.S.; Volpe, J.J.; Kinney, H.C. Arrested Oligodendrocyte Lineage Progression During Human Cerebral White Matter Development: Dissociation Between the Timing of Progenitor Differentiation and Myelination. *J. Neuropathol. Exp. Neurol.* **2002**, *61*, 197–211. <https://doi.org/10.1093/jnen/61.2.197>.
42. Segovia, K.N.; McClure, M.; Moravec, M.; Luo, N.L.; Wan, Y.; Gong, X.; Riddle, A.; Craig, A.; Struve, J.; Sherman, L.S.; et al. Arrested oligodendrocyte lineage maturation in chronic perinatal white matter injury. *Ann. Neurol.* **2008**, *63*, 520–530. <https://doi.org/10.1002/ana.21359>.
43. French, H.M.; Reid, M.; Mamontov, P.; Simmons, R.A.; Grinspan, J.B. Oxidative stress disrupts oligodendrocyte maturation. *J. Neurosci. Res.* **2009**, *87*, 3076–3087. <https://doi.org/10.1002/jnr.22139>.
44. Figueras, F.; Caradeux, J.; Crispi, F.; Eixarch, E.; Peguero, A.; Gratacos, E. Diagnosis and surveillance of late-onset fetal growth restriction. *Am. J. Obstet. Gynecol.* **2018**, *218*, S790–S802.e1. <https://doi.org/10.1016/j.ajog.2017.12.003>.
45. Figueras, F.; Gratacos, E. An integrated approach to fetal growth restriction. *Best Pract. Res. Clin. Obstet. Gynaecol.* **2017**, *38*, 48–58. <https://doi.org/10.1016/j.bpobgyn.2016.10.006>.

46. Maršál, K. Obstetric management of intrauterine growth restriction. *Best Pract. Res. Clin. Obstet. Gynaecol.* **2009**, *23*, 857–870. <https://doi.org/10.1016/j.bpobgyn.2009.08.011>.
47. Sukanuma, H.; Arai, Y.; Kitamura, Y.; Hayashi, M.; Okumura, A.; Shimizu, T. Maternal docosahexaenoic acid-enriched diet prevents neonatal brain injury. *Neuropathology* **2010**, *30*, 597–605. <https://doi.org/10.1111/j.1440-1789.2010.01114.x>.
48. Bernardo, A.; Giammarco, M.L.; De Nuccio, C.; Ajmone-Cat, M.A.; Visentin, S.; De Simone, R.; Minghetti, L. Docosahexaenoic acid promotes oligodendrocyte differentiation via PPAR- $\gamma$  signalling and prevents tumor necrosis factor- $\alpha$ -dependent maturational arrest. *Biochim. et Biophys. Acta (BBA)—Mol. Cell Biol. Lipids* **2017**, *1862*, 1013–1023. <https://doi.org/10.1016/j.bbalip.2017.06.014>.
49. Gustafson, K.M.; Carlson, S.E.; Colombo, J.; Yeh, H.-W.; Shaddy, D.J.; Li, S.; Kerling, E.H. Effects of docosahexaenoic acid supplementation during pregnancy on fetal heart rate and variability: A randomized clinical trial. *Prostaglandins Leukot. Essent. Fat. Acids* **2013**, *88*, 331–338. <https://doi.org/10.1016/j.plefa.2013.01.009>.
50. Mozurkewich, E.L.; Clinton, C.M.; Chilimigras, J.L.; Hamilton, S.E.; Allbaugh, L.J.; Berman, D.R.; Marcus, S.M.; Romero, V.C.; Treadwell, M.C.; Keeton, K.L.; et al. The Mothers, Omega-3, and Mental Health Study: A double-blind, randomized controlled trial. *Am. J. Obstet. Gynecol.* **2013**, *208*, 313.e1–313.e9. <https://doi.org/10.1016/j.ajog.2013.01.038>.
51. Reiter, R.J.; Tan, D.X.; Korkmaz, A.; Rosales-Corral, S.A. Melatonin and stable circadian rhythms optimize maternal, placental and fetal physiology. *Hum. Reprod. Update* **2014**, *20*, 293–307. <https://doi.org/10.1093/humupd/dmt054>.
52. Berbets, A. Melatonin, placental growth factor and placental hormones at placental insufficiency. *Cell Organ Transpl.* **2019**, *7*, 103–107. <https://doi.org/10.22494/cot.v7i2.98>.
53. Berbets, A.M.; Davydenko, I.S.; Barbe, A.M.; Konkov, D.H.; Albota, O.M.; Yuzko, O.M. Melatonin 1A and 1B Receptors' Expression Decreases in the Placenta of Women with Fetal Growth Restriction. *Reprod. Sci.* **2021**, *28*, 197–206. <https://doi.org/10.1007/s43032-020-00285-5>.
54. Castillo-Melendez, M.; Yawno, T.; Sutherland, A.; Jenkin, G.; Wallace, E.M.; Miller, S.L. Effects of Antenatal Melatonin Treatment on the Cerebral Vasculature in an Ovine Model of Fetal Growth Restriction. *Dev. Neurosci.* **2017**, *39*, 323–337. <https://doi.org/10.1159/000471797>.
55. Olivier, P.; Fontaine, R.H.; Loron, G.; Van Steenwinckel, J.; Biran, V.; Massonneau, V.; Kaindl, A.; Dalous, J.; Charriaut-Marlangue, C.; Aigrot, M.-S.; et al. Melatonin Promotes Oligodendroglial Maturation of Injured White Matter in Neonatal Rats. *PLoS ONE* **2009**, *4*, e7128. <https://doi.org/10.1371/journal.pone.0007128>.
56. Palmer, K.R.; Mockler, J.C.; Davies-Tuck, M.L.; Miller, S.L.; Goergen, S.K.; Fahey, M.C.; Anderson, P.J.; Groom, K.M.; Wallace, E.M. Protect-me: A parallel-group, triple blinded, placebo-controlled randomised clinical trial protocol assessing antenatal maternal melatonin supplementation for fetal neuroprotection in early-onset fetal growth restriction. *BMJ Open* **2019**, *9*, e028243. <https://doi.org/10.1136/bmjopen-2018-028243>.
57. Klose, J.; Pahl, M.; Bartmann, K.; Bendt, F.; Blum, J.; Dolde, X.; Förster, N.; Holzer, A.-K.; Hübenenthal, U.; Keßel, H.E.; et al. Neurodevelopmental toxicity assessment of flame retardants using a human DNT in vitro testing battery. *Cell Biol. Toxicol.* **2021**, *5*, 1–45. <https://doi.org/10.1007/s10565-021-09603-2>.
58. Kilby, M.D.; Gittoes, N.; McCabe, C.; Verhaeg, J.; Franklyn, J.A. Expression of thyroid receptor isoforms in the human fetal central nervous system and the effects of intrauterine growth restriction. *Clin. Endocrinol.* **2000**, *53*, 469–477. <https://doi.org/10.1046/j.1365-2265.2000.01074.x>.
59. LaFranchi, S.H. Thyroid Function in Preterm/Low Birth Weight Infants: Impact on Diagnosis and Management of Thyroid Dysfunction. *Front. Endocrinol.* **2021**, *12*, 371. <https://doi.org/10.3389/fendo.2021.666207>.
60. van de Looij, Y.; Ginet, V.; Chatagner, A.; Toulotte, A.; Somm, E.; Hüppi, P.S.; Sizonenko, S.V. Lactoferrin during lactation protects the immature hypoxic-ischemic rat brain. *Ann. Clin. Transl. Neurol.* **2014**, *1*, 955–967. <https://doi.org/10.1002/acn3.138>.
61. Bashmakov, Y.K.; Petyaev, I.M.; Chalyk, N.E.; Klochkov, V.A.; Pristensky, D.V.; Chernyshova, M.P.; Kyle, N.H. Pharmacokinetics and oxidation parameters in volunteers supplemented with microencapsulated docosahexaenoic acid. *Int. J. Appl. Basic Med. Res.* **2018**, *8*, 148–154. [https://doi.org/10.4103/ijabmr.ijabmr\\_367\\_17](https://doi.org/10.4103/ijabmr.ijabmr_367_17).
62. Harpsøe, N.G.; Andersen, L.P.H.; Gögenur, I.; Rosenberg, J. Clinical pharmacokinetics of melatonin: A systematic review. *Eur. J. Clin. Pharmacol.* **2015**, *71*, 901–909. <https://doi.org/10.1007/s00228-015-1873-4>.
63. Gonzalez-Candia, A.; Veliz, M.; Araya, C.; Quezada, S.; Ebensperger, G.; Serón-Ferré, M.; Reyes, R.V.; Llanos, A.J.; Herrera, E.A. Potential adverse effects of antenatal melatonin as a treatment for intrauterine growth restriction: Findings in pregnant sheep. *Am. J. Obstet. Gynecol.* **2016**, *215*, 245.e1–245.e7. <https://doi.org/10.1016/j.ajog.2016.02.040>.
64. Nair, A.B.; Jacob, S. A simple practice guide for dose conversion between animals and human. *J. Basic Clin. Pharm.* **2016**, *7*, 27–31. <https://doi.org/10.4103/0976-0105.177703>.
65. Zehnder, A.M.; Hawkins, M.G.; Trestrail, E.A.; Holt, R.W.; Kent, M.S. Calculation of body surface area via computed tomography-guided modeling in domestic rabbits (*Oryctolagus cuniculus*). *Am. J. Veter Res.* **2012**, *73*, 1859–1863. <https://doi.org/10.2460/ajvr.73.12.1859>.



#### 4.4 Lactoferrin prevents adverse effects of intrauterine growth restriction (IUGR) on neurite length: investigations in an in vitro rabbit neurosphere model

**Britta Anna Kühne**<sup>1,2</sup>, Lara Gutiérrez Vázquez<sup>1</sup>, Estela Sánchez Lamelas<sup>1</sup>, Laia Guardia-Escote<sup>1</sup>, Laura Pla<sup>2</sup>, Carla Loreiro<sup>2,3</sup>, Eduard Gratacós<sup>2,3,4</sup>, Marta Barenys<sup>1,†</sup> and Miriam Illa<sup>\*,2,5,†</sup>

<sup>1</sup> Grup de Recerca en Toxicologia (GRET) i INSA-UB, Departament de Farmacologia, Toxicologia i Química Terapèutica, Facultat de Farmàcia i Ciències de l'Alimentació, Universitat de Barcelona, 08028 Barcelona, Spain

<sup>2</sup> BCNatal | Fetal Medicine Research Center (Hospital Clínic and Hospital Sant Joan de Déu), Universitat de Barcelona, 08028 Barcelona, Spain

<sup>3</sup> Institut d'Investigacions Biomèdiques August Pi i Sunyer (IDIBAPS), 08036 Barcelona, Spain

<sup>4</sup> Center for Biomedical Research on Rare Diseases (CIBER-ER), 08036 Barcelona, Spain

<sup>5</sup> Institut de Recerca Sant Joan de Déu, 08950 Esplugues de Llobregat, Spain

<sup>†</sup> These authors contributed equally to this work and share last authorship

\* Correspondence: Dr. Miriam Illa

|                       |                                    |
|-----------------------|------------------------------------|
| Journal               | Frontiers in cellular neuroscience |
| Impact Factor 2020    | 5.505                              |
| Quartile              | Q1 in Neurosciences                |
| Type of authorship    | First Author                       |
| Status of publication | To be submitted                    |

## Summary

We aimed to characterize alterations in neuronal development in fetuses complicated with intrauterine growth restriction (IUGR) and to discover strategies to ameliorate adverse neurodevelopment effects by using a recently established rabbit *in vitro* neurosphere culture. IUGR was surgically induced in pregnant rabbits by ligation of placental vessels in one uterine horn, while the contralateral horn remained as control. At this timepoint, rabbits were randomly assigned to receive either no treatment, docosahexaenoic acid (DHA), melatonin (MEL), or lactoferrin (LF) until C-section. Neurospheres consisting of neural progenitor cells were obtained from control and IUGR pups and comparable analyzed for the ability to differentiate into neurons, extent neurite length, form dendritic branching or synapses. We established for the very first time a protocol to cultivate control and IUGR rabbit neurospheres not only for 5 days but under long-term conditions up to 14 days under differentiation conditions. We revealed that IUGR significantly increased the neurite length after 5 days cultivation *in vitro*. This result agrees with previous *in vivo* results from our group: IUGR rabbits presented a more complex dendritic arborization of neurons in the frontal cortex. MEL, DHA, and sialic acid (SA) the main metabolite of LF, were exposed *in vitro* to neurospheres obtained from untreated rabbit mums. MEL, DHA, and SA decreased the IUGR-induced length of primary dendrites, however, only SA was able to reduce the total neurite length to control level in IUGR neurospheres. SA's parent compound LF was able to prevent abnormal neurite extension after prenatal administration *in vivo* and was therefore identified as the most promising therapy against IUGR induced adverse outcome on neuronal development.

# Lactoferrin prevents adverse effects of intrauterine growth restriction (IUGR) on neurite length: investigations in an *in vitro* rabbit neurosphere model

Running title: Lactoferrin prevents IUGR induced neurite length

**Britta Anna Kühne**<sup>1,2</sup>, **Lara Gutiérrez Vázquez**<sup>1</sup>, **Estela Sánchez Lamelas**<sup>1</sup>, **Laia Guardia-Escote**<sup>1</sup>, **Laura Pla**<sup>2</sup>, **Carla Loreiro**<sup>2,3</sup>, **Eduard Gratacós**<sup>2,3,4</sup>, **Marta Barenys**<sup>1,†</sup> and **Miriam Illa**<sup>2,5,\*</sup>,<sup>†</sup>

<sup>1</sup> Grup de Recerca en Toxicologia (GRET) i INSA-UB, Departament de Farmacologia, Toxicologia i Química Terapèutica, Facultat de Farmàcia i Ciències de l'Alimentació, Universitat de Barcelona, 08028 Barcelona, Spain

<sup>2</sup> BCNatal | Fetal Medicine Research Center (Hospital Clínic and Hospital Sant Joan de Déu), Universitat de Barcelona, 08028 Barcelona, Spain

<sup>3</sup> Institut d'Investigacions Biomèdiques August Pi i Sunyer (IDIBAPS), 08036 Barcelona, Spain

<sup>4</sup> Center for Biomedical Research on Rare Diseases (CIBER-ER), 08036 Barcelona, Spain

<sup>5</sup> Institut de Recerca Sant Joan de Déu, 08950 Esplugues de Llobregat, Spain

† These authors contributed equally to this work and share last authorship

## \* Correspondence:

Dr. Miriam Illa

[miriamil@clinic.cat](mailto:miriamil@clinic.cat)

**Keywords: Fetal Growth Restriction (FGR), Neural Progenitor Cells, Neurogenesis, *in vitro* Techniques, Sialic acid, Melatonin, DHA.**

## 1 Abstract

We aimed to characterize alterations in neuronal development in fetuses complicated with intrauterine growth restriction (IUGR) and to discover strategies to ameliorate adverse neurodevelopment effects by using a recently established rabbit *in vitro* neurosphere culture. IUGR was surgically induced in pregnant rabbits by ligation of placental vessels in one uterine horn, while the contralateral horn remained unaffected for normal growth (control). At this timepoint, rabbits were randomly assigned to receive either no treatment, docosahexaenoic acid (DHA), melatonin (MEL), or lactoferrin (LF) until c-section. Neurospheres consisting of neural progenitor cells were obtained from control and IUGR pups and comparable analyzed for the ability to differentiate into neurons, extent neurite length, form dendritic branching or synapses. We established for the very first time a protocol to cultivate control and IUGR rabbit neurospheres not only for 5 days but under long-

35 term conditions up to 14 days under differentiation conditions. We revealed that IUGR significantly  
36 increased the neurite length after 5 days cultivation *in vitro*. This result agrees with previous *in vivo*  
37 results from our group: IUGR rabbits presented a more complex dendritic arborization of neurons in  
38 the frontal cortex. MEL, DHA, and sialic acid (SA) the main metabolite of LF, were exposed *in vitro*  
39 to neurospheres obtained from untreated rabbit mums. MEL, DHA, and SA decreased the IUGR-  
40 induced length of primary dendrites, however, only SA was able to reduce the total neurite length to  
41 control level in IUGR neurospheres. SA's parent compound LF was able to prevent abnormal neurite  
42 extension after prenatal administration *in vivo* and was therefore identified as the most promising  
43 therapy against IUGR induced adverse outcome on neuronal development.

44

## 45 2 Introduction

46 Intrauterine growth restriction (IUGR) is defined as a significant decrease in fetal growth rate  
47 resulting in a birth weight below the 10<sup>th</sup> percentile of the corresponding gestational age (Sharma,  
48 Shastri and Sharma, 2016). The prevalence accounts for 5-10% of all pregnancies, and amounts to  
49 approximately 600.000 cases in Europe, being therefore a serious health problem (Kady and Gardosi,  
50 2004). Placental insufficiency, the main cause of IUGR, chronically decreases the blood flow and  
51 nutrient supply to the developing fetus resulting in an unfavorable *in utero* environment with chronic  
52 hypoxia conditions. This situation results to a wide range of abnormal trajectories of brain  
53 development including grey (GM) and white matter (WM) injury (Esteban *et al.*, 2010; Pla *et al.*,  
54 2020), which are associated with short- and long-term neurodevelopmental damage and cognitive  
55 dysfunctions (Mwaniki *et al.*, 2012; Bataille *et al.*, 2014; Eixarch *et al.*, 2016). This WM injury is  
56 tightly related to impaired oligodendrocyte development and myelination (Tolcos *et al.*, 2011;  
57 Eixarch *et al.*, 2012; Reid *et al.*, 2012; Rideau Batista Novais *et al.*, 2016), while GM impairment  
58 often emerges from altered neuronal connectivity including irregular neurite and dendritic processes  
59 in cerebellar cortex and hippocampus, as discovered in sheep, guinea pig and rabbit models of IUGR  
60 (Dieni and Rees, 2003; Piorkowska *et al.*, 2014; Pla *et al.*, 2020). Previous investigations of our  
61 group unraveled IUGR induced impaired oligodendrogenesis in an *in vitro* rabbit neurospheres  
62 model, which correlates very well with clinical outcomes of WM injury (Kühne *et al.*, 2022). In the  
63 current study, we have directed our focus on investigating neuronal development using the same  
64 model but studying differentiation of neurons, their neurite outgrowth followed by dendritic  
65 branching and network formation *in vitro*.

66 Currently, there is no efficient neuroprotective treatment to avoid deleterious consequences related to  
67 IUGR (Lees *et al.*, 2022). Several clinical and experimental assessments give evidence that early  
68 postnatal approaches like breastfeeding (Rao *et al.*, 2007), individualized newborn developmental  
69 care and assessment program (Als *et al.*, 2012), and environmental enrichment (Illa *et al.*, 2018) can  
70 partially ameliorate the neurodevelopmental impairment caused by IUGR. However, all these  
71 strategies have been applied after birth, at a time point when adverse effects of IUGR on brain  
72 development have already occurred. We hypothesize that a treatment applied during the prenatal  
73 period, a "critical window of opportunity" (Susan L. Andersen, 2003), is probably more effective.  
74 But to discover efficacious neuroprotective treatments, it is essential to first deepen the understanding  
75 of the mechanisms behind neurostructural changes underlying fetal programming due to IUGR, and  
76 for that, to have a good experimental model is indispensable.

77 Eixarch et al. developed an experimental IUGR model in pregnant rabbits mimicking placental  
78 insufficiency leading to neurodevelopmental symptoms of IUGR which highly correlates with

79 clinical outcomes including postnatal functional and structural discrepancies (Eixarch *et al.*, 2009,  
80 2012). Previous studies using this animal model discovered neonatal as well as long-term persistence  
81 of brain reorganization and changes in cerebral network organization induced by IUGR (Eixarch *et al.*,  
82 2012; Illa *et al.*, 2013; Bataille *et al.*, 2014). These results agreed with clinical investigations that  
83 one year old infants who suffered IUGR also present alterations in structural brain connectivity based  
84 on connectomics studies (Bataille *et al.*, 2012). The species rabbit was selected due to its higher  
85 similarity to human neurodevelopment compared to other species according to a precocial score  
86 established by Workman *et al.* (Workman *et al.*, 2013). Rabbits resemble humans in terms of  
87 circulatory changes during gestation, placentation, and brain maturation which occurs primarily  
88 postnatally in both species (Derrick *et al.*, 2004; Carter, 2007; Workman *et al.*, 2013). Combining  
89 clinical findings with the neurological changes observed in rabbits indicates that the rabbit IUGR  
90 model is a suitable model to assess IUGR-induced alterations in humans (Bassan *et al.*, 2000;  
91 Eixarch *et al.*, 2009, 2011; Barenys *et al.*, 2021). To understand better which basic cellular processes  
92 are altered during brain development under IUGR, our group recently established an *in vitro* model  
93 based on primary rabbit neuronal progenitor cells (NPCs) (Barenys *et al.*, 2021). In this model, rabbit  
94 NPCs obtained from control and IUGR pups are cultured as three-dimensional (3D) cell aggregates  
95 known as neurospheres. Neurospheres are able to imitate basic courses of brain development such as  
96 NPC proliferation, migration and differentiation into the brain effector cells neurons,  
97 oligodendrocytes and astrocytes (Moors *et al.*, 2007, 2009; Breier *et al.*, 2010; Gassmann *et al.*,  
98 2010; Schreiber *et al.*, 2010; Barenys *et al.*, 2017). Because of its 3D structure encompassing  
99 multiple cell types, the neurosphere model is a valuable test system for studying a wide range of  
100 neurodevelopmental processes guided by a broad variety of cellular pathways (Gassmann *et al.*,  
101 2010, 2014; Baumann *et al.*, 2016; Barenys *et al.*, 2017, 2021; Dach *et al.*, 2017; Masjosthusmann *et al.*,  
102 2019). In a cost-efficient and animal-reducing way, with this system we were able to test a much  
103 wider concentration range of potential therapies *in vitro* compared to classical *in vivo* experiments.  
104 Besides, on the day of IUGR induction, mother animals were administered to potential therapies *in*  
105 *vivo* to subsequently discover prenatal effects of tested compounds in the neurosphere model *in vitro*.  
106 A detailed description of the experimental setup is displayed in Fig. 1.

107 By using the rabbit neurosphere assay, our group revealed previously IUGR-induced adversity on the  
108 differentiation rate of pre-myelinating oligodendrocytes and discovered two therapies,  
109 docosahexaenoic acid (DHA), and melatonin (MEL) reverting the reduced oligodendrocyte  
110 population after *in vitro* exposure and prevent the neurodevelopmental damage after *in vivo*  
111 administration to the pregnant rabbit (Kühne *et al.*, 2022). This previous study, demonstrated that the  
112 novel rabbit *in vitro* neurosphere assay is able to accurately predict the *in vivo* outcome regarding  
113 oligodendrocyte differentiation (Kühne *et al.*, 2022). Besides from improving IUGR- induced  
114 impaired oligodendrogenesis (Kühne *et al.*, 2022), DHA is also described to facilitate myelin  
115 formation, neurotransmitter synthesis, and sustaining synaptogenesis and neuronal network  
116 (Greenberg, Bell and Ausdal, 2008; Gil-Sánchez *et al.*, 2010; Lauritzen *et al.*, 2016), while MEL is  
117 depicted to reduce fetoplacental oxidative stress and white- and grey-matter damage in a sheep model  
118 of placental insufficiency (Rees, Harding and Walker, 2011; Miller *et al.*, 2014). Lactoferrin (LF), a  
119 sialic acid (SA)-rich glycoprotein, was considered as a promising candidate as it enhances neuronal  
120 growth, synaptic connectivity as well as placental development (Lopez, Kelleher and Lönnerdal,  
121 2008; Wang, 2016). We selected MEL, DHA, and LF (or its main metabolite SA *in vitro* due to  
122 limited solubility of LF) due to their promising potential to improve impaired neurogenesis and we  
123 further assessed their safety and efficacy on the neuronal endpoints: Neuron differentiation, neurite  
124 length, number of dendrites per neuron, as well as cell viability.

125

126 **3 Material and methods**

127 **3.1 IUGR induction**

128 All animal experimentation procedures were approved by the Ethics Committee for Animal  
129 Experimentation (CEEAA) of the University of Barcelona. All protocols were accepted by the  
130 Department of Environment and Housing of the Generalitat de Catalunya with the license number  
131 11126, date of approval 24/5/2021, and the procedure CEEA number OB 340/19 SJD. The method of  
132 IUGR induction was previously described in Eixarch et al. (2009). Briefly, IUGR was induced at the  
133 25<sup>th</sup> gestational day (GD) in pregnant New Zealand rabbits by surgical ligation of 40-50% of the  
134 uteroplacental vessels of each gestational sac of one uterine horn, while the contralateral horn was  
135 left for normal growth. Caesarean section was carried out at GD 30 to obtain IUGR and control pups.

136 **3.2 Administration of therapies in vivo**

137 On the day of IUGR induction animals were assigned to 4 different groups: without (w/o)  
138 administration, or with administration of MEL, DHA, or LF. The therapies were daily administered  
139 to the pregnant rabbit by releasing the solution with a syringe in the throat from the day of IUGR  
140 induction (GD 25) until the day of caesarean section (GD 30). Specific doses were determined as  
141 followed: MEL (10 mg /kg bw/day), DHA (37 mg/kg bw/day) and Lf (166 mg/kg bw/day). We refer  
142 to (Kühne *et al.*, 2022) for a detailed description about *in vivo* treatment calculations and supplier.  
143 For all treatment groups, the inclusion criteria for PND0 IUGR pups was a birth weight lower and for  
144 control pups higher than the 25<sup>th</sup> percentile (39.7 g, (Barenys *et al.*, 2021)). The number and birth  
145 weight of PND0 rabbits from each group was equal to the animals described in (Kühne *et al.*, 2022),  
146 briefly 12 control and 10 IUGR pups from the group w/o were included, 2 control and 2 IUGR rabbit  
147 pups were included for each treatment group. 4 independent experiments were performed from one  
148 rabbit pup's brain.

149 **3.3 Neurosphere preparation**

150 The *in vitro* neurosphere culture was generated directly after decapitation at postnatal day 0 (PND0).  
151 Neural progenitor cells (NPCs) were isolated from rabbits' whole brains by dissection, mechanical  
152 dissociation, digestion (20 min incubation with papain 20 U/ml at 37°C), mechanical homogenization  
153 into a cell suspension, and centrifugation (10 min at 1200 rpm). The cell pellet obtained was  
154 resuspended in 1 ml of freezing medium (1:1; volume of pellet: volume of freezing medium  
155 [consisting in 70% (v/v) proliferation medium, 20% (v/v) fetal calf serum and 10% (v/v) DMSO])  
156 and immediately stored at -80°C. Each cryo-vial was thawed by brief immersion in a 37°C water  
157 bath, and cells were transferred to 15 mL of proliferation medium preconditioned at 37°C and 5%  
158 CO<sub>2</sub> for two hours, and gentle resuspension. The cell suspension was centrifuged (10 min, 1200  
159 rpm), supernatant discarded and cells transferred to Poly-HEMA coated dishes filled with  
160 proliferation medium [consisting in DMEM and Hams F12 3:1 supplemented with 2% B27, and 20  
161 ng/ml epidermal growth factor (EGF) and recombinant human fibroblast growth factor 2 (FGF2), 100  
162 U/mL penicillin, and 100 µg/mL streptomycin] supplemented with Rho kinase (ROCK) inhibitor Y-  
163 276322 at a final concentration of 10 µM. Half of the volume of proliferation medium per petri dish  
164 was exchanged every 2-3 days by proliferation medium without ROCK inhibitor.

165 **3.4 Neurosphere Plating**

166 IUGR and control brains derived neurospheres formed in the proliferation medium were always  
167 cultured in parallel. Two days before starting experiments, proliferating neurospheres were

## Lactoferrin prevents IUGR induced neurite length

168 mechanically chopped to a size of 0.2 mm (McIlwain tissue chopper) to ensure homogeneous  
169 neurosphere size and spherical shape. On the experiment plating day, 0.3 mm diameter neurospheres  
170 were selected and transferred in 8-chamber slides (Falcon) previously coated with Laminin/PDL  
171 containing differentiation medium [consisting in DMEM and Hams F12 3:1 supplemented with N2  
172 (Invitrogen), penicillin and streptomycin (100 U/mL and 100 µg/mL)]. The medium of 7-, and 14-  
173 day experiments were supplemented with 1% fetal calf serum (FCS). Half of the medium was  
174 renewed every 2-3 days. NPCs plated on a Laminin/PDL coated surface radially migrated out of the  
175 sphere core and differentiated into effector cells. Each chamber contained five (5-day experiment) or  
176 six (7- and 14-day experiment) neurospheres representing replicates within one experiment, and at  
177 least three independent experiments were performed for every endpoint and exposure condition.

### 178 3.5 Therapy exposure in vitro

179 Compounds for neuroprotective therapy testing were dissolved in their corresponding vehicle  
180 depending on their maximum solubility (Table 1) and subsequently in differentiation medium. The  
181 effect of the potential therapies was assessed after 5 days of differentiation.

182

183 **Table 1. Therapy exposure in vitro.** The concentration range of potential therapies and their solubility  
184 is indicated, as well as the maximum tolerated concentration (MTC) established in Kühne et al. (2022).  
185 The maximum solvent concentration was 0.1% (v/v) DMSO.

| Therapy (synonym) | CAS Number | Solubility    | Concentration <i>in vitro</i> | MTC   |
|-------------------|------------|---------------|-------------------------------|-------|
| MEL               | 73-31-4    | 100 µM (DMSO) | 3 – 1 – 0.3 – 0.1 µM          | 3 µM  |
| DHA               | 6217-54-5  | 300 µM (DMSO) | 10 – 3 – 1 – 0.3 – 0.1 µM     | 10 µM |
| SA                | 131-48-6   | 30 µM (DMSO)  | 10 – 3 – 1 – 0.3 – 0.1 µM     | 30 µM |

186

### 187 3.6 Immunocytochemistry

188 After 5, 7 or 14 days under differentiation conditions, neurospheres were fixed with PFA 4% for 30  
189 minutes at 37°C, washed twice with PBS and stored in PBS until immunostained. Neuronal staining  
190 after 5 and 7 days: Neurospheres were incubated with a primary antibody solution containing 10%  
191 goat serum and 1:100 rabbit IgG anti-βIII-tubulin antibody (R&D Systems) in PBS-T (PBS  
192 containing 0.1% Triton X-100) for 1h at 37°C. After three washing steps with PBS, slides were  
193 incubated with secondary antibody solution containing 2% goat serum (Sigma), 1:100 Hoechst 33258  
194 and 1:200 Alexa 546 anti-rabbit IgG in PBS for 30 minutes at 37°C. Co-Staining of neurons and  
195 synapses after 14 days: Neurospheres were incubated for 1 h at 37°C, with a primary antibody  
196 solution containing goat serum as blocking solution (10%), rabbit anti-βIII-tubulin IgG antibody  
197 (1:100), mouse anti-synapsin1 IgG antibody and PBS-T. After three washes with PBS, slides were  
198 incubated with secondary antibody solution containing 2% goat serum (Sigma), 1:100 Hoechst  
199 33258, Alexa 488 anti-rabbit IgG (1:100), Alexa 546 anti-mouse IgG (1:100) and PBS for 30 minutes  
200 at 37°C. After incubation with the respective antibody solution and three washing steps with PBS,

201 slides were mounted with Acqua Poly/Mount (Polysciences Inc.) and stored at 4°C until image  
202 acquisition.

### 203 **3.7 Image acquisition and analysis of neuronal endpoints**

204 The endpoints “% of neurons”, “number of dendrites per neuron” and “neurite length” were analyzed  
205 after 5, 7 and 14 days of differentiation, whereas “synaptogenesis” was only assessed after 14 days  
206 (Fig. 1). EGF [20 ng/ml] was used as a positive control for neuronal differentiation. Neurospheres  
207 were fixed, immunocytostained and image analysis was carried out by taking two images of each  
208 migration area with a BX61 microscope (Olympus, Japan) and using the ImageJ/Fiji 1.53q software.  
209 The number of nuclei (Hoechst staining) representing the total amount of cells were automatically  
210 counted using ImageJ/Fiji 1.53q software and neurons ( $\beta$ III-tubulin+ cells) were manually counted.  
211 To determine the % of neurons the number of neurons was normalized to the number of nuclei.

212 The number of dendrites/neuron and their distances from the soma (neurite length) were manually  
213 measured by using ImageJ 1.53q after 5 days of differentiation. After 7 and 14 days, the number of  
214 dendrites/neuron and neurite length were assessed with the “Sholl analysis” of the ImageJ/Fiji 1.53q  
215 software (Binley *et al.*, 2014; Bird and Cuntz, 2019). The total amount of dendrites was classified in  
216 primary, secondary, or tertiary dendrites depending on their point of division. The primary dendrites  
217 are born from the soma, the secondary ones from the primaries and so on. The tool “Sholl analysis”  
218 allowed us to trace manually the different paths of dendrites calculating dendritic branching and  
219 length.

220 After 14 days the ability to generate synapses was analyzed. Synaptic puncta were defined as the  
221 synapse marker Synapsin1 co-localized with  $\beta$ III-Tubulin+ cells. Synaptogenesis (synapsin-1+  
222 neurons [%]) was determined by the number of neurons with synapsin-1+ puncta normalized by the  
223 total number of neurons. Analysis was evaluated in 5-6 neurospheres/condition, minimum 10  
224 neurons/neurosphere in at least 3 independent experiments.

### 225 **3.8 Cell viability**

226 The cell viability was assessed with the CellTiter-Blue® cell viability assay (Promega). This assay is  
227 based on the measurement of mitochondrial reductase activity of living cells by conversion of  
228 resazurin to the fluorescent product resorufin. After 2 h of incubation with the reagent (1:3), medium  
229 was placed in a 96-well plate and read with FLUOstar Optima microplate reader. Neurospheres  
230 exposed to 10% DMSO (2 h) were used as lysis control.

### 231 **3.9 Statistics**

232 Statistical analysis was performed using GraphPad Prism v9. The difference between two samples  
233 was calculated with a two-tailed student’s t-test. Concentration-dependent effects were analyzed  
234 using one-way ANOVA. Time-course experiments including the comparisons of two groups were  
235 assessed by performing a two-way ANOVA. One-way and two-way ANOVA analysis was always  
236 followed by post-hoc test Bonferroni’s multiple comparison test. The significance threshold was  
237 established at \*  $p \leq 0.05$ .

238

239

240



241 **4 Results**242 **4.1 IUGR increases neurite length after 5 days in vitro**

243 Neurospheres were prepared from 12 control and 10 IUGR rabbit pups with a significantly reduced  
 244 body weight in the IUGR group as described in Kühne et al. (2022). Previous results from our group  
 245 testing the impact of IUGR in the rabbit neurosphere model after 3 days in culture determined no  
 246 difference between control and IUGR on the endpoint ‘% neurons’ (Barenys *et al.*, 2021). In the  
 247 current study, we investigated the impact of IUGR on neuronal endpoints after 5 days *in vitro* to  
 248 unravel if changes may occur at a later timepoint but we confirmed that the percentage of neurons  
 249 was also not significantly different between control and IUGR at this timepoint (Fig. 2A displays  
 250 representative pictures of neurons stained with the neuronal marker  $\beta$ III-tubulin in the migration area  
 251 of control and IUGR neurospheres after 5 days *in vitro*. Fig. 2B, Control:  $2.25 \pm 0.39$  % vs IUGR:  
 252  $2.34 \pm 0.25$  %,  $p=0.800$ ). The positive control EGF significantly decreased the % of neurons in both  
 253 groups (Fig. 2B, Control:  $0.21 \pm 0.08$  %; IUGR:  $0.15 \pm 0.04$  %), while significantly rising the  
 254 viability (Supplementary Fig. 1A), proving that the system is flexible and can react to external  
 255 stimuli known to keep cells in a proliferating instead of in a differentiating status. The endpoint  
 256 ‘neurite length’ was measured by the distance from the soma to the neurite end, and the ‘number of  
 257 dendrites per neuron’ revealed the degree of dendritic arborization. After 5 days in culture, neurons  
 258 of control and IUGR neurospheres developed mainly primary dendrites and significantly fewer  
 259 secondary dendrites per neuron ( $1.39$  control primary vs  $0.12$  control secondary dendrites/neuron,  
 260  $p<0.0001$  (FIG. 2D)). Importantly, the total neurite length was significantly increased in IUGR  
 261 neurospheres compared to the respective control value (Fig. 2C, total control:  $29.82 \pm 2.84$  vs. IUGR:  
 262  $36.03 \pm 3.46$   $\mu$ m,  $p=0.011$ ). From the total neurite, the length of the primary dendrites arising directly  
 263 from the soma was significantly increased in IUGR neurospheres too (Fig. 2C, primary control:  
 264  $28.50 \pm 2.71$  vs. IUGR:  $34.81 \pm 3.48$   $\mu$ m,  $p=0.006$ ), whereas secondary dendrites arising from the  
 265 primary dendrites were not significantly different compared to control (Fig. 2C, secondary control:  
 266  $1.36 \pm 0.35$  vs. IUGR:  $1.19 \pm 0.16$   $\mu$ m.  $p=0.943$ ). The number of dendrites per neuron did not vary  
 267 between control and IUGR after 5 days, neither the total number nor the number of primary or  
 268 secondary dendrites (Fig. 2D, total control:  $1.51 \pm 0.09$  vs. IUGR:  $1.44 \pm 0.05$  dendrites/neuron,  
 269  $p=0.353$ ).

270 **4.2 IUGR increases the % of neurons after 14 days in a time-dependent manner**

271 We established for the very first time the maintenance of rabbit control and IUGR neurospheres  
 272 under long-term differentiation conditions (maximum time in culture previously described was 5  
 273 days *in vitro* (Barenys *et al.*, 2021)) and examined if the neuronal morphology or network formation  
 274 may be altered over time (Fig. 3). Representative pictures of neurospheres cultured for 7 and 14 days  
 275 *in vitro* revealed that both groups (IUGR and control) developed  $\beta$ III-tubulin+ cells and after 14 days  
 276 also the pre-synaptic marker synapsin-1+ (Fig. 3A-B). In a time-course experiment, the percentage of  
 277  $\beta$ III-tubulin+ cells was slightly increased in the IUGR group compared to the control after 7 days.  
 278 Remarkably, after 14 days, the percentage of neurons in IUGR neurospheres exceeded to a  
 279 significant extent the percentage of neurons in the control group (Fig. 3C, Control:  $4.43 \pm 0.98$  % vs.  
 280 IUGR:  $8.82 \pm 2.61$  %,  $p=0.005$ ). By using this time-course approach we discovered that the neuronal  
 281 differentiation rate is significantly faster in IUGR compared to control (Fig. 3C, difference between  
 282 the slopes of control and IUGR:  $p=0.013$ ), without affecting the viability at any timepoint indicating  
 283 a specific effect on neuronal development by excluding a cytotoxic effect (Supplementary Fig. 1B-  
 284 C). The total neurite length and number of dendrites per neuron increased over time in both groups,

285 control and IUGR, demonstrating a more complex neuronal morphology with extended neurites and  
286 more branched dendrites from 5 to 14 days (Fig. 3D-E).

287 After 14 days, the percentage of neurons developing pre-synaptic puncta (synapsin-1+ neurons) was  
288 measured to determine the degree of synaptogenesis (Fig. 3B IV-V arrows, 3F). However, no  
289 significant difference in the synaptic formation between control and IUGR was discovered (Fig. 3F,  
290 Control:  $15.23 \pm 9.97$  % vs IUGR:  $27.45 \pm 11.36$  %,  $p=0.277$ ).

291 To investigate the development of neurite length and dendritic arborization in more detail, we  
292 measured not only the total number and length but also primary, secondary, and tertiary dendrites  
293 after 7 and 14 days *in vitro* (Fig. 4). While NPCs cultured for 5 days only formed neurons with  
294 primary and secondary dendrites (Fig. 2C-D), NPCs cultured for 7 and 14 days established a more  
295 advanced neuronal phenotype including tertiary dendrites (Fig. 4). Representative pictures display the  
296 measurement of neurite length and the number of primary, secondary and tertiary dendrites of control  
297 and IUGR neurons after 7 and 14 days using the 'Sholl analysis' (Fig. 4B and D). Primary dendrites  
298 from neurons of both groups (control and IUGR) significantly extended their length over time from 7  
299 to 14 days, whereas only the IUGR group significantly increased the number of primary dendrites  
300 over time (Fig. 4A). Secondary dendrites of neurons of both groups increased their number from 7 to  
301 14 days, while only the control group significantly increased the length of secondary dendrites (Fig.  
302 4C). Tertiary dendrites from neurons of both groups did not significantly expand their length or  
303 number over time.

### 304 4.3 Assessment of potential therapies after 5 days *in vitro*

305 We selected the timepoint 5 days *in vitro* for further assessments of potential therapies, because our  
306 results at this time-point correlate very well with the situation described *in vivo* in a previous study  
307 investigating structural brain changes in a rabbit model of IUGR (Pla *et al.*, 2020). This study  
308 observed a more advanced dendritic morphology in the frontal cortex of IUGR compared to control  
309 animals (Pla *et al.*, 2020).

310 With the aim to revert adverse effects on neurogenesis induced by IUGR, we evaluated the safety and  
311 efficacy of 3 potential therapies MEL, DHA, and SA on the neuronal endpoints ' % of neurons ',  
312 ' neurite length ', and ' number of dendrites per neuron ', as well as cell viability. In a previous study of  
313 our group using rabbit neurospheres, the maximum tolerated concentration (MTC) from MEL, DHA,  
314 and SA was determined in control neurospheres with the following criteria: viability was not lower  
315 than 70% of the solvent control (SC), migration distance and % of oligodendrocytes were not  
316 significantly reduced (Kühne *et al.*, 2022). In the current approach, the additional criteria to set the  
317 MTC was ' no significant adverse effect on any on the tested neuronal endpoints ' in control  
318 neurospheres. Control neurospheres were exposed to potential therapies in a concentration-dependent  
319 manner for 5 days under differentiation conditions *in vitro* (Fig. 5). None of the tested therapies  
320 adversely disturbed the tested endpoints and the MTC of each compound was set at the highest tested  
321 concentration for each compound, which was in accordance with the results in Kühne *et al.* (2022)  
322 and presented in table 1.

323 The main interest was to find a concentration of the selected therapies which reverts the adverse  
324 effects of IUGR bringing it to control values *in vitro*. The cell viability determined by metabolic  
325 activity was always performed in the same experiments to distinguish between a specific effect and a  
326 cytotoxic effect (Supplementary Fig. 2). IUGR neurospheres were exposed to increasing  
327 concentrations of the selected therapies up to their MTC (table 1). MEL, DHA, and SA did not  
328 significantly interfere with the % neurons at any of the tested concentrations neither in control nor in

IUGR neurospheres (Fig. 6A). Our focus lied on decreasing the neurite length of the IUGR group because the total neurite length and the length of primary dendrites were significantly increased by IUGR after 5 days *in vitro*. MEL did not significantly reduce the total neurite length in IUGR neurospheres in none of the tested concentrations (Fig. 6B). However, the lowest (0.1  $\mu\text{M}$ ) and the highest (3  $\mu\text{M}$ ) concentration of MEL significantly reduced the length of primary dendrites by presenting a stronger effect in the lowest concentration (Fig. 6C, 0.1  $\mu\text{M}$  MEL  $20.70 \pm 2.86 \mu\text{m}$  vs. SC  $34.81 \pm 3.48 \mu\text{m}$ ,  $p=0.004$ ). MEL induced a non-monotonic response without showing a concentration-dependent effect or impact on the total neurite length, that is why MEL was not considered as the most favorable therapy against IUGR induced adverse effects on neurite length. Likewise, DHA did not present a significant reduction in the total neurite length at any of the tested concentrations (Fig. 6B). Nevertheless, DHA showed a concentration-dependent effect on primary dendrites decreasing its length significantly to  $20.06 \pm 1.21 \mu\text{m}$  compared to SC ( $p=0.001$ ) with 1  $\mu\text{M}$  DHA (Fig. 6C). Even though DHA showed a positive effect on primary dendrites, the total length of neurites could not be improved. On the contrary, the exposure of SA to IUGR neurospheres prompted a concentration-dependent effect on total neurites and primary dendrites by significantly reducing their length. While 10  $\mu\text{M}$  SA significantly decreased the total neurite length ( $21.03 \pm 0.75 \mu\text{m}$  vs. SC  $36.03 \pm 3.46 \mu\text{m}$ ,  $p=0.05$ ), 1  $\mu\text{M}$  SA significantly reduced the length of primary dendrites ( $20.33 \pm 3.68 \mu\text{m}$ ,  $p=0.006$ ). The total number of dendrites per neuron was not altered by any of the tested therapies (Fig. 6D), neither the number of primary nor of secondary dendrites per neuron (Fig. 6E). Based on these findings, SA was selected to be the best candidate in reverting induced neurite length induced by IUGR *in vitro*.

#### 4.4 Administration of therapies *in vivo* – evaluation *in vitro*

To investigate the transferability of the *in vitro* results to the situation *in vivo*, we randomly assigned pregnant rabbits to different groups and administered MEL, DHA, or LF daily from the day of IUGR induction until c-section. SA is the main metabolite of LF, and therefore not SA but the parent compound LF was selected for the treatment *in vivo*. The body weight of the PND0-IUGR pups from all treatment groups was significantly lower than from the respective control group the same as in non-treated animals (w/o), suggesting that the treatments have no effect on the body weight (see table 1 in Kühne et al. (2022)).

Neurospheres were obtained from control and IUGR pup's whole brain delivered from the different treatment groups and analyzed for neuronal endpoints *in vitro*. The cell viability determined by the metabolic activity was not significantly reduced compared to the control value in all treatment groups of neurospheres obtained from control and IUGR pups (Supplementary Fig. 3). The % of neurons was not significantly different between control and IUGR neurospheres obtained from pups from all treatment groups, which is in accordance with the effect observed *in vitro* (Fig. 7A). Fig. 7B and C display the total neurite length and number of dendrites of all treatment groups and the respective lower graphics the length and number of primary and secondary dendrites per neuron. Neurospheres obtained from IUGR pups prenatally administered to MEL did not display any improvement in neurite length, neither the total neurite length nor the length of primary or secondary dendrites (Fig. 7B). Likewise, the prenatal administration of DHA to the pregnant rabbit could not prevent the adverse effect of IUGR on total neurite length, primary or secondary dendrites (Fig. 7B). However, neurospheres from IUGR pups delivered from LF-treated rabbits presented a significant reduction in the total neurite length compared to the non-treated IUGR group (LF total:  $23.71 \pm 0.64 \mu\text{m}$  vs. w/o total:  $36.03 \pm 3.46 \mu\text{m}$ ,  $p=0.049$ , Fig. 7B). The length of primary dendrites was also significantly reduced in IUGR neurospheres of the LF group compared to primary dendrites of the non-treated IUGR group (LF primary:  $22.23 \pm 1.10 \mu\text{m}$  vs. w/o primary:  $34.81 \pm 3.48 \mu\text{m}$ ,  $p=0.0045$ ), while the

375 length of secondary dendrites remained unaffected. In control neurospheres from the LF group, the  
376 neurite length of total and primary dendrites stayed on the level of w/o control neurospheres.  
377 Remarkably, these results follow the results of the *in vitro* exposure to SA, the main metabolite of LF  
378 (Fig. 6B-C). Finally, the total number of dendrites per neuron did not differ between any treatment  
379 group and non-treated group (Fig. 7C). None of the tested therapies influenced the number of  
380 primary or secondary dendrites per neuron, which was also in line with our *in vitro* results (Fig. 6D-  
381 E).

382 Taking into account all results presented, the *in vitro* neurosphere assay correctly predicted the  
383 outcome of both, positive and negative results of the *in vivo* administration for the endpoints ‘% of  
384 neurons’, ‘total neurite length’ and ‘total number of dendrites’ or ‘number of primary and secondary  
385 dendrites’. Merely the *in vitro* results of ‘length of primary and secondary dendrites’ after exposure  
386 to MEL and DHA was not in accordance with the results of the prenatal *in vivo* treatment. Our  
387 findings revealed LF as the most promising therapy to prevent neurite extension caused by IUGR.  
388 This result is consistent with the *in vitro* results, where SA improved IUGR-induced neurite length.  
389 These results support the neurosphere assay as a compelling instrument for predicting neuronal  
390 endpoints *in vivo*.

## 391 5 Discussion

392 We used a previously established rabbit neurosphere model mimicking brain development of IUGR  
393 affected babies (Barenys *et al.*, 2021). The *in vitro* neurosphere system has been revealed to  
394 reproduce the clinical situation of WM injury by reducing the percentage of pre-oligodendrocytes in  
395 the IUGR group *in vitro* by accurately predicting the outcome *in vivo* with respect to  
396 oligodendrogenesis, which makes it a powerful and consistent tool to assess IUGR induced  
397 neurological alterations (Kühne *et al.*, 2022). In this study, we assessed the impact of IUGR on  
398 neuronal development after 5, 7 and 14 days and synaptogenesis after 14 days *in vitro*, as well as the  
399 safety and efficacy of potential therapies *in vitro* and after *in vivo* administration.

400 IUGR neurospheres presented a significant increase in the total neurite length as well as in the length  
401 of primary dendrites after 5 days *in vitro*. These results correlate very well with a previous *in vivo*  
402 study of our group, where neurons presented a more complex branched morphology in the frontal  
403 cortex of IUGR rabbit pups (PND1). Tertiary, quaternary and quinary dendritic branches were  
404 significantly increased in the IUGR versus the control group (Pla *et al.*, 2020). With the same *in vivo*  
405 rabbit model, diffusion tensor imaging parameter were assessed revealing reduced fractional  
406 anisotropy (FA) in several brain regions of WM and GM including the frontal cortex of IUGR  
407 animals (Eixarch *et al.*, 2012). A decrease in cortical FA is associated with an increase in dendritic  
408 expansion and branching of neurons (McKinstry *et al.*, 2002) and may explain the advanced neurite  
409 length in our IUGR *in vitro* culture. A recent study by our group provides evidence for an underlying  
410 molecular mechanism: IUGR neurospheres present a significant higher expression of the adhesion  
411 molecule integrin- $\beta$ 1 at gene and protein level (Kühne *et al.*, under submission). Integrin- $\beta$ 1 interacts  
412 with the extracellular matrix (ECM) protein laminin allowing the migration of NPCs to a distal  
413 destination and the alignment of glial cell in brain and cerebellar cortex (Graus-Porta *et al.*, 2001;  
414 Förster *et al.*, 2002; Richard Belvindrah *et al.*, 2007; Barenys *et al.*, 2017; Kühne *et al.*, 2019).  
415 Integrin- $\beta$ 1 is not only involved in migration but also in the extension of neurite length and  
416 arborization in the developing brain as studies have shown that integrin- $\beta$ 1 deficiency in cells from  
417 partial knock-out mice were not able to evolve dendritic branching (Marrs *et al.*, 2006; R. Belvindrah  
418 *et al.*, 2007), integrin- $\beta$ 1 blocking or inhibitor experiments reduced or avoided neurite extension and  
419 branching on laminin (Moresco *et al.*, 2005; Warren *et al.*, 2012; Ortiz-Romero *et al.*, 2018). A

## Lactoferrin prevents IUGR induced neurite length

420 further perspective experiment to prove the underlying mechanism would be to plate control and  
421 IUGR neurospheres on an ECM with decreasing laminin concentrations to discover whether the  
422 extended neurite length decreases with declining laminin concentrations. However, the increased  
423 expression of integrin- $\beta$ 1 in the IUGR culture gives explanation for our findings of increased neurite  
424 length after IUGR induction.

425 We successfully established for the very first time the maintenance of the rabbit neurosphere culture  
426 not only for 5 days, but also for 7 and 14 days under differentiation conditions. Both, control and  
427 IUGR neurospheres developed a more complex neuronal phenotype over time including more  
428 dendrites and longer neurites. This outcome demonstrates that our rabbit neurosphere system is able  
429 to reflect spatiotemporal processes of brain development with increasing complexity of the nervous  
430 system as described for human neurospheres (Kim *et al.*, 2006). After 14 days, both groups were able  
431 to develop the pre-synaptic marker synapsin-1, demonstrating the formation of a neuronal network.  
432 These results indicate a faster network expansion in the rabbit compared to human neurosphere  
433 culture because neurons of primary human NPCs did not develop this marker until 28 days under  
434 differentiation conditions and human induced pluripotent stem cells (hiPSCs) developed synaptic  
435 markers at first after 28 days in culture forming an electrically active neuronal network (Hofrichter *et al.*,  
436 2017; Nimtz *et al.*, 2020). However, it was challenging to maintain rabbit neurospheres for more  
437 than 7 days under differentiation conditions, and it was necessary to supplement the medium with  
438 FCS, which is known to improve viability but also induce neuronal development in rabbit  
439 neurospheres (Barenys *et al.*, 2021). In the time-course experiment, the percentage of neurons in  
440 IUGR significantly exceeded the % of neurons in control neurospheres after 14 days. This increase in  
441 percentage of neurons is not in line with what was described *in vivo* (Pla *et al.*, 2020), thus we  
442 decided not to focus on this timepoint of the study in the current publication. If IUGR neurospheres  
443 need to be kept under restricted oxygen and nutrients supply *in vitro* for long-term culture to keep  
444 being a correct model to study IUGR needs further clarification. We did not find a difference in the  
445 synaptogenesis between control and IUGR, but to our knowledge, a IUGR induced disturbance of  
446 neuronal function including signal transmissions has never been studied yet in an *in vitro* model of  
447 IUGR.

448 To date no efficient treatment is available to improve adverse brain development occurring from  
449 IUGR, and neuroprotective therapies are urgently needed to be applied prenatally during the “critical  
450 window of opportunity” to protect or correct IUGR-induced brain damage (Susan L Andersen, 2003).  
451 Our rabbit model mimics the situation of late-onset IUGR, which is the most critical instance  
452 encompassing the highest incidence of IUGR cases with a very small time window between  
453 diagnosis and intervention (Figueras and Gratacos, 2017; Figueras *et al.*, 2018). For the safety and  
454 efficacy testing of potential therapies MEL, DHA, and LF or its main metabolite SA we chose the  
455 timepoint 5 days under differentiation conditions, because our results highly corresponds to the  
456 results of the *in vivo* study that IUGR animals produced a more branched neuronal phenotype in the  
457 frontal cortex than the control group (Pla *et al.*, 2020). Regarding the safety of the selected therapies,  
458 none of the tested concentrations *in vitro* or after prenatal administration *in vivo* exhibited an adverse  
459 effect on viability or neuronal endpoints in control neurospheres indicating safe concentrations *in vitro*  
460 and a safe maternal dose *in vivo*. These results comply with the safety assessment of all tested  
461 compounds on the endpoint oligodendrogenesis as previously calculated in Kühne *et al.* (2022). In  
462 this earlier study, we identified MEL and DHA as the most promising therapies to prevent and revert  
463 adverse effects on oligodendrogenesis, while LF did not change impaired oligodendrocyte  
464 differentiation after IUGR induction (Kühne *et al.*, 2022). The hormone MEL is a highly effective  
465 antioxidant, which readily crosses the placental and blood-brain barrier (BBB) reducing fetoplacental  
466 oxidative stress and decreased white- and grey-matter damage in different models of IUGR (Rees,

## Lactoferrin prevents IUGR induced neurite length

467 Harding and Walker, 2011; Miller *et al.*, 2014; Castillo-Melendez *et al.*, 2017). DHA is a long-chain  
468 omega-3 polyunsaturated fatty acid that is an important component of brain membrane  
469 phospholipids, which contributes to neuronal differentiation and signaling and accelerate myelination  
470 (Greenberg, Bell and Ausdal, 2008; Gil-Sánchez *et al.*, 2010; Lauritzen *et al.*, 2016). By exposure to  
471 different concentrations of MEL, DHA, and SA to IUGR neurospheres *in vitro*, all three tested  
472 compounds could revert the IUGR-induced length of primary dendrites, however, merely SA was  
473 able to decrease the total neurite length in IUGR neurospheres. After *in vivo* administration only LF  
474 could prevent the neurite elongation in IUGR neurospheres and was therefore considered as the best  
475 candidate for the protection of neuronal development.

476 LF is an iron-binding, SA-rich glycoprotein known to act as anti-bacterial and anti-inflammatory  
477 compound protecting the development of brain and cognitive function (Wang, 2016). LF was  
478 reported to protect against immature brain injury by recovering cerebral GM and WM destruction in  
479 a rat model of hypoxia-ischemia after maternal supplementation with LF (van de Looij *et al.*, 2014).  
480 SA is a monosaccharide that plays a key role in the synthesis of brain gangliosides and sialylated  
481 glycoproteins including polysialic acid (Poly-SA), which binds to the neural cell adhesion molecule  
482 (NCAM) and is crucial for the neurodevelopment (Weinhold *et al.*, 2005; Bonfanti, 2006; Wang,  
483 2016). Burgess *et al.* (2007) discovered in an *in vitro* primary embryonic rat cell culture, that poly-  
484 SA limits the neurite elongation of septal neurons by preventing the interactions between integrin- $\beta$ 1  
485 and laminin. The other way around, a removal of poly-SA enhances the laminin and integrin- $\beta$ 1  
486 interaction, which was responsible for neurite outgrowth. Another group reported that a removal of  
487 poly-SA facilitated the development of immature neurons in adult mice (Coviello *et al.*, 2021).  
488 Strikingly, functional antibody blocking of integrin- $\beta$ 1 completely eliminated neurite outgrowth on  
489 laminin (Burgess *et al.*, 2007). These results are in line with our investigations revealing an  
490 overexpression of integrin- $\beta$ 1 in IUGR NPCs (Kühne *et al.*, under submission) along with elongated  
491 neurite length in IUGR neurospheres, which could be reverted due to SA exposure *in vitro* and  
492 prevented by LF administration *in vivo*.

493 In summary, we established for the first time the sustainment of the rabbit neurosphere culture until  
494 14 days under differentiation conditions with increasing complexity of neuronal length and branching  
495 up to network formation including synaptogenesis, mimicking spatiotemporal characteristics of brain  
496 development. IUGR neurospheres presented a significant increase in neurite length compared to  
497 control neurospheres after 5 days *in vitro*. The underlying mechanism of this effect in the IUGR  
498 group, as previously discovered in Kühne *et al.* (under submission), could be attributed to an increase  
499 in the adhesion molecule integrin- $\beta$ 1, which promotes neurite outgrowth and branching.

500 Strongly supporting this hypothesis, SA was able to revert *in vitro*, and LF to prevent *in vivo* the  
501 induced neurite length in IUGR neurospheres. Whereas MEL and DHA could not improve the IUGR  
502 induced total neurite extension neither *in vitro* nor after prenatal treatment *in vivo*. Therefore, LF has  
503 been selected as the most promising therapy due to its neuroprotective capacity. For future  
504 applications in the clinical field it may be of high interest to develop a combined supplementation  
505 during pregnancy including DHA as protective agent against impaired oligodendrocyte  
506 differentiation (Kühne *et al.*, 2022) and LF to prevent IUGR-induced adverse effects on neuronal  
507 development.

508

509

### 510 **Conflict of Interest**

511 The authors declare that the research was conducted in the absence of any commercial or financial  
512 relationships that could be construed as a potential conflict of interest.

### 513 **Author Contributions**

514 Britta Anna Kühne: Conceptualization; Data curation; Formal analysis; Investigation; Methodology;  
515 Visualization; Validation; Writing - original draft; Lara Gutiérrez Vázquez: Formal analysis;  
516 Investigation; Methodology; Visualization; Estela Sánchez Lamelas: Formal analysis; Investigation;  
517 Visualization; Laia Guardia-Escote: Data curation; Formal analysis; Investigation; Laura Pla:  
518 Methodology; Carla Loreiro: Methodology; Eduard Gratacós: Resources; Funding acquisition; Marta  
519 Barenys: Conceptualization; Data curation; Formal analysis; Investigation; Project administration;  
520 Supervision; Validation; Visualization; Writing - review & editing; Miriam Illa: Funding acquisition;  
521 Methodology; Project administration; Supervision; Writing - review & editing;

### 522 **Funding**

523 This study has been funded by Instituto de Salud Carlos III through the project "PI18/01763" (Co-  
524 funded by European Regional Development Fund/European Social Fund) "Investing in your future").  
525 B.A.K. received a scholarship from Fundació Bosch i Gimpera (project number: 300155).

### 526 **Acknowledgments**

527 Figure 1 were created with BioRender.com (accessed on 20 May 2022, license number:  
528 SZ23XTEBMR). C.L. received the support the Health Department of the Catalan Government (grant  
529 n° SLT006/17/00325).

### 530 **Data Availability Statement**

531 The data that support the findings of this study are available from the corresponding author upon  
532 reasonable request.

533

### 534 **References**

535 Als, H. *et al.* (2012) 'NIDCAP improves brain function and structure in preterm infants with severe  
536 intrauterine growth restriction', *Journal of Perinatology*, 32(10), pp. 797–803. doi:  
537 10.1038/jp.2011.201.

538 Andersen, Susan L (2003) 'Trajectories of brain development: point of vulnerability or window of  
539 opportunity?', *Neuroscience & Biobehavioral Reviews*, 27(1–2), pp. 3–18. doi: 10.1016/S0149-  
540 7634(03)00005-8.

541 Andersen, Susan L. (2003) 'Trajectories of brain development: Point of vulnerability or window of  
542 opportunity?', *Neuroscience and Biobehavioral Reviews*, 27(1–2), pp. 3–18. doi: 10.1016/S0149-  
543 7634(03)00005-8.

544 Barenys, M. *et al.* (2017) 'Epigallocatechin gallate (EGCG) inhibits adhesion and migration of neural  
545 progenitor cells in vitro', *Archives of Toxicology*. doi: 10.1007/s00204-016-1709-8.

## Lactoferrin prevents IUGR induced neurite length

- 546 Barenys, M. *et al.* (2021) ‘Rabbit neurospheres as a novel in vitro tool for studying  
547 neurodevelopmental effects induced by intrauterine growth restriction’, *STEM CELLS Translational*  
548 *Medicine*, 10(2), pp. 209–221. doi: 10.1002/sctm.20-0223.
- 549 Bassan, H. *et al.* (2000) ‘Experimental intrauterine growth retardation alters renal development’,  
550 *Pediatric Nephrology*, 15(3–4), pp. 192–195. doi: 10.1007/s004670000457.
- 551 Batalle, D. *et al.* (2012) ‘Altered small-world topology of structural brain networks in infants with  
552 intrauterine growth restriction and its association with later neurodevelopmental outcome’,  
553 *NeuroImage*. Elsevier Inc., 60(2), pp. 1352–1366. doi: 10.1016/j.neuroimage.2012.01.059.
- 554 Batalle, D. *et al.* (2014) ‘Long-term reorganization of structural brain networks in a rabbit model of  
555 intrauterine growth restriction’, *NeuroImage*. Elsevier Inc., 100, pp. 24–38. doi:  
556 10.1016/j.neuroimage.2014.05.065.
- 557 Baumann, J. *et al.* (2016) ‘Comparative human and rat neurospheres reveal species differences in  
558 chemical effects on neurodevelopmental key events’, *Archives of Toxicology*. 2015/07/29. Modern  
559 Risk Assessment and Sphere Biology, IUF - Leibniz Research Institute for Environmental Medicine,  
560 Auf’m Hennekamp 50, 40225, Duesseldorf, Germany. Modern Risk Assessment and Sphere Biology,  
561 IUF - Leibniz Research Institute for Environmental Medicine: Springer Berlin Heidelberg, 90(6), pp.  
562 1415–1427. doi: 10.1007/s00204-015-1568-8.
- 563 Belvindrah, Richard *et al.* (2007) ‘ $\beta$ 1 integrins in radial glia but not in migrating neurons are essential  
564 for the formation of cell layers in the cerebral cortex’, *Journal of Neuroscience*, 27(50), pp. 13854–  
565 13865.
- 566 Belvindrah, R. *et al.* (2007) ‘ $\beta$ 1 Integrins in Radial Glia But Not in Migrating Neurons Are Essential  
567 for the Formation of Cell Layers in the Cerebral Cortex’, *Journal of Neuroscience*, 27(50), pp.  
568 13854–13865. doi: 10.1523/JNEUROSCI.4494-07.2007.
- 569 Binley, K. E. *et al.* (2014) ‘Sholl analysis: A quantitative comparison of semi-automated methods’,  
570 *Journal of Neuroscience Methods*. Elsevier B.V., 225, pp. 65–70. doi:  
571 10.1016/j.jneumeth.2014.01.017.
- 572 Bird, A. D. and Cuntz, H. (2019) ‘Dissecting Sholl Analysis into Its Functional Components’, *Cell*  
573 *Reports*. ElsevierCompany., 27(10), pp. 3081-3096.e5. doi: 10.1016/j.celrep.2019.04.097.
- 574 Bonfanti, L. (2006) ‘PSA-NCAM in mammalian structural plasticity and neurogenesis.’, *Progress in*  
575 *neurobiology*, 80(3), pp. 129–64. doi: 10.1016/j.pneurobio.2006.08.003.
- 576 Breier, J. M. *et al.* (2010) ‘Neural progenitor cells as models for high-throughput screens of  
577 developmental neurotoxicity: State of the science’, *Neurotoxicology and Teratology*. Elsevier B.V.,  
578 32(1), pp. 4–15. doi: 10.1016/j.ntt.2009.06.005.
- 579 Burgess, A. *et al.* (2007) ‘Polysialic acid limits septal neurite outgrowth on laminin’, *Brain Research*,  
580 1144(1), pp. 52–58. doi: 10.1016/j.brainres.2007.01.072.
- 581 Carter, A. M. (2007) ‘Animal Models of Human Placentation - A Review’, *Placenta*. IFPA and  
582 Elsevier Ltd, 28(SUPPL.), pp. S41–S47. doi: 10.1016/j.placenta.2006.11.002.



## Lactoferrin prevents IUGR induced neurite length

- 583 Castillo-Melendez, M. *et al.* (2017) 'Effects of Antenatal Melatonin Treatment on the Cerebral  
584 Vasculature in an Ovine Model of Fetal Growth Restriction', *Developmental Neuroscience*, 39(1–4),  
585 pp. 323–337. doi: 10.1159/000471797.
- 586 Coviello, S. *et al.* (2021) 'Psa depletion induces the differentiation of immature neurons in the  
587 piriform cortex of adult mice', *International Journal of Molecular Sciences*, 22(11). doi:  
588 10.3390/ijms22115733.
- 589 Dach, K. *et al.* (2017) 'BDE-99 impairs differentiation of human and mouse NPCs into the  
590 oligodendroglial lineage by species-specific modes of action', *Scientific Reports*, 7(March), pp. 1–11.  
591 doi: 10.1038/srep44861.
- 592 Derrick, M. *et al.* (2004) 'Preterm Fetal Hypoxia-Ischemia Causes Hypertonia and Motor Deficits in  
593 the Neonatal Rabbit: A Model for Human Cerebral Palsy?', *Journal of Neuroscience*, 24(1), pp. 24–  
594 34. doi: 10.1523/JNEUROSCI.2816-03.2004.
- 595 Dieni, S. and Rees, S. (2003) 'Dendritic morphology is altered in hippocampal neurons following  
596 prenatal compromise', *Journal of Neurobiology*, 55(1), pp. 41–52. doi: 10.1002/neu.10194.
- 597 Eixarch, E. *et al.* (2009) 'An experimental model of fetal growth restriction based on selective  
598 ligation of uteroplacental vessels in the pregnant rabbit', *Fetal Diagnosis and Therapy*, 26(4), pp.  
599 203–211. doi: 10.1159/000264063.
- 600 Eixarch, E. *et al.* (2011) 'Impact on fetal mortality and cardiovascular Doppler of selective ligation of  
601 uteroplacental vessels compared with undernutrition in a rabbit model of intrauterine growth  
602 restriction', *Placenta*. Elsevier Ltd, 32(4), pp. 304–309. doi: 10.1016/j.placenta.2011.01.014.
- 603 Eixarch, E. *et al.* (2012) 'Neonatal neurobehavior and diffusion MRI changes in brain reorganization  
604 due to intrauterine growth restriction in a rabbit model', *PLoS ONE*, 7(2). doi:  
605 10.1371/journal.pone.0031497.
- 606 Eixarch, E. *et al.* (2016) 'Motor and cortico-striatal-thalamic connectivity alterations in intrauterine  
607 growth restriction', *American Journal of Obstetrics and Gynecology*. Elsevier Inc., 214(6), pp.  
608 725.e1-725.e9. doi: 10.1016/j.ajog.2015.12.028.
- 609 Esteban, F. J. *et al.* (2010) 'Fractal-dimension analysis detects cerebral changes in preterm infants  
610 with and without intrauterine growth restriction', *NeuroImage*, 53(4), pp. 1225–1232. doi:  
611 10.1016/j.neuroimage.2010.07.019.
- 612 Figueras, F. *et al.* (2018) 'Diagnosis and surveillance of late-onset fetal growth restriction', *American  
613 Journal of Obstetrics and Gynecology*. Elsevier, 218(2), pp. S790-S802.e1. doi:  
614 10.1016/j.ajog.2017.12.003.
- 615 Figueras, F. and Gratacos, E. (2017) 'An integrated approach to fetal growth restriction', *Best  
616 Practice and Research: Clinical Obstetrics and Gynaecology*. Elsevier Ltd, 38, pp. 48–58. doi:  
617 10.1016/j.bpobgyn.2016.10.006.
- 618 Förster, E. *et al.* (2002) 'Reelin, disabled 1, and  $\beta$ 1 integrins are required for the formation of the  
619 radial glial scaffold in the hippocampus', *Proceedings of the National Academy of Sciences of the  
620 United States of America*, 99(20), pp. 13178–13183. doi: 10.1073/pnas.202035899.

## Lactoferrin prevents IUGR induced neurite length

- 621 Gassmann, K. *et al.* (2014) 'BDE-47 and 6-OH-BDE-47 modulate calcium homeostasis in primary  
622 fetal human neural progenitor cells via ryanodine receptor-independent mechanisms', *Archives of*  
623 *Toxicology*, 88(8), pp. 1537–1548. doi: 10.1007/s00204-014-1217-7.
- 624 Gassmann, Kathrin *et al.* (2010) 'Species-specific differential AhR expression protects human neural  
625 progenitor cells against developmental neurotoxicity of PAHs', *Environmental health perspectives*,  
626 118(11), pp. 1571–1577.
- 627 Gil-Sánchez, A. *et al.* (2010) 'Maternal-fetal in vivo transfer of [<sup>13</sup>C]docosahexaenoic and other  
628 fatty acids across the human placenta 12 h after maternal oral intake', *The American Journal of*  
629 *Clinical Nutrition*, 92(1), pp. 115–122. doi: 10.3945/ajcn.2010.29589.
- 630 Graus-Porta, D. *et al.* (2001) 'β1-class integrins regulate the development of laminae and folia in the  
631 cerebral and cerebellar cortex', *Neuron*, 31(3), pp. 367–379.
- 632 Greenberg, J. A., Bell, S. J. and Ausdal, W. Van (2008) 'Omega-3 Fatty Acid supplementation  
633 during pregnancy.', *Reviews in obstetrics & gynecology*, 1(4), pp. 162–169.
- 634 Hofrichter, M. *et al.* (2017) 'Comparative performance analysis of human iPSC-derived and primary  
635 neural progenitor cells (NPC) grown as neurospheres in vitro', *Stem Cell Research*. The Authors, 25,  
636 pp. 72–82. doi: 10.1016/j.scr.2017.10.013.
- 637 Illa, M. *et al.* (2013) 'Long-Term Functional Outcomes and Correlation with Regional Brain  
638 Connectivity by MRI Diffusion Tractography Metrics in a Near-Term Rabbit Model of Intrauterine  
639 Growth Restriction', *PLoS ONE*, 8(10). doi: 10.1371/journal.pone.0076453.
- 640 Illa, M. *et al.* (2018) 'Early Environmental Enrichment Enhances Abnormal Brain Connectivity in a  
641 Rabbit Model of Intrauterine Growth Restriction', *Fetal Diagnosis and Therapy*, 44(3), pp. 184–193.  
642 doi: 10.1159/000481171.
- 643 Kady, S. M. and Gardosi, J. (2004) 'Perinatal mortality and fetal growth restriction', *Best Practice*  
644 *and Research: Clinical Obstetrics and Gynaecology*, 18(3), pp. 397–410. doi:  
645 10.1016/j.bpobgyn.2004.02.009.
- 646 Kim, H.-T. *et al.* (2006) 'Human neurospheres derived from the fetal central nervous system are  
647 regionally and temporally specified but are not committed', *Experimental Neurology*, 199(1), pp.  
648 222–235. doi: 10.1016/j.expneurol.2006.03.015.
- 649 Kühne, B. A. *et al.* (2019) 'Comparison of migration disturbance potency of epigallocatechin gallate  
650 (EGCG) synthetic analogs and EGCG PEGylated PLGA nanoparticles in rat neurospheres', *Food*  
651 *and Chemical Toxicology*, 123. doi: 10.1016/j.fct.2018.10.055.
- 652 Kühne, B. A. *et al.* (2022) 'Docosahexaenoic Acid and Melatonin Prevent Impaired  
653 Oligodendrogenesis Induced by Intrauterine Growth Restriction (IUGR)', *Biomedicines*, 10(5). doi:  
654 10.3390/biomedicines10051205.
- 655 Lauritzen, L. *et al.* (2016) 'DHA Effects in Brain Development and Function', (December 2015), pp.  
656 1–17. doi: 10.3390/nu8010006.
- 657 Lees, C. C. *et al.* (2022) 'Clinical Opinion: The diagnosis and management of suspected fetal growth

## Lactoferrin prevents IUGR induced neurite length

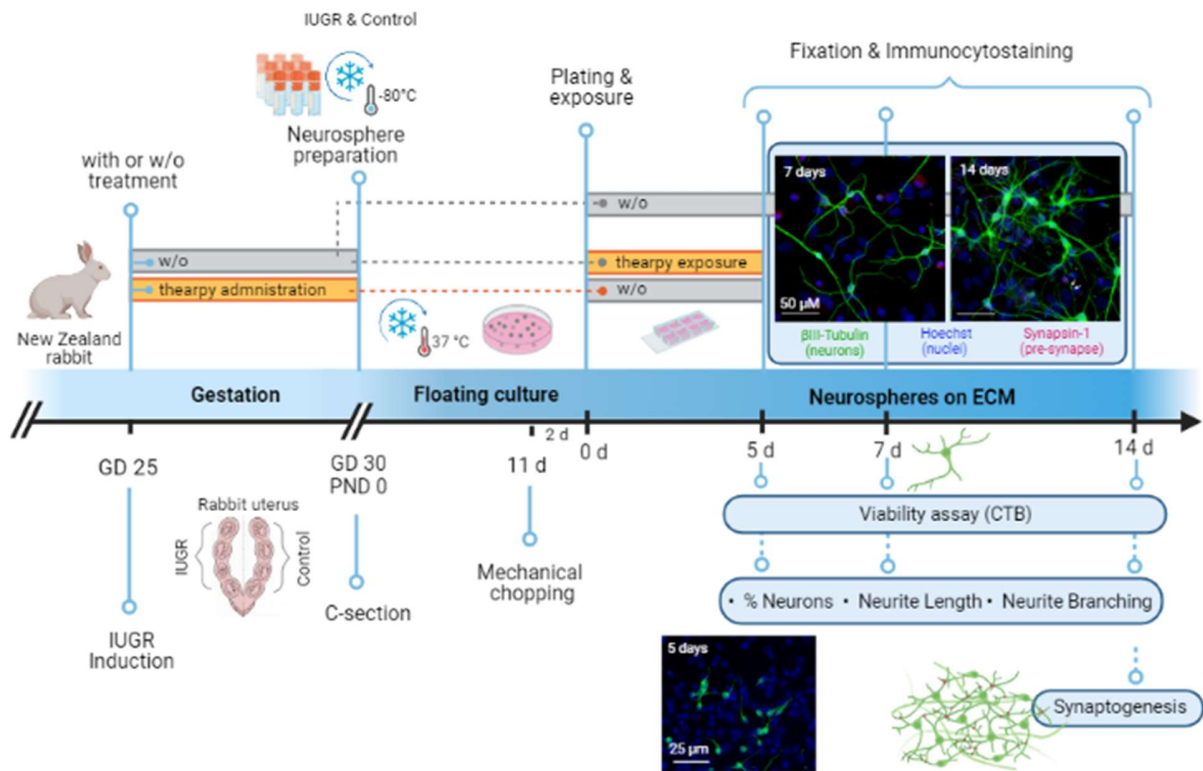
- 658 restriction: an evidence-based approach', *American Journal of Obstetrics and Gynecology*. Elsevier  
659 Inc., 226(3), pp. 366–378. doi: 10.1016/j.ajog.2021.11.1357.
- 660 van de Looij, Y. *et al.* (2014) 'Lactoferrin during lactation protects the immature hypoxic-ischemic  
661 rat brain', *Annals of Clinical and Translational Neurology*, 1(12), pp. 955–967. doi:  
662 10.1002/acn3.138.
- 663 Lopez, V., Kelleher, S. L. and Lönnerdal, B. (2008) 'Lactoferrin receptor mediates apo- but not holo-  
664 lactoferrin internalization via clathrin-mediated endocytosis in trophoblasts', *Biochemical Journal*,  
665 411(2), pp. 271–278. doi: 10.1042/BJ20070393.
- 666 Marrs, G. S. *et al.* (2006) 'Dendritic arbors of developing retinal ganglion cells are stabilized by  $\beta$ 1-  
667 integrins', *Molecular and Cellular Neuroscience*, 32(3), pp. 230–241. doi:  
668 10.1016/j.mcn.2006.04.005.
- 669 Masjosthusmann, S. *et al.* (2019) 'Arsenite interrupts neurodevelopmental processes of human and  
670 rat neural progenitor cells: The role of reactive oxygen species and species-specific antioxidative  
671 defense', *Chemosphere*. Elsevier Ltd, 235, pp. 447–456. doi: 10.1016/j.chemosphere.2019.06.123.
- 672 McKinsty, R. C. *et al.* (2002) 'Radial organization of developing preterm human cerebral cortex  
673 revealed by non-invasive water diffusion anisotropy MRI', *Cerebral Cortex*, 12(12), pp. 1237–1243.  
674 doi: 10.1093/cercor/12.12.1237.
- 675 Miller, S. L. *et al.* (2014) 'Antenatal antioxidant treatment with melatonin to decrease newborn  
676 neurodevelopmental deficits and brain injury caused by fetal growth restriction', *Journal of Pineal*  
677 *Research*, 56(3), pp. 283–294. doi: 10.1111/jpi.12121.
- 678 Moors, M. *et al.* (2007) 'ERK-dependent and -independent pathways trigger human neural progenitor  
679 cell migration', *Toxicology and Applied Pharmacology*, 221(1), pp. 57–67. doi:  
680 10.1016/j.taap.2007.02.018.
- 681 Moors, M. *et al.* (2009) 'Human neurospheres as three-dimensional cellular systems for  
682 developmental neurotoxicity testing', *Environmental Health Perspectives*, 117(7), pp. 1131–1138.
- 683 Moresco, E. M. Y. *et al.* (2005) 'Integrin-mediated dendrite branch maintenance requires Ablson  
684 (Abl) family kinases.', *The Journal of neuroscience : the official journal of the Society for*  
685 *Neuroscience*, 25(26), pp. 6105–18. doi: 10.1523/JNEUROSCI.1432-05.2005.
- 686 Mwaniki, M. K. *et al.* (2012) 'Long-term neurodevelopmental outcomes after intrauterine and  
687 neonatal insults: a systematic review', *The Lancet*, 379(9814), pp. 445–452. doi: 10.1016/S0140-  
688 6736(11)61577-8.
- 689 Nimtz, L. *et al.* (2020) 'Characterization and application of electrically active neuronal networks  
690 established from human induced pluripotent stem cell-derived neural progenitor cells for  
691 neurotoxicity evaluation', *Stem Cell Research*, 45, p. 101761. doi: 10.1016/j.scr.2020.101761.
- 692 Ortiz-Romero, P. *et al.* (2018) 'Epigallocatechin-3-gallate improves cardiac hypertrophy and short-  
693 term memory deficits in a Williams-Beuren syndrome mouse model', *PLOS ONE*. Edited by P. A. da  
694 Costa Martins, 13(3), p. e0194476. doi: 10.1371/journal.pone.0194476.

## Lactoferrin prevents IUGR induced neurite length

- 695 Piorkowska, K. *et al.* (2014) ‘Synaptic development and neuronal myelination are altered with  
696 growth restriction in fetal guinea pigs’, *Developmental Neuroscience*, 36(6), pp. 465–476. doi:  
697 10.1159/000363696.
- 698 Pla, L. *et al.* (2020) ‘Structural Brain Changes during the Neonatal Period in a Rabbit Model of  
699 Intrauterine Growth Restriction’, *Developmental Neuroscience*, 42(5–6), pp. 217–229. doi:  
700 10.1159/000512948.
- 701 Rao, M. *et al.* (2007) ‘Effect of breastfeeding on cognitive development of infants born small for  
702 gestational age’, *Acta Paediatrica*, 91(3), pp. 267–274. doi: 10.1111/j.1651-2227.2002.tb01713.x.
- 703 Rees, S., Harding, R. and Walker, D. (2011) ‘The biological basis of injury and neuroprotection in  
704 the fetal and neonatal brain’, *International Journal of Developmental Neuroscience*, 29(6), pp. 551–  
705 563. doi: 10.1016/j.ijdevneu.2011.04.004.
- 706 Reid, M. V. *et al.* (2012) ‘Delayed myelination in an intrauterine growth retardation model is  
707 mediated by oxidative stress upregulating bone morphogenetic protein 4’, *Journal of Neuropathology  
708 and Experimental Neurology*, 71(7), pp. 640–653. doi: 10.1097/NEN.0b013e31825cfa81.
- 709 Rideau Batista Novais, A. *et al.* (2016) ‘Transcriptomic Regulations in Oligodendroglial and  
710 Microglial Cells Related to Brain Damage following Fetal Growth Restriction’, (April). doi:  
711 10.1002/glia.2307.
- 712 Schreiber, T. *et al.* (2010) ‘Polybrominated diphenyl ethers induce developmental neurotoxicity in a  
713 human in vitro model: Evidence for endocrine disruption’, *Environmental Health Perspectives*,  
714 118(4), pp. 572–578. doi: 10.1289/ehp.0901435.
- 715 Sharma, D., Shastri, S. and Sharma, P. (2016) ‘Intrauterine Growth Restriction: Antenatal and  
716 Postnatal Aspects’, *Clinical Medicine Insights: Pediatrics*, 10, p. CMPed.S40070. doi:  
717 10.4137/CMPed.S40070.
- 718 Tolcos, M. *et al.* (2011) ‘Intrauterine growth restriction affects the maturation of myelin’,  
719 *Experimental Neurology*. Elsevier B.V., 232(1), pp. 53–65. doi: 10.1016/j.expneurol.2011.08.002.
- 720 Wang, B. (2016) ‘Molecular Determinants of Milk Lactoferrin as a Bioactive Compound in Early  
721 Neurodevelopment and Cognition’, *The Journal of Pediatrics*, 173, pp. S29–S36. doi:  
722 10.1016/j.jpeds.2016.02.073.
- 723 Warren, M. S. *et al.* (2012) ‘Integrin  $\beta 1$  signals through Arg to regulate postnatal dendritic  
724 arborization, synapse density, and behavior’, *Journal of Neuroscience*, 32(8), pp. 2824–2834.
- 725 Weinhold, B. *et al.* (2005) ‘Genetic ablation of polysialic acid causes severe neurodevelopmental  
726 defects rescued by deletion of the neural cell adhesion molecule.’, *The Journal of biological  
727 chemistry*, 280(52), pp. 42971–7. doi: 10.1074/jbc.M511097200.
- 728 Workman, A. D. *et al.* (2013) ‘Modeling transformations of neurodevelopmental sequences across  
729 mammalian species.’, *The Journal of neuroscience : the official journal of the Society for  
730 Neuroscience*, 33(17), pp. 7368–83. doi: 10.1523/JNEUROSCI.5746-12.2013.

731

## Lactoferrin prevents IUGR induced neurite length

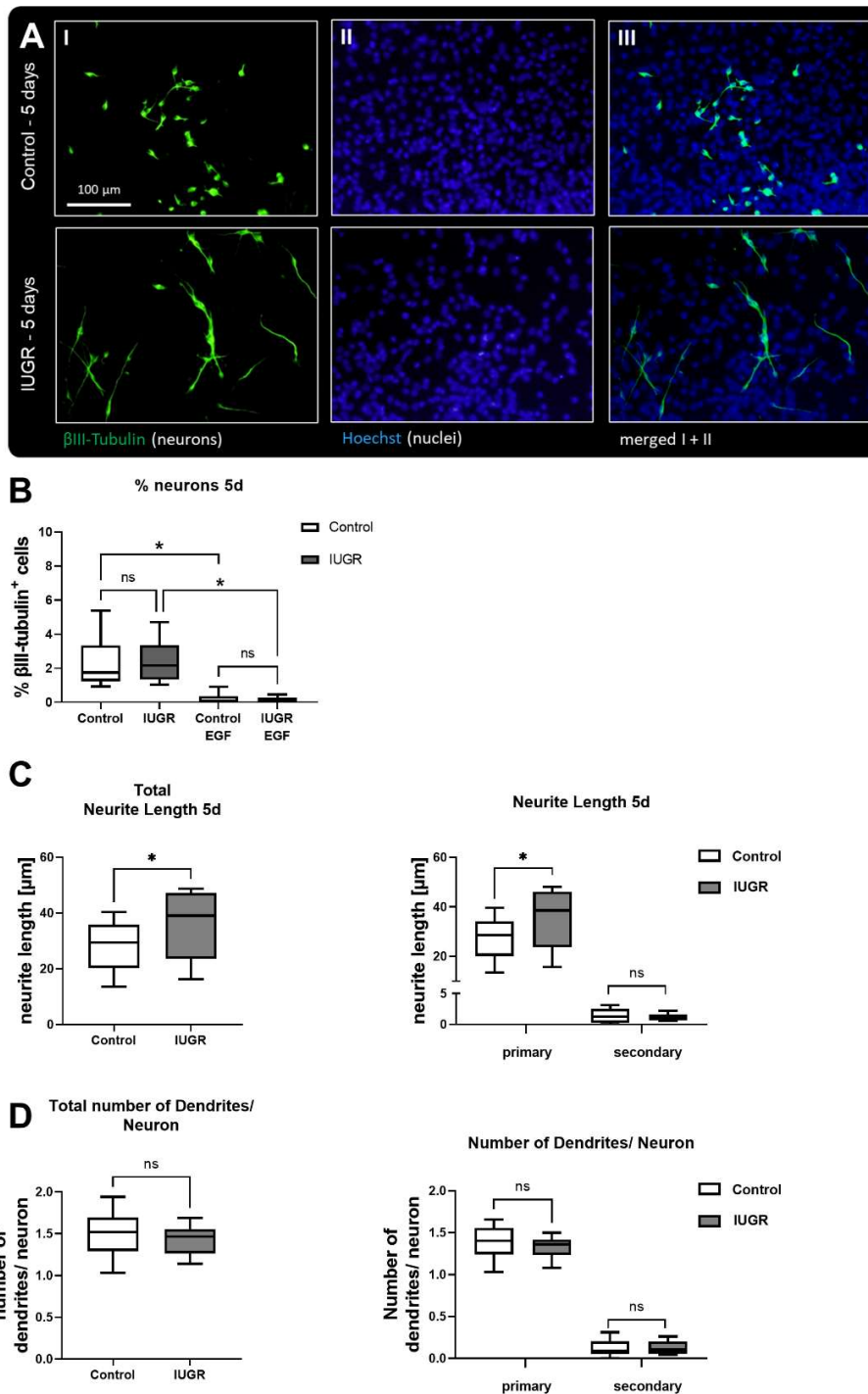


732

733 **Figure 1. Experimental setup.** At gestational day 25, IUGR was induced in one uterine horn of  
 734 pregnant New Zealand rabbits, while the contralateral horn remained as control. Rabbits were kept  
 735 until C-section on GD30 with or without (w/o) administration of therapies. Neurospheres were obtained  
 736 from control and IUGR rabbit pup's whole brain on PND0 and stored at -80°C. Proliferating  
 737 neurospheres were cultivated in a floating culture until mechanical chopping after 11 days. After 2  
 738 days neurosphere were plated on an 8-chamber slide previously coated with PDL/Laminin with or w/o  
 739 exposure to therapies under differentiation conditions. The following endpoints were analyzed after 5,  
 740 7 or 14 days: Viability, % neurons, neurite length, neurite branching (determined by the number of  
 741 dendritic branching per neuron). Synaptogenesis determined by the % of synapsin-1+ neurons was  
 742 analyzed after 14 days. The effect of therapies on neurogenesis was assessed after 5 days under  
 743 differentiation conditions. Rectangle bars = time of administration or exposure, blue circle = endpoints.  
 744 w/o = without, GD = gestational day, PND = postnatal day, c-section = cesarean section, ECM =  
 745 extracellular matrix, CTB = cell titer blue. Created with BioRender.com

746

## Lactoferrin prevents IUGR induced neurite length

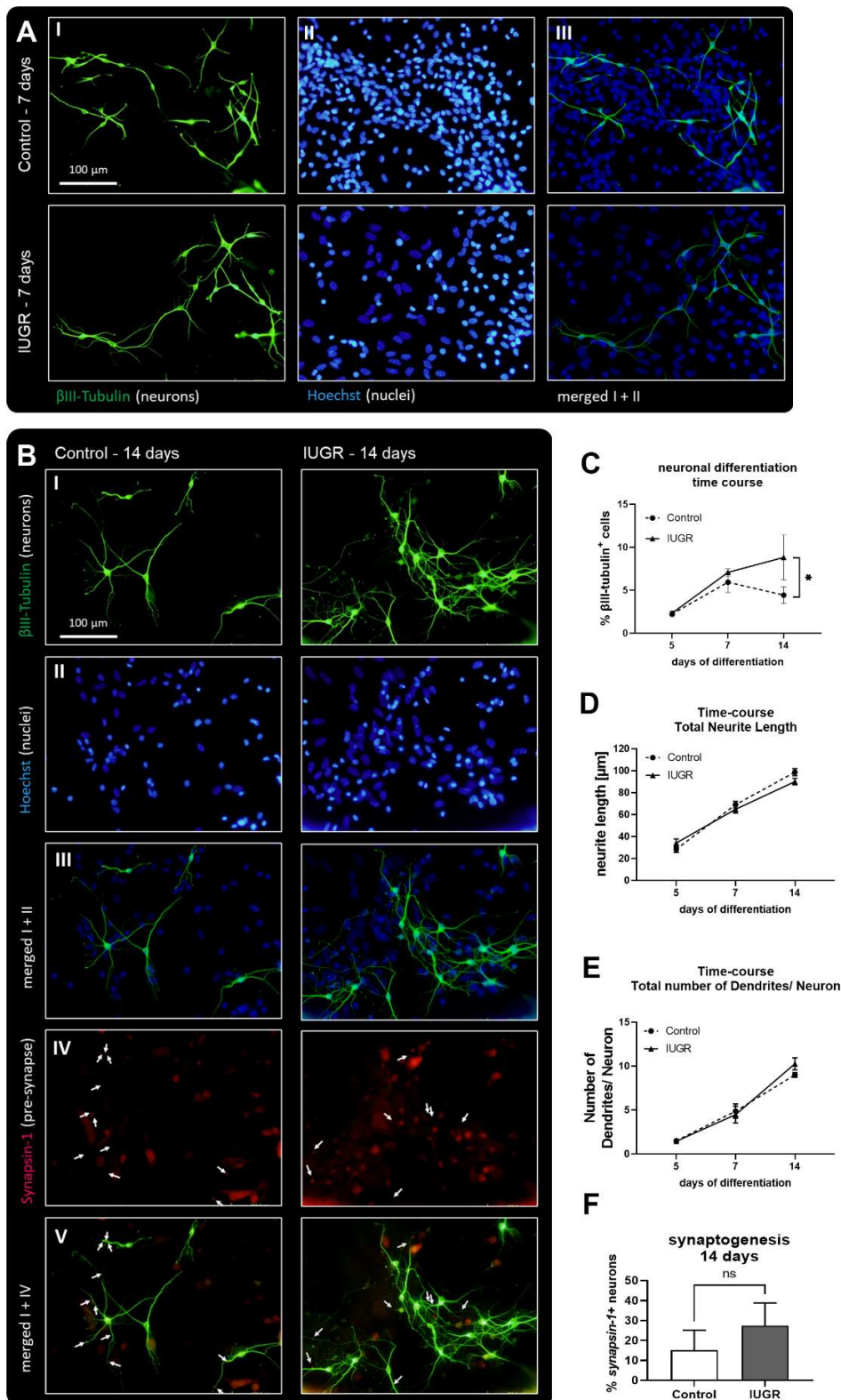


747

748 **Figure 2. Neuronal development after 5 days in vitro.** (A) Representative pictures of neuronal  
 749 marker βIII-Tubulin (I, green), nuclei marker Hoechst 33258 (II, blue) and merged (III) in control and  
 750 IUGR neurospheres after 5 days under differentiation conditions. Control and IUGR neurospheres were  
 751 tested for (B) % neurons, including the positive control EGF [20 ng/ml], (C) neurite length and (D)  
 752 number of dendrites/neurons. Mean ± SEM; \*  $p \leq 0.05$ , ns: not significant.

753

## Lactoferrin prevents IUGR induced neurite length



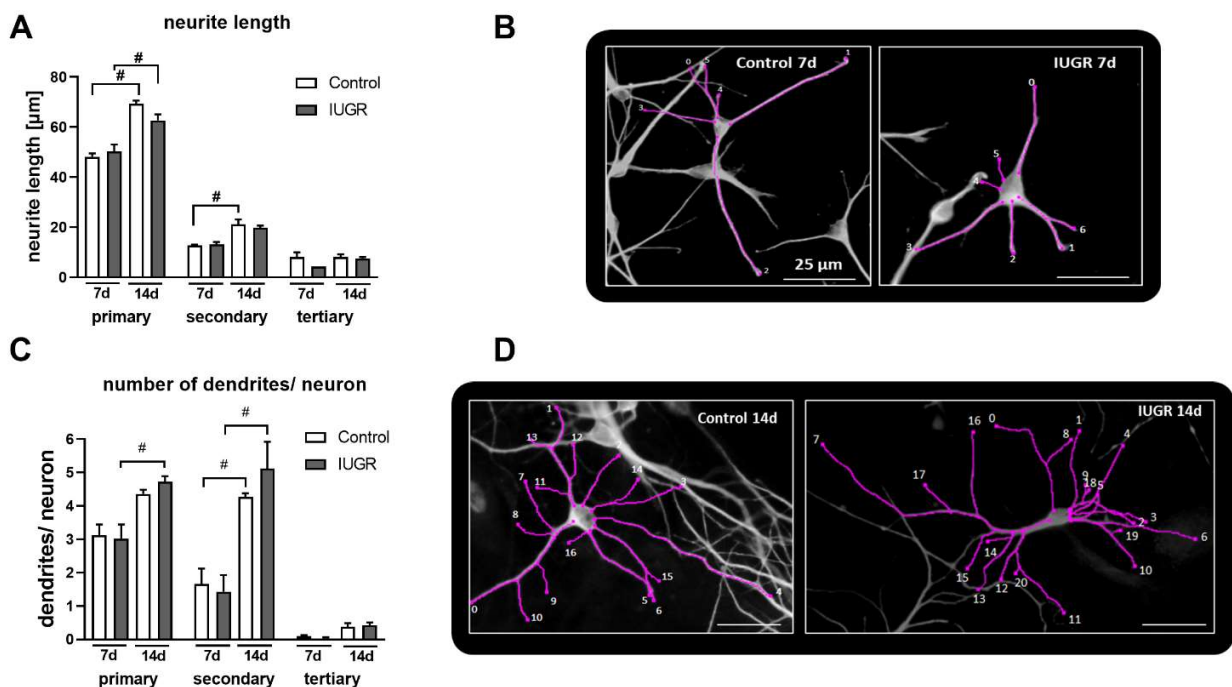
754

755 **Figure 3. Neuronal development and network formation.** (A) 7 days of neuronal differentiation in  
 756 control and IUGR neurospheres. Representative pictures of neuronal marker βIII-Tubulin (I, green),  
 757 nuclei marker Hoechst 33258 (II, blue) and merged (III). (B) 14 days of neuronal differentiation control

## Lactoferrin prevents IUGR induced neurite length

758 and IUGR neurospheres. Representative pictures of (I) Neuronal marker  $\beta$ III-Tubulin (green), (II)  
 759 nuclei marker Hoechst 33258 (blue), (III) merged picture of neuronal and nuclei staining, (IV) pre-  
 760 synaptic marker Synapsin-1, (V) merged picture of neuronal and synaptic staining. Scale bar = 100  
 761  $\mu$ m. (C) Time course of neuronal differentiation from 3 to 14 days of differentiation [%  $\beta$ III-Tubulin  
 762 positive cells], (D) Time course of total neurite length/ neuron from 5-14 days. (E) Time course of total  
 763 number of dendrites/neuron from 5-14 days. (F) Synaptogenesis: Rabbit neurospheres obtained from  
 764 control and IUGR pups were cultured for 14 days and comparatively tested for the ability to generate  
 765 synapses. Synaptogenesis (synapsin-1+ neurons [%]) was determined by the number of neurons with  
 766 synapsin-1 positive puncta normalized by the total number of neurons. Analysis was evaluated in 6  
 767 neurospheres/condition, minimum 10 neurons/neurosphere in 3 independent experiments. Mean  $\pm$   
 768 SEM; \*  $p \leq 0.05$ , ns: not significant.

769



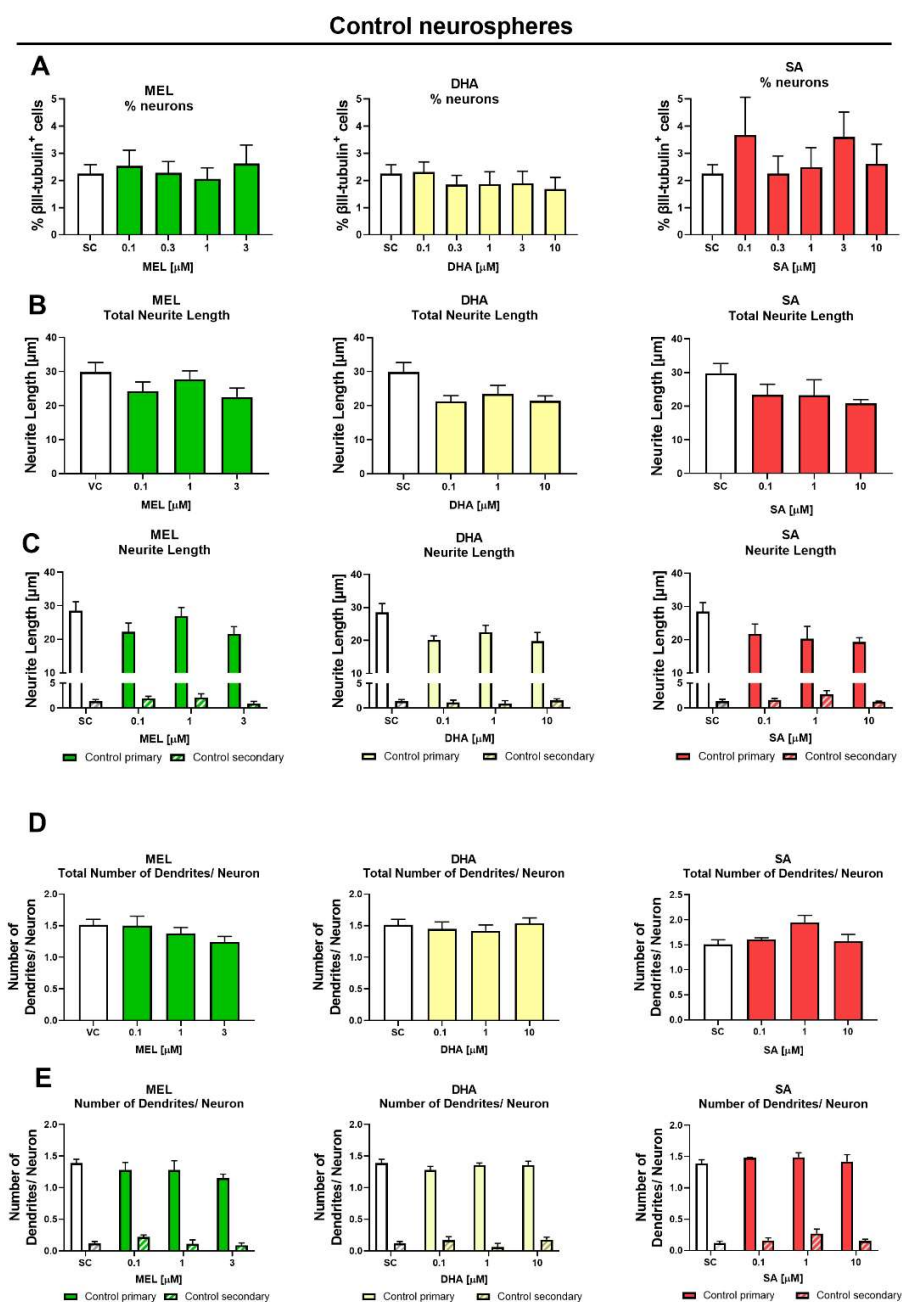
770

771 **Figure 4. Length and number of primary, secondary and tertiary dendrites per neuron after 7**  
 772 **and 14 days.** Control and IUGR neurospheres were cultured for 7 or 14 days and comparatively tested  
 773 for the (A) neurite length of primary, secondary and tertiary dendrites, (C) number of primary,  
 774 secondary and tertiary dendrites/ neuron, (B, D) Example of 'Sholl analysis' of a control (left) and  
 775 IUGR (right) neuron with traced and counted dendrites, after 7 and 14 days of differentiation, scale bar  
 776 = 25  $\mu$ m. Analysis was evaluated in 6 neurospheres/condition, minimum 10 neurons/neurosphere in at  
 777 least 3 independent experiments. \*  $p \leq 0.05$  control vs. IUGR. #:  $p \leq 0.05$  7d vs. 14d.

778



## Lactoferrin prevents IUGR induced neurite length



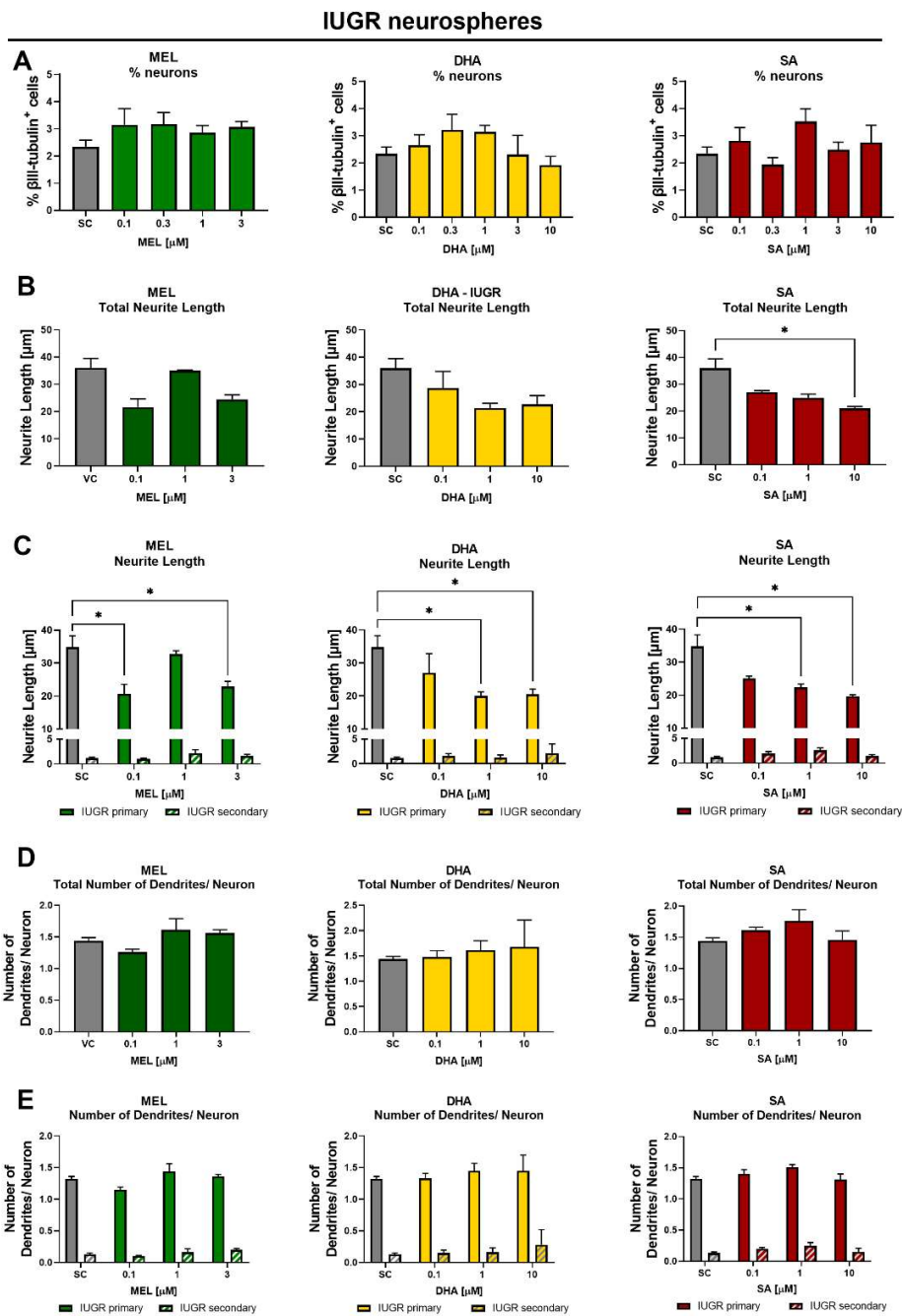
779

780 **Figure 5. Exposure to potential therapies in vitro – evaluation in vitro:** Safety assessment of  
 781 therapies on neuronal endpoints. Control neurospheres were tested for (A) % neurons [% βIII-tubulin+  
 782 cells], (B) total neurite length, (C) length of primary and secondary dendrites, (D) total number of  
 783 dendrites/neuron, and (E) number of primary and secondary dendrites/neuron and exposed to  
 784 increasing concentrations of Melatonin (MEL, green), DHA (yellow), or Sialic Acid (SA, red). Mean  
 785 ± SEM.

786

787

## Lactoferrin prevents IUGR induced neurite length



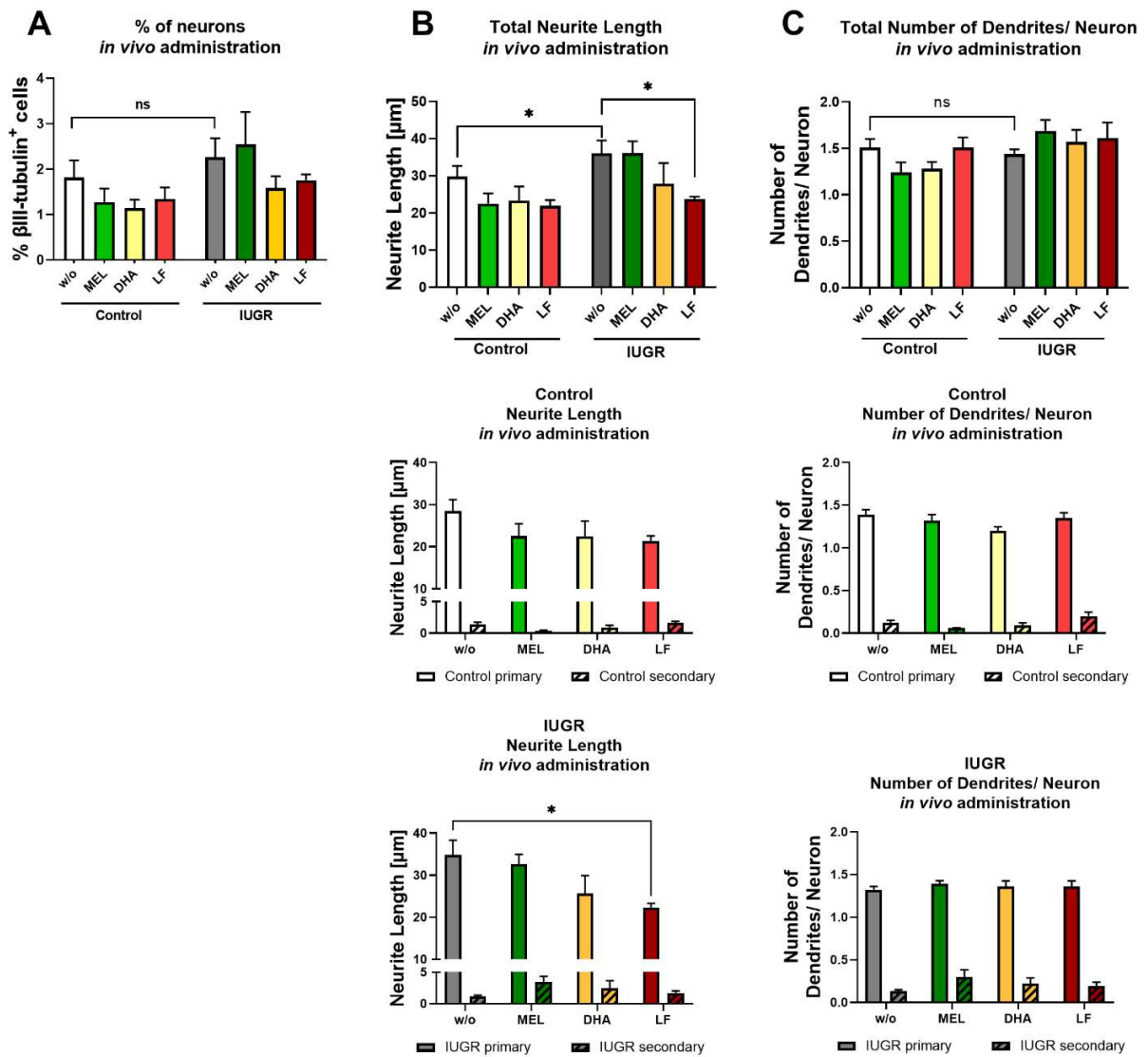
788

789 **Figure 6. Exposure to potential therapies in vitro – evaluation in vitro:** Effect of therapies on  
 790 neuronal endpoints. IUGR neurospheres were tested for (A) % neurons [%  $\beta$ III-tubulin+ cells], (B)  
 791 total neurite length, (C) length of primary and secondary dendrites, (D) total number of  
 792 dendrites/neuron, and (E) number of primary and secondary dendrites/neuron and exposed to  
 793 increasing concentrations of Melatonin (MEL, green), DHA (yellow), or Sialic Acid (SA, red). Mean  
 794  $\pm$  SEM; \*  $p \leq 0.05$  SC vs treatment.

795

796

797



798

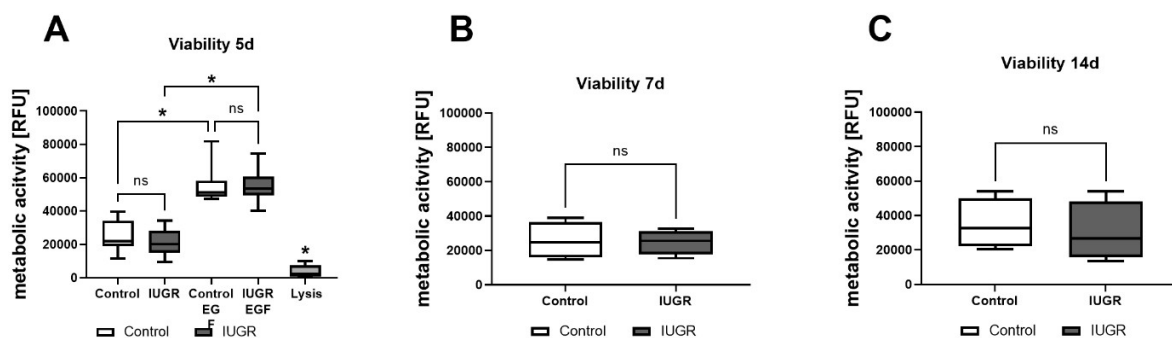
799 **Figure 7. Administration of potential therapies in vivo – evaluation in vitro.** Pregnant rabbits were  
 800 administrated to no treatment (w/o) or to MEL (10 mg /kg bw/day, green), DHA (37 mg/kg bw/day,  
 801 yellow) or LF (166 mg/kg bw/day, red) at the day of IUGR induction until cesarean section.  
 802 Neurospheres obtained from Control and IUGR pups were tested for (A) % neuronal differentiation  
 803 (%  $\beta$ III-tubulin+ cells), (B) total neurite length and below length of primary and secondary dendrites  
 804 in control and IUGR neurospheres (C) total number of dendrites/ neuron and below number of primary  
 805 and secondary dendrites in control and IUGR neurospheres; Mean  $\pm$  SEM; \*  $p \leq 0.05$ , ns: not significant.

806

807

808

*Supplementary Material*

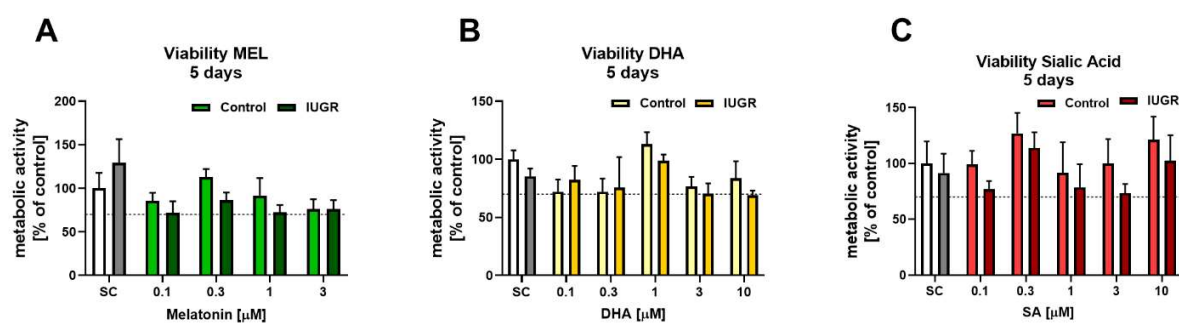


809

810 **Supplementary Figure 1. Viability of control and IUGR neurospheres: 5, 7 and 14 days in vitro.**  
 811 Control and IUGR neurospheres were tested for viability determined by metabolic activity after (A)  
 812 5, (B) 7, and (C) 14 days under differentiation condition, including positive controls Lysis [10 %  
 813 DMSO]. Mean ± SEM; \*  $p \leq 0.05$ , ns: not significant.

814

815

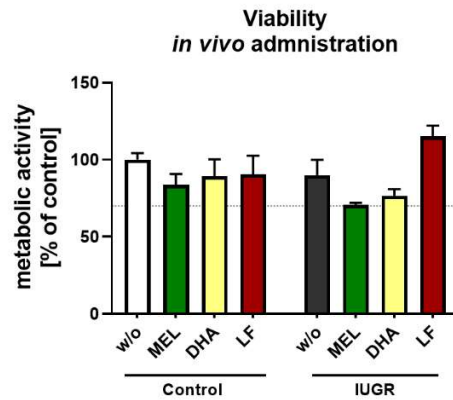


816

817 **Supplementary Figure 2. Exposure to therapies in vitro – evaluation after 5 days in vitro: Safety**  
 818 **assessment of potential therapies in viability.** Control and IUGR neurospheres were tested for viability  
 819 determined by metabolic activity after 5 days under differentiation condition and exposure to  
 820 increasing concentrations of (A) Melatonin (MEL), (B) DHA, (C) Sialic Acid (SA). Dotted line: 70%  
 821 metabolic activity. Mean ± SEM.

822

## Lactoferrin prevents IUGR induced neurite length



823

824 **Supplementary Figure 3. Administration of therapies in vivo – evaluation after 5 days in vitro:**  
825 Safety assessment of potential therapies in viability. Pregnant rabbits were administrated to no  
826 treatment (w/o) or to MEL (10 mg /kg bw/day, green), DHA (37 mg/kg bw/day, yellow) or LF (166  
827 mg/kg bw/day, red) at the day of IUGR induction until cesarean section. Neurospheres obtained from  
828 Control and IUGR pups were tested for viability determined by metabolic activity; black dotted line:  
829 70% metabolic activity. Mean  $\pm$  SEM.

830

831

#### 4.5 Comparison of migration disturbance potency of epigallocatechin gallate (EGCG) synthetic analogs and EGCG PEGylated PLGA nanoparticles in rat neurospheres

**Britta Anna Kühne**<sup>1</sup>, Teresa Puig<sup>2</sup>, Santiago Ruiz-Martínez<sup>2</sup>, Joan Crous-Masó<sup>2,3</sup>, Marta Planas<sup>3</sup>, Lidia Feliuc<sup>3</sup>, Amanda Cano<sup>4,5,6</sup>, Maria Luisa García<sup>4,5</sup>, Ellen Fritsche<sup>7</sup>, Joan M. Llobet<sup>1,8</sup>, Jesús Gómez-Catalán<sup>1,8</sup>, Marta Barenys<sup>1,8</sup>

<sup>1</sup> Department of Pharmacology, Toxicology and Therapeutic Chemistry, Faculty of Pharmacy and Food Sciences, University of Barcelona, 08028, Barcelona, Spain

<sup>2</sup> New Therapeutic Targets Laboratory (TargetsLab), Department of Medical Sciences, University of Girona, Girona Institute for Biomedical Research, 17003, Girona, Spain

<sup>3</sup> LIPPSO, Department of Chemistry, University of Girona, 17003, Girona, Spain

<sup>4</sup> Department of Pharmacy, Pharmaceutical Technology and Physical Chemistry, Faculty of Pharmacy and Food Sciences, University of Barcelona, 08028, Barcelona, Spain

<sup>5</sup> Institute of Nanoscience and Nanotechnology (IN2UB), 08028, Barcelona, Spain

<sup>6</sup> Biomedical Research Networking Centre in Neurodegenerative Diseases (CIBERNED), 28031, Madrid, Spain

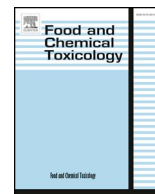
<sup>7</sup> IUF – Leibniz Research Institute for Environmental Medicine, 40225, Düsseldorf, Germany

<sup>8</sup> Institut de Recerca en Nutrició i Seguretat Alimentària de la UB (INSA-UB), 08921, Santa Coloma de Gramenet, Spain

|                       |  |
|-----------------------|--|
| Journal               | Food and Chemical Toxicology   |
| Impact Factor 2019    | 4.679  |
| Quartile              | Q1 (and D1) Food science and technology  |
| Type of authorship    | First author   |
| Status of publication | Published: Food and Chemical Toxicology 123 (2019 Jan) 195-204<br>DOI: 10.1016/j.fct.2018.10.055 |

## Summary

Epigallocatechin gallate (EGCG), the main catechin of green tea, is described to have potential health benefits in several fields like oncology, neurology, or cardiology. Currently, it is also under pre-clinical investigation as a potential therapeutic or preventive treatment during pregnancy against developmental adverse effects induced by toxic substances. However, the safety of EGCG during pregnancy is unclear due to its proven adverse effects on neural progenitor cells' (NPCs) migration. As lately several strategies have arisen to generate new therapeutic agents derived from EGCG, we have used the rat 'Neurosphere Assay' to characterize and compare the effects of EGCG structurally related compounds and EGCG PEGylated PLGA nanoparticles on a neurodevelopmental key event: NPCs migration. Compounds structurally related to EGCG induce the same pattern of NPCs migration alterations (decreased migration distance, decreased formation of migration corona, chaotic orientation of cellular processes and decreased migration of neurons at higher concentrations). The potency of the compounds does not depend on the number of galloyl groups, and small structure variations can imply large potency differences. Due to their lower toxicity observed in vitro in NPCs, 4,4'-bis[(3,4,5-trihydroxybenzoyl)oxy]-1,1'-biphenyl and EGCG PEGylated PLGA nanoparticles are suggested as potential future therapeutic or preventive alternatives to EGCG during prenatal period.



## Comparison of migration disturbance potency of epigallocatechin gallate (EGCG) synthetic analogs and EGCG PEGylated PLGA nanoparticles in rat neurospheres



Britta A. Kühne<sup>a</sup>, Teresa Puig<sup>b</sup>, Santiago Ruiz-Martínez<sup>b</sup>, Joan Crous-Masó<sup>b,c</sup>, Marta Planas<sup>c</sup>, Lidia Feliu<sup>c</sup>, Amanda Cano<sup>d,e,f</sup>, Maria Luisa García<sup>d,e</sup>, Ellen Fritsche<sup>g</sup>, Joan M. Llobet<sup>a,h</sup>, Jesús Gómez-Catalán<sup>a,h,\*</sup>, Marta Barenys<sup>a,h,\*\*</sup>

<sup>a</sup> Department of Pharmacology, Toxicology and Therapeutic Chemistry, Faculty of Pharmacy and Food Sciences, University of Barcelona, 08028, Barcelona, Spain

<sup>b</sup> New Therapeutic Targets Laboratory (TargetsLab), Department of Medical Sciences, University of Girona, Girona Institute for Biomedical Research, 17003, Girona, Spain

<sup>c</sup> LIPPSO, Department of Chemistry, University of Girona, 17003, Girona, Spain

<sup>d</sup> Department of Pharmacy, Pharmaceutical Technology and Physical Chemistry, Faculty of Pharmacy and Food Sciences, University of Barcelona, 08028, Barcelona, Spain

<sup>e</sup> Institute of Nanoscience and Nanotechnology (IN2UB), 08028, Barcelona, Spain

<sup>f</sup> Biomedical Research Networking Centre in Neurodegenerative Diseases (CIBERNED), 28031, Madrid, Spain

<sup>g</sup> IUF – Leibniz Research Institute for Environmental Medicine, 40225, Düsseldorf, Germany

<sup>h</sup> Institut de Recerca en Nutrició i Seguretat Alimentària de la UB (INSA-UB), 08921, Santa Coloma de Gramenet, Spain

### ARTICLE INFO

#### Keywords:

Food supplements  
Neural progenitor cells  
Migration  
Neurospheres  
Developmental neurotoxicity

### ABSTRACT

Epigallocatechin gallate (EGCG), the main catechin of green tea, is described to have potential health benefits in several fields like oncology, neurology or cardiology. Currently, it is also under pre-clinical investigation as a potential therapeutic or preventive treatment during pregnancy against developmental adverse effects induced by toxic substances. However, the safety of EGCG during pregnancy is unclear due to its proven adverse effects on neural progenitor cells' (NPCs) migration. As lately several strategies have arisen to generate new therapeutic agents derived from EGCG, we have used the rat 'Neurosphere Assay' to characterize and compare the effects of EGCG structurally related compounds and EGCG PEGylated PLGA nanoparticles on a neurodevelopmental key event: NPCs migration. Compounds structurally-related to EGCG induce the same pattern of NPCs migration alterations (decreased migration distance, decreased formation of migration corona, chaotic orientation of cellular processes and decreased migration of neurons at higher concentrations). The potency of the compounds does not depend on the number of galloyl groups, and small structure variations can imply large potency differences. Due to their lower toxicity observed *in vitro* in NPCs, 4,4'-bis[(3,4,5-trihydroxybenzoyl)oxy]-1,1'-biphenyl and EGCG PEGylated PLGA nanoparticles are suggested as potential future therapeutic or preventive alternatives to EGCG during prenatal period.

**Abbreviations:** CEEA, Ethic Committee for Animal Experimentation; cMINC, circular migration inhibition of neural crest cells; CTB, CellTiter-Blue Reagent; DMEM, Dulbecco's Modified Eagle Medium; DMSO, dimethyl sulfoxide; DNT, developmental neurotoxicity; EC<sub>50</sub>, 50% effective concentration; EE, encapsulation efficiency; EGC, epigallocatechin; EGCG, epigallocatechin gallate; EGF, epidermal growth factor; FASN, fatty acid synthase; rrFGF, rat recombinant fibroblast growth factor; G37, 1,4-bis[(3,4,5-trihydroxybenzoyl)oxy]naphthalene; G56, 4,4'-bis[(3,4,5-trihydroxybenzoyl)oxy]-1,1'-biphenyl; M1, 4-hydroxy-2-naphthyl 3,4,5-trihydroxybenzoate; M2, 3-hydroxy-1-naphthyl 3,4,5-trihydroxybenzoate; Nano-EGCG, EGCG PEGylated-PLGA nanoparticles; NPCs, neural progenitor cells; PBS, phosphate buffered saline; PDL, poly-D-lysine; PEG, polyethylene glycol; PEGylated-PLGA nanoparticles, polyethylene glycosylated poly (lactic-co-glycolic acid); PFA, paraformaldehyde; PI, polydispersity index; PLGA, poly (lactic-co-glycolic acid); PLGA-PEG, poly (lactic-co-glycolic acid)-polyethylene glycol; PND1, postnatal day 1; Z<sub>av</sub>, average particle size; ZP, zeta potential

\* Corresponding author. Department of Pharmacology, Toxicology and Therapeutic Chemistry, Faculty of Pharmacy and Food Sciences, University of Barcelona, 08028, Barcelona, Spain.

\*\* Corresponding author. Department of Pharmacology, Toxicology and Therapeutic Chemistry, Faculty of Pharmacy and Food Sciences, University of Barcelona, 08028, Barcelona, Spain.

E-mail addresses: [jesusgomez@ub.edu](mailto:jesusgomez@ub.edu) (J. Gómez-Catalán), [mbarenys@ub.edu](mailto:mbarenys@ub.edu) (M. Barenys).

<https://doi.org/10.1016/j.fct.2018.10.055>

Received 1 August 2018; Received in revised form 22 October 2018; Accepted 23 October 2018

Available online 25 October 2018

0278-6915/ © 2018 Elsevier Ltd. All rights reserved.



## 1. Introduction

Efforts towards improving nutritional status of pregnant women require the involvement of a wide range of specialists, among them toxicologists, as efficacy testing of nutritional supplementation should always be accompanied of safety evaluations. Several national and multinational studies report on the intake of herbal-based supplements during pregnancy with high variation on the reported percentages (reviewed by Barenys et al., 2017b) and describe that ‘health promotion’ is one of the ten most commonly reported reasons among pregnant women for using herbal-based supplements (Kennedy et al., 2013). As these substances are not subject to classical risk assessment evaluations, their general toxicities might be known, but there is a lack of information on specific toxicities concerning subtle endpoints like developmental neurotoxicity (DNT) (Barenys et al., 2017b).

Epigallocatechin gallate (EGCG) is the most abundant catechin in green tea (Rothwell et al., 2013). It is present in herbal-based food supplements which can be easily purchased online, in food shops or in supermarkets without the advice of health professionals. It has been described to have several potential health benefits (Hollman et al., 1999; Singh et al., 2011; Yang et al., 2009) driven by its actions on numerous cellular targets involved in cell proliferation, adhesion, and migration (Mineva et al., 2013; Shankar et al., 2008; Singh et al., 2011; Suzuki and Isemura, 2001), but these cellular processes are also essential for correct brain development (Holmes and McCabe, 2001), suggesting a hazardous potential for EGCG on neurodevelopment.

In a previous study using human and rat neurospheres we have shown that EGCG inhibits adhesion and migration of neural progenitor cells (NPCs) and that at higher concentrations it also produces a reduction of the number of migrating young neurons *in vitro*, without affecting NPC proliferation (Barenys et al., 2017a). An independent research group has recently reproduced these migration alteration effects in a different test model (cMINC) showing that EGCG also inhibits human neural crest cells migration *in vitro* (Nyffeler et al., 2017). Besides being a freely-available food-supplement, EGCG is also intensively studied at a preclinical level as a potential prenatal treatment to decrease developmental adverse effects induced by toxic substances, i.e. prevention of the neurodevelopmental adverse effects related to the fetal alcohol syndrome (Long et al., 2010; Tiwari et al., 2010), or adverse outcomes related with genetic diseases like cardiac hypertrophy and short-term memory deficits associated with Williams-Beuren syndrome (Ortiz-Romero et al., 2018) and reduction of craniofacial features associated with Down syndrome (McElyea et al., 2016).

Even if EGCG stimulates an elevated interest for therapies in adults or during prenatal development, it displays poor bioavailability and limited stability under physiological conditions (Krupkova et al., 2016; Puig et al., 2009; Turrado et al., 2012), therefore in the last years several strategies have arisen to generate new therapeutical agents derived from EGCG to overcome these limitations: e.g. the use of polyethylene glycosylated poly (lactic-co-glycolic-acid) (PEGylated-PLGA) nanoparticles to encapsulate EGCG or the synthesis of EGCG analogues. Here we tested such EGCG alternatives in the ‘Neurosphere Assay’ to assess their potency to disturb (1) NPC migration distance (2) the formation of the migration corona (3) cellular process orientation angle, and (4) neuronal migration. In our study we included the original compound EGCG, EGCG PEGylated-PLGA nanoparticles (Nano-EGCG), the polyphenolic compounds G37 and G56 with two galloyl units and a naphthyl or a biphenyl moiety, respectively, and M1 and M2 with one galloyl group (Fig. 1). The inclusion of the latter was motivated by the results in our previous study where we observed that the natural catechin with only one galloyl group epigallocatechin (EGC, CAS: 970-74-1) disturbed the adhesion of NPCs less potently than EGCG (Barenys et al., 2017a). These five compounds: Nano-EGCG, G37, G56, M1, and M2, have already been tested for some beneficial effects related with, for example, their anticancer, anti-seizure, antibacterial and/or analgesic activity (Cano et al., 2018; Crous-Masó et al., 2018; Xifró et al.,

2015), yet their potential to interfere with neurodevelopmental processes like migration needs evaluation before they are tested as prenatal therapies or prenatal nutritional supplements.

## 2. Material and methods

### 2.1. Reagents

(–)-Epigallocatechin-3-gallate (EGCG, CAS 989-51-5, purity > 98%) was purchased from TransMIT PlantMetaChem (Giessen, Germany). 4-Hydroxy-2-naphthyl 3,4,5-trihydroxybenzoate (M1), 3-hydroxy-1-naphthyl 3,4,5-trihydroxybenzoate (M2), 1,4-bis[(3,4,5-trihydroxybenzoyl)oxy]naphthalene (G37) and 4,4′-bis[(3,4,5-trihydroxybenzoyl)oxy]-1,1′-biphenyl (G56) were synthesized as detailed by Crous-Masó et al. (2018) by the LIPPSO group at the University of Girona at a purity > 90%. Stock solutions of EGCG and its four derivatives were dissolved at a final working concentration of 0.01% DMSO.

Poly (lactic-co-glycolic acid)-polyethylene glycol (PLGA-PEG) 5% was purchased from Evonik Co. (Evonik Co., Birmingham, USA). 1.5 mg/mL EGCG loaded PEGylated-PLGA nanoparticles were prepared at the laboratory of the ‘Nanostructured systems for controlled drug delivery’ research group as described in Cano et al. (2018). Briefly, the formulation with 1.5 mg/ml of EGCG, 14 mg/ml of PLGA-PEG and Tween<sup>®</sup> 80 1.5% led to a monodisperse population (polydispersity index: PI < 0.1) of particles with an average particle size ( $Z_{av}$ ) of  $168.5 \pm 9.9$  nm and an encapsulation efficiency (EE) higher than 95%. The formulation showed a zeta potential (ZP) value ( $-23.3 \pm 5.3$  mV). As the nanocarrier was formulated by the double emulsion method using Tween<sup>®</sup> 80 as surfactant, working solutions of Nano-EGCG were prepared at a final concentration of 0.1% Tween<sup>®</sup> 80.

### 2.2. Ethics statement

The acquisition of brain tissue for preparation of neurospheres was approved by the Ethic Committee for Animal Experimentation of the University of Barcelona (CEEA) with license number OB 341/17.

### 2.3. Proliferating cell culture establishment and maintenance

See Fig. 2 for a graphical representation of the experimental approach. Rat neural progenitor cells (NPCs) were isolated from whole brain of two postnatal day 1 (PND1) pups as previously described in Baumann et al. (2014). NPCs were cultivated as a floating culture in a humidified incubator at 37 °C and 5% CO<sub>2</sub> in B27-proliferation medium [Dulbecco’s Modified Eagle Medium (DMEM) and Hams F12 (3:1) with B27-supplement (Invitrogen GmbH, Karlsruhe, Germany), 20 ng/mL Epidermal growth factor (EGF, Biosource, Karlsruhe, Germany), 10 ng/mL recombinant rat fibroblast growth factor (rrFGF, R&D Systems, Wiesbaden-Nordenstadt, Germany), 100 U/mL penicillin and 100 µg/mL streptomycin (PAN-Biotech)]. Every 2–3 days half of the medium was replaced with fresh B27-proliferation medium. As soon as neurospheres reached a certain size of 0.5–0.6 mm in diameter they were passaged mechanically with a tissue chopper (McIlwain) to maintain their proliferative character. NPCs were chopped 3–4 days before plating on a poly-D-lysine/laminin-coated surface in an 8-chamber slide to perform the differentiation assay as described below.

### 2.4. Differentiation conditions and chemical exposure

Studies of migration and differentiation were performed under differentiation conditions as described elsewhere (Baumann et al., 2014). Briefly, NPCs were plated onto a coated surface of poly-D-lysine (PDL; 0.1 mg/mL, Sigma Aldrich) and laminin (5 µg/mL, Sigma Aldrich) in an 8-chamber slide filled with N2 differentiation medium [Dulbecco’s modified Eagle medium (DMEM) and Hams F12 (3:1) supplemented

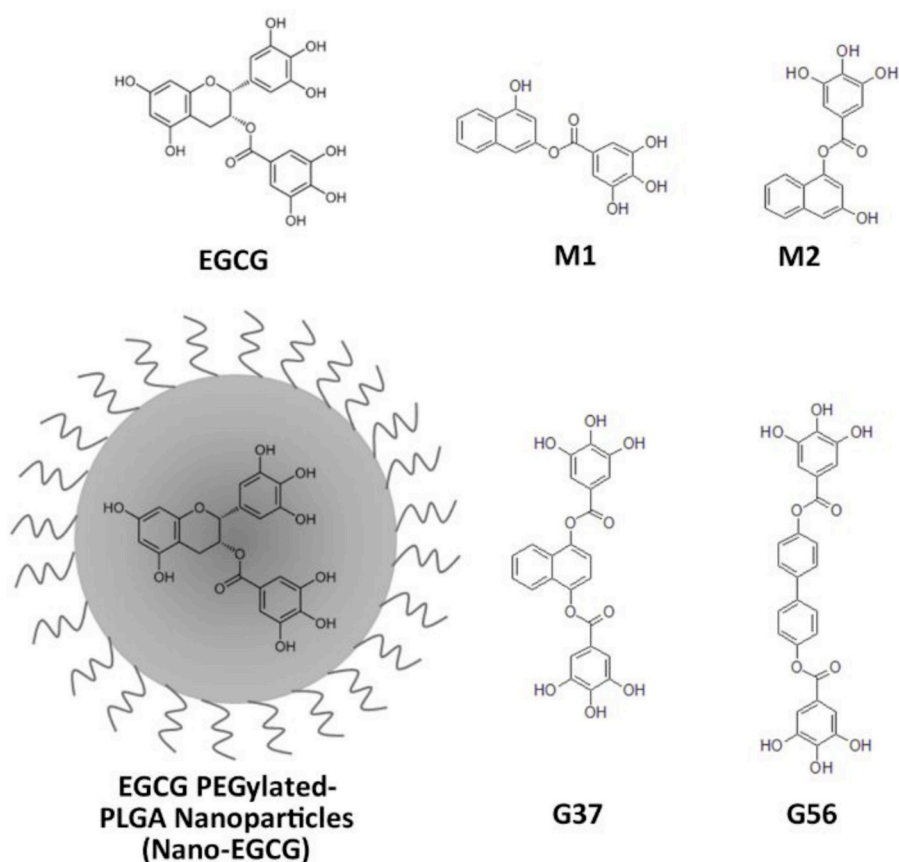


**Fig. 1. Chemical structure of the tested compounds.** EGCG (458.375 g/mol): epigallocatechin gallate; M1 (312.27 g/mol): 4-hydroxy-2-naphthyl 3,4,5-trihydroxybenzoate; M2 (312.27 g/mol): 3-hydroxy-1-naphthyl 3,4,5-trihydroxybenzoate; EGCG PEGylated-PLGA Nanoparticles (Nano-EGCG); G37 (464.38 g/mol): 1,4-bis[(3,4,5-trihydroxybenzoyl)oxy]naphthalene; G56 (490.42 g/mol): 4,4'-bis[(3,4,5-trihydroxybenzoyl)oxy]-1,1'-biphenyl.

with N2 (Invitrogen GmBH, Karlsruhe, Germany), 100 U/mL penicillin, and 100 µg/mL streptomycin (PAN-Biotech) in absence of the growth factors EGF and FGF]. 3–4 days after chopping five neurospheres of diameter 0.3 mm were placed on the surface of each chamber and

exposed for 24 h to EGCG, Nano-EGCG, G37, G56, M1 or M2 at increasing concentrations (1, 5 and 10 µM) at 37 °C in a humidified 5% CO<sub>2</sub> incubator. Solvent controls were plated containing the same solvent concentrations then the tested compounds: 0.01% DMSO as

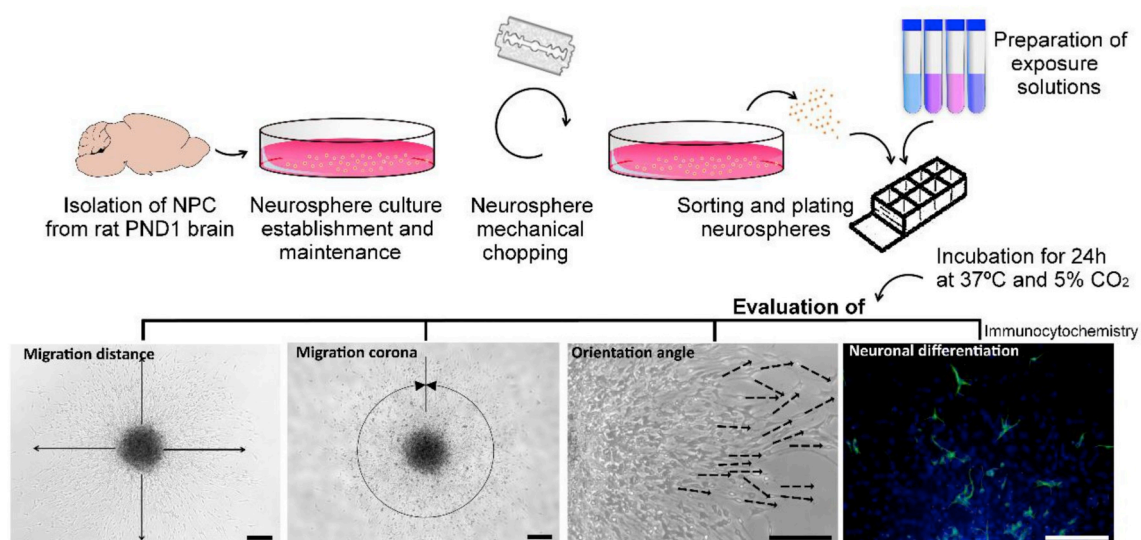


**Fig. 2. Graphical representation of the experimental approach.** **Migration distance.** Phase-contrast image of the whole migration area of a rat neurosphere after 24 h of culture on a PDL/laminin coated surface. Migration distance measurement in 4 perpendicular radii from the neurosphere edge to the furthest migrated cells is exemplified with 4 arrows. **Migration corona.** Phase-contrast image of the whole migration area of a rat neurosphere after 24 h of culture on a PDL/laminin coated surface. The angle of the corona with presence of migrating cells surrounding the neurosphere core is represented with an arrow. **Orientation angle.** Phase-contrast image of the right side of the migration area of a rat neurosphere after 24 h of culture on a PDL/laminin coated surface. Measurement of 20 orientation angles is represented with discontinuous arrows. **Neuronal differentiation.** Fluorescent microscope image of the upper part of the migration area of a rat neurosphere after 24 h of culture on a PDL/laminin coated surface, fixation and immunocytochemistry. Blue: nuclei staining (Hoechst), green: neuronal marker (βIII-tubulin). Scale bars: 100 µm. (For interpretation of the references to color in this figure legend, the reader is referred to the Web version of this article.)

solvent control for EGCG, G37, G56, M1 and M2 and 0.1% Tween<sup>®</sup>80 as solvent control for Nano-EGCG. EGF (20 ng/mL) was used as a positive control, since this concentration significantly increases migration and inhibits neuronal differentiation (Schmuck et al., 2017). Three to four independent experiments were performed for every endpoint and treatment.

## 2.5. Migration

All migration experiments were performed under differential conditions and were analyzed after an exposure time of 24 h. To evaluate the individual endpoints the whole migration area of each neurosphere was visualized using a high performance phase-contrast microscope (Nikon Eclipse TS100) and pictures were taken with a monochrome camera (Imaging Source DMK 51AU02).

### 2.5.1. Migration distance

The radial migration distance of each neurosphere was measured as described in Baumann et al. (2014) and Moors et al. (2007). Briefly, the radius in four perpendicular angles from the edge of the neurosphere core to the furthest migrated cells was measured by using the ImageJ software. Subsequently the mean of the four radii was calculated to obtain the migration distance of each sphere.

### 2.5.2. Corona of migrating cells

The corona of migrating cells around the sphere core was calculated by manual measurement of the angles of the area covered with cells of the total corona around a sphere core (360°). The sum of all angles around the neurospheres covered by cells was calculated.

### 2.5.3. Orientation angle measurement

NPCs migrate in a specific orientation angle within the migration area which was manually analyzed in two frames (406.5 μm × 284.8 μm) per neurosphere. This orientation angle was measured in respect to the perpendicular direction from the sphere core for approximately 300 cell processes per concentration and experiment and subsequently plotted in a color-coded polar plot using MatLab R2017b version.

## 2.6. Viability testing

Viability was assessed directly after capturing pictures for the migration assay (24 h after exposure) by means of Alamar Blue Assay using the CellTiter-Blue Reagent (CTB) (Promega, Mannheim, Germany) as described in Baumann et al. (2014).

## 2.7. Immunocytochemistry

After 24 h of exposure and subsequently viability testing cells were fixed overnight in 4% paraformaldehyde (PFA) at 4 °C. On the following day cells were washed with 1x Phosphate Buffered Saline (PBS) and stored in PBS at 4 °C until immunofluorescence staining was performed. To stain the cell nuclei and differentiated neurons within the migration area, neurospheres were incubated for 1 h at 37 °C with 10% goat serum and rabbit-anti-β(III)-tubulin first antibody (1:200; Sigma-Aldrich) in 1x PBS with 0.1% (v/v) Triton-X 100 (PBS-T) followed by 30 min incubation at 37 °C with 2% goat serum, 1% Hoechst 33258 (Sigma-Aldrich) and anti-rabbit Alexa Fluor 546 secondary antibody (1:200; Sigma-Aldrich) in 1x PBS. Two images of the stained migrating area of each neurosphere were taken under a Nikon Eclipse TS100 fluorescence microscope. The number of Hoechst-positive cell nuclei was determined with the “Analyze Particle” command of ImageJ software (Schneider et al., 2012). βIII-tubulin<sup>+</sup> cells were quantified by manual counting in all images and expressed as percentage of the total number of cell nuclei within the two pictures corresponding to one neurosphere.

## 2.8. Statistics

Statistical analysis was performed with the Software GraphPad Prism, Version 7, by one-way ANOVA, followed by Bonferroni's test in the one compound concentration-response experiments. Two-way ANOVA, followed by Bonferroni's post hoc test was carried out to compare two compounds concentration-response curves. For each evaluated compound 50% effective concentrations (EC<sub>50</sub>) were calculated by applying a nonlinear sigmoidal dose-response inhibition curve fit with variable slope to the obtained data points (with constrains top = 100, bottom = 0). Two-way ANOVA, followed by Bonferroni's post hoc test was also performed to determine the significance between angle-orientation variation and concentration. Student's t-test was used to compare the results between the two solvent controls and multiple student's t-test was applied to determine the significance between angle-orientation variation and concentration between the two solvent controls. Significance threshold in all statistical analysis was fixed at  $p < 0.05$ .

## 3. Results

In a previous study, EGCG exposure for 24 h disturbed migration of NPCs in both human and rat neurospheres (Barenys et al., 2017a). As there were no significant differences in sensitivity towards adverse EGCG effects between both species, we tested EGCG and five different related-substances in only one model: the rat neurospheres. To follow the same approach of that study, we chose the same exposure period (24 h), the same exposure concentration range (1–10 μM) and the same solvent control concentration (0.01% DMSO) in all cases except in the nanoparticulated formulation Nano-EGCG where the solvent control needed to be 0.1% Tween<sup>®</sup>80, the surfactant used to ensure the optimal physicochemical characteristics of the developed nanosystem (Cano et al., 2018). As 0.1% Tween<sup>®</sup>80 was never used as solvent control in the ‘Neurosphere Assay’ before, we present in Supplementary Figure 1 the comparison of the raw values obtained for all evaluated endpoints for 0.01% DMSO and 0.1% Tween<sup>®</sup>80 controls, showing no statistically significant differences for any migration- or neuronal differentiation-related endpoint and a significant increase in cell viability detected by means of Alamar-Blue assay in the 0.1% Tween<sup>®</sup>80 group which indicates that this solvent concentration is not cytotoxic for NPCs in culture.

The compounds selected to be included in this study were a nano-formulation of EGCG, and four EGCG structurally-related compounds including one (M1 and M2) or two (G37 and G56) galloyl groups (Fig. 1). The tested compounds displayed different potencies in disturbing NPC migration distance after 24 h of exposure. G37 and M2 produced significant decreases of migration distance at 5 μM, G56 and M1 caused this effect at the maximum concentration tested (10 μM), while Nano-EGCG did not significantly reduce the migration distance (Fig. 3). G56, M1, M2 and Nano-EGCG displayed a significantly different concentration-response curve from the one of EGCG (Fig. 3).

Besides decreasing the migration distance, we observed the previously described characteristic effect of EGCG disturbing the migration pattern by induction of gaps and branches in the migration area (Fig. 3). This effect, which so far has only been reported after exposure to catechin related compounds or to a functional beta1-integrin antibody, can be assessed by measuring the angle of the corona surrounding each neurosphere core with presence of migrating cells, irrespective of the distance of migration from the neurosphere core as published before for EGCG evaluation (Barenys et al., 2017a) and previously described in a different developmental neurotoxicity test using stem cells and measuring the neural outgrowth surrounding embryoid bodies (Theunissen et al., 2011). When the angle of the corona surrounded by migrating cells was measured, the tested compounds displayed very similar potencies than in the migration distance assay: G37 and M2 significantly decreased the angle of corona at 5 μM, while G56 and M1 only

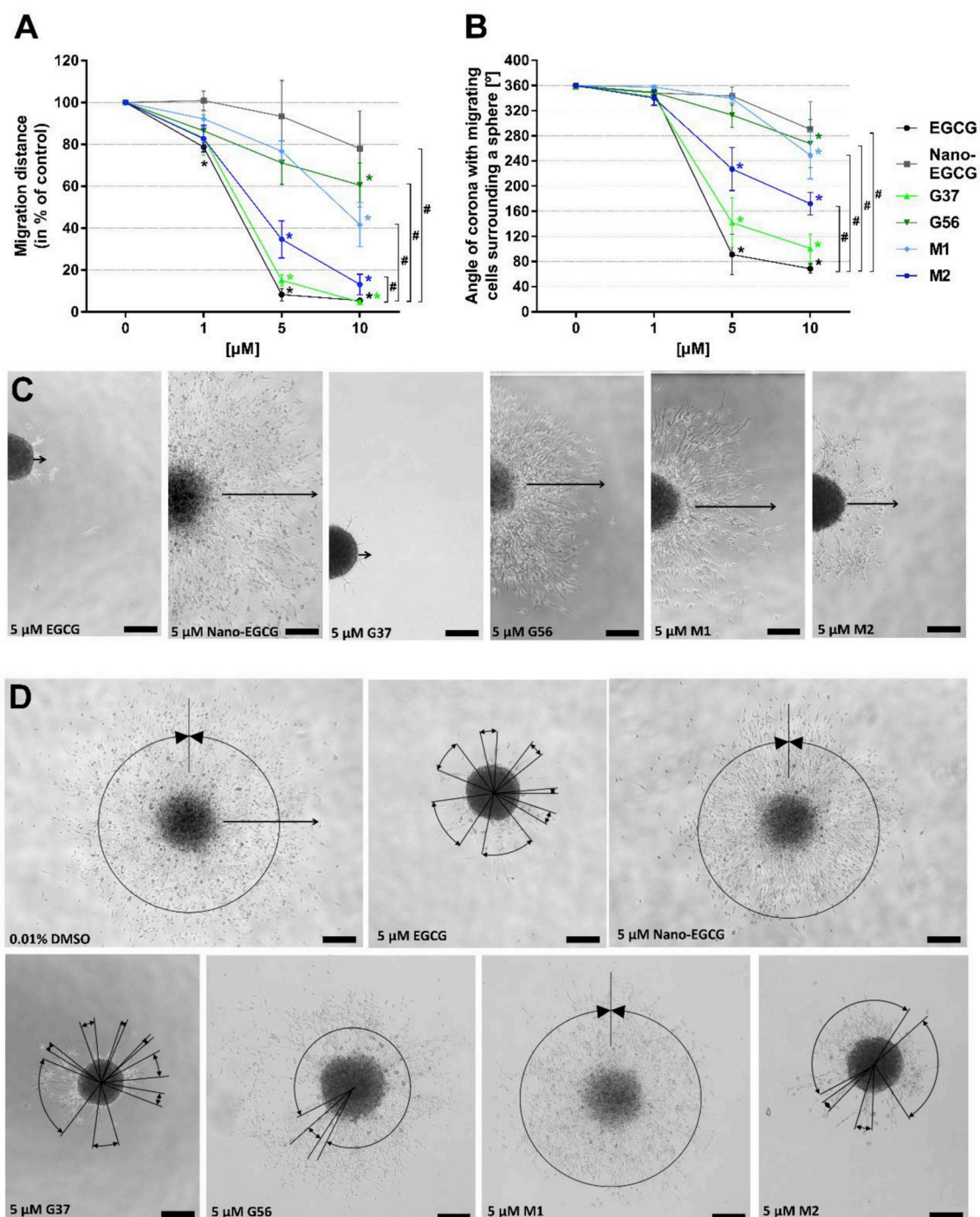


**Fig. 3.** EGCG, Nano-EGCG and structurally related compounds display different potencies in disturbing NPC migration distances and the formation of the migration corona. Rat neurospheres were cultured for 24 h with increasing concentrations of EGCG, Nano-EGCG, G37, G56, M1 and M2. Migration distance (A) and the angle of the corona with presence of migrating cells surrounding the neurosphere core (B) were evaluated in five neurospheres/concentration in four independent experiments. Results are presented as mean  $\pm$  SEM in % of respective solvent control (DMSO 0.01% for EGCG, G37, G56, M1 and M2 or 0.1% Tween<sup>®</sup>80 for Nano-EGCG), and mean  $\pm$  SEM angle values in degrees, respectively. \* $p < 0.05$  versus respective solvent control by one-way ANOVA and Bonferroni test. # $p < 0.05$  versus EGCG concentration-response curve by two-way ANOVA. C. Representative phase-contrast images of neurospheres exposed to 5  $\mu$ M of each test compound for 24 h showing part of their migration area with one of the measured distances indicated with an arrow. D. Representative phase-contrast images of neurospheres exposed to solvent control 0.01% DMSO, or 5  $\mu$ M of all tested compounds for 24 h showing the full migration area and the measured angles of corona with migrating cells around a sphere (In solvent control picture D, an arrow indicating the measured migration distance is also included for comparison with C). Scale bars: 100  $\mu$ m.

presented significant effects at 10  $\mu$ M and Nano-EGCG did not induce a significant reduction of the endpoint (Fig. 3). Also in this case, when concentration-response curves of each compound were compared to the one of EGCG, all tested compounds displayed a significantly different curve profile than EGCG except G37 (Fig. 3).

To better compare the potencies of the effects among all compounds, 50% effective concentrations ( $EC_{50}$ ) were calculated for the two previously presented endpoints as well as for viability results by applying a nonlinear sigmoidal dose response curve fit to the obtained data points (Fig. 4).  $EC_{50}$  values were above the tested concentrations

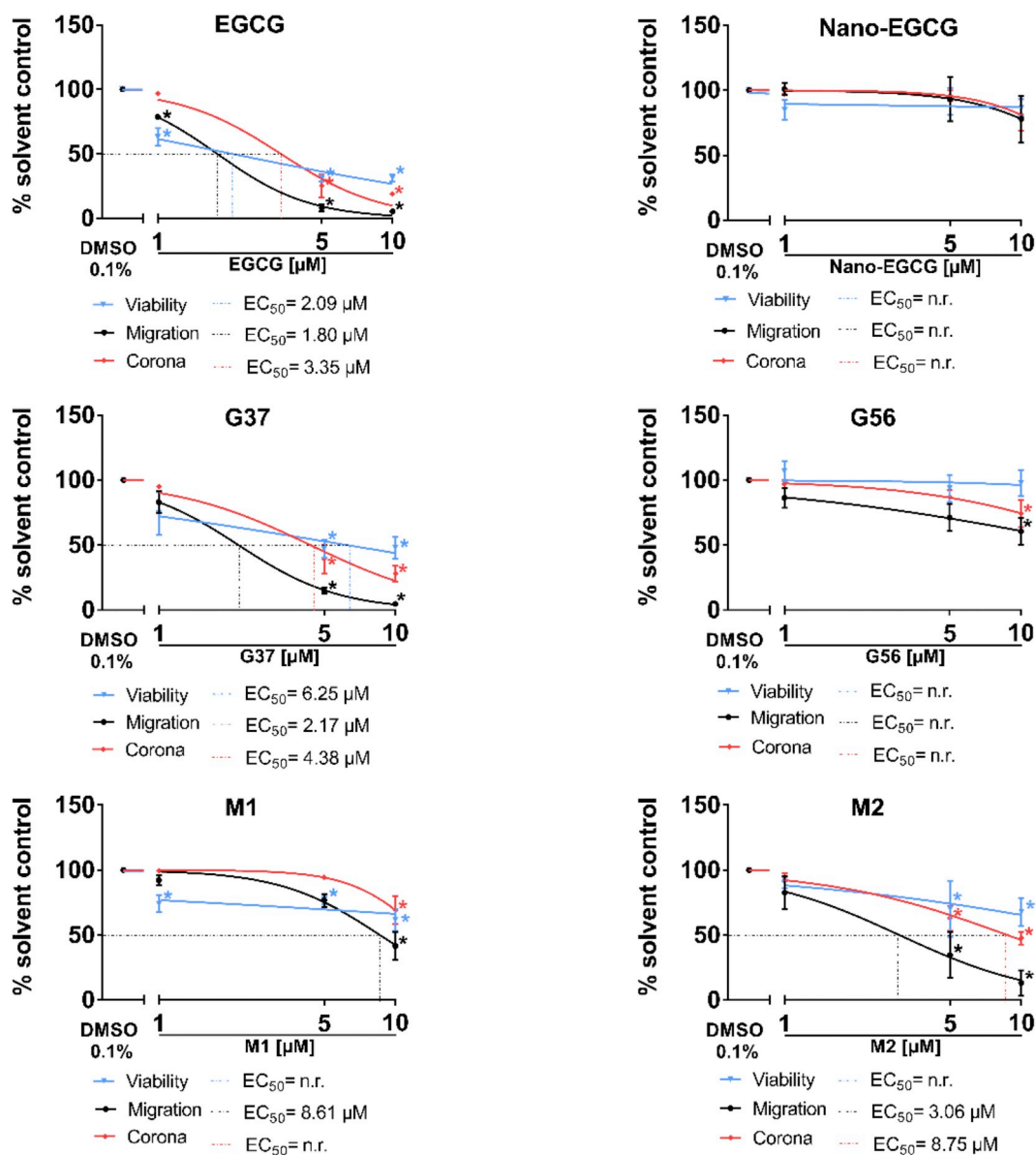


**Fig. 4.** EGCG structurally related compounds display different potencies in disturbing NPCs migration related endpoints. Rat neurospheres were cultured for 24 h with increasing concentrations of EGCG, Nano-EGCG, G37, G56, M1 and M2. Blue (viability), black (migration) and orange lines (angle of corona with migrating cells) represent the nonlinear sigmoidal dose response curve fitted to the data points of four independent experiments using GraphPad Prism v7. Data points represent the mean  $\pm$  SEM in % of respective solvent control (DMSO 0.01% for EGCG, G37, G56, M1 and M2 or 0.1% Tween<sup>®</sup>80 for Nano-EGCG). n. r.: not reached. \* $p < 0.05$  versus respective solvent control by one-way ANOVA and Bonferroni test. (For interpretation of the references to color in this figure legend, the reader is referred to the Web version of this article.)

for all endpoints for G56 and Nano-EGCG. For M1, EC<sub>50</sub> values were also above the tested concentrations for all endpoints except for migration where it was 8.61 μM. In contrast, G37 presented EC<sub>50</sub> values of the same magnitude than EGCG while M2 displayed approximately two times higher EC<sub>50</sub> values for the endpoints migration distance and corona formation. Viability curves representing metabolic activity measured with the Alamar Blue Assay showed that EC<sub>50</sub> values were not reached in any compound except for EGCG and G37. A very recent study shows that migration distance or pattern can define the magnitude of signal of viability assays like the Alamar Blue Assay because the metabolizing rate is related to number of cells in the migration area (Fritsche et al., 2018). Therefore it is not surprising that EGCG and G37, the two compounds with the strongest effect in migration distance and migration pattern are the only ones reaching an EC<sub>50</sub> in the Alamar Blue Assay. In that study, to discard a direct cytotoxic effect of EGCG in NPCs a different assay not directly dependent on cell number was applied:

FACS analyses identifying annexinV/Propidium Iodide positive cells clearly showed that EGCG does not cause cell death (Fritsche et al., 2018).

A complementary approach to evaluate the effect of EGCG on the migration of NPCs is to measure the orientation angle of the cell migrating processes in a fixed area. As cells migrate radially from the neurosphere core, cellular processes of solvent control neurospheres were mainly oriented between 0° and  $\pm 30^\circ$  angles toward the reference axis (for a schematic representation of the measurement method the reader is referred to Barenys et al., 2017a). In contrast, as previously observed, 24 h EGCG exposure caused a chaotic orientation of processes with a significantly increased percentage of cells between  $\pm 30^\circ$  and  $\pm 60^\circ$  angles. In this case, at higher concentrations, a significant increase in the percentage of cells oriented between  $\pm 60^\circ$  and  $\pm 90^\circ$  angles was also observed, while Nano-EGCG did not change the orientation of cell processes at any tested concentration (Fig. 5).

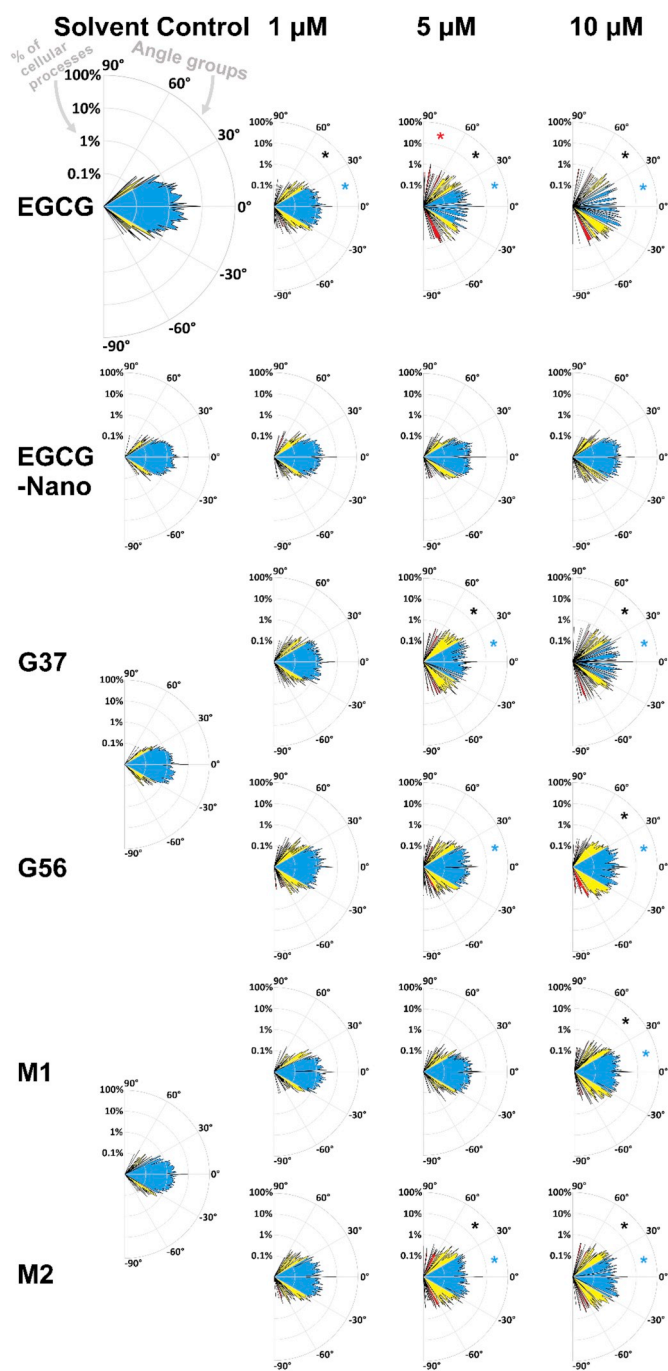


**Fig. 5.** EGCG, Nano-EGCG and structurally related compounds display different effects on the orientation of migrating cells processes. Color-coded polar plot displaying the orientation of cellular processes in relation to the reference axis after exposure of rat neurospheres to increasing concentrations of EGCG, Nano-EGCG, G37, G56, M1 and M2 during 24 h. Blue: angles from  $-30$  to  $30^\circ$ , yellow: angles from  $30^\circ$  to  $60^\circ$  and  $-30^\circ$  to  $-60^\circ$ , red: angles from  $60^\circ$  to  $90^\circ$  and  $-60^\circ$  to  $-90^\circ$ . Results are expressed in percentage of the total angles measured (vertical axis represents percentage in logarithmic scale). Data representing 3 independent experiments, where the angle of 240 cell processes in average per concentration and experiment were measured. \* $p < 0.05$  versus respective solvent control angle group by two-way ANOVA and Bonferroni analysis (EGCG, G37, G56, M1 and M2 solvent control: 0.01% DMSO; Nano-EGCG solvent control: 0.1% Tween<sup>®</sup>80). (For interpretation of the references to color in this figure legend, the reader is referred to the Web version of this article.)

For the other four tested compounds, in all cases the disturbance effect induced was less potent than after exposure to EGCG, as no significant effects were observed at 1  $\mu\text{M}$  and there was no significant increase in the percentage of cells oriented between  $\pm 60^\circ$  and  $\pm 90^\circ$  angles after exposure to any of the compounds tested. Again, when comparing among them four, the effect was more potent after exposure to G37 and M2 than after exposure to G56 or M1, which was not inducing significant effects until 10  $\mu\text{M}$ .

As in the ‘Neurosphere Assay’ the radial glial scaffold is normally used by young neurons to migrate away from the sphere core, we finally evaluated if the alterations in cell orientation had an impact in the percentage of migrating neurons, as previously observed with EGCG in human NPC (Barenys et al., 2017a). Similar to previous results in human neurospheres, after 24 h of exposure, EGCG induced a significant reduction in the percentage of neurons in the migration area also of rat neurospheres only at the highest concentration tested (10  $\mu\text{M}$ ; Fig. 6) (Barenys et al., 2017a). From all other compounds tested, only M2 induced a significant decrease in the percentage of neurons at concentrations even lower than EGCG (1  $\mu\text{M}$ ), while G37 and M1 showed a trend to reduction without reaching statistical significance (ANOVA  $p$  value = 0.06 and 0.07 respectively). Again, Nano-EGCG and G56 had no adverse effect on the endpoint studied at any concentration.

#### 4. Discussion

The within-laboratory variability of the results obtained with the ‘Neurosphere Assay’ in control or exposed neurospheres has already been published in several articles performed by different operators over a long time (Baumann et al., 2016; Fritsche et al., 2005; Moors et al., 2009; Schmuck et al., 2017). In addition historical control values of the different endpoints of the neurosphere assay were summarized (Baumann et al., 2015). But so far, the transferability of the method in a second laboratory was not shown. In the present work, we reproduce the results previously published for solvent control (DMSO 0.01%) and EGCG exposed neurospheres in a different laboratory (University of Barcelona) of a different country (Spain), with different equipment and using neurospheres gained from a different rat strain (Sprague-Dawley). The values obtained in control culture conditions in this new lab fulfill the quality requirements previously published (Baumann et al., 2016, 2014) and EGCG exposure disturbed NPC migration by inducing the same pattern of alterations: significantly reduced migration distance, significantly decreased angle of corona with presence of migrating cells, significantly disturbed orientation of migrating cells’ processes, and at higher concentrations reduced neuronal migration. The transferability of results among laboratories is a requirement of the retrospective validation process of new methods in toxicology described by Hartung et al. (2004), which outlines the path to evaluate the validity of a new test on the basis of a modular validation approach and which was already used for example to retrospectively validate the *in vitro* micronucleus test (Corvi et al., 2008). According to the recommendations on test readiness criteria for new approach methods in toxicology (Bal-Price et al., 2018) the present results contribute to prove the robustness of the ‘Neurosphere Assay’ (criteria 9c-interlab) and bring forward its readiness.

The main aim of this study was to compare the effects of EGCG on NPC migration with the ones induced by the structurally related compounds G37, G56, M1, M2 and Nano-EGCG, developed as new therapeutic strategies. The overall evaluation of the endpoints shows a consistent pattern of different potencies of the tested compounds:

EGCG  $\approx$  G37 > M2 > M1  $\approx$  G56 > Nano-EGCG

Several studies have shown that EGCG can bind to laminin (Peter et al., 2017; Suzuki and Isemura, 2001) and disturb the adhesion of cells to the extracellular matrix (Bracke et al., 1987; Chen et al., 2003;

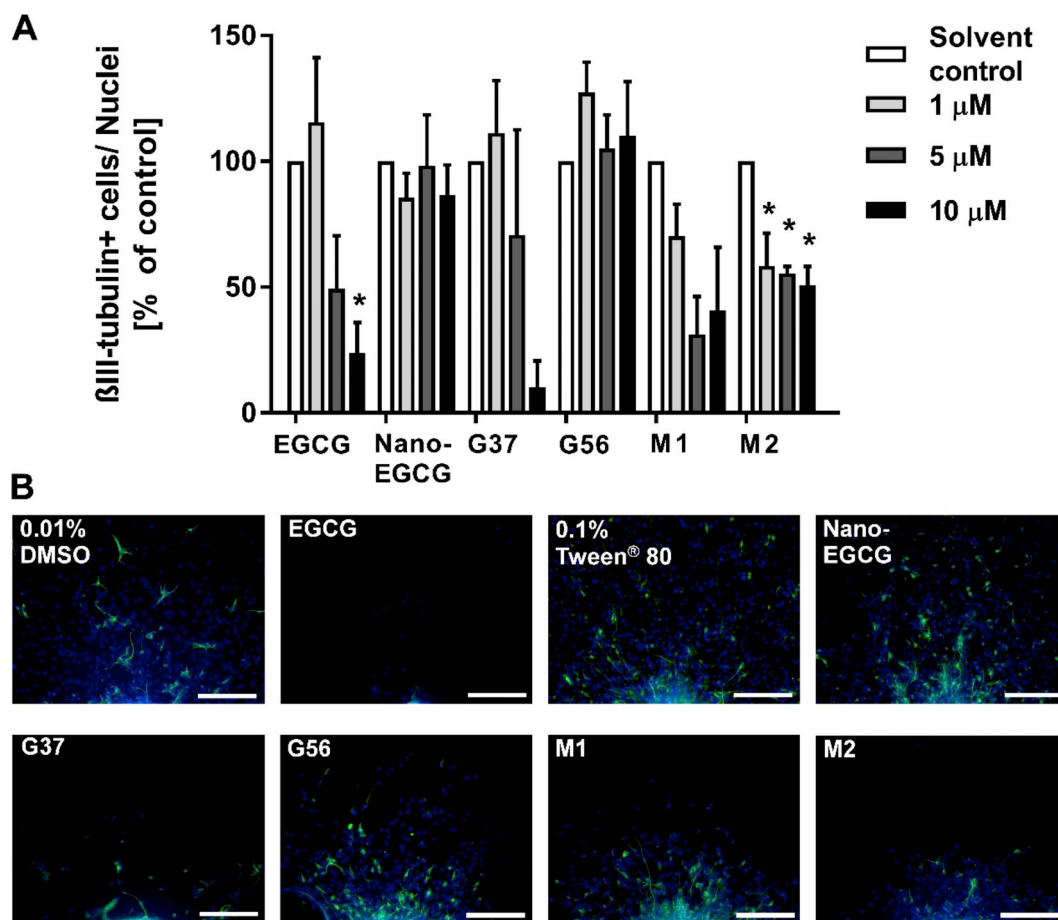


**Fig. 6.** EGCG structurally related compounds display different potencies in disturbing the migration of young neurons. **A.** Rat neurospheres were cultured for 24 h with increasing concentrations of EGCG, Nano-EGCG, G37, G56, M1 and M2. The number of  $\beta$ III-tubulin<sup>+</sup> cells was manually counted in two areas per neurosphere and five neurospheres per concentration in three independent experiments and divided by the total number of nuclei in the two areas. Results represent the mean  $\pm$  SEM in % of respective solvent control (DMSO 0.01% for EGCG, G37, G56, M1 and M2 or 0.1% Tween® 80 for Nano-EGCG). \* $p < 0.05$  versus respective solvent control by one-way ANOVA and Bonferroni test. **B.** Representative pictures of neurospheres exposed to 10  $\mu$ M of the tested compounds and their respective solvent controls. Blue: nuclei staining (Hoechst), green: neuronal marker ( $\beta$ III-tubulin). Scale bars: 100  $\mu$ m. (For interpretation of the references to color in this figure legend, the reader is referred to the Web version of this article.)

Suzuki and Isemura, 2001) finally leading to an altered cell migration pattern (Bal-Price et al., 2017; Barenys et al., 2017a; Nyffeler et al., 2017). The structural moieties inducing this altered cell migration seemed to be galloyl/pyrogallol groups because in a previous study, catechins lacking these residues did not disrupt cell adhesion (Barenys et al., 2017a). In that study we postulated that compounds with only one galloyl or pyrogallol moiety would disturb NPC migration less potently than compounds including two of them. With the results of the present work we can refute this hypothesis, as M2 with only one galloyl moiety disturbs migration more potently ( $EC_{50\text{migration-M2}} = 3.06 \mu\text{M}$ ) than G56 with two ( $EC_{50\text{migration-G56}} = \text{not reached}$ ). The current results also indicate that variations in the main structure can cause large differences in migration disturbance potency as G37 and G56 include both two galloyl groups but G37 with a naphthyl unit disturbs migration more potently than G56 with a biphenyl one ( $EC_{50\text{migration-G37}} = 2.17 \mu\text{M} < EC_{50\text{migration-G56}} = \text{not reached}$ ).

Hence, the structural interplay between galloyl groups and other aromatic ring groups within the same molecule seems to determine laminin binding capacity that masks integrin binding sites. To unravel the precise structures necessary for exerting these effects, more compounds structurally related to EGCG need to be tested in this assay.

To compare the EGCG-related compounds' potencies at an *in vivo* relevant concentration-range all compounds were tested between 1 and 10  $\mu$ M (reviewed by Barenys et al., 2017b). Concentrations of EGCG in human plasma within this range have already been described after

EGCG supplements intake (Shanafelt et al., 2009; Ullmann et al., 2003), however, a 5 or 10  $\mu$ M concentration would not be achievable in individuals with a non-supplemented diet (Skibola and Smith, 2000). When tested at this range of concentrations, compounds G37 and M2 disturbed some endpoints with an  $EC_{50} < 5 \mu\text{M}$ . G56 and M1 significantly disturbed migration distance and the formation of the migration corona only at 10  $\mu$ M and for G56  $EC_{50}$  values were not reached within the tested concentrations. For these compounds, concentrations around 10  $\mu$ M are not expected to be achieved in the developing brain *in vivo*, as pharmacokinetic studies in pregnant rats indicate that for example total EGCG is found at approximately eight times lower concentrations in the fetal brain than in maternal plasma (Chu et al., 2006). However, pharmacokinetic studies in pregnant animals with G37, G56, M1, M2 or Nano-EGCG have not been performed yet. In this sense, even if 10  $\mu$ M EGCG already induce a total response in migration, and higher concentrations would exceed *in vivo* relevance, the addition of a 20  $\mu$ M concentration for some of the other tested compounds would have strengthened the calculation of  $EC_{50}$  values. According to our results, M1 and G56 would seem good candidates to develop therapeutic or preventive strategies for pregnant women, however, M1 induces a non-significant decrease in migration of young neurons after 24 h ( $p = 0.07$ ) which could be expected to become stronger after longer exposures. As G56 does not induce any reduction in this endpoint either, G56 would seem a better alternative than M1. Other studies have shown that G56 is significantly more effective than EGCG in reducing thermal

hyperalgesia in a chronic constriction nerve injury mice model, that it displays strongest inhibition of lipogenic enzyme fatty acid synthase (FASN) than EGCG and that compared to the control group it does not cause significant changes on body weight neither alterations in hepatic, renal or hematological function markers at daily doses of 50 and 75 mg/kg (Xifró et al., 2015).

Furthermore, the nanoformulation of EGCG did not disturb any of the evaluated endpoints in this study ( $EC_{50s}$  = not reached for any endpoint). It is expected that in this particular case EGCG presents a more sustained release to the medium than when neurospheres are exposed to the free drug as this is precisely one of the aims of nanoencapsulating a compound, to contribute to a slower delivery of the drug. This sustained delivery might be responsible of a decreased concentration in the medium and a decreased interaction of the compound with the cells of the sphere or with the extracellular matrix, and therefore be responsible of a decrease or in this case an avoidance of adverse effects. The fact that a different solvent control was used while testing Nano-EGCG (0.1% Tween<sup>®</sup>80) did not influence the outcome, as the results of this solvent control are comparable with the ones of the solvent control used for G37, G56, M1 and M2 (0.01% DMSO; Supplementary Figure 1). This comparison also contributes to identify Tween<sup>®</sup>80 as a usable solvent control in the ‘Neurosphere Assay’, which might be of relevance due to its common use to develop nanoparticulated systems. Based on our results, Nano-EGCG could also be a potentially useful alternative to EGCG for developmental therapies. Previously published studies showed that Nano-EGCG significantly reduced the number and the intensity of epileptic episodes in mice more than the administration of the free drug (Cano et al., 2018).

Finally, it is important to remark that compounds containing galloyl moieties should be suspected to disturb the neurodevelopmental key event ‘NPC migration’, and therefore, developmental neurotoxicity relevant evaluations should be included in the process of developing new medical drugs structurally-related with this family.

In summary, we can conclude that several compounds structurally-related to EGCG that are designed as its new therapeutical alternatives, induce the same pattern of alterations in the migration of NPCs than EGCG and some of them do it with the same potency (G37). In general, the potency of the effects of these compounds does not necessarily depend on the number of galloyl groups present in the molecule. This study suggests G56 and Nano-EGCG as potential therapeutic or preventive alternatives to EGCG for the prenatal period but further comprehensive evaluations of the neurodevelopmental effects of these compounds are needed to confirm their safety.

## 5. Conflicts of interest

The authors declare no conflict of interest.

## Acknowledgements

The authors acknowledge the financial support from the University of Girona (MPCUdG2016/036) and the support of the Catalanian government (2017SGR00385). This work was also supported partially by Spanish grants from Fundación Ramón Areces and Instituto de Salud Carlos III (PI1400329). B.K. acknowledges the support of the Erasmus + EU Programme and A.C. acknowledges the support of the Generalitat de Catalunya for the PhD scholarship FI-DGR (CVE-DOGC-B-14206020-2014).

## Transparency document

Transparency document related to this article can be found online at <https://doi.org/10.1016/j.fct.2018.10.055>.

## Appendix A. Supplementary data

Supplementary data to this article can be found online at <https://doi.org/10.1016/j.fct.2018.10.055>.

## References

- Bal-Price, A., Lein, P.J., Keil, K.P., Sethi, S., Shafer, T., Barenys, M., Fritsche, E., Sachana, M., Meek, M.E., 2017. Developing and applying the adverse outcome pathway concept for understanding and predicting neurotoxicity. *Neurotoxicology* 59, 240–255. <https://doi.org/10.1016/j.neuro.2016.05.010>.
- Bal-Price, A., Hogberg, H.T., Crofton, K.M., Daneshian, M., FitzGerald, R.E., Fritsche, E., Heinonen, T., Hougaard Bennekou, S., Klima, S., Piersma, A.H., Sachana, M., Shafer, T.J., Terron, A., Monnet-Tschudi, F., Viviani, B., Waldmann, T., Westerink, R.H.S., Wilks, M.F., Witters, H., Zurich, M.G., Leist, M., 2018. Recommendation on Test Readiness Criteria for New Approach Methods in Toxicology: Exemplified for Developmental Neurotoxicity. *ALTEX*. <https://doi.org/10.14573/altex.1712081>.
- Barenys, M., Gassmann, K., Baksmeier, C., Heinz, S., Reverte, I., Schmuck, M., Temme, T., Bendt, F., Zschauer, T.-C., Rockel, T.D., Unfried, K., Wätjen, W., Sundaram, S.M., Heuer, H., Colomina, M.T., Fritsche, E., 2017a. Epigallocatechin gallate (EGCG) inhibits adhesion and migration of neural progenitor cells in vitro. *Arch. Toxicol.* 91. <https://doi.org/10.1007/s00204-016-1709-8>.
- Barenys, M., Masjosthusmann, S., Fritsche, E., 2017b. Is intake of flavonoid-based food supplements during pregnancy safe for the developing child? A literature review. *Curr. Drug Targets* 18. <https://doi.org/10.2174/1389450116666150804110049>.
- Baumann, J., Barenys, M., Gassmann, K., Fritsche, E., 2014. Comparative human and rat “neurosphere assay” for developmental neurotoxicity testing. *Curr. Protoc. Toxicol.* 1. <https://doi.org/10.1002/0471140856.tx1221s59>.
- Baumann, J., Dach, K., Barenys, M., Giersiefer, S., Goniwiecha, J., Lein, P.J., Fritsche, E., 2015. Application of the Neurosphere Assay for DNT Hazard Assessment: Challenges and Limitations. Humana Press, Totowa, NJ, pp. 1–29. [https://doi.org/10.1007/7653\\_2015\\_49\\_LB-ref1](https://doi.org/10.1007/7653_2015_49_LB-ref1).
- Baumann, J., Gassmann, K., Masjosthusmann, S., DeBoer, D., Bendt, F., Giersiefer, S., Fritsche, E., 2016. Comparative human and rat neurospheres reveal species differences in chemical effects on neurodevelopmental key events. *Arch. Toxicol.* 90, 1415–1427. <https://doi.org/10.1007/s00204-015-1568-8>.
- Bracke, M.E., Castronovo, V., Van Cauwenberge, R.M., Coopman, P., Vakaet, L.J., Strojny, P., Foidart, J.M., Mareel, M.M., 1987. The anti-invasive flavonoid (+)-catechin binds to laminin and abrogates the effect of laminin on cell morphology and adhesion. *Exp. Cell Res.* 173, 193–205.
- Cano, A., Ettcheto, M., Espina, M., Auladell, C., Calpena, A.C., Folch, J., Barenys, M., Sánchez-López, E., Camins, A., García, M.L., 2018. Epigallocatechin-3-gallate loaded PEGylated-PLGA nanoparticles: a new anti-seizure strategy for temporal lobe epilepsy. *Nanomed. Nanotechnol. Biol. Med.* 14. <https://doi.org/10.1016/j.nano.2018.01.019>.
- Chen, C.-N., Liang, C.-M., Lai, J.-R., Tsai, Y.-J., Tsay, J.-S., Lin, J.-K., 2003. Capillary electrophoretic determination of theanine, caffeine, and catechins in fresh tea leaves and oolong tea and their effects on rat neurosphere adhesion and migration. *J. Agric. Food Chem.* 51, 7495–7503. <https://doi.org/10.1021/jf034634b>.
- Chu, K.O., Wang, C.C., Chu, C.Y., Chan, K.P., Rogers, M.S., Choy, K.W., Pang, C.P., 2006. Pharmacokinetic studies of green tea catechins in maternal plasma and fetuses in rats. *J. Pharmacol. Sci.* 95, 1372–1381. <https://doi.org/10.1002/jps.20594>.
- Corvi, R., Albertini, S., Hartung, T., Hoffmann, S., Maurici, D., Pfuhler, S., van Benthem, J., Vanparys, P., 2008. ECVAM retrospective validation of in vitro micronucleus test (MNT). *Mutagenesis* 23, 271–283. <https://doi.org/10.1093/mutage/gen010>.
- Crous-Masó, J., Palomeras, S., Relat, J., Camó, C., Martínez-Garza, U., Planas, M., Feliu, L., Puig, T., 2018. (–)-Epigallocatechin 3-gallate synthetic analogues inhibit fatty acid synthase and show anticancer activity in triple negative breast cancer. *Molecules* 23. <https://doi.org/10.3390/molecules23051160>.
- Fritsche, E., Cline, J.E., Nguyen, N.-H., Scanlan, T.S., Abel, J., 2005. Polychlorinated biphenyls disturb differentiation of normal human neural progenitor cells: clue for involvement of thyroid hormone receptors. *Environ. Health Perspect.* 113, 871–876.
- Fritsche, E., Barenys, M., Klose, J., Masjosthusmann, S., Nimtz, L., Schmuck, M., Wuttke, S., Tigges, J., 2018. Current availability of stem cell-based in vitro methods for Developmental Neurotoxicity (DNT) testing. *Toxicol. Sci.* 165 (1), 21–30. <https://doi.org/10.1093/toxsci/kfy178>.
- Hartung, T., Bremer, S., Casati, S., Coecke, S., Corvi, R., Fortaner, S., Gribaldo, L., Halder, M., Hoffmann, S., Roi, A.J., Prieto, P., Sabbioni, E., Scott, L., Worth, A., Zuang, V., 2004. A modular approach to the ECVAM principles on test validity. *Altern. Lab. Anim.* 32, 467–472.
- Hollman, P.C., Feskens, E.J., Katan, M.B., 1999. Tea flavonols in cardiovascular disease and cancer epidemiology. *Proc. Soc. Exp. Biol. Med.* 220, 198–202.
- Holmes, G.L., McCabe, B., 2001. Brain development and generation of brain pathologies. *Int. Rev. Neurobiol.* 45, 17–41.
- Kennedy, D.A., Lupattelli, A., Koren, G., Nordeng, H., 2013. Herbal Medicine Use in Pregnancy: Results of a Multinational Study.
- Krupkova, O., Ferguson, S.J., Wuertz-Kozak, K., 2016. Stability of (–)-epigallocatechin gallate and its activity in liquid formulations and delivery systems. *J. Nutr. Biochem.* 37, 1–12. <https://doi.org/10.1016/j.jnutbio.2016.01.002>.
- Long, L., Li, Y., Wang, Y.D., He, Q.Y., Li, M., Cai, X.D., Peng, K., Li, X.P., Xie, D., Wen, Y.L., Yin, D.L., Peng, Y., 2010. The preventive effect of oral EGCG in a fetal alcohol spectrum disorder mouse model. *Alcohol Clin. Exp. Res.* 34, 1929–1936. <https://doi.org/10.1111/j.1530-0277.2010.01282.x>.
- McElyea, S.D., Starbuck, J.M., Tumbleson-Brink, D.M., Harrington, E., Blazek, J.D.,



- Ghoneima, A., Kula, K., Roper, R.J., 2016. Influence of prenatal EGCG treatment and Dyrk1a dosage reduction on craniofacial features associated with Down syndrome. *Hum. Mol. Genet.* 25, 4856–4869. <https://doi.org/10.1093/hmg/ddw309>.
- Mineva, N.D., Paulson, K.E., Naber, S.P., Yee, A.S., Sonenshein, G.E., 2013. Epigallocatechin-3-gallate inhibits stem-like inflammatory breast cancer cells. *PLoS One* 8, e73464. <https://doi.org/10.1371/journal.pone.0073464>.
- Moors, M., Cline, J.E., Abel, J., Fritsche, E., 2007. ERK-dependent and -independent pathways trigger human neural progenitor cell migration. *Toxicol. Appl. Pharmacol.* 221, 57–67. <https://doi.org/10.1016/j.taap.2007.02.018>.
- Moors, M., Rockel, T.D., Abel, J., Cline, J.E., Gassmann, K., Schreiber, T., Schuwald, J., Weinmann, N., Fritsche, E., 2009. Human neurospheres as three-dimensional cellular systems for developmental neurotoxicity testing. *Environ. Health Perspect.* 117, 1131–1138. <https://doi.org/10.1289/ehp.0800207>.
- Nyffeler, J., Dolde, X., Krebs, A., Pinto-Gil, K., Pastor, M., Behl, M., Waldmann, T., Leist, M., 2017. Combination of multiple neural crest migration assays to identify environmental toxicants from a proof-of-concept chemical library. *Arch. Toxicol.* 91, 3613–3632. <https://doi.org/10.1007/s00204-017-1977-y>.
- Ortiz-Romero, P., Borralleras, C., Bosch-Morato, M., Guivernau, B., Albericio, G., Munoz, F.J., Perez-Jurado, L.A., Campuzano, V., 2018. Epigallocatechin-3-gallate improves cardiac hypertrophy and short-term memory deficits in a Williams-Beuren syndrome mouse model. *PLoS One* 13, e0194476. <https://doi.org/10.1371/journal.pone.0194476>.
- Peter, B., Farkas, E., Forgacs, E., Saftics, A., Kovacs, B., Kurunzi, S., Szekacs, I., Csampai, A., Bosze, S., Horvath, R., 2017. Green tea polyphenol tailors cell adhesivity of RGD displaying surfaces: multicomponent models monitored optically. *Sci. Rep.* 7, 42220. <https://doi.org/10.1038/srep42220>.
- Puig, T., Turrado, C., Benhamú, B., Aguilar, H., Relat, J., Ortega-Gutiérrez, S., Casals, G., Marrero, P.F., Urruticoechea, A., Haro, D., López-Rodríguez, M.L., Colomer, R., 2009. Novel inhibitors of fatty acid synthase with anticancer activity. *Clin. Canc. Res.* 15, 7608–7615. <https://doi.org/10.1158/1078-0432.CCR-09-0856>.
- Schneider, C.A., Rasband, W.S., Eliceiri, K.W., 2012. NIH Image to ImageJ: 25 years of image analysis. *Nat. methods* 9 (7), 671–675.
- Rothwell, J.A., Perez-Jimenez, J., Neveu, V., Medina-Remon, A., M'hiri, N., Garcia-Lobato, P., Manach, C., Knox, C., Eisner, R., Wishart, D.S., Scalbert, A., 2013. Phenol-explorer 3.0: a major update of the phenol-explorer database to incorporate data on the effects of food processing on polyphenol content. *Database* 2013. <https://doi.org/10.1093/database/bat070>.
- Schmuck, M.R., Temme, T., Dach, K., de Boer, D., Barenys, M., Bendt, F., Mosig, A., Fritsche, E., 2017. Omnisphero: a high-content image analysis (HCA) approach for phenotypic developmental neurotoxicity (DNT) screenings of organoid neurosphere cultures in vitro. *Arch. Toxicol.* 91, 2017–2028. <https://doi.org/10.1007/s00204-016-1852-2>.
- Shanafelt, T.D., Call, T.G., Zent, C.S., LaPlant, B., Bowen, D.A., Roos, M., Secreto, C.R., Ghosh, A.K., Kabat, B.F., Lee, M.-J., Yang, C.S., Jelinek, D.F., Erlichman, C., Kay, N.E., 2009. Phase I trial of daily oral Polyphenon E in patients with asymptomatic Rai stage 0 to II chronic lymphocytic leukemia. *J. Clin. Oncol.* 27, 3808–3814. <https://doi.org/10.1200/JCO.2008.21.1284>.
- Shankar, S., Ganapathy, S., Hingorani, S.R., Srivastava, R.K., 2008. EGCG inhibits growth, invasion, angiogenesis and metastasis of pancreatic cancer. *Front. Biosci.* 13, 440–452.
- Singh, B.N., Shankar, S., Srivastava, R.K., 2011. Green tea catechin, epigallocatechin-3-gallate (EGCG): mechanisms, perspectives and clinical applications. *Biochem. Pharmacol.* 82, 1807–1821. <https://doi.org/10.1016/j.bcp.2011.07.093>.
- Skibola, C.F., Smith, M.T., 2000. Potential health impacts of excessive flavonoid intake. *Free Radic. Biol. Med.* 29, 375–383.
- Suzuki, Y., Isemura, M., 2001. Inhibitory effect of epigallocatechin gallate on adhesion of murine melanoma cells to laminin. *Cancer Lett.* 173, 15–20.
- Theunissen, P.T., Pennings, J.L.A., Robinson, J.F., Claessen, S.M.H., Kleinjans, J.C.S., Piersma, A.H., 2011. Time-response evaluation by transcriptomics of methylmercury effects on neural differentiation of murine embryonic stem cells. *Toxicol. Sci.* 122, 437–447. <https://doi.org/10.1093/toxsci/kfr134>.
- Tiwari, V., Kuhad, A., Chopra, K., 2010. Epigallocatechin-3-gallate ameliorates alcohol-induced cognitive dysfunctions and apoptotic neurodegeneration in the developing rat brain. *Int. J. Neuropsychopharmacol.* 13, 1053–1066. <https://doi.org/10.1017/S146114571000060X>.
- Turrado, C., Puig, T., García-Cárceles, J., Artola, M., Benhamú, B., Ortega-Gutiérrez, S., Relat, J., Oliveras, G., Blancafort, A., Haro, D., Marrero, P.F., Colomer, R., López-Rodríguez, M.L., 2012. New synthetic inhibitors of fatty acid synthase with anticancer activity. *J. Med. Chem.* 55, 5013–5023. <https://doi.org/10.1021/jm2016045>.
- Ullmann, U., Haller, J., Decourt, J.P., Girault, N., Girault, J., Richard-Caudron, A.S., Pineau, B., Weber, P., 2003. A single ascending dose study of epigallocatechin gallate in healthy volunteers. *J. Int. Med. Res.* 31, 88–101. <https://doi.org/10.1177/147323000303100205>.
- Xifró, X., Vidal-Sancho, L., Boadas-Vaello, P., Turrado, C., Alberch, J., Puig, T., Verdú, E., 2015. Novel epigallocatechin-3-gallate (EGCG) derivative as a new therapeutic strategy for reducing neuropathic pain after chronic constriction nerve injury in mice. *PLoS One* 10, 1–15. <https://doi.org/10.1371/journal.pone.0123122>.
- Yang, C.S., Wang, X., Lu, G., Picinich, S.C., 2009. Cancer prevention by tea: animal studies, molecular mechanisms and human relevance. *Nat. Rev. Canc.* 9, 429–439. <https://doi.org/10.1038/nrc2641>.

## 4.6 Application of the adverse outcome pathway to identify changes in prenatal brain programming after exposure to EGCG

**Britta Anna Kühne**<sup>1,2</sup>, Elisabet Teixidó<sup>1</sup>, Miren Ettcheto<sup>3,4</sup>, Teresa Puig<sup>5</sup>, Marta Planas<sup>6</sup>, Lidia Feliu<sup>6</sup>, Laura Pla<sup>2</sup>, Victoria Campuzano<sup>7</sup>, Eduard Gratacós<sup>2</sup>, Ellen Fritsche<sup>8</sup>, Miriam Illa<sup>2,†</sup>, Marta Barenys<sup>1,\*,†</sup>

<sup>1</sup> Grup de Recerca en Toxicologia (GRET) i INSA-UB, Departament de Farmacologia, Toxicologia i Química Terapèutica, Facultat de Farmàcia i Ciències de l'Alimentació, Universitat de Barcelona, 08028 Barcelona, Spain

<sup>2</sup> BCNatal-Barcelona Center for Maternal-Fetal and Neonatal Medicine (Hospital Clínic and Hospital Sant Joan de Déu), Fetal i+D Fetal Medicine Research Center, IDIBAPS, University of Barcelona, Center for Biomedical Research on Rare Diseases (CIBER-ER), Barcelona, Spain.

<sup>3</sup> Institute of Neuroscience, University of Barcelona, Barcelona, Spain

<sup>4</sup> Biomedical Research Networking Centre in Neurodegenerative Diseases (CIBERNED), Madrid, Spain; Department of Pharmacology, Toxicology and Therapeutic Chemistry, Faculty of Pharmacy and Food Sciences, University of Barcelona, Spain

<sup>5</sup> New Therapeutic Targets Laboratory (TargetsLab), Department of Medical Sciences, University of Girona, Girona Institute for Biomedical Research, 17003, Girona, Spain.

<sup>6</sup> LIPPSO, Department of Chemistry, University of Girona, 17003, Girona, Spain.

<sup>7</sup> Department of Biomedical Sciences, University of Barcelona School of Medicine and Health Sciences and Center for Biomedical Research on Rare Diseases (CIBER-ER), 08036 Barcelona (Spain).

<sup>8</sup> IUF-Leibniz Research Institute for Environmental Medicine, Düsseldorf, Germany.

† These authors contributed equally to this work and share last authorship

\* Corresponding author: Dr. Marta Barenys

|                       |  |
|-----------------------|--|
| Journal               | Food and Chemical Toxicology               |
| Impact Factor 2020    | 6.023                                      |
| Quartile              | Q1 (and D1) in Food science and technology |
| Type of authorship    | First author                               |
| Status of publication | Submitted 22.07.2022                       |

## Summary

Following a multi-disciplinary approach integrating information from several experimental models we have collected new evidence supporting, expanding and redesigning the AOP “Disrupted laminin/int- $\beta$ 1 interaction leading to decreased cognitive function”. Investigations *in vitro* in rabbit and rat neurospheres and *in vivo* in mice exposed to EGCG (epigallocatechin-gallate) during neurodevelopment are combined with *in vitro* evaluations in neural progenitor cells overexpressing int- $\beta$ 1 and literature information from int- $\beta$ 1 deficiency models. We have discovered for the first time that neural progenitor cells from intrauterine growth restricted (IUGR) animals overexpress int- $\beta$ 1 at gene and protein level and due to this change in prenatal brain programming they respond differently than control neurospheres to the exposure of EGCG, a compound triggering neural progenitor cell migration alterations. We have also identified that EGCG developmental exposure has deleterious effects on neuronal branching and arborisation *in vitro* and *in vivo*. Our results warn that a thorough developmental neurotoxicity characterization of this and other catechin-based food supplements is needed before recommending their consumption during pregnancy.

# Application of the adverse outcome pathway to identify molecular changes in prenatal brain programming induced by IUGR: discoveries after EGCG exposure

Britta Anna Kühne<sup>1,2</sup>, Elisabet Teixidó<sup>1</sup>, Miren Ettcheto<sup>3,4</sup>, Teresa Puig<sup>5</sup>, Marta Planas<sup>6</sup>, Lidia Feliu<sup>6</sup>, Laura Pla<sup>2</sup>, Victoria Campuzano<sup>7</sup>, Eduard Gratacós<sup>2</sup>, Ellen Fritsche<sup>8</sup>, Miriam Illa<sup>2,†</sup>, Marta Barenys<sup>1,\*,†</sup>

<sup>1</sup> Grup de Recerca en Toxicologia (GRET) i INSA-UB, Departament de Farmacologia, Toxicologia i Química Terapèutica, Facultat de Farmàcia i Ciències de l'Alimentació, Universitat de Barcelona, 08028 Barcelona, Spain

<sup>2</sup> BCNatal-Barcelona Center for Maternal-Fetal and Neonatal Medicine (Hospital Clínic and Hospital Sant Joan de Déu), Fetal i+D Fetal Medicine Research Center, IDIBAPS, University of Barcelona, Center for Biomedical Research on Rare Diseases (CIBER-ER), Barcelona, Spain.

<sup>3</sup> Institute of Neuroscience, University of Barcelona, Barcelona, Spain

<sup>4</sup> Biomedical Research Networking Centre in Neurodegenerative Diseases (CIBERNED), Madrid, Spain; Department of Pharmacology, Toxicology and Therapeutic Chemistry, Faculty of Pharmacy and Food Sciences, University of Barcelona, Spain

<sup>5</sup> New Therapeutic Targets Laboratory (TargetsLab), Department of Medical Sciences, University of Girona, Girona Institute for Biomedical Research, 17003, Girona, Spain.

<sup>6</sup> LIPPSO, Department of Chemistry, University of Girona, 17003, Girona, Spain.

<sup>7</sup> Department of Biomedical Sciences, University of Barcelona School of Medicine and Health Sciences and Center for Biomedical Research on Rare Diseases (CIBER-ER), 08036 Barcelona (Spain).

<sup>8</sup> IUF-Leibniz Research Institute for Environmental Medicine, Düsseldorf, Germany.

† These authors contributed equally to this work and share last authorship

\* Corresponding author:

Dr. Marta Barenys

GRET, INSA-UB and Toxicology Unit, Pharmacology, Toxicology and Therapeutic Chemistry Department, Faculty of Pharmacy, University of Barcelona, Barcelona, Spain.

Av. Joan XXIII, 27-31

08028 Barcelona (Spain)

E-Mail: [mbarenys@ub.edu](mailto:mbarenys@ub.edu)

## Author's contributions:

Britta Anna Kühne: Conceptualization; Data curation; Formal analysis; Investigation; Methodology; Visualization; Validation; Writing - original draft; Elisabet Teixidó: Data curation; Formal analysis; Software; Miren Ettcheto: Methodology; Formal analysis; Investigation; Teresa Puig: Resources; Marta Planas: Resources; Lidia Feliu: Resources; Laura Pla: Methodology; Victoria Campuzano: Data curation; Formal analysis; Investigation; Methodology; Validation; Eduard Gratacós: Resources; Funding acquisition; Ellen Fritsche: Validation; Writing - review & editing; Miriam Illa: Funding acquisition; Methodology; Project administration; Supervision; Writing - review & editing; Marta Barenys:

Conceptualization; Data curation; Formal analysis; Investigation; Project administration; Supervision; Validation; Visualization; Writing - original draft; Writing - review & editing

Keywords: Embryonic and Fetal Development, Fetal Growth Restriction (FGR), Progenitor Cells, Neurogenesis, Neurosphere Model, epigallocatechin gallate (EGCG); developmental neurotoxicity (DNT).

Abbreviations: AOP, Adverse outcome pathway; BMP7, Bone Morphogenetic Protein 7; CA1, Cornu ammonis; CEEA, Ethic Committee for Animal Experimentation; cKE, contrary/compensating key event; CTB, CellTiter-Blue Reagent; DMEM, Dulbecco's Modified Eagle Medium; DMSO, dimethyl sulfoxide; DNT, Developmental neurotoxicity; EC50, 50% effective concentration; ECG, Epicatechingallate; ECM, extracellular matrix; EGC, Epigallocatechin; EGCG, Epigallocatechin gallate; EGF, Epidermal growth factor; FGF2, Fibroblast growth factor 2; G56, 4,4'-bis[(3,4,5-trihydroxybenzoyl)oxy]-1,1'-biphenyl; GD, gestational day; GFAP, glial fibrillary acidic protein; HPLC, High Performance Liquid Chromatography; int- $\beta$ 1, Integrin- $\beta$ 1; int- $\beta$ 4, Integrin- $\beta$ 4; IUGR, Intrauterine growth restriction; KEs, Key events; KNIME, Konstanz Information Miner; MIE, Molecular initiating event; NOEAL, No Observed Adverse Effect Level; NPCs, Neural progenitor cells; OECD, Organisation for Economic Co-operation and Development; OL, Oligodendrocytes; PBS, Phosphate buffered saline; PDL, Poly-D-lysine; PFA, Paraformaldehyde; PND0, Postnatal day 0; poly-HEMA, Polyhydroxyethylmethacrylate; qRT-PCR, Quantitative real-time polymerase chain reaction; ROCK, Rho kinase; SC, Solvent control; SM, Supplementary material; SO, Stratum oriens; SR, Stratum radiatum.

## Abstract

Following a multi-disciplinary approach integrating information from several experimental models we have collected new evidence supporting, expanding and redesigning the AOP "Disrupted laminin/int- $\beta$ 1 interaction leading to decreased cognitive function". Investigations *in vitro* in rabbit and rat neurospheres and *in vivo* in mice exposed to EGCG (epigallocatechin-gallate) during neurodevelopment are combined with *in vitro* evaluations in neural progenitor cells overexpressing int- $\beta$ 1 and literature information from int- $\beta$ 1 deficiency models. We have discovered for the first time that neural progenitor cells from intrauterine growth restricted (IUGR) animals overexpress int- $\beta$ 1 at gene and protein level and due to this change in prenatal brain programming they respond differently than control neurospheres to the exposure of EGCG, a compound triggering neural progenitor cell migration alterations. We have also identified that EGCG developmental exposure has deleterious effects on neuronal branching and arborisation *in vitro* and *in vivo*. Our results warn that a thorough developmental neurotoxicity characterization of this and other catechin-based food supplements is needed before recommending their consumption during pregnancy.

## 1. Introduction

Epigallocatechin gallate (EGCG), the most abundant catechin in green tea, is currently being broadly studied as a promising treatment for several diseases including Alzheimer' and Parkinson's disease, cancer, obesity or inflammation (Cano et al., 2019; Pervin et al., 2018). EGCG has even been proposed as a possible treatment during pregnancy to prevent/ treat alterations of brain development due to Down's syndrome (Catuara-Solarz et al., 2016; Souchet et al., 2019; Stagni et al., 2021, 2016), or fetal alcoholic syndrome (Almeida-Toledano et al., 2021; Long et al., 2010; Tiwari et al., 2010). However, the safety of EGCG during prenatal development is still unclear because it has not been subject to classical risk assessment evaluations (Abdel-Rahman et al., 2011) and comprehensive information on specific toxicities concerning subtle endpoints like developmental neurotoxicity (DNT) is missing (Barenys et al., 2016a). Previous studies using the Neurosphere Assay shed light on the potential neurodevelopmental toxic effects of EGCG proving adverse effects on neural progenitor cell' (NPC) migration and unravelling the mechanism behind it: the binding of EGCG to the extracellular matrix protein laminin, which prevents the interaction of the integrin- $\beta$ 1 (int- $\beta$ 1) cell adhesion molecule with laminin (Barenys et al., 2016b, 2017; Kühne et al., 2019; Peter et al., 2017; Suzuki and Isemura, 2001).

However, the dose makes the poison, so in the present study, we investigated in the Neurosphere Assay if 5-, 50- or 500-times lower concentrations of EGCG would no longer have this DNT effect and could be safely used as a neuroprotective prenatal therapy. In parallel we tested the same concentrations of a synthetic analogue of EGCG named 4,4'-bis[(3,4,5-trihydroxybenzoyl)oxy]-1,1'-biphenyl or G56 with the same purpose, because it was previously selected in the Neurosphere Assay as the safest among a group of synthetic analogues regarding NPC migration and it was suggested to be the best candidate for potential future therapeutic or preventive alternatives to EGCG during the prenatal period (Kühne et al., 2019).

For both compounds we didn't only evaluate their safety, but also their efficacy as neuroprotective agents at this lower concentration range. In this case and based on the known antioxidant activity of EGCG we studied their use as neuroprotective prenatal therapies during intrauterine growth restriction (IUGR) (Barenys et al., 2021). IUGR is a widespread disorder during development defined as a significant reduction of fetal growth rate mainly due to placental insufficiency (Kady and Gardosi, 2004). This condition leads to fetal development under chronic hypoxia resulting in white matter injury due to myelination defects and in a significant reduction in oligodendrogenesis (Barenys et al., 2021; Kühne et al., 2022; Reid et al., 2012; Rideau Batista Novais et al., 2016; Tolcos et al., 2011). In the long run, IUGR can manifest in severe neurodevelopmental sequelae like neurocognitive disorders, learning disabilities, attention deficit hyperactivity disorder, or autism spectrum disorder (Abel et al., 2013; Illa et al., 2013; Leitner et al., 2007; Mwaniki et al., 2012). Hence it was reasonable to test the widely used green tea component EGCG and the alternative G56 on the critical neurodevelopmental endpoints of migration and OL differentiation. To study the neuroprotective potential of EGCG and G56 to rescue IUGR induced oligodendrogenesis defects, we used a novel 3D rabbit neurosphere model, which mimics the basic processes of brain development of control and IUGR rabbit pups including NPC proliferation, migration and differentiation (Barenys et al., 2021; Baumann et al., 2014; Moors et al., 2009). The species rabbit was chosen due to its similarity to human placentation and perinatal brain development (Barenys et al., 2021; Drobyshevsky et al., 2014; Workman et al., 2013) and because it was previously proven to reflect better the neurodevelopmental alterations observed in humans than the rodent species (Batalle et al., 2012, 2014; Eixarch et al., 2012; Illa et al., 2013).

Based on the obtained results with EGCG and G56 in control and IUGR rabbit neurospheres, we further explored the consequences of EGCG exposure to dendrite formation and continued building a previously postulated adverse outcome pathway (AOP) complementing it with a

combination of key events (KEs) related with both endpoint, cell migration and dendrite formation.

## **2. Material and Methods**

### **2.1. IUGR induction**

All animal procedures were approved by the Ethics Committee for Animal Experimentation (CEEAA) of the University of Barcelona and all protocols were accepted by the Department of Environment and Housing of the 'Generalitat de Catalunya' (license number: 11126, date of approval: 24/5/2021, procedure CEEA number: OB 340/19 SJD). The IUGR induction were performed in pregnant New Zealand rabbit according to the procedure previously described in Eixarch et al., (2009). Briefly, on gestational day (GD) 25, IUGR was induced by surgical ligation of 40-50% of the uterine vessels of each gestational sac of one uterine horn whereas the parallel horn remained as control for normal growth. On GD 30, IUGR and control pups were born under caesarean section and the birth weight was measured. In this study, the inclusion criteria for postnatal day (PND) 0 rabbit pups was the same that was previously used in Barenys et al., (2021): for IUGR pups a birth weight lower and for control pups a birth weight higher than the 25<sup>th</sup> percentile (39.7 g).

### **2.2. Neurosphere preparation**

The neurosphere culture was prepared from whole brains of control and IUGR PND0 rabbit pups. The body weight of the pups was measured after caesarean section. The average birth weight of IUGR rabbit pups was significantly lower than the weight of control pups (control  $47.7 \pm 19.5$  g vs IUGR  $28.1 \pm 11.4$  g, Fig. S1). Neural progenitor cells (NPCs) isolation from PND0 rabbit brains was performed as previously explained in Barenys et al. (2021), Kühne et al. (2022) and detailed in Pla et al. (2022). In brief, meninges and olfactory bulbs were carefully removed from the brain followed by mechanical cutting and enzymatic digestion with papain 20 U/mL for 20 min at 37°C. Cell suspension was generated by mechanical homogenization and centrifugation for 10 min at



1200 rpm. Afterwards the cell pellet was resuspended in freezing medium (1:1; volume of pellet: volume of freezing medium [consisting in 70% (v/v) proliferation medium, 20% (v/v) fetal calf serum and 10% (v/v) DMSO]) and immediately stored at  $-80^{\circ}\text{C}$ . A detailed description of the thawing protocol can be found in Pla et al. (2022). After thawing, NPCs were cultured for 11 days in proliferation medium on Petri dishes coated with poly-HEMA at  $37^{\circ}\text{C}$  and 5%  $\text{CO}_2$ . Proliferation medium consists of DMEM and Hams F12 3:1 supplemented with 2% B27, and 20 ng/mL epidermal growth factor (EGF) including recombinant human fibroblast growth factor (FGF2), 100 U/mL penicillin, and 100  $\mu\text{g}/\text{mL}$  streptomycin, supplemented with 10  $\mu\text{M}$  Rho kinase (ROCK) inhibitor Y-276322. Subsequently, half of the medium was renewed every 2–3 days without ROCK supplements.

### 2.3. Neurosphere assay

After 11 days of proliferation, neurospheres were mechanically chopped to 0.2 mm size (McIlwain tissue chopper) and incubated at  $37^{\circ}\text{C}$  and 5%  $\text{CO}_2$  for 2–3 days until they reached a size of 0.3 mm. For every endpoint of migration and differentiation, 5 neurospheres per condition were plated as replicates in a dice position in one well of an 8-chamber slide coated with PDL/Laminin. Each chamber contained 500  $\mu\text{L}$  of differentiation medium consisting of DMEM and Hams F12 3:1 supplemented with N2 (Invitrogen), penicillin, and streptomycin (100 U/mL and 100  $\mu\text{g}/\text{mL}$ ). At least three independent experiments were performed for every endpoint and exposure.

#### 2.3.1. Testing of EGCG and G56

EGCG and G56 were dissolved in DMSO and subsequently in differentiation medium with a maximum solvent concentration of 0.01% DMSO. The highest tested concentration was 1  $\mu\text{M}$  followed by 1:10 dilution. NPCs exposed to the solvent control (SC), or compound were incubated for 72 h or 120 h depending on the endpoint to analyse. After 72 h of differentiation 50% of the medium was replaced by fresh exposure medium.

### 2.3.2. Migration distance assay

Radial glial migration was measured as previously described in Baumann et al. (2014). Briefly, after 72 h and 120 h under differentiation conditions, bright-field pictures were taken from each neurosphere [EX-H30 camera (Casio, Japan)]. Migration distance [ $\mu\text{m}$ ] was measured on four right-angled sides from the neurospheres core until the furthest migrated cell using ImageJ 1.53a software.

### 2.3.3. Corona formation of migrating cells

After 72 h under differentiation conditions, the angles of cells covering the migration corona around the sphere core was manually measured, being  $360^\circ$  the total corona of migrating cells. The sum of all angles surrounding the sphere core was calculated, as previously described in Kühne et al. (2019).

### 2.3.4. Viability testing

Cell viability was assessed after 120 h of differentiation using CellTiter-Blue<sup>®</sup> (CTB) reagent (Promega). In every experiment a lysis control was included by exposing neurospheres to 10% DMSO for 2 h. For a detailed description refer to Pla et al. (2022).

### 2.3.5. Oligodendrocyte differentiation assay

The OL immunocytostaining was performed after viability assessment as described in (Kühne et al., 2022; Pla et al., 2022). Briefly, after 120 h of exposure neurospheres were fixed with 4% PFA. Slides were washed with PBS and incubated with the 1<sup>st</sup> antibody solution overnight at  $4^\circ\text{C}$  (1:200 mouse IgM anti-O4 (R&D Systems), 10% goat serum in PBS) and after washing with the 2<sup>nd</sup> antibody solution for 30 min at  $37^\circ\text{C}$  (1:200 anti-mouse IgG Alexa Fluor<sup>®</sup> 488 (Invitrogen), 2% goat serum and 1% Hoechst 33258 (Sigma Aldrich)). Images from the upper and lower part from each neurosphere were taken with a BX61 microscope (Olympus, Japan). The number of O4+ cells and nuclei were automatically counted using a high-content workflow from KNIME<sup>®</sup> version

4.4.0 (Berthold et al., 2007), and subsequently normalized by the number of nuclei (KNIME® workflow adapted from the “High content Screening” workflow of KNIME created by Christian Dietz. Our workflow is available in KNIME®-hub: [https://hub.knime.com/elisabet\\_t/spaces/Public/latest/Counting%20OL~fVnKIrqqJhzW8qjf](https://hub.knime.com/elisabet_t/spaces/Public/latest/Counting%20OL~fVnKIrqqJhzW8qjf). A statistical comparison with manual evaluation can be found in supplementary material SM1 and Fig. S2).

#### 2.3.6. qRT-PCR

RNA isolation and cDNA synthesis was performed from control and IUGR neurospheres after 5 days under differentiation conditions followed by qRT-PCR using self-designed primer sequences for *int-β1* and *int-β4* for the species rabbit (table S1). A detailed description is described in SM2.

#### 2.3.7. Western blot

NPCs under proliferating conditions obtained from control and IUGR animals were thawed, 2x centrifuged at 163 rcf for 10 min to discard the supernatant and the remaining pellet was homogenized for protein expression analyses of *int-β1* and *int-β4* by using the western blot technique. A detailed description of the western blot method is explained in SM3.

#### 2.4. Neurite length in rat neurosphere assay

For details on the performance of the rat neurosphere assay the reader is referred to Kühne et al. (2019). Briefly, rat neurospheres were cultured under differentiation conditions for 24 h on PDL/Laminin coated 8-chamber slides, and subsequently fixed and immunostained for βIII-tubulin+ cells (neurons) and Hoechst 33258 (nuclei). After 24 h exposure to SC (0.01% DMSO) or EGCG [1 μM] the neurite length from 20 neurons (βIII-tubulin+ cells) per neurosphere was manually measured using ImageJ 1.53a software.

#### 2.5. Dendrite length after developmental administration of EGCG in vivo

Animal procedures were approved by the Committee of Ethical Animal Experimentation (CEEA-PRBB; Protocol Number: VCU-14-1665) and the Generalitat of Catalonia (Protocol Number: DAAM-8101) in accordance with the guidelines of the European Communities Directive 86/609/EEC. For a description of the *in vivo* study the reader is referred to Ortiz-Romero et al. (2018). Briefly, treatment was started in pregnant female mice at postcoitum by dissolving EGCG in drinking water freshly prepared from a green tea extract (Mega Green Tea Extract, decaffeinated, from Life Extension®, USA, EGCG content by HPLC 326,25 mg) every 48–60 hours. Animals drank EGCG (2.5-3 mg per day) until sacrifice at 8 weeks old. After cardiac perfusion with 1x PBS followed by 4% PFA, brains were removed and postfixed in 4% PFA for 24 h at 4°C, in PBS for 24 h at 4°C and, afterwards, crioprotected in 30% sucrose for 24 h at 4°C. Finally, serial coronal sections (150 µm) of brain were collected on a glass slide and directly mounted with Mowiol. For morphological analysis of the stratum radiatum (SR) and stratum oriens (SO), 1360x1024 images of CA1 hippocampus were obtained with an Olympus DP71 camera attached to an Olympus BX51 microscopy with an Olympus U-RFL-T source of fluorescence at 4x magnification. Measures from six hippocampal sections per animal were averaged. For spine density and spine length analyses we obtained 1024x1024 pixel confocal fluorescent image stacks from coronal tissue sections of using a TCS SP2 LEICA confocal microscope. Measurements were performed according to a previously published method in Borralleras et al. (2016).

## 2.6. Behavioural tests

All experiments were performed during the light phase of the dark/light cycle by researchers unaware of the different experimental groups. At the level of the task apparatus there was a constant illumination of about <10 lux. In all tests each apparatus was cleaned with a diluted ethanol solution after each mouse.

### 2.6.1. Social interaction test

We used the same previously described test in Borralleras et al. (2016), conducted in an open field. First, an empty wire cup-container was placed in the centre of the arena. The subject mouse was allowed to explore the arena, and the amount of time sniffing the empty container was measured for 5 minutes. Next, an intruder mouse was held in the container and, again, the amount of time nose to nose sniffing was measured for 5 minutes.

#### 2.6.2. Marble-burying test

The test was conducted in a polycarbonate rat cage filled with bedding to a depth of 5 cm and lightly tamped down. A regular pattern of 20 glass marbles (five rows of four marbles) was placed on the surface of the bedding prior to each test. An individual animal was placed in each cage. The number of buried marbles (>2/3 marble covered) was counted every five minutes for 20 minutes.

#### 2.7. Statistics

Statistical analysis was performed using GraphPad Prism v9. Two groups were compared with two-way ANOVA followed by post-hoc Tukey's multiple comparison test. The difference between two groups was calculated with a two-tailed Student's t-test. The significance threshold was established at  $p < 0.05$ .

### 3. Results

#### 3.1. Safety and efficacy testing of EGCG and G56 in the Neurosphere Assay.

##### 3.1.1. Safety testing

A fundamental neurodevelopmental key event previously found to be affected by EGCG exposure at 5 and 10  $\mu\text{M}$  is NPC radial migration, including the migration distance and its corona formation (Barenys et al., 2017). Therefore, to test the safety of lower concentrations, we analysed the effects of EGCG and G56 on neurospheres derived from control and IUGR brains. After 3 days *in vitro* exposure to the highest tested concentration of EGCG [1  $\mu\text{M}$ ], control

neurospheres had a significantly reduced migration distance ( $62.4 \pm 4.9$  % of SC), whereas migration was not disturbed in IUGR neurospheres ( $102.9 \pm 6.8$  % of SC; Fig. 1A and B). This result remained the same after 5 days *in vitro* (Suppl. Fig. S3). Thus, after exposure to  $1 \mu\text{M}$  of EGCG, the migration distance of control and IUGR neurospheres was significantly different (Fig. 1A) because the controls were affected but IUGR neurospheres were not. Similarly, EGCG [ $1 \mu\text{M}$ ] significantly reduced the corona formation surrounding the sphere core in control neurospheres ( $313^\circ \pm 12.9^\circ$  vs  $360^\circ$  of SC), but not in IUGR neurospheres ( $347^\circ \pm 13.0^\circ$  vs  $360^\circ$  in SC; Fig. 1B). G56 did not significantly interfere with the migration distance or corona formation at any tested concentration in both groups, control or IUGR (Fig. 1C and D), which shows, as described before, that this EGCG derivative is safer than the parent compound (Kühne et al., 2019). After exposure to EGCG or G56, cell viability determined by metabolic activity was not significantly affected (Fig. 1D).

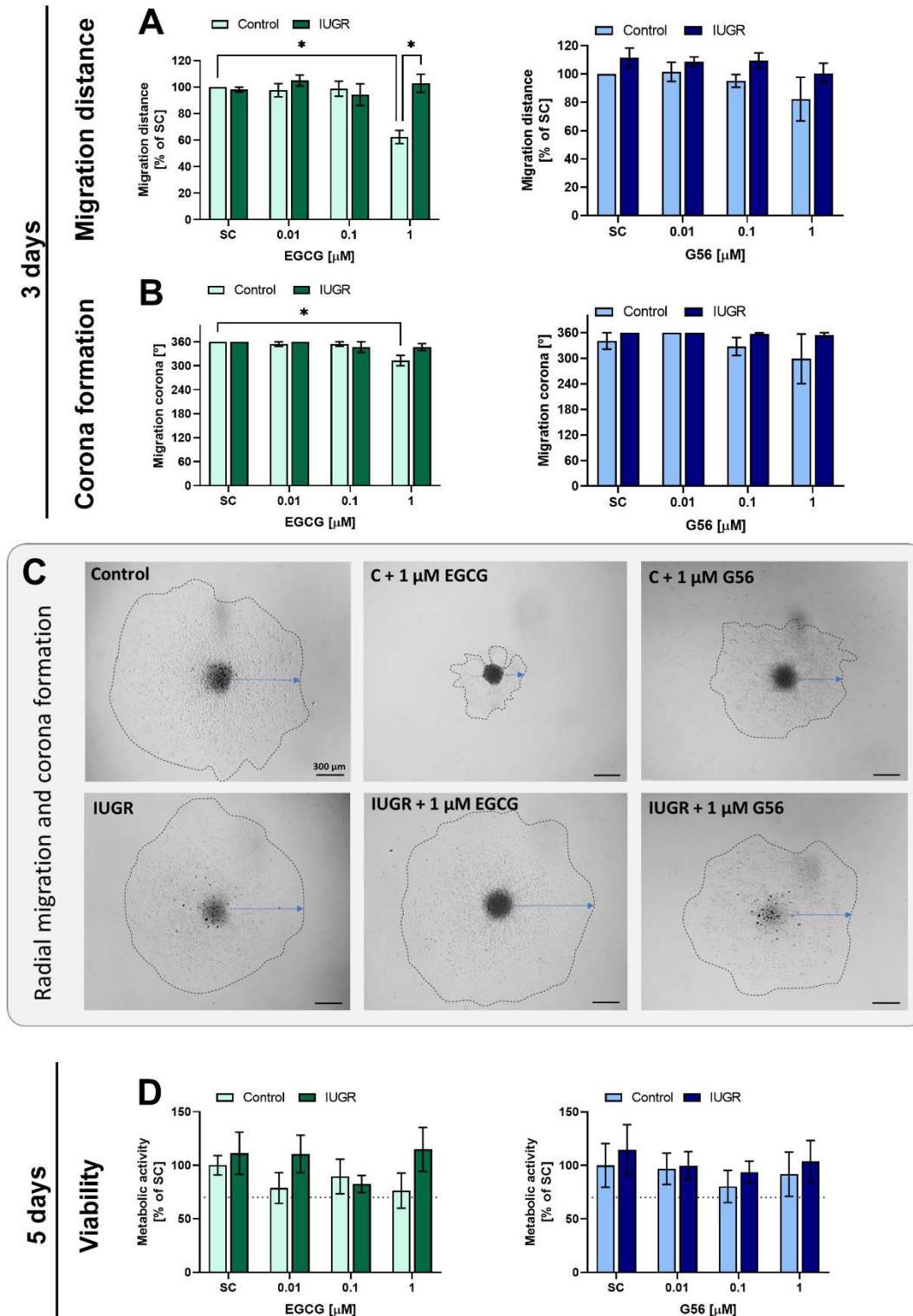


**Figure 1. EGCG disturbs migration in control but not in IUGR neurospheres.** Rabbit neurospheres obtained from Control and IUGR pups were comparatively analysed for each endpoint. Migration pattern was analysed after 3 days under differentiation conditions. (A) Migration distance [ $\mu\text{m}$ ] after exposure to EGCG (green) and G56 (blue). (B) Formation of migration corona [ $^{\circ}$ ] after exposure to EGCG (green) and G56 (blue). (C) Representative pictures of migrated neural progenitor cells (NPCs) after 3 days in vitro of control and IUGR neurospheres with and without exposure to 1  $\mu\text{M}$  EGCG or G56, arrow: migration distance, dotted line: corona formation. (D) Cell viability determined by metabolic activity after exposure to EGCG (green) and G56 (blue). Analysis was evaluated in five neurospheres/condition in at least three independent experiments. Mean  $\pm$  SEM, \*:  $p < 0.05$ .

### 3.1.2. Efficacy testing

Within the migration area, NPCs differentiated under control conditions to  $7.9 \pm 0.8$  % oligodendrocytes (OLs). NPCs obtained from IUGR brains had a significantly reduced ability to differentiate to OLs ( $4.6 \pm 0.5$  IUGR) compared to control (Fig. 2A-C), reproducing previous findings of our group (Kühne et al., 2022). We observed that none of the tested concentrations of EGCG or G56 could significantly increase OL differentiation, neither in control nor in IUGR neurospheres. The endpoint-specific positive control BMP7 significantly reduced OL differentiation to  $1.3 \pm 0.6$  % (Suppl. Fig. S4). With these results it was clear that neither EGCG nor G56 is a good candidate to be used as a neuroprotective therapy to prevent or treat white matter alterations induced by IUGR.

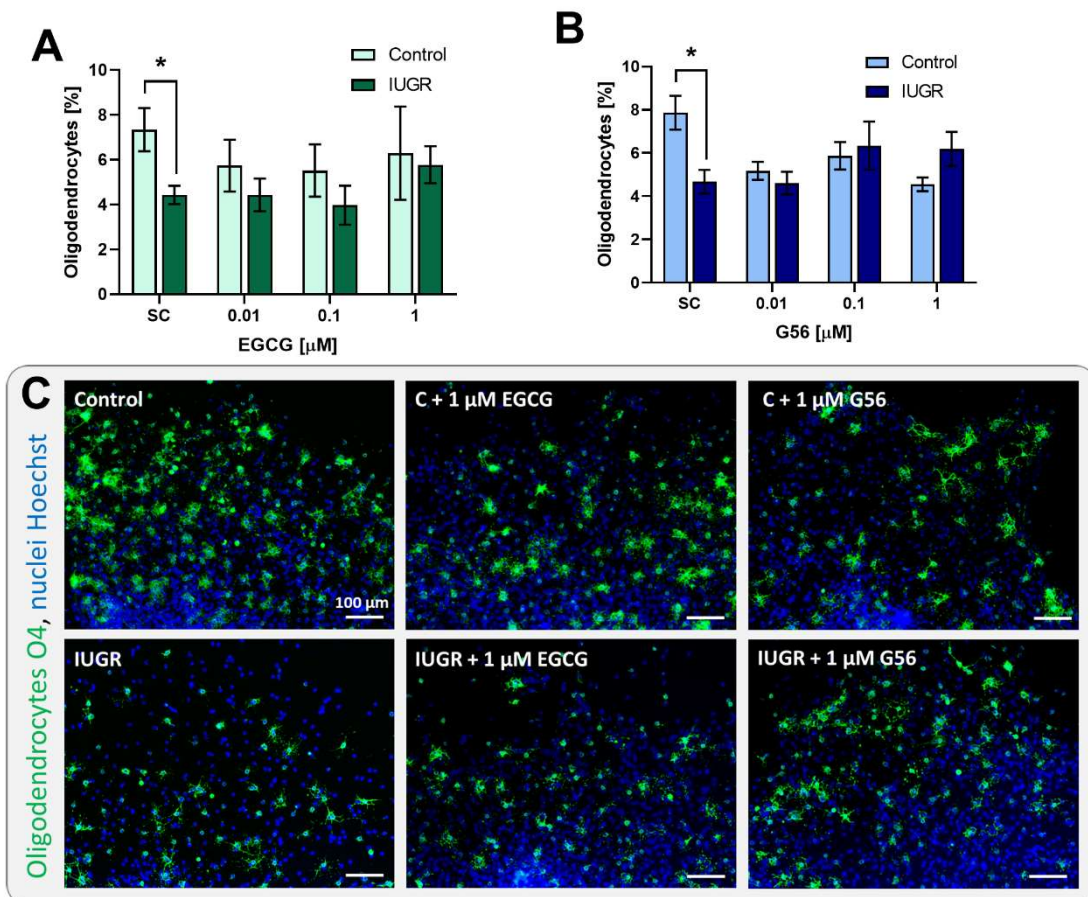


**Figure 2.** Lack of efficacy of EGCG or G56 upon decreased oligodendrocyte differentiation in IUGR neurospheres. Rabbit neurospheres obtained from control and IUGR pups were comparatively analysed for each endpoint. Oligodendrocyte differentiation after 5 days exposed to (A) EGCG and (B) G56. (C) Representative pictures of control and IUGR neurospheres exposed to the 1 $\mu$ M EGCG or G56, oligodendrocyte marker O4 (green) and Hoechst 33258



(blue), Scale bar = 100  $\mu$ m. Analysis was evaluated in five neurospheres/condition in at least three independent experiments. Mean  $\pm$  SEM, \*:  $p < 0.05$ .

### 3.2. IUGR neural /progenitor cells overexpress int- $\beta$ 1

Since we identified a significant difference in susceptibility to migration effects between control and IUGR neurospheres, being the IUGR less sensitive, we analysed the gene expression of subunit int- $\beta$ 1 in control and IUGR neurospheres, because previous studies revealed that EGCG interferes with the laminin/ int- $\beta$ 1 interaction leading to a disturbed migration pattern (Barenys et al., 2017). We also analysed the expression of int- $\beta$ 4 since this is another integrin subunit known to bind to laminin (Barczyk et al., 2010; Humphries et al., 2006) but it is not involved in the mechanism of action of EGCG disturbed migration (Barenys et al., 2017). Our qRT-PCR results confirmed that in the IUGR group, the expression of int- $\beta$ 1 was significantly increased to a 10-fold higher amount than in the control (control 1.14 vs IUGR 10.97,  $p=0.047$ , Fig. 3A). No significant difference was observed in the fold-change expression of int- $\beta$ 4 between control and IUGR (control 1.09 vs IUGR 1.08,  $p=0.964$ , Fig. 3A). In line with these results, a significant increase in int- $\beta$ 1 protein to a 3.5-fold higher amount than in control was observed in IUGR NPCs (control 1.00 vs IUGR 3.49,  $p=0.0465$ , Fig. 3B) and no significant difference was observed in the fold-change expression of int- $\beta$ 4 protein between control and IUGR (control 1.00 vs IUGR 1.05,  $p=0.8116$  Fig. 3B).

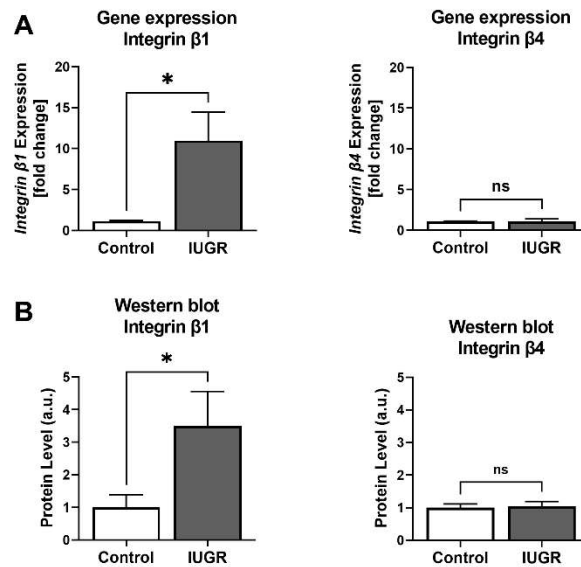


**Figure 3. Overexpression of *int-β1* in IUGR neurospheres on gene and protein level.** (A) qRT-PCR from *int-β1* and *int-β4* expression in control and IUGR neurospheres after 5 days of differentiation (five neurospheres/condition). (B) Western blot analysis from control and IUGR proliferating NPCs. Analysis was evaluated in at least three independent experiments. Mean ± SEM, \*:  $p < 0.05$ , ns: not significant.

### 3.3. Neurodevelopmental EGCG exposure has deleterious effects on neurites

Besides being involved in cell adhesion and migration, *int-β1* is crucial for other neurodevelopmental processes like neurite length and arborization (Belvindrah et al., 2007; Marrs et al., 2006). Knowing that, and linking this information with the fact that IUGR animals present a higher arborization of neurons (Pla et al., 2020), we wondered if EGCG could also affect neurite length and arborization during neurodevelopment. We first analysed *in vitro* the neurite length of neurons exposed for 24 h to EGCG [1 μM] in a neurosphere culture using the pictures of a previous study (Kühne et al., 2019). Indeed, the neurite length *in vitro* was significantly reduced after EGCG exposure compared to the solvent control ( $51.0 \pm 2.7 \mu\text{m}$  SC vs  $42.0 \pm 3.9 \mu\text{m}$  EGCG,  $p=0.0138$ , Fig. 4A-B). In a next step we searched for evidence of the relevance of this effect *in vivo* in the literature and we found an article performed in mice indicating that one of the experimental groups was exposed to EGCG during gestation and the postnatal period (Ortiz-Romero et al., 2018). Since the results of control animals exposed to EGCG on dendritic length

for this specific group were not included in that publication (the publication was focusing on the effects of EGCG in a Williams-Beuren syndrome mouse model), we contacted the authors obtained the raw data of controls and controls exposed to EGCG and we present the results here. In this case the dendritic length was analysed at postnatal week 8 after administration of EGCG from postcoitum until sacrifice. Indeed, the dendritic length of CA1 cortical neurons in the stratum radiatum (SR) and stratum oriens (SO) decreased significantly in the EGCG group compared to the untreated group (SR:  $225.9 \pm 4.0$  vs  $197.2 \pm 2.5$ ; SO:  $130.1 \pm 1.6$  vs  $100.1 \pm 1.4$  Fig. 4C-D), without affecting birth weight or brain weight (Suppl. Fig. S5).

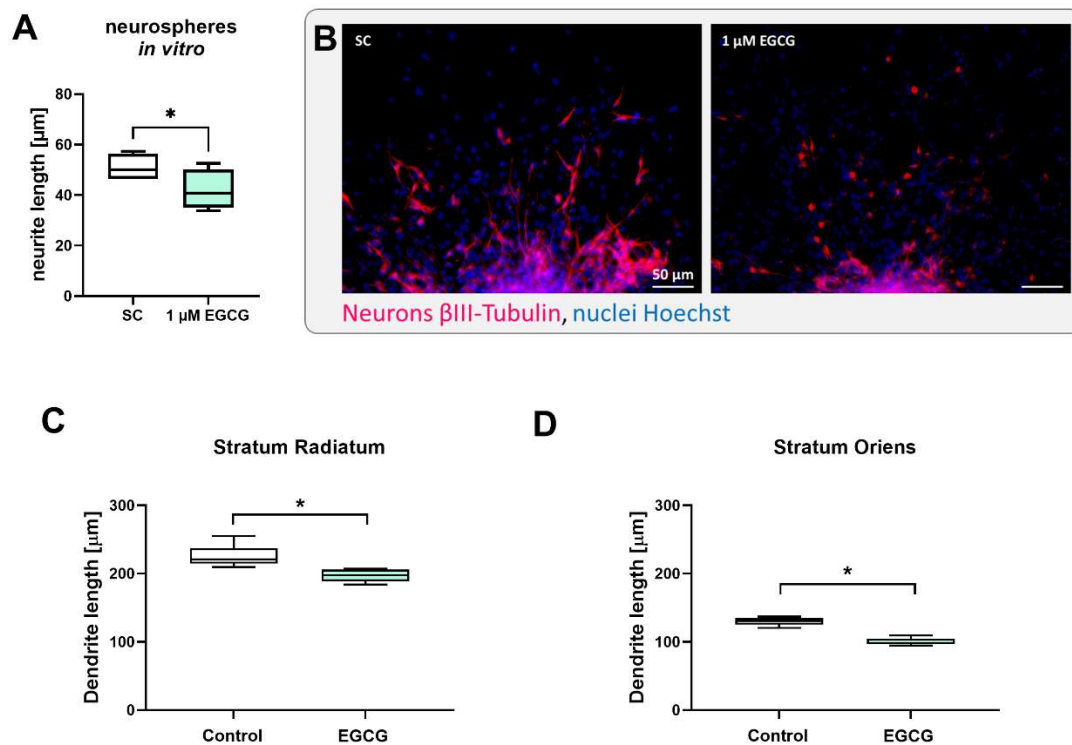
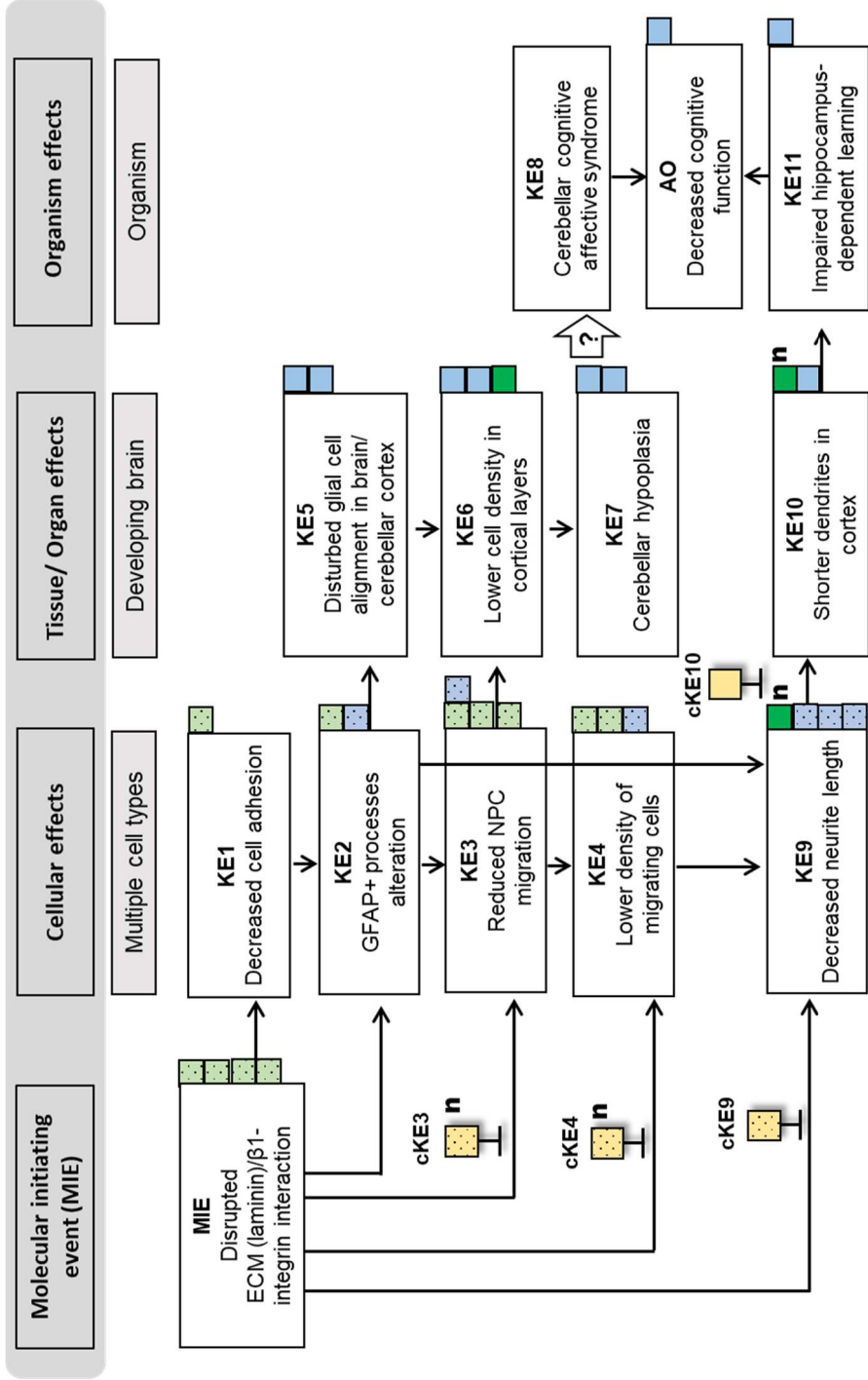


**Figure 4. Neurodevelopmental exposure to EGCG decreases neurite length in vivo and in vitro.** (A) *In vitro* neurite length measurement in rat neurospheres exposed for 24h to solvent control (SC) or 1  $\mu\text{M}$  EGCG; (B) representative images of rat neurospheres stained for neurons with  $\beta\text{III-Tubulin}$  (red) and nuclei with Hoechst 33258 (blue), Scale bar = 50  $\mu\text{m}$ . (C) *In vivo* dendrite length measurement of CA1 cortical neurons in stratum radiatum and (D) stratum oriens with and without developmental administration of EGCG to mice; boxplot represented in Tukey's style (Median, and 25th and 75th percentiles), \*:  $p < 0.05$ .

### 3.4. Integration in an adverse outcome pathway (AOP) concept

By combining previous results from the literature with our novel investigations, we bring new evidence supporting, expanding and redesigning the previously postulated AOP “Binding to the extracellular matrix protein laminin leading to decreased cognitive function.” (Klose et al., 2022) which is now entitled: “Disrupted laminin/int- $\beta$ 1 interaction leading to decreased cognitive function” (Fig. 5). Our new design includes information from three kind of experimental data obtained 1) after exposure to EGCG (in green), 2) from an int- $\beta$ 1 deficiency in partial int- $\beta$ 1 knock-out animals or via blocking experiments with int- $\beta$ 1 antibody (in blue), and 3) from an overexpression of int- $\beta$ 1 due to IUGR (in yellow). Moreover, we bring together evidence at both levels, *in vivo* (blank box) and *in vitro* (dotted box).



Chemical binding to laminin  
EGCG

Integrin-β1 deficiency

Partial knock-out/blocking with antibody, peptides or toxin

Overexpression of integrin-β1  
IUGR

*In vivo*

*In vitro*

Hypothetical linkage

Established mechanistic linkage with quantitative or semi-quantitative data

cKE: contrary/compensating effects

n New results from present publication

Green tea extract

**Figure 5. AOP “Disrupted laminin/ int-β1 interaction leading to decreased cognitive function”.** The AOP frame begins with a MIE leading to a cascade of KEs on cellular and tissue/organ level and results ultimately in an AO at the organism level. Every little box refers to a publication including the MIE, interference with a KE or AO respectively, either *in vivo* (blank box) or *in vitro* (dotted box). The interference of KEs was due to EGCG exposure or administration (green) or int-β1 deficiency due to partial knock-out or blocking experiments with int-β1 antibody, specific peptides, or toxins (blue). The yellow boxes present a contrary/compensating effect in IUGR models exhibiting an overexpression of int-β1 (yellow). n: new results including in the present paper; AOP: adverse outcome pathway; MIE: molecular initiating event; KE: key event; AO: adverse outcome.

#### References Legend:

Chemical binding to laminin: (Barenys et al., 2017; Lo et al., 2007; Suzuki and Isemura, 2001)

Int-β1 deficiency: (Barenys et al., 2017; Belvindrah et al., 2007; Graus-Porta et al., 2001)

Overexpression of int-β1: Fig. 3 A & B

#### References KEs

MIE (Barenys et al., 2017; Lo et al., 2007; Melgarejo et al., 2009; Park et al., 2010)

KE1 (Barenys et al., 2017)

KE2 (Barenys et al., 2017; Belvindrah et al., 2007)

KE3 (Barenys et al., 2017 (green and blue); Chen et al., 2003; Kühne et al., 2019)

KE4 (Barenys et al., 2017; Kühne et al., 2019)

KE5 (Belvindrah et al., 2007; Graus-Porta et al., 2001)

KE6 (Belvindrah et al., 2007; El-Borm and Abd El-Gaber, 2021; Graus-Porta et al., 2001)

KE7 (Frick et al., 2012; Robel et al., 2009)

KE8 (hypothetical)

KE9 Green (n): Fig. 4A & B; (Belvindrah et al., 2007; Marrs et al., 2006; Moresco et al., 2005)

KE10 Green (n): Fig. 4C & D; (Warren et al., 2012)

KE11 (Warren et al., 2012)

AO (Warren et al., 2012)

#### References contrary/ compensating effects (cKE):

cKE3: Fig. 1A

cKE4: Fig. 1B

cKE9: (Kühne et al., in preparation: IUGR increased neurite length)

cKE10: (Pla et al., 2020)

The AOP begins with a disrupted laminin- int-β1 interaction (MIE (Barenys et al., 2017; Lo et al., 2007; Melgarejo et al., 2009; Park et al., 2010)) due to a chemical, in this case EGCG, binding to laminin (Barenys et al., 2017; Lo et al., 2007; Suzuki and Isemura, 2001). As previously described, this interference causes decreased adhesion of NPC's *in vitro* (KE1 (Barenys et al., 2017; Graus-Porta et al., 2001)) and GFAP+ processes alterations (KE2 (Barenys et al., 2017; Belvindrah et al., 2007)), which leads to a reduced migration distance (KE3 (Barenys et al., 2017; Chen et al., 2003; Kühne et al., 2019)) and a reduced corona formation with a lower density of migrating cells (KE4 (Barenys et al., 2017; Kühne et al., 2019)). Our new results in IUGR neurospheres exposed to

EGCG support this previously established chain of KEs, because KE3 and KE4 are not present if cells overexpress int- $\beta$ 1 (cKE3 and cKE4; Fig. 1A and B). The altered GFAP+ processes (KE2) are an *in vitro* observation after EGCG exposure but also an effect described in cell cultures from mice lacking the expression of int- $\beta$ 1 subunit in radial glial cells, which was linked with the same effect (disturbed glial cell alignment in the developing brain cortex) in brain sections of these mice (KE5 (Belvindrah et al., 2007; Graus-Porta et al., 2001)). As a result of this alteration in GFAP+ processes outgrowth, the same main effect has been described *in vitro* and *in vivo*: a lower cell density in the migration area (*in vitro*; KE4) or in cortical layers (KE6 (Belvindrah et al., 2007; El-Borm and Abd El-Gaber, 2021; Graus-Porta et al., 2001)). A preliminary indication that EGCG could also produce this effect is given by the fact that prenatal exposure to green tea extract leads to a decreased number of cells in the cerebellar cortex and cerebellum (El-Borm and Abd El-Gaber, 2021), but a study with only EGCG exposure at doses not producing significant decreases in body weight of the pups should be performed to confirm these results. As a consequence, another key event at organ level already described after int- $\beta$ 1 knock-out induction in glial cells, leading to cerebellar hypoplasia (KE7 (Frick et al., 2012; Robel et al., 2009)), but the behavioural consequences of this group of KEs, are to the best of our knowledge, not explored after integrin beta 1/laminin disruption. The behavioural consequence of cerebellar hypoplasia described in the literature is “cerebellar cognitive affective syndrome” (KE8 (Basson and Wingate, 2013)), but this remains as a hypothetical linkage in our AOP.

Our new results have opened a second branch in this AOP related to adverse effects on neurite growth due to the same MIE: disrupted interaction between ECM (laminin) and  $\beta$ 1-integrin. At the *in vitro* level there were already several evidence: 1) int- $\beta$ 1 deficiency in cultures of partial knock-out mice cells decreases neurite length (KE9 (Belvindrah et al., 2007; Marrs et al., 2006)), 2) int- $\beta$ 1 blocking peptide  $\beta$ 1P reduces the length of neurites on laminin (KE10 (Belvindrah et al., 2007; Marrs et al., 2006)) and, 3) int- $\beta$ 1 inhibitor toxin echistatin eliminates neurite branching and elongation of cortical neurons on laminin (Moresco et al., 2005). Again, our investigations

in IUGR neurospheres support this link because neurons obtained from IUGR neurospheres, overexpressing *int-β1*, present longer neurites (cKE9; Kühne et al., in preparation). Moreover, the *in vivo* relevance of this AOP part was already demonstrated in mice lacking *int-β1* in excitatory forebrain neurons and failing to elaborate dendritic arborization (KE10 (Ortiz-Romero et al., 2018; Warren et al., 2012)), while IUGR animals overexpressing integrin beta 1 present more complex dendrite arborization than controls (cKE10). Thanks to this AOP approach, we could build all these connections between the KEs and finally demonstrate for the first time that EGCG *in vitro* exposure decreases neurite length (Fig. 4A and B) and EGCG *in vivo* developmental exposure impairs dendritic arborization and decreases dendrite length in the hippocampus (Fig. 4C and D). The AO described in mice lacking *int-β1* in excitatory forebrain neurons was cognitive deficits, specifically impaired hippocampus-dependent learning measured by the novel object recognition test (KE11 (Warren et al., 2012)), so the expected AO would be “decreased cognitive function” after developmental exposure to EGCG.

#### **4. Discussion**

We have discovered a significant increase in the expression of *int-β1* in IUGR neurospheres, at both gene expression and protein expression level, which enables a better adhesion of NPCs to the ECM and an appropriate migration phenotype under exposure to EGCG at concentrations disturbing migration in control neurospheres. This finding unravels one of the probably several molecular adaptations that brains suffer when developing under chronic mild hypoxic conditions. To the best of our knowledge, this is the first time that this molecular change is identified in IUGR brains, and the implications of this finding are very relevant because it can explain some of the neurodevelopmental alterations described after IUGR *in vivo*, as for example the changes in neuronal arborization. Other authors have described a marked upregulation of integrin  $\alpha6\beta1$  or  $\alpha5\beta1$  in brain endothelial cells (Halder et al., 2018; Li et al., 2010) or increases in astrocyte end-feet adhesion molecules such as integrin  $\alpha6\beta4$  in adult brains after chronic mild



hypoxia (Li et al., 2010) or increases in the expression of laminin-associated integrins  $\alpha6\beta1$  or  $\alpha7\beta1$  in mature neurons after nerve injury, which promote axonal regeneration in a mature nerve system (Nieuwenhuis et al., 2018), so it is not surprising that changes in adhesion molecules also occur in developing brains under IUGR induced by chronic mild hypoxic conditions.

During brain development integrins are involved in laminin adhesion and in axonal growth and pathfinding (Myers et al., 2011). Several studies clearly support that *int-β1* increases extension and complexity of dendritic branching of cortical neurons (Moresco et al., 2005; Warren et al., 2012) and previous studies of our group have discovered that IUGR rabbit pups present a significantly higher complexity of dendritic branches in the frontal cortex *in vivo* (Pla et al., 2020). Therefore, it is plausible to postulate that the increased *int-β1* expression in rabbit IUGR NPCs might underlie this increased dendritic arborization in IUGR brains. Although further studies need to be done to unequivocally link this mechanism with the histological outcome observed in IUGR pups, our discovery gives insights of an *int-β1* mediated mechanism in neurogenesis and opens the door for a better characterization of changes in prenatal brain programming induced by IUGR.

This discovery was possible thanks to the previous existence of a putative AOP: “Binding to the extracellular matrix protein laminin leading to decreased cognitive function” (Klose et al., 2022), which was submitted to the OECD in 2019. Creating AOP-structured collections of molecular/cellular/organ/organism-event networks underlying human biology responding to toxic insults (named as toxicological ontology (Baker et al., 2018; Desprez et al., 2019; Heusinkveld et al., 2021)) is an extremely powerful strategy because it allows to cross information from different fields, in this case developmental neurotoxicity, developmental biology, and developmental physiopathology, to identify the molecular events behind specific

cellular effects and finally design experiments which are directly aimed to evaluate the relevant KE or AO while saving animals, time and resources because the search is more directed.

Our results support and expand the previously submitted AOP, and after combining them with the literature results, we can say that compared to the previous one, the new version of the AOP: 1) is more chemically agnostic, 2) includes a new branch of key events, and 3) is more specific at the organ and organism level. Since we have found evidence of other compounds following the same chain of KEs (mainly blocking peptides or spider toxins) but not having the same MIE (which was previously defined as “binding compound to laminin” (Bal-Price et al., 2016)) to make the AOP more chemically agnostic, as required per definition in AOPs (Bal-Price and Meek, 2017), we have changed the MIE to a broader definition: “disrupted laminin/integrin beta-1 interaction”, which encompasses both situations: those where the interaction is disrupted due to lower laminin availability and those due to lower integrin beta-1 availability. As a consequence, the title of the AOP has also changed to: “Disrupted laminin/integrin beta-1 interaction leading to decreased cognitive function”. Thanks to the cross-linked information in this AOP we could also identify a new adverse effect of developmental exposure to EGCG, and we have therefore included a new branch of events related to adverse effects on neurite outgrowth, which could be independent or related to the glial effects described in the other branch of the AOP. We have characterized for the first time adverse effects on dendritic length of CA1 neurons in the stratum radiatum and stratum oriens in mouse brains after developmental exposure to EGCG *in vivo*. In accordance, EGCG reduced the neurite length in a neurosphere culture after 24h of exposure, so both *in vitro* and *in vivo* evidence are added to this new branch of the AOP. The interrelationship between both branches is suspected because Belvindrah et al., discovered that “the defect in neurite outgrowth of  $\alpha$ 1-integrin-deficient neurons is rescued when glial cells express  $\beta$ 1 integrins and undergo normal morphological differentiation, suggesting that the perturbations in neurite outgrowth are a secondary consequence of defects in glial cells” (Belvindrah et al., 2007), however, after *in vitro* or *in vivo* exposure to EGCG it is not

possible to distinguish if the effect is direct or secondary. By including this information together with new evidence supporting the glial branch, we have made the AOP more specific at the organ and organism level: we have collected evidence *in vivo* for both branches, we have identified a more specific and more probable organ effect for the glial branch “cerebellar hypoplasia” (based on *int-β1* knock-out induction in glial cells, leading to cerebellar hypoplasia in mice (Robel 2009 and Frick 2012)), and identified which behavioural alteration is probably disturbed due to the neurite outgrowth effects, impaired hippocampus-dependent learning (based on previous publications revealing that a selective loss of *int-β1* in excitatory neurons leads to this effects measured with the Novel Object Recognition test (Warren et al., 2012)). The final AO of both branches would still be “decreased cognitive function”, as previously described in the AOP (Klose et al., 2022). It is true that the evidence *in vivo* is based on green tea extract exposure studies instead of only EGCG exposure studies, so there is still the need to confirm this relationship, but one important aspect is that the new branch could have even more relevance *in vivo* than the previous one because adverse effects in animals appear at lower doses of green tea extract, and of EGCG. In the lower case the dose is 2.5-3 mg/animal/day, which is a dose within the range of the recommended doses in pre-clinical and clinical studies (Almeida-Toledano et al., 2021; Souchet et al., 2019; [www.clinicaltrials.gov](http://www.clinicaltrials.gov), 2022).

Altogether, our investigations strongly suggest that EGCG can produce developmental neurotoxicity and they are the basis for future studies required to confirm the postulated AO of this pathway. From our work, it is clear that there is the need to do an *in vivo* study in mice exposed to EGCG, to green tea extract (with an equivalent dose of EGCG) or to water where behavioural alterations in the Novel Object Recognition test and cerebellar hypoplasia and “Cerebellar cognitive affective syndrome” are evaluated. Performing behavioural tests, such as anxiety-like behaviour tests or sociability tests has not shown any effects in the present study (see Suppl. Fig. S6 including non-significant results of the marble burying test and social interaction test), but the dose used was low and these effects could still appear at higher doses.

Given the high importance EGCG prenatal exposure is acquiring in the last years in the preclinical field for the treatment of several diseases (Almeida-Toledano et al., 2021; Ortiz-Romero et al., 2018; Souchet et al., 2019), it is of utmost importance to clarify its possible neurodevelopmental toxicity and to perform a correct risk assessment evaluation depending on the dose of exposure. Since the quantitative aspect of the proposed AOP is still missing, the inclusion of different doses of EGCG would be required to identify a NOAEL. The idea of including two groups, one exposed to EGCG and one to the green tea extract relies on the already mentioned fact that all results *in vivo* included in the current version of the AOP are based on studies where EGCG was administered as a green tea extract and because in these extracts several catechins are present. Other catechins like EGC (epigallocatechin) or ECG (epicatechingallate) have been shown to produce the same KEs than EGCG *in vitro* (Barenys et al., 2017), so an additive effect among them can be expected and would be important to be identified.

Our work also contributes to future evaluation of chemicals triggering the same KEs, which would be expected to have the same MIE and induce the same AO. So far, several compounds or plant extracts have been proved to potentially trigger migration disturbance (KE3 – KE4) with the same specific phenotype than EGCG: Lei Gong Teng extract (another Chinese herbal medicine) (Klose et al., 2022), and two synthetic analogues of EGCG including G37 (1,4-bis[(3,4,5-trihydroxybenzoyl)oxy]naphthalene) and M2 (3-hydroxy-1-naphthyl 3,4,5-trihydroxybenzoate) (Kühne et al., 2019). For future substances suspected to be candidates to follow this AOP, a simultaneous *in vitro* evaluation of KE3, KE4 and KE9 in a neurosphere model could be enough to evaluate the potency of the compound in comparison to EGCG and to assess the suitability of its use during pregnancy, avoiding the unnecessary use of animal experiments. Using this strategy, we give evidence here that another analogue of EGCG named G56 does not adversely affect these key events and can therefore be considered as a safer alternative to EGCG during pregnancy, in this specific DNT aspect. However, neither G56 nor EGCG could rescue the decrease in oligodendrocyte differentiation induced by IUGR, so despite being safer, this

compound would still not be a promising neuroprotective treatment in this condition. The oligodendrocyte differentiation evaluation was performed for the first time using a high-content workflow of KNIME® adapted from the “High content Screening” workflow of KNIME created by Christian Dietz for oligodendrocyte automatic counting (see link in Material and Method 2.3.5). We have proved that our workflow results are statistically comparable to those obtained with our manual counting (see Suppl. Fig. S4), and we contribute to the field by sharing this workflow in open access to make the evaluation of this endpoint faster, easier because it can be used in manually taken fluorescence microscope pictures, and cheaper because no expensive evaluation software is needed (see link in Material and Method 2.3.5).

## **5. Conclusions**

We have discovered for the first time that IUGR neurospheres overexpress int-β1 and they respond differently than control neurospheres to the exposure of a compound triggering migration alterations. Because int-β1 is involved in NPC migration but also in axonal growth and neuronal branching, and IUGR animals have branching alterations, we strongly think that our discovery is bringing relevant new insights to the characterization of IUGR-induced neurodevelopmental alterations.

On top of that, we have also discovered that EGCG developmental exposure has deleterious effects on neuronal branching and arborization. This important finding warns for a further DNT thorough characterization of this and other food supplement compounds before recommending them as prenatal treatments.

Finally, our study contributes to demonstrate that the neurosphere assay is well suited for hazard assessment of DNT, that the results obtained with this technique correlate well with *in vivo* evidence and that when they are combined with gene/protein expression analyses they are powerful tools for building AOPs which ultimately allow a better comprehension of the DNT effect or related neurodevelopmental diseases.

## Acknowledgments.

This study has been funded by Instituto de Salud Carlos III through the project "PI18/01763" (co-funded by European Regional Development Fund, "A way to make Europe"), from "LaCaixa" Foundation under grant agreements LCF/PR/GN14/10270005 and LCF/PR/GN18/10310003, and from AGAUR under grant 2017 SGR n° 1531. B.A.K. received a scholarship from Fundació Bosch i Gimpera (project number: 300155).

## 6. References

- Abdel-Rahman, A., Anyangwe, N., Carlacci, L., Casper, S., Danam, R.P., Enongene, E., Erives, G., Fabricant, D., Gudi, R., Hilmas, C.J., 2011. The safety and regulation of natural products used as foods and food ingredients. *Toxicol. Sci.* 123, 333–348.
- Abel, K.M., Dalman, C., Svensson, A.C., Susser, E., Dal, H., Idring, S., Webb, R.T., Rai, D., Magnusson, C., 2013. Deviance in Fetal Growth and Risk of Autism Spectrum Disorder. *Am. J. Psychiatry* 170, 391–398. <https://doi.org/10.1176/appi.ajp.2012.12040543>
- Almeida-Toledano, L., Andreu-Fernández, V., Aras-López, R., García-Algar, Ó., Martínez, L., Gómez-Roig, M.D., 2021. Epigallocatechin Gallate Ameliorates the Effects of Prenatal Alcohol Exposure in a Fetal Alcohol Spectrum Disorder-Like Mouse Model. *Int. J. Mol. Sci.* 22, 715. <https://doi.org/10.3390/ijms22020715>
- Baker, N., Boobis, A., Burgoon, L., Carney, E., Currie, R., Fritsche, E., Knudsen, T., Laffont, M., Piersma, A.H., Poole, A., Schneider, S., Daston, G., 2018. Building a developmental toxicity ontology. *Birth Defects Res.* 110, 502–518. <https://doi.org/10.1002/bdr2.1189>
- Bal-Price, A., Lein, P.J., Keil, K.P., Sethi, S., Shafer, T., Barenys, M., Fritsche, E., Sachana, M., Meek, M.E.B., 2016. Developing and applying the adverse outcome pathway concept for understanding and predicting neurotoxicity. *Neurotoxicology.* <https://doi.org/10.1016/j.neuro.2016.05.010>
- Bal-Price, A., Meek, M.E. (Bette., 2017. Adverse outcome pathways: Application to enhance mechanistic understanding of neurotoxicity. *Pharmacol. Ther.* 179, 84–95. <https://doi.org/10.1016/j.pharmthera.2017.05.006>
- Barczyk, M., Carracedo, S., Gullberg, D., 2010. Integrins. *Cell Tissue Res.* 339, 269–280.
- Barenys, M., Gassmann, K., Baksmeier, C., Heinz, S., Reverte, I., Schmuck, M., Temme, T., Bendt, F., Zschau, T.C., Rockel, T.D., Unfried, K., Wätjen, W., Sundaram, S.M., Heuer, H., Colomina, M.T., Fritsche, E., 2017. Epigallocatechin gallate (EGCG) inhibits adhesion and migration of neural progenitor cells in vitro. *Arch. Toxicol.* <https://doi.org/10.1007/s00204-016-1709-8>
- Barenys, M., Illa, M., Hofrichter, M., Loreiro, C., Pla, L., Klose, J., Kühne, B.A., Gómez-Catalán, J.,

- Braun, J.M., Crispi, F., Gratacós, E., Fritsche, E., 2021. Rabbit neurospheres as a novel in vitro tool for studying neurodevelopmental effects induced by intrauterine growth restriction. *Stem Cells Transl. Med.* 10, 209–221. <https://doi.org/10.1002/sctm.20-0223>
- Barenys, M., Masjosthusmann, S., Fritsche, E., 2016a. Is Intake of Flavonoid-Based Food Supplements During Pregnancy Safe for the Developing Child? A Literature Review. *Curr. Drug Targets* 18, 196–231. <https://doi.org/10.2174/1389450116666150804110049>
- Barenys, M., Masjosthusmann, S., Fritsche, E., 2016b. Is Intake of Flavonoid-Based Food Supplements During Pregnancy Safe for the Developing Child? A Literature Review. *Curr. Drug Targets*. <https://doi.org/10.2174/1389450116666150804110049>
- Basson, M.A., Wingate, R.J., 2013. Congenital hypoplasia of the cerebellum: developmental causes and behavioral consequences. *Front. Neuroanat.* 7, 29. <https://doi.org/10.3389/fnana.2013.00029>
- Batalle, D., Eixarch, E., Figueras, F., Muñoz-Moreno, E., Bargallo, N., Illa, M., Acosta-Rojas, R., Amat-Roldan, I., Gratacos, E., 2012. Altered small-world topology of structural brain networks in infants with intrauterine growth restriction and its association with later neurodevelopmental outcome. *Neuroimage* 60, 1352–1366. <https://doi.org/10.1016/j.neuroimage.2012.01.059>
- Batalle, D., Muñoz-Moreno, E., Arbat-Plana, A., Illa, M., Figueras, F., Eixarch, E., Gratacos, E., 2014. Long-term reorganization of structural brain networks in a rabbit model of intrauterine growth restriction. *Neuroimage* 100, 24–38. <https://doi.org/10.1016/j.neuroimage.2014.05.065>
- Baumann, J., Barenys, M., Gassmann, K., Fritsche, E., 2014. Comparative Human and Rat “Neurosphere Assay” for Developmental Neurotoxicity Testing. *Curr. Protoc. Toxicol.* 59, 12.21. 1-12.21. 24. <https://doi.org/10.1002/0471140856.tx1221s59>
- Belvindrah, R., Graus-Porta, D., Goebbels, S., Nave, K.-A., Muller, U., 2007.  $\beta$ 1 Integrins in Radial Glia But Not in Migrating Neurons Are Essential for the Formation of Cell Layers in the Cerebral Cortex. *J. Neurosci.* 27, 13854–13865. <https://doi.org/10.1523/JNEUROSCI.4494-07.2007>
- Berthold, M.R., Cebon, N., Dill, F., Gabriel, T.R., Kötter, T., Meinl, T., Ohl, P., Sieb, C., Thiel, K., Wiswedel, B., 2007. {KNIME}: The {K}onstanz {I}nformation {M}iner, in: *Studies in Classification, Data Analysis, and Knowledge Organization (GfKL 2007)*. Springer.
- Borralleras, C., Mato, S., Amédée, T., Matute, C., Mulle, C., Pérez-Jurado, L.A., Campuzano, V., 2016. Synaptic plasticity and spatial working memory are impaired in the CD mouse model of Williams-Beuren syndrome. *Mol. Brain* 9, 76. <https://doi.org/10.1186/s13041-016-0258-7>
- Cano, A., Ettcheto, M., Chang, J.H., Barroso, E., Espina, M., Kühne, B.A., Barenys, M., Auladell, C., Folch, J., Souto, E.B., Camins, A., Turowski, P., García, M.L., 2019. Dual-drug loaded nanoparticles of Epigallocatechin-3-gallate (EGCG)/Ascorbic acid enhance therapeutic efficacy of EGCG in a APPswe/PS1dE9 Alzheimer’s disease mice model. *J. Control. Release* 301, 62–75. <https://doi.org/10.1016/j.jconrel.2019.03.010>
- Catuara-Solarz, S., Espinosa-Carrasco, J., Erb, I., Langohr, K., Gonzalez, J.R., Notredame, C., Dierssen, M., 2016. Combined Treatment With Environmental Enrichment and (-)-Epigallocatechin-3-Gallate Ameliorates Learning Deficits and Hippocampal Alterations in a Mouse Model of Down Syndrome. *eNeuro* 3. <https://doi.org/10.1523/ENEURO.0103-16.2016>

- Chen, C.N., Liang, C.M., Lai, J.R., Tsai, Y.J., Tsay, J.S., Lin, J.K., 2003. Capillary Electrophoretic Determination of Theanine, Caffeine, and Catechins in Fresh Tea Leaves and Oolong Tea and Their Effects on Rat Neurosphere Adhesion and Migration. *J. Agric. Food Chem.* <https://doi.org/10.1021/jf034634b>
- Desprez, B., Birk, B., Blaauboer, B., Boobis, A., Carmichael, P., Cronin, M.T.D., Curie, R., Daston, G., Hubesch, B., Jennings, P., Klaric, M., Kroese, D., Mahony, C., Ouédraogo, G., Piersma, A., Richarz, A.-N., Schwarz, M., van Benthem, J., van de Water, B., Vinken, M., 2019. A mode-of-action ontology model for safety evaluation of chemicals: Outcome of a series of workshops on repeated dose toxicity. *Toxicol. Vitro*. 59, 44–50. <https://doi.org/10.1016/j.tiv.2019.04.005>
- Drobyshevsky, A., Jiang, R., Derrick, M., Luo, K., Tan, S., 2014. Functional correlates of central white matter maturation in perinatal period in rabbits. *Exp. Neurol.* 261, 76–86. <https://doi.org/10.1016/j.expneurol.2014.06.021>
- Eixarch, E., Batalle, D., Illa, M., Muñoz-Moreno, E., Arbat-Plana, A., Amat-Roldan, I., Figueras, F., Gratacos, E., 2012. Neonatal neurobehavior and diffusion MRI changes in brain reorganization due to intrauterine growth restriction in a rabbit model. *PLoS One* 7, e31497. <https://doi.org/10.1371/journal.pone.0031497>
- Eixarch, E., Figueras, F., Hernández-Andrade, E., Crispi, F., Nadal, A., Torre, I., Oliveira, S., Gratacós, E., 2009. An experimental model of fetal growth restriction based on selective ligation of uteroplacental vessels in the pregnant rabbit. *Fetal Diagn. Ther.* 26, 203–211. <https://doi.org/10.1159/000264063>
- El-Borm, H.T., Abd El-Gaber, A.S., 2021. Effect of prenatal exposure of green tea extract on the developing central nervous system of rat fetuses; histological, immune-histochemical and ultrastructural studies. *Saudi J. Biol. Sci.* 28, 4704–4716. <https://doi.org/10.1016/j.sjbs.2021.04.084>
- Frick, A., Grammel, D., Schmidt, F., Pöschl, J., Priller, M., Pagella, P., von Bueren, A.O., Peraud, A., Tonn, J.C., Herms, J., Rutkowski, S., Kretschmar, H.A., Schüller, U., 2012. Proper cerebellar development requires expression of  $\beta 1$ -integrin in Bergmann glia, but not in granule neurons. *Glia* 60, 820–832. <https://doi.org/10.1002/glia.22314>
- Graus-Porta, D., Blaess, S., Senften, M., Littlewood-Evans, A., Damsky, C., Huang, Z., Orban, P., Klein, R., Schittny, J.C., Müller, U., 2001.  $\beta 1$ -class integrins regulate the development of laminae and folia in the cerebral and cerebellar cortex. *Neuron* 31, 367–379.
- Halder, S.K., Kant, R., Milner, R., 2018. Chronic mild hypoxia increases expression of laminins 111 and 411 and the laminin receptor  $\alpha 6\beta 1$  integrin at the blood-brain barrier. *Brain Res.* 1700, 78–85. <https://doi.org/10.1016/j.brainres.2018.07.012>
- Heusinkveld, H.J., Staal, Y.C.M., Baker, N.C., Daston, G., Knudsen, T.B., Piersma, A., 2021. An ontology for developmental processes and toxicities of neural tube closure. *Reprod. Toxicol.* 99, 160–167. <https://doi.org/10.1016/j.reprotox.2020.09.002>
- Humphries, J.D., Byron, A., Humphries, M.J., 2006. Integrin ligands at a glance. *J. Cell Sci.* 119, 3901–3903. <https://doi.org/10.1242/jcs.03098>
- Illa, M., Eixarch, E., Batalle, D., Arbat-Plana, A., Muñoz-Moreno, E., Figueras, F., Gratacos, E., 2013. Long-Term Functional Outcomes and Correlation with Regional Brain Connectivity by MRI Diffusion Tractography Metrics in a Near-Term Rabbit Model of Intrauterine Growth Restriction. *PLoS One* 8. <https://doi.org/10.1371/journal.pone.0076453>



- Kady, S.M., Gardosi, J., 2004. Perinatal mortality and fetal growth restriction. *Best Pract. Res. Clin. Obstet. Gynaecol.* 18, 397–410. <https://doi.org/10.1016/j.bpobgyn.2004.02.009>
- Klose, J., Li, L., Pahl, M., Bendt, F., Hübenthal, U., Jüngst, C., Petzsch, P., Schauss, A., Köhrer, K., Leung, P.C., Wang, C.C., Koch, K., Tigges, J., Fan, X., Fritsche, E., 2022. Application of the adverse outcome pathway concept for investigating developmental neurotoxicity potential of Chinese herbal medicines by using human neural progenitor cells in vitro. *Cell Biol. Toxicol.* <https://doi.org/10.1007/s10565-022-09730-4>
- Kühne, B.A., Puig, T., Ruiz-Martínez, S., Crous-Masó, J., Planas, M., Feliu, L., Cano, A., García, M.L., Fritsche, E., Llobet, J.M., Gómez-Catalán, J., Barenys, M., 2019. Comparison of migration disturbance potency of epigallocatechin gallate (EGCG) synthetic analogs and EGCG PEGylated PLGA nanoparticles in rat neurospheres. *Food Chem. Toxicol.* 123. <https://doi.org/10.1016/j.fct.2018.10.055>
- Kühne, B.A., Vázquez-Aristizabal, P., Fuentes-Amell, M., Pla, L., Loreiro, C., Gómez-Catalán, J., Gratacós, E., Illa, M., Barenys, M., 2022. Docosahexaenoic Acid and Melatonin Prevent Impaired Oligodendrogenesis Induced by Intrauterine Growth Restriction (IUGR). *Biomedicines* 10. <https://doi.org/10.3390/biomedicines10051205>
- Leitner, Y., Fattal-Valevski, A., Geva, R., Eshel, R., Toledano-Alhadeef, H., Rotstein, M., Bassan, H., Radianu, B., Bitchonsky, O., Jaffa, A.J., Harel, S., 2007. Neurodevelopmental outcome of children with intrauterine growth retardation: A longitudinal, 10-Year prospective study. *J. Child Neurol.* 22, 580–587. <https://doi.org/10.1177/0883073807302605>
- Li, L., Welser, J. V., Dore-Duffy, P., del Zoppo, G.J., Lamanna, J.C., Milner, R., 2010. In the hypoxic central nervous system, endothelial cell proliferation is followed by astrocyte activation, proliferation, and increased expression of the alpha 6 beta 4 integrin and dystroglycan. *Glia* 58, 1157–67. <https://doi.org/10.1002/glia.20995>
- Lo, H.-M., Hung, C.-F., Huang, Y.-Y., Wu, W.-B., 2007. Tea polyphenols inhibit rat vascular smooth muscle cell adhesion and migration on collagen and laminin via interference with cell–ECM interaction. *J. Biomed. Sci.* 14, 637–645. <https://doi.org/10.1007/s11373-007-9170-6>
- Long, L., Li, Y., Wang, Y.D., He, Q.Y., Li, M., Cai, X.D., Peng, K., Li, X.P., Xie, D., Wen, Y.L., Yin de, L., Peng, Y., 2010. The preventive effect of oral EGCG in a fetal alcohol spectrum disorder mouse model. *Alcohol Clin Exp Res* 34, 1929–1936. <https://doi.org/10.1111/j.1530-0277.2010.01282.x>
- Marrs, G.S., Honda, T., Fuller, L., Thangavel, R., Balsamo, J., Lilien, J., Dailey, M.E., Arregui, C., 2006. Dendritic arbors of developing retinal ganglion cells are stabilized by  $\beta$ 1-integrins. *Mol. Cell. Neurosci.* 32, 230–241. <https://doi.org/10.1016/j.mcn.2006.04.005>
- Melgarejo, E., Medina, M.A., Sanchez-Jimenez, F., Urdiales, J.L., 2009. Epigallocatechin gallate reduces human monocyte mobility and adhesion in vitro. *Br J Pharmacol* 158, 1705–1712. <https://doi.org/10.1111/j.1476-5381.2009.00452.x>
- Moors, M., Rockel, T.D., Abel, J., Cline, J.E., Gassmann, K., Schreiber, T., Schuwald, J., Weinmann, N., Fritsche, E., 2009. Human neurospheres as three-dimensional cellular systems for developmental neurotoxicity testing. *Environ. Health Perspect.* 117, 1131–8. <https://doi.org/10.1289/ehp.0800207>
- Moresco, E.M.Y., Donaldson, S., Williamson, A., Koleske, A.J., 2005. Integrin-mediated dendrite branch maintenance requires Abelson (Abl) family kinases. *J. Neurosci.* 25, 6105–18. <https://doi.org/10.1523/JNEUROSCI.1432-05.2005>

- Mwaniki, M.K., Atieno, M., Lawn, J.E., Newton, C.R., 2012. Long-term neurodevelopmental outcomes after intrauterine and neonatal insults: a systematic review. *Lancet* 379, 445–452. [https://doi.org/10.1016/S0140-6736\(11\)61577-8](https://doi.org/10.1016/S0140-6736(11)61577-8)
- Myers, J.P., Santiago-Medina, M., Gomez, T.M., 2011. Regulation of axonal outgrowth and pathfinding by integrin-ecm interactions. *Dev. Neurobiol.* 71, 901–923. <https://doi.org/10.1002/dneu.20931>
- Nieuwenhuis, B., Haenzi, B., Andrews, M.R., Verhaagen, J., Fawcett, J.W., 2018. Integrins promote axonal regeneration after injury of the nervous system. *Biol. Rev.* 93, 1339–1362. <https://doi.org/10.1111/brv.12398>
- Ortiz-Romero, P., Borralleras, C., Bosch-Morató, M., Guivernau, B., Albericio, G., Muñoz, F.J., Pérez-Jurado, L.A., Campuzano, V., 2018. Epigallocatechin-3-gallate improves cardiac hypertrophy and short-term memory deficits in a Williams-Beuren syndrome mouse model. *PLoS One* 13, e0194476. <https://doi.org/10.1371/journal.pone.0194476>
- Park, J.H., Yoon, J.H., Kim, S.A., Ahn, S.G., Yoon, J.H., 2010. (-)-Epigallocatechin-3-gallate inhibits invasion and migration of salivary gland adenocarcinoma cells. *Oncol Rep* 23, 585–590.
- Pervin, M., Unno, K., Ohishi, T., Tanabe, H., Miyoshi, N., Nakamura, Y., 2018. Beneficial Effects of Green Tea Catechins on Neurodegenerative Diseases. *Molecules* 23, 1–17. <https://doi.org/10.3390/molecules23061297>
- Peter, B., Farkas, E., Forgacs, E., Saftics, A., Kovacs, B., Kurunczi, S., Szekacs, I., Csampai, A., Bosze, S., Horvath, R., 2017. Green tea polyphenol tailors cell adhesivity of RGD displaying surfaces: multicomponent models monitored optically. *Sci. Rep.* 7, 42220. <https://doi.org/10.1038/srep42220>
- Pla, L., Illa, M., Loreiro, C., Lopez, M.C., Vázquez-Aristizabal, P., Kühne, B.A., Barenys, M., Eixarch, E., Gratacós, E., 2020. Structural Brain Changes during the Neonatal Period in a Rabbit Model of Intrauterine Growth Restriction. *Dev. Neurosci.* 42, 217–229. <https://doi.org/10.1159/000512948>
- Pla, L., Kühne, B.A., Guardia-Escote, L., Vázquez-Aristizabal, P., Loreiro, C., Flick, B., Gratacós, E., Barenys, M., Illa, M., 2022. Protocols for the evaluation of neurodevelopmental alterations in rabbit models in vitro and in vivo. *Front. Toxicol.* <https://doi.org/10.3389/ftox.2022.918520>
- Reid, M. V., Murray, K.A., Marsh, E.D., Golden, J.A., Simmons, R.A., Grinspan, J.B., 2012. Delayed myelination in an intrauterine growth retardation model is mediated by oxidative stress upregulating bone morphogenetic protein 4. *J. Neuropathol. Exp. Neurol.* 71, 640–653. <https://doi.org/10.1097/NEN.0b013e31825cfa81>
- Rideau Batista Novais, A., Pham, H., Van de Looij, Y., Bernal, M., Mairesse, J., Zana-taieb, E., Colella, M., Jarreau, P., Gressens, P., Pansiot, J., Dumont, F., Charriaut-marlangue, C., Tanter, M., Demene, C., Vaiman, D., Baud, O., 2016. Transcriptomic Regulations in Oligodendroglial and Microglial Cells Related to Brain Damage following Fetal Growth Restriction. <https://doi.org/10.1002/glia.2307>
- Robel, S., Mori, T., Zoubaa, S., Schlegel, J., Sirko, S., Faissner, A., Goebbels, S., Dimou, L., Götz, M., 2009. Conditional deletion of  $\beta$ 1-integrin in astroglia causes partial reactive gliosis. *Glia* 57, 1630–1647. <https://doi.org/10.1002/glia.20876>
- Souchet, B., Duchon, A., Gu, Y., Dairou, J., Chevalier, C., Daubigney, F., Nalesso, V., Créau, N.,

- Yu, Y., Janel, N., Herault, Y., Delabar, J.M., 2019. Prenatal treatment with EGCG enriched green tea extract rescues GAD67 related developmental and cognitive defects in Down syndrome mouse models. *Sci. Rep.* 9, 3914. <https://doi.org/10.1038/s41598-019-40328-9>
- Stagni, F., Giacomini, A., Emili, M., Trazzi, S., Guidi, S., Sassi, M., Ciani, E., Rimondini, R., Bartesaghi, R., 2016. Short- and long-term effects of neonatal pharmacotherapy with epigallocatechin-3-gallate on hippocampal development in the Ts65Dn mouse model of Down syndrome. *Neuroscience* 333, 277–301. <https://doi.org/10.1016/j.neuroscience.2016.07.031>
- Stagni, F., Guidi, S., Bartesaghi, R., 2021. Chapter 53 - Epigallocatechin-3-gallate: Linking the neurogenesis, hippocampus, and Down syndrome, in: *Factors Affecting Neurodevelopment*. Elsevier, pp. 619–630. <https://doi.org/10.1016/B978-0-12-817986-4.00053-5>
- Suzuki, Y., Isemura, M., 2001. Inhibitory effect of epigallocatechin gallate on adhesion of murine melanoma cells to laminin. *Cancer Lett.* 173, 15–20. [https://doi.org/10.1016/S0304-3835\(01\)00685-1](https://doi.org/10.1016/S0304-3835(01)00685-1)
- Tiwari, V., Kuhad, A., Chopra, K., 2010. Epigallocatechin-3-gallate ameliorates alcohol-induced cognitive dysfunctions and apoptotic neurodegeneration in the developing rat brain. *Int J Neuropsychopharmacol* 13, 1053–1066. <https://doi.org/10.1017/s146114571000060x>
- Tolcos, M., Bateman, E., O'Dowd, R., Markwick, R., Vrijssen, K., Rehn, A., Rees, S., 2011. Intrauterine growth restriction affects the maturation of myelin. *Exp. Neurol.* 232, 53–65. <https://doi.org/10.1016/j.expneurol.2011.08.002>
- Warren, M.S., Bradley, W.D., Gourley, S.L., Lin, Y.-C., Simpson, M.A., Reichardt, L.F., Greer, C.A., Taylor, J.R., Koleske, A.J., 2012. Integrin  $\beta 1$  signals through Arg to regulate postnatal dendritic arborization, synapse density, and behavior. *J. Neurosci.* 32, 2824–34. <https://doi.org/10.1523/JNEUROSCI.3942-11.2012>
- Workman, A.D., Charvet, C.J., Clancy, B., Darlington, R.B., Finlay, B.L., 2013. Modeling transformations of neurodevelopmental sequences across mammalian species. *J. Neurosci.* 33, 7368–83. <https://doi.org/10.1523/JNEUROSCI.5746-12.2013>
- www.clinicaltrials.gov, 2022. Database of privately and publicly funded clinical studies conducted around the world. [WWW Document]. URL [www.clinicaltrials.gov](http://www.clinicaltrials.gov)

## Supplementary material

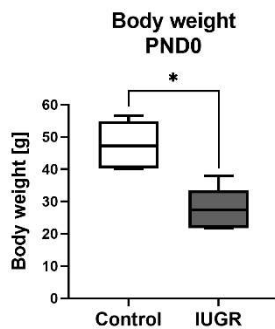


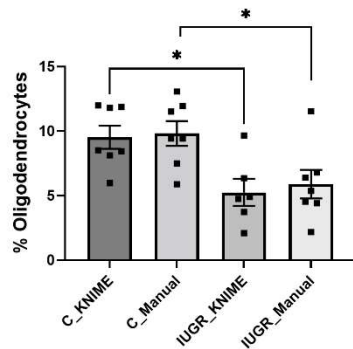
*Figure S 1. Body weight of control and IUGR rabbit pups at PND0. Rabbit pups used to prepare neurospheres were weighted at PND0; n=6 controls and n=6 IUGR. Boxplot represented in Tukey's style (Median, and 25th and 75th percentiles), \*:  $p < 0.05$ .*

### SM1 – Establishment of KNIME high-content screening workflow to count OLS

For the establishment of the automatic counting of OLS using the program KNIME, we compared the results between manual and automatic cell count. Figure S2 A illustrates that the automatic (KNIME) and manual counting present the same effect: A significant decrease in % OLS in the IUGR compared to the control group. Figure S2 B shows two estimation plots illustrating the mean of difference between automatic (KNIME) and manual cell count of control (left) and IUGR (right). The estimation plot presents the magnitude of an effect along with a 95% confidence interval (CI). The left x-axis scales the % OLS, each point of the left side represents one independent experiment of automatic cell count (blue) connected to its respective manual cell count (red). The right x-axis scales the confidence interval of the mean of difference, by representing the difference between both groups in each black point. In control and IUGR neurospheres, the pairing between automatic and manual counting was significantly effective (CI  $p < 0.05$ ), which means the cell counts are statistically comparable. Therefore, the automatic counting of OLS with KNIME was considered as reliable. Our workflow is available in KNIME®-hub:

[https://hub.knime.com/elisabet\\_t/spaces/Public/latest/Counting%20OL~fVnKirqqJhzW8qjf](https://hub.knime.com/elisabet_t/spaces/Public/latest/Counting%20OL~fVnKirqqJhzW8qjf).

### A KNIME vs manual cell count



### B

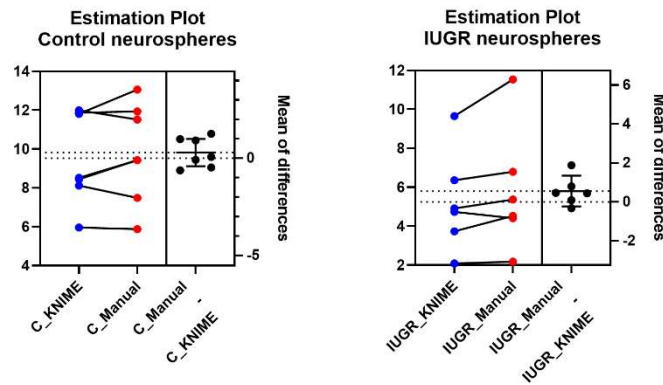


**Figure S 2. KNIME vs. manual cell count of Oligodendrocytes.** (A) Effect of control and IUGR on % OLs counted either automatic (KNIME) or manual using ImageJ. Each square represents one independent experiment. (B) Two estimation plots illustrating the difference between KNIME and manual counting in control (left) or IUGR neurospheres (right). Left side of the plot: Each point represents one independent experiment analysed with 5 neurospheres per condition, blue: automatic, red: manual counting. Right plotted side: each black point represents the mean of difference between KNIME and manual counting.

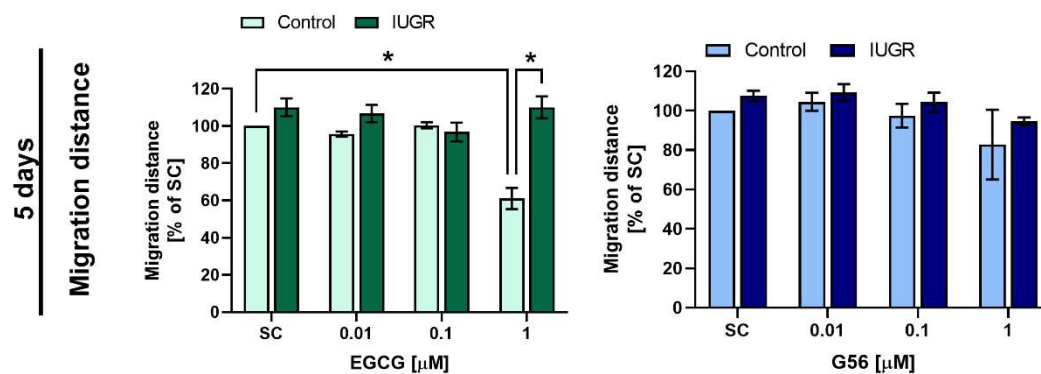


**Figure S 3. EGCG and G56 effects on migration pattern after 5 days in vitro.** Rabbit neurospheres obtained from Control and IUGR pups were comparatively analysed after 5 days under differentiation conditions in vitro. Migration distance [% of SC] after exposure to EGCG (green) and G56 (blue).

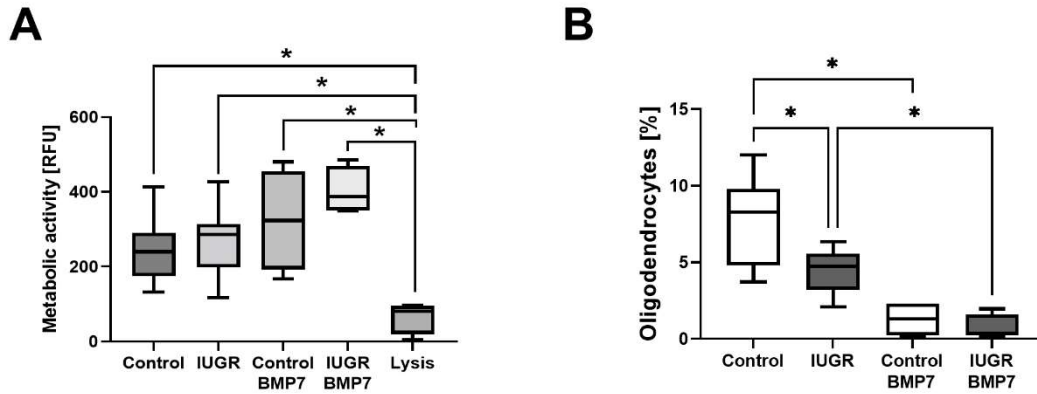


**Figure S 4.** Viability and OL differentiation of control and IUGR rabbit neurospheres after 5 days differentiation with or without exposure to their respective positive control. (A) Cell viability determined by metabolic activity after exposure to BMP7 [100 ng/mL] or lysis control (10% DMSO). (B) OL differentiation, positive control: BMP7 [100 ng/mL]. Boxplot represented in Tukey's style (Median, and 25th and 75th percentiles), \*:  $p < 0.05$ .

## SM2 – qRT PCR.

After 11 days of proliferation, IUGR and control pup's derived neurospheres were chopped to 0.1 mm pieces and resuspended in differentiation medium. 700-800 pieces were placed in a PDL/Laminin coated well on a 24-Well-plate in triplicates containing 1 mL differentiation medium for 5 days. After 72h of cultivation 50% of the medium was renewed. After 5 days RNA was isolated (RNeasy Mini Kit, Qiagen, Hilden, Germany) and cDNA was transcribed (Quantitect Reverse Transcription Kit, Qiagen) according to the manufacturer instructions. Primer sequences were designed using NCBI Primer-BLAST (Table S1). qRT-PCR was performed using QuantiFast SYBR Green PCR Kit (Qiagen) and the AriaMx Real-Time PCR instrument with the software Agilent Aria Software v1.6. The thermal profile included a hot start for 7 min at 95°C, 47 amplification cycles comprising 10 min at 95°C for denaturation, 35 min at 60°C for annealing and 20 min at 72°C for extension, followed by a melting step for the dissociation of PCR products for 30 min at 75°C and 30 min at 99°C. Gene expression was evaluated by using the cycle threshold (Ct) value from each sample. Relative fold gene expression of the gene of interest (GOI) was assessed by the  $\Delta\Delta C_t$  method:

$$1) \Delta C_t = C_t (\text{GOI}) - C_t (\beta \text{ actin})$$

- 2) MEAN of the  $\Delta Ct$  values of the solvent control (SC) triplicates
- 3)  $\Delta\Delta Ct = \Delta Ct (\text{sample}) - \text{MEAN } \Delta Ct (\text{SC})$
- 4) relative GOI expression =  $2^{-\Delta\Delta Ct}$

Mean and SEM of the qRT-PCR analysis was calculated from at least three independent experiments.

**Table S 1 Primer sequences** designed with [NCBI Blast Primer design](#)

|  | Species | Forward primer                   | Reverse primer                   |
|--|---------|----------------------------------|----------------------------------|
| <b><i>Integrin beta 1</i></b>          | rabbit  | 5'-TGT GAT CGC TCC AAT GGC TT-3' | 5'-ATT TTC AAA GCC TGC ACC GC-3' |
| <b><i>Integrin beta 4</i></b>          | rabbit  | 5'-ATC CCT GAA AGT GAG CTG GC-3' | 5'-TTG TAA GGC ACG TTC TCG CT-3' |
| <b><i><math>\beta</math>-actin</i></b> | rabbit  | 5'-TCC CTG GAG AAG AGC TAC GA-3' | 5'-GTA CAG GTC CTT GCG GAT GT-3' |

### SM3 – Western blot.

Pellets were homogenized in RIPA lysis buffer system with protease inhibitors included (SC-24948, Santa Cruz Biotechnology) and they were centrifuged at full speed for 10 min at 4°C after a 2 h incubation at the same temperature. The supernatant was recovered and frozen at –80°C until use. Sample protein concentration was determined using the Bradford Protein Assay Kit (Bio-Rad). For immunoblot assays, 10  $\mu$ g per sample were separated by SDS-PAGE on 10% acrylamide gels at constant 120 V and transferred to polyvinylidene difluoride sheets (Immobilon®-P Transfer Membrane; IPVH00010; Merck Millipore Ltd., USA) at constant 200 mA for 120 min. After, membranes were blocked for 1 h with 5% non-fat milk dissolved in TBS-T buffer (0.5 mM Tris; NaCl, Tween® 20 (P1379, Sigma-Aldrich, USA), pH 7.5), washed with TBS-T 3 times for 5 min and incubated with int- $\beta$ 1 (BD Pharmingen™ 555003) or int- $\beta$ 4 (EMD Millipore Corp. MAB2059) antibody, overnight (O/N) at 4°C. Subsequently, blots were washed in TBS-T buffer and incubated at room temperature for 1 h with secondary goat anti-mouse (Invitrogen 31460) antibody. Finally, results were obtained through chemiluminescence detection using the Pierce® ECL Western Blotting Substrate (#32106, Thermo Scientific, USA), a

Bio-Rad Universal Hood II Molecular Imager and the Image Lab v5.2.1 software (Bio-Rad laboratories). Measurements were expressed in arbitrary units and all results were normalized with  $\beta$ -actin loading control (A5441, Sigma)

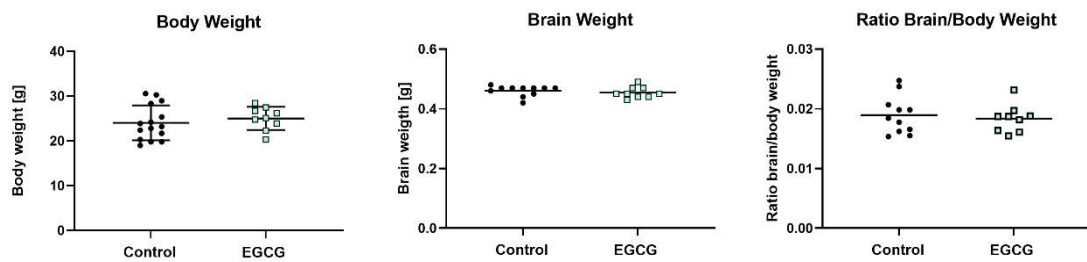


**Figure S 5. Mouse body, brain, and ratio brain/body weight.** Body and brain weight of postnatal week 8 mice exposed or not to EGCG during development. Results presented as single values in dots (controls) or squares (EGCG treated) and mean  $\pm$ SD.

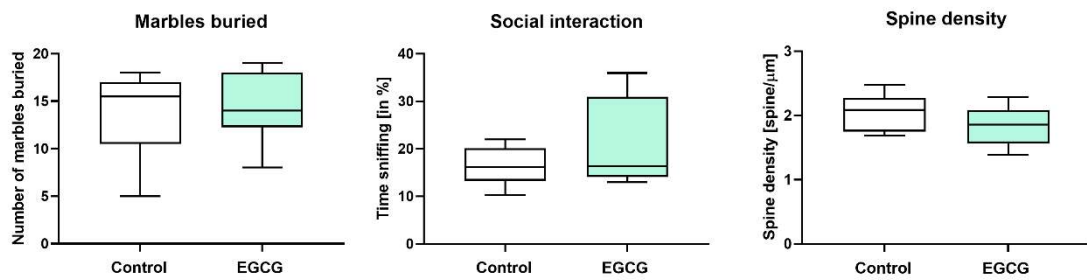


**Figure S 6. Behaviour of mice with or without developmental administration to EGCG.** Number of marbles buried evaluated after 20 minutes. Boxplot represented in Tukey's style (Median, and 25th and 75th percentiles), \*:  $p < 0.05$ .



## Summary of results

The present thesis includes seven manuscripts summarized here:

The first manuscript 3.1 (Pla et al., 2022) “Protocols for the evaluation of neurodevelopmental alterations in rabbit models *in vitro* and *in vivo*” is a methodological paper including new protocols for the *in vivo* and *in vitro* evaluation of neurodevelopmental alterations in the rabbit species. It critically discusses why the rabbit species is relevant for the evaluation of neurodevelopmental alterations in particular cases. The publication points out that rabbits have a higher similarity to humans than rodent regarding (1) the timing of brain- and white matter maturation, (2) the complexity of the brain structure, and (3) extraembryonic membranes, placenta development and circulatory changes during gestation. The established protocols cover the majority of endpoints currently required in DNT OECD TG 426 (OECD, 2007), plus the *in vitro* rabbit ‘Neurosphere Assay’ for compound testing or mechanistic studies helping to reduce the number of animals.

The manuscript 4.1 (Pla et al., 2020) “Structural Brain Changes during the Neonatal Period in a Rabbit Model of Intrauterine Growth Restriction” describes IUGR induced changes in neurodevelopment during the neonatal period of rabbits. PND1 IUGR pups had a significantly higher stillbirth rate and lower body weight, accompanied by poorer functional outcomes compared to the control group. The lower birth weight correlated significantly with lower density of OLs in the WM of the corpus callosum, whereas no differences were observed between control and IUGR in the density of microglia and astrocytes. In addition, the study revealed a higher number of distal dendrites in the frontal cortex of IUGR brains. Of note, the detected changes in brain histology are consistent with the *in vitro* results obtained with the neurosphere assay in Manuscript 4.2, 4.3, 4.4, and 4.5.

The manuscript 4.2. (Barenys et al., 2021) “Rabbit neurospheres as a novel *in vitro* tool for studying neurodevelopmental effects induced by intrauterine growth restriction a novel *in vitro* rabbit neurosphere model” characterizes neurodevelopmental effects induced by IUGR and includes the establishment of the preparation of NPCs growing as neurospheres from whole brain of PND0 control and IUGR rabbit pups. Rabbit NPCs appeared to be suitable for characterizing previously unknown changes in basic neurogenesis processes induced by IUGR at the cellular level. Exposure of established positive controls demonstrated that the neurosphere system is flexible and can respond to external stimuli. Moreover, the ability of rabbit NPCs to proliferate, migrate, and differentiate into neurons, astrocytes, and OLs was proven for the first time and compared between control and IUGR. Neurospheres derived from IUGR brains have a significantly lower percentage of OLs, while no significant adverse effects were found in the other neurodevelopmental endpoints tested. The publication clearly demonstrates that the novel rabbit neurosphere model opens the door to test

potential therapies for brain development disrupted by IUGR in a more mechanistic approach by reducing the number of animals and resources.

The manuscript 4.3. (Kühne et al., 2022) “Docosahexaenoic Acid and Melatonin Prevent Impaired Oligodendrogenesis Induced by Intrauterine Growth Restriction (IUGR)” provides insights into alterations in oligodendrogenesis in fetuses with IUGR and therapeutic strategies to prevent or treat impaired OLs using the novel *in vitro* rabbit neurosphere model. In the IUGR culture, the percentage of OLs was reduced due to a slower OL differentiation rate, which correlates very well with clinical outcomes of IUGR induced white matter injury. Five potential therapies were screened *in vitro*, namely DHA, melatonin (MEL), zinc, T3 and sialic acid (SA), the main metabolite of Lactoferrin (LF). DHA and MEL were identified as the most effective therapies to treat IUGR induced OL alterations *in vitro* and selected together with LF for further *in vivo* prenatal administration. The *in vitro* neurospheres assay predicted in all tested cases the outcome of the maternal *in vivo* treatment, making it a reliable and consistent model to select new neuroprotective therapies in a fast, economic, and ethical way. Moreover, the study suggests the *in vitro* neurospheres assay as a powerful tool to assess the safety and efficacy of potential therapies by determining the MTC and mEC *in vitro*.

The manuscript 4.4. (Kühne et al., to be submitted) “Lactoferrin prevents adverse effects of intrauterine growth restriction (IUGR) on neurite length: investigations in an *in vitro* rabbit neurosphere model” deals with the impact of IUGR on processes of neuronal differentiation, number of dendrites, neurite length and network formation including synaptogenesis in the *in vitro* rabbit neurosphere culture. IUGR induced significantly longer neurite length compared to control after 5 days in culture. The efficacy and safety of the neuroprotective candidates DHA, MEL and LF/SA was assessed in neurospheres after direct *in vitro* exposure or after maternal administration. LF was identified as the most effective agent against IUGR induced neurite extension after prenatal *in vivo* administration and SA after *in vitro* exposure. All tested concentrations of the potential therapies were considered as safe regarding NPC viability, migration, and differentiation. The study points out, that understanding how neuronal development is changed by IUGR, and therefore a mechanistically driven search of therapies will facilitate and make more efficient the discovery and development of new therapies in the future.

The manuscript 4.5. (Kühne et al., 2019) “Comparison of migration disturbance potency of epigallocatechin gallate (EGCG) synthetic analogs and EGCG PEGylated PLGA nanoparticles in rat neurospheres” involves the evaluation of DNT effects of EGCG, synthetic analogs (G37, G56, M1, and M2) and EGCG PEGylated PLGA nanoparticles (Nano-EGCG) in rat control neurospheres. EGCG, the most abundant catechin of green tea, is considered as a promising neuroprotective therapy but EGCG has been shown to disturb NPC migration, corona formation and orientation angles as well as the migration of young neurons. In this study, a chemical hazard characterization of structurally related

compounds was approached to find a safer alternative. Different potencies of adverse effects on the key event 'NPC migration' were observed: EGCG  $\approx$  G37 > M2 > M1  $\approx$  G56 > Nano-EGCG. The compounds G56 and Nano-EGCG may serve as safer prenatal nutritional supplements or potential therapeutic alternatives to EGCG based on their lower toxicity outcome tested with the rat neurosphere assay.

The manuscript 4.6. (Kühne et al., submitted) "Application of the adverse outcome pathway to identify molecular changes in prenatal brain programming induced by IUGR: discoveries after EGCG exposure" is based on previous studies discovering that EGCG binds to the extracellular matrix protein laminin, which prevents the interaction of the cell adhesion molecule int- $\beta$ 1 with laminin, resulting in a disturbed NPC migration pattern (Barenys et al., 2016, 2017; Kühne et al., 2019; Peter et al., 2017; Suzuki and Isemura, 2001). Strikingly, in IUGR neurospheres the EGCG induced adverse effect on NPC migration was not observed. The manuscript reveals that IUGR neurospheres overexpress int- $\beta$ 1 and respond differently than control neurospheres to the exposure of a compound triggering migration alterations. Because int- $\beta$ 1 is not only involved in NPC migration but also in axonal growth and neuronal branching, the study suggests that int- $\beta$ 1 has decisive influence on the IUGR induced neurite length extension (manuscript 4.1. (Pla et al., 2020) and 4.4 (Kühne et al., 2022 to be submitted). The generated results, in combination with data from the literature, were integrated into a putative AOP framework entitled "Disrupted laminin/ int- $\beta$ 1 interaction leading to decreased cognitive function".

## Supervisors' report

Hereby, we Dr. Marta Barenys and Dr. Míriam Illa, as PhD supervisors of Britta A. Kühne, state that:

This thesis includes in its main part 5 accepted scientific publications and 2 manuscripts submitted or to be submitted to peer-reviewed scientific journals. These 7 pieces of work belong to the topic "Safety and efficacy investigations for new prenatal neuroprotective therapies. Applications in a model of intrauterine growth restriction (IUGR)" and have been developed within the frame of the PhD work of the candidate Britta A. Kühne.

A summary of the 7 pieces of work included in this thesis indicating the publication year, the impact factor of the Journal according to the Journal of Citation Reports (JCR), the position of the Journal in the field (according to the JCR) in quartile or decile, the indication of whether Britta A. Kühne is first author of the publication or not, and whether the publication has been used by another author for another PhD thesis work, is included in Table R1. Besides that, the participation of Britta A. Kühne in each manuscript/publication is detailed in Table R2.

**Table R1. Summary of the manuscripts/publications included in the thesis of Britta A. Kühne:**

| Thesis section | Manuscript / Publication  | Publication year | IF    | D/Q | First author? | Used for another PhD thesis? |
|----------------|---|------------------|-------|-----|---------------|------------------------------|
| 3.1            | Protocols for the evaluation of neurodevelopmental alterations in rabbit models in vitro and in vivo                            | 2022             | no IF | -   | Yes (shared)  | No                           |
| 4.1            | Structural Brain Changes during the Neonatal Period in a Rabbit Model of Intrauterine Growth Restriction                        | 2020             | 2.984 | Q2  | No            | Yes (by L. Pla)              |
| 4.2            | Rabbit neurospheres as a novel in vitro tool for studying neurodevelopmental effects induced by intrauterine growth restriction | 2021             | 6.940 | Q1  | No            | Yes (by J. Klose)            |
| 4.3            | Docosahexaenoic Acid and Melatonin Prevent Impaired Oligodendrogenesis Induced by Intrauterine Growth Restriction (IUGR)        | 2022             | 6.081 | Q1  | Yes           | No                           |
| 4.4            | Lactoferrin prevents adverse effects of intrauterine growth restriction (IUGR)  | To be submitted  | -     | -   | Yes           | No                           |

on neurite length: investigations in an  
in vitro rabbit neurosphere model

|     |  |           |       |    |     |    |
|-----|--|-----------|-------|----|-----|----|
| 4.5 | Comparison of migration disturbance potency of epigallocatechin gallate (EGCG) synthetic analogs and EGCG PEGylated PLGA nanoparticles in rat neurospheres | 2019      | 4.679 | D1 | Yes | No |
| 4.6 | Application of the adverse outcome pathway to identify changes in prenatal brain programming after exposure to EGCG  | submitted | -     | -  | Yes | No |

*Table R1. D1: 1st decile; D/Q: decile or quartile; IF: impact factor; Q1: first quartile; (-): not applicable; Highlighted in blue: articles accepted for publication in 1st decile or 1st quartile Journals in which B.A.K is 1st author, and which have not been used for the doctoral thesis of other candidates.*

The articles included in this thesis fulfill the requirements of the Biomedicine PhD Program of the University of Barcelona for the thesis to be submitted as a “Thesis by compilation” because the articles (4.3) “Docosahexaenoic Acid and Melatonin Prevent Impaired Oligodendrogenesis Induced by Intrauterine Growth Restriction (IUGR)” and (4.5) “Comparison of migration disturbance potency of epigallocatechin gallate (EGCG) synthetic analogs and EGCG PEGylated PLGA nanoparticles in rat neurospheres”:

- have already been accepted for publication in a Q1 (4.3) or D1 (4.5) Journal according to JCR rankings
- are authored by Britta A. Kühne in the first position (single first author)
- have not been used for the doctoral thesis of any other candidate.

**Table R2. Summary of the contributions of Britta A. Kühne to the manuscripts included in this thesis:**

| Thesis section | Manuscript   | Contribution of Britta A. Kühne   |
|----------------|--|---|
| 3.1            | Protocols for the evaluation of neurodevelopmental alterations in rabbit models in vitro and in vivo   | Protocols reproducibility assessment, data analysis and interpretation, manuscript writing, visualization.  |
| 4.1            | Structural Brain Changes during the Neonatal Period in a Rabbit Model of Intrauterine Growth Restriction   | Methodology and investigation.  |
| 4.2            | Rabbit neurospheres as a novel in vitro tool for studying neurodevelopmental effects induced by intrauterine growth restriction                            | Data analysis and interpretation, manuscript writing.   |
| 4.3            | Docosahexaenoic Acid and Melatonin Prevent Impaired Oligodendrogenesis Induced by Intrauterine Growth Restriction (IUGR)                                   | Conceptualization, methodology, validation, formal analysis, investigation, data curation, manuscript writing, visualization, project administration. |
| 4.4            | Intrauterine growth restriction (IUGR) increases neurite length: investigations in an in vitro rabbit neurosphere model                                    | Conception and design, collection and assembly of data, data analysis and interpretation, manuscript writing.   |
| 4.5            | Comparison of migration disturbance potency of epigallocatechin gallate (EGCG) synthetic analogs and EGCG PEGylated PLGA nanoparticles in rat neurospheres | Conceptualization, methodology, validation, formal analysis, investigation, data curation, manuscript writing, visualization.                         |
| 4.6            | Application of the adverse outcome pathway to identify changes in prenatal brain programming after exposure to EGCG  | Conceptualization, methodology, validation, formal analysis, investigation, data curation, manuscript writing, visualization.                         |

*Table R2. D1: Highlighted in blue: articles accepted for publication in 1st decile or 1st quartile Journals in which B.A.K is 1st author, and which have not been used for the doctoral thesis of other candidates.*

Besides the manuscripts included in the main part of the thesis, other publications of Britta A. Kühne obtained in collaboration with other research groups and contributing to topics not directly related to her thesis have been included in the Annex and their details are summarized in table R3.

**Table R3. Summary of the manuscripts/publications included in the Annex of Britta A. Kühne's thesis:**

| Thesis section | Manuscript / Publication   | Publication year | IF    | D/Q |
|----------------|--|------------------|-------|-----|
| 8.1            | Docosahexaenoic acid and lactoferrin effects on the brain and placenta in a rabbit model of intrauterine growth restriction  | submitted        | -     | -   |
| 8.2            | Epigallocatechin-3-gallate PEGylated poly(lactic-co-glycolic) acid nanoparticles mitigate striatal pathology and motor deficits in 3-nitropropionic acid intoxicated mice  | 2021             | 5.037 | Q1  |
| 8.3            | Dual-drug loaded nanoparticles of Epigallocatechin-3-gallate (EGCG) / Ascorbic acid enhance therapeutic efficacy of EGCG in a APPswe/PS1dE9 Alzheimer's disease mice model | 2019             | 7.727 | D1  |
| 8.4            | Literature review and appraisal on alternative neurotoxicity testing methods   | 2018             | no IF | -   |

*Table R3. D1: 1st decile; D/Q: decile or quartile; IF: impact factor; Q1: first quartile; (-): (-): not applicable.*

## 5 Discussion

### 5.1 The need of new prenatal therapies

IUGR is among the most frequent disorders during pregnancy affecting 5-10% of all pregnancies (Kady and Gardosi, 2004), being abnormal placental function the most common cause, which reduces placental blood flow leading to fetal development under chronic hypoxia. The development of the brain is composed of several highly regulated processes that must occur in a correct spatiotemporal order from early pre- until postnatal fetal growth. This long process of complex neurogenesis is therefore extremely susceptible to an unfavorable intrauterine situation and already mild continuous developmental hypoxia can cause a wide range of adverse effects on the central nervous system. Currently, there is no therapy to be applied at the prenatal period preventing or reverting the neurological insults that arise from IUGR (Fleiss et al., 2019; Tolcos et al., 2017). The only prenatal treatment is preterm delivery, which involves a good management in timing of delivery including balancing the risk between adverse intrauterine environment and prematurity (Figueras and Gardosi, 2011). Although researchers and clinicians have made tremendous efforts to generate preclinical data to support translation of therapies into clinical trials, no conclusively effective therapy has yet been found as reviewed in Fleiss et al. (2019). For example, a small study recruiting early and late IUGR cases has reported increased birth weight after administrating dydrogesterone to the pregnant woman, a synthetic progestogen playing an important role in pregnancy maintenance (Zarean et al., 2018). Despite promising results, this was a single-center study with no postnatal follow-up and thus, requires further analysis (Fleiss et al., 2019) and cautious assessment of possible delayed endocrine disrupting effects of the therapy. A more extensive international study involving multiple centers, the STRIDER-UK study, tested sildenafil (a selective inhibitor of phosphodiesterase 5 used to treat erectile dysfunction and pulmonary arterial hypertension) in women with severe early-onset IUGR, but sildenafil did neither prolong nor improve IUGR-complicated pregnancy (Sharp et al., 2018). Even though this study included many patients without reported side-effects of the drug, it could not adequately evaluate therapeutical consequences because of a high mortality in the cohort (Smith, 2018). Numerous animal studies suggest that maternally administered creatine can increase its placental transfer, which improves fetal survival and alters brain development in a hypoxic intrauterine environment (Adcock et al., 2002; Ireland et al., 2011, 2008). Although creatine is considered as a presumptive therapy to prevent or reduce the adverse effects of IUGR, no intervention studies have yet been conducted in pregnant women (Fleiss et al., 2019). To overcome the hurdles impeding the therapy progress, it was crucial to establish a reliable model to discover and develop neuroprotective strategies for impaired brain development to be applied during the prenatal phase, the “critical window of opportunity”. The thesis aimed to establish a novel *in vitro* rabbit neurospheres model of



IUGR to discover so far unknown mechanisms of potential therapies on a cellular level, unraveling its safety (DNT potential) and efficacy.

## 5.2 The rabbit *in vitro* neurosphere model

Eixarch et al. established the rabbit *in vivo* disease model of IUGR, which has been proved to present cardiovascular Doppler changes similar to those observed in human IUGR cases, reduced birth weight and a higher brain to birth weight ratio ((Eixarch et al., 2011, 2009), Manuscript 4.1 (Pla et al., 2020)). The rabbit species was chosen because it mimics human conditions better than other animal models according to a “precocial score” for neurodevelopment and has become the favorable species in translational medicine for neurodevelopmental studies (Manuscript 3.1 (Pla et al., 2022) (Derrick et al., 2004; Eixarch et al., 2012b; Workman et al., 2013)). Its brain development occurs largely perinatal by building complex brain structures and starting the myelination process postnatally similar to human (Barenys et al., 2021; Drobyshevsky et al., 2014; Workman et al., 2013), whereas the rodent brain develops mainly during the prenatal period (Chini and Hanganu-Opatz, 2021) (Fig. 3). Furthermore, rabbits are more similar to humans in terms of placental circulation and placental transfer as well as the development of extraembryonic membranes (Carter, 2007; Eixarch et al., 2009; Pla et al., 2022). However, conducting developmental studies with rabbits entails some constraints compared to smaller test animals such as mouse and rat, because rabbits need more room space, and the gestation period is longer which means more time, costs, and higher usage of test compounds. *In vivo* studies entail a large number of animals over a long period of time and notwithstanding often leading to a high variability in results. Manuscript 3.1 (Pla et al., 2022) critically discussed steps in protocols and limitations of techniques while giving orientation on expected results by using positive controls. The manuscript 3.1 points out in which particular cases it is relevant to use the *in vivo* rabbit model, such as for behavioral, memory and sensory function, and learning tests during the neonatal and long-term period as well as in the test guidelines OECD TG 414 (OECD, 2018a). To refine and reduce the use of animals, it was from importance to develop a reliable *in vitro* system that captures a wide complexity of the developmental neuronal system. In the current study a rabbit and a rabbit IUGR neurosphere model were established (Manuscript 3.1 (Pla et al., 2022) and 4.2. (Barenys et al., 2021)) opening the door to investigate the effects of IUGR on cell functions characteristic of the developing brain, and to test potential neuroprotective therapies or chemicals in a more time- and cost-efficient way than the classical *in vivo* studies. Neurospheres were prepared from the rabbit *in vivo* model mimicking placental insufficiency by selective ligation of uteroplacental vessels in late pregnancy, which is associated with a mild and chronic late-onset IUGR. Late-onset IUGR has a higher incidence and a larger etiologic contribution to adverse outcomes than early-onset IUGR (Table 1), and therefore it was crucial to characterize the neurodevelopmental abnormalities that result from late-onset IUGR to

minimize adverse fetal programming. Illa et al., and Eixarch et al., identified subtle changes in brain GM and WM structure of rabbit fetuses growing under these mild and chronic hypoxia conditions in fixed whole brains, which are difficult to perceive *in vivo* (Eixarch et al., 2012b; Illa et al., 2013). These subtle differences occurring from mild late-onset IUGR were observed in brain regions associated to anxiety, attention, memory, and long-term functional impairments (Eixarch et al., 2012b; Illa et al., 2013). These findings highlight the need to investigate the underlying mechanisms at a cellular level to find target-directed drugs using an appropriate *in vitro* system.

Neurospheres have been used for many years as a model to study central nervous disorders including Alzheimer, Parkinson, demyelinating diseases, epilepsy and glioma (da Silva Siqueira et al., 2021), and the 'Neurosphere Assay' has previously been established for several species rat, mouse, and human (Barenys et al. 2021; Baumann et al. 2014; Gassmann et al. 2010; Masjosthusmann et al. 2018). In recent years, neurospheres have been characterized at the molecular and cellular levels to confirm their suitability for evaluating neurodevelopmental endpoints. NPCs growing as neurospheres have multipotent and self-renewal properties regardless of regional origin of the brain and are able to maintain their molecular expression for each unique brain region across several *in vitro* passages (Hitoshi et al., 2002; Kim et al., 2006). Flow cytometry analyses revealed that proliferating primary human NPCs express nestin and SOX2, which confirms their progenitor character whose expression decreases under differentiation conditions and progressive migration (Hofrichter et al., 2017; Schmuck et al., 2017). The migration assay revealed that after 3 days rabbit NPCs cover a distance from ca. 700  $\mu\text{m}$ , and differentiate while migrating into  $\beta\text{III-Tubulin}^+$  neurons, O4<sup>+</sup> OLs and GFAP<sup>+</sup> astrocytes as it occurs in human neurospheres (Manuscript 4.1 (Barenys et al., 2021)(Baumann et al., 2016)). After 14 days under differentiation conditions, the rabbit culture presented long extension and dendritic branching of  $\beta\text{III-tubulin}^+$  cells as well as network formation (Manuscript 4.4). Immunocytochemical staining confirmed the process of synaptogenesis by the pre-synaptic marker SYNAPSIN-1, which was aligned with  $\beta\text{III-tubulin}^+$  cells. Rabbit neurospheres developed synaptic markers after 14 days, whereas neurons of human primary NPCs did not develop synaptic markers after 28 days under differentiation conditions (Hofrichter et al., 2017), which indicates a faster network expansion in the rabbit compared to the human culture. In order to prove the functionality of the neuronal network in future, rabbit NPCs can be cultured on microelectrode arrays (MEAs). This technology measures the electrical activity in real-time at different locations of neurons (Hofrichter et al., 2017; Nimtz et al., 2020). By using MEAs, Hofrichter et al., discovered that neurospheres from human induced pluripotent stem cells form synapses and functional neuronal networks after 28 days of differentiation (Hofrichter et al., 2017). The MEA-technique is a novel tool with great potential as part of an *in vitro* testing battery and would cover a further essential endpoint of brain development that has so far not been included in the rabbit neurosphere system.

To prove that rabbit neurospheres are able to detect changes induced during the phase of neurodevelopment without being oversensitive, they were exposed to increasing concentrations of two compounds, a positive and a negative control, following the recommendations of Crofton et al. (2011). One is a known neurodevelopmental toxicant in humans and animals, methylmercury chloride (MeHgCl; positive control) and the other a compound known to have no effects on neurodevelopment in humans and animals, saccharine (negative control (Aschner et al., 2017)). The neurosphere model was proven to detect the known neurotoxicant MeHgCl and was not adversely affected by the negative control saccharine (Manuscript 4.2 (Barenys et al., 2021)). Therefore, the rabbit neurosphere system is sensitive, because it can detect known toxicants and is specific because it is not overreacting to innocuous compounds.

The 'Neurosphere Assay' covers a broad variety of endpoints mimicking basic processes of the vast complexity of brain development in a temporal context and has therefore the potential to be part of an *in vitro* testing battery. The culture can be used to characterize effects on a cellular level to fill disparities in translational approaches by shifting from apical *in vivo* testing to pathway analysis *in vitro*. It is worth noting, that such an *in vitro* testing battery would not be intended to directly replace *in vivo* test guidelines, but could inform regulatory approaches for decision-making in the assessment of chemicals and drugs (Sachana et al., 2021). In this sense, the *in vitro* 'Neurosphere Assay' can be used to screen numerous chemicals in a wide concentration range for their neuroprotective or DNT potential and to prioritize them for follow-up studies.

### 5.3 Effects of IUGR on brain development

By exploring the impact of IUGR, we identified an adverse effect on oligodendrogenesis *in vitro* (Manuscript 4.2 (Barenys et al., 2021), 4.3 (Kühne et al., 2022)) and in brain histology studies *in vivo* (Manuscript 4.1 (Pla et al., 2020)). We discovered that the differentiation already of early pre-myelinated OLs is disturbed by IUGR resulting in a maturation delay of OLs compared to control. Several studies in rodents with induced prenatal hypoxia-ischemia confirmed the myelination insult by a failed maturation from OPC or pre-myelinating OL (Back et al., 2002a; Stephen A. Back, 2017; Segovia et al., 2008). Back et al reported that a chronic ischemic injury in fetal humans is the leading cause of cerebral myelination disturbance by targeting late OL progenitor cells, which leads to WM injury in humans (Back et al., 2002b). Newly generated pre-OLs are the predominant OL population during late gestation, the timepoint of IUGR induction, and are especially vulnerable to free radicals, while more mature OLs appeared to be more resilient against unfavorable in-utero environment. Our findings follow clinical observation indicating WM injury in IUGR children, which makes the model a reliable tool for studying potential therapies aiming to increase the maturation of the OL lineage.

IUGR induced the prolongation of neurites *in vitro* (Manuscript 4.4 (Kühne et al., to be submitted)), and in accordance more branched dendrites *in vivo* (Manuscript 4.1 (Pla et al., 2020)). Our results revealed that IUGR neurospheres have a significantly higher expression of the adhesion molecule int- $\beta$ 1 than control neurospheres. Int- $\beta$ 1 is involved in neurodevelopmental processes like neurite length and arborization (Belvindrah et al., 2007; Marrs et al., 2006), which might be the underlying mechanism for an increased neurite length. Additionally, we unraveled that IUGR neurospheres react differently than control neurospheres to a compound initiating migration alteration (Manuscript 4.6 (Kühne et al., submitted)). Besides from neuronal development, int- $\beta$ 1 is crucial for NPC migration by its adhesion to the extracellular matrix protein laminin and an interference with the laminin/ int- $\beta$ 1 interaction leads to a disturbed migration pattern (Barenys et al., 2017). Because int- $\beta$ 1 is implied in NPC migration but also in axonal growth and neuronal branching (Belvindrah et al., 2007; Marrs et al., 2006), this discovery can give valuable insights to the characterization of IUGR-induced neurodevelopmental alterations. To prove the hypothesized mode of action in future, experiments should be performed with reduced laminin concentrations to see if the IUGR neurospheres develop neurite length and arborization as well as migration pattern comparable to the control group.

#### 5.4 Potential therapies

In the present study, we have applied the neurosphere model for drug screening of the potential therapies and its safety: DHA, MEL, T3, zinc, SA/LF, and EGCG, EGCG derivatives (G37, G56, M1, and M2) and EGCG PEGylated PLGA nanoparticles (Nano-EGCG) (Manuscript 4.3, 4.4, 4.5, 4.6).

DHA, an omega-3 fatty acid, is maternally released via the uteroplacental circulation, forms an important constituent of brain membrane phospholipids and is crucial for fetal neurodevelopment (Gil-Sánchez et al., 2010; Lauritzen et al., 2016). However, most pregnant women do not regularly integrate an adequate quantity of omega-3 fatty acids in their diet. (Greenberg et al., 2008). Manuscript 4.3 (Kühne et al., 2022) revealed an increase of percentage of OLs after *in vitro* exposure to DHA and after its prenatal administration in rabbits. In a preprint publication by Illa et al. (Manuscript 9.1), DHA significantly improved reduced pre-OL in a histological assessment of rabbit IUGR brains ((Illa et al., n.d.) to be resubmitted). In accordance, maternal DHA supplementation in a rat model prevented neonatal brain injury by reducing oxidative stress and apoptotic neuronal death (Suganuma et al., 2010). Other studies support that DHA enhances the differentiation of OL progenitors into mature OL in demyelinating diseases (Bernardo et al., 2017). MEL, like DHA, could revert the reduced level of OLs *in vitro* and were able to prevent pathological effects secondary to IUGR by administration during rabbit's pregnancy, which was discovered in Manuscript 4.3 (Kühne et al., 2022). MEL is produced in the placenta and ovary, where it works as a free radical scavenger and

potent antioxidant and has an essential function in placental homeostasis and fetal maturation (Reiter et al., 2014b). Studies about pregnancies complicated with placental insufficiency revealed a significantly declined MEL level in maternal blood (Berbets, 2019) and a significantly reduced expression of MEL receptors in the placenta (Berbets et al., 2021b). Until today there was only one pilot clinical trial of oral MEL administration to women with IUGR (Miller et al., 2014). However, in our experiments, neither DHA nor MEL improved IUGR induced alterations in neurite length in the neurosphere culture described in Manuscript 4.4 (Kühne et al., to be submitted). Both compounds did not adversely affect any of the tested endpoints related to neuronal development at the effective concentration for the prevention of OL adverse effects, and therefore, this concentration can be considered as safe for those endpoints after *in vitro* exposure and *in vivo* administration. The results from Manuscript 4.3 (Kühne et al., 2022) together with the evidence from the literature strongly suggest that DHA and MEL are promising antenatal neuroprotective therapies promoting fetal pre-OL differentiation and should be brought into the clinical field to prenatally prevent/revert IUGR-induced white matter damage.

An *in vitro* exposure to T3 significantly increased the percentage of pre-OL in IUGR neurospheres (Manuscript 4.3 (Kühne et al., 2022)), which is in accordance with enhanced OL differentiation and myelination in rodent and human neurospheres after T3 exposure (Dach et al., 2017; Klose et al., 2021a). However, T3 was not prioritized in our study for *in vivo* maternal administration due to possible complications altering the maternal T3 level and thus, due to expected difficulties in the translation to the clinical field (Fumarola et al., 2011; Kilby et al., 2000). Remarkably, zinc did not significantly increase the percentage of OLs in IUGR neurospheres but in control neurospheres. This treatment was discarded for further investigations in the IUGR model, but these results could be useful for other researchers aiming to increase the percentage of OLs in other disease models (Manuscript 4.3 (Kühne et al., 2022)).

LF, an iron-binding glycoprotein with antioxidant and anti-inflammatory properties, is described to support neuronal development, maintain neuronal integrity and increase neuronal density during brain development (Wang, 2016). Hence, we expected an impact of LF on neurogenesis. The lactic compound LF presented solubility problems *in vitro*, but its main metabolite SA significantly reduced the IUGR induced neurite extension and in accordance LF after maternal treatment *in vivo*, whereas LF and SA did not show a protective effect on OL differentiation (Manuscript 4.3 (Kühne et al., 2022), Manuscript 4.4 (Kühne et al., to be submitted)). In another preliminary study, histological brain slices, obtained from rabbit pups prenatally treated with LF, did not show an improvement in pre-OLs, but interestingly, significantly reduced the total dendritic length and number of neuronal intersections

(Manuscript 9.1 (Illa et al., n.d.)). Illa et al., also suggest that LF may improve the observed higher number of dendrites and longer neurite length in IUGR infants (Illa et al., n.d.).

Epigallocatechin gallate (EGCG), the most abundant catechin in green tea, has been proposed as a possible treatment during pregnancy to prevent/ treat alterations of brain development induced by Down's syndrome (Catuara-Solarz et al., 2016; Souchet et al., 2019; Stagni et al., 2021, 2016), or by fetal alcoholic syndrome (Almeida-Toledano et al., 2021; Long et al., 2010; Tiwari et al., 2010), among other diseases. Despite its therapeutic effects, manuscript 4.5 (Kühne et al., 2019) and other studies using the 'Neurosphere Assay' shed light on potential neurodevelopmental toxic effects of EGCG proving adverse effects on NPC migration and unraveling the mechanism behind: the binding of EGCG to the extracellular matrix protein laminin, which prevents the interaction of the int- $\beta$ 1 cell adhesion molecule with laminin (Barenys et al., 2016, 2017; Kühne et al., 2019; Peter et al., 2017; Suzuki and Isemura, 2001). NPC migration is a fundamental KE during cortical brain development, in which migrating radial glial cells form a scaffold used by neurons to migrate to distal regions in cortical layers, and an impairment can significantly disrupt brain structure and function (Borrell and Götz, 2014; Klose et al., 2022). While EGCG exposure affected the phenotype of NPC migration presenting an irregular pattern with gaps and reduced spacing in control neurospheres, strikingly, IUGR neurospheres did not suffer any alteration in their migration distance or pattern after EGCG exposure. Manuscript 4.6 (Kühne et al., submitted) revealed a significant overexpression of int- $\beta$ 1 in IUGR at gene and protein levels, which is strongly suspected to improve migration impairment secondary to EGCG exposure. In addition to the involvement of int- $\beta$ 1 in cell adhesion and migration, int- $\beta$ 1 is also critical for other neurodevelopmental processes such as neurite length and branching (Belvindrah et al., 2007; Marrs et al., 2006). We have observed a reduced neurite length *in vitro* and accordingly a decreased dendrite length in the hippocampus *in vivo* after EGCG exposure (Manuscript 4.6 (Kühne et al., submitted)). LF/SA could revert this effect (Manuscript 4.4 (Kühne et al., to be submitted)), Burgess et al. (2007) discovered in an *in vitro*, that poly-SA limits the neurite elongation of neurons by preventing the interactions between int- $\beta$ 1 and laminin (Burgess et al., 2007), which gives indications about the underlining mode-of-action.

The alteration of the migration pattern of the NPC caused by EGCG prompted us to prioritize EGCG analogues in the search for safer alternatives for possible clinical applications (Manuscript 4.5 (Kühne et al., 2019)). The global assessment of the endpoints: migration distance, migration corona formation, cellular process orientation angles, and migrating neurons showed a consistent array of different potencies of the tested compounds. The study suggests G56, a synthetic compound structurally related to EGCG, and nano capsulated EGCG as prospective therapeutic or preventive alternatives to EGCG due to its lower toxicity potential in NPC migration disturbances. Subsequently, non-toxic

concentrations of G56 and EGCG were applied to IUGR neurospheres to test their potential in improving OL impairment, but neither G56 nor EGCG enhanced the differentiation of OLs (Manuscript 4.6 (Kühne et al., submitted)). Although EGCG could not rescue OL impairment in IUGR neurospheres, a logical consequence of the results would be to test EGCG as a neuroprotective agent against IUGR-induced neurite extension at safe concentrations not decreasing migration ( $\leq 100$  nM) in future experiments. However, since other tested candidates like LF or DHA have a safer profile according to the Neurosphere Assay, EGCG studies would not be prioritized.

## 5.5 Shifting from *in vivo* to *in vitro* in DNT

Standard DNT testing is performed according to *in vivo* US-EPA or OECD TG (EPA, 1998; OECD, 2007) and non-clinical safety studies for the conduct of human clinical trials are conducted according to ICH guideline M3(R2) EMA (2009). These guidelines are based on animal models, being rat the preferred species for prenatal neurodevelopmental toxicity. The testing guidelines are complex and extremely resource intensive in terms of materials, time, cost, and animal use, which results in poor implementation of *in vivo* DNT guidelines and a serious lack of DNT hazard information for chemicals globally (Crofton et al., 2012; Fritsche et al., 2018c; Lein et al., 2005; Leist and Hartung, 2013). A literature review by Grandjean and Landrigan (2006) estimated 202 known human neurotoxicants, of which only 6 are known to be toxic to human neurodevelopment, although these numbers were expanded to 214 and 12 in a subsequent assessment eight years later, it was noted that the discovery of new neurodevelopmental hazards is much slower than for adult neurotoxicants (Grandjean and Landrigan, 2014; P Grandjean, 2006). The comprehensive *in vivo* DNT guidelines combined with the paradigm shift in toxicity (Gibb, 2008) are prompting to move from apical endpoint measurements *in vivo* to the development of new relevant alternative methods not only for hazard and risk assessment but also for drug development initiated by scientists in industry, academia, and regulatory bodies (Bal-Price, 2018; Bal-Price et al., 2015; EFSA, 2013; Fritsche et al., 2018c, 2017, 2015). A key driver in this shift is the effort to embed mechanistic knowledge linking *in vitro* and *in vivo* results in a structured AOP framework initiated by the OECD in 2012 (Sachana and Leinala, 2017).

## 5.6 Integration of results in an AOP framework

A mixture of dynamic *in vitro*, kinetic and epidemiological/clinical studies assembled in an integrated approach (e.g. AOP and IATA) is a key attempt to describe mechanistic pathways and hazards of chemicals (Hartung, 2018). The mechanism of EGCG as a chemical inducing the MIE “disrupted laminin-

β1-integrin interaction” (MIE (Barenys et al., 2017; Lo et al., 2007; Melgarejo et al., 2009; Park et al., 2010)) was integrated in an AOP framework and organized in a putative AOP, facilitating the understanding of the underlining mode of action (Manuscript 4.6 (Kühne et al., submitted)). The here designed AOP extends the putative AOP “disrupted laminin-b1-integrin interaction leading to developmental neurotoxicity”, which was already submitted to the OECD in 2019 (Bal-Price et al., 2017). An AOP concept connects mechanistic information leading to an adverse outcome by integrating various types of information such as *in silico*, *in chemico*, *in vitro* and *in vivo* data for hazard and risk assessment strategies and regulatory purposes (Leist et al., 2017; OECD, 2018b; Sakuratani et al., 2018). AOPs can be used to inform integrated approaches for decision making such as “Integrated Approaches to Testing and Assessment” (IATA) by providing (1) plausible and transparent data and making uncertainties explicit, (2) conceptual framework coordinating information at different levels of biological organization, (3) categorizing key events based on chemical and biological activities, (4) describing data’s weight of evidence by the plausibility of the underlining literature (Sakuratani et al., 2018). Still, using AOPs promoting IATA approaches in DNT remains challenging because most DNT approaches analyzing several KEs but lacking plausible MIE (Bal-Price et al., 2017; Barenys et al., 2020; Chen et al., 2020; Klose et al., 2021a; Li et al., 2019). In this study, the developed AOP includes a clear MIE based on data with high grade of confidence leading to KEs mechanistically linked with quantitative or semi-quantitative data. The interpretation of the relationship between chemical induced MIE/KE resulting in a pathological outcome on organism level represent another challenge. The here described MIE is followed by two arms, one is dealing with migration disturbance and the second with alteration in neuronal development terminating in the AO “decreased cognitive function”. More evidence on the AO “decreased cognitive function” is needed, which is only based on one publication (Warren et al., 2012) discovering learning disabilities *in vivo* after initiating the described MIE. Klose et al discovered another chemical, the Chinese herbal medicine Lei Gong Teng (LGT), which triggers the same MIE as EGCG leading to the same AO due to the KEs “disturbed cortical radial glia alignment and migration” by using human neurospheres (Klose et al., 2022). This putative AOP detects aligned KEs and strengthens the weight of evidence of the here described AOP.

However, a putative AOP alone is not sufficient for regulatory decisions, but crucial to collect data and to order them in a framework outlining uncertainties and to lay the foundation for a quantitative AOP. The framework serves as a communication tool between researcher and regulatory bodies in a clear and transparent way and may inform approaches addressing biomedical challenges, safety assessments for drug development, systemic toxicology and simulation of clinical trials (Ankley et al., 2010; Carusi et al., 2018). The importance of AOPs becomes clear when one considers that they have been evolved in the context of regulatory toxicology, but that the potential stakeholder community has already become broader than chemical risk assessor (reviewed in (Carusi et al., 2018)).



Stakeholders from different groups such as society/NGOs, governmental agencies, academia, and industry are involved in different topic areas of research and development (e.g.: basic research, environmental quality, medicine/ health, pharma/ drug discovery, chemical safety), and those stakeholder can make use of AOPs for the ecosystem's health, drug development, disease diagnosis and prevention, and risk assessment and management (Carusi et al., 2018).

An *in vitro* approach like the neurosphere system seems to reflect sufficiently trigger points (MIEs) and crucial steps in a mechanistic pathway (KEs). On regulatory level, the neurosphere model may inform integrated approaches for hazard-based decisions by extending putative AOP frameworks.

## 5.7 Extrapolation from *in vitro* to *in vivo* in human

By modelling a situation, the plausible concern is the extrapolation to the whole organism *in vivo* predicting how the entire body would react after injury or exposure to a test substance (Bale et al., 2014; Hartung, 2018). Different information resources provide for the extrapolation to the real-life situation in human by crosslinking different models and levels of complexity including *in vitro*, *in vivo*, clinical, and epidemiological studies (Hartung, 2018). A model simplifying a complex situation can naturally not cover the multifaceted reaction of an entire organism, but a sophisticated model does not automatically make a better system, while a simpler model can directly approach critical endpoints (Hartung, 2018). The neurosphere approach, as a control or disease model, allows to test toxico- and pharmacodynamics of compounds by describing its interaction with a target and its biological effects on brain development, in relatively simple, cost- and animal-reduced way (Baumann et al., 2016; Dach et al., 2017; Klose et al., 2021b). However, the species-specific variations should always be considered when testing pharmaceuticals or chemicals. The 'Neurosphere Assay' has been established with several species enabling a comparison of time-matched neurodevelopmental endpoints between rat, mouse, rabbit, and human (Barenys et al., 2021; Baumann et al., 2014; Gassmann et al., 2010; Masjosthusmann et al., 2018b). Species differences can be studied and represented by using a parallelogram approach described in (Baumann et al., 2016), which is used for the extrapolation of exposure concentration from the chosen species to humans. The approach depicts that existing animal *in vivo* data are compared to *in vitro* data from the same species illustrating *in vivo/in vitro* similarities or differences (Baumann et al., 2016). The animal *in vitro* data are compared to human *in vitro* data to detect interspecies differences, allowing the extrapolation to the situation in human (Baumann et al., 2016). Rabbit neurospheres were obtained from pups with or without prenatal exposure through the mother animal, which allows the direct comparison of chemical induced neurodevelopmental outcomes *in vitro* and *in vivo*. Hereafter, rabbit *in vitro* data should ideally be compared to human *in*

*vitro* data to discover interspecies variations, allowing the calculation of a possible effect in human *in vivo* (Baumann et al., 2016). Human NPCs (hNPCs) are commercially available from healthy individuals, but hNPCs from IUGR fetuses are an extremely limited material and therefore not profitable for comprehensive mechanistic examinations or efficacy testing of potential neuroprotective therapies (Barenys et al., 2021). In future, an *in vitro* induced IUGR hNPC system could be considered as a model to further prove the safety of the proposed effective concentration of neuroprotective therapies detected in rabbit neurospheres.

Overall, it is remarkable that the *in vitro* rabbit neurosphere assay established in Manuscript 4.2 (Barenys et al., 2021) predicted regarding the endpoint oligodendrogenesis the *in vivo* outcome of the tested potential neuroprotective candidates, for both, positive and negative effects (analyzed after exposure to LF, DHA, and MEL). The good agreement of the *in vitro* vs. the *in vivo* treatment increases the reliability of the model and reinforces its use for further drug screening.

## 6 Conclusions

Overall conclusion:

A novel *in vitro* rabbit neurosphere model was established, which can mimic basic processes of brain development proliferation, migration, differentiation, synaptogenesis, and network formation. A significantly lower percentage of OL due to a slower differentiation rate was identified in IUGR neurospheres, which fits very well to the clinical outcome of IUGR induced white matter alterations. Moreover, the neurite length was significantly elongated in IUGR neurospheres. The safety and efficacy from a plateau of potential neuroprotective drugs were analyzed, by toxicological and pharmacological assessment using the novel *in vitro* rabbit neurosphere model. This study revealed two major compounds, DHA and MEL, as promising therapies against adverse neurodevelopmental outcomes in oligodendrogenesis of IUGR, and LF against IUGR induced effects on neurons (neurite length extension). We hypothesize that this increased neurite length is due to an increased int- $\beta$ 1 expression in the IUGR culture and LF or SA reduces neurite length due to a possible interaction between int- $\beta$ 1 and laminin. In future studies, it will be also important to measure the impact and safety of the tested therapies not only in neurodevelopment, but also in terms of general developmental parameters.

Specific conclusions:

1. We have established an *in vitro* neurosphere model derived from control and IUGR rabbit pup's whole brain, in which NPCs are able to proliferate, migrate, differentiate into neurons, oligodendrocytes, and astrocytes, and in which neurite length, dendritic branching and network formation including synaptogenesis can be evaluated.
2. We have characterized the following main differences in basic processes of neurogenesis induced by IUGR:
  - *In vitro*, OL differentiation was significantly decreased due to a slower differentiation rate in IUGR neurospheres compared with the control group.
  - *In vivo*, the significantly lower body weight of IUGR pups correlated with the density of OLs in the WM of the corpus callosum.
  - IUGR induced significantly longer neurites compared with control after 5 days *in vitro* and a significantly higher percentage of neurons over time after 14 days.
  - Accordingly, *in vivo* evaluation of the IUGR animals showed a higher number of distal dendrites in the frontal cortex.
  - IUGR NPCs have a significantly higher expression of int- $\beta$ 1 at gene and protein level

- IUGR NPCs respond differently than controls to the exposure of environmental compounds disturbing neurodevelopment.
- 3. We have determined the MTC of DHA at 10  $\mu\text{M}$  and of MEL at 3  $\mu\text{M}$ , whereas SA/LF, zinc, and T3 did not present an adverse effect at any of the tested concentrations. EGCG's MTC was established at 0.1  $\mu\text{M}$ , because 1  $\mu\text{M}$  EGCG presented adverse effects on NPC migration. Different potencies of EGCG and synthetic analogues were observed, revealing G56 and Nano-EGCG as possible safe alternatives to EGCG due to their lower toxicity on NPC migration.

The most Effective Concentration of DHA, MEL and T3 were determined at 1  $\mu\text{M}$  and 0.1 nM. The antenatal DHA and MEL treatment during pregnancy is effective in preventing or reverting poor oligodendrocyte differentiation arising from IUGR.

- 4. The *in vitro* rabbit neurosphere assay predicted in the endpoints cell viability, oligodendrogenesis, % of neurons, total neurite length and dendritic arborization, the outcome after prenatal administration *in vivo* of the tested potential neuroprotective candidates, for both positive and negative effects.
- 5. We have shown for the first time an adverse effect *in vivo* after developmental exposure to EGCG.
- 6. We developed the putative AOP "Disrupted laminin- $\beta$ 1-integrin interaction leading to developmental neurotoxicity", integrating the discovered results about IUGR induced changes in neurodevelopment.

## 7 References

- Abdel-Rahman, A., Anyangwe, N., Carlacci, L., Casper, S., Danam, R.P., Enongene, E., Erives, G., Fabricant, D., Gudi, R., Hilmas, C.J., 2011. The safety and regulation of natural products used as foods and food ingredients. *Toxicol. Sci.* 123, 333–348.
- Adamo, A.M., Oteiza, P.I., 2010. Zinc deficiency and neurodevelopment: The case of neurons. *BioFactors* 36, 117–124. <https://doi.org/https://doi.org/10.1002/biof.91>
- Adcock, K.H., Nedelcu, J., Loenneker, T., Martin, E., Wallimann, T., Wagner, B.P., 2002. Neuroprotection of Creatine Supplementation in Neonatal Rats with Transient Cerebral Hypoxia-Ischemia. *Dev. Neurosci.* 24, 382–388. <https://doi.org/10.1159/000069043>
- Almeida-Toledano, L., Andreu-Fernández, V., Aras-López, R., García-Algar, Ó., Martínez, L., Gómez-Roig, M.D., 2021. Epigallocatechin Gallate Ameliorates the Effects of Prenatal Alcohol Exposure in a Fetal Alcohol Spectrum Disorder-Like Mouse Model. *Int. J. Mol. Sci.* 22, 715. <https://doi.org/10.3390/ijms22020715>
- Als, H., Duffy, F.H., McAnulty, G., Butler, S.C., Lightbody, L., Kosta, S., Weisenfeld, N.I., Robertson, R., Parad, R.B., Ringer, S.A., Blickman, J.G., Zurakowski, D., Warfield, S.K., 2012. NICHD improves brain function and structure in preterm infants with severe intrauterine growth restriction. *J. Perinatol.* 32, 797–803. <https://doi.org/10.1038/jp.2011.201>
- Andersen, Susan L., 2003. Trajectories of brain development: point of vulnerability or window of opportunity? *Neurosci. Biobehav. Rev.* 27, 3–18. [https://doi.org/10.1016/S0149-7634\(03\)00005-8](https://doi.org/10.1016/S0149-7634(03)00005-8)
- Andersen, Susan L., 2003. Trajectories of brain development: point of vulnerability or window of opportunity? *Neurosci. Biobehav. Rev.* 27, 3–18. [https://doi.org/10.1016/S0149-7634\(03\)00005-8](https://doi.org/10.1016/S0149-7634(03)00005-8)
- Ankley, G.T., Bennett, R.S., Erickson, R.J., Hoff, D.J., Hornung, M.W., Johnson, R.D., Mount, D.R., Nichols, J.W., Russom, C.L., Schmieder, P.K., Serrano, J.A., Tietge, J.E., Villeneuve, D.L., 2010. Adverse outcome pathways: a conceptual framework to support ecotoxicology research and risk assessment. *Environ. Toxicol. Chem.* 29, 730–741. <https://doi.org/10.1002/etc.34>
- Aschner, M., Ceccatelli, S., Daneshian, M., Fritsche, E., Hasiwa, N., Hartung, T., Hogberg, H.T., Leist, M., Li, A., Mundi, W.R., Padilla, S., Piersma, A.H., Bal-Price, A., Seiler, A., Westerink, R.H., Zimmer, B., Lein, P.J., 2017. Reference compounds for alternative test methods to indicate developmental neurotoxicity (DNT) potential of chemicals: example lists and criteria for their selection and use. *ALTEX* 34, 49–74. <https://doi.org/10.14573/altex.1604201>
- Aykul, S., Martinez-Hackert, E., 2016. Determination of half-maximal inhibitory concentration using biosensor-based protein interaction analysis. *Anal. Biochem.* 508, 97–103. <https://doi.org/10.1016/j.ab.2016.06.025>
- Back, Stephen A, 2017. White Matter Injury in the Preterm Infant: Pathology and Mechanisms HHS Public Access Author manuscript, *Acta Neuropathol.* <https://doi.org/10.1007/s00401-017-1718-6.White>

- Back, Stephen A., 2017. White matter injury in the preterm infant: pathology and mechanisms. *Acta Neuropathol.* 134, 331–349. <https://doi.org/10.1007/s00401-017-1718-6>
- Back, S.A., 2001. Late oligodendrocyte progenitors coincide with the developmental window of vulnerability for human perinatal white matter injury. *J. Neurosci.* 21, 1302–1312.
- Back, S.A., Han, B.H., Luo, N.L., Chricton, C.A., Xanthoudakis, S., Tam, J., Arvin, K.L., Holtzman, D.M., 2002a. Selective vulnerability of late oligodendrocyte progenitors to hypoxia-ischemia. *J. Neurosci.* 22, 455–463. <https://doi.org/10.1523/jneurosci.22-02-00455.2002>
- Back, S.A., Luo, N.L., Borenstein, N.S., Volpe, J.J., Kinney, H.C., 2002b. Arrested oligodendrocyte lineage progression during human cerebral white matter development: Dissociation between the timing of progenitor differentiation and myelinogenesis. *J. Neuropathol. Exp. Neurol.* 61, 197–211. <https://doi.org/10.1093/jnen/61.2.197>
- Baird, T.J., Caruso, M.J., Gauvin, D. V., Dalton, J.A., 2019. NOEL and NOAEL: A retrospective analysis of mention in a sample of recently conducted safety pharmacology studies. *J. Pharmacol. Toxicol. Methods* 99, 106597. <https://doi.org/10.1016/j.vascn.2019.106597>
- Bal-Price, A., 2018. Recommendation on Test Readiness Criteria for New Approach Methods in Toxicology: Exemplified for Developmental Neurotoxicity. *ALTEX* 35. <https://doi.org/10.14573/altex.1712081>
- Bal-Price, A., Crofton, K.M., Leist, M., Allen, S., Arand, M., Buetler, T., Delrue, N., FitzGerald, R.E., Hartung, T., Heinonen, T., Hogberg, H., Bennekou, S.H., Lichtensteiger, W., Oggier, D., Paparella, M., Axelstad, M., Piersma, A., Rached, E., Schilter, B., Schmuck, G., Stoppini, L., Tongiorgi, E., Tiramani, M., Monnet-Tschudi, F., Wilks, M.F., Ylikomi, T., Fritsche, E., 2015. International STakeholder NETwork (ISTNET): creating a developmental neurotoxicity (DNT) testing road map for regulatory purposes. *Arch. Toxicol.* 89, 269–287. <https://doi.org/10.1007/s00204-015-1464-2>
- Bal-Price, A., Lein, P.J., Keil, K.P., Sethi, S., Shafer, T., Barenys, M., Fritsche, E., Sachana, M., Meek, M.E. (Bette., 2017. Developing and applying the adverse outcome pathway concept for understanding and predicting neurotoxicity. *Neurotoxicology* 59, 240–255. <https://doi.org/10.1016/j.neuro.2016.05.010>
- Bal-Price, A., Meek, M.E. (Bette., 2017. Adverse outcome pathways: Application to enhance mechanistic understanding of neurotoxicity. *Pharmacol. Ther.* 179, 84–95. <https://doi.org/10.1016/j.pharmthera.2017.05.006>
- Bale, A.S., Kenyon, E., Flynn, T.J., Lipscomb, J.C., Mendrick, D.L., Hartung, T., Patton, G.W., 2014. Symposium report: Correlating in vitro data to in vivo findings for risk assessment. *ALTEX* 31, 79–90. <https://doi.org/10.14573/altex.1310011>
- Barateiro, A., Fernandes, A., 2014. Temporal oligodendrocyte lineage progression: In vitro models of proliferation, differentiation and myelination. *Biochim. Biophys. Acta - Mol. Cell Res.* 1843, 1917–1929. <https://doi.org/10.1016/j.bbamcr.2014.04.018>
- Barenys, M., Gassmann, K., Baksmeier, C., Heinz, S., Reverte, I., Schmuck, M., Temme, T., Bendt, F., Zschauer, T.C., Rockel, T.D., Unfried, K., Wätjen, W., Sundaram, S.M., Heuer, H., Colomina, M.T., Fritsche, E., 2017. Epigallocatechin gallate (EGCG) inhibits adhesion and migration of neural progenitor cells in vitro. *Arch. Toxicol.* <https://doi.org/10.1007/s00204-016-1709-8>

- Barenys, M., Illa, M., Hofrichter, M., Loreiro, C., Pla, L., Klose, J., Kühne, B.A., Gómez-Catalán, J., Braun, J.M., Crispi, F., Gratacós, E., Fritsche, E., 2021. Rabbit neurospheres as a novel in vitro tool for studying neurodevelopmental effects induced by intrauterine growth restriction. *Stem Cells Transl. Med.* 10, 209–221. <https://doi.org/10.1002/sctm.20-0223>
- Barenys, M., Masjosthusmann, S., Fritsche, E., 2016. Is Intake of Flavonoid-Based Food Supplements During Pregnancy Safe for the Developing Child? A Literature Review. *Curr. Drug Targets.* <https://doi.org/10.2174/1389450116666150804110049>
- Barenys, M., Reverte, I., Masjosthusmann, S., Gómez-Catalán, J., Fritsche, E., 2020. Developmental neurotoxicity of MDMA. A systematic literature review summarized in a putative adverse outcome pathway. *Neurotoxicology* 78, 209–241. <https://doi.org/10.1016/j.neuro.2019.12.007>
- Baschat, A.A., 2014. Neurodevelopment after fetal growth restriction. *Fetal Diagn. Ther.* 36, 136–142. <https://doi.org/10.1159/000353631>
- Bassan, H., Leider Trejo, L., Kariv, N., Bassan, M., Berger, E., Fattal, A., Gozes, I., Harel, S., 2000. Experimental intrauterine growth retardation alters renal development. *Pediatr. Nephrol.* 15, 192–195. <https://doi.org/10.1007/s004670000457>
- Batalle, D., Eixarch, E., Figueras, F., Muñoz-Moreno, E., Bargallo, N., Illa, M., Acosta-Rojas, R., Amat-Roldan, I., Gratacos, E., 2012. Altered small-world topology of structural brain networks in infants with intrauterine growth restriction and its association with later neurodevelopmental outcome. *Neuroimage* 60, 1352–1366. <https://doi.org/10.1016/j.neuroimage.2012.01.059>
- Batalle, D., Muñoz-Moreno, E., Arbat-Plana, A., Illa, M., Figueras, F., Eixarch, E., Gratacos, E., 2014. Long-term reorganization of structural brain networks in a rabbit model of intrauterine growth restriction. *Neuroimage* 100, 24–38. <https://doi.org/10.1016/j.neuroimage.2014.05.065>
- Baud, O., Berkane, N., 2019. Hormonal changes associated with intra-uterine growth restriction: Impact on the developing brain and future neurodevelopment. *Front. Endocrinol. (Lausanne)*. 10, 1–9. <https://doi.org/10.3389/fendo.2019.00179>
- Baud, O., Daire, J.-L., Dalmaz, Y., Fontaine, R.H., Krueger, R.C., Sebag, G., Evrard, P., Gressens, P., Verney, C., 2004. Gestational Hypoxia Induces White Matter Damage in Neonatal Rats: A New Model of Periventricular Leukomalacia. *Brain Pathol.* 14, 1–10. <https://doi.org/10.1111/j.1750-3639.2004.tb00492.x>
- Baumann, J., Barenys, M., Gassmann, K., Fritsche, E., 2014. Comparative Human and Rat “Neurosphere Assay” for Developmental Neurotoxicity Testing. *Curr. Protoc. Toxicol.* 59, 1–24. <https://doi.org/10.1002/0471140856.tx1221s59>
- Baumann, J., Gassmann, K., Masjosthusmann, S., DeBoer, D., Bendt, F., Giersiefer, S., Fritsche, E., 2016. Comparative human and rat neurospheres reveal species differences in chemical effects on neurodevelopmental key events. *Arch. Toxicol.* 90, 1415–1427. <https://doi.org/10.1007/s00204-015-1568-8>
- Baumann, N., Pham-Dinh, D., 2001. Biology of oligodendrocyte and myelin in the mammalian central nervous system. *Physiol. Rev.* 81, 871–927.

- Belvindrah, R., Graus-Porta, D., Goebbels, S., Nave, K.-A., Müller, U., 2007.  $\beta$ 1 Integrins in Radial Glia But Not in Migrating Neurons Are Essential for the Formation of Cell Layers in the Cerebral Cortex. *J. Neurosci.* 27, 13854–13865. <https://doi.org/10.1523/JNEUROSCI.4494-07.2007>
- Berbets, A., 2019. Melatonin, placental growth factor and placental hormones at placental insufficiency. *Cell Organ Transplantology* 7, 103–107. <https://doi.org/10.22494/cot.v7i2.98>
- Berbets, A.M., Davydenko, I.S., Barbe, A.M., Konkov, D.H., Albota, O.M., Yuzko, O.M., 2021a. Melatonin 1A and 1B Receptors' Expression Decreases in the Placenta of Women with Fetal Growth Restriction. *Reprod. Sci.* 28, 197–206. <https://doi.org/10.1007/s43032-020-00285-5>
- Berbets, A.M., Davydenko, I.S., Barbe, A.M., Konkov, D.H., Albota, O.M., Yuzko, O.M., 2021b. Melatonin 1A and 1B Receptors' Expression Decreases in the Placenta of Women with Fetal Growth Restriction. *Reprod. Sci.* 28, 197–206. <https://doi.org/10.1007/s43032-020-00285-5>
- Bergles, D.E., Richardson, W.D., 2016. Oligodendrocyte development and plasticity. *Cold Spring Harb. Perspect. Biol.* 8, 1–27. <https://doi.org/10.1101/cshperspect.a020453>
- Bernal, J., 2016. Thyroid hormone regulated genes in cerebral cortex development. *J. Endocrinol.* 232, R83–R97. <https://doi.org/10.1530/JOE-16-0424>
- Bernal, J., 2005. The Significance of Thyroid Hormone Transporters in the Brain. *Endocrinology* 146, 1698–1700. <https://doi.org/10.1210/en.2005-0134>
- Bernal, J., 2002. Action of thyroid hormone in brain. *J. Endocrinol. Invest.* 25, 268–288. <https://doi.org/10.1007/BF03344003>
- Bernardo, A., Giammarco, M.L., De Nuccio, C., Ajmone-Cat, M.A., Visentin, S., De Simone, R., Minghetti, L., 2017. Docosahexaenoic acid promotes oligodendrocyte differentiation via PPAR- $\gamma$  signalling and prevents tumor necrosis factor- $\alpha$ -dependent maturational arrest. *Biochim. Biophys. Acta - Mol. Cell Biol. Lipids* 1862, 1013–1023. <https://doi.org/10.1016/j.bbalip.2017.06.014>
- Bernstein, I.M., Horbar, J.D., Badger, G.J., Ohlsson, A., Golan, A., 2000. Morbidity and mortality among very-low-birth-weight neonates with intrauterine growth restriction. *Am. J. Obstet. Gynecol.* 182, 198–206. [https://doi.org/10.1016/S0002-9378\(00\)70513-8](https://doi.org/10.1016/S0002-9378(00)70513-8)
- Billon, N., Jolicoeur, C., Tokumoto, Y., Vennström, B., Raff, M., 2002. Normal timing of oligodendrocyte development depends on thyroid hormone receptor alpha 1 (TR $\alpha$ 1). *EMBO J.* 21, 6452–6460. <https://doi.org/10.1093/emboj/cdf662>
- Billon, N., Tokumoto, Y., Forrest, D., Raff, M., 2001. Role of thyroid hormone receptors in timing oligodendrocyte differentiation. *Dev. Biol.* 235, 110–120. <https://doi.org/10.1006/dbio.2001.0293>
- Blair, E.M., Nelson, K.B., 2015. Fetal growth restriction and risk of cerebral palsy in singletons born after at least 35 weeks' gestation. *Am. J. Obstet. Gynecol.* 212, 520.e1–7. <https://doi.org/10.1016/j.ajog.2014.10.1103>
- Borrell, V., Götz, M., 2014. Role of radial glial cells in cerebral cortex folding. *Curr. Opin.*



Neurobiol. 27, 39–46. <https://doi.org/10.1016/j.conb.2014.02.007>

Breier, J.M., Gassmann, K., Kayser, R., Stegeman, H., De Groot, D., Fritsche, E., Shafer, T.J., 2010. Neural progenitor cells as models for high-throughput screens of developmental neurotoxicity: State of the science. *Neurotoxicol. Teratol.* 32, 4–15. <https://doi.org/10.1016/j.ntt.2009.06.005>

Burgess, A., Weng, Y.Q., Ypsilanti, A.R., Cui, X., Caines, G., Aubert, I., 2007. Polysialic acid limits septal neurite outgrowth on laminin. *Brain Res.* 1144, 52–58. <https://doi.org/10.1016/j.brainres.2007.01.072>

Buser, J.R., Segovia, K.N., Dean, J.M., Nelson, K., Beardsley, D., Gong, X., Luo, N.L., Ren, J., Wan, Y., Riddle, A., McClure, M.M., Ji, X., Derrick, M., Hohimer, A.R., Back, S.A., Tan, S., 2010. Timing of appearance of late oligodendrocyte progenitors coincides with enhanced susceptibility of preterm rabbit cerebral white matter to hypoxia-ischemia. *J. Cereb. Blood Flow Metab.* 30, 1053–1065. <https://doi.org/10.1038/jcbfm.2009.286>

Calafat, A.M., Needham, L.L., Silva, M.J., Lambert, G., 2004. Exposure to Di-(2-Ethylhexyl) Phthalate Among Premature Neonates in a Neonatal Intensive Care Unit. *Pediatrics* 113, e429–e434. <https://doi.org/10.1542/peds.113.5.e429>

Cano, A., Ettcheto, M., Chang, J.H., Barroso, E., Espina, M., Kühne, B.A., Barenys, M., Auladell, C., Folch, J., Souto, E.B., Camins, A., Turowski, P., García, M.L., 2019. Dual-drug loaded nanoparticles of Epigallocatechin-3-gallate (EGCG)/Ascorbic acid enhance therapeutic efficacy of EGCG in a APP<sup>swe</sup>/PS1<sup>dE9</sup> Alzheimer's disease mice model. *J. Control. Release* 301, 62–75. <https://doi.org/10.1016/j.jconrel.2019.03.010>

Cano, A., Ettcheto, M., Espina, M., Auladell, C., Calpena, A.C., Folch, J., Barenys, M., Sánchez-López, E., Camins, A., García, M.L., 2018. Epigallocatechin-3-gallate loaded PEGylated-PLGA nanoparticles: A new anti-seizure strategy for temporal lobe epilepsy. *Nanomedicine Nanotechnology, Biol. Med.* 14, 1073–1085. <https://doi.org/10.1016/j.nano.2018.01.019>

Cano, A., Ettcheto, M., Espina, M., Auladell, C., Folch, J., Kühne, B.A., Barenys, M., Sánchez-López, E., Souto, E.B., García, M.L., Turowski, P., Camins, A., 2021. Epigallocatechin-3-gallate PEGylated poly(lactic-co-glycolic) acid nanoparticles mitigate striatal pathology and motor deficits in 3-nitropropionic acid intoxicated mice. *Nanomedicine (Lond)*. 16, 19–35. <https://doi.org/10.2217/nnm-2020-0239>

Carter, A.M., 2007. Animal Models of Human Placentation - A Review. *Placenta* 28, S41–S47. <https://doi.org/10.1016/j.placenta.2006.11.002>

Carusi, A., Davies, M.R., De Grandis, G., Escher, B.I., Hodges, G., Leung, K.M.Y., Whelan, M., Willett, C., Ankley, G.T., 2018. Harvesting the promise of AOPs: An assessment and recommendations. *Sci. Total Environ.* 628–629, 1542–1556. <https://doi.org/10.1016/j.scitotenv.2018.02.015>

Castillo-Melendez, M., Yawno, T., Sutherland, A., Jenkin, G., Wallace, E.M., Miller, S.L., 2017. Effects of Antenatal Melatonin Treatment on the Cerebral Vasculature in an Ovine Model of Fetal Growth Restriction. *Dev. Neurosci.* 39, 323–337. <https://doi.org/10.1159/000471797>

Catuara-Solarz, S., Espinosa-Carrasco, J., Erb, I., Langohr, K., Gonzalez, J.R., Notredame, C.,

- Dierssen, M., 2016. Combined Treatment With Environmental Enrichment and (-)-Epigallocatechin-3-Gallate Ameliorates Learning Deficits and Hippocampal Alterations in a Mouse Model of Down Syndrome. *eNeuro* 3. <https://doi.org/10.1523/ENEURO.0103-16.2016>
- Chapman, K.L., Holzgrefe, H., Black, L.E., Brown, M., Chellman, G., Copeman, C., Couch, J., Creton, S., Gehen, S., Hoberman, A., Kinter, L.B., Madden, S., Mattis, C., Stemple, H.A., Wilson, S., 2013. Pharmaceutical toxicology: Designing studies to reduce animal use, while maximizing human translation. *Regul. Toxicol. Pharmacol.* 66, 88–103. <https://doi.org/10.1016/j.yrtph.2013.03.001>
- Chen, H., Chidboy, M.A., Robinson, J.F., 2020. Retinoids and developmental neurotoxicity: Utilizing toxicogenomics to enhance adverse outcome pathways and testing strategies. *Reprod. Toxicol.* 96, 102–113. <https://doi.org/10.1016/j.reprotox.2020.06.007>
- Chini, M., Hanganu-Opatz, I.L., 2021. Prefrontal Cortex Development in Health and Disease: Lessons from Rodents and Humans. *Trends Neurosci.* 44, 227–240. <https://doi.org/10.1016/j.tins.2020.10.017>
- Crispi, F., Bijnens, B., Figueras, F., Bartrons, J., Eixarch, E., Le Noble, F., Ahmed, A., Gratacós, E., 2010. Fetal growth restriction results in remodeled and less efficient hearts in children. *Circulation* 121, 2427–2436. <https://doi.org/10.1161/CIRCULATIONAHA.110.937995>
- Crofton, K.M., Mundy, W.R., 2021. External Scientific Report on the Interpretation of Data from the Developmental Neurotoxicity In Vitro Testing Assays for Use in Integrated Approaches for Testing and Assessment. *EFSA Support. Publ.* 18. <https://doi.org/10.2903/sp.efsa.2021.en-6924>
- Crofton, K.M., Mundy, W.R., Lein, P.J., Bal-Price, A., Coecke, S., Seiler, A.E.M., Knaut, H., Buzanska, L., Goldberg, A., 2011. Developmental neurotoxicity testing: recommendations for developing alternative methods for the screening and prioritization of chemicals. *ALTEX* 28, 9–15. <https://doi.org/10.14573/altex.2011.1.009>
- Crofton, K.M., Mundy, W.R., Shafer, T.J., 2012. Developmental neurotoxicity testing: A path forward. *Congenit. Anom. (Kyoto)*. 52, 140–146. <https://doi.org/10.1111/j.1741-4520.2012.00377.x>
- Crovetto, F., Crispi, F., Scazzocchio, E., Mercade, I., Meler, E., Figueras, F., Gratacos, E., 2014. First-trimester screening for early and late small-for-gestational-age neonates using maternal serum biochemistry, blood pressure and uterine artery Doppler. *Ultrasound Obstet. Gynecol.* 43, 34–40. <https://doi.org/10.1002/uog.12537>
- Crupi, R., Marino, A., Cuzzocrea, S., 2013. n-3 Fatty Acids: Role in Neurogenesis and Neuroplasticity. *Curr. Med. Chem.* 20, 2953.
- Cruz-Lemini, M., Crispi, F., Van Mieghem, T., Pedraza, D., Cruz-Martínez, R., Acosta-Rojas, R., Figueras, F., Parra-Cordero, M., Deprest, J., Gratacós, E., 2012. Risk of perinatal death in early-onset intrauterine growth restriction according to gestational age and cardiovascular doppler indices: A multicenter study. *Fetal Diagn. Ther.* 32, 116–122. <https://doi.org/10.1159/000333001>
- Cruz-Martinez, R., Figueras, F., Hernandez-Andrade, E., Oros, D., Gratacos, E., 2011. Changes in myocardial performance index and aortic isthmus and ductus venosus Doppler in term,

- small-for-gestational age fetuses with normal umbilical artery pulsatility index. *Ultrasound Obstet. Gynecol.* 38, 400–405. <https://doi.org/10.1002/uog.8976>
- da Silva Siqueira, L., Majolo, F., da Silva, A.P.B., da Costa, J.C., Marinowic, D.R., 2021. Neurospheres: a potential in vitro model for the study of central nervous system disorders. *Mol. Biol. Rep.* 48, 3649–3663. <https://doi.org/10.1007/s11033-021-06301-4>
- Dach, K., 2015. Mechanistic studies on the developmental neurotoxicity of polybrominated diphenyl ethers ( PBDEs ) in human and murine 3D in vitro models.
- Dach, K., Bendt, F., Huebenthal, U., Giersiefer, S., Lein, P.J., Heuer, H., Fritsche, E., 2017. BDE-99 impairs differentiation of human and mouse NPCs into the oligodendroglial lineage by species-specific modes of action. *Sci. Rep.* 7, 1–11. <https://doi.org/10.1038/srep44861>
- De Souza, A.S., Fernandes, F.S., Tavares Do Carmo, M. das G., 2011. Effects of maternal malnutrition and postnatal nutritional rehabilitation on brain fatty acids, learning, and memory. *Nutr. Rev.* 69, 132–144. <https://doi.org/10.1111/j.1753-4887.2011.00374.x>
- Delcour, M., Olivier, P., Chambon, C., Pansiot, J., Russier, M., Liberge, M., Xin, D., Gestreau, C., Alescio-Lautier, B., Gressens, P., Verney, C., Barbe, M.F., Baud, O., Coq, J.O., 2012. Neuroanatomical, sensorimotor and cognitive deficits in adult rats with white matter injury following prenatal ischemia. *Brain Pathol.* 22, 1–16. <https://doi.org/10.1111/j.1750-3639.2011.00504.x>
- Derrick, M., Luo, N.L., Bregman, J.C., Jilling, T., Ji, X., Fisher, K., Gladson, C.L., Beardsley, D.J., Murdoch, G., Back, S.A., Tan, S., 2004. Preterm Fetal Hypoxia-Ischemia Causes Hypertonia and Motor Deficits in the Neonatal Rabbit: A Model for Human Cerebral Palsy? *J. Neurosci.* 24, 24–34. <https://doi.org/10.1523/JNEUROSCI.2816-03.2004>
- Dieni, S., Rees, S., 2003. Dendritic morphology is altered in hippocampal neurons following prenatal compromise. *J. Neurobiol.* 55, 41–52. <https://doi.org/10.1002/neu.10194>
- Dorato, M.A., Engelhardt, J.A., 2005. The no-observed-adverse-effect-level in drug safety evaluations: Use, issues, and definition(s). *Regul. Toxicol. Pharmacol.* 42, 265–274. <https://doi.org/10.1016/j.yrtph.2005.05.004>
- Drobyshevsky, A., Jiang, R., Derrick, M., Luo, K., Tan, S., 2014. Functional correlates of central white matter maturation in perinatal period in rabbits. *Exp. Neurol.* 261, 76–86. <https://doi.org/10.1016/j.expneurol.2014.06.021>
- EFSA, 2013. Scientific Opinion on the developmental neurotoxicity potential of acetamiprid and imidacloprid. *EFSA J.* 11, 47. <https://doi.org/10.2903/j.efsa.2013.3471>
- Egaña-Ugrinovic, G., Sanz-Cortes, M., Figueras, F., Bargalló, N., Gratacós, E., 2013. Differences in cortical development assessed by fetal MRI in late-onset intrauterine growth restriction. *Am. J. Obstet. Gynecol.* 209, 126.e1-126.e8. <https://doi.org/10.1016/j.ajog.2013.04.008>
- Eixarch, E., Batalle, D., Illa, M., Muñoz-Moreno, E., Arbat-Plana, A., Amat-Roldan, I., Figueras, F., Gratacos, E., 2012a. Neonatal neurobehavior and diffusion MRI changes in brain reorganization due to intrauterine growth restriction in a rabbit model. *PLoS One* 7, e31497. <https://doi.org/10.1371/journal.pone.0031497>
- Eixarch, E., Batalle, D., Illa, M., Muñoz-Moreno, E., Arbat-Plana, A., Amat-Roldan, I., Figueras,

- F., Gratacos, E., 2012b. Neonatal neurobehavior and diffusion MRI changes in brain reorganization due to intrauterine growth restriction in a rabbit model. *PLoS One* 7. <https://doi.org/10.1371/journal.pone.0031497>
- Eixarch, E., Figueras, F., Hernández-Andrade, E., Crispi, F., Nadal, A., Torre, I., Oliveira, S., Gratacós, E., 2009. An experimental model of fetal growth restriction based on selective ligation of uteroplacental vessels in the pregnant rabbit. *Fetal Diagn. Ther.* 26, 203–211. <https://doi.org/10.1159/000264063>
- Eixarch, E., Hernandez-Andrade, E., Crispi, F., Illa, M., Torre, I., Figueras, F., Gratacos, E., 2011. Impact on fetal mortality and cardiovascular Doppler of selective ligation of uteroplacental vessels compared with undernutrition in a rabbit model of intrauterine growth restriction. *Placenta* 32, 304–309. <https://doi.org/10.1016/j.placenta.2011.01.014>
- Eixarch, E., Meler, E., Iraola, A., Illa, M., Crispi, F., Hernandez-Andrade, E., Gratacos, E., Figueras, F., 2008. Neurodevelopmental outcome in 2-year-old infants who were small-for-gestational age term fetuses with cerebral blood flow redistribution. *Ultrasound Obstet. Gynecol.* 32, 894–899. <https://doi.org/10.1002/uog.6249>
- Eixarch, E., Muñoz-Moreno, E., Bargallo, N., Batalle, D., Gratacos, E., 2016. Motor and corticostriatal-thalamic connectivity alterations in intrauterine growth restriction. *Am. J. Obstet. Gynecol.* 214, 725.e1-725.e9. <https://doi.org/10.1016/j.ajog.2015.12.028>
- Ejaredar, M., Nyanza, E.C., Ten Eycke, K., Dewey, D., 2015. Phthalate exposure and childrens neurodevelopment: A systematic review. *Environ. Res.* 142, 51–60. <https://doi.org/10.1016/j.envres.2015.06.014>
- Ekor, M., 2014. The growing use of herbal medicines: issues relating to adverse reactions and challenges in monitoring safety. *Front. Pharmacol.* 4. <https://doi.org/10.3389/fphar.2013.00177>
- Elitt, C.M., Fahrni, C.J., Rosenberg, P.A., 2019. Zinc homeostasis and zinc signaling in white matter development and injury. *Neurosci. Lett.* 707, 134247. <https://doi.org/10.1016/j.neulet.2019.05.001>
- EPA, 1998. Health Effects Test Guidelines OPPTS 870.6300 Developmental Neurotoxicity Study Public Draft 14.
- Fernández, M., Paradisi, M., Del Vecchio, G., Giardino, L., Calzà, L., 2009. Thyroid hormone induces glial lineage of primary neurospheres derived from non-pathological and pathological rat brain: implications for remyelination-enhancing therapies. *Int. J. Dev. Neurosci.* 27, 769–778. <https://doi.org/10.1016/j.ijdevneu.2009.08.011>
- Fernández, V., Llinares-Benadero, C., Borrell, V., 2016. Cerebral cortex expansion and folding: what have we learned? *EMBO J.* 35, 1021–1044. <https://doi.org/10.15252/embj.201593701>
- Ferrazzi, E., Bozzo, M., Rigano, S., Bellotti, M., Morabito, A., Pardi, G., Battaglia, F.C., Galan, H.L., 2002. Temporal sequence of abnormal Doppler changes in the peripheral and central circulatory systems of the severely growth-restricted fetus. *Ultrasound Obstet. Gynecol.* 19, 140–146. <https://doi.org/10.1046/j.0960-7692.2002.00627.x>

- Figueras, F., Caradeux, J., Crispi, F., Eixarch, E., Peguero, A., Gratacos, E., 2018. Diagnosis and surveillance of late-onset fetal growth restriction. *Am. J. Obstet. Gynecol.* 218, S790-S802.e1. <https://doi.org/10.1016/j.ajog.2017.12.003>
- Figueras, F., Gardosi, J., 2011. Intrauterine growth restriction: New concepts in antenatal surveillance, diagnosis, and management. *Am. J. Obstet. Gynecol.* 204, 288–300. <https://doi.org/10.1016/j.ajog.2010.08.055>
- Figueras, F., Gratacos, E., 2017. An integrated approach to fetal growth restriction. *Best Pract. Res. Clin. Obstet. Gynaecol.* 38, 48–58. <https://doi.org/10.1016/j.bpobgyn.2016.10.006>
- Figueras, F., Gratacós, E., 2014. Update on the diagnosis and classification of fetal growth restriction and proposal of a stage-based management protocol. *Fetal Diagn. Ther.* 36, 86–98. <https://doi.org/10.1159/000357592>
- Figueras, F., Oros, D., Cruz-Martinez, R., Padilla, N., Hernandez-Andrade, E., Botet, F., Costas-Moragas, C., Gratacos, E., 2009. Neurobehavior in term, small-for-gestational age infants with normal placental function. *Pediatrics* 124. <https://doi.org/10.1542/peds.2008-3346>
- Firestone, M., Kavlock, R., Zenick, H., Kramer, M., 2010. The U.S. environmental protection agency strategic plan for evaluating the toxicity of chemicals. *J. Toxicol. Environ. Heal. - Part B Crit. Rev.* 13, 139–162. <https://doi.org/10.1080/10937404.2010.483178>
- Fischi-Gómez, E., Vasung, L., Meskaldji, D.-E., Lazeyras, F., Borradori-Tolsa, C., Hagmann, P., Barisnikov, K., Thiran, J.-P., Hüppi, P.S., 2015. Structural Brain Connectivity in School-Age Preterm Infants Provides Evidence for Impaired Networks Relevant for Higher Order Cognitive Skills and Social Cognition. *Cereb. Cortex* 25, 2793–2805. <https://doi.org/10.1093/cercor/bhu073>
- Fleiss, B., Murray, D.M., Bjorkman, S.T., Wixey, J.A., 2021. Editorial: Pathomechanisms and Treatments to Protect the Preterm, Fetal Growth Restricted and Neonatal Encephalopathic Brain. *Front. Neurol.* 12. <https://doi.org/10.3389/fneur.2021.755617>
- Fleiss, B., Wong, F., Brownfoot, F., Shearer, I.K., Baud, O., Walker, D.W., Gressens, P., Tolcos, M., 2019. Knowledge gaps and emerging research areas in intrauterine growth restriction-associated brain injury. *Front. Endocrinol. (Lausanne)*. 10, 1–24. <https://doi.org/10.3389/fendo.2019.00188>
- Fouron, J., Gosselin, J., Amiel-tison, C., Infante-rivard, C., 2001. Correlation between prenatal velocity waveforms in the aortic isthmus and neurodevelopmental outcome between the ages of 2 and 4 years 630–636. <https://doi.org/10.1067/mob.2001.110696>
- Fritsche, E., Alm, H., Baumann, J., Geerts, L., Håkansson, H., Masjosthusmann, S., Witters, H., 2015. Literature review on in vitro and alternative Developmental Neurotoxicity (DNT) testing methods. *EFSA Support. Publ.* 12. <https://doi.org/10.2903/sp.efsa.2015.EN-778>
- Fritsche, E., Barenys, M., Klose, J., Masjosthusmann, S., Nimtz, L., Schmuck, M., Wuttke, S., Tigges, J., 2018a. Development of the Concept for Stem Cell-Based Developmental Neurotoxicity Evaluation. *Toxicol. Sci.* 165, 14–20. <https://doi.org/10.1093/toxsci/kfy175>
- Fritsche, E., Barenys, M., Klose, J., Masjosthusmann, S., Nimtz, L., Schmuck, M., Wuttke, S., Tigges, J., 2018b. Current availability of stem cell-Based in vitro methods for developmental neurotoxicity (DNT) testing. *Toxicol. Sci.* 165, 21–30.

<https://doi.org/10.1093/toxsci/kfy178>

- Fritsche, E., Crofton, K.M., Hernandez, A.F., Hougaard Bennekou, S., Leist, M., Bal-Price, A., Reaves, E., Wilks, M.F., Terron, A., Solecki, R., Sachana, M., Gourmelon, A., 2017. OECD/EFSA workshop on developmental neurotoxicity (DNT): The use of non-animal test methods for regulatory purposes. *ALTEX* 34, 311–315. <https://doi.org/10.14573/altex.1701171>
- Fritsche, E., Grandjean, P., Crofton, K.M., Aschner, M., Goldberg, A., Heinonen, T., Hessel, E.V.S., Hogberg, H.T., Bennekou, S.H., Lein, P.J., Leist, M., Mundy, W.R., Paparella, M., Piersma, A.H., Sachana, M., Schmuck, G., Solecki, R., Terron, A., Monnet-Tschudi, F., Wilks, M.F., Witters, H., Zurich, M.G., Bal-Price, A., 2018c. Consensus statement on the need for innovation, transition and implementation of developmental neurotoxicity (DNT) testing for regulatory purposes. *Toxicol. Appl. Pharmacol.* 354, 3–6. <https://doi.org/10.1016/j.taap.2018.02.004>
- Fumarola, A., Di Fiore, A., Dainelli, M., Grani, G., Carbotta, G., Calvanese, A., 2011. Therapy of hyperthyroidism in pregnancy and breastfeeding. *Obstet. Gynecol. Surv.* 66, 378–385. <https://doi.org/10.1097/OGX.0b013e31822c6388>
- Gangwal, S., Reif, D.M., Mosher, S., Egeghy, P.P., Wambaugh, J.F., Judson, R.S., Hubal, E.A.C., 2012. Incorporating exposure information into the toxicological prioritization index decision support framework. *Sci. Total Environ.* 435–436, 316–325. <https://doi.org/10.1016/j.scitotenv.2012.06.086>
- Gardosi, J., Kady, S.M., McGeown, P., Francis, A., Tonks, A., 2005. Classification of stillbirth by relevant condition at death (ReCoDe): population based cohort study. *BMJ* 331, 1113–1117. <https://doi.org/10.1136/bmj.38629.587639.7C>
- Gassmann, K., Abel, J., Bothe, H., Haarmann-Stemmann, T., Merk, H.F., Quasthoff, K.N., Rockel, T.D., Schreiber, T., Fritsche, E., 2010. Species-Specific Differential AhR Expression Protects Human Neural Progenitor Cells against Developmental Neurotoxicity of PAHs. *Environ. Health Perspect.* 118, 1571–1577. <https://doi.org/10.1289/ehp.0901545>
- Geva, R., Eshel, R., Leitner, Y., Valevski, A.F., Harel, S., 2006. Neuropsychological outcome of children with intrauterine growth restriction: a 9-year prospective study. *Pediatrics* 118, 91–100. <https://doi.org/10.1542/peds.2005-2343>
- Ghassabian, A., Bongers-Schokking, J.J., Henrichs, J., Jaddoe, V.W.V., Visser, T.J., Visser, W., De Muinck Keizer-Schrama, S.M.P.F., Hooijkaas, H., Steegers, E.A.P., Hofman, A., Verhulst, F.C., Van Der Ende, J., De Rijke, Y.B., Tiemeier, H., 2011. Maternal thyroid function during pregnancy and behavioral problems in the offspring: The generation R study. *Pediatr. Res.* 69, 454–459. <https://doi.org/10.1203/PDR.0b013e3182125b0c>
- Gibb, S., 2008. Toxicity testing in the 21st century: A vision and a strategy. *Reprod. Toxicol.* 25, 136–138. <https://doi.org/10.1016/j.reprotox.2007.10.013>
- Gil-Sánchez, A., Larqué, E., Demmelmair, H., Acien, M.I., Faber, F.L., Parrilla, J.J., Koletzko, B., 2010. Maternal-fetal in vivo transfer of [<sup>13</sup>C]docosahexaenoic and other fatty acids across the human placenta 12 h after maternal oral intake. *Am. J. Clin. Nutr.* 92, 115–122. <https://doi.org/10.3945/ajcn.2010.29589>
- Gilchrist, C., Cumberland, A., Walker, D., Tolcos, M., 2018. Intrauterine growth restriction and

- development of the hippocampus: implications for learning and memory in children and adolescents. *Lancet Child Adolesc. Heal.* 2, 755–764. [https://doi.org/10.1016/S2352-4642\(18\)30245-1](https://doi.org/10.1016/S2352-4642(18)30245-1)
- Gordijn, S.J., Beune, I.M., Thilaganathan, B., Papageorgiou, A., Baschat, A.A., Baker, P.N., Silver, R.M., Wynia, K., Ganzevoort, W., 2016. Consensus definition of fetal growth restriction: a Delphi procedure. *Ultrasound Obstet. Gynecol.* 48, 333–339. <https://doi.org/10.1002/uog.15884>
- Grandjean, P., Landrigan, P.J., 2014. Neurobehavioural effects of developmental toxicity. *Lancet Neurol.* 13, 330–338. [https://doi.org/10.1016/S1474-4422\(13\)70278-3](https://doi.org/10.1016/S1474-4422(13)70278-3)
- Grandjean, P., Landrigan, P.J., 2006. Developmental neurotoxicity of industrial chemicals. *Lancet (London, England)* 368, 2167–2178. [https://doi.org/10.1016/S0140-6736\(06\)69665-7](https://doi.org/10.1016/S0140-6736(06)69665-7)
- Greenberg, J.A., Bell, S.J., Ausdal, W. Van, 2008. Omega-3 Fatty Acid supplementation during pregnancy. *Rev. Obstet. Gynecol.* 1, 162–169.
- GRIT Study Group, 2003. A randomised trial of timed delivery for the compromised preterm fetus: short term outcomes and Bayesian interpretation. *BJOG* 110, 27–32. [https://doi.org/10.1016/s1470-0328\(02\)02514-4](https://doi.org/10.1016/s1470-0328(02)02514-4)
- Haddow, J.E., Palomaki, G.E., Allan, W.C., Williams, J.R., Knight, G.J., Gagnon, J., O’Heir, C.E., Mitchell, M.L., Hermos, R.J., Waisbren, S.E., Faix, J.D., Klein, R.Z., 1999. Maternal Thyroid Deficiency during Pregnancy and Subsequent Neuropsychological Development of the Child. *N. Engl. J. Med.* 341, 549–555. <https://doi.org/10.1056/NEJM199908193410801>
- Hartung, T., 2018. Perspectives on In Vitro to In Vivo Extrapolations. *Appl. Vitro. Toxicol.* 4, 305–316. <https://doi.org/10.1089/aivt.2016.0026>
- Heinonen, K., Räikkönen, K., Pesonen, A.K., Andersson, S., Kajantie, E., Eriksson, J.G., Wolke, D., Lano, A., 2010. Behavioural symptoms of attention deficit/hyperactivity disorder in preterm and term children born small and appropriate for gestational age: A longitudinal study. *BMC Pediatr.* 10, 91. <https://doi.org/10.1186/1471-2431-10-91>
- Hitoshi, S., Tropepe, V., Ekker, M., van der Kooy, D., 2002. Neural stem cell lineages are regionally specified, but not committed, within distinct compartments of the developing brain. *Development* 129, 233–244. <https://doi.org/10.1242/dev.129.1.233>
- Hofrichter, M., Nimtz, L., Tigges, J., Kabiri, Y., Schröter, F., Royer-Pokora, B., Hildebrandt, B., Schmuck, M., Epanchintsev, A., Theiss, S., Adjaye, J., Egly, J.M., Krutmann, J., Fritsche, E., 2017. Comparative performance analysis of human iPSC-derived and primary neural progenitor cells (NPC) grown as neurospheres in vitro. *Stem Cell Res.* 25, 72–82. <https://doi.org/10.1016/j.scr.2017.10.013>
- Howard, B.M., Mo, Z., Filipovic, R., Moore, A.R., Antic, S.D., Zecevic, N., 2008. Radial glia cells in the developing human brain. *Neuroscientist* 14, 459–473. <https://doi.org/10.1177/1073858407313512>
- Huttner, W.B., Kosodo, Y., 2005. Symmetric versus asymmetric cell division during neurogenesis in the developing vertebrate central nervous system. *Curr. Opin. Cell Biol.* 17, 648–657. <https://doi.org/10.1016/j.ceb.2005.10.005>

- ICH M3 (R2) EMA, 2009. ICH M3 (R2) - Non-clinical Safety studies for the conduct of human clinical trials and marketing authorisation for pharmaceuticals. ICH Guidel. 3, 31.
- ICH5(R3), 2020. International Council for Harmonisation of Technical Requirements for Pharmaceuticals for Human Use - DETECTION OF REPRODUCTIVE AND DEVELOPMENTAL TOXICITY FOR HUMAN PHARMACEUTICALS. ICH Saf. Guidel. 41, 1–120.
- Illa, M., Brito, V., Pla, L., Eixarch, E., Arbat-Plana, A., Batallé, D., Muñoz-Moreno, E., Crispi, F., Udina, E., Figueras, F., Ginés, S., Gratacós, E., 2018. Early Environmental Enrichment Enhances Abnormal Brain Connectivity in a Rabbit Model of Intrauterine Growth Restriction. *Fetal Diagn. Ther.* 44, 184–193. <https://doi.org/10.1159/000481171>
- Illa, M., Eixarch, E., Batalle, D., Arbat-Plana, A., Muñoz-Moreno, E., Figueras, F., Gratacos, E., 2013. Long-Term Functional Outcomes and Correlation with Regional Brain Connectivity by MRI Diffusion Tractography Metrics in a Near-Term Rabbit Model of Intrauterine Growth Restriction. *PLoS One* 8. <https://doi.org/10.1371/journal.pone.0076453>
- Illa, M., Pla, L., Loreiro, C., Miranda, C., Mayol, M., Kühne, B.A., Barenys, M., Eixarch, E., Gratacós, E., n.d. Docosahexaenoic Acid and Lactoferrin Effects on the Brain and Placenta in a Rabbit Model of Intrauterine Growth Restriction. *PLoS One*.
- Ireland, Z., Castillo-Melendez, M., Dickinson, H., Snow, R., Walker, D.W., 2011. A maternal diet supplemented with creatine from mid-pregnancy protects the newborn spiny mouse brain from birth hypoxia. *Neuroscience* 194, 372–379. <https://doi.org/10.1016/j.neuroscience.2011.05.012>
- Ireland, Z., Dickinson, H., Snow, R., Walker, D.W., 2008. Maternal creatine: does it reach the fetus and improve survival after an acute hypoxic episode in the spiny mouse (*Acomys cahirinus*)? *Am. J. Obstet. Gynecol.* 198, 431.e1-431.e6. <https://doi.org/10.1016/j.ajog.2007.10.790>
- Jacobsson, B., Ahlin, K., Francis, A., Hagberg, G., Hagberg, H., Gardosi, J., 2008. Cerebral palsy and restricted growth status at birth: Population-based case-control study. *BJOG An Int. J. Obstet. Gynaecol.* 115, 1250–1255. <https://doi.org/10.1111/j.1471-0528.2008.01827.x>
- Jakovcevski, I., Filipovic, R., Mo, Z., Rakic, S., Zecevic, N., 2009. Oligodendrocyte development and the onset of myelination in the human fetal brain. *Front. Neuroanat.* 3, 5. <https://doi.org/10.3389/neuro.05.005.2009>
- James, S.R., Franklyn, J.A., Kilby, M.D., 2007. Placental transport of thyroid hormone. *Best Pract. Res. Clin. Endocrinol. Metab.* 21, 253–264. <https://doi.org/10.1016/j.beem.2007.03.001>
- Judge, M.P., Harel, O., Lammi-Keefe, C.J., 2007. Maternal consumption of a docosahexaenoic acid-containing functional food during pregnancy: Benefit for infant performance on problem-solving but not on recognition memory tasks at age 9 mo. *Am. J. Clin. Nutr.* <https://doi.org/10.1093/ajcn/85.6.1572>
- Kady, S.M., Gardosi, J., 2004. Perinatal mortality and fetal growth restriction. *Best Pract. Res. Clin. Obstet. Gynaecol.* 18, 397–410. <https://doi.org/10.1016/j.bpobgyn.2004.02.009>
- Kerlin, R., Bolon, B., Burkhardt, J., Francke, S., Greaves, P., Meador, V., Popp, J., 2016. Scientific and Regulatory Policy Committee: Recommended (“Best”) Practices for Determining,



- Communicating, and Using Adverse Effect Data from Nonclinical Studies. *Toxicol. Pathol.* 44, 147–162. <https://doi.org/10.1177/0192623315623265>
- Kilby, M.D., Gittoes, N., McCabe, C., Verhaeg, J., Franklyn, J.A., 2000. Expression of thyroid receptor isoforms in the human fetal central nervous system and the effects of intrauterine growth restriction. *Clin. Endocrinol. (Oxf)*. 53, 469–477. <https://doi.org/10.1046/j.1365-2265.2000.01074.x>
- Kim, H.-T., Kim, I.-S., Lee, I.-S., Lee, J.-P., Snyder, E.Y., In Park, K., 2006. Human neurospheres derived from the fetal central nervous system are regionally and temporally specified but are not committed. *Exp. Neurol.* 199, 222–235. <https://doi.org/10.1016/j.expneurol.2006.03.015>
- Klose, J., Li, L., Pahl, M., Bendt, F., Hübenthal, U., Jüngst, C., Petzsch, P., Schauss, A., Köhrer, K., Leung, P.C., Wang, C.C., Koch, K., Tigges, J., Fan, X., Fritsche, E., 2022. Application of the adverse outcome pathway concept for investigating developmental neurotoxicity potential of Chinese herbal medicines by using human neural progenitor cells in vitro. *Cell Biol. Toxicol.* <https://doi.org/10.1007/s10565-022-09730-4>
- Klose, J., Pahl, M., Bartmann, K., Bendt, F., Blum, J., Dolde, X., Förster, N., Holzer, A.-K., Hübenthal, U., Keßel, H.E., Koch, K., Masjosthusmann, S., Schneider, S., Stürzl, L.-C., Woeste, S., Rossi, A., Covaci, A., Behl, M., Leist, M., Tigges, J., Fritsche, E., 2021a. Neurodevelopmental toxicity assessment of flame retardants using a human DNT in vitro testing battery. *Cell Biol. Toxicol.* 5, 1–45. <https://doi.org/10.1007/s10565-021-09603-2>
- Klose, J., Tigges, J., Masjosthusmann, S., Schmuck, K., Bendt, F., Hübenthal, U., Petzsch, P., Köhrer, K., Koch, K., Fritsche, E., 2021b. TBBPA targets converging key events of human oligodendrocyte development resulting in two novel AOPs. *ALTEX* 38, 215–234. <https://doi.org/10.14573/altex.2007201>
- Krewski, D., Andersen, M.E., Mantus, E., Zeise, L., 2009. Toxicity testing in the 21st century: Implications for human health risk assessment: Perspective. *Risk Anal.* 29, 474–479. <https://doi.org/10.1111/j.1539-6924.2008.01150.x>
- Kuhn, S., Gritti, L., Crooks, D., Dombrowski, Y., 2019. Oligodendrocytes in Development, Myelin Generation and Beyond. *Cells* 8, 1424. <https://doi.org/10.3390/cells8111424>
- Kühne, B.A., Puig, T., Ruiz-Martínez, S., Crous-Masó, J., Planas, M., Feliu, L., Cano, A., García, M.L., Fritsche, E., Llobet, J.M., Gómez-Catalán, J., Barenys, M., 2019. Comparison of migration disturbance potency of epigallocatechin gallate (EGCG) synthetic analogs and EGCG PEGylated PLGA nanoparticles in rat neurospheres. *Food Chem. Toxicol.* 123. <https://doi.org/10.1016/j.fct.2018.10.055>
- Kühne, B.A., Vázquez-Aristizabal, P., Fuentes-Amell, M., Pla, L., Loreiro, C., Gómez-Catalán, J., Gratacós, E., Illa, M., Barenys, M., 2022. Docosahexaenoic Acid and Melatonin Prevent Impaired Oligodendrogenesis Induced by Intrauterine Growth Restriction (IUGR). *Biomedicines* 10. <https://doi.org/10.3390/biomedicines10051205>
- Lackman, F., Capewell, V., Gagnon, R., Richardson, B., 2001. Fetal umbilical cord oxygen values and birth to placental weight ratio in relation to size at birth. *Am. J. Obstet. Gynecol.* 185, 674–682. <https://doi.org/10.1067/mob.2001.116686>
- Ladd, F.V.L., Ladd, A.A.B.L., Ribeiro, A.A.C.M., Costa, S.B.C., Coutinho, B.P., Feitosa, G.A.S., de

- Andrade, G.M., Maurício de Castro-Costa, C., Magalhães, C.E.C., Castro, I.C., Oliveira, B.B., Guerrant, R.L., Lima, A.Â.M., Oriá, R.B., 2010. Zinc and glutamine improve brain development in suckling mice subjected to early postnatal malnutrition. *Nutrition* 26, 662–670. <https://doi.org/https://doi.org/10.1016/j.nut.2009.11.020>
- LaFranchi, S.H., 2021. Thyroid Function in Preterm/Low Birth Weight Infants: Impact on Diagnosis and Management of Thyroid Dysfunction. *Front. Endocrinol. (Lausanne)*. 12. <https://doi.org/10.3389/fendo.2021.666207>
- LaFranchi, S.H., Austin, J., 2007. How Should We Be Treating Children with Congenital Hypothyroidism? *J. Pediatr. Endocrinol. Metab.* 20, 559–578. <https://doi.org/10.1515/JPEM.2007.20.5.559>
- Landers, K., Richard, K., 2017. Traversing barriers – How thyroid hormones pass placental, blood-brain and blood-cerebrospinal fluid barriers. *Mol. Cell. Endocrinol.* 458, 22–28. <https://doi.org/10.1016/j.mce.2017.01.041>
- Larroque, B., Bertrais, S., Czernichow, P., Léger, J., 2001. School difficulties in 20-year-olds who were born small for gestational age at term in a regional cohort study. *Pediatrics* 108, 111–115. <https://doi.org/10.1542/peds.108.1.111>
- Lauritzen, L., Brambilla, P., Mazzocchi, A., Harsløf, L.B.S., Ciappolino, V., Agostoni, C., 2016. DHA Effects in Brain Development and Function 1–17. <https://doi.org/10.3390/nu8010006>
- Lee, J.Y., Petratos, S., 2016. Thyroid Hormone Signaling in Oligodendrocytes: from Extracellular Transport to Intracellular Signal. *Mol. Neurobiol.* 53, 6568–6583. <https://doi.org/10.1007/s12035-016-0013-1>
- Lees, C.C., Romero, R., Stampalija, T., Dall’Asta, A., DeVore, G.A., Prefumo, F., Frusca, T., Visser, G.H.A., Hobbins, J.C., Baschat, A.A., Bilardo, C.M., Galan, H.L., Campbell, S., Maulik, D., Figueras, F., Lee, W., Unterscheider, J., Valensise, H., Da Silva Costa, F., Salomon, L.J., Poon, L.C., Ferrazzi, E., Mari, G., Rizzo, G., Kingdom, J.C., Kiserud, T., Hecher, K., 2022. Clinical Opinion: The diagnosis and management of suspected fetal growth restriction: an evidence-based approach. *Am. J. Obstet. Gynecol.* 226, 366–378. <https://doi.org/10.1016/j.ajog.2021.11.1357>
- Lein, P., Silbergeld, E., Locke, P., Goldberg, A.M., 2005. In vitro and other alternative approaches to developmental neurotoxicity testing (DNT). *Environ. Toxicol. Pharmacol.* 19, 735–744. <https://doi.org/10.1016/j.etap.2004.12.035>
- Leist, M., Ghallab, A., Graepel, R., Marchan, R., Hassan, R., Bennekou, S.H., Limonciel, A., Vinken, M., Schildknecht, S., Waldmann, T., Danen, E., van Ravenzwaay, B., Kamp, H., Gardner, I., Godoy, P., Bois, F.Y., Braeuning, A., Reif, R., Oesch, F., Drasdo, D., Höhme, S., Schwarz, M., Hartung, T., Braunbeck, T., Beltman, J., Vrieling, H., Sanz, F., Forsby, A., Gadaleta, D., Fisher, C., Kelm, J., Fluri, D., Ecker, G., Zdrzil, B., Terron, A., Jennings, P., van der Burg, B., Dooley, S., Meijer, A.H., Willighagen, E., Martens, M., Evelo, C., Mombelli, E., Taboureau, O., Mantovani, A., Hardy, B., Koch, B., Escher, S., van Thriel, C., Cadenas, C., Kroese, D., van de Water, B., Hengstler, J.G., 2017. Adverse outcome pathways: opportunities, limitations and open questions. *Arch. Toxicol.* 91, 3477–3505. <https://doi.org/10.1007/s00204-017-2045-3>

- Leist, M., Hartung, T., 2013. Inflammatory findings on species extrapolations: humans are definitely no 70-kg mice. *Arch. Toxicol.* 87, 563–567. <https://doi.org/10.1007/s00204-013-1038-0>
- Li, J., Settivari, R., LeBaron, M.J., Marty, M.S., 2019. An industry perspective: A streamlined screening strategy using alternative models for chemical assessment of developmental neurotoxicity. *Neurotoxicology* 73, 17–30. <https://doi.org/10.1016/j.neuro.2019.02.010>
- Linderkamp, O., Janus, L., Linder, R., Skoruppa, D.B., 2009. Time Table of Normal Foetal Brain Development. *Int. J. Prenat. Perinat. Psychol. Med.* 21, 4–16.
- Lo, H.-M., Hung, C.-F., Huang, Y.-Y., Wu, W.-B., 2007. Tea polyphenols inhibit rat vascular smooth muscle cell adhesion and migration on collagen and laminin via interference with cell–ECM interaction. *J. Biomed. Sci.* 14, 637–645. <https://doi.org/10.1007/s11373-007-9170-6>
- Lodygensky, G.A., Seghier, M.L., Warfield, S.K., Tolsa, C.B., Sizonenko, S., Lazeyras, F., Hüppi, P.S., 2008. Intrauterine growth restriction affects the preterm infant’s hippocampus. *Pediatr. Res.* 63, 438–443. <https://doi.org/10.1203/PDR.0b013e318165c005>
- Long, L., Li, Y., Wang, Y.D., He, Q.Y., Li, M., Cai, X.D., Peng, K., Li, X.P., Xie, D., Wen, Y.L., Yin de, L., Peng, Y., 2010. The preventive effect of oral EGCG in a fetal alcohol spectrum disorder mouse model. *Alcohol Clin Exp Res* 34, 1929–1936. <https://doi.org/10.1111/j.1530-0277.2010.01282.x>
- Mackay, D., Smith, G., Dobbie, R., Cooper, S.-A., Pell, J., 2013. Obstetric factors and different causes of special educational need: retrospective cohort study of 407 503 schoolchildren. *BJOG An Int. J. Obstet. Gynaecol.* 120, 297–308. <https://doi.org/10.1111/1471-0528.12071>
- Marasciulo, F., Orabona, R., Fratelli, N., Fichera, A., Valcamonico, A., Ferrari, F., Odicino, F.E., Sartori, E., Prefumo, F., 2021. Preeclampsia and late fetal growth restriction. *Minerva Obstet. Gynecol.* 73, 435–441. <https://doi.org/10.23736/S2724-606X.21.04809-7>
- Marrs, G.S., Honda, T., Fuller, L., Thangavel, R., Balsamo, J., Lilien, J., Dailey, M.E., Arregui, C., 2006. Dendritic arbors of developing retinal ganglion cells are stabilized by  $\beta$ 1-integrins. *Mol. Cell. Neurosci.* 32, 230–241. <https://doi.org/10.1016/j.mcn.2006.04.005>
- Masjosthusmann, S., Barenys, M., El-Gamal, M., Geerts, L., Gerosa, L., Gorreja, A., Kühne, B., Marchetti, N., Tigges, J., Viviani, B., Witters, H., Fritsche, E., 2018a. Literature review and appraisal on alternative neurotoxicity testing methods. *EFSA Support. Publ.* 15. <https://doi.org/10.2903/sp.efsa.2018.en-1410>
- Masjosthusmann, S., Becker, D., Petzuch, B., Klose, J., Siebert, C., Deenen, R., Barenys, M., Baumann, J., Dach, K., Tigges, J., Hübenthal, U., Köhrer, K., Fritsche, E., 2018b. A transcriptome comparison of time-matched developing human, mouse and rat neural progenitor cells reveals human uniqueness. *Toxicol. Appl. Pharmacol.* 354, 40–55. <https://doi.org/10.1016/j.taap.2018.05.009>
- Masjosthusmann, S., Blum, J., Bartmann, K., Dolde, X., Holzer, A., Stürzl, L., Keßel, E.H., Förster, N., Dönmez, A., Klose, J., Pahl, M., Waldmann, T., Bendt, F., Kisitu, J., Suci, I., Hübenthal, U., Mosig, A., Leist, M., Fritsche, E., 2020. Establishment of an a priori protocol for the implementation and interpretation of an in-vitro testing battery for the assessment of

developmental neurotoxicity. EFSA Support. Publ. 17.  
<https://doi.org/10.2903/sp.efsa.2020.en-1938>

- Masjosthusmann, S., Siebert, C., Hübenthal, U., Bendt, F., Baumann, J., Fritsche, E., 2019. Arsenite interrupts neurodevelopmental processes of human and rat neural progenitor cells: The role of reactive oxygen species and species-specific antioxidative defense. *Chemosphere* 235, 447–456. <https://doi.org/10.1016/j.chemosphere.2019.06.123>
- Mathur, N B, Agarwal, D.K., 2015. Zinc supplementation in preterm neonates and neurological development: A randomized controlled trial. *Indian Pediatr.* 52, 951–955. <https://doi.org/10.1007/s13312-015-0751-6>
- Mathur, N. B., Agarwal, D.K., 2015. Zinc supplementation in preterm neonates and neurological development: A randomized controlled trial. *Indian Pediatr.* 52, 951–955. <https://doi.org/10.1007/s13312-015-0751-6>
- Mato, S., Sánchez-Gómez, M.V., Bernal-Chico, A., Matute, C., 2013. Cytosolic zinc accumulation contributes to excitotoxic oligodendroglial death. *Glia* 61, 750–764. <https://doi.org/10.1002/glia.22470>
- McKinstry, R.C., Mathur, A., Miller, J.H., Ozcan, A., Snyder, A.Z., Schefft, G.L., Almlı, C.R., Shiran, S.I., Conturo, T.E., Neil, J.J., 2002. Radial organization of developing preterm human cerebral cortex revealed by non-invasive water diffusion anisotropy MRI. *Cereb. Cortex* 12, 1237–1243. <https://doi.org/10.1093/cercor/12.12.1237>
- Melgarejo, E., Medina, M.A., Sanchez-Jimenez, F., Urdiales, J.L., 2009. Epigallocatechin gallate reduces human monocyte mobility and adhesion in vitro. *Br J Pharmacol* 158, 1705–1712. <https://doi.org/10.1111/j.1476-5381.2009.00452.x>
- Miller, S.L., Huppi, P.S., Mallard, C., 2016. The consequences of fetal growth restriction on brain structure and neurodevelopmental outcome. *J. Physiol.* 594, 807–823. <https://doi.org/10.1113/JP271402>
- Miller, S.L., Yawno, T., Alers, N.O., Castillo-Melendez, M., Supramaniam, V.G., Vanzyl, N., Sabaretnam, T., Loose, J.M., Drummond, G.R., Walker, D.W., Jenkin, G., Wallace, E.M., 2014. Antenatal antioxidant treatment with melatonin to decrease newborn neurodevelopmental deficits and brain injury caused by fetal growth restriction. *J. Pineal Res.* 56, 283–294. <https://doi.org/10.1111/jpi.12121>
- Mineva, N.D., Paulson, K.E., Naber, S.P., Yee, A.S., Sonenshein, G.E., 2013. Epigallocatechin-3-Gallate Inhibits Stem-Like Inflammatory Breast Cancer Cells. *PLoS One* 8, e73464. <https://doi.org/10.1371/journal.pone.0073464>
- Moors, M., Cline, J.E., Abel, J., Fritsche, E., 2007. ERK-dependent and -independent pathways trigger human neural progenitor cell migration. *Toxicol. Appl. Pharmacol.* 221, 57–67. <https://doi.org/10.1016/j.taap.2007.02.018>
- Moors, M., Rockel, T.D., Abel, J., Cline, J.E., Gassmann, K., Schreiber, T., Schuwald, J., Weinmann, N., Fritsche, E., 2009. Human neurospheres as three-dimensional cellular systems for developmental neurotoxicity testing. *Environ. Health Perspect.* 117, 1131–8. <https://doi.org/10.1289/ehp.0800207>
- Muller, P.Y., Milton, M.N., 2012. The determination and interpretation of the therapeutic

- index in drug development. *Nat. Rev. Drug Discov.* 11, 751–761. <https://doi.org/10.1038/nrd3801>
- Mwaniki, M.K., Atieno, M., Lawn, J.E., Newton, C.R., 2012. Long-term neurodevelopmental outcomes after intrauterine and neonatal insults: a systematic review. *Lancet* 379, 445–452. [https://doi.org/10.1016/S0140-6736\(11\)61577-8](https://doi.org/10.1016/S0140-6736(11)61577-8)
- National Toxicology Program, 2022. Definition Adverse Outcome Pathways [WWW Document]. URL <https://ntp.niehs.nih.gov/whatwestudy/niceatm/comptox/ct-aop/aop.html>
- Nimtz, L., Hartmann, J., Tigges, J., Masjosthusmann, S., Schmuck, M., Keßel, E., Theiss, S., Köhrer, K., Petzsch, P., Adjaye, J., Wigmann, C., Wieczorek, D., Hildebrandt, B., Bendt, F., Hübenthal, U., Brockerhoff, G., Fritsche, E., 2020. Characterization and application of electrically active neuronal networks established from human induced pluripotent stem cell-derived neural progenitor cells for neurotoxicity evaluation. *Stem Cell Res.* 45, 101761. <https://doi.org/10.1016/j.scr.2020.101761>
- Nuttall, J.R., Oteiza, P.I., 2012. Zinc and the ERK kinases in the developing brain. *Neurotox. Res.* 21, 128–141. <https://doi.org/10.1007/s12640-011-9291-6>
- Nyffeler, J., Dolde, X., Krebs, A., Pinto-Gil, K., Pastor, M., Behl, M., Waldmann, T., Leist, M., 2017. Combination of multiple neural crest migration assays to identify environmental toxicants from a proof-of-concept chemical library. *Arch. Toxicol.* 91, 3613–3632. <https://doi.org/10.1007/s00204-017-1977-y>
- O’Keeffe, M.J., O’Callaghan, M., Williams, G.M., Najman, J.M., Bor, W., 2003. Learning, Cognitive, and Attentional Problems in Adolescents Born Small for Gestational Age. *Pediatrics* 112, 301–307. <https://doi.org/10.1542/peds.112.2.301>
- OECD, 2022. Guidance on Evaluation of Data from the Developmental Neurotoxicity ( DNT ) In-Vitro Testing Battery Original Draft : July 2021 Revised Draft : May 2022.
- OECD, 2018a. Test No. 414: Prenatal Developmental Toxicity Study. <https://doi.org/https://doi.org/https://doi.org/10.1787/9789264070820-en>
- OECD, 2018b. Users Handbook supplement to the Guidance Document for developing and assessing Adverse Outcome Pathways, OECD Series on Adverse Outcome Pathways, No. 1, OECD Publishing, Paris. Organ. Econ. Co-operation Dev. Publ. <https://doi.org/https://doi.org/10.1787/5jlv1m9d1g32-en>
- OECD, 2017. Guidance Document for the Use of Adverse Outcome Pathways in Developing Integrated Approaches to Testing and Assessment (IATA), Series on Testing and Assessment No. 206, OECD Series on Testing and Assessment. OECD. <https://doi.org/10.1787/44bb06c1-en>
- OECD, 2007. Test No. 426: Developmental Neurotoxicity Study, OECD Guidelines for the Testing of Chemicals, Section 4. OECD. <https://doi.org/10.1787/9789264067394-en>
- Olivier, P., Baud, O., Evrard, P., Gressens, P., Verney, C., 2005. Prenatal ischemia and white matter damage in rats. *J. Neuropathol. Exp. Neurol.* 64, 998–1006. <https://doi.org/10.1097/01.jnen.0000187052.81889.57>
- Olivier, P., Fontaine, R.H., Loron, G., Van Steenwinckel, J., Biran, V., Massonneau, V., Kaindl,

- A., Dalous, J., Charriaut-Marlangue, C., Aigrot, M.S., Pansiot, J., Verney, C., Gressens, P., Baud, O., 2009. Melatonin promotes oligodendroglial maturation of injured white matter in neonatal rats. *PLoS One* 4. <https://doi.org/10.1371/journal.pone.0007128>
- Oros, D., Figueras, F., Cruz-Martinez, R., Meler, E., Munmany, M., Gratacos, E., 2011. Longitudinal changes in uterine, umbilical and fetal cerebral Doppler indices in late-onset small-for-gestational age fetuses. *Ultrasound Obstet. Gynecol.* 37, 191–195. <https://doi.org/10.1002/uog.7738>
- Oros, D., Figueras, F., Cruz-Martinez, R., Padilla, N., Meler, E., Hernandez-Andrade, E., Gratacos, E., 2010. Middle versus anterior cerebral artery doppler for the prediction of perinatal outcome and neonatal neurobehavior in term small-for-gestational-age fetuses with normal umbilical artery doppler. *Ultrasound Obstet. Gynecol.* 35, 456–461. <https://doi.org/10.1002/uog.7588>
- P Grandjean, P.L., 2006. Developmental neurotoxicity of industrial chemicals. *Lancet* 368, 2167–2178. [https://doi.org/10.1016/S0140-6736\(06\)69665-7](https://doi.org/10.1016/S0140-6736(06)69665-7)
- Padilla, N., Junqué, C., Figueras, F., Sanz-Cortes, M., Bargalló, N., Arranz, A., Donaire, A., Figueras, J., Gratacos, E., 2014. Differential vulnerability of gray matter and white matter to intrauterine growth restriction in preterm infants at 12 months corrected age. *Brain Res.* 1545, 1–11. <https://doi.org/10.1016/j.brainres.2013.12.007>
- Park, J.H., Yoon, J.H., Kim, S.A., Ahn, S.G., Yoon, J.H., 2010. (-)-Epigallocatechin-3-gallate inhibits invasion and migration of salivary gland adenocarcinoma cells. *Oncol Rep* 23, 585–590.
- Paul, S.M., Mytelka, D.S., Dunwiddie, C.T., Persinger, C.C., Munos, B.H., Lindborg, S.R., Schacht, A.L., 2010. How to improve RD productivity: The pharmaceutical industry's grand challenge. *Nat. Rev. Drug Discov.* 9, 203–214. <https://doi.org/10.1038/nrd3078>
- Pedroso, M.A., Palmer, K.R., Hodges, R.J., Costa, F. da S., Rolnik, D.L., 2018. Uterine artery doppler in screening for preeclampsia and fetal growth restriction. *Rev. Bras. Ginecol. e Obstet.* 40, 287–293. <https://doi.org/10.1055/s-0038-1660777>
- Pervin, M., Unno, K., Ohishi, T., Tanabe, H., Miyoshi, N., Nakamura, Y., 2018. Beneficial Effects of Green Tea Catechins on Neurodegenerative Diseases. *Molecules* 23, 1–17. <https://doi.org/10.3390/molecules23061297>
- Peter, B., Farkas, E., Forgacs, E., Saftics, A., Kovacs, B., Kurunczi, S., Szekacs, I., Csampai, A., Bosze, S., Horvath, R., 2017. Green tea polyphenol tailors cell adhesivity of RGD displaying surfaces: multicomponent models monitored optically. *Sci. Rep.* 7, 42220. <https://doi.org/10.1038/srep42220>
- Piorkowska, K., Thompson, J., Nygard, K., Matuszewski, B., Hammond, R., Richardson, B., 2014. Synaptic development and neuronal myelination are altered with growth restriction in fetal guinea pigs. *Dev. Neurosci.* 36, 465–476. <https://doi.org/10.1159/000363696>
- Pla, L., Illa, M., Loreiro, C., Lopez, M.C., Vázquez-Aristizabal, P., Kühne, B.A., Barenys, M., Eixarch, E., Gratacós, E., 2020. Structural Brain Changes during the Neonatal Period in a Rabbit Model of Intrauterine Growth Restriction. *Dev. Neurosci.* 42, 217–229. <https://doi.org/10.1159/000512948>

- Pla, L., Kühne, B.A., Guardia-Escote, L., Vázquez-Aristizabal, P., Loreiro, C., Flick, B., Gratacós, E., Barenys, M., Illa, M., 2022. Protocols for the evaluation of neurodevelopmental alterations in rabbit models in vitro and in vivo. *Front. Toxicol.* <https://doi.org/10.3389/ftox.2022.918520>
- Pop, V.J., Kuijpers, J.L., van Baar, A.L., Verkerk, G., van Son, M.M., de Vijlder, J.J., Vulsma, T., Wiersinga, W.M., Drexhage, H.A., Vader, H.L., 1999. Low maternal free thyroxine concentrations during early pregnancy are associated with impaired psychomotor development in infancy. *Clin. Endocrinol. (Oxf)*. 50, 149–155. <https://doi.org/10.1046/j.1365-2265.1999.00639.x>
- Radke, E.G., Braun, J.M., Nachman, R.M., Cooper, G.S., 2020. Phthalate exposure and neurodevelopment: A systematic review and meta-analysis of human epidemiological evidence. *Environ. Int.* 137. <https://doi.org/10.1016/j.envint.2019.105408>
- Ramenghi, L.A., Martinelli, A., De Carli, A., Brusati, V., Mandia, L., Fumagalli, M., Triulzi, F., Mosca, F., Cetin, I., 2011. Cerebral Maturation in IUGR and Appropriate for Gestational Age Preterm Babies. *Reprod. Sci.* 18, 469–475. <https://doi.org/10.1177/19337191110388847>
- Rao, M., Hediger, M., Levine, R., Naficy, A., Vik, T., 2007. Effect of breastfeeding on cognitive development of infants born small for gestational age. *Acta Paediatr.* 91, 267–274. <https://doi.org/10.1111/j.1651-2227.2002.tb01713.x>
- Reid, M. V., Murray, K.A., Marsh, E.D., Golden, J.A., Simmons, R.A., Grinspan, J.B., 2012. Delayed myelination in an intrauterine growth retardation model is mediated by oxidative stress upregulating bone morphogenetic protein 4. *J. Neuropathol. Exp. Neurol.* 71, 640–653. <https://doi.org/10.1097/NEN.0b013e31825cfa81>
- Reiter, R.J., Tan, D.X., Korkmaz, A., Rosales-Corral, S.A., 2014a. Melatonin and stable circadian rhythms optimize maternal, placental and fetal physiology. *Hum. Reprod. Update* 20, 293–307. <https://doi.org/10.1093/humupd/dmt054>
- Reiter, R.J., Tan, D.X., Korkmaz, A., Rosales-Corral, S.A., 2014b. Melatonin and stable circadian rhythms optimize maternal, placental and fetal physiology. *Hum. Reprod. Update* 20, 293–307. <https://doi.org/10.1093/humupd/dmt054>
- Richter, H.G., Hansell, J.A., Raut, S., Giussani, D.A., 2009. Melatonin improves placental efficiency and birth weight and increases the placental expression of antioxidant enzymes in undernourished pregnancy. *J. Pineal Res.* 46, 357–364. <https://doi.org/10.1111/j.1600-079X.2009.00671.x>
- Rideau Batista Novais, A., Pham, H., Van de Looij, Y., Bernal, M., Mairesse, J., Zana-taieb, E., Colella, M., Jarreau, P., Gressens, P., Pansiot, J., Dumont, F., Charriaut-marlangue, C., Tanter, M., Demene, C., Vaiman, D., Baud, O., 2016. Transcriptomic Regulations in Oligodendroglial and Microglial Cells Related to Brain Damage following Fetal Growth Restriction. <https://doi.org/10.1002/glia.2307>
- Rodriguez, C., Mayo, J.C., Sainz, R.M., Antolin, I., Herrera, F., Martin, V., Reiter, R.J., 2004. Regulation of antioxidant enzymes: a significant role for melatonin. *J. Pineal Res.* 36, 1–9. <https://doi.org/10.1046/j.1600-079X.2003.00092.x>
- Rolando, C., Taylor, V., 2014. Neural Stem Cell of the Hippocampus. *Development, Physiology*

- Regulation, and Dysfunction in Disease., 1st ed, Current Topics in Developmental Biology. Elsevier Inc. <https://doi.org/10.1016/B978-0-12-416022-4.00007-X>
- Ruan, Y.W., Zou, B., Fan, Y., Li, Y., Lin, N., Zeng, Y.S., Gao, T.M., Yao, Z., Xu, Z.C., 2006. Dendritic plasticity of CA1 pyramidal neurons after transient global ischemia. *Neuroscience* 140, 191–201. <https://doi.org/10.1016/j.neuroscience.2006.01.039>
- Russell, W., Burch, R., 1959. The principles of humane experimental technique [WWW Document].
- Sachana, M., Leinala, E., 2017. Approaching chemical safety assessment through application of integrated approaches to testing and assessment: Combining mechanistic information derived from adverse outcome pathways and alternative methods. *Appl. Vit. Toxicol.* 3, 227–233. <https://doi.org/10.1089/aivt.2017.0013>
- Sachana, M., Shafer, T.J., Terron, A., 2021. Toward a better testing paradigm for developmental neurotoxicity: Oecd efforts and regulatory considerations. *Biology (Basel)*. 10, 1–11. <https://doi.org/10.3390/biology10020086>
- Sakuratani, Y., Horie, M., Leinala, E., 2018. Integrated Approaches to Testing and Assessment: OECD Activities on the Development and Use of Adverse Outcome Pathways and Case Studies. *Basic Clin. Pharmacol. Toxicol.* 123, 20–28. <https://doi.org/10.1111/bcpt.12955>
- Sanz-Cortés, M., Figueras, F., Bargalló, N., Padilla, N., Amat-Roldan, I., Gratacós, E., 2010. Abnormal brain microstructure and metabolism in small-for-gestational-age term fetuses with normal umbilical artery Doppler. *Ultrasound Obstet. Gynecol.* 36, 159–165. <https://doi.org/10.1002/uog.7724>
- Savchev, S., Figueras, F., Sanz-Cortés, M., Cruz-Lemini, M., Triunfo, S., Botet, F., Gratacós, E., 2014. Evaluation of an optimal gestational age cut-off for the definition of early-and late-onset fetal growth restriction. *Fetal Diagn. Ther.* 36, 99–105. <https://doi.org/10.1159/000355525>
- Schmuck, M., Temme, T., Heinz, S., Baksmeier, C., Mosig, A., Colomina, M.T., Barenys, M., Fritsche, E., 2014. Automatic counting and positioning of 5-bromo-2-deoxyuridine (BrdU) positive cells in cortical layers of rat brain slices. *Neurotoxicology* 43, 127–133. <https://doi.org/10.1016/j.neuro.2014.02.005>
- Schmuck, M.R., Temme, T., Dach, K., de Boer, D., Barenys, M., Bendt, F., Mosig, A., Fritsche, E., 2017. Omnisphero: a high-content image analysis (HCA) approach for phenotypic developmental neurotoxicity (DNT) screenings of organoid neurosphere cultures in vitro. *Arch. Toxicol.* 91, 2017–2028. <https://doi.org/10.1007/s00204-016-1852-2>
- Schoonover, C.M., Seibel, M.M., Jolson, D.M., Stack, M.J., Rahman, R.J., Jones, S.A., Mariash, C.N., Anderson, G.W., 2004. Thyroid hormone regulates oligodendrocyte accumulation in developing rat brain white matter tracts. *Endocrinology* 145, 5013–5020. <https://doi.org/10.1210/en.2004-0065>
- Schreiber, T., Gassmann, K., Götz, C., Hübenthal, U., Moors, M., Krause, G., Merk, H.F., Nguyen, N.H., Scanlan, T.S., Abel, J., Rose, C.R., Fritsche, E., 2010. Polybrominated diphenyl ethers induce developmental neurotoxicity in a human in vitro model: Evidence for endocrine disruption. *Environ. Health Perspect.* 118, 572–578. <https://doi.org/10.1289/ehp.0901435>



- Scientific Committee on Emerging and Newly-Identified Health Risks, 2016. Scientific Committee on Emerging and Newly-Identified Health Risks SCENIHR Opinion on The safety of medical devices containing DEHP- plasticized PVC or other plasticizers on neonates and other groups possibly at risk ( 2015 update ). <https://doi.org/10.2772/45179>
- Sebastiani, G., Navarro-Tapia, E., Almeida-Toledano, L., Serra-Delgado, M., Paltrinieri, A.L., García-Algar, Ó., Andreu-Fernández, V., 2022. Effects of Antioxidant Intake on Fetal Development and Maternal/Neonatal Health during Pregnancy. *Antioxidants* 11, 648. <https://doi.org/10.3390/antiox11040648>
- Segovia, K.N., McClure, M., Moravec, M., Ning, L.L., Wan, Y., Gong, X., Riddle, A., Craig, A., Struve, J., Sherman, L.S., Back, S.A., 2008. Arrested oligodendrocyte lineage maturation in chronic perinatal white matter injury. *Ann. Neurol.* 63, 520–530. <https://doi.org/10.1002/ana.21359>
- Shankar, S., Ganapathy, S., Hingorani, S.R., Srivastava, R.K., 2008. EGCG inhibits growth, invasion, angiogenesis and metastasis of pancreatic cancer. *Front. Biosci.* 13, 440–452.
- Sharma, D., Shastri, S., Sharma, P., 2016. Intrauterine Growth Restriction: Antenatal and Postnatal Aspects. *Clin. Med. Insights Pediatr.* 10, CMPed.S40070. <https://doi.org/10.4137/CMPed.S40070>
- Sharp, A., Cornforth, C., Jackson, R., Harrold, J., Turner, M.A., Kenny, L.C., Baker, P.N., Johnstone, E.D., Khalil, A., von Dadelszen, P., Papageorghiou, A.T., Alfirevic, Z., Agarwal, U., Willis, E., Mammarella, S., Masson, G., Aquilina, J., Greco, E., Higgins, S., Vinayagam, D., Shaw, L., Stephens, L., Howe, D., Rand, A., Patni, S., Mousa, T., Rabab, A., Russell, H., Hannon, T., Fenn, A., Kilby, M., Selman, T., David, A., Spencer, R., Cohen, K., Breeze, A., McKelvey, A., Impey, L., Loannou, C., Stock, S., Poon, L., Pasupathy, D., Webster, L., Bugg, G., 2018. Maternal sildenafil for severe fetal growth restriction (STRIDER): a multicentre, randomised, placebo-controlled, double-blind trial. *Lancet Child Adolesc. Heal.* 2, 93–102. [https://doi.org/10.1016/S2352-4642\(17\)30173-6](https://doi.org/10.1016/S2352-4642(17)30173-6)
- Shea, K.M., 2003. Pediatric Exposure and Potential Toxicity of Phthalate Plasticizers. *Pediatrics* 111, 1467–1474. <https://doi.org/10.1542/peds.111.6.1467>
- Sheppard, P.A.S., Choleris, E., Galea, L.A.M., 2019. Structural plasticity of the hippocampus in response to estrogens in female rodents. *Mol. Brain* 12, 22. <https://doi.org/10.1186/s13041-019-0442-7>
- Shi, D.-D., Guo, J. -j., Zhou, L., Wang, N., 2018. Epigallocatechin gallate enhances treatment efficacy of oral nifedipine against pregnancy-induced severe pre-eclampsia: A double-blind, randomized and placebo-controlled clinical study. *J. Clin. Pharm. Ther.* 43, 21–25. <https://doi.org/10.1111/jcpt.12597>
- Sienkiewicz, M., Jaśkiewicz, A., Tarasiuk, A., Fichna, J., 2021. Lactoferrin: an overview o its main functions, immunomodulatory and antimicrobial role, and clinical significance. *Crit. Rev. Food Sci. Nutr.* 0, 1–18. <https://doi.org/10.1080/10408398.2021.1895063>
- Silbereis, J.C., Pochareddy, S., Zhu, Y., Li, M., Sestan, N., 2016. The Cellular and Molecular Landscapes of the Developing Human Central Nervous System. *Neuron* 89, 248. <https://doi.org/10.1016/j.neuron.2015.12.008>

- Singh, B.N., Shankar, S., Srivastava, R.K., 2011. Green tea catechin, epigallocatechin-3-gallate (EGCG): mechanisms, perspectives and clinical applications. *Biochem Pharmacol* 82, 1807–1821. <https://doi.org/10.1016/j.bcp.2011.07.093>
- Smith, G.C.S., 2018. The STRIDER trial: one step forward, one step back. *Lancet Child Adolesc. Heal.* 2, 80–81. [https://doi.org/10.1016/S2352-4642\(17\)30176-1](https://doi.org/10.1016/S2352-4642(17)30176-1)
- Somm, E., Larvaron, P., Van De Looij, Y., Toulotte, A., Chatagner, A., Faure, M., Métaïron, S., Mansourian, R., Raymond, F., Gruetter, R., Wang, B., Sizonenko, S. V., Hüppi, P.S., 2014. Protective effects of maternal nutritional supplementation with lactoferrin on growth and brain metabolism. *Pediatr. Res.* 75, 51–61. <https://doi.org/10.1038/pr.2013.199>
- Souchet, B., Duchon, A., Gu, Y., Dairou, J., Chevalier, C., Daubigney, F., Nalesso, V., Créau, N., Yu, Y., Janel, N., Herault, Y., Delabar, J.M., 2019. Prenatal treatment with EGCG enriched green tea extract rescues GAD67 related developmental and cognitive defects in Down syndrome mouse models. *Sci. Rep.* 9, 3914. <https://doi.org/10.1038/s41598-019-40328-9>
- Stagni, F., Giacomini, A., Emili, M., Trazzi, S., Guidi, S., Sassi, M., Ciani, E., Rimondini, R., Bartesaghi, R., 2016. Short- and long-term effects of neonatal pharmacotherapy with epigallocatechin-3-gallate on hippocampal development in the Ts65Dn mouse model of Down syndrome. *Neuroscience* 333, 277–301. <https://doi.org/10.1016/j.neuroscience.2016.07.031>
- Stagni, F., Guidi, S., Bartesaghi, R., 2021. Chapter 53 - Epigallocatechin-3-gallate: Linking the neurogenesis, hippocampus, and Down syndrome, in: *Factors Affecting Neurodevelopment*. Elsevier, pp. 619–630. <https://doi.org/10.1016/B978-0-12-817986-4.00053-5>
- Stiles, J., Jernigan, T.L., 2010. The basics of brain development. *Neuropsychol. Rev.* 20, 327–348. <https://doi.org/10.1007/s11065-010-9148-4>
- Suganuma, H., Arai, Y., Kitamura, Y., Hayashi, M., Okumura, A., Shimizu, T., 2010. Maternal docosahexaenoic acid-enriched diet prevents neonatal brain injury. *Neuropathology* 30, 597–605. <https://doi.org/10.1111/j.1440-1789.2010.01114.x>
- Suzuki, Y., Isemura, M., 2001. Inhibitory effect of epigallocatechin gallate on adhesion of murine melanoma cells to laminin. *Cancer Lett.* 173, 15–20. [https://doi.org/10.1016/S0304-3835\(01\)00685-1](https://doi.org/10.1016/S0304-3835(01)00685-1)
- Swanson, D., Block, R., Mousa, S.A., 2012. Omega-3 fatty acids EPA and DHA: Health benefits throughout life. *Adv. Nutr.* 3, 1–7. <https://doi.org/10.3945/an.111.000893>
- Szajewska, H., 2011. The role of meta-analysis in the evaluation of the effects of early nutrition on mental and motor development in children. *Am. J. Clin. Nutr.* 94, 1889–1895. <https://doi.org/10.3945/ajcn.110.000653>
- Tiwari, V., Kuhad, A., Chopra, K., 2010. Epigallocatechin-3-gallate ameliorates alcohol-induced cognitive dysfunctions and apoptotic neurodegeneration in the developing rat brain. *Int J Neuropsychopharmacol* 13, 1053–1066. <https://doi.org/10.1017/s146114571000060x>
- Tolcos, M., Bateman, E., O’Dowd, R., Markwick, R., Vrijisen, K., Rehn, A., Rees, S., 2011. Intrauterine growth restriction affects the maturation of myelin. *Exp. Neurol.* 232, 53–

65. <https://doi.org/10.1016/j.expneurol.2011.08.002>
- Tolcos, M., Petratos, S., Hirst, J.J., Wong, F., Spencer, S.J., Azhan, A., Emery, B., Walker, D.W., 2017. Blocked, delayed, or obstructed: What causes poor white matter development in intrauterine growth restricted infants? *Prog. Neurobiol.* 154, 62–77. <https://doi.org/10.1016/j.pneurobio.2017.03.009>
- Tolsa, C.B., Zimine, S., Warfield, S.K., Freschi, M., Rossignol, A.S., Lazeyras, F., Hanquinet, S., Pfizenmaier, M., Hüppi, P.S., 2004. Early alteration of structural and functional brain development in premature infants born with intrauterine growth restriction. *Pediatr. Res.* 56, 132–138. <https://doi.org/10.1203/01.PDR.0000128983.54614.7E>
- Turan, O.M., Turan, S., Gungor, S., Berg, C., Moyano, D., Gembruch, U., Nicolaidis, K.H., Harman, C.R., Baschat, A.A., 2008. Progression of Doppler abnormalities in intrauterine growth restriction. *Ultrasound Obstet. Gynecol.* 32, 160–167. <https://doi.org/10.1002/uog.5386>
- van de Looij, Y., Ginet, V., Chatagner, A., Toulotte, A., Somm, E., Hüppi, P.S., Sizonenko, S. V., 2014. Lactoferrin during lactation protects the immature hypoxic-ischemic rat brain. *Ann. Clin. Transl. Neurol.* 1, 955–967. <https://doi.org/10.1002/acn3.138>
- Van De Looij, Y., Larpin, C., Cabungcal, J.H., Sanches, E.F., Toulotte, A., Do, K.Q., Sizonenko, S. V., 2019. Nutritional intervention for developmental brain damage: Effects of lactoferrin supplementation in hypocaloric induced intrauterine growth restriction rat pups. *Front. Endocrinol. (Lausanne)*. 10, 1–14. <https://doi.org/10.3389/fendo.2019.00046>
- Van Vliet, E.D.S., Reitano, E.M., Chhabra, J.S., Bergen, G.P., Whyatt, R.M., 2011. A review of alternatives to di (2-ethylhexyl) phthalate-containing medical devices in the neonatal intensive care unit. *J. Perinatol.* 31, 551–560. <https://doi.org/10.1038/jp.2010.208>
- Van Vliet, E.O.G., De Kieviet, J.F., Van Der Voorn, J.P., Been, J. V., Oosterlaan, J., Van Elburg, R.M., 2012. Placental pathology and long-term neurodevelopment of very preterm infants. *Am. J. Obstet. Gynecol.* 206, 489.e1-489.e7. <https://doi.org/10.1016/j.ajog.2012.03.024>
- Verkauskiene, R., Figueras, F., Deghmoun, S., Chevenne, D., Gardosi, J., Levy-Marchal, M., 2008. Birth weight and long-term metabolic outcomes: Does the definition of smallness matter? *Horm. Res.* 70, 309–315. <https://doi.org/10.1159/000157878>
- Villeneuve, D.L., Crump, D., Garcia-Reyero, N., Hecker, M., Hutchinson, T.H., LaLone, C.A., Landesmann, B., Lettieri, T., Munn, S., Nepelska, M., Ottinger, M.A., Vergauwen, L., Whelan, M., 2014. Adverse outcome pathway development II: Best practices. *Toxicol. Sci.* 142, 321–330. <https://doi.org/10.1093/toxsci/kfu200>
- Vlot, A.H.C., de Witte, W.E.A., Danhof, M., van der Graaf, P.H., van Westen, G.J.P., de Lange, E.C.M., 2018. Target and Tissue Selectivity Prediction by Integrated Mechanistic Pharmacokinetic-Target Binding and Quantitative Structure Activity Modeling. *AAPS J.* 20, 1–14. <https://doi.org/10.1208/s12248-017-0172-7>
- Volpe, J.J., 2000. Overview: Normal and abnormal human brain development. *Ment. Retard. Dev. Disabil. Res. Rev.* 6, 1–5. [https://doi.org/10.1002/\(SICI\)1098-2779\(2000\)6:1<1::AID-MRDD1>3.0.CO;2-J](https://doi.org/10.1002/(SICI)1098-2779(2000)6:1<1::AID-MRDD1>3.0.CO;2-J)

- Wang, B., 2016. Molecular Determinants of Milk Lactoferrin as a Bioactive Compound in Early Neurodevelopment and Cognition. *J. Pediatr.* 173, S29–S36. <https://doi.org/10.1016/j.jpeds.2016.02.073>
- Warren, M.S., Bradley, W.D., Gourley, S.L., Lin, Y.-C., Simpson, M.A., Reichardt, L.F., Greer, C.A., Taylor, J.R., Koleske, A.J., 2012. Integrin  $\beta$ 1 signals through Arg to regulate postnatal dendritic arborization, synapse density, and behavior. *J. Neurosci.* 32, 2824–34. <https://doi.org/10.1523/JNEUROSCI.3942-11.2012>
- Whitebread, S., Hamon, J., Bojanic, D., Urban, L., 2005. Keynote review: In vitro safety pharmacology profiling: an essential tool for successful drug development. *Drug Discov. Today* 10, 1421–1433. [https://doi.org/10.1016/S1359-6446\(05\)03632-9](https://doi.org/10.1016/S1359-6446(05)03632-9)
- Williams, F., Watson, J., Ogston, S., Hume, R., Willatts, P., Visser, T., 2012. Mild Maternal Thyroid Dysfunction at Delivery of Infants Born  $\leq$ 34 Weeks and Neurodevelopmental Outcome at 5.5 Years. *J. Clin. Endocrinol. Metab.* 97, 1977–1985. <https://doi.org/10.1210/jc.2011-2451>
- Workman, A.D., Charvet, C.J., Clancy, B., Darlington, R.B., Finlay, B.L., 2013. Modeling transformations of neurodevelopmental sequences across mammalian species. *J. Neurosci.* 33, 7368–83. <https://doi.org/10.1523/JNEUROSCI.5746-12.2013>
- Wurtman, R.J., Cansev, M., Ulus, I.H., 2009. Synapse formation is enhanced by oral administration of uridine and DHA, the circulating precursors of brain phosphatides. *J. Nutr. Heal. Aging* 13, 189–197. <https://doi.org/10.1007/s12603-009-0056-3>
- Yassa, M.A., 2020. hippocampus [WWW Document]. *Encycl. Br.* URL <https://www.britannica.com/science/hippocampus> (accessed 6.6.22).
- Zarean, E., Mostajeran, F., Dayani, Z., 2018. Effect of Dydrogesterone on the Outcome of Idiopathic Intrauterine Growth Restriction: A Double-blind Clinical Trial Study. *Adv. Biomed. Res.* 7, 93. [https://doi.org/10.4103/abr.abr\\_250\\_16](https://doi.org/10.4103/abr.abr_250_16)
- Zgheib, E., Gao, W., Limonciel, A., Aladjov, H., Yang, H., Tebby, C., Gayraud, G., Jennings, P., Sachana, M., Beltman, J.B., Bois, F.Y., 2019. Application of three approaches for quantitative AOP development to renal toxicity. *Comput. Toxicol.* 11, 1–13. <https://doi.org/10.1016/j.comtox.2019.02.001>
- Zhang, W., Hu, X., Yang, W., Gao, Y., Chen, J., 2010. Omega-3 polyunsaturated fatty acid supplementation confers long-term neuroprotection against neonatal hypoxic-ischemic brain injury through anti-inflammatory actions. *Stroke* 41, 2341–2347. <https://doi.org/10.1161/STROKEAHA.110.586081>
- Zhang, Y., Aizenman, E., DeFranco, D.B., Rosenberg, P.A., 2007. Intracellular Zinc Release, 12-Lipoxygenase Activation and MAPK Dependent Neuronal and Oligodendroglial Death. *Mol. Med.* 13, 350–355. <https://doi.org/10.2119/2007-00042.Zhang>
- Zong, L., Wei, X., Gou, W., Huang, P., Lv, Y., 2017. Zinc improves learning and memory abilities of fetal growth restriction rats and promotes trophoblast cell invasion and migration via enhancing STAT3-MMP-2/9 axis activity. *Oncotarget* 8, 115190–115201. <https://doi.org/10.18632/oncotarget.23122>

## 8 Annex

### 8.1 Docosahexaenoic acid and lactoferrin effects on the brain and placenta in a rabbit model of intrauterine growth restriction

Miriam Illa <sup>1,2</sup>, Laura Pla <sup>1</sup>, Carla Loreiro <sup>3</sup>, Christina Miranda <sup>1</sup>, Montse Mayol <sup>1</sup>, **Britta Anna Kühne** <sup>1,4</sup>, Marta Barenys <sup>4</sup>, Elisenda Eixarch <sup>1,5,6</sup>, Eduard Gratacós <sup>1,3,5,6</sup>

<sup>1</sup> BCNatal | Fetal Medicine Research Center (Hospital Clínic and Hospital Sant Joan de Déu), Universitat de Barcelona, Barcelona, Spain,

<sup>2</sup> Institut d'Investigacions Biomèdiques August Pi i Sunyer (IDIBAPS), Barcelona, Spain,

<sup>3</sup> GRET, INSA-UB and Toxicology Unit, Pharmacology, Toxicology and Therapeutical Chemistry Department, Faculty of Pharmacy, University of Barcelona, Barcelona, Spain,

<sup>4</sup> Institut de Recerca Sant Joan de Déu, Esplugues de Llobregat, Spain

|                       |                       |
|-----------------------|-----------------------|
| Journal               | PLoS ONE              |
| Impact Factor 2020    | 3.240                 |
| Quartile              | Q1                    |
| Type of authorship    | Co-author             |
| Status of publication | Submitted: 29.07.2022 |

## Summary

Intrauterine growth restriction (IUGR) is associated with suboptimal perinatal outcomes and neurodevelopment in the offspring. We hypothesize that prenatal supplementation with docosahexaenoic acid (DHA) or lactoferrin (Lf) would ameliorate these consequences. At 25 days of gestation, IUGR was surgically induced in pregnant rabbits, which were randomized as follows: no treatment, or DHA or Lf administration. DHA or Lf were administered orally once per day. Five days later, animals were delivered obtaining controls, untreated IUGR, IUGR treated with DHA and IUGR treated with Lf, and the associated placentas. At postnatal day 1, a functional evaluation was performed and, thereafter, brains were obtained. Neuronal arborization in the prefrontal cortex and the density of pre-oligodendrocytes in the corpus callosum were then evaluated. Untreated IUGR pups presented a higher percentage of stillbirth, lower birth weight, and poorer neurobehavioral performance in comparison with control pups, and these are associated with structural changes in brain and placenta. Regarding treated IUGR animals, although no significant improvements were detected in perinatal data, functional and structural effects were observed in either the brain or the placenta. DHA and Lf supplements in a rabbit model of IUGR were related to neurodevelopmental improvements and an amelioration of the placental changes.

# **Docosahexaenoic acid and lactoferrin effects on the brain and placenta in a rabbit model of intrauterine growth restriction**

Miriam Illa<sup>a,b</sup> ¶<sup>\*</sup>, Laura Pla<sup>a</sup> ¶, Carla Loreiro<sup>a,c</sup>, Cristina Miranda<sup>a</sup>, Montse Mayol<sup>a</sup>, Britta Anna Kühne<sup>a,d</sup>, Marta Barenys<sup>d</sup>, Eduard Gratacós<sup>a,b,c,e</sup>, Elisenda Eixarch<sup>a,c,e</sup>

<sup>a</sup>BCNatal | Fetal Medicine Research Center (Hospital Clínic and Hospital Sant Joan de Déu), Universitat de Barcelona, Barcelona, Spain

<sup>b</sup>Institut de Recerca Sant Joan de Déu, Esplugues de Llobregat, Spain

<sup>c</sup>Institut d'Investigacions Biomèdiques August Pi i Sunyer (IDIBAPS), Barcelona, Spain

<sup>d</sup>GRET, INSA-UB and Toxicology Unit, Pharmacology, Toxicology and Therapeutical Chemistry Department, Faculty of Pharmacy, University of Barcelona, Barcelona, Spain

<sup>e</sup>Centre for Biomedical Research on Rare Diseases (CIBER-ER), Barcelona, Spain

¶¶These authors contributed equally to this work.

Corresponding Author:

E-mail: [miriamil@clinic.cat](mailto:miriamil@clinic.cat) (MI)

# 1. Introduction

Intrauterine growth restriction (IUGR) is defined as a significant reduction in the fetal growth rate affecting 7–10% of all pregnancies in developed countries[1]. One of the most prevalent causes of IUGR is placental insufficiency, which represents one of the major causes of perinatal morbidity and mortality[2]. IUGR has been related to poorer functional performance in the neonatal period[3,4], persisting during childhood and adolescence[5,6]. Although the exact structural substrate underlying neurodevelopmental impairments in IUGR is still under evaluation, different studies have suggested that abnormal oligodendrocyte maturation and neuronal arborization could be key processes[7–11]. Despite the clear impact of this condition, there are no effective therapies to either reverse IUGR or prevent its neurodevelopmental consequences.

Clinical and experimental evidence suggests that early postnatal strategies such as breastfeeding[12], an individualized newborn developmental care and assessment program[13], and environmental enrichment[14] can partially ameliorate the neurodevelopmental impairment caused by IUGR. However, all these strategies have been applied after birth, when the adverse effects of IUGR on brain development have already been consolidated. We hypothesized that a strategy applied during the prenatal period, a “critical window of opportunity”[15], could have a more pronounced effect. Among potential therapies that could be applied during the prenatal period, docosahexaenoic acid (DHA) and lactoferrin (Lf) emerge as potential candidates. Previous evidences have demonstrated their neuroprotective role in several neurological disorders such as Parkinson’s disease and schizophrenia, and after perinatal insults such as acute hypoxic-ischemic events[16–19]. DHA, a long-chain polyunsaturated fatty acid, plays a fundamental role in central nervous system development and transfers across the placenta to reach the fetal circulation[20,21] and fetal brain[22]. Lf is a sialic acid-rich glycoprotein that also crosses the placenta and blood–brain barrier and has been involved in modulating cell-to-cell interactions and neuronal



27 outgrowth[23]. In addition, preliminary evidence has linked both therapies with some positive  
28 effects on placental development. Reduced oxidative stress and placental apoptosis has been  
29 previously described in omega-3 supplemented pregnancies[24,25], whereas Lf has been  
30 involved in cytotrophoblast endothelial cell invasion and placental vasculature  
31 enhancement[26,27]. Furthermore, a key factor of DHA and lactoferrin supplements is that  
32 they are normal bioactive components of a great diversity of foods and maternal milk, and  
33 consequently can be safely used as supplements[28].

34 Despite all these evidences of the positive effect of DHA and Lf on brain and placental  
35 development, no previous studies have evaluated the potential neuroprotective role or  
36 placental effects of these two therapies in a well characterized model of placental insufficiency.  
37 We previously demonstrated the functional and structural brain sequels and placental  
38 histological alterations related to IUGR by using a surgical IUGR rabbit model[29]. In this study  
39 we aimed to evaluate the neuroprotective effects of DHA and Lf in the brain at the functional  
40 and structural level and in the placenta structure in this animal model. For this purpose, density  
41 of pre-oligodendrocytes (pre-OLs) in the corpus callosum (CC), neuronal arborization in the  
42 frontal cortex, and placenta structure in prenatally treated IUGR animals with DHA or Lf were  
43 evaluated and this data was compared with the already published data in untreated IUGR  
44 rabbit animals[29].

45

## 46 **2. Materials and Methods**

### 47 **2.1 IUGR induction, experimental groups, and therapy** 48 **administration**

49 All procedures were performed following all the applicable regulations and guidelines  
50 of the Animal Experimental Ethics Committee (CEEA) of the University of Barcelona and were  
51 approved with the license number 03/17. The animals were provided by a certified commercial  
52 farm (Granja San Bernardo) and were acclimated at least for one week before surgery. Their

53 clinical condition was assessed by veterinary staff before starting the study. The animals were  
54 housed following local standards. All surgery was performed under general anesthesia, and  
55 all efforts were made to minimize suffering. Also, animal work has been conducted fulfilling  
56 ARRIVE's guidelines and reported accordingly[30].

57 At 25 days of gestation, a total of 19 pregnant rabbits were subjected to the IUGR  
58 induction protocol. Sample size was calculated taking into account the mortality related to the  
59 IUGR model following previous experience in the group[7,14,31,32] to include the required  
60 number of animals for each analysis (see each paragraph for detailed information). IUGR was  
61 induced by ligating 40-50% of the uteroplacental vessels of each gestational sac, whereas  
62 non-ligated gestational sacs provided normally-grown controls as previously described [31]. At  
63 the time of IUGR induction, the pregnant rabbits were randomly assigned to 3 groups: no  
64 treatment (n = 9), treatment with DHA (n = 5) and treatment with Lf (n = 5). At 30 days of  
65 gestation, cesarean section was performed obtaining living and stillborn animals and their  
66 placentas. Normally-grown controls and untreated IUGR pups were obtained from untreated  
67 mothers, whereas IUGR-DHA and IUGR-Lf pups were obtained from mothers treated with  
68 DHA or Lf, respectively. All the experimental groups were contemporaneous, were evaluated  
69 following similar protocols and by the same examiners (M.I., L.P). Functional and structural  
70 data from untreated IUGR and normally-grown controls had been discussed and published in  
71 a previous paper[7]. The present work focuses in the evaluation of the potential protective  
72 effects of DHA and Lf prenatally in IUGR. To this end, already published data from the  
73 untreated IUGR animals were used as a positive control in this study. After cesarean section,  
74 mothers were sacrificed by an overdose of pentobarbital.

75 DHA or Lf were orally administered to the pregnant rabbits once per day from day 25  
76 until the day of the cesarean section. The therapy was administered using a syringe to  
77 cautiously release the solution into the mouth. The specific dose of DHA (37 mg/kg/day) and  
78 Lf (166 mg/kg/day) was calculated taking into account previous evidence[19,33]. Doses were

79 adjusted with the formula for interspecies translation based on the body surface area  
80 (BSA)[34], obtained as follows:

$$81 \quad BSA(m^2) = 9.9x \frac{\text{rabbit weight (g)}}{10\,000}$$

82

83 and on the Km value, obtained by:

$$84 \quad k_m = \frac{\text{body weight (kg)}}{BSA}$$

85 Finally, the formula used for interspecies translation was as follows[35]:

$$86 \quad HED (mg/kg) = \text{known dose (mg/kg)}_x \frac{k_m \text{ animal of known dose}}{\text{rabbit } K_m}$$

87 The DHA was obtained from Rendon Europe Laboratories and was presented in 3 g 100%  
88 pure powder from Microalga oil Schizochytrium sp. The Lf administrated was bovine Lf  
89 containing a low concentration of iron (9.2 mg of iron per 100 g of protein) and was obtained  
90 from Farmalabor.

91

## 92 **2.2 Functional evaluation**

93 Due to differences in the mortality rate obtained in the experimental groups, the final  
94 sample included in the functional evaluation differed between groups: 12 untreated IUGR, 18  
95 IUGR-DHA, and 19 IUGR-Lf. At postnatal day 1, functional variables that previously  
96 demonstrated to be altered in IUGR[29] were evaluated in all offspring following the previous  
97 methodology described by Derrick et al.[36]. Briefly, at postnatal day 1, general motor skills,  
98 tone, reflexes, and olfactory sensitivity were evaluated in all offspring. For each animal, the  
99 testing was videotaped and variables were scored on a scale of 0 to 3 (0 = worst and 3 = best),  
100 except for tone, which was scored (0–4) according to the Ashworth scale[37] by two blinded  
101 observers (MI, LP). A detailed explanation of how each variable was assessed is given above.

102 The first part of evaluation lasted 1 minute and included the evaluation of: i. Animal  
103 posture; ii. Righting reflex (number of times the animal turned prone from the supine position

104 in 10 tries); iii. Tone (assessed by an active flexion and extension of the fore limbs and hind  
105 limbs); ii. Circular motion (evaluation of the range of movements and jumping); iii. Hind limb  
106 locomotion (assessed by grading the amount of spontaneous movement of the hind limbs); iv.  
107 Intensity of the movements; v. Duration of the movements; vi. Lineal movement (number of  
108 times the animal crossed a perpendicular line of 15 cm when walking straight); vii. The mean  
109 of the shortest fore–hind paw distance (evaluated when the animal walks in a straight line).

110 After this first minute of evaluation, suck and swallow, head turning, and olfaction were  
111 evaluated: i. Suck and swallow (assessed by the introduction of formula (Lactadiet with omega  
112 3; Royal Animal) into the pup's mouth with a plastic pipette); ii. Head turning (assessed by  
113 observing the head and body movements associated with the suction reflex); iii. Olfaction  
114 (counting the time in seconds the animal moves the nose away from a cotton swab soaked  
115 with pure ethanol when this was placed close to the nose). The score grading used for each  
116 variable is detailed in Supplementarial Table 1 (S1 Table).

117

## 118 **2.3 Sample collection**

119 After the cesarean section, placentas were obtained, carefully washed in saline  
120 solution, weighed, fixed for 24 hours in 10% formalin and embedded in paraffin.

121 After functional evaluation, newborns were weighed and sacrificed by decapitation after  
122 the administration of ketamine (35 mg/kg) and xylazine (5mg/kg) intramuscularly. All brains  
123 were carefully dissected and fixed according to the analysis performed. Four brains from each  
124 group were randomly selected for the Golgi-Cox staining protocol and were processed  
125 according to it (detailed below). The other brains (11 untreated IUGR, 14 IUGR-DHA, 15 IUGR-  
126 DHA) were fixed for 24 hours in 10% formalin, dehydrated for 48 hours with sucrose 30% and  
127 finally frozen at  $-80^{\circ}\text{C}$ .

128

## 129 **2.4 Histological procedures**

### 130 **2.4.1 Placenta**

131 Five placentas from each group were randomly selected for histological evaluation  
132 based on findings from previous work in pregnant rabbits[7]. All the placentas were evaluated  
133 except one from the IUGR-DHA group, in which the analysis could not be performed owing to  
134 technical problems with the processing. Two consecutive slices (4  $\mu$ m) of each placenta from  
135 paraffin blocks were stained following a hematoxylin and eosin standard protocol. The  
136 pathologist was blinded to the experimental groups. The analyses were performed on two  
137 different regions of the placenta: the decidua basalis (maternal part) and the labyrinth zone  
138 (fetal part). Ischemia, necrosis, fibrin, and calcifications were assessed in the decidua, while  
139 ischemia, vascular collapse, congestion, and calcifications were evaluated in the labyrinth  
140 zone. Ischemia and fibrin were expressed as a percentage, necrosis was assessed by the  
141 presence of karyorrhexis and karyolysis, and the remaining variables were evaluated with a  
142 semiquantitative system that graded each lesion from 0 to 5. The grading criteria followed  
143 were: 0) Unremarkable; 1) Minimal; 2) Mild; 3) Moderate; 4) Marked; 5) Severe.

144

### 145 **2.4.2 O4-immunoreactive oligodendrocytes**

146 Eight formalin-fixed brains per group were selected for the O4-immunoreactive  
147 oligodendrocyte evaluation. The sample size for oligodendrocyte evaluation was calculated  
148 taking into consideration previous studies with the same animal model[7,32]. Three coronal  
149 sections of 40  $\mu$ m per animal at the level of the genu CC and with reference to the bregma  
150 were obtained and processed as previously described[7]. Briefly, slices were incubated  
151 overnight with anti-oligodendrocyte marker O4 (1:50, Chemicon) followed by 1% Hoechst  
152 33258 (1:1000, Thermofischer) incubation for cellular nucleus visualization. Finally, slices were  
153 incubated with the specific secondary antibody conjugated to 488 Alexa Fluor (1:400,  
154 MoBitec). Immunoreactive sites were observed under the confocal microscope and images  
155 were taken as previously described[7]. The number of the total cell nuclei (stained with  
156 Hoechst) and the number of cells with fluorescent staining around the nucleus (O4-

157 immunoreactive oligodendrocytes) were counted using the software ImageJ. O4-  
158 immunoreactive oligodendrocyte density (immune-reactive cells/mm<sup>2</sup>) was then calculated.  
159 The evaluation for each experimental group was blinded for the evaluator (LP). The anti-O4  
160 antibody was selected as a marker for the latter stages of oligodendrocyte maturation (O4-  
161 OL), which include pre-OLs, pre-myelinating OL, and myelinating OL[38]. Since pre-OL cells  
162 are the most predominant oligodendrocytes in rabbits at the day of evaluation, we assumed  
163 that the O4 marker used mainly stained the pre-OL cells[39].

164

### 165 **2.4.3 Neuronal arborization (Golgi-Cox staining)**

166 Four brains per group were included in the neuronal arborization analyses, similarly to  
167 previous studies[7,8]. Neuronal arborization evaluation was performed as previously  
168 described[7]. Briefly, vibratome was used to obtain 100 µm serial and coronal sections that  
169 were processed for Golgi-Cox impregnation with the FD Rapid Golgi Stain kit (FD  
170 Neurotechnologies Inc.). Coronal slices with reference to the bregma were observed under  
171 ×40 objective magnification in an AF6000 epifluorescence microscope. Five pyramidal  
172 neurons that fulfilled the inclusion criteria from the frontal cortex (at the level of premotor cortex)  
173 per brain hemisphere were selected randomly and one image per neuron was obtained. In  
174 order to obtain the dendritic tree of each neuron, different Z-stacks per each image were  
175 needed. The inclusion criteria were: pyramidal neurons within layer II and III and complete  
176 filling of the dendritic tree with well-defined endings. The evaluation for each experimental  
177 group was blinded for the evaluators (LP, MM). The parameters evaluated were: i) area of the  
178 soma (obtained by manual delineation of the shape of the neuronal soma in a 2D image); ii)  
179 total basal dendritic length (obtained after performing manual delineation of the length of each  
180 basal dendrite and then calculating the sum of all lengths from all basal dendritic branches);  
181 iii) basal dendritic complexity, including number of dendrites (obtained by manual counting)  
182 and number of intersections for each Sholl ring (following the sholl analyses technic previously

183 published [40] and standardized in our model [7]). The study design is summarized in Figure 1  
184 (Fig 1).

185

186 **Fig 1. Study design.** 1A) DHA or Lf administration to the pregnant rabbits; 1B) Unilateral  
187 ligation of 40–50% of uteroplacental vessels at 25 days of pregnancy; 1C) Living newborns  
188 and placenta at 30 days of pregnancy on the day of the cesarean section; Neurobehavioral  
189 evaluation of righting reflex (2A), smelling test (2B), locomotion (2C) and sucking and  
190 swallowing (2D) performed at +1 postnatal day; 3A O4-immunoreactive oligodendrocyte  
191 density evaluation in the CC; 3B) Neuronal arborization analyses in the frontal cortex.

192

193

## 194 **2.5 Statistical analyses**

195 The software packages STATA 14.0 and GraphPad 5 were used for statistical analyses  
196 and graphical representation. For quantitative variables, normality was assessed by the  
197 Shapiro-Wilk test and homoscedasticity was determined by Levene's Test, except for variables  
198 with more than 30 observations (Golgi-Cox variables) for which normal distribution was already  
199 assumed. For ordinal variables, non-normal distribution was assumed. The descriptives of the  
200 variables were expressed as mean and standard deviation (SD) for normal distributions,  
201 whereas median and interquartile range (IQR) were used for non-normal distributions and  
202 ordinal variables. Appropriate statistical tests were used according to the variable: ANOVA  
203 with Dunnett's multiple comparison test was used for continuous variables (birth weight,  
204 placental ischemia and fibrin deposition, some functional variables, pre-OL and arborization  
205 parameters), Kruskal-Wallis with Dunn's multiple comparison test for ordinal variables  
206 (placental calcifications, collapse and congestion and some functional variables) and chi-  
207 squared for binary variables (survival). Statistical significance was declared at  $p < 0.05$  in all  
208 variables evaluated.

209

## 210 3. Results

### 211 3.1 Perinatal data

212 Untreated IUGR animals presented a significantly reduction of survival along with a lower birth  
213 weight in comparison to controls [7]. In comparison with untreated IUGR animals, treated IUGR  
214 did not present any statistical improvement in stillbirth and birth weight, independently of the  
215 treatment group (stillbirth: untreated IUGR 42%; IUGR-DHA 57%,  $p=0.03$ ; IUGR-Lf 53%,  $p=$   
216  $0.11$ ; birth weight: untreated IUGR 38.65 g (9.84); IUGR-DHA 40.4 g (6.81),  $p=0.39$ ; IUGR-Lf  
217 37.7 g (7.93),  $p=1.00$ ).

218

### 219 3.2 Functional results

220 Animals prenatally treated with DHA (IUGR-DHA) presented a significant improvement in  
221 righting reflex, intensity, sucking and swallowing and head turning, with no improvement in the  
222 circular motion variable. Regarding IUGR-Lf group, a significant improvement in sucking and  
223 swallowing was observed with no significant improvement in the rest of variables (Table 1).

224

225 **Table 1. Functional results in the study groups.**

| Variables                  | Untreated IUGR (n=12) | IUGR-DHA (n = 18) | IUGR-Lf (n= 19) |
|----------------------------|-----------------------|-------------------|-----------------|
| Righting reflex, num       | 8 (5)                 | 10 (0)*           | 6 (4)           |
| Circular motion, sc        | 1 (2)                 | 2 (1)             | 2 (1)           |
| Intensity, sc              | 2 (1)                 | 3 (0)*            | 2 (1)           |
| Sucking and swallowing, sc | 1 (2)                 | 3 (1)*            | 3 (0)*          |
| Head turning, sc           | 2 (2)                 | 3 (0) *           | 3 (1)           |

226 Results are given as a median and interquartile range (median (IQR)). Abbreviations: num:

227 number; sc: score \* $p<0.05$



228

229 **3.3 Placental findings**

230 No differences were observed in the placental weight across groups (untreated IUGR: 5.23 g;  
 231 IUGR-DHA: 4.96 g; IUGR-Lf: 5.05 g). Overall, DHA and Lf groups presented a significant  
 232 reduction of the percentage of ischemia in the decidua basalis in comparison to untreated  
 233 IUGR. In addition, IUGR-Lf group showed a significant decrease in ischemia and, a reduction  
 234 of vascular collapse accompanied by an increase in vascular channel dilation in the labyrinth  
 235 zone in comparison with untreated IUGR (Table 2 and Fig 2).

236

237 **Table 2. Placental histopathological findings in the study groups.**

| DECIDUA BASALIS     |                       |                 |                |
|---------------------|-----------------------|-----------------|----------------|
| Variables           | Untreated IUGR (n= 5) | IUGR-DHA (n= 5) | IUGR-Lf (n= 5) |
| Ischemia (%)        | 99.8 (0.45)           | 88.3 (5.69)*    | 89.0 (9.62)*   |
| Necrosis (Y/N)      | Y                     | Y               | Y              |
| Fibrin (%)          | 4.40 (0.55)           | 4.25 (0.50)     | 4.40 (0.55)    |
| Calcification (0-5) | 3 (3.5)               | 3 (1.5)         | 2 (1.5)        |
| LABYRINTH ZONE      |                       |                 |                |
| Variables           | Untreated IUGR (n= 5) | IUGR-DHA (n= 5) | IUGR-Lf (n= 5) |
| Ischemia (%)        | 96.0 (1.73)           | 97.0 (2.45)     | 89.0 (4.18)*   |
| Collapse (0–5)      | 3 (0)                 | 2 (1.5)         | 0 (1.5)*       |
| Congestion (0–5)    | 0 (0)                 | 0 (1.5)         | 4 (1.5)*       |
| Calcification (0–5) | 4 (4)                 | 3 (1.5)         | 4 (1.5)        |

238 Results are mean and standard deviation (mean (SD)) for continuous variables (expressed as  
 239 a percentage) and median and interquartile range (median(IQR)) for ordinal variables  
 240 (expressed as a semiquantitative grading system, score = 0–5). The nomenclature of Y (yes)  
 241 or N (no) was used for the variable of necrosis. \*p<0.05

242

243 **Fig 2. Placenta histological findings in the study groups.** A. Representative images of  
244 calcification (arrow) in decidua basalis among the study groups. B. Representative images of  
245 vascular channel congestion (arrow) in the labyrinth zone among the study groups.  
246 Abbreviations: IUGR = intrauterine growth restriction, DHA = docosahexaenoic acid, Lf =  
247 Lactoferrin

248

### 249 **3.4 O4-immunoreactive oligodendrocyte results**

250 A significant increase in the percentage of O4-immunoreactive oligodendrocytes  
251 density (immune-reactive cells/mm<sup>2</sup>) was observed in the IUGR-DHA group in comparison  
252 with the untreated IUGR group (DHA vs untreated IUGR: 1.13 cells/mm<sup>2</sup> (0.18) vs 0.86  
253 cells/mm<sup>2</sup> (0.21),  $p = 0.04$ ). No statistical differences were observed in the IUGR-Lf groups  
254 when comparing to untreated IUGR (shown in Fig 3).

#### **Fig 3. O4-immunoreactive oligodendrocytes in the CC in the study groups.**

255 \*  $p < 0.05$  between the untreated IUGR and IUGR-DHA.

Abbreviations: untreated IUGR = intrauterine growth restriction with no treatment; IUGR-DHA  
= intrauterine growth restriction treated with DHA; IUGR-Lf = intrauterine growth restriction  
treated with Lf.

256

### 257 **3.5 Neuronal arborization**

258 IUGR-DHA group showed higher values in the total dendritic length, area of soma and number  
259 of intersections per Sholl ring (shown in Fig 4 and Table 3) and a significant increase in the  
260 number of primary and secondary dendrites, with no significant changes in the more distal  
261 dendrites when compared with the pups of untreated animals (shown in Fig 4 and Table 3).  
262 The IUGR-Lf animals presented a decrease in the majority of the neuronal arborization

263 parameters when compared with the pups of untreated IUGR (shown in Figs 4 and 5 and Table  
264 3).

265

266 **Fig 4. Number of intersections per Sholl ring in the study groups.**

267 \*  $p < 0.05$  between the untreated IUGR and IUGR-DHA

268 #  $p < 0.05$  between the untreated IUGR and IUGR-Lf .

269 Abbreviations: untreated IUGR = intrauterine growth restriction with no treatment; IUGR-DHA

270 = intrauterine growth restriction treated with DHA; IUGR-Lf = intrauterine growth restriction

271 treated with Lf.

272

273 **Fig 5. Number of each basal dendritic branch in the frontal cortex in the study groups.**

274 Statistical significance was declared at  $p < 0.05$  between untreated IUGR and IUGR-DHA or

275 IUGR-Lf (\*).

276 Abbreviations: untreated IUGR = intrauterine growth restriction with no treatment; IUGR-DHA

277 = intrauterine growth restriction treated with DHA; IUGR-Lf = intrauterine growth restriction

278 treated with Lf.

279

280 **Table 3. Dendritic arborization parameters in the study groups.**

| Variables                             | Untreated IUGR ( $n = 40$ ) | IUGR-DHA ( $n = 40$ ) | IUGR-Lf ( $n = 40$ ) |
|---------------------------------------|-----------------------------|-----------------------|----------------------|
| Area of soma, $\mu\text{m}^2$         | 366.97 (76.7)               | 446.1 (165.0)*        | 313.8 (95.2)         |
| Total intersections, no.              | 47.03 (13.4)                | 52.3 (16.3)           | 34.2 (7.74)*         |
| Total dendritic length, $\mu\text{m}$ | 623.01 (173.3)              | 723.8 (230.8)*        | 472.1 (121.3)*       |
| Primary dendrites, no.                | 6.83 (1.71)                 | 8.95 (2.50)*          | 7.60 (2.07)          |
| Secondary dendrites, no.              | 7.65 (2.17)                 | 9.70 (3.38)*          | 7.48 (2.49)          |
| Tertiary dendrites, no.               | 4.75 (2.30)                 | 3.93 (2.83)           | 2.85 (2.43)*         |

|                           |             |              |              |
|---------------------------|-------------|--------------|--------------|
| Quaternary dendrites, no. | 2.10 (2.35) | 1.43 (2.10)  | 0.83 (1.28)* |
| Quinary dendrites, no.    | 0.75 (1.26) | 0.43 (0.98)  | 0.10 (0.44)* |
| Senary dendrites, no.     | 0.30 (0.97) | 0.00 (0.00)* | 0.00 (0.00)* |

281 Results are expressed as mean and standard deviation. \*p<0.05

282

## 283 4. Discussion

284 The present study explores the functional and structural effects on fetal  
285 neurodevelopment and placental insufficiency of the maternal administration of DHA and Lf in  
286 pregnancies complicated by IUGR. In this study we reported that maternal supplementation  
287 with DHA present protective effects in the brain, whereas Lf effect seemed to be more confined  
288 in the placenta in the form of IUGR secondary to placental insufficiency.

289

### 290 4.1 Perinatal data and placental evaluation

291 Our data showed that prenatal administration of DHA and Lf in an IUGR rabbit model  
292 was not related to improvements in survival and birth weight. These results are in line with  
293 previous studies showing no improvements in birth weight, nor in fetal survival after Omega-3  
294 supplementation in human IUGR pregnancies[41] and after Lf supplementation in an IUGR rat  
295 model[42].

296 Regarding the histological findings in the placenta, DHA was related with a reduction  
297 in the proportion of ischemia in the decidua basalis. This is in line with previous experimental  
298 data that showed a reduction in the placental oxidative stress in the placenta of normal  
299 pregnancies of rats supplemented with an omega-3 diet [24]. In the clinical setting, reduced  
300 placental apoptosis has been described in normal pregnancies after DHA administration[25].  
301 In the same line, Lf group showed a reduction in the proportion of ischemia in the decidua  
302 basalis and in the labyrinth zone. Furthermore, significant vascular channel dilation in

303 comparison with the placentas of untreated IUGR animals was observed. This finding could  
304 be explained by the fact that Lf, especially apoLf, enhances matrix metalloproteinase-2  
305 expression in the cytotrophoblast, which promotes endothelial cell invasion[26] and increases  
306 placental vasculature[27]. However, this improvement did not lead to an improvement in  
307 perinatal outcomes, perhaps due to the fact that Lf only improved the vasculature with no  
308 significant effects on fibrin deposition and necrosis, which could be determinants of perinatal  
309 outcomes. Further studies including fetal and maternal Doppler evaluations and specific  
310 vascular immunohistochemistry or matrix metalloproteinase-2 expression detection would be  
311 of help in evaluating the meaning of these findings.

312

## 313 **4.2 Neurodevelopmental effects of the perinatal** 314 **administration of DHA in IUGR**

315 Overall, our data demonstrated the positive effect of DHA in ameliorating the functional  
316 and structural brain changes induced by IUGR in the neonatal period. Maternal administration  
317 of DHA was associated with functional improvements in most of the functional variables that  
318 have been demonstrated to be impaired in the untreated IUGR animals, similar to those  
319 previously reported in a neonatal acute hypoxic-ischemic[43] and in transient focal cerebral  
320 ischemia[44] mouse models.

321 Regarding structural brain results, we observed a significant improvement of the pre-  
322 OLs in the DHA group. These results are in line with previous findings described by our group  
323 in an in vitro IUGR rabbit neurosphere model, where the impairment of OL differentiation was  
324 reversed after the administration of DHA [45]. Besides, previous evidence in other animal  
325 models suggests a protective role of Omega 3 in preserving myelin and oligodendrocytes in a  
326 mouse model of traumatic brain injury[46], promoting remyelination in a rat model of  
327 periventricular leukomalacia[47] and after neonatal hypoxia and ischemia in rats[18].  
328 Concerning IUGR, postnatal nutrient supply including DHA has shown increased white matter

329 (WM) volume in IUGR piglets[48] and improved WM maturation in human babies born  
330 prematurely [49]. The improvement in pre-OLs observed after DHA supplementation in the CC  
331 might explain the functional improvements detected, since Pre-OLs act as a reservoir of cells  
332 for later differentiation and myelination processes and these have been described to be  
333 essential for normal motor circuit function[50].

334         Regarding neuronal arborization, our results also suggest a protective role of DHA on  
335 several parameters. These results are in the same direction with previous data showing  
336 positive effects of Omega 3 fatty acids on dendritic arborization and new spine formation in the  
337 hippocampus during normal ageing[51,52] and on neurite length and branching in hippocampal  
338 embryonic neuronal cell cultures[53,54]. Interestingly, previous literature has demonstrated the  
339 link between enhanced neuronal dendritic growth in the motor cortex with motor functional  
340 improvements[55]. In this study, neuronal arborization has been evaluated in the frontal  
341 cortex, which has been involved in associative learning in rabbits[56]. Therefore, the functional  
342 correspondence of these neuronal arborization results in the frontal cortex might be assessed  
343 by evaluating other functional domains, rather than motor and reflex variables, such as social  
344 interaction, anxiety traits, or cognition.

345

### 346 **4.3 Neurodevelopmental effects of the perinatal** 347 **administration of Lf in IUGR**

348         Maternal administration of Lf was associated with significant improvements in sucking  
349 and swallowing functional variable of the pups compared with untreated IUGR pups. This could  
350 not be contrasted with previous evidence as there is a lack of functional data reported in  
351 hypoxic-ischemia and IUGR studies evaluating the neuroprotective role of Lf in this setting.

352         At a structural level, in our study Lf seemed to have no effect in the pre-OL cell  
353 population. This finding is aligned with the previous study described by our group in the IUGR  
354 rabbit neurosphere model, where no OL improvement was observed after the administration

355 of Lf[45]. On the contrary, these findings go against previous evidence in which a positive effect  
356 of Lf on the oligodendrocyte lineage was described, although the effect was in earlier stages  
357 of oligodendrocyte development: oligodendrocyte precursor NG2+[57]. It should be noted that  
358 we only included the evaluation of O4+ immunoreactivity oligodendrocytes. The evaluation of  
359 earlier oligodendrocyte stages (such as NG2+) would be required in future studies to further  
360 evaluate the real role of Lf in the WM in our animal model. Regarding the neuronal arborization  
361 results, the prenatal administration of Lf also had a limited effect, with a significant reduction  
362 in the area of soma, total number of intersections, total dendritic length, and number of tertiary,  
363 quaternary, and quinary dendrites in comparison with IUGR pups born to untreated mothers.  
364 Although previous data regarding the specific effect of Lf on neuronal arborization at the same  
365 neonatal age as in our study are not available, the positive effects of Lf on neuroplasticity, cell  
366 migration, and the differentiation of neuronal progenitor cells during the postnatal period in  
367 piglets have been described[23,58]. Similarly, Lf demonstrated a tendency to improve  
368 synaptogenesis in a hypocaloric IUGR rat model supplemented with Lf during gestation and  
369 lactation at postnatal day 7[57]. Future evaluation of more mature stages of neuronal  
370 connectivity in our animal model such as dendrite spine formation and synaptogenesis would  
371 provide additional insight regarding the mechanisms by which Lf exerts its neuroprotective role  
372 as suggested in previous studies.

373         Regarding the decrease in the more distal dendrites observed in the IUGR-Lf, we  
374 speculate that Lf might avoid the compensatory mechanism described in our previous paper  
375 in IUGR pups of untreated mothers in which a significant increase of the more distal dendrites  
376 was obtained in comparison with normally-grown pups[7,59].

377

## 378 **4.4 Strengths and limitations**

379         Among the strengths of the study was the use of a well described experimental  
380 model[31,60,61] that has consistently shown to reproduce the perinatal (birth weight and  
381 survival rate) and neurodevelopmental effects of IUGR in humans. In addition, among all the

382 animal species used in investigations of IUGR, the rabbit has been described as presenting  
383 higher similarities to humans in terms of brain maturation in comparison with other species,  
384 making this a reliable model for obtaining data that is translational to humans[62]. Also, the  
385 use of an experimental model allowed extensive functional and neurostructural analysis to  
386 span a significant life period of the animals. Another strength of the study is that the DHA and  
387 Lf effect has been evaluated at different levels: through histology of the placenta, in functional  
388 evaluation, and through WM and grey matter (GM) assessments, giving robustness to the  
389 conclusions of the effects of these therapies on our model.

390 We acknowledge that there are limitations in the study. Lack of a true control or sham  
391 group is a major limitation as no baseline comparison could be done. Although DHA and Lf did  
392 not present any effect in control neurospheres from our IUGR in vitro model[45], future in vivo  
393 studies including normally grown animals prenatally treated with DHA or Lf should be  
394 considered. In reference to the histological findings of the placenta, additional stainings  
395 including specific vascular markers (eg. VEGF, CD31) would give additional insights in the  
396 results obtained in this paper. Another limitation of the study was that histological analyses  
397 were restricted to the frontal cortex and CC. Other brain regions such as the hippocampus or  
398 ventricular zone have been documented to be key structures altered in IUGR[63,64] and would  
399 therefore be interesting to evaluate. Although the molecular mechanisms and pathways  
400 involved in the effects of DHA and Lf are beyond the scope of this study, the description of the  
401 molecular mechanisms by which both therapies exert their neuroprotective role would be  
402 useful in understanding the differences in the structural effects of both therapies. Finally, we  
403 acknowledge that sex is an important factor in brain development. However, gender could not  
404 be assessed in the study groups, as this could not be clearly identified at neonatal stage.

405

## 406 **5. Conclusions**



407           In summary, our study provides novel insights into the potential protective effects of  
408 DHA and Lf administered to mothers with pregnancies affected by IUGR due to placental  
409 insufficiency during the prenatal period. We demonstrated that DHA supplementation had a  
410 positive effect on brain development ameliorating the brain changes induced by IUGR with  
411 some positive impact into the placental insufficiency. On the contrary, Lf seemed to have a  
412 more relevant effect in ameliorating the placental changes rather than having a significant  
413 neuroprotective effect in our IUGR model. Finally, results obtained in this study support the  
414 implementation of clinical studies testing the potential role of DHA and Lf as neuroprotective  
415 strategies in IUGR.

## 6. References

- [1] Kady SM, Gardosi J. Perinatal mortality and fetal growth restriction. *Best Pract Res Clin Obstet Gynaecol* 2004;18:397–410.
- [2] Malhotra A, Allison BJ, Castillo-Melendez M, Jenkin G, Polglase GR, Miller SL. Neonatal morbidities of fetal growth restriction: Pathophysiology and impact. *Front Endocrinol (Lausanne)* 2019;10:1–18.
- [3] Figueras F, Oros D, Cruz-Martinez R, Padilla N, Hernandez-Andrade E, Botet F, et al. Neurobehavior in term, small-for-gestational age infants with normal placental function. *Pediatrics* 2009;124:e934–41.
- [4] Feldman R, Eidelman AI. Neonatal state organization, neuromaturation, mother-infant interaction, and cognitive development in small-for-gestational-age premature infants. *Pediatrics* 2006;118:e869-78.
- [5] Leitner Y, Fattal-Valevski A, Geva R, Eshel R, Toledano-Alhadeif H, Rotstein M, et al. Neurodevelopmental outcome of children with intrauterine growth retardation: A longitudinal, 10-Year prospective study. *J Child Neurol* 2007;22:580–7.
- [6] Tideman E, Mar KS, Ley D. Cognitive function in young adults following intrauterine growth restriction with abnormal fetal aortic blood flow. *Ultrasound Obs Gynecol* 2007;29:614–8.
- [7] Pla L, Illa M, Loreiro C, Lopez MC, Vázquez-Aristizabal P, Anna B, et al. Structural brain changes at the neonatal period in a rabbit model of Intrauterine Growth Restriction. *Dev Neurosci* 2020.
- [8] Dean JM, McClendon E, Hansen K, Azimi-Zonooz A, Chen K, Riddle A, et al. Prenatal Cerebral Ischemia Disrupts MRI-Defined Cortical Microstructure Through Disturbances in Neuronal Arborization. *Sci Transl Med* 2013;5:168ra7-168ra7.
- [9] Dieni S, Rees S. Dendritic morphology is altered in hippocampal neurons following prenatal compromise. *J Neurobiol* 2003;55:41–52.

- [10] Back SA, Han BH, Luo NL, Chricton CA, Xanthoudakis S, Tam J, et al. Selective vulnerability of late oligodendrocyte progenitors to hypoxia- ischemia. *J Neurosci* 2002;22:455–63.
- [11] Tolcos M, Bateman E, O’Dowd R, Markwick R, Vrijisen K, Rehn A, et al. Intrauterine growth restriction affects the maturation of myelin. *Exp Neurol* 2011;232:53–65.
- [12] Rao MR, Hediger ML, Levine RJ, Naficy a B, Vik T. Effect of breastfeeding on cognitive development of infants born small for gestational age. *Acta Paediatr* 2002;91:267–74.
- [13] Als H, Duffy FH, McAnulty G, Butler SC, Lightbody L, Kosta S, et al. NIDCAP improves brain function and structure in preterm infants with severe intrauterine growth restriction. *J Perinatol* 2012;32:797–803.
- [14] Illa M, Brito V, Pla L, Eixarch E, Arbat-Plana A, Batallé D, et al. Early Environmental Enrichment Enhances Abnormal Brain Connectivity in a Rabbit Model of Intrauterine Growth Restriction. *Fetal Diagn Ther* 2018;44:184–93.
- [15] Andersen SL. Trajectories of brain development : point of vulnerability or window of opportunity? *Neurosci Biobehav Rev* 2003;27:3–18.
- [16] Rousseau E, Michel PP, Hirsch EC. The Iron-Binding Protein Lactoferrin Protects Vulnerable Dopamine Neurons from Degeneration by Preserving Mitochondrial Calcium Homeostasis. *Mol Pharmacol* 2013;84:888–98.
- [17] Zugno AI, Chipindo HL, Volpato AM, Budni J, Steckert A V, Oliveira MB De, et al. Omega-3 prevents behavior response and brain oxidative damage in the ketamine model of schizophrenia. *Neuroscience* 2014;259:223–31.
- [18] Arteaga O, Revuelta M, Urigüen L, Martínez-Millán L, Hilario E, Álvarez A. Docosahexaenoic Acid Reduces Cerebral Damage and Ameliorates Long-Term Cognitive Impairments Caused by Neonatal Hypoxia-Ischemia in Rats. *Mol Neurobiol* 2016;54:7137–55.
- [19] Looij Y Van De, Ginet V, Chatagner A, Toulotte A, Somm E, Hüppi PS, et al.

- Lactoferrin during lactation protects the immature hypoxic- ischemic rat brain. *Ann Clin Transl Neurol* 2014;1:955–67.
- [20] Innis SM. Essential Fatty Acid Transfer and Fetal Development. *Placenta* 2005;26:S70–5.
- [21] Gil-Sánchez A, Larqué E, Demmelmair H, Acien MI, Faber FL, Parrilla JJ, et al. Maternal-fetal in vivo transfer of [<sup>13</sup>C]docosahexaenoic and other fatty acids across the human placenta 12 h after maternal oral intake. *Am J Clin Nutr* 2010;92:115–22.
- [22] Ikeno M, Okumura A, Hayakawa M, Kitamura Y, Suganuma H, Yamashiro Y, et al. Fatty acid composition of the brain of intrauterine growth retardation rats and the effect of maternal docosahexaenoic acid enriched diet. *Early Hum Dev* 2009;85:733–5.
- [23] Wang B. Molecular Determinants of Milk Lactoferrin as a Bioactive Compound in Early Neurodevelopment and Cognition. *J Pediatr* 2016;173:S29–36.
- [24] Jones ML, Mark PJ, Mori TA, Keelan JA, Waddell BJ. Maternal Dietary Omega-3 Fatty Acid Supplementation Reduces Placental Oxidative Stress and Increases Fetal and Placental Growth in the Rat. *Biol Reprod* 2013;88:37, 1–8.
- [25] Wietrak E, Kamiński K, Leszczyńska-Gorzela B, Oleszczuk J. Effect of Docosahexaenoic Acid on Apoptosis and Proliferation in the Placenta: Preliminary Report. *Biomed Res Int* 2015;2015.
- [26] Lopez V, Kelleher SL, Lönnerdal B. Lactoferrin receptor mediates apo- but not holo-lactoferrin internalization via clathrin-mediated endocytosis in trophoblasts. *Biochem J* 2008;411:271–8.
- [27] Chen J, Khalil RA. Matrix Metalloproteinases in Normal Pregnancy and Preeclampsia. *Prog Mol Biol Transl Sci* 2017;148:87–165.
- [28] Boquien CY. Human milk: An ideal food for nutrition of preterm newborn. *Front Pediatr* 2018;6:1–9.
- [29] Pla L, Illa M, Loreiro C, Lopez MC, Vázquez-Aristizabal P, Kühne BA, et al. Structural

- Brain Changes during the Neonatal Period in a Rabbit Model of Intrauterine Growth Restriction. *Dev Neurosci* 2021;42:217–29.
- [30] du Sert NP, Hurst V, Ahluwalia A, Alam S, Avey MT, Baker M, et al. The arrive guidelines 2.0: Updated guidelines for reporting animal research. *PLoS Biol* 2020;18:e300041.
- [31] Eixarch E, Figueras F, Hernández-Andrade E, Crispi F, Nadal A, Torre I, et al. An experimental model of fetal growth restriction based on selective ligation of uteroplacental vessels in the pregnant rabbit. *Fetal Diagn Ther* 2009;26:203–11.
- [32] Barenys M, Illa M, Hofrichter M, Loreiro C, Pla L, Klose J, et al. Rabbit neurospheres as a novel in vitro tool for studying neurodevelopmental effects induced by intrauterine growth restriction (IUGR). *Stem Cells Transl Med* 2020;10:1–13.
- [33] Greenberg JA, Bell SJ, Ausdal W Van. Omega-3 Fatty Acid Supplementation During Pregnancy. *Rev Obstet Gynecol* 2008;1:162–9.
- [34] Zehnder AM, Hawkins MG, Trestrail EA, Holt RW, Kent MS. Calculation of body surface area via computed tomography–guided modeling in domestic rabbits (*Oryctolagus cuniculus*). *Am J Vet Res* 2012;73:1859–63.
- [35] Anroop B, Nair SJ. A simple practice guide for dose conversion between animals and human. *J Basic Clin Pharm* 2016;7:27–31.
- [36] Derrick M, Luo NL, Bregman JC, Jilling T, Ji X, Fisher K, et al. Preterm Fetal Hypoxia–Ischemia Causes Hypertonia and Motor Deficits in the Neonatal Rabbit: A Model for Human Cerebral Palsy? *J Neurosci* 2004;24:24–34.
- [37] Damiano DL, Quinlivan JM, Owen BF, Payne P, Nelson KC, Abel MF. What does the Ashworth scale really measure and are instrumented measures more valid and precise? *Dev Med Child Neurol* 2002;44:112–8.
- [38] Kuhn S, Gritti L, Crooks D, Dombrowski Y. Oligodendrocytes in Development, Myelin Generation and Beyond. *Cells* 2019;8:1424.
- [39] Saadani-makki F, Kannan S, Lu X, Janisse J, Dawe E, Edwin S, et al. Intrauterine

- administration of endotoxin leads to motor deficits in a rabbit model: a link between prenatal infection and cerebral palsy. *Am J Obstet Gynecol* 2008;199:651. e1-651. e7.
- [40] Sholl D a. Dendritic organization in the neurons of the visual and motor cortices of the cat. *J Anat* 1953;87:387–406.
- [41] Saccone G, Berghella V, Maruotti GM, Sarno L, Martinelli P. Omega-3 supplementation during pregnancy to prevent recurrent intrauterine growth restriction: Systematic review and meta-analysis of randomized controlled trials. *Ultrasound Obstet Gynecol* 2015;46:659–64.
- [42] Somm E, Larvaron P, van de Looij Y, Toulotte A, Chatagner A, Faure M, et al. Protective effects of maternal nutritional supplementation with lactoferrin on growth and brain metabolism. *Pediatr Res* 2014;75:51–61.
- [43] Mayurasakorn K, Niatsetskaya Z V, Sosunov SA, Williams JJ, Zirpoli H, Vlasakov I, et al. DHA but Not EPA Emulsions Preserve Neurological and Mitochondrial Function after Brain Hypoxia-Ischemia in Neonatal Mice. *PLoS One* 2016;11:e0160870.
- [44] Jian X post-stroke therapeutic regimen with omega-3 polyunsaturated fatty acids that promotes white matter integrity and beneficial microglial responses after cerebral ischemia, Pu H, Hu X, Wei Z, Hong D, Zhang W, et al. A post-stroke therapeutic regimen with omega-3 polyunsaturated fatty acids that promotes white matter integrity and beneficial microglial responses after cerebral ischemia. *Transl Stroke Res* 2016;7:548–61.
- [45] Kühne BA, Vázquez.Aristizabal P, Fuentes-Amella M, Pla L, Loreiro C, Gómez-Catalán J et al. Docosahexaenoic acid and Melatonin prevent impaired oligodendrogenesis induced by Intrauterine growth restriction. *Biomedicines* 2022; 10, 1205.
- [46] Pu H, Guo Y, Zhang W, Huang L, Wang G, Liou AK, et al. Omega-3 polyunsaturated fatty acid supplementation improves neurologic recovery and attenuates white matter injury after experimental traumatic brain injury. *J Cereb Blood Flow Metab*

- 2013;33:1474–84.
- [47] Tuzun F, Kumral A, Dilek M, Ozbal S, Ergur B, Yesilirmak DC, et al. Maternal omega-3 fatty acid supplementation protects against lipopolysaccharide-induced white matter injury in the neonatal rat brain. *J Matern Neonatal Med* 2012;25:849–54.
- [48] Caputo MP, Williams JN, Drnevich J, Radlowski EC, Larsen RJ, Sutton BP, et al. Hydrolyzed Fat Formula Increases Brain White Matter in Small for Gestational Age and Appropriate for Gestational Age Neonatal Piglets. *Front Pediatr* 2020;8:32.
- [49] Strømme K, Blakstad EW, Moltu SJ, Almaas AN, Westerberg AC, Amlien IK, et al. Enhanced nutrient supply to very low birth weight infants is associated with improved white matter maturation and head growth. *Neonatology* 2015;107:68–75.
- [50] Pepper RE, Pitman KA, Cullen CL, Young KM. How do cells of the oligodendrocyte lineage affect neuronal circuits to influence motor function, memory and mood? *Front Cell Neurosci* 2018;12:1–14.
- [51] Cutuli D. Functional and Structural Benefits Induced by Omega-3 Polyunsaturated Fatty Acids During Aging. *Curr Neuropharmacol* 2017;15:534–42.
- [52] Crupi R, Marino A, Cuzzocrea S. n-3 Fatty Acids : Role in Neurogenesis and Neuroplasticity. *Curr Med Chem* 2013;20:2953–63.
- [53] Calderon F, Kim HY. Docosahexaenoic acid promotes neurite growth in hippocampal neurons. *J Neurochem* 2004;90:979–88.
- [54] Carbone BE, Abouleish M, Watters KE, Vogel S, Ribic A, Schroeder OHU, et al. Synaptic Connectivity and Cortical Maturation Are Promoted by the  $\omega$ -3 Fatty Acid Docosahexaenoic Acid. *Cereb Cortex* 2020;30:226–40.
- [55] Biernaskie J, Corbett D. Enriched Rehabilitative Training Promotes Improved Forelimb Motor Function and Enhanced Dendritic Growth after Focal Ischemic Injury. *J Neurosci* 2001;21:5272–80.
- [56] Woodruff-Pak DS, Agelan A, Valle L Del. A rabbit model of Alzheimer’s disease: Valid at neuropathological, cognitive, and therapeutic levels. *J Alzheimer’s Dis*

- 2011;11:371–83.
- [57] Looij Y Van De, Larpin C, Cabungcal JH, Sanches EF, Toulotte A, Do KQ, et al. Nutritional intervention for developmental brain damage: Effects of lactoferrin supplementation in hypocaloric induced intrauterine growth restriction rat pups. *Front Endocrinol (Lausanne)* 2019;10:1–14.
- [58] Chen Y, Zheng Z, Zhu X, Shi Y, Li FAT, Wang B. Lactoferrin Promotes Early Neurodevelopment and Cognition in Postnatal Piglets by Upregulating the BDNF Signaling Pathway and Polysialylation. *Mol Neurobiol* 2015;52:256–69.
- [59] Ruan Y, Zou B, Fan Y, Li Y, Lin N, Zeng Y, et al. Dendritic plasticity of CA1 pyramidal neurons after transient global ischemia. *Neuroscience* 2006;140:191–201.
- [60] Eixarch E, Batalle D, Illa M, Muñoz-Moreno E, Arbat-Plana A, Amat-Roldan I, et al. Neonatal neurobehavior and diffusion MRI changes in brain reorganization due to intrauterine growth restriction in a rabbit model. *PLoS One* 2012;7:e31497.
- [61] Illa M, Eixarch E, Muñoz-Moreno E, Batalle D, Leal-Campanario R, Gruart A, et al. Neurodevelopmental Effects of Undernutrition and Placental Underperfusion in Fetal Growth Restriction Rabbit Models. *Fetal Diagn Ther* 2017;42:189–97.
- [62] Workman AD, Charvet CJ, Clancy B, Darlington RB, Finlay BL. Modeling transformations of neurodevelopmental sequences across mammalian species. *J Neurosci* 2013;33:7368–83.
- [63] Lodygensky GA, Seghier ML, Warfield SK, Tolsa CB, Sizonenko S, Lazeyras F, et al. Intrauterine growth restriction affects the preterm infant's hippocampus. *Pediatr Res* 2008;63:438–43.
- [64] Ruff CA, Faulkner SD, Rumajogee P, Beldick S, Foltz W, Corrigan J, et al. The extent of intrauterine growth restriction determines the severity of cerebral injury and neurobehavioural deficits in rodents. *PLoS One* 2017;12:e0184653.

## 7. Supporting information



**S1 Table. Functional evaluation — score grading in the study groups.**

## 8.2 Epigallocatechin-3-gallate PEGylated poly(lactic-co-glycolic) acid nanoparticles mitigate striatal pathology and motor deficits in 3-nitropropionic acid intoxicated mice

Amanda Cano <sup>1,2,3</sup>, Miren Ettcheto <sup>3,4,5</sup>, Marta Espina <sup>1,2</sup>, Carmen Auladell <sup>6</sup>, Jaume Folch <sup>3,5</sup>, **Britta A Kühne** <sup>4</sup>, Marta Barenys <sup>4</sup>, Elena Sánchez-López <sup>1,2,3</sup>, Eliana B Souto <sup>7,8</sup>, Maria Luisa García <sup>1,2</sup>, Patric Turowski <sup>9</sup>, Antonio Camins <sup>3,4</sup>

<sup>1</sup> Department of Pharmacy, Pharmaceutical Technology & Physical Chemistry, Faculty of Pharmacy & Food Sciences, University of Barcelona, Barcelona, Spain.

<sup>2</sup> Institute of Nanoscience & Nanotechnology (IN2UB), Barcelona, Spain.

<sup>3</sup> Biomedical Research Networking Centre in Neurodegenerative Diseases (CIBERNED), Madrid, Spain.

<sup>4</sup> Department of Pharmacology, Toxicology & Therapeutic Chemistry, Faculty of Pharmacy & Food Sciences, University of Barcelona, Spain.

<sup>5</sup> Unit of Biochemistry & Pharmacology, Faculty of Medicine & Health Sciences, University of Rovira i Virgili, Reus (Tarragona), Spain.

<sup>6</sup> Department of Cellular Biology, Physiology & Immunology, Faculty of Biology, University of Barcelona, Spain.

<sup>7</sup> Department of Pharmaceutical Technology, Faculty of Pharmacy, University of Coimbra, Coimbra, Portugal.

<sup>8</sup> CEB - Centre of Biological Engineering, University of Minho, Campus de Gualtar 4710-057 Braga, Portugal.

<sup>9</sup> UCL Institute of Ophthalmology, University College of London, London, UK.

|                       |  |
|-----------------------|--|
| Journal               | Nanomedicine   |
| Impact Factor 2020    | 5.307  |
| Quartile              | Q1   |
| Type of authorship    | Co-author  |
| Status of publication | Nanomedicine (Lond) (2021 Jan) 19-35<br>DOI: 10.2217/nnm-2020-0239 |

## Summary

**Aim:** To compare free and nanoparticle (NP)-encapsulated epigallocatechin-3-gallate (EGCG) for the treatment of Huntington's disease (HD)-like symptoms in mice.

**Materials & methods:** EGCG was incorporated into PEGylated poly(lactic-co-glycolic) acid NPs with ascorbic acid (AA). HD-like striatal lesions and motor deficit were induced in mice by 3-nitropropionic acid-intoxication. EGCG and EGCG/AA NPs were co-administered and behavioral motor assessments and striatal histology performed after 5 days.

**Results:** EGCG/AA NPs were significantly more effective than free EGCG in reducing motor disturbances and depression-like behavior associated with 3-nitropropionic acid toxicity. EGCG/AA NPs treatment also mitigated neuroinflammation and prevented neuronal loss.

**Conclusion:** NP encapsulation enhances therapeutic robustness of EGCG in this model of HD symptomatology. Together with our previous findings, this highlights the potential of EGCG/AA NPs in the symptomatic treatment of neurodegenerative diseases.

**Keywords:** 3-nitropropionic acid; Huntington's disease; PLGA-PEG; epigallocatechin-3-gallate; neurodegenerative diseases; polymeric nanoparticles.

## Lay abstract

Huntington's disease (HD) is a debilitating neurodegenerative disease that affects around 5–10/100,000 individuals in developed countries. It is caused by genetic alterations in the huntingtin (htt) gene. Efforts are being made to find treatments which will correct the genetic alterations or their consequences; however, none of these options are yet available to patients. Thus, therapies that improve the symptoms of HD, which include motor dysfunction and a wide range of behavioral disturbances, are also needed. Epigallocatechin-3-gallate (EGCG) is a powerful compound extracted from the green tea plant that may possess beneficial effects for HD patients, but whose therapeutic success is limited because of its chemical instability. In this study, we show that encasing EGCG in nano-sized capsules makes it much more efficient in reducing motor deficits and depression-like behavior in a mouse model of HD-like neurodegeneration. Importantly, behavioral improvement was also associated with a reduction of nerve cell damage. These results, together with previous findings using nano-encapsulated EGCG in mouse models of Alzheimer's disease and epilepsy, highlight their potential effectiveness for treating the symptoms of neurodegenerative diseases.

## Epigallocatechin-3-gallate PEGylated poly(lactic-co-glycolic) acid nanoparticles mitigate striatal pathology and motor deficits in 3-nitropropionic acid intoxicated mice

Amanda Cano<sup>a,b,c,#</sup>, Miren Ettcheto<sup>c,d,e</sup>, Marta Espina<sup>a,b</sup>, Carmen Auladell<sup>f</sup>, Jaume Folch<sup>c,e</sup>, Britta A. Kühne<sup>d</sup>, Marta Barenys<sup>d</sup>, Elena Sánchez-López<sup>a,b,c</sup>, Eliana B. Souto<sup>g,h</sup>, Maria Luisa García<sup>a,b,\*</sup>, Patric Turowski<sup>i,\*</sup>, Antoni Camins<sup>c,d,\*</sup>

<sup>a</sup> Department of Pharmacy, Pharmaceutical Technology and Physical Chemistry, Faculty of Pharmacy and Food Sciences, University of Barcelona, Spain.

<sup>b</sup> Institute of Nanoscience and Nanotechnology (IN2UB), Barcelona, Spain.

<sup>c</sup> Biomedical Research Networking Centre in Neurodegenerative Diseases (CIBERNED), Madrid, Spain.

<sup>d</sup> Department of Pharmacology, Toxicology and Therapeutic Chemistry, Faculty of Pharmacy and Food Sciences, University of Barcelona, Spain.

<sup>e</sup> Unit of Biochemistry and Pharmacology, Faculty of Medicine and Health Sciences, University of Rovira i Virgili, Reus (Tarragona), Spain.

<sup>f</sup> Department of Cellular Biology, Physiology and Immunology, Faculty of Biology, University of Barcelona, Spain.

<sup>g</sup> Department of Pharmaceutical Technology, Faculty of Pharmacy, University of Coimbra, Coimbra, Portugal.

<sup>h</sup> CEB - Centre of Biological Engineering, University of Minho, Campus de Gualtar 4710-057 Braga, Portugal.

<sup>i</sup> UCL Institute of Ophthalmology, University College of London, United Kingdom.

\* Senior co-authors

# Corresponding author:

**Amanda Cano**, Department of Pharmacy, Pharmaceutical Technology and Physical Chemistry, Faculty of Pharmacy and Food Sciences. Av Joan XXIII, 27-31, 08017.

University of Barcelona, Barcelona, Spain.

E-mail address: [acanofernandez@ub.edu](mailto:acanofernandez@ub.edu)

### Key words

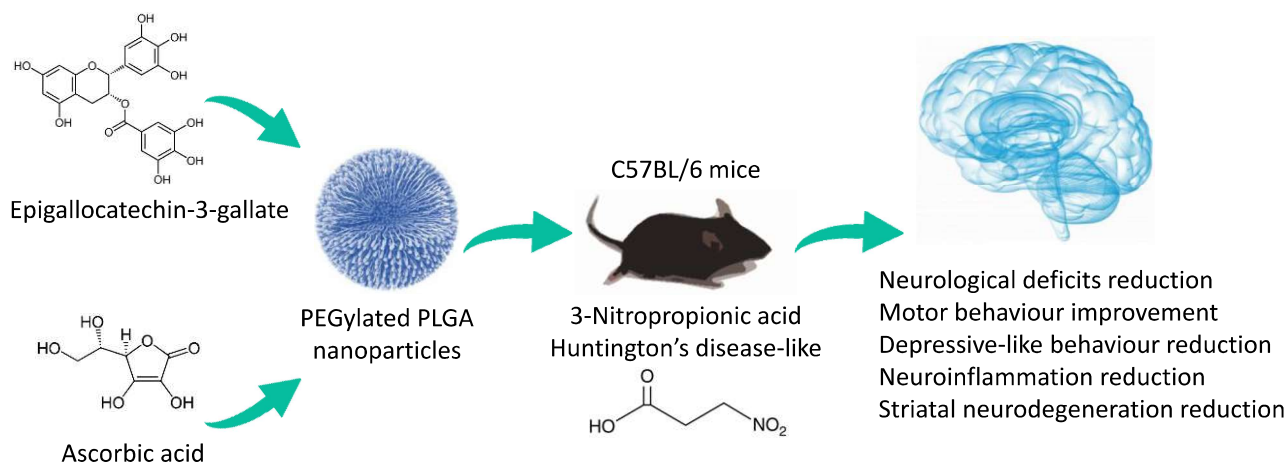
Epigallocatechin-3-gallate; polymeric nanoparticles; PLGA-PEG; 3-nitropropionic acid; Huntington's disease; neurodegenerative diseases.

### Abbreviations

3-NP, 3-nitropropionic acid; AA, ascorbic acid; ASOs, antisense oligonucleotides; BWT, Beam walk test; DALYs, disability-adjusted life year; EE, encapsulation efficiency; EGCG, Epigallocatechin-3-gallate; FDA, Food and Drug Administration; FJC, Fluoro-Jade C; GFAP, glial fibrillary acidic protein; HD, Huntington's disease; *HTT*, Huntingtin; mHTT, mutant HTT protein; ND, neurodegenerative diseases; NPs, nanoparticles; NPCs, neuronal progenitor cells; OFT, open field test; OxHb, oxidized hemoglobin; PDI, polydispersity index; PEG, polyethylene glycol; PFA, paraformaldehyde; PLGA, poly (lactic-co-glycolic acid); TEM, transmission electron microscopy; TST, tail suspension test; XRD, X-ray diffraction;  $Z_{av}$ , mean average size; ZP, zeta potential.

Link to original article: <https://www.futuremedicine.com/doi/10.2217/nnm-2020-0239>

## Graphical Abstract



## Abstract

**Aims:** To compare free and nanoparticle (NP)-encapsulated epigallocatechin-3-gallate for the treatment of Huntington's disease (HD)-like symptoms in mice.

**Material and Methods:** EGCG was incorporated into PEGylated PLGA NPs with AA. HD-like striatal lesions and motor deficit were induced in mice by 3-NP-intoxication. EGCG and EGCG/AA NPs were co-administered and behavioral motor assessments and striatal histology performed after 5 days.

**Results:** EGCG/AA NPs were significantly more effective than free EGCG in reducing motor disturbances and depression-like behaviour associated with 3-NP toxicity. EGCG/AA NPs treatment also mitigated neuroinflammation and prevented neuronal loss.

**Conclusion:** NP encapsulation enhances therapeutic robustness of EGCG in this model of HD symptomatology. Together with our previous findings, this highlights the potential of EGCG/AA NPs in the symptomatic treatment of neurodegenerative diseases.

## 1. Introduction

Neurodegenerative diseases are increasingly prevalent in developed countries [1]. Huntington's disease (HD), an autosomal neurodegenerative disease, is mainly characterized by a motor dysfunction accompanied by behavioural disturbances ranging from irritability, apathy to depression and cognitive decline [2]. Specifically in HD, a region of repetitive CAG trinucleotides in exon 1, which encodes a polyglutamine stretch normally varying between 6 and 35 in length, is expanded, resulting in polyglutamine stretches exceeding 38 repetitions and leading to varying degrees of HTT protein misfolding [3]. Misfolded HTT often aggregates, forming insoluble amyloid-like deposits, which possess cytotoxic activity and eventually induce cell death. Although disease-causing *HTT* variants are expressed from birth in all tissues of all HD patients, only the nervous system is ultimately affected by this misfolded protein response and only in later stages of life [4]. The most affected brain area is the corticostriatal region, indicating that striatal neurons are disproportionately sensitive [5]. However, despite these mechanistic insights, the consequences of *HTT* polymorphisms and the normal physiological role of HTT remain poorly understood [6].

Currently, HD affects ca. 5-10/100,000 individuals in developed countries with recent rises potentially linked to an increase in mutation rates [7]. HD is a chronic pathology without cure, with affected individuals expected to survive for 15–20 years after the onset of first symptoms [8]. Current efforts to find an effective HD cure are still at the stage of pre-clinical or clinical testing. These include; HTT-lowering therapies with focus on reducing transcript or protein accumulation through the use of antisense oligonucleotides (ASOs) or siRNA; regulating homeostasis of mutant HTT protein by inhibiting aggregation or promoting the HTT clearance; and reducing neuroinflammation. Additionally, much research also focuses on finding symptomatic treatment of HD [9–12]. Indeed, the only two drugs currently approved by the *Food and Drug Administration* (FDA) for the treatment of HD belong to this latter therapeutic class. Both tetrabenazine and its deuterated derivative SD-809 (deutetabenazine) suppress specific symptoms of HD, namely spasmodic involuntary movements, commonly known as “chorea”. However, they also lead to serious adverse effects, such as deterioration of pre-existing depressions in patients.[13].

Phytochemicals have potential for neuroprotection and neurodegenerative diseases [14]. In this regard, epigallocatechin-3-gallate (EGCG), which is its most abundant polyphenol constituent of the green tea plant *Camellia sinensis*, has attracted considerable interest in recent years [15]. Many beneficial effects of the green tea plant,

*Camellia sinensis*, have been attributed to EGCG, which is its most abundant polyphenol constituent [16]. A number of hydroxyls groups and aromatic rings significantly contribute to the potent antioxidant activity of EGCG [16]. However, they are also responsible for the low physicochemical stability of EGCG, which, together with low intestinal absorption, significantly reduces its bioavailability and thus currently compromises its promising therapeutic potential [17].

Nanosystems used to develop controlled drug delivery systems, include many types of vehicles, core matrices and particle sizes. Their most important characteristics are the ability to increase the physicochemical stability of encapsulated compounds, improve drugs solubility and bioavailability problems, sustained release, control their pharmacokinetic, reduction of adverse effects and targeting to a specific organ [18]. Currently, polymeric nanoparticles (NPs) are among the most explored vehicles in nanomedicine, specifically those composed of poly (lactic-co-glycolic acid) (PLGA) matrices [19,20]. Polymeric NPs can be formulated as nanospheres or nanocapsules, depending on the structural arrangement of the polymer. Nanocapsules have a liquid core surrounded by a polymer cover, whereas nanospheres are entirely composed of a polymeric matrix. Importantly, whereas the active, vectorised compound is dissolved in the liquid core of nanocapsules, it is dispersed in the intramatrix space or adsorbed on the surface of nanospheres [21]. Furthermore, PLGA NPs are frequently surface modified using polyethylene glycol (PEG), leading to improved aqueous solubility and reduced immunogenicity, which are both thought to contribute to lower rates of NP clearance and increased long term NPs stability [22].

We have previously shown that incorporation of EGCG into PEGylated PLGA nanoparticles improves bioavailability and effectiveness and renders it more effective in treating seizures in a mouse model of temporal lobe epilepsy [23]. Further improvement of this nanosystem is achieved by additional co-loading of the NPs with ascorbic acid (AA) [24]. Oral administration of such EGCG/AA NPs improves pharmacokinetics in the circulation and crucially higher EGCG levels in the brain of mice, resulting in improved therapeutic efficacy in a mouse model of Alzheimer's disease [24]. In light of this clear therapeutic potential of EGCG in attenuating neurodegeneration, it is noteworthy that EGCG also inhibits the aggregation of mHTT protein in a dose-dependent manner *in vitro*, and leads to morphological and behavioral improvements in transgenic HD flies [25]. Here, we tested if EGCG and EGCG/AA NPs have therapeutic benefit in mice intoxicated with 3-nitropropionic acid (3-NP). This mitochondrial toxin causes bilateral striatal lesions in the brain and has been extensively used to model HD- like motor deficit

symptoms [26]. Collectively, our data showed that EGCG formulated in NPs was more effective than free EGCG in correcting cellular and behavioural dysfunction in this mouse HD model.

## **2. Materials and Methods**

### **2.1 Preparation of NPs**

EGCG/AA NPs were prepared by double emulsion method and optimized with a central composite factorial design as previously described [24]. Briefly, the internal water phase ( $W_1$ ) composed by 1 ml of MQ water with EGCG (Capotchem Hangzhou, P.R.China) and AA (Sigma Aldrich, Madrid, Spain) was emulsified with the organic phase, 1.5 ml of ethyl acetate containing a dissolved amount of PLGA-PEG 5% (O) (Evonik Co., Birmingham, USA). The simple emulsion ( $W_1/O$ ) was obtained by an ultrasounds cycle (Ultrasounds probe Sonics&Materials, INC. Newtown, USA) at 37% amplitude during 30s. Then, 2 ml of the external water phase ( $W_2$ ), composed by Tween<sup>®</sup>80 2.5% as surfactant (Sigma Aldrich, Madrid, Spain), were added to the simple  $W_1/O$  emulsion and subjected to an extra ultrasounds cycle at the same amplitude for 3 min to lead to the formation of the double emulsion ( $W_1/O/W_2$ ). The entire procedure was carried out in an ice bath. Finally, 2 ml of an aqueous solution of 0.04% Tween<sup>®</sup>80 was added dropwise to stabilize the emulsion and the organic solvent was evaporated by stirring during 24 h (**Figure 1A**).

### **2.2 Transmission electron microscopy**

Transmission electron microscopy (TEM) was used to confirm the morphological properties of the developed NPs. Samples were diluted (1:10) and fixed on the surface of activated copper grids (UV light). To visualize the particles, NPs were subjected to negative staining with uranyl acetate (2%). Images were taken on a Jeol 1010 microscope (Jeol USA, MA, USA).

### **2.3 X-ray diffraction**

EGCG/AA NPs were ultracentrifuged (Optima<sup>®</sup> LE-BOK Ultracentrifuge, Beckman, USA) at 25,000 g, 15 °C for 15 min, and the pellet dried and pulverized to obtain the dry powder samples.

X-ray diffraction (XRD) was used to evaluate the crystalline status of EGCG/AA NPs components. Pulverized samples were placed in polyester films and exposed to CuK<sup>α</sup> radiation (45 kV, 40 mA,  $\lambda = 1.5418 \text{ \AA}$ ) in a range ( $2\theta$ ) from 2 °C to 60 °C and a measuring time of 200 s per step.



## **2.4 Cellular in vitro assays**

### **2.4.1 Hemolysis**

Hemolysis tests were performed as described elsewhere [23]. Briefly, blood from C57BL/6 mice was extracted by maxillofacial puncture and collected in heparinized tubes. Samples were centrifuged at 4,000 rpm for 5 min and erythrocytes were re-suspended in 0.9 % NaCl. Then, triplicate samples of 1 ml of free EGCG or NPs formulations were incubated with 100 µl of erythrocyte suspensions for 30 min, 6 or 12 h in a shaking water bath at 37 °C. Distilled water and 0.9% NaCl were used as positive and negative controls, respectively. Finally, oxidation of released hemoglobin (OxHb) was promoted by exposing samples to light and its absorbance was measured with a GE Healthcare Genequant 1300 spectrophotometer at 540 nm. Up to 10% of hemolysis was considered as non-toxic.

### **2.4.2 Cytotoxicity**

The cytotoxicity of EGCG/AA NPs was evaluated in PC12 and GPNT cells, widely-used culture models for neuronal and brain microvascular endothelial cells, respectively [27,28]. Both naive and differentiated PC12 cells were used to account for potential differences in susceptibility between proliferative and differentiated states [29,30]. Differentiated and undifferentiated PC12, as well as confluent GPNTs were exposed to increasing concentrations of EGCG/AA NPs for 24 h. PC12 viability was measured by means of Alamar Blue assay (Promega) in a FluoStar Optima Plate Reader (BMG Labtech, USA) at 544/590 nm. GPNTs viability was analysed by measuring the absorbance of MTT reduction in a Safire microplate reader (Tecan, Reading, UK) at 540 nm.

## **2.5 In vivo tests**

### **2.5.1 Animals, experimental groups and treatment schedule**

Every effort was made to reduce the number of animals and minimize animal suffering. All procedures involving animals were conducted in strict accordance with the European Community Council Directive 86/609/EEC, EU Directive 2010/63/EU for animal experiments, the procedures established by the Department d'Agricultura, Ramaderia i Pesca of the Generalitat de Catalunya and approved by the local ethical committee (University of Barcelona). Male C57BL/6 mice (6 weeks, 21–25 g) were purchased from Envigo® (Europe region, Spain). They were kept at 23 °C with a 12 h light-dark cycle and had access to food and water *ad libitum*. 3-NP was used to induce HD-like symptoms [31,32]. After environmental adaptation, animals were randomly

divided into four groups (with at least 8 mice per group): saline control group (CTRL), 3-NP control group (3-NP), 3-NP + free EGCG treated group (free EGCG) and 3-NP + EGCG/AA NPs treated group (EGCG/AA NPs). Mice were injected intraperitoneally (i.p.) with EGCG or EGCG/AA NPs (containing 50 mg/kg of EGCG) and 1 h later with 3-NP (70 mg/kg) (Sigma Aldrich, Madrid) every day for 5 days. Equal volumes of saline were injected in control groups. At the end of the treatments, behavioural tests were performed (**Figure S1 of Supplementary material**).

### 2.5.2 Beam walk test

Beam walk tests (BWT) were performed as described Babu *et al.* with some modifications [33]. Briefly, motor performance was assessed by measuring the ability of mice to traverse a horizontal wood beam (1 cm x 80 cm) suspended 50 cm above a padded surface. The day before the test, animals were allowed to cross the beam 3 times for training purposes. Maximum test time was 60 s. Latency to cross the beam, speed, distance travelled, immobility periods and falls were recorded.

### 2.5.3 Open field test

Open field tests (OFT) were conducted as described in previous studies [32]. Briefly, exploratory and spontaneous locomotor activities of mice were tested in the center of a 50 cm diameter platform surrounded by 30 cm walls. After allowing 5 min for the mice to adapt to the novel environment, motor activities were recorded during a 10 min session. The ambulation distance and mean speed was recorded using SMART V3.0 (Panlab Harvard Apparatus, Germany) video tracking system. The test area was thoroughly wiped with a cloth containing ethanol solution 70% after each session to prevent any bias from olfactory cues.

### 2.5.4 Tail suspension test

The tail suspension test (TST) was selected as a measure of depression-like behaviour [32,34]. Mice tail ends were fixed to a raised structure 50 cm from the ground and animals were hung upside down such that their bodies were suspended during a six-min session. Immobility time was scored during the final 4 min of the session as the time that mice spent hanging in an immobile position without any desire to free themselves.

### 2.5.5 Neurological scoring (movement analysis)

Movement analysis was used to derive a neurological scoring as previously described Ludolph *et al.* [35]. Briefly, neurological deficits on day 5 were evaluated on a 0-4 scale as follows: normal behaviour (0), general slowness of displacement resulting

from mild hind limb impairment (1), marked gait abnormalities and incoordination (2), hind limb paralysis (3), movement incapacity resulting from fore limb and hind limb impairment (4).

## **2.6 Ex vivo assays**

### *2.6.1 Immunohistochemistry assay*

At the end of treatments and behavioural assays, mice were sacrificed by i.p. injection of ketamine:xylazine (100 mg:10 mg/kg, respectively) and perfusion with PFA 4%. Brains were removed and maintained at 4 °C in a 30 % sucrose PFA solution until coronal sections of 20 µm of thickness were cut using a cryostat (Leica Microsystems, Wetzlar, Germany). Brain slices were subjected to immunohistochemistry as described elsewhere [23]. Primary polyclonal antibody against glial fibrillary acidic protein (GFAP) (1:1000; Dako Chemicals, Glostrup, Denmark) and secondary antibody AlexaFluor 594 goat anti-rabbit (Red, 1:1000; Life Technologies, Cambridge, UK) were used. Image acquisition was carried out using an epifluorescence microscope (BX41, Olympus, Germany) equipped with MercuryShortArc HBO™ 103 W/2 laser; Olympus DP70 camera; UPlanFI 20x/0.50 Ph1, UPlanFI 10x/0.30 Ph1 and Plan 4x/0.10 lenses; Olympus DP Controller 1.1.1.65 software).

### *2.6.2 Fluoro-Jade C histochemistry*

Fluoro-Jade C (FJC) staining was performed to evaluate neurodegeneration as described elsewhere [36]. Briefly, brain slides were immersed in 0.06 g/l of KMnO<sub>4</sub> and transferred to the staining solution containing 0.1 % of acetic acid and 0.0001% of FJC for 30 minutes in the dark. Then, the slides were dried, submerged in xylene and mounted on gelatin-coated glass with DPX mounting media. Samples were imaged using an epifluorescence microscope (Olympus BX61).

### *2.6.3 Nissl staining*

Nissl staining has been widely used to detect neuronal degeneration in different models of HD [37,38]. Brain coronal sections (20 µm thick) were rinsed with PBS, transferred to gelatin-coated glass and air dried for 24 h. Subsequently, slides were hydrated by consecutive immersion in 90 % EtOH, 70 % EtOH, and distilled water before staining with cresyl violet 0.1%. Slides were then washed twice with distilled water and dehydrated by consecutive immersion in 70 %, 90% and 100 % EtOH, and then twice in xylene. Finally, slides were air dried and covered using DPX. Stained sections were

analysed using an Olympus BX61 microscope and stained neuronal cells were manually counted in a double-blind setup.

## 2.7 Statistical analysis

All quantitative data were processed using GraphPad 6.0 Prism and analysed for normal distribution using the D'Agostino & Pearson omnibus normality test. For normally distributed data groups comparisons were performed by one-way ANOVA followed by Tukey post hoc tests. All other data was analysed by non-parametric one-way Kruskal-Wallis test followed by Dunn's multiple comparisons. Statistical significant difference was set at  $P < 0.05$  (\*).

## 3. Results

### 3.1 Physicochemical characteristics of optimized EGCG/AA NPs formulation

EGCG/AA NPs were previously optimized, thus leading to a formulation composed by 2.5 mg/ml of EGCG, 2.5 mg/ml of AA and 14 mg/ml of PLGA-PEG [24]. This composition results in particles with an average size ( $Z_{av}$ ) of  $124.8 \pm 5.2$  nm, monodisperse population with a polydispersity index (PDI) of  $0.054 \pm 0.013$  and a zeta potential (ZP) of  $-15.7 \pm 1.7$  mV. Such EGCG/AA NPs release almost 50% of the loaded drug in sustained fashion from the polymeric matrix at 24 h, and EGCG stability is significantly increased due to the incorporation of EGCG into the developed nanocarrier [24].

Additional TEM analyses showed that EGCG/AA NPs were perfectly spherical, possessed a smooth surface and did not display any aggregation phenomenon (**Figure 1B**). Moreover, the PEGylated cover was clearly identified by TEM (Figure 1B, inset). All physicochemical EGCG/AA NPs characteristics are summarized in **Table 1**.

The crystalline or amorphous state of substances is one of the physicochemical characteristics that strongly determines their biopharmaceutical behaviour. EGCG and AA displayed intense sharp peaks at diffraction angles, suggesting properties of both drugs typical of crystallization. Major XRD experimental peaks of 95% pure EGCG correlated with those obtained from literature [39] [experimental (literature)]: 5.13 (5.72), 8.46 (8.63), 10.30 (10.40), 12.09 (11.99), 17.00 (16.99), 20.70 (20.66), 24.51 (24.66), 29.47 (29.65). Free EGCG and AA showed XRD profiles of crystalline compounds. PLGA-PEG exhibited an amorphous pattern typical of copolymers. Empty and drug-loaded NPs displayed similar XRD profiles to PLGA-PEG polymer profile alone, indicating that new covalent bonds were not created between EGCG or AA and PLGA-PEG. Thus, these results demonstrate that both EGCG and AA were properly

encapsulated inside the polymeric matrix, maintaining their crystallinity, and by inference, their effectiveness (**Figure 1C**).

### **3.2 Cellular viability assays**

Hemolysis assays were performed and showed that both free and loaded-EGCG led to less than 10 % erythrocyte breakdown for assay times up to 12 h and free EGCG, AA and EGCG/AA NPs at concentrations up to 2.5 mg/ml (**Figure 2A, Table S1 of Supplementary material**). Brain endothelial GPNT cells treated with increasing concentrations of EGCG/AA NPs for 24 h remained viable, with only some insignificant reduction in cell viability at very high EGCG concentrations (450 µg/ml for 24 h). (**Figure 2B**). Undifferentiated PC12 showed no reduction in viability in presence of up to 300 µg/ml NP-formulated EGCG (**Figure 2C**). In contrast, when cultured under differentiating conditions, PC12 cells were more sensitive. Cell viability diminished in response to EGCG/AA NPs at concentration greater than 80 µg/mL. However, it never dropped below 50% within the concentration range tested and consequently, a half maximal inhibitory concentration (IC50) could not be determined.

### **3.3 EGCG/NPs ameliorated 3-NP-induced neurological deficits**

Neurological deficits induced by 3-NP toxicity were evaluated by movement analysis. 3-NP resulted in clear motor abnormalities, with these mice displaying an average neurological score of nearly 3, corresponding to hind limb paralysis (**Figure 3A**). These mice generally exhibited slowness, motor incoordination and common hind limb paralysis. Importantly, more than 50% of 3-NP mice exhibited score values higher than 3, with two of them being completely immobile. Treatment of 3-NP mice with free EGCG resulted in a significant improvement in the neurological score, with none of the treated animals showing any sign of hind limb paralysis or inability to move. EGCG/NP treatment was even more effective; this treatment group displayed a score value close to 0.

### **3.4 EGCG/AA NPs on 3-NP reduced depression-like behaviour**

Time spent in immobility in the TST was used to evaluate potential depression. By this measure, as illustrated in **Figure 3B**, EGCG possessed a potent antidepressant effect in 3-NP HD-induced mice.

### **3.5 EGCG/AA NPs improved 3-NP induced motor disturbances**

We used 3-NP intoxicated mice to model symptoms of HD and evaluate the effectiveness of EGCG to reduce associated motor disturbances. BWT and OFT are

useful tests to evaluate motor skills, balance and fine coordination, and have been widely used to analyse motor alterations in a variety of different HD mouse models [31,40,41]. When subjected to a BWT assay, more than 55% of 3-NP mice fell from the beam, as opposed to none in the untreated control group (**Table 2**). None of the EGCG/AA NPs treated 3-NP mice exhibited any fall, either. **Figure 3C** shows the typical loss of gait posture observed in 3-NP mice and its absence in animals that were also treated with EGCG/AA NPs. Significantly, 3-NP mice took on average ca. 20 times longer to cross the beam than untreated littermates (**Figure 3D**). EGCG/AA NPs, but not free EGCG treatment significantly reduced crossing time; with average crossing times being close to those of control animals. The distance travelled on the beam was reduced ca. 2-fold in mice subjected to 3-NP but was within control values with animals treated with either free and NP-formulated EGCG (**Figures 3E**). 3-NP-treated mice also travelled at much reduced speed. In contrast, with EGCG/AA NPs but not free EGCG treatment these 3-NP mice travelled again at control speeds (**Figures 3F**). In summary EGCG/AA NPs treatment significantly ameliorated performance of 3-NP mice in BWT. A clear improvement in agility of movements, coordination, body posture and gait, all very similar to those control littermates, was also observed as illustrated in the accompanying video (**Supplementary material**).

OFT, also frequently used to analyse motor disturbances in mice [42] confirmed our BWT observations. Intoxication with 3-NP led to significant reduction in the movement distance and speed of mice. EGCG/AA NPs treatment prevented these deficiencies, and significantly more so than free drug. (**Figure 3G, 3H**). All detailed data obtained in the behavioural tests are summarised in **Table 2**.

### **3.6 EGCG/AA NPs reduce astrogliosis**

Neuroinflammation was evaluated by analysing astrocyte activation and concomitant enhanced GFAP expression by immunohistochemistry [43]. In both, the caudoputamen and hippocampal regions, 3-NP intoxication led to enhanced astrocyte reactivity, as well as changes in cell morphology, with dendritic alterations clearly evident (**Figure 4A**). Both free and NPs-loaded EGCG administration reversed 3-NP-induced astrocyte reactivity in both brain regions. Whilst free EGCG did not normalize cell and dendrite morphology completely, EGCG/AA NPs treatment clearly did. Quantitative analysis confirmed that EGCG/AA NPs treatment significantly reduced the number of reactive astrocyte in 3-NP mice, not instead the free drug (**Figure 4B**).

### **3.7 EGCG/AA NPs reduce striatum neuronal death**

FJC and Nissl staining were used as measures for neurodegeneration [38,44,45]. FJC showed that the brain area most affected by 3-NP intoxication was the dorsal striatum. Here, 3-NP mice clearly showed an intense FJC signal compared to control littermates, which barely displayed any sign of staining (**Figure 5A**). Both free and NPs-loaded EGCG treatments strongly reduced 3-NP-induced FJC staining. However, quantification of affected area showed that only EGCG/AA NPs appeared to be significant compared to those non-treated littermates.

Strong differences in Nissl brain staining between control and 3-NP-intoxicated mice were found in the lateral septal complex and the caudoputamen, both in frontal midbrain sections. As shown in **Figure 5B**, the total number of striatal neurons in Nissl-stained sections was significantly decreased in the 3-NP group. Brains of these animals also displayed deformation of the neuronal body and dendrites, typical alterations of neuronal morphology associated with neurodegenerative processes [37,38,46,47]. Striatal neuronal loss in 3-NP mice compared to control littermates ranged from between ca. 75% in the caudoputamen of midbrain sections to ca. 44 % and 48% in the caudoputamen and lateral septal complex of frontal brain sections, respectively. Free EGCG treatment was not able to significantly reduced 3-NP-induced neuronal loss in the analysed areas. Significantly, EGCG/AA NPs nearly completely prevented neuronal loss in the caudoputamen striatum, with neuronal cell loss completely absent and ca. 18% in the caudoputamen of middle and frontal brain, respectively, and ca. 18% in the lateral septal complex of frontal brain (see also Supplementary **Table S2**).

#### 4. Discussion

HD is a disabling ND caused by autosomal dominant mutations in the *HTT* gene that are related with nerve cell death. Despite this clear genetic link, there is no effective cure to date. Nevertheless, therapeutic strategies targeting the *HTT* gene and its expression are increasingly explored, with some at advanced stage. Currently, two types of ASOs are in clinical development for HD: the allele-specific ASOs, WVE-120101 (NCT03225833) and WVE-120102 (NCT03225846) and the non-allele specific ASO, IONIS HTRRx (NCT02519036) [8]. However, in line with many other ND, HD management and cures are generally recognised to require a multi-target approach, with those focusing on HD neurological symptoms continuing to be important, either as principal or adjunct treatment option [8].

Amongst phytochemicals, EGCG has increasingly drawn interest as a potential therapeutic due to its natural origin and its many beneficial properties [15]. In its free form, the therapeutic use of EGCG is limited because of limitation in bioavailability.

Nevertheless, there is increasing evidence that EGCG may be beneficial for diseases without effective treatments and unclear etiology, such as HD. Indeed, some studies have already evaluated the effect of EGCG in pre-clinical models of HD. Ehrnhoefer *et al.* carried out a study in an *in vitro* yeast model and transgenic flies of HD [25]. This study reported for the first time that EGCG can beneficially modulate HTT protein misfolding, resulting in a decrease of protein aggregation and cytotoxicity, and improvement of motor function. Likewise, Kumar and colleagues evaluated the effect of EGCG in 3-NP-intoxicated rats [48]. In this case, authors report that EGCG is able to restore the glutathione system and improve memory processes. Lastly, in 2015 a phase II clinical trial of 12-month EGCG treatment in HD patients was initiated (NCT01357681). Its primary outcome evaluates changes of cognitive functions; however, results are not yet available.

Our study focused on EGCG loaded into PEGylated PLGA NPs under an antioxidant environment. Our previous studies show that the incorporation of EGCG into this nanocarrier results in an improvement of drug physicochemical stability and an enhanced EGCG bioavailability, as well as its sustained release from the polymeric matrix [24]. PEGylation of this polymer matrix and the use of Tween<sup>®</sup>80 as surfactant were specifically selected to develop these NPs since available evidence indicates that these components act as enhancers of NPs penetration to the brain [49,50]. Likewise, the biocompatibility, biodegradability, safety, easy elimination and surface modification versatility of PLGA provide a matrix with many advantages for the delivery of different drugs with widely different chemical characteristics in biomedical applications [51,52]. Our results here also demonstrated that the developed nanocarrier efficiently incorporates EGCG into the polymeric matrix, preserves the crystallinity properties of both drugs, and thus combined with a small  $Z_{av}$ , monodisperse population, high negative surface charge and elevated loading capacity give rise to the appropriated characteristics for drug enhanced brain delivery.

EGCG/AA NPs did not display relevant cytotoxicity towards blood, neuronal and brain endothelial cells, and this was in full agreement with studies using similar nanocarriers [23,53]. In particular, the polymer on its own appears to have little effect on cells at the low concentrations present *in vivo* [24]. We also showed here that high concentrations of free or loaded EGCG, or empty NPs did not affect the integrity of red blood cells, again in line with previous studies [54–56]. No cytotoxicity of EGCG/AA NPs was detectable in cultured brain GPNT endothelial cells or undifferentiated PC12 neuronal cells. In accordance with results reported by Asaki *et al.* showing that



differentiated PC12 are typically more sensitive [29], we found that differentiated PC12 exhibited some sensitivity towards EGCG/AA NPs. However, this was only seen at concentrations above 80 µg/ml ( $p < 0.05$ ); a concentration, which was never reached in vivo: even if all of the 50 mg/kg we injected i.p. into mice was in the circulation, this would translate to less than 1 mg/ml in the blood. We have previously shown that this nanosystem does not accumulate in the brain at more than 1/1000 of the circulating concentration [24], i.e. in the present at 1 µg/ml as a theoretical maximum and well below any cytotoxicity seen in differentiated PC12 cells. This confirmed that EGCG can be safely used in a neuronal environment, with protective effects of EGCG in (6-OHDA)-induced Parkinson's disease model in PC12 cells also previously reported [57].

We chose to assess the effectiveness of EGCG and EGCG/AA NPs in 3-NP intoxicated mice, which, whilst not faithfully reproducing the genetically driven pathology and aetiology of HD, have been used extensively to model striatal lesions and motor deficit reminiscent of HD [26,31,58]. Using this model, we were able to show for the first time that the prophylactic administration of EGCG significantly improved the motor performance of 3-NP intoxicated. Significantly, whilst treatment with free EGCG positively affected some measures of motor performance such as distance travelled in BWT and speed in OFT, it was the treatment with the NP-encapsulated EGCG, which led to normal motor behaviour in all measured parameters of BWT and OFT. Furthermore, we noted normalisation of behavioural traits associated with depression by treatment with both free and encapsulated EGCG. Previous studies have already shown the beneficial effects of EGCG on locomotion in different animal models. HD is categorized in a *less common neurological disorders* group, together with motor dystrophies, such as Duchenne muscular dystrophy [59]. Thus, In 2012, Nakae and collaborators reported that oral administration of EGCG to *mdx* mice, a mild phenotype model of Duchenne muscular dystrophy, significantly increases the locomotor activities [60]. Other have also reported that chronic EGCG treatment improves motor performance in motor neurodegenerative diseases, such as amyotrophic lateral sclerosis [61]. The present study adds to this body of evidence and, in addition, demonstrates clear therapeutic superiority of using EGCG stabilised and protected in a nanocarrier, such as in our EGCG/AA NPs.

*In vivo* results also showed a reduction of 3-NP-induced neurotoxicity in mice when EGCG was co-administered with the 3-NP. The presence of AA (used at 50 mg/kg in our experiments) may have also contributed to mitigating symptoms of 3-NP toxicity: a previous study shows that AA at 100 mg/kg protects somewhat from 3-NP-induced

oxidative damage [62]. However, given the demonstrated and greater overall effectiveness of free EGCG [15] and AA-free EGCG NPs [23] in models of NDs, a direct neuroprotective effect of AA can probably be discounted in favour of its EGCG stabilising function. Importantly, we found again that overall EGCG was significantly more effective when used formulated as EGCG/AA NPs. EGCG-enhanced brain function as suggested by our behavioural assays was correlated by cytological observation, since EGCG reduced 3-NP-induced astrogliosis and neurodegeneration in the hippocampus and the striatum. Furthermore, EGCG was clearly neuroprotective in the striatum. The involvement of striatum in motor functions, especially the caudoputamen region, is widely recognised, as well as the relation between striatal neuronal loss and HD motor impairment [63–65]. Accordingly, we observed reduced neurodegeneration in the caudoputamen and the lateral septal complex; most significantly when EGCG/AA NPs were used. Importantly, these cytological observations correlated well with improved motor performance observed in these mice. EGCG also protects motor neurons in other models, such a transgenic mice model of amyotrophic lateral sclerosis or cultures of rat spinal cords [66,67]. Overall our results show that neuroprotection through EGCG treatment translated into strongly improved motor behaviour in a rodent preclinical model of HD.

## 5. Conclusions

In summary, the current study adds to increasing evidence of significantly improved pharmacological effectivity of EGCG when co-loaded with AA into PLGA-PEG NPs. Indeed, NP encapsulation clearly renders EGCG more robust for *in vivo* application and thus EGCG/AA NPs will facilitate future pre-clinical studies assessing the effectiveness of this phytochemical in ND. In 3-NP-induced HD-like mice, EGCG/AA NPs effectively restored locomotor performance and overall neurological score. It also reduced depression-like behaviour, neuroinflammation and neurodegeneration. Our study did not elucidate if EGCG/AA NP affected *HTT* driven pathology; more elaborate genetic models are required for that. Nevertheless, our data highlighted the potential benefits of this novel NP formulation to manage neurological symptoms of HD and thus, we also propose that EGCG/AA NPs could be a novel and promising adjuvant for the symptomatic treatment of a wide range of ND, and HD in particular.

## Summary Points

- Epigallocatechin-3-gallate (EGCG) is the most abundant polyphenol of the tea plant and has previously shown to possess beneficial effects in HD, but its therapeutic instability compromises its therapeutic success.

- We have previously demonstrated that the encapsulation of EGCG into PLGA-PEG nanoparticles (NPs) improved EGCG stability and penetration into the brain, as well as improve drug effectiveness in other ND.
- In this study, EGCG-loaded NPs were administered to 3-nitropropionic acid (3-NP)-intoxicated mice, an accepted animal model of HD, to evaluate the potential effectiveness of developed nanocarrier in this ND.
- EGCG-loaded NPs were significantly more effective than free EGCG in reducing motor disturbances, depression-like behaviour, neuroinflammation and striatal neuronal loss.
- Thus, we propose EGCG-loaded NPs as a promising therapeutic adjuvant in the management of HD symptomatology.

### Financial support

This work was supported by the Spanish Ministry of Economy and Competitiveness (SAF2017-84283-R), CB06/05/0024 (CIBERNED) and the European Regional Development Funds. AC<sup>a,b,c</sup>, ME<sup>a,b</sup>, ESL<sup>a,b,c</sup> and MLG<sup>a,b</sup> belong to 2017SGR-1477. ME<sup>c,d,e</sup>, CA<sup>f</sup>, and AC<sup>c,d</sup> belong to 2017SGR-625.

### Acknowledgements

Authors acknowledge the support of the Spanish Ministry of Science, Innovation and Universities, Biomedical Research Networking Centre in Neurodegenerative Diseases (CIBERNED) and European Regional Development Funds.

### Conflict of interest

None of the authors have any conflicts of interest including any financial, personal or other relationships with other people or organizations. All authors have reviewed the contents of the manuscript being submitted, approved its contents and validated the accuracy of the data.

### References

**Reference note:** indicated references are ‘\*’ – of interest and “\*\*” – of considerable interest.

1. **\*\*Wyss-coray T. Ageing, neurodegeneration and brain rejuvenation. *Nature*. 539(7628), 180–186 (2016).**

*Comprehensive and well described explanation of neurodegeneration and its development.*

2. Handley RR, Reid SJ, Patassini S, *et al.* Metabolic disruption identified in the Huntington 's disease transgenic sheep model. *Nature Publishing Group*. 11(6:20681), 1–11 (2016).
3. Jiang Y, Chadwick SR, Lajoie P. Endoplasmic reticulum stress : The cause and solution to Huntington' s disease ? *Brain Research*. 1648, 650–657 (2016).
4. Gövert F, Schneider S. Huntington's disease and Huntington's disease-like syndromes: an overview. *Curr Opin Neurol*. 26(4), 420–7 (2013).

5. Margulis J, Finkbeiner S. Proteostasis in striatal cells and selective neurodegeneration in Huntington's disease. *Front Cell Neurosci.* 8, 1–9 (2014).
6. Bates G, Dorsey R, Gusella J, et al. Huntington's disease. *Nat Rev Dis Primers.* 23(1), 15005 (2015).
7. Rawlins MD, Wexler NS, Wexler AR, et al. The Prevalence of Huntington's Disease. *Neuroepidemiology.* 46, 144–153 (2016).
8. Mestre TA. Recent advances in the therapeutic development for Huntington's disease. *Parkinsonism and Related Disorders.* 59, 125–130 (2019).
9. Stahl CM, Feigin A. Medical, Surgical, and Genetic Treatment of Huntington Disease. *Neurol Clin.* 8(2), 367–378 (2020).
10. Shannon KM. Recent Advances in the Treatment of Huntington's Disease: Targeting DNA and RNA. *CNS Drugs.* 34(3), 219–228 (2020).
11. **\*\*Kumar A, Kumar V, Singh K, et al. Therapeutic Advances for Huntington's Disease. *Brain Sci.* 10(1), 43 (2020).**

*Global vision of recent findings in Huntington therapeutic approach.*

12. Costa-Valadão PA, Santos KBS, Ferreira E Vieira TH, et al. Inflammation in Huntington's disease: A few new twists on an old tale. *J Neuroimmunol.* 348, 577380 (2020).
13. Frank S, Testa C, Stamlor D, et al. Effect of Deutetrabenazine on Chorea Among Patients With Huntington Disease: A Randomized Clinical Trial. *JAMA.* 316(1), 40–50 (2016).
14. Khan A, Jahan S, Imtiyaz Z, et al. Neuroprotection: Targeting Multiple Pathways by Naturally Occurring Phytochemicals. *Biomedicines.* 8(8), 284 (2020).
15. **\*Chowdhury A, Sarkar J, Chakraborti T, Pramanik PK, Chakraborti S. Protective role of epigallocatechin-3-gallate in health and disease : A perspective. *Biomedicine et Pharmacotherapy.* 78, 50–59 (2016).**

*Comprehensive and well described explanation of epigallocatechin-3-gallate multifactorial benefits.*

16. Singh BN, Shankar S, Srivastava RK. Green tea catechin , epigallocatechin-3-gallate ( EGCG ): Mechanisms , perspectives and clinical applications Catechin backbone. *Biochemical Pharmacology.* 82(12), 1807–1821 (2011).
17. Krupkova O, Ferguson SJ, Wuertz-kozak K. Stability of (–)-epigallocatechin gallate and its activity in liquid formulations and delivery systems. *The Journal of Nutritional Biochemistry.* 37, 1–12 (2016).
18. Yun Y., Lee B., Park K, Lafayette W. Controlled Drug Delivery: Historical perspective for the next generation. *J Control Release.* 219, 2–7 (2015).
19. **\*\*El-say KM, El-sawy HS. Polymeric nanoparticles : Promising platform for drug delivery. *International Journal of Pharmaceutics.* 528(1–2), 675–691 (2017).**

*Complete and well described explanation of polymeric nanoparticles as promising vectors for drug delivery.*

20. Cano A, Sánchez-López E, Etcheto M, et al. Current advances in the development of novel polymeric nanoparticles for the treatment of neurodegenerative diseases. *Nanomedicine (London).* 15(12), 1239–1261 (2020).
21. Cano A, Espina M, García ML. Recent Advances on Antitumor Agents-loaded Polymeric and Lipid-based Nanocarriers for the Treatment of Brain Cancer. *Current Pharmaceutical Design.* 26(12), 1316–1330 (2020).
22. Soo J, Xu Q, Kim N, Hanes J, Ensign LM. PEGylation as a strategy for improving nanoparticle-based drug and gene delivery. *Advanced Drug Delivery Reviews.* 99, 28–51

(2016).

23. **\*Cano A, Ettcheto M, Espina M, et al. Epigallocatechin-3-gallate loaded PEGylated-PLGA nanoparticles: A new anti-seizure strategy for temporal lobe epilepsy. *Nanomedicine: Nanotechnology, Biology, and Medicine*. 14(4), 1073–1085 (2018).**

*Previous relevant findings of EGCG NPs effectiveness in other neurodegenerative diseases.*

24. **\*Cano A, Ettcheto M, Chang J, et al. Dual-drug loaded nanoparticles of Epigallocatechin-3-gallate ( EGCG )/ Ascorbic acid enhance therapeutic efficacy of EGCG in a APP<sup>swe</sup> / PS1<sup>dE9</sup> Alzheimer' s disease mice model. *Journal of Controlled Release*. 301, 62–75 (2019).**

*Previous relevant findings of EGCG NPs effectiveness in other neurodegenerative diseases.*

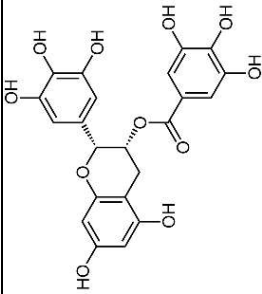
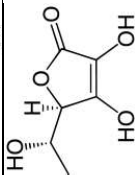
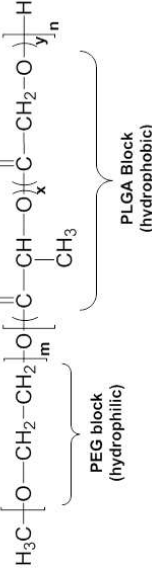
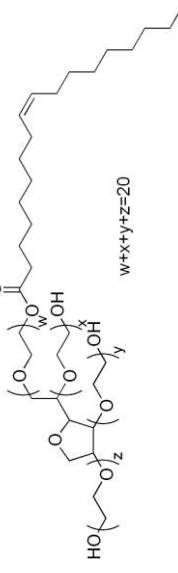
25. Ehrnhoefer DE, Duennwald M, Markovic P, et al. Green tea ( 2 ) -epigallocatechin-gallate modulates early events in huntingtin misfolding and reduces toxicity in Huntington ' s disease models. *Human Molecular Genetics*. 15(18), 2743–2751 (2006).
26. Chandra R, Reddy S, Reddy S, et al. Neuroprotective activity of tetramethylpyrazine against 3-nitropropionic acid induced Huntington ' s disease-like symptoms in rats. *Biomedicine & Pharmacotherapy*. 105, 1254–1268 (2018).
27. Waetzig V, Ri J, Cordt J, et al. Neurodegenerative effects of azithromycin in differentiated PC12 cells. *European Journal of Pharmacology*. 809, 1–12 (2017).
28. Dragoni S, Hudson N, Kenny B, et al. Endothelial MAPKs Direct ICAM-1 Signaling to Divergent Inflammatory Functions. *The Journal of Immunology*. 2(19), 4074–4085 (2017).
29. Asaki NS, Aba NB, Atsuo MM. Cytotoxicity of Reactive Oxygen Species and Related Agents Toward Undifferentiated and Differentiated Rat Phenochromocytoma PC12 Cells. *Biol. Pharm. Bull.* 24, 515–519 (2001).
30. Ekshyyan O, Aw TY. Decreased susceptibility of differentiated PC12 cells to oxidative challenge: relationship to cellular redox and expression of apoptotic protease activator factor-1. *Cell Death and Differentiation*. 12, 1066–1077 (2005).
31. Dhadde SB, Nagakannan P, Roopesh M, et al. Effect of embelin against 3-nitropropionic acid-induced Huntington' s disease in rats. *Biomedicine et Pharmacotherapy*. 77, 52–58 (2016).
32. Wang L, Wang J, Yang L, et al. Effect of Praeruptorin C on 3-nitropropionic acid induced Huntington' s disease-like symptoms in mice. *Biomedicine et Pharmacotherapy*. 86, 81–87 (2017).
33. Babu S, Vijayan R, Sekar S, Mani S. Simultaneous blockade of NMDA receptors and PARP-1 activity synergistically alleviate immunoexcitotoxicity and bioenergetics in 3-nitropropionic acid intoxicated mice: Evidences from memantine and 3- aminobenzamide interventions. *European Journal of Pharmacology*. 803, 148–158 (2017).
34. Chmielarz P, Kreiner G, Kuśmierczyk J, et al. Depressive-like immobility behavior and genotype × stress interactions in male mice of selected strains in male mice of selected strains. *The International Journal on the Biology of Stress*. 3890, 1–8 (2016).
35. Ludolph A, He F, Spencer P, Hammerstad J, Sabri M. 3-Nitropropionic acid-exogenous animal neurotoxin and possible human striatal toxin. *Canadian Journal of Neurological Sciences*. 18(4), 492–498 (1991).
36. Gu Q, Schmued LC, Sarkar S, Paule MG, Raymick B. One-step labeling of degenerative neurons in unfixed brain tissue samples using Fluoro-Jade C. *Journal of Neuroscience Methods*. 208(1), 40–43 (2012).
37. Turmaine M, Raza A, Mahal A, Mangiarini L, Bates GP, Davies SW. Nonapoptotic neurodegeneration in a transgenic mouse model of Huntington ' s disease. *PNAS*. 97(14), 14–18 (2000).

38. Lallani SB, Villalba RM, Chen Y, Smith Y, Chan AWS. Striatal Interneurons in Transgenic Nonhuman Primate Model of Huntington ' s Disease. *Nature Scientific Reports*. 9(1), 3528 (2019).
39. Bureau I. Polymorphs of cocrystals of epigallocatechin gallate and caffeine (W O 2017 / 040809). 2(12), [PATENT REGISTRATION] (2017).
40. Carter RJ, Morton AJ, Dunnett SB. Motor Coordination and Balance in Rodents. *Current Protocols in Neuroscience*. 8(12), 1–14 (2001).
41. Luong TN, Carlisle HJ, Southwell A, Patterson PH. Assessment of Motor Balance and Coordination in Mice using the Balance Beam. *Journal of Visualized Experiments*. 10(49), 2376 (2011).
42. Seibenhener ML, Wooten MC. Use of the Open Field Maze to Measure Locomotor and Anxiety-like Behavior in Mice. *Journal of Visualized Experiments*. , e52434 (2015).
43. Hanisch U, Kettenmann H. Microglia : active sensor and versatile effector cells in the normal and pathologic brain. *Nature neuroscience*. 10(11), 1387–1394 (2007).
44. Ehara A, Ueda S. Application of Fluoro-Jade C in Acute and Chronic Neurodegeneration Models : Utilities and Staining Differences. *Acta Histochem Cytochem*. 42(6), 171–179 (2009).
45. Gutiérrez IL, González-Prieto M, García-Bueno B, Caso JR, Leza JC, Madrigal JLM. Alternative Method to Detect Neuronal Degeneration and Amyloid b Accumulation in Free-Floating Brain Sections With Fluoro-Jade. *ASN Neuro Methods*. 10, 1–7 (2018).
46. Loh DH, Kudo T, Truong D, Wu Y, Colwell CS. The Q175 Mouse Model of Huntington ' s Disease Shows Gene Dosage- and Age-Related Decline in Circadian Rhythms of Activity and Sleep. *PLOS ONE*. 8(7), 1–13 (2013).
47. Cicchetti F, Saporta S, Hauser RA, et al. Neural transplants in patients with Huntington ' s disease undergo disease-like neuronal degeneration. *PNAS*. 106(30), 12483–12488 (2009).
48. Kumar P, Kumar A. Effect of lycopene and epigallocatechin-3-gallate against 3-nitropropionic acid induced cognitive dysfunction and glutathione depletion in rat : A novel nitric oxide mechanism. *Food and Chemical Toxicology*. 47(10), 2522–2530 (2009).
49. Nance EA, Woodworth GF, Sailor KA, et al. A Dense Poly(ethylene glycol) Coating Improves Penetration of Large Polymeric Nanoparticles within Brain Tissue. *Sci Transl Med*. 4(149), 1–19 (2012).
50. Sun W, Xie C, Wang H, Hu Y. Specific role of polysorbate 80 coating on the targeting of nanoparticles to the brain. *Biomaterials*. 25, 3065–3071 (2004).
51. Zhang K, Tang X, Zhang J, et al. PEG – PLGA copolymers : Their structure and structure-in fl uenced drug delivery applications. *Journal of Controlled Release*. 183, 77–86 (2014).
52. Sharma S, Parmar A, Kori S, Sandhir R. PLGA-based nanoparticles : A new paradigm in biomedical applications. *Trends in Analytical Chemistry*. 80, 30–40 (2016).
53. Sánchez-lópez E, Ettcheto M, Egea MA, et al. New potential strategies for Alzheimer ' s disease prevention : pegylated biodegradable dexibuprofen nanospheres administration to APPswe / PS1dE9. *Nanomedicine: Nanotechnology, Biology, and Medicine*. 13(3), 1171–1182 (2017).
54. Moses K, Pepple D, Singh P, Moses K, Pepple D, Singh P. The Protective Effect of Epigallocatechin-3-gallate on Paraquat-induced Haemolysis of Erythrocyte Membrane. *West Indian Med J*. 64(3), 186–188 (2015).
55. Raval JS, Fontes J, Banerjee U, Yazer MH, Mank E, Palmer AF. Ascorbic acid improves membrane fragility and decreases haemolysis during red blood cell storage. *Transfusion Medicine*. 23, 87–93 (2013).

56. Martins LG, Rubiana NM khalil, Mainardes M. PLGA Nanoparticles and Polysorbate-80-Coated PLGA Nanoparticles Increase the In vitro Antioxidant Activity of Melatonin. *Current Drug Delivery*. 15(4), 554–563 (2018).
  57. Nie G, Cao Y, Zhao B. Protective effects of green tea polyphenols and their major component, (-)-epigallocatechin-3-gallate (EGCG), on 6-hydroxydopamine-induced apoptosis in PC12 cells. *Redox Rep*. 7, 171–177 (2002).
  58. Hoshi A, Tsunoda A, Yamamoto T, Tada M, Kakita A. Increased neuronal and astroglial aquaporin-1 immunoreactivity in rat striatum by chemical preconditioning with 3-nitropropionic acid. *Neuroscience Letters*. 626, 48–53 (2016).
  59. Feigin VL, Abajobir AA, Abate KH, et al. Global , regional , and national burden of neurological disorders during 1990 – 2015: a systematic analysis for the Global Burden of Disease Study 2015. *Lancet neurology*. 16, 877–897 (2017).
  60. Nakae Y, Dorchie OM, Ritter C, Ruegg UT. Quantitative evaluation of the beneficial effects in the mdx mouse of epigallocatechin gallate , an antioxidant polyphenol from green tea. *Histochem Cell Biol*. 137, 811–827 (2012).
  61. Koh S, Mok S, Young H, et al. The effect of epigallocatechin gallate on suppressing disease progression of ALS model mice. *Neuroscience Letters*. 395, 103–107 (2006).
  62. Rodríguez-Martínez E, Rugerio-Vargas C, Rodríguez AI, Borgonio-Pérez G, Rivas-Arancibia S. Antioxidant effects of taurine, vitamin C, and vitamin E on oxidative damage in hippocampus caused by the administration of 3-nitropropionic acid in rats. *Int J Neurosci*. 114(9), 1133–1145 (2004).
  63. Isomura Y, Takekawa T, Harukuni R, et al. Reward-Modulated Motor Information in Identified Striatum Neurons. *The Journal of Neuroscience*. 33(25), 10209–10220 (2013).
  64. **\*Guo Z, Rudow G, Pletnikova O, et al. Striatal neuronal loss correlates with clinical motor impairment in Huntington’s disease. *Mov Disord*. 27(11), 1379–1386 (2012).**
- Comprehensive and well described explanation of the relation between striatal neuronal loss and Huntington’s diseases motor disturbances.*
65. Morigaki R, Goto S. Striatal Vulnerability in Huntington’s Disease: Neuroprotection Versus Neurotoxicity. *Brain Sciences*. 7, 63 (2017).
  66. Xu Z, Chen AES, Li AEX, Luo G, Li AEL, Le AEW. Neuroprotective Effects of ( - ) - Epigallocatechin-3-gallate in a Transgenic Mouse Model of Amyotrophic Lateral Sclerosis. *Neurochem Res*. 31, 1263–1269 (2006).
  67. Yu J, Jia Y, Guo Y, et al. Epigallocatechin-3-gallate protects motor neurons and regulates glutamate level. *FEBS Letters*. 584(13), 2921–2925 (2010).

## Tables

Table 1. Physicochemical characteristics of optimized formulation of EGCG/AA NPs.

| Compound        | Chemical structure  | Molecular weight (g/mol) | Concentration (mg/ml) | EGCG/AA NPs physicochemical characteristics        | EGCG/AA NPs morphological characteristics                |
|-----------------|---|--------------------------|-----------------------|--|--|
| <b>EGCG</b>     |    | 458,372                  | 2.5                   | $Z_{av}$ 124.8 ± 5.2 nm                            |  |
| <b>AA</b>       |    | 176,12                   | 2.5                   | $PI$ 0.054 ± 0.013                                 | Spherical shape, smooth surface, well defined PEG cover. |
| <b>PLGA-PEG</b> |   | 80.2 kDa                 | 14                    | $ZP$ -15.7 ± 1.7 mV                                |  |
| <b>Tween®80</b> |  | 1.310                    | 1.016 %               | $EE_{EGCG}$ 97.1 ± 2.4 %<br>$EE_{AA}$ 94.3 ± 1.6 % |  |



**Table 2.** Behavioural test results of EGCG/AA NPs treatment of 3-NP-induced HD mice.

| Behavioural test            | Analysed conditions     | Experimental groups |                   |                     |                       |
|-----------------------------|-------------------------|---------------------|-------------------|---------------------|-----------------------|
|                             |                         | CTRL<br>(n=8)       | 3-NP<br>(n=12)    | Free EGCG<br>(n=10) | EGCG/AA NPs<br>(n=10) |
| <b>Beam walk</b>            | Falls                   | 0                   | 7                 | 2                   | 0                     |
|                             | Time for crossing (sec) | 3.857 ± 0.806       | 25.262 ± 14.796   | 26.239 ± 6.693      | 9.950 ± 7.998         |
|                             | Distance (cm)           | 80.0 ± 0.0          | 41.8 ± 29.0       | 69.1 ± 12.3         | 79.7 ± 1.1            |
|                             | Speed (cm/sec)          | 21.4 ± 3.4          | 3.2 ± 2.4         | 3.0 ± 1.9           | 15.1 ± 6.0            |
| <b>Open field</b>           | Total distance (cm)     | 3161.9 ± 445.1      | 1143.9 ± 567.9    | 2146.9 ± 659.8      | 2936.9 ± 795.8        |
|                             | Speed (cm/sec)          | 5.2 ± 0.7           | 1.9 ± 0.9         | 3.5 ± 1.1           | 4.9 ± 1.3             |
|                             | Time at border (sec)    | 290.813 ± 36.340    | 397.198 ± 125.067 | 266.653 ± 84.793    | 199.87 ± 47.757       |
| <b>Tail suspension</b>      | Immobility (sec)        | 99.9 ± 31.8         | 165.5 ± 43.0      | 99.9 ± 38.2         | 90.5 ± 31.1           |
| <b>Neurological scoring</b> | Score 0-4               | 0.000 ± 0.000       | 2.788 ± 0.958     | 1.600 ± 1.039       | 0.333 ± 0.497         |

## Figures

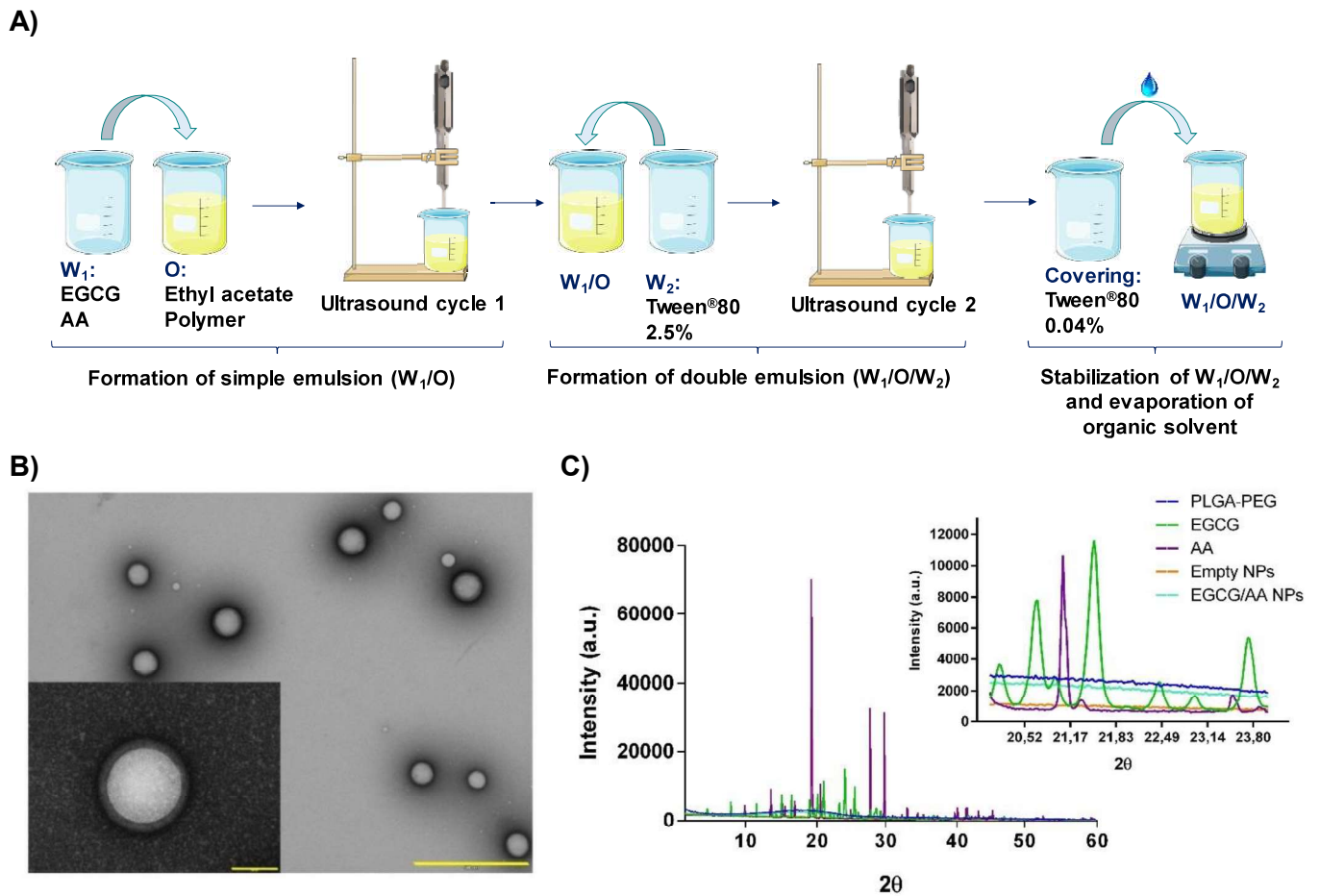


**Figure 1. EGCG/AA NPs preparation method and additional physicochemical characterization. (A)** Scheme of preparation of EGCG/AA NPs by the double emulsion method. Polymeric matrix: PLGA-PEG; loaded drugs: EGCG and AA; Surfactant: Tween®80. **(B)** EGCG/AA NPs morphology as revealed by TEM Scale bars 100/500 nm. **(C)** XRD profiles of different components of EGCG/AA NPs formulation, including an expanded view on the right of the 20  $\theta$  to 30  $\theta$  region.

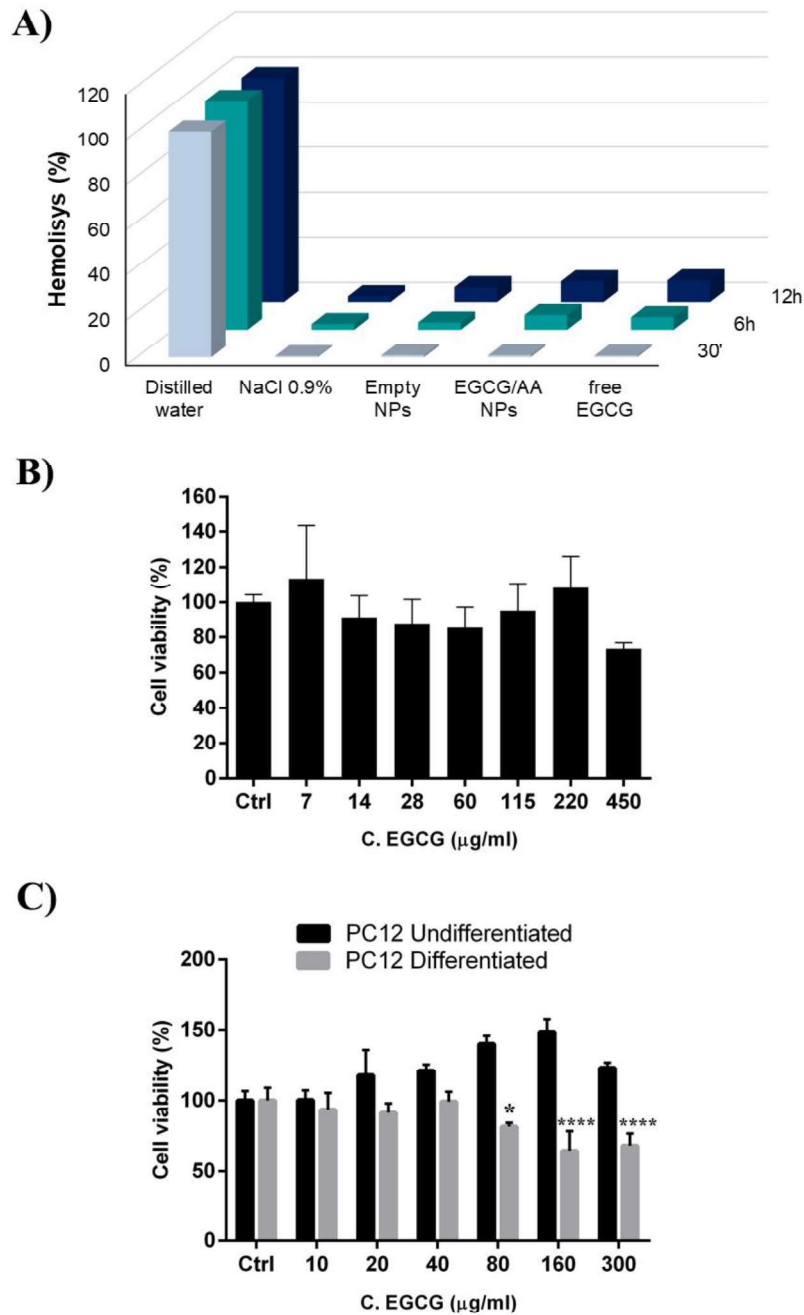


**Figure 2. Cell viability in response to EGCG/AA NPs.** (A) Hemolysis test results of EGCG/AA NPs and their constituents. Absorbance of released OxHb from erythrocytes was used to quantify hemolysis. Final concentrations of compounds were: EGCG/AA NPs: 2.5 mg/ml of EGCG, 2.5 mg/ml of AA and 14 mg/ml of PLGA-PEG; Empty NPs: 14 mg/ml of PLGA-PEG; free EGCG: 2.5 mg/ml (B) Cytotoxicity of EGCG/AA NPs measured by MTT assay in GPNT brain endothelial cell line. Cells were treated for 24 h with increasing amount of EGCG/AA NPs. Cell viability is expressed as a function of final EGCG concentrations (added as EGCG/AA NPs). Shown are normalised mean  $\pm$  SD (n=3). (C) Cytotoxicity of EGCG/AA NPs measured by Alamar Blue assays in differentiated and undifferentiated PC12 neuronal cells. Cell viability is expressed as a function of final EGCG concentration (added as EGCG/AA NPs). Shown are normalised mean  $\pm$  SD (n=3). One-way ANOVA statistical analysis followed by Bonferroni's multiple comparison test was performed. Statistical significance is expressed as  $p < 0.05$  \*;  $p < 0.0001$  \*\*\*\*.

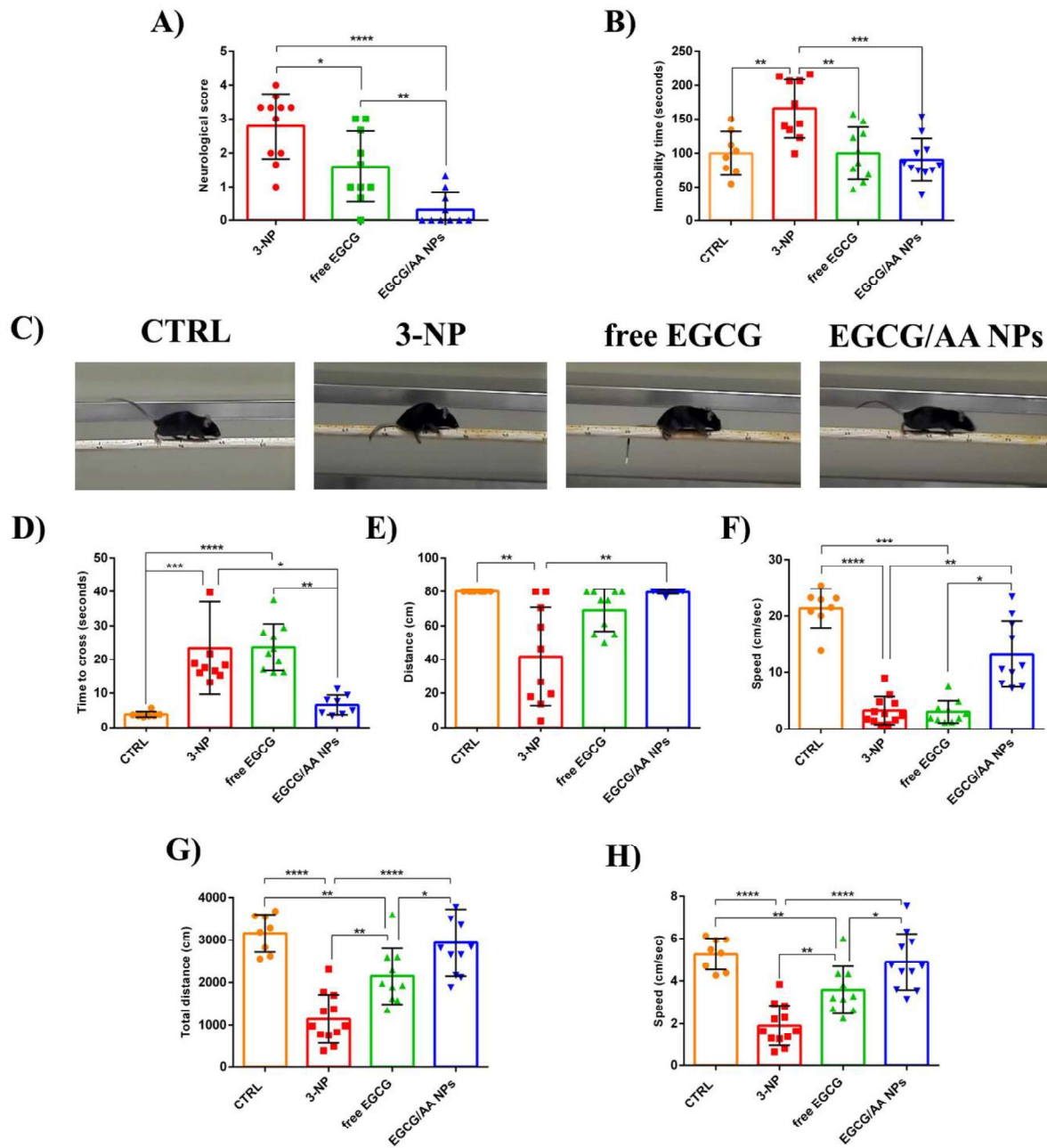


**Figure 3. Behavioural tests in 3-NP intoxicated mice and effect of EGCG.** 2 months-old C57BL/6 mice were i.p. injected daily with free and loaded EGCG (50 mg/kg/day) and with 3-NP (70 mg/kg/day) during 5 days. **(A)** Neurological score of the different experimental groups. **(B)** Time spent immobile in TST by the different experimental groups. **(C-F)** Assessment of animals by BWT. Typical gait posture of different groups in the BWT **(C)**. Quantification of time spent by animals to cross the complete beam **(D)**; of the total travel distance **(E)**, and of the mean speed **(F)** of different experimental groups in BWT. **(G-H)** Assessment by OFT results. Shown are the total travel distance **(G)** and the mean speed **(H)** of different experimental groups. One-way ANOVA statistical analysis followed by Tukey post hoc test was performed for panels **A**, **B**, **G** and **H**. One-way Kruskal-Wallis non-parametric statistical analysis followed by a Dunn's multiple comparisons test was performed for panels **D-F**. Statistical significance is expressed as  $p < 0.05$  \*,  $p < 0.01$  \*\*,  $p < 0.001$  \*\*\*,  $p < 0.0001$  \*\*\*\*.

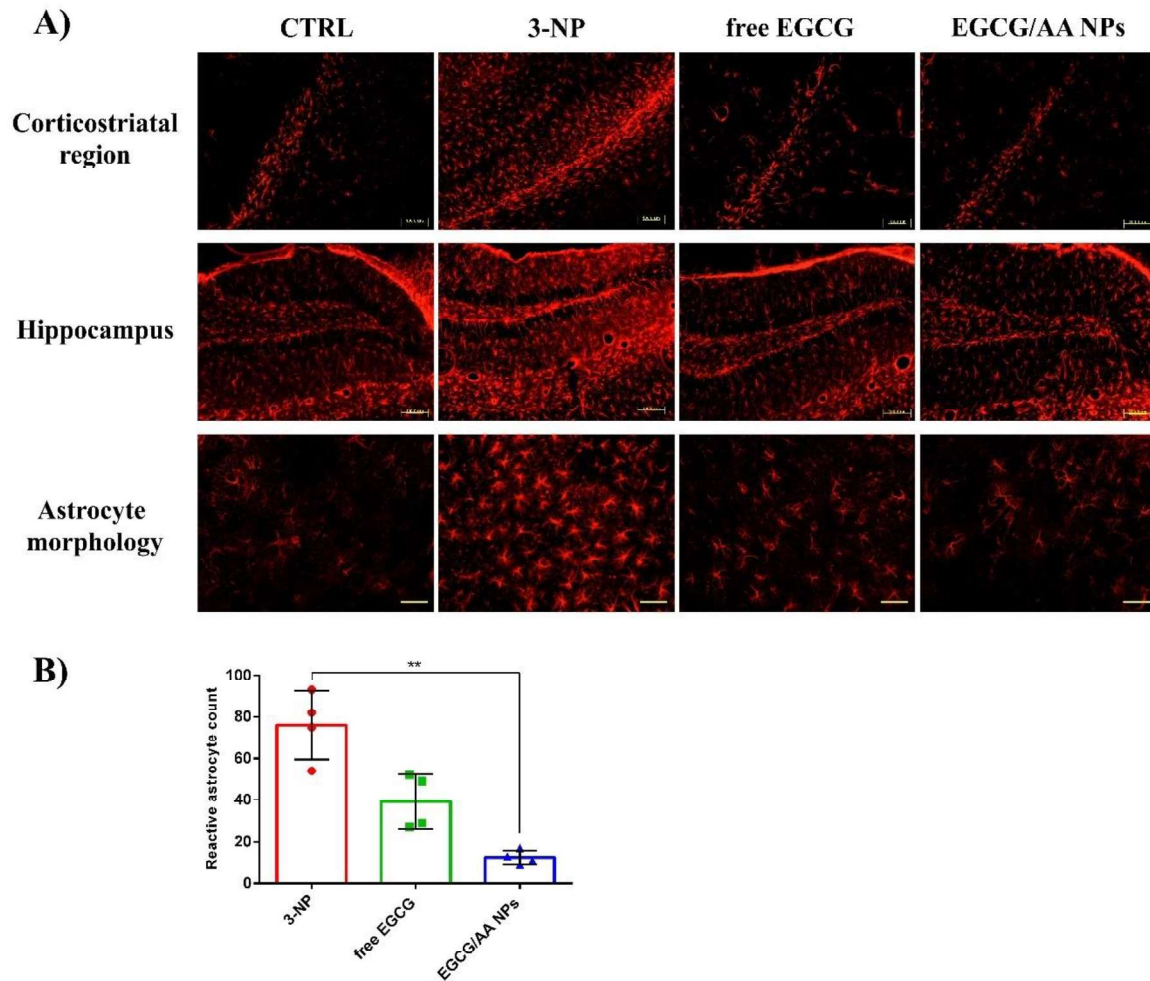


**Figure 4. Astrogliosis in 3-NP intoxicated mice and effect of EGCG.** 3-NP intoxication and EGCG treatments were performed as described for Figure 3. At the end of day 5, animals were sacrificed by perfusion with 4% PFA and brains were sectioned. GFAP immunostaining was performed on 20  $\mu$ m coronal sections. **A)** *Dentate gyrus* of hippocampus and corticostriatal region are shown. Scale bar 100  $\mu$ m. The bottom panels show astrocyte morphology of corticostriatal region of different experimental groups. Scale bar, 50  $\mu$ m. (n=4/group). Images of each series have been acquired using identical settings. **B)** Quantitative analysis of reactive astrocytes in corticostriatal brain region of the different experimental groups. Analysis performed from images of corticostriatal region with scale bar of 50  $\mu$ m. (n=4/group). One-way Kruskal-Wallis non-parametric statistical analysis followed by a Dunn's multiple comparisons test was performed for panel **B**. Statistical significance is expressed as  $p < 0.01$  \*\*.

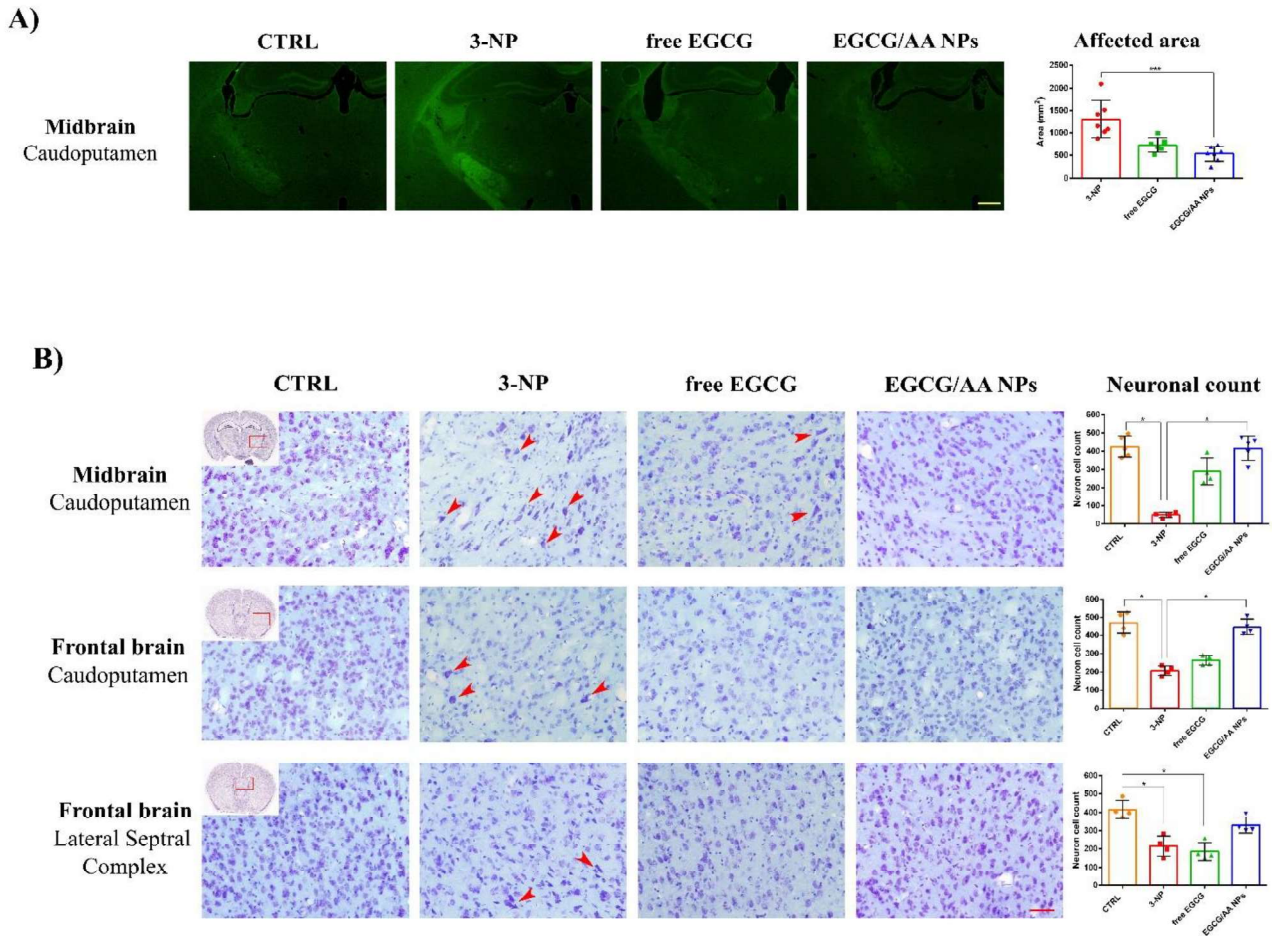


**Figure 5. Effect of free and loaded EGCG on 3-NP-induced neurodegeneration. (A)** As described for Figure 4, except that coronal sections were stained using FJC. Caudoputamen area of midbrain section are shown. Scale bar, 500  $\mu$ m. Images of each series have been acquired using identical settings. Shown on the right is the quantification of FJC staining area as normalised mean cell count  $\pm$  SD ( $n=6$ /group). **(B)** As described for Figure 4, except that Nissl staining was performed on 20  $\mu$ m coronal sections. Striatal areas of frontal and midbrain section are shown. Red arrows point out morphological alterations of stained cells. Scale bar, 50  $\mu$ m. Images of each series have been acquired using identical settings. Shown on the right are the quantifications of mean neuronal cell counts  $\pm$  SD ( $n=4$ /group). One-way Kruskal-Wallis non-parametric statistical analysis followed by a Dunn's multiple comparisons test was performed for all quantifications in panels A and B. Statistical significance is expressed as  $p<0.05$  \*.

### 8.3 Dual-drug loaded nanoparticles of Epigallocatechin-3-gallate (EGCG) / Ascorbic acid enhance therapeutic efficacy of EGCG in a APPswe/PS1dE9 Alzheimer's disease mice model

Amanda Cano <sup>a,b,c,d</sup>, Miren Ettcheto <sup>c,e,f</sup>, Jui-Hsien Chang <sup>d</sup>, Emma Barroso <sup>e,g,h</sup>, Marta Espina <sup>a,b</sup>, Britta A. Kühne <sup>e</sup>, Marta Barenys <sup>e</sup>, Carmen Auladell <sup>i</sup>, Jaume Folch <sup>c,f</sup>, Eliana B. Souto <sup>j,k</sup>, Antoni Camins <sup>c,e,1</sup>, Patric Turowski <sup>d</sup>, Maria Luisa García <sup>a,b</sup>

<sup>a</sup> Department of Pharmacy, Pharmaceutical Technology and Physical Chemistry, Faculty of Pharmacy and Food Sciences, University of Barcelona, Spain

<sup>b</sup> Institute of Nanoscience and Nanotechnology (IN2UB), Barcelona, Spain

<sup>c</sup> Biomedical Research Networking Centre in Neurodegenerative Diseases (CIBERNED), Madrid, Spain

<sup>d</sup> UCL Institute of Ophthalmology, University College of London, United Kingdom.

<sup>e</sup> Department of Pharmacology, Toxicology and Therapeutic Chemistry, Faculty of Pharmacy and Food Sciences, University of Barcelona, Spain

<sup>f</sup> Unit of Biochemistry and Pharmacology, Faculty of Medicine and Health Sciences, University of Rovira i Virgili, Reus, Tarragona, Spain

<sup>g</sup> Biomedical Research Center in Diabetes and Associated Metabolic Diseases (CIBERDEM)-Health Institute Carlos III, Barcelona, Spain

<sup>h</sup> Research Institute-Hospital Sant Joan de Déu, Esplugues de Llobregat, Barcelona, Spain

<sup>i</sup> Department of Cellular Biology, Physiology and Immunology, Faculty of Biology, University of Barcelona, Spain

<sup>j</sup> Department of Pharmaceutical Technology, Faculty of Pharmacy, University of Coimbra, Coimbra, Portugal

<sup>k</sup> REQUIMTE/LAQV, Group of Pharmaceutical Technology, Faculty of Pharmacy, University of Coimbra, Coimbra, Portugal

|                       |  |
|-----------------------|--|
| Journal               | Journal of Controlled Release  |
| Impact Factor 2019    | 7.727  |
| Quartile              | D1   |
| Type of authorship    | Co-author  |
| Status of publication | J Control Release 310 (2019 May) 62–75<br>DOI: 10.1016/j.jconrel.2019.03.010 |

## Summary

Epigallocatechin-3-gallate (EGCG) is a candidate for treatment of Alzheimer's disease (AD) but its inherent instability limits bioavailability and effectiveness. We found that EGCG displayed increased stability when formulated as dual-drug loaded PEGylated PLGA nanoparticles (EGCG/AA NPs). Oral administration of EGCG/AA NPs in mice resulted in EGCG accumulation in all major organs, including the brain. Pharmacokinetic comparison of plasma and brain accumulation following oral administration of free or EGCG/AA NPs showed that, whilst in both cases initial EGCG concentrations were similar, long-term (5-25 h) concentrations were ca. 5 fold higher with EGCG/AA NPs. No evidence was found that EGCG/AA NPs utilised a specific pathway across the blood-brain barrier (BBB). However, EGCG, empty NPs and EGCG/AA NPs all induced tight junction disruption and opened the BBB in vitro and ex vivo. Oral treatment of APP<sup>swe</sup>/PS1<sup>dE9</sup> (APP/PS1) mice, a familial model of AD, with EGCG/AA NPs resulted in a marked increase in synapses, as judged by synaptophysin (SYP) expression, and reduction of neuroinflammation as well as amyloid  $\beta$  (A $\beta$ ) plaque burden and cortical levels of soluble and insoluble A $\beta$ (1-42) peptide. These morphological changes were accompanied by significantly enhanced spatial learning and memory. Mechanistically, we propose that stabilisation of EGCG in NPs complexes and a destabilized BBB led to higher therapeutic EGCG concentrations in the brain. Thus EGCG/AA NPs have the potential to be developed as a safe and strategy for the treatment of AD.





## Dual-drug loaded nanoparticles of Epigallocatechin-3-gallate (EGCG)/Ascorbic acid enhance therapeutic efficacy of EGCG in a APPswe/PS1dE9 Alzheimer's disease mice model

Amanda Cano<sup>a,b,c,d</sup>, Miren Ettcheto<sup>c,e,f</sup>, Jui-Hsien Chang<sup>d</sup>, Emma Barroso<sup>e,g,h</sup>, Marta Espina<sup>a,b</sup>, Britta A. Kühne<sup>e</sup>, Marta Barenys<sup>e</sup>, Carmen Auladell<sup>i</sup>, Jaume Folch<sup>c,f</sup>, Eliana B. Souto<sup>j,k</sup>, Antoni Camins<sup>c,e,1</sup>, Patric Turowski<sup>d,\*,1</sup>, Maria Luisa García<sup>a,b,\*1</sup>

<sup>a</sup> Department of Pharmacy, Pharmaceutical Technology and Physical Chemistry, Faculty of Pharmacy and Food Sciences, University of Barcelona, Spain

<sup>b</sup> Institute of Nanoscience and Nanotechnology (IN2UB), Barcelona, Spain

<sup>c</sup> Biomedical Research Networking Centre in Neurodegenerative Diseases (CIBERNED), Madrid, Spain

<sup>d</sup> UCL Institute of Ophthalmology, University College of London, United Kingdom

<sup>e</sup> Department of Pharmacology, Toxicology and Therapeutic Chemistry, Faculty of Pharmacy and Food Sciences, University of Barcelona, Spain

<sup>f</sup> Unit of Biochemistry and Pharmacology, Faculty of Medicine and Health Sciences, University of Rovira i Virgili, Reus, Tarragona, Spain

<sup>g</sup> Biomedical Research Center in Diabetes and Associated Metabolic Diseases (CIBERDEM)-Health Institute Carlos III, Barcelona, Spain

<sup>h</sup> Research Institute-Hospital Sant Joan de Déu, Esplugues de Llobregat, Barcelona, Spain

<sup>i</sup> Department of Cellular Biology, Physiology and Immunology, Faculty of Biology, University of Barcelona, Spain

<sup>j</sup> Department of Pharmaceutical Technology, Faculty of Pharmacy, University of Coimbra, Coimbra, Portugal

<sup>k</sup> REQUIMTE/LAQV, Group of Pharmaceutical Technology, Faculty of Pharmacy, University of Coimbra, Coimbra, Portugal

### ARTICLE INFO

#### Keywords:

Epigallocatechin gallate  
EGCG  
Polymeric nanoparticles  
PLGA-PEG  
Alzheimer's disease  
APP/PS1 mice

### ABSTRACT

Epigallocatechin-3-gallate (EGCG) is a candidate for treatment of Alzheimer's disease (AD) but its inherent instability limits bioavailability and effectiveness. We found that EGCG displayed increased stability when formulated as dual-drug loaded PEGylated PLGA nanoparticles (EGCG/AA NPs). Oral administration of EGCG/AA NPs in mice resulted in EGCG accumulation in all major organs, including the brain. Pharmacokinetic comparison of plasma and brain accumulation following oral administration of free or EGCG/AA NPs showed that, whilst in both cases initial EGCG concentrations were similar, long-term (5–25 h) concentrations were ca. 5 fold higher with EGCG/AA NPs. No evidence was found that EGCG/AA NPs utilised a specific pathway across the blood-brain barrier (BBB). However, EGCG, empty NPs and EGCG/AA NPs all induced tight junction disruption and opened the BBB in vitro and ex vivo. Oral treatment of APPswe/PS1dE9 (APP/PS1) mice, a familial model of AD, with EGCG/AA NPs resulted in a marked increase in synapses, as judged by synaptophysin (SYP) expression, and reduction of neuroinflammation as well as amyloid  $\beta$  ( $A\beta$ ) plaque burden and cortical levels of soluble and insoluble  $A\beta_{(1-42)}$  peptide. These morphological changes were accompanied by significantly enhanced spatial learning and memory. Mechanistically, we propose that stabilisation of EGCG in NPs complexes and a destabilized BBB led to higher therapeutic EGCG concentrations in the brain. Thus EGCG/AA NPs have the potential to be developed as a safe and strategy for the treatment of AD.

**Abbreviations:** AA, ascorbic acid;  $A\beta$ , amyloid- $\beta$ ; APP/PS1, APPswe/PS1dE9; BBB, blood-brain barrier; BMVECs, brain microvascular endothelial cells; EE, encapsulation efficiency; EGCG, epigallocatechin-3-gallate; EGCG/AA NPs, dual-drug loading PEGylated PLGA nanoparticles of EGCG and AA; EGCG/AA NPs-Rho, EGCG/AA NPs covalently labelled with Rhodamine 110; FITC-dextran, Fluorescein isothiocyanate-dextran; FTIR, Fourier transform infrared spectroscopy; GFAP, glial fibrillary acidic protein; HPLC, high performance liquid chromatography; IL-6, interleukin 6; iNOS, inducible nitric oxide synthase; i.p., intraperitoneal; MWM, Morris Water Maze; NOR, Novel Object Recognition; NPs, nanoparticles; PDI, polydispersity index; PEG, Polyethylene glycol; PFA, paraformaldehyde; PLGA, poly(lactic-co-glycolic acid); Rho, Rhodamine 110; SYN, Synaptophysin; TEER, transendothelial electric resistance; ThS, Thioflavin-S; TNF $\alpha$ , tumor necrosis factor  $\alpha$ ; WT, wild-type; XRD, X ray diffraction;  $Z_{av}$ , average particle size; ZP, zeta potential

\* Correspondence to: Maria Luisa García, Department of Pharmacy, Pharmaceutical Technology and Physical Chemistry, Faculty of Pharmacy and Food Sciences, University of Barcelona, Barcelona, Spain.

\*\* Correspondence to: Patric Turowski, UCL Institute of Ophthalmology, University College of London, London, UK.

E-mail addresses: [p.turowski@ucl.ac.uk](mailto:p.turowski@ucl.ac.uk) (P. Turowski), [marisagarcia@ub.edu](mailto:marisagarcia@ub.edu), [rdcm@ub.edu](mailto:rdcm@ub.edu) (M.L. García).

<sup>1</sup> Senior co-authors have contributed equally.

<https://doi.org/10.1016/j.jconrel.2019.03.010>

Received 23 April 2018; Received in revised form 8 March 2019; Accepted 10 March 2019

Available online 13 March 2019

0168-3659/© 2019 The Authors. Published by Elsevier B.V. This is an open access article under the CC BY license

(<http://creativecommons.org/licenses/by/4.0/>).

## 1. Background

AD is the most common form of dementia worldwide [1] and involves 60–80% of all reported dementias. It is characterized by cognitive decline and, ultimately, by an incapacitation of basic functions, such as swallowing or walking that leads to death [2]. In 2005, the *Delphi Consensus Study* predicted that, by the year 2020, 42.3 million people in the world will have developed dementia, and that by 2040 this number will have doubled [3]. This increase in dementia cases will be accompanied by a large economic burden, which currently stands at around a trillion dollar worldwide [4].

The incidence of AD increases with age, but its exact etiology remains unknown. The main hypothesis of pathogenesis focuses on the alteration in the amyloidogenic pathway and Tau hyperphosphorylation. This is based on observations of increased accumulation of A $\beta$  plaques and induction of formation of neurofibrillary tangles in the brain, respectively, both of which can lead to neuronal death and subsequent dementia [5]. In the last decade, it has been described that alterations in both pathways are closely related to the onset of the disease, but also that other physiological alterations such as the deregulation of cholesterol homeostasis, insulin signaling, neuroinflammatory processes, mitochondrial alterations or oxidative stress contribute to the pathogenesis of this multifactorial disorder [6,7].

Due to its unknown etiology and the late appearance of the first symptoms (which are detected when neurodegeneration is already established), early diagnosis and effective treatment are very challenging [8,9]. Currently, the only drugs approved for AD treatment are the acetylcholinesterase inhibitors donepezil, galantamine and rivastigmine, and the NMDA receptor antagonist memantine, for mild to moderate and moderate to severe stages, respectively [1,5]. However, since none of these drugs stop the progression of the disease, novel therapeutic approaches for the treatment of AD are urgently needed [5].

A number of new pharmacological strategies for AD have been described [10–12]. One of them focuses on EGCG, the most abundant polyphenol of green tea plant *Camellia sinensis* [13]. This catechin has a strong chelating and antioxidant activity, due to two gallo catechol rings which can directly remove free radicals with high efficacy [14].

EGCG has demonstrated therapeutic effectiveness in several diseases, such as Down's syndrome, cancer and a variety of neurological disorders [15–17] and is considered a safe molecule [18]. Some cases of liver damage with EGCG consumptions higher than 800 mg/day have been reported, but in most cases these are attributed to idiosyncratic reactions [18].

With regard to AD, pre-clinical and clinical trials have shown that EGCG can act at different steps, such as inhibiting TAU aggregation, reducing A $\beta$  accumulation, suppressing tumor necrosis factor  $\alpha$  (TNF $\alpha$ ), inducible nitric oxide synthase (iNOS) or interleukin 6 (IL-6) expression, or even protecting mitochondrial function [19–22]. However, EGCG possesses many pharmacological disadvantages, in particular high instability, resulting in low EGCG bioavailability and, consequently, its effectiveness [23,24]. EGCG degradation is primarily caused by oxidation of the polyphenolic structure. Thus, potent antioxidant molecules, such as ascorbic acid (AA), are frequently added to reverse this effect. In addition to scavenging oxygen and protecting double bonds, AA also adds anti-inflammatory properties to resulting formulations [25,26].

Another strategy to reduce degradation of drugs is their incorporation into nanostructured systems. In recent years, the use of nanotechnology as a therapeutic strategy for targeting and drug delivery has been widely explored for diseases such as cancer, diabetes or neurodegenerative disorders [27–29].

Among several types of nanocarriers, polymeric NPs have been widely exploited for drug delivery and targeting, due to their versatility and production facilities. These nanosystems display a high loading capacity of a range of chemically different drugs. In addition, they offer

the possibility of attaching molecules to their surface for targeting, therefore representing an optimal alternative for the administration of drugs [30,31]. Due to its biocompatibility, biodegradability and non-toxicity, poly (lactic-co-glycolic acid) (PLGA) is one of the most commonly used polymers for the preparation of NPs [32]. Additionally, surface PEGylation of polymeric NPs is often used to enhance in vivo half-life. Surface tailoring NPs with polyethylene glycol (PEG) chains reduces aggregation, improves aqueous solubility and minimizes opsonisation, resulting in demonstrably lower immunogenicity and enhanced long term stability of the nanosystem [33,34].

We hypothesized that loading of EGCG in PEGylated PLGA NPs will improve physicochemical stability of the molecule and, consequently, its bioavailability and therapeutic efficacy. Thus, the aims of this work were to develop and characterize PEGylated PLGA NPs of EGCG under an AA antioxidant environment and to evaluate their effectiveness in a APP/PS1 double transgenic mouse model.

## 2. Materials and methods

### 2.1. Preparation of EGCG/AA NPs

EGCG/AA NPs were prepared by the double emulsion method [35] in three steps (Supplementary Fig. S1). (i) EGCG (Capotchem Hangzhou, P.R.China) and AA (Sigma Aldrich, Madrid, Spain) were dissolved in 1 ml of an aqueous phase ( $W_1$ ) at pH 3.5 and emulsified with 1.5 ml of an oil phase (O) composed of ethyl acetate containing the dissolved polymeric matrix (PLGA with a 5% of PEG content) (Evonik Co., Birmingham, USA). A simple emulsion ( $W_1/O$ ) was prepared by ultrasound using an ultrasounds probe (Sonics&Materials, INC. Newtown, USA) at 37% amplitude during 30 s. (ii) 2 ml of Tween®80 2.5% (pH 4.5) ( $W_2$ ) (Sigma Aldrich, Madrid, Spain) was added to  $W_1/O$  and the mixture again subjected to ultrasound (37% amplitude) for 3 min, to yield a double emulsion ( $W_1/O/W_2$ ). The entire procedure was carried out on ice. (iii) 2 ml of Tween®80 0.04% was added dropwise to stabilize the emulsion. Finally, the organic solvent was evaporated by stirring for 24 h, resulting in a final volume of 5 ml.

### 2.2. Optimization

Final formulation of EGCG/AA NPs with optimal physicochemical characteristics was found using a 2<sup>3</sup> central composite factorial design allowing optimisation with a minimum number of experiments providing maximum information. A total of 16 experiments were run as described above in triplicate, with varying concentrations of EGCG, AA and polymer (independent variables). The surfactant concentration was left fixed, intended for chronic administration, in order to increase at maximum nanocarrier stability and enhance tissue penetration [36]. The dependent variables included average particle size ( $Z_{av}$ ), polydispersity index (PDI), zeta potential (ZP) and entrapment efficiency (EE). The predicted response Y can be obtained from the non-linear quadratic model equation as follows Eq. (1),

$$Y = \beta_0 + \beta_1 X_1 + \beta_2 X_2 + \beta_3 X_3 + \beta_{11} X_1^2 + \beta_{22} X_2^2 + \beta_{33} X_3^2 + \beta_{12} X_1 X_2 + \beta_{13} X_1 X_3 + \beta_{23} X_2 X_3 \quad (1)$$

where Y is the measured response,  $\beta_0$  the intercept,  $\beta_1$  to  $\beta_3$  the linear coefficients,  $\beta_{11}$ ,  $\beta_{22}$  and  $\beta_{33}$  the square coefficients,  $\beta_{12}$ ,  $\beta_{23}$  and  $\beta_{23}$  the interaction coefficients and  $X_1$ ,  $X_2$  and  $X_3$  are the independent studied factors. Statgraphics Plus (16.1.18) was used to compute these models and the effect of the factors was statically evaluated by analysis of variance (ANOVA).

### 2.3. In vitro drug release

The release profile of EGCG from the polymeric matrix was determined by bulk-equilibrium direct dialysis as described by Fanguero

et al., with some modifications [37]. Briefly, 10 ml of EGCG/AA NPs were placed in a dialysis bag (Medicell International Ltd. MWCO 12–14,000) and dialysed against 140 ml of release medium, composed of EtOH (25%, v/v), Transcutol®P (5%, v/v) and AA (0.25% w/v), pH 3 (to ensure compound stability and mimic the acid environment of the stomach). 1 ml samples were withdrawn at regular time intervals during 24 h from the release medium and EGCG content analysed by HPLC as described elsewhere [38]. Total volume of release medium was kept constant by replacement with fresh buffer throughout the experiment.

#### 2.4. Stability study

Stability of drug and NPs was carried out for: 1) the formulation of EGCG-AA NPs; 2) EGCG in water; 3) EGCG in an aqueous solution of AA 0.25%; and 4) EGCG within the NPs formulation at storage temperatures of 4 and 25 °C.

The stability study of NPs was performed with the optical analyser Turbiscan®Lab (Formulation, L'Union, France) as described elsewhere [39]. Samples were scanned every hour for a period of 24 h. This process was repeated every month.  $Z_{av}$ , PDI and ZP of were also measured monthly.

Drug content of the NPs over time was measured at predefined times. 300 µl of acetonitrile was added to 50 µl of EGCG/AA NPs to break the polymer structure. Then, the total amount of EGCG was determined by HPLC [38]. EGCG in water and AA 0.25% solution was also assessed by direct HPLC measurement. EGCG concentrations were derived by extrapolation to a standard curve of EGCG at 25–500 µg/ml.

#### 2.5. Interaction studies

EGCG/AA NPs were ultracentrifuged (Optima® LE-BOK Ultracentrifuge, Beckman, USA) at 25,000 g, 15 °C, for 15 min. Resulting pellets were dried and pulverized.

#### 2.6. FTIR

In order to evaluate potentially new bonds generated in the manufacturing process of EGCG/AA NPs a Fourier transform infrared (FTIR) study of different components was carried out. For this, a Nicolet iZ10 with an ATR diamond and DTGS detector (Thermo Scientific) was used. 3 mg of powdered sample was added to 100 mg of KBr and scanned at 500–4000  $\text{cm}^{-1}$  in an inert nitrogen/argon atmosphere.

#### 2.7. Differential scanning calorimetry

Differential scanning calorimetry (DSC) was carried out as previously described [40]. Briefly, samples were weighed (1–3 mg) in a perforated aluminium pan and analysed in a TA 4000 system (Mettler, Greifensee, Switzerland) equipped with a DSC 25 cell. Heating was performed under a nitrogen atmosphere and a flow rate of 10 °C/min (40–280 °C). Thermograms were analysed with STARE V 9.01 dB software (Mettler, Greifensee, Switzerland).

#### 2.8. Nanoparticles transport across the BBB *in vitro*

Primary brain microvascular endothelial cells (BMVECs) were isolated from rat cortical grey matter microvessels as described elsewhere [41] and seeded onto collagen IV/fibronectin coated Transwells® (12 mm, Costar 3401, Sigma Aldrich, UK) at high density (6 rat brains per 50  $\text{cm}^2$ ). BMVECs were cultured in EBM®-2 MV (Lonza, UK) supplemented with 5 µg/ml puromycin during the initial 3 days, until transendothelial electric resistance (TEER) was above 200  $\Omega/\text{cm}^2$  (after 2–3 weeks).

In order to measure transport across this *in vitro* BBB, EGCG/AA NPs were covalently labelled with Rhodamine 110 (Sigma Aldrich,

Madrid, Spain) (12 mg/g of labelled polymer) as previously described [42,43] to produce EGCG/AA NPs-Rho. These were then added at increasing concentrations to the apical side of primary rat BMVECs grown on Transwell® filters. 50 µl of medium were removed from the basal chamber (and replaced by fresh medium) at 20 min intervals for 24 h. Fluorescence was measured in a Safire microplate reader (Tecan, Reading, UK) at 496/520 nm.

#### 2.9. Effect of EGCG/AA NPs on the *in vitro* BBB

Flux of 4 kDa fluorescein (FITC dextran) (Sigma Aldrich, UK) across primary rat BMVECs was measured as described previously [41]. Baseline flux was recorded for 2 h at which point free or encapsulated EGCG was added to the apical chamber and flux recorded for another 2–3 h. Changes of flux were expressed as linear changes of flux before and after addition of EGCG or NPs samples.

Alternatively, primary rat BMVECs were seeded on collagen type IV/fibronectin gold-coated ECIS 8W10E electrode arrays (Applied Biophysics) and real-time impedance changes and extrapolated TEER measured in response to EGCG and NPs treatments [41].

#### 2.10. Rat BMVECs staining

Monolayer of rat primary BMVECs grown on collagen IV/fibronectin coated Transwell® filters were treated with free or encapsulated EGCG. After 2 h, cells were fixed with –20 °C MeOH and then stained for Cldn-5 (1200, Thermo Fisher Scientific, UK) and nuclear DNA (Bisbenzimidazole) exactly as previously described [41]. Images were acquired on a Zeiss Axioskop 2 (Cambridge, UK) using a Hamamatsu camera and HCImage software (Hamamatsu Photonics, Hertfordshire, UK).

#### 2.11. Effect of EGCG/AA NPs on the neurovascular unit *ex vivo*

Rats were asphyxiated using CO<sub>2</sub> and immediately processed for bilateral carotid arteries cannulation. The head was first perfused with heparin (300 U/ml in isotonic saline) and then with cardioplegic solution (10 mM MgCl<sub>2</sub>, 110 mM NaCl, 8 mM KCl, 10 mM HEPES, 1 mM CaCl<sub>2</sub>, 10 µM isoproterenol), known to protect blood-neural barriers [44]. Perfusates containing Evans Blue (5 g/l in 10% BSA) in cardioplegic solution with or without EGCG or NPs at various concentrations were administered simultaneously via both carotid cannulae under equal delivery pressure (thus avoiding mixing at the Circle of Willis). After 1 h incubation, the drug-containing perfusates were washed out and brains were fixed with 4% PFA (w/v in PBS) for 24 h before sectioning and imaging of Evans Blue accumulation in brain areas on an Olympus SZX16 stereomicroscope.

#### 2.12. *In vivo* studies

6 months-old male APP/PS1 and control wild type C57BL/6 (WT) mice were used [45]. These transgenic mice express a Swedish (K594M/N595L) mutation of a chimeric mouse/human APP (mo/huAPP695swe), together with the human exon-9-deleted variant of PS1 (PS1-dE9), all of which leads to high expression of Aβ peptide. Animal groups and treatments timelines are shown in Fig. S2 of Supplementary material. Daily EGCG treatments were provided orally in the drinking water at a dose of 40 mg/kg (free or encapsulated). All animals were kept under controlled temperature, humidity and light conditions and given access to food and water *ad libitum*. Every effort was made to reduce the number of animals and minimize animal suffering. Mice were treated in accordance with the European Community Council Directive 86/609/EEC, the procedures established by the Department d'Agricultura, Ramaderia i Pesca of the Generalitat de Catalunya and approved by the local ethical committee (University of Barcelona).

### 2.13. In vivo biodistribution of EGCG/AA NPs

WT mice were given a single dose of 40 mg/kg of EGCG/AA NPs-Rho (expressed in EGCG concentration) or a corresponding dose of free Rhodamine (2.7 mg/kg) by oral gavage. After 24 h they were divided in two groups and sacrificed by: (i) cardiac perfusion with PFA 4% (previously anesthetized by intraperitoneal (i.p.) injection of sodium pentobarbital 80 mg/kg) and (ii) cervical dislocation. From the first group, brain coronal sections of 20  $\mu$ m of thickness were cut on a cryostat (Leica Microsystems, Wetzlar, Germany) for rhodamine visualization under an epifluorescence microscope (Olympus BX61, Barcelona, Spain). From the second group, different organs were collected and processed to determine the biodistribution of EGCG/AA NPs by detecting the EGCG amount by LC-MS-MS as described elsewhere [46]. All measurements were run in triplicate.

### 2.14. Pharmacokinetic assay

40 mg/kg of EGCG/AA NPs (expressed as EGCG concentration) and free EGCG were administered to WT mice by oral gavage. To evaluate the pharmacokinetic profile, animals were anesthetized with isoflurane and sacrificed by cardiac puncture at different time intervals. Blood and brain were collected to measure EGCG amount by LC-MS-MS. Samples processing was performed as described Chen et al. with some modifications [47]. Briefly, blood samples were centrifuged at 4,000 g during 4 min at 4 °C, plasma was removed, extracted with ethyl acetate twice and resuspended in 20% AA, 10% acetonitrile. Brains were weighed, homogenized in 20% AA, 0.5 mg/ml Na<sub>2</sub>EDTA, PBS 0.4 M and centrifuged at 16,000 g during 10 min at 4 °C. Then, supernatant was extracted the same as those plasma samples. All measurements were run in triplicate.

### 2.15. Behavioural test

#### 2.15.1. Morris water maze

Morris water maze (MWM) test was performed in a circular tank with latex white water and a platform, which was kept in the same position during all the experiment, submerged 1 cm below the water surface. Temperature and intensity of light were kept at 25  $\pm$  2 °C and 30 lx throughout all the days. The procedure was based on six training days (1 min per trial) and one test day. On the test day, the platform was removed and the mouse was placed in the tank in the quadrant opposite to where the platform used to be for 1 min. The behavioural

data were acquired and analysed using SMART V3.0 (Panlab Harvard Apparatus, Germany) video tracking system.

#### 2.15.2. Novel object recognition

Novel object recognition (NOR) test was used as indicator of cognitive impairment [48]. Briefly, in a first phase of habituation (days 1–3), mice were placed in an open field (without any object) to familiarize themselves with. On day 4, two identical objects were placed at equidistance and the exploration time of each one was recorded. On the day of the test the same process was repeated by changing one of the familiar objects to a different one (novel object). The duration of each trial was 10 min. The results of the test were expressed as (eq. 2):

$$\text{Exploration time (\%)} = \frac{\text{Exploration time of new object (s)}}{\text{Total exploration time (s)}} \cdot 100 \quad (2)$$

#### 2.15.3. Immunohistochemistry and Thioflavin-S staining

At the end of treatments and behavioural studies, mice were sacrificed by i.p. injection of ketamine/xylazine (100/10 mg/kg, respectively) and perfusion with 4% PFA. Brains were removed and maintained at 4 °C in 30% sucrose, 4% PFA solution until they were cut in 20  $\mu$ m coronal sections using a cryostat (Leica Microsystems, Wetzlar, Germany). Sections were stained as described elsewhere [40]. Primary polyclonal antibodies against glial fibrillary acidic protein (GFAP) (1:1000; Dako Chemicals, Glostrup, Denmark) and Synaptophysin (SYN) (1200, Dako Products, Sta. Clara, CA, USA) and secondary antibodies AlexaFluor 594 goat anti-rabbit (Red, 1:1000; Life Technologies, Cambridge, UK) and AlexaFluor 488 goat anti-mouse (Green, 1:1000; Life Technologies, Cambridge, UK), were used. Image acquisition was carried out with an epifluorescence microscope (BX41, Olympus, Germany).

To detect A $\beta$  plaques in brain slides, Thioflavin-S (ThS) staining was performed as described elsewhere [49]. Briefly, brain sections were incubated with 5 ml of ThS 0.3% and washed twice with 10 ml of EtOH 50% and PBS. Slides were mounted with Fluoromount on gelatin-coated glass microscope and observed under the epifluorescence microscope. Plaque quantification was carried out using the same areas, focusing on the hippocampus and cortical area.

#### 2.15.4. Evaluation of $\beta$ -amyloid peptides levels

Measurement of A $\beta$ <sub>(1-42)</sub> peptides in cortical tissues was carried out using a commercially available human ELISA according to manufacturer's guideline kit (Cat # KHB3441; Invitrogen, Camarillo, CA, USA).

**Table 1**

Optimization study results of EGCG/AA NPs by 2<sup>3</sup> central composite factorial design.

| Factorial points | C.EGCG      |         | C. AA       |         | C.PLGA-PEG  |         | Z <sub>av</sub><br>(nm) | PDI               | ZP<br>(mV)      | EGCG EE<br>(%) | AA EE<br>(%)   |
|------------------|-------------|---------|-------------|---------|-------------|---------|-------------------------|-------------------|-----------------|----------------|----------------|
|                  | Coded level | (mg/ml) | Coded level | (mg/ml) | Coded level | (mg/ml) |                         |                   |                 |                |                |
| F1               | -1          | 2       | -1          | 2       | -1          | 12      | 126.5 $\pm$ 4.1         | 0.063 $\pm$ 0.019 | -17.8 $\pm$ 0.5 | 94.4 $\pm$ 4.5 | 91.1 $\pm$ 2.1 |
| F2               | 1           | 3       | -1          | 2       | -1          | 12      | 174.7 $\pm$ 11.4        | 0.060 $\pm$ 0.004 | -19.9 $\pm$ 0.6 | 97.5 $\pm$ 3.2 | 90.5 $\pm$ 6.1 |
| F3               | -1          | 2       | 1           | 3       | -1          | 12      | 121.7 $\pm$ 0.9         | 0.070 $\pm$ 0.001 | -13.6 $\pm$ 0.8 | 96.1 $\pm$ 1.2 | 90.3 $\pm$ 2.7 |
| F4               | 1           | 3       | 1           | 3       | -1          | 12      | 185.1 $\pm$ 8.2         | 0.586 $\pm$ 0.085 | -16.1 $\pm$ 2.1 | 97.8 $\pm$ 1.3 | 92.5 $\pm$ 1.1 |
| F5               | -1          | 2       | -1          | 2       | 1           | 16      | 126.5 $\pm$ 6.1         | 0.067 $\pm$ 0.003 | -14.5 $\pm$ 0.8 | 96.5 $\pm$ 1.3 | 94.2 $\pm$ 4.2 |
| F6               | 1           | 3       | -1          | 2       | 1           | 16      | 144.6 $\pm$ 27.1        | 0.255 $\pm$ 0.110 | -20.7 $\pm$ 2.3 | 97.9 $\pm$ 2.8 | 95.1 $\pm$ 1.2 |
| F7               | -1          | 2       | 1           | 3       | 1           | 16      | 134.1 $\pm$ 5.0         | 0.050 $\pm$ 0.012 | -14.9 $\pm$ 1.6 | 96.8 $\pm$ 2.4 | 95.8 $\pm$ 3.1 |
| F8               | 1           | 3       | 1           | 3       | 1           | 16      | 176.5 $\pm$ 18.9        | 0.183 $\pm$ 0.098 | -17.1 $\pm$ 3.5 | 98.0 $\pm$ 0.8 | 97.0 $\pm$ 1.3 |
| Axial points     |             |         |             |         |             |         |                         |                   |                 |                |                |
| F9               | -1.68       | 1.66    | 0           | 2.5     | 0           | 14      | 119.6 $\pm$ 5.9         | 0.076 $\pm$ 0.006 | -12.6 $\pm$ 0.8 | 95.9 $\pm$ 4.5 | 93.9 $\pm$ 1.2 |
| F10              | 1.68        | 3.34    | 0           | 2.5     | 0           | 14      | 512.4 $\pm$ 64.0        | 0.293 $\pm$ 0.126 | -11.5 $\pm$ 0.8 | 97.2 $\pm$ 2.6 | 95.5 $\pm$ 2.1 |
| F11              | 0           | 2.5     | -1.68       | 1.66    | 0           | 14      | 277.4 $\pm$ 20.9        | 0.284 $\pm$ 0.207 | -18.2 $\pm$ 0.8 | 96.4 $\pm$ 1.9 | 90.6 $\pm$ 2.4 |
| F12              | 0           | 2.5     | 1.68        | 3.34    | 0           | 14      | 135.0 $\pm$ 10.1        | 0.062 $\pm$ 0.015 | -12.5 $\pm$ 0.1 | 97.1 $\pm$ 1.3 | 95.3 $\pm$ 0.6 |
| F13              | 0           | 2.5     | 0           | 2.5     | -1.68       | 10.64   | 186.7 $\pm$ 2.3         | 0.169 $\pm$ 0.064 | -14.1 $\pm$ 1.6 | 96.3 $\pm$ 2.1 | 90.1 $\pm$ 2.4 |
| F14              | 0           | 2.5     | 0           | 2.5     | 1.68        | 17.36   | 129.7 $\pm$ 4.3         | 0.061 $\pm$ 0.006 | -18.3 $\pm$ 0.4 | 95.7 $\pm$ 3.1 | 96.9 $\pm$ 0.7 |
| Central points   |             |         |             |         |             |         |                         |                   |                 |                |                |
| F15              | 0           | 2.5     | 0           | 2.5     | 0           | 14      | 124.8 $\pm$ 5.2         | 0.054 $\pm$ 0.013 | -15.1 $\pm$ 1.7 | 97.1 $\pm$ 2.4 | 94.3 $\pm$ 1.6 |
| F16              | 0           | 2.5     | 0           | 2.5     | 0           | 14      | 129.6 $\pm$ 5.2         | 0.063 $\pm$ 0.013 | -15.7 $\pm$ 1.7 | 96.5 $\pm$ 2.4 | 96.1 $\pm$ 1.7 |

A $\beta$  content of cortical extracts homogenates was expressed in picograms of A $\beta$  per milligrams of total protein [45].

### 2.15.5. Statistical analysis

Data are presented as the mean  $\pm$  S.D. One-way ANOVA followed by Tukey post hoc test was performed for groups comparison using GraphPad 6.0 Prism. Statistical significance was set at  $p < 0.05$  (\*).

## 3. Results

### 3.1. Optimization and physicochemical characteristics of EGCG/AA NPs

Physicochemical characteristics of 16 formulations tested in the  $2^3$  composite central factorial design are shown in Table 1. From this an optimal formulation was chosen consisting of 2.5 mg/ml of EGCG, 2.5 mg/ml of AA and 14 mg/ml of PLGA-5% PEG. Tween®80 concentration of the aqueous phase  $W_2$  and outer covering was 2.5 and 0.04% (i.e. resulting in a final concentration of 1.016% of surfactant). EGCG/AA NPs optimized in this way exhibited a monodisperse population (PDI  $0.054 \pm 0.013$ ) with a  $Z_{av}$  of  $124.8 \pm 5.2$  nm. The response surface showed a direct relationship of EGCG concentration and  $Z_{av}$  and PDI; both decreasing as the amount of EGCG decreased (Fig. 1A and B). The optimized formulation showed a ZP of ca.  $-15$  mV (Fig. 1C). EGCG EE was higher than 97%, slightly decreasing at low concentrations of PLGA-PEG (Fig. 1D). AA EE value was higher than 94%.

### 3.2. Interaction studies

No covalent bonds were observed between both drugs and polymer in line with our previous studies [40]. EGCG FTIR profile exhibited typical peaks at 1543, 1690 and  $3356\text{ cm}^{-1}$  which correspond to C–C stretch in aromatic ring, a C=O group that links the trihydroxybenzoate and chroman groups and an OH group attached to the aromatic ring, respectively [50]. AA exhibited intense bands at 1322 and  $1674\text{ cm}^{-1}$ , which correspond to the enol hydroxyl group and the stretching vibration of the C=C group, respectively [51]. PLGA-PEG showed a peak at  $1743\text{ cm}^{-1}$  corresponding to the C–O stretching vibration of the carbonyl groups of lactic and glycolic acid. Intense bands were also detected between 2900 and  $2950\text{ cm}^{-1}$  due to the C–H stretching of PLGA-PEG [52]. Drug-loaded NPs exhibited a very similar FTIR profile to polymer, as well as empty NPs, but not as EGCG FTIR pattern. The encapsulation of the drug was evident by an important decrease of the absorbance in the EGCG/AA NPs profile against the polymer profile (Fig. S3A of Supplementary material).

EGCG and AA exhibited similar DSC profiles due to their common crystalline chemical structure (Fig. S3B of Supplementary material). Endothermic peaks of melting transition at 225 and 195 °C, respectively, more intense in the case of AA, were observed. These peaks were followed by an exothermic peak at 235 °C in both cases, which is related to the melting process of the drugs. Drug-loaded NPs and empty NPs DSC profiles were similar to that of polymer itself, suggesting that both molecules may converge to an amorphous or disordered crystalline form which led to their inclusion inside the NPs [50].

These results suggest that both EGCG and AA were dissolved in the form of a molecular dispersion and successfully included into the PLGA-PEG matrix.

### 3.3. NP formulated EGCG displays improved physicochemical stability

EGCG/AA NPs were stored at either 4 °C and 25 °C for extended periods. Backscattering profiles were established to determine stability (Fig. 2A and B). The formulation only became instable after 4 mo of storage at 25 °C. At this time, it was also noted that coloration of the normally white sample turned brown, presumably due to the oxidation of both drugs. Furthermore a precipitate appeared presumably due to

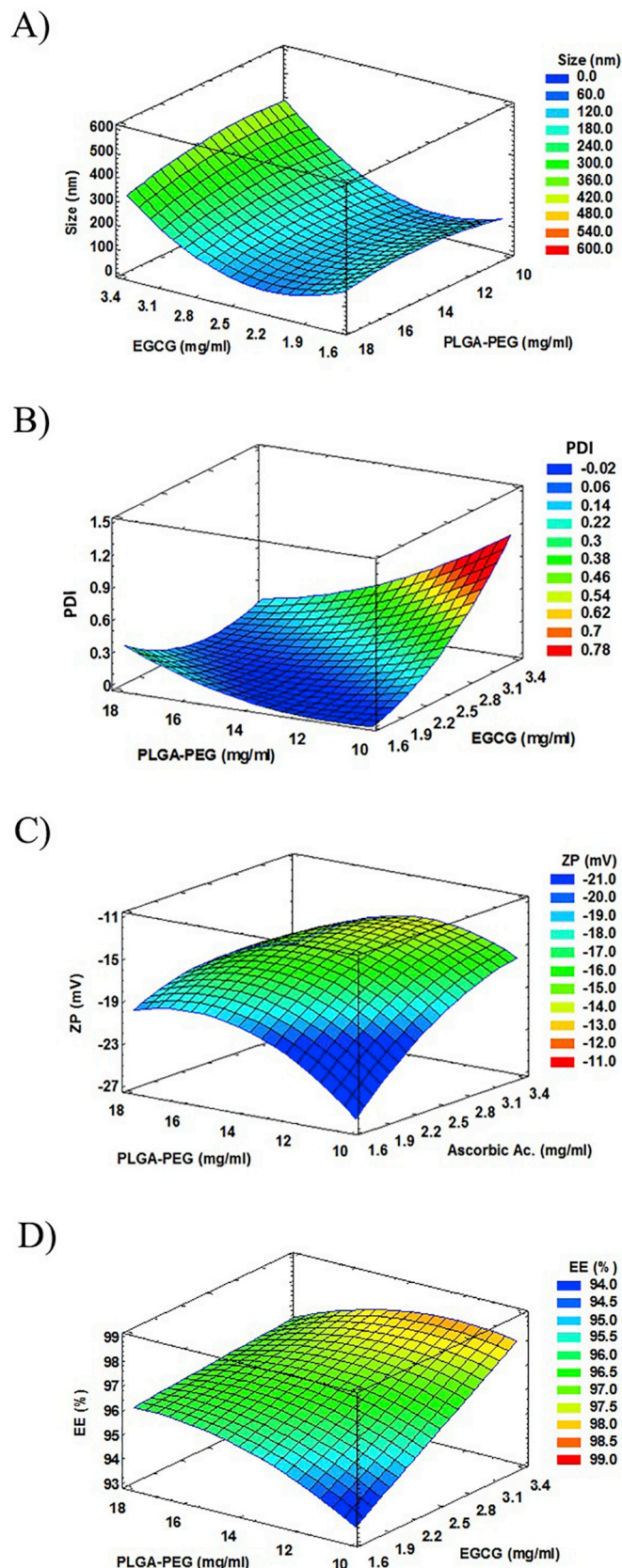


Fig. 1. Results of EGCG/AA NPs optimization study. (A) Response surface of size at fixed value of AA 2.5 mg/ml. Optimized value  $124.8 \pm 5.2$  nm. (B) Response surface of PDI at fixed value of AA 2.5 mg/ml. Optimized value  $0.054 \pm 0.013$ . (C) Response surface of ZP at fixed value of EGCG 2.5 mg/ml. Optimized value  $-15.1 \pm 1.7$  mV. (D) Response surface of EGCG EE at fixed value of AA 2.5 mg/ml. Optimized value  $97.1 \pm 2.4$  (%).

degradation of the polymeric matrix [53] (Fig. S4 of Supplementary material). By contrast, EGCG/AA NPs stored at 4 °C remained stable for up to 11 months.  $Z_{av}$ , PDI and ZP measurements confirmed these results (Table S1 of Supplementary material).

HPLC measurements showed that free EGCG suffered fast degradation when it was dissolved in aqueous solutions. The half-life of EGCG in water was ca. 3 and 8 days at 25 °C and 4 °C, respectively, in accordance with a previous report by Proniuk et al. [54]. The addition of AA 0.25% increased half-life of the drug to ca. 9 and 15 days at 25 °C and 4 °C, respectively. In contrast, EGCG incorporated in EGCG/AA NPs maintained at least 80% of its integrity for 1 mo at both temperatures (Fig. 2C).

### 3.4. In vitro drug release profile

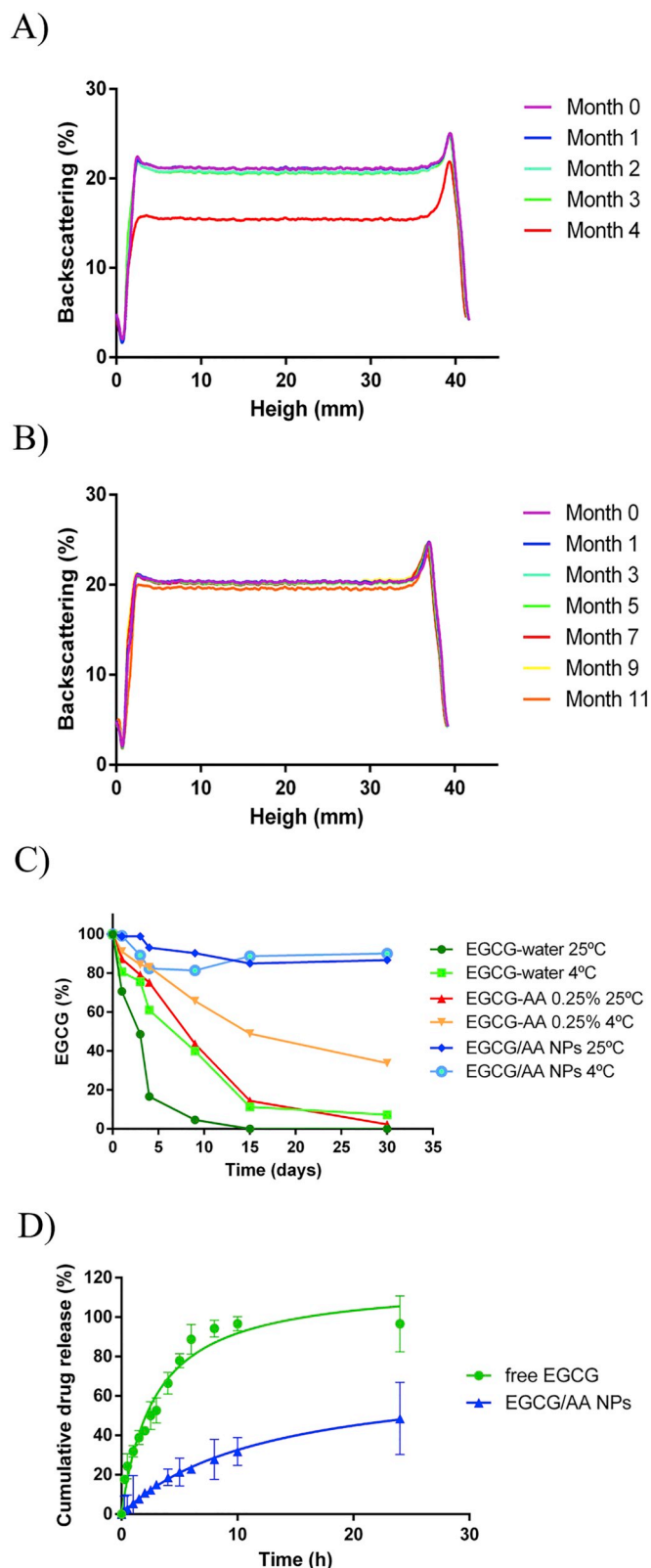
One of the main advantages of polymeric controlled drug delivery systems is sustained release of encapsulated drugs, which is usually governed by a diffusion/degradation process [53]. The drug release profile of EGCG/AA NPs was determined in vitro by dialysis against a release medium at acid pH, taking into consideration the EGCG instability at neutral pH and, in preparation of oral use of EGCG/AA in mice (see below), the acid environment of the stomach [55–57]. When free EGCG was dialysed, its concentration in the dialysate reached the theoretical equilibrium concentration after about 10 h (Fig. 2D). In contrast only 23% of EGCG had been released from EGCG/AA NPs to the dialysate at that time. After 24 h, NPs had released almost 50% of EGCG. Taken together this indicated that our NP formulation displayed characteristics of sustained release.

### 3.5. In vivo biodistribution and EGCG pharmacokinetics

3 months-old C57BL/6 mice were treated with a single oral dose of EGCG/AA NPs 40 mg/kg. After 24 h EGCG content was determined in various organs (Fig. 3A). EGCG had accumulated strongly in the liver. Whilst in the brain, EGCG concentration was ca. 10 times lower, brain accumulation constituted ca. 0.025% of the administered EGCG. Pharmacokinetic profiles of EGCG were established after an oral administration both of EGCG/AA NPs and free EGCG (Fig. 3B and C, Table 2). After 1 h, maximal EGCG plasma concentrations were very similar under both conditions ( $1078.976 \pm 242.238$  ng/ml for free EGCG v.  $842.590 \pm 78.911$  ng/ml for EGCG/AA NPs). Thereafter, whilst a rapid decrease in plasma EGCG concentration was observed in mice administered with free EGCG (to  $60.267 \pm 40.150$  ng/ml after 24 h), EGCG plasma concentration stabilised at ca. 500 ng/ml (with  $361.346 \pm 156.176$  ng/ml at 24 h) in mice treated with EGCG/AA NPs. Analysis of AUC of plasma EGCG concentrations revealed significant differences with  $10,270.624 \pm 123.564$  h.ng/ml following oral treatment with EGCG/AA NPs and only  $4509.790 \pm 65.411$  h.ng/ml following free EGCG.

A similar pharmacokinetic profile was observed in the brain of these mice. EGCG reached maximal concentration of  $0.908 \pm 0.162$  ng/mg when it was administered encapsulated in NPs, as compared to  $0.826 \pm 0.206$  ng/mg following free form administration. Again cerebral EGCG concentrations stabilised at a significantly higher concentrations following EGCG/AA NPs, with EGCG concentrations of  $0.561 \pm 0.119$  ng/mg and  $0.111 \pm 0.022$  ng/mg at 24 h, following treatment with EGCG/AA NPs and free EGCG, respectively. AUC analyses showed  $14.410 \pm 3.511$  and  $6.426 \pm 0.811$  h.ng/mg following encapsulated and free administration, respectively. Overall these data indicated that NPs stabilised circulating EGCG and consequently cerebral accumulation of the drug.

EGCG brain penetration was investigated indirectly by histochemical analysis in mice following a single oral dose of EGCG/AA NPs-Rho. Inspection of fixed coronal sections revealed discrete accumulation of Rhodamine structures, which were ca. 5–15  $\mu$ m in size in various areas of the brain (Fig. 3D) (shown are the *dentatus gyrus* of hippocampus and



(caption on next page)

**Fig. 2.** Stability and in vitro drug release results. (A) Backscattering profile of EGCG/AA NPs at 25 °C showed nanovehicle instability after 4 months. (B) Backscattering profile of EGCG/AA NPs stored at 4 °C did not show any instability for up to 11 months. (C) EGCG chemical stability in different solutions, formulations and storage temperatures. EGCG showed a significant increase in the stability after the addition of AA to the medium and its incorporation into PEGylated PLGA NPs. (D) In vitro drug release of EGCG/AA NPs and free EGCG. In each condition 25 mg of EGCG were dialysed in a total volume of 150 ml. Thus 0.167 mg/ml was 100% of the maximal equilibrium concentration. Cumulative drug release from EGCG/AA NPs at 24 h = 48.6%. Data shown was from triplicate experiments.

cortex). In contrast, mice treated with free Rhodamine showed a diffused staining in the brain.

### 3.6. Effect of EGCG/AA NPs on BBB integrity

NPs have been proposed to facilitate or even open a specific transport route across the BBB [58,59]. Passage of EGCG/AA NPs-Rho was assessed using rat primary BMVECs, a well-established in vitro model of BBB [41]. Added apically at concentrations of 15 of 15, 50, 150 and 500 µg/ml EGCG/AA NPs-Rho crossed BBB cell monolayers in concentration dependent manner (Fig. 4A), initially being mostly linear but then plateauing when reaching the equilibrium concentration (kinetically fitting an exponential one-phase association model).

Free EGCG at and above 15 µg/ml, EGCG/AA NPs at and above EGCG concentration of 15 µg/ml as well as empty NPs at equivalent concentrations induced significantly enhanced 4 kDa dextran flux in cultured primary rat BMVECs (Fig. 4B). They also induced disruption of BMVEC electrical barrier indicating that tight junctions were affected (Fig. 4C). Indeed, immunohistochemical analysis showed that junctional Claudin-5 was lost from primary BMVEC monolayers treated with increasing concentrations of free EGCG, empty and EGCG/AA NPs (Fig. 4D). Excessive leakage was also observed in rat ex vivo brains in

response to free EGCG, empty NPs and EGCG/AA NPs at and above concentrations (or equivalents) of 150 µg/ml (Fig. 4E), indicating that EGCG and empty NPs themselves could disrupt the BBB.

### 3.7. EGCG/AA NPs increase synaptic expression in APP/PS1 mice

We next investigated the therapeutic effect of EGCG/AA NPs in APP/PS1 mice. Synaptic loss, as evidenced by decreased SYN immunoreactivity in the hippocampus area of patients with early and established AD and demented individuals, correlates with the development of neuropathology and severe cognitive deficit [60]. APP/PS1 mice showed reduction of SYN staining in the CA3 region of hippocampus. In contrast, APP/PS1 mice, treated with either free or NPs formulated EGCG, displayed enhanced SYN staining. In fact, EGCG/AA NPs group showed even higher SYN staining than the WT group (Fig. 5A). 3D surface mapping analysis confirmed these results (Fig. 5B).

### 3.8. EGCG/AA NPs reduce neuroinflammation and Aβ plaque/peptide burden in APP/PS1 mice

Neuroinflammation with accompanying accumulation of Aβ plaques plays a crucial role in the pathogenesis of AD [61]. Astrocyte activation and concomitant enhanced GFAP expression have been widely used as a neuroinflammatory indicator [62]. Neuroinflammation and Aβ plaque accumulation was assessed in WT and APP/PS1 mice by Th-S and GFAP staining (Fig. 6A). Hippocampal and cortical areas of APP/PS1 mice displayed much stronger GFAP reactivity as well as altered morphology when compared to that of WT littermates. Treatment of APP/PS1 mice with free EGCG had little effect on GFAP expression. However, EGCG/AA NPs treatment strongly reduced GFAP reactivity, with observed levels similar to those of WT littermates. APP/PS1 mice showed Aβ plaques accumulation in these cerebral areas analysed. Whilst treatment with either free or NP encapsulated EGCG showed

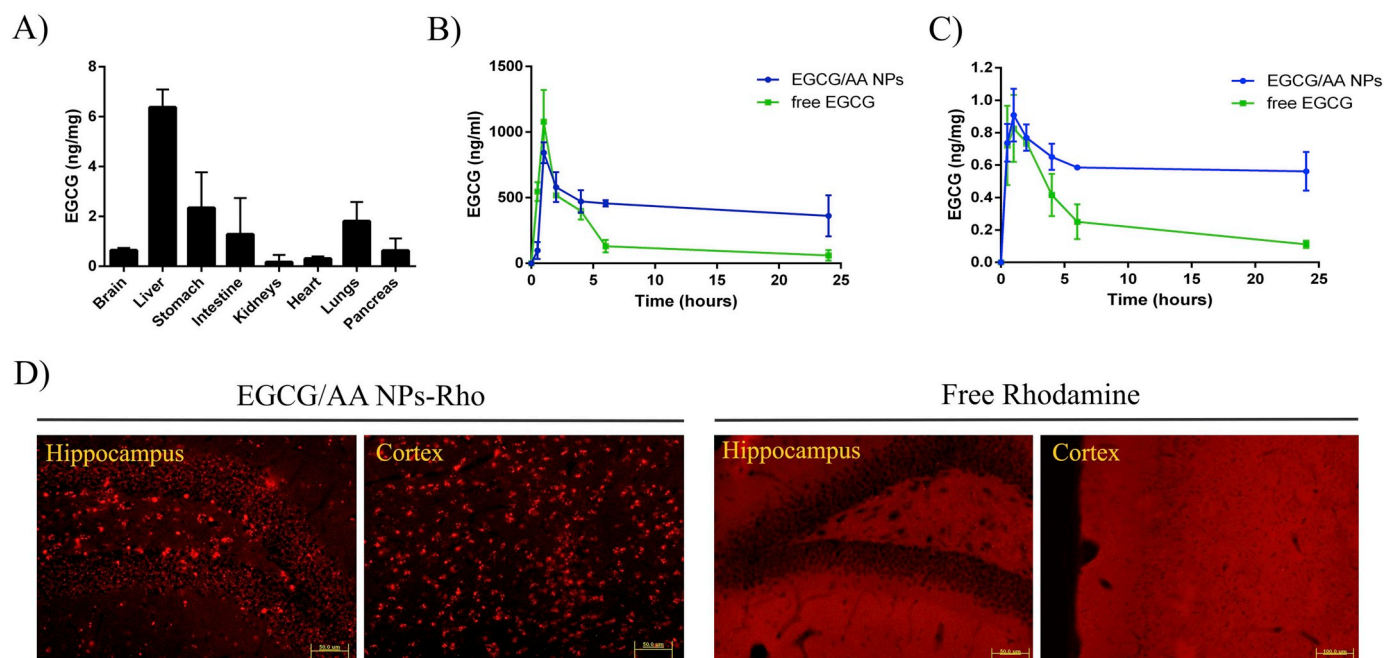


**Fig. 3.** In vivo biodistribution and pharmacokinetics of EGCG/AA NPs. 3 months-old C57BL/6 WT mice were treated with a single oral dose of EGCG/AA NPs and EGCG/AA NPs-Rho 40 mg/kg. (A) Histograms show biodistribution of EGCG in brain, liver, stomach, intestine, kidneys, heart, lungs and pancreas of mice after 24 h of EGCG/AA NPs administration. Data expressed as EGCG amount per mg of tissue. Mean administered volume of EGCG/AA NPs was 448 µl (1.120 mg). Mean brain EGCG concentration was 0.6 ng/ml. With mean brain weight of 470 mg this represented 0.025% of administered EGCG. (B) Plasma and (C) brain pharmacokinetic profile of EGCG following single oral dose administration of free EGCG or EGCG/AA NPs (40 mg/kg). Data expressed as EGCG amount per ml of plasma and EGCG amount per mg of tissue, respectively. (D) Rhodamine detection in the *dentatus gyrus* of the hippocampus and the cortex of mice treated with EGCG/AA NPs-Rho (40 mg/kg) or free Rhodamine (2.7 mg/kg). Scale bar 50 µm.

**Table 2**

Pharmacokinetic parameters of an oral gavage administration of EGCG/AA NPs and free EGCG 40 mg/kg in 3 months-old C57BL/6 mice. Non-compartmental model.

| Parameter         | EGCG/AA NPs         | Free EGCG          | Unit    | EGCG/AA NPs      | Free EGCG      | Unit    |
|-------------------|---------------------|--------------------|---------|------------------|----------------|---------|
|                   | Plasm               |                    |         | Brain            |                |         |
| AUC <sup>a</sup>  | 10270.624 ± 123.564 | 4509.790 ± 65.411  | h.ng/ml | 14.410 ± 3.511   | 6.426 ± 0.811  | h.ng/mg |
| C <sub>max</sub>  | 842.590 ± 78.911    | 1078.976 ± 242.238 | ng/ml   | 0.908 ± 0.162    | 0.826 ± 0.206  | ng/mg   |
| T <sub>max</sub>  | 1.000 ± 0.000       | 1.000 ± 0.000      | h       | 1.000 ± 0.000    | 1.000 ± 0.000  | h       |
| λ <sub>z</sub>    | 0.013 ± 0.007       | 0.0871 ± 0.006     | 1/h     | 0.005 ± 0.003    | 0.058 ± 0.006  | 1/h     |
| HL λ <sub>z</sub> | 52.360 ± 9.024      | 7.956 ± 0.625      | h       | 128.144 ± 16.051 | 12.025 ± 1.009 | h       |
| V <sub>z</sub> /F | 1850.574 ± 75.166   | 2503.858 ± 100.021 | ml      | NA               | NA             | ml      |
| Cl/F              | 24.498 ± 7.212      | 218.1483 ± 46.854  | ml/h    | NA               | NA             | ml/h    |
| MRT <sup>∞</sup>  | 75.415 ± 6.341      | 9.489 ± 0.079      | h       | 184.687 ± 11.267 | 14.860 ± 2.362 | h       |

<sup>a</sup> AUC was measured between 0 and 24 h.

reduction of Aβ plaques in the hippocampus, the reduction was significantly greater in the EGCG/AA NPs treated group (Fig. 6B). Cortical Aβ plaque count revealed that both treatments were equally effective in reducing the number of Aβ plaques (Fig. 6C).

Soluble and insoluble Aβ42 peptide was quantified in cortical extracts of APP/PS1 mice by ELISA. Oral EGCG/AA NPs treatment led to a significant reduction of both soluble and insoluble Aβ42 peptide in the cortex (Fig. 6D and E). However, treatment with free EGCG did not show any significant reduction in either Aβ42 peptide population. Taken together these data indicated that EGCG/AA NPs were more effective in reducing neuroinflammation and pathological Aβ accumulation in APP/PS1 mice.

### 3.9. EGCG/AA NPs improve EGCG effectiveness on spatial memory and learning process in APP/PS1 mice

The behaviour of APP/PS1 transgenic mice was assessed following EGCG treatment for 3 mo. Mice were subjected to a MWM test as measure for learning ability and spatial memory mechanisms [63]. APP/PS1 mice displayed significantly longer escape latency time than WT control mice. Following treatment with free or NPs formulated EGCG, APP/PS1 mice showed a significant decrease in escape latency time during the training phase (Fig. 7A). On the day of the test, EGCG/AA NPs treated APP/PS1 mice showed a significantly reduced escape latency time, which was similar to WT mice (Fig. 7B). Free EGCG treatment also significantly reduced escape latency on the test day, however it was still significantly longer than that of EGCG/AA NPs treated APP/PS1 mice. APP/PS1 also showed significantly reduced exploration time in the target quadrant. Exploration time was significantly enhanced with either EGCG treatment (Fig. 7C). Additionally, the time spent in the border area was analysed as indicator of the anxiety level. Results revealed that both treated groups significantly displayed reduced border exploration time, nearly at levels of WT controls (Fig. 7D).

### 3.10. EGCG/AA NPs improve EGCG effect on cognitive process in APP/PS1 mice

The NOR test, which is based on the natural tendency of mice to explore new objects and environments is widely used in the evaluation of short- and long-term cognitive deficits in AD [48]. APP/PS1 mice were treated with EGCG/AA NPs or free EGCG for 12 weeks. Assessment by NOR test showed a significant improvement in performance in both treated groups. Significantly, the EGCG/AA NPs group performed even better results than the free drug group, with similar NOR scores than those observed in the WT group (Fig. 7E). Taken together these data indicated that EGCG/AA NPs offered a significant treatment advantage over free EGCG.

## 4. Discussion

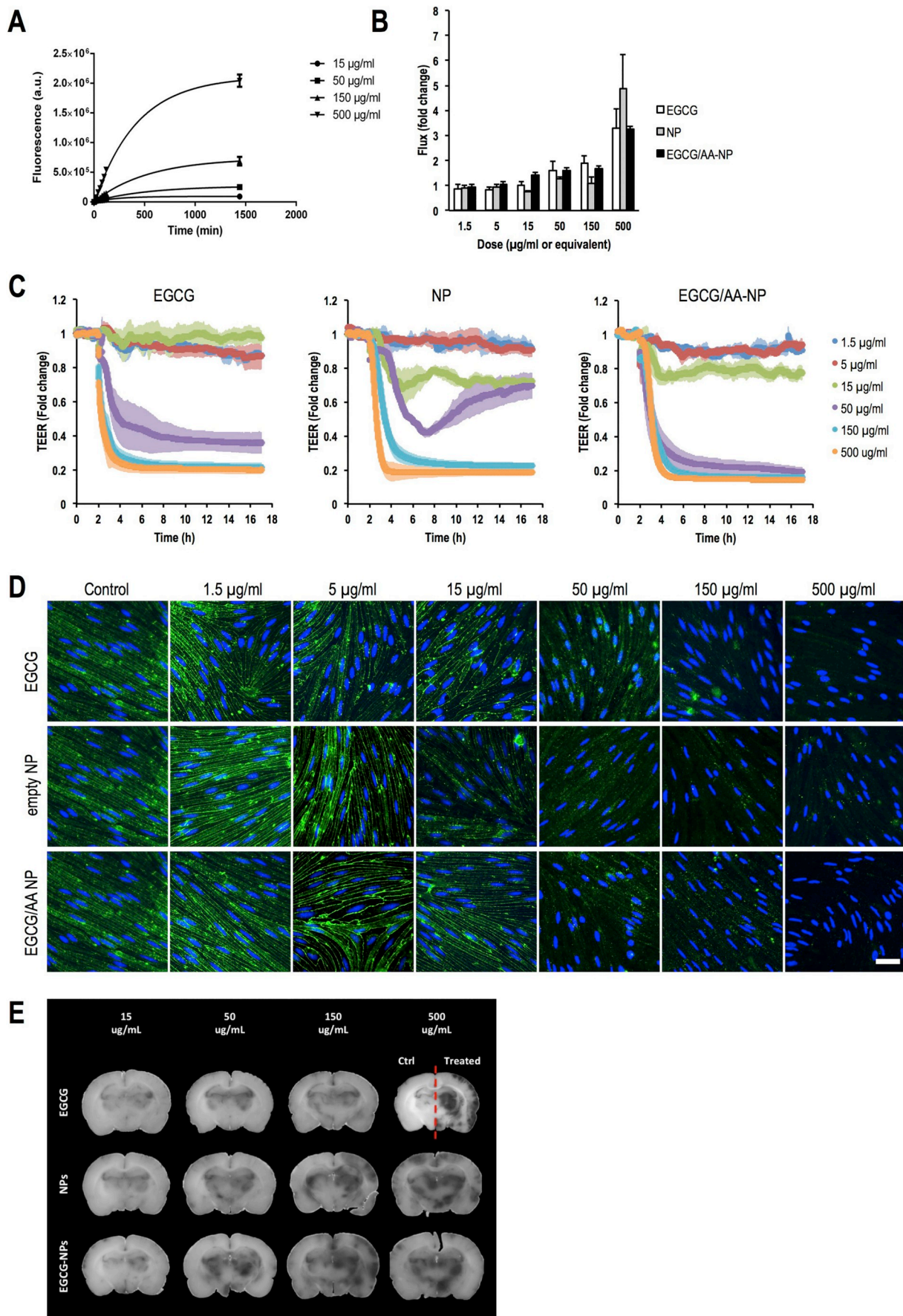
Neurodegeneration and dementia associated with AD is the result of many cytological and biochemical alterations in the brain [1]. There are currently no effective treatments and in this context, our study focused on developing EGCG as a new therapeutic option for AD. Specially we opted to address this drug's inherent chemical instability and resulting low bioavailability [24] by incorporating it into polymeric NPs. Nanovehicle incorporation stabilised EGCG, produced a better pharmacokinetic profile of EGCG with higher concentrations in the brain and, in APP/PS1 mice, was more effective in reducing neuroinflammation and Aβ accumulation and in improving cognitive deficits.

We chose to formulate EGCG in polymeric nanostructures of PLGA based matrix. PLGA was one of the first polymers approved by US Food and Drug Administration for biomedical applications because of its biocompatibility, biodegradability and non-toxicity [64]. Overall, the biocompatibility and safety of PLGA NPs has been demonstrated and does not involve a risk of peripheral side effects [72,73]. PLGA is widely used in nanomedicine for brain diseases, since it possesses a great versatility in its manufacture, physicochemical properties and functionalization [65]. Likewise, PEGylated polymeric matrix was used, since it is well described that the coating with PEG enhance a rapid spread of carried drugs within brain tissue [66]. Conjugation of PEG to the NPs surface may also contribute to an enhanced penetration across the intestinal barrier, since PEGylation has been described to increase the permeability coefficient of solid lipid nanoparticles by 1.5–2 times and their resulting bioavailability by 1.99 to 7.5 times [67]. Additionally, our EGCG/AA NPs were formulated with Tween®80 as surfactant (final concentration 1.016%) since this has been reported to facilitate brain uptake of a number of drugs [68]. Lastly, we chose to incorporate AA together with EGCG in NPs with the aim to provide a stabilizing, antioxidant environment. AA, together with EGCG, may also mitigate potential local inflammatory response [69,70], which has been ascribed to hydrolytic degradation products derived from PLGA during chronic administration [71]. We have used similar EGCG PLGA NPs before, albeit at lower drug and surfactant concentration and without AA, with demonstrable therapeutic benefits in a mouse model of epilepsy [40].

Our optimized formulation of EGCG/AA NPs significantly enhanced shelf stability of EGCG, in particular in an aqueous environment and demonstrated adequate properties for enhanced brain delivery. With our formulation, we achieved small Z<sub>av</sub>, monomodal population and negative surface charge, which contributes to enhance the stability of NPs due to the increase of repulsion forces. In fact, PLGA matrix commonly suffers surface erosion and is degraded through a hydrolytic cleavage of its polyester backbone, resulting in smaller structures of byproducts, which also contains encapsulated drug [74]. These processes give rise to a reduction of particle size, which could also contribute to the enhancement of encapsulated drug penetration.

Importantly, EGCG showed an adequate and sustained release profile from the polymeric nanostructures, indicating suitability for long-term treatment. Taken together EGCG/AA NPs showed the desired





(caption on next page)

**Fig. 4.** Effect of EGCG formulations on in vitro models (A) Flux of 15, 50, 150 and 500  $\mu\text{g/ml}$  of EGCG/AA NPs-Rho across primary rat BMVECs within the initial 2 h. Data are shown as mean  $\pm$  SD. At 1440 min values of each data set showed statistical difference to each of the other groups ( $p < 0.001$ , ANOVA). (B) FITC-dextran flux across primary rat BMVECs in the presence of 1.5, 5, 15, 50, 150 and 500  $\mu\text{g/ml}$  EGCG, EGCG/AA NPs and equivalent amounts of empty NPs. Flux rates in the absence of drug were normalised to 1. Data are shown as mean  $\pm$  SEM. (C) Normalised TEER real time measurement of BMVECs monolayer in response to 1.5, 5, 15, 50, 150 and 500  $\mu\text{g/ml}$  EGCG, EGCG/AA NPs and equivalent amounts of empty NPs (added at 2 h). Shown are mean  $\pm$  SEM. (D) Claudin-5 (green) and DNA (blue) staining of BMVECs monolayer after exposure to 1.5, 5, 15, 50, 150 and 500  $\mu\text{g/ml}$  EGCG, EGCG/AA NPs and equivalent amounts of empty NPs for 1 h. Scale bar 10  $\mu\text{m}$ . (E) Evans Blue/Albumin leakage response in ex vivo rat brains treated on the indicated side with 1.5, 5, 15, 50, 150 and 500  $\mu\text{g/ml}$  EGCG, EGCG/AA NPs or equivalent amounts of empty NPs for 1 h. (For interpretation of the references to color in this figure legend, the reader is referred to the web version of this article.)

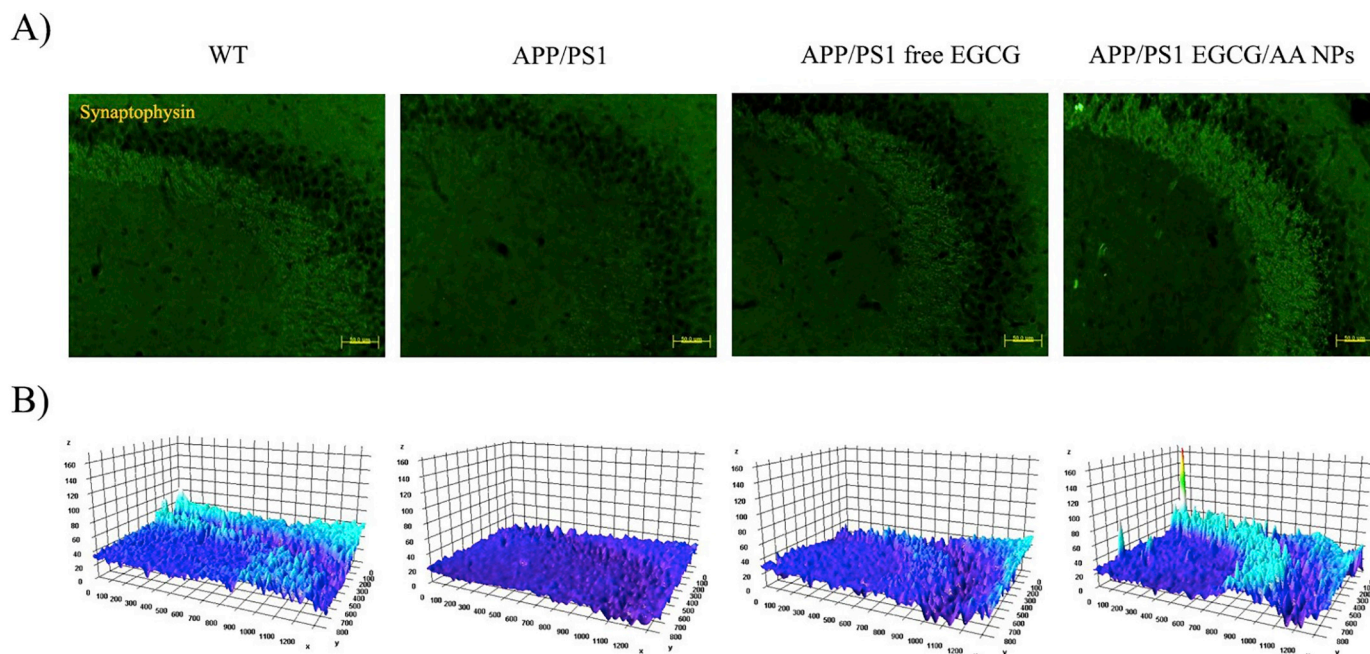


**Fig. 5.** Effect of EGCG treatments on SYN expression. 3 months-old APP/PS1 mice were orally treated with EGCG/AA NPs or free EGCG 40 mg/kg/day for 3 months. At 6 months, animals were sacrificed by perfusion with 4% PFA and brains were cut with a cryostat. SYN immunostaining was performed on 20  $\mu\text{m}$  coronal sections. (A) SYN staining of CA3 hippocampus region. Scale bar 50  $\mu\text{m}$ . (B) 3D surface mapping analysis of SYN staining. Interactive 3D surface Plot v 2.4, Image J. Zones with synaptic labeling of the EGCG/AA NPs treated mice exhibited a tridimensional relief and color intensity higher to those of the WT group.

characteristics of enhanced stability, sustained release and physico-chemical properties compatible with brain penetration.

A number of reports describe enhanced drug transport to the brain when using non-ligand coated PLGA NP [59,65,75,76]. However, the mechanism underlying these observation remains disputed [58]. Experimental data shows that PEG coating and the use of surfactants such as Tween are important for NP formulated drug passage across the BBB [66,68]. There is clear evidence that PLGA NPs with a  $Z_{\text{av}}$  of around 100 nm can be specifically transported through BBB endothelial cells by absorptive transcytosis [58,59,77]. However, it is unclear if such transcytosis events, observed at relatively scarce numbers, contribute in a quantitative manner to the measured drug concentrations in the brain [58]. In the present study we have not investigated the transport of intact NPs across the BBB directly. When using EGCG/AA NP-Rho we observed concentration-dependent passage of Rhodamine across the BBB in vitro, which appeared entirely diffusion controlled, suggesting that flux occurred through gaps in the BBB. Similarly, Rhodamine aggregates were observed in the hippocampus and the cortex when EGCG/AA NP-Rho were administered in vivo. Since Rhodamine was coupled covalently to the PLGA matrix, it is likely that intact NPs or their hydrolytic degradation products crossed the BBB. Diameters of Rhodamine clusters in the brain ranged from 5 to 15  $\mu\text{m}$ , suggesting aggregation of the NPs and/or their uptake by resident or migrating phagocytic cells.

Significantly, we can report here that each of the constituent components of EGCG/AA NPs affected BBB integrity in vitro and ex vivo, suggesting that ultimately free or nanomaterial formulated EGCG penetrated the BBB through destabilized junctions, which was in complete

agreement with our EGCG/AA NPs-Rho data. Whilst junction destabilization in our models was only measurable at concentrations several fold higher than what was observed in the plasma in vivo, it is likely that lower EGCG/AA NPs constituent concentrations also affected BBB integrity. In addition, given that the nanomaterial appeared aggregated when detected in the brain, it is also possible that high localized concentrations of aggregated material led to severe localized tight junction disruption and breach of the BBB similarly to what we observed in cultured BMVEC. In addition, it is well established that AD pathology involves a dysfunctional BBB with an enhanced permeability [78,79]. Indeed, APP/PS1 mice showed enhanced perivascular IgG accumulation indicating a dysfunctional BBB (Fig. S5 of Supplementary material). This contributes to the penetration of many molecules which would not normally cross the BBB under healthy conditions [80]. Therefore, we propose that quantitative uptake of EGCG to the brain occurred through a destabilized BBB.

Irrespective of the transport route, our study shed light on possibly the most therapeutically important property of EGCG-loaded NPs: when administered as PLGA-PEG nanomaterial, EGCG exhibited pharmacokinetic profile with significantly enhanced residence time in blood stream and brain tissue. When provided orally to mice either free or as EGCG/AA NPs, EGCG accumulated rapidly in the blood, reaching peak plasma concentrations of around 1  $\mu\text{g/ml}$  within 1 h of administration. Importantly, peak concentrations measured were similar in both cases, indicating that the same absorption route from the GI tract to the blood was used and that PLGA NPs did not specifically enhance GI uptake. GI absorption of tea catechins, appears to involve active transport [81]. Importantly, longer term plasma concentrations were ca. 5 times higher

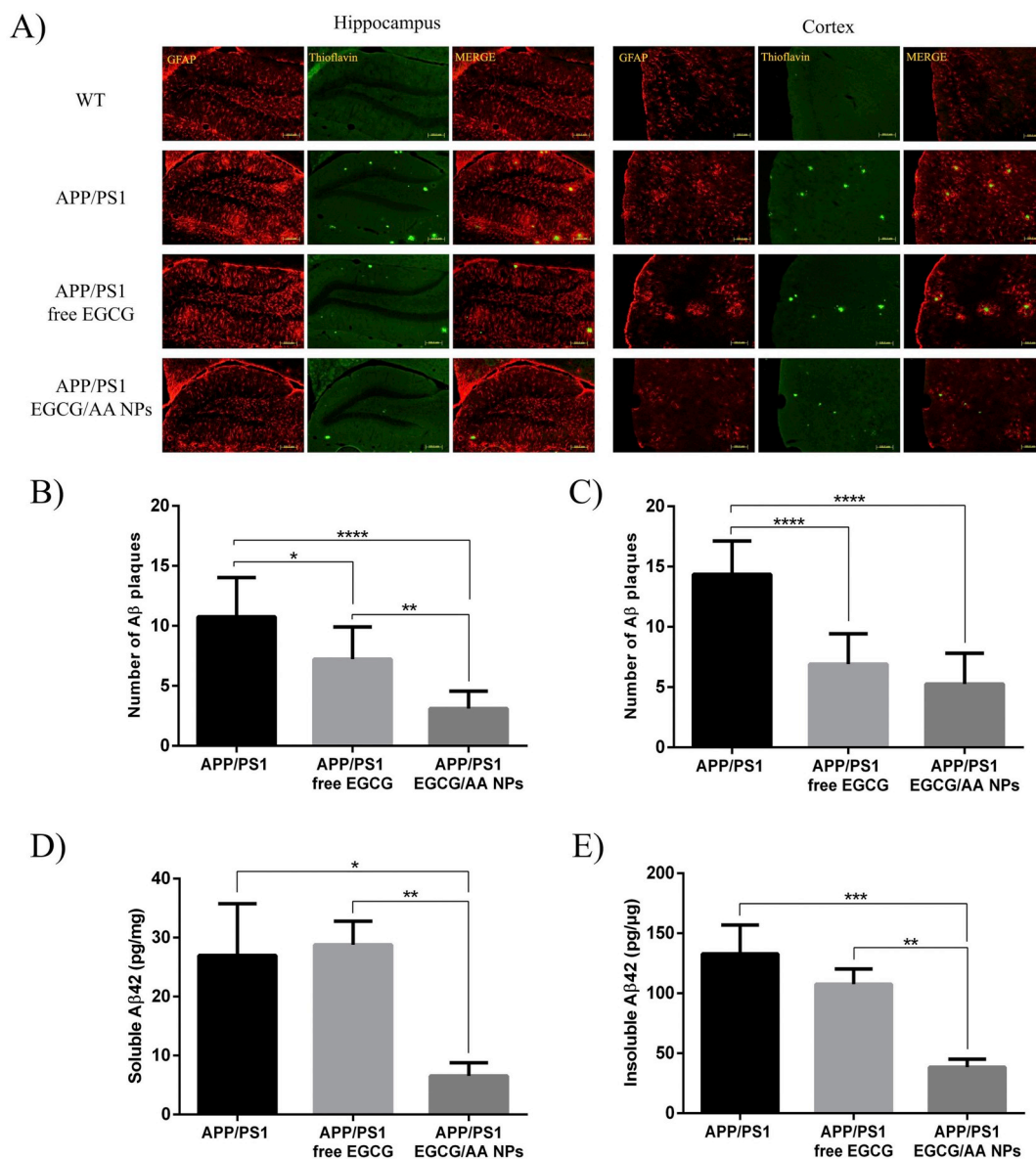


**Fig. 6.** Effect of EGCG treatments on neuroinflammation and A $\beta$  plaque/peptide burden. (A) 3 months-old APP/PS1 mice were orally treated with EGCG/AA NPs or free EGCG 40 mg/kg/day for 3 months. At 6 months, animals were sacrificed by perfusion with 4% PFA and brains were cut with a cryostat. GFAP and ThS immunostaining was performed on 20  $\mu$ m coronal sections. *Dentate gyrus* of hippocampus and cortex area are shown. Scale bar 100  $\mu$ m. Images of ThS staining of 100  $\mu$ m coronal sections of perfused animals were used for A $\beta$  plaques depositions count. Histograms show A $\beta$  plaques depositions count at (B) hippocampus and (C) cortex area. In ELISA kit, animals were sacrificed by cervical dislocation, and brain cortices were homogenized. Histograms show (D) soluble and (E) insoluble amounts of A $\beta_{(1-42)}$  peptide expressed as pg/mg of total protein. ANOVA analysis of data is included in the table S2 of the supplementary material.

in animals treated with EGCG/AA NPs, suggesting less degradation (either chemical or in the liver). This pharmacokinetic profile was mirrored in the brains of treated animals, where peak EGCG concentrations were also observed after around 1 h. Again subsequently, concentrations fell rapidly but remained much higher in animals having received EGCG/AA NPs as opposed to free EGCG. Importantly, relative brain EGCG concentrations were similar to those in the plasma (see footnote<sup>2</sup>), indicating that pharmacokinetic profile of EGCG in the brain was a direct consequence of that in the plasma. Overall our results strongly suggested that brain uptake of EGCG occurred through destabilized BBB endothelial junctions by diffusion and was enhanced due to greater stability and dwell time in the blood.

<sup>2</sup> Assuming a density of 1.04 g/ml, mean brain concentration was ca. 624 ng/ml, which was very similar to mean blood concentration (see Fig. 3B and C).

Previous studies have shown that different treatments with EGCG improved the memory process in AD animals models [16]. Lee et al. demonstrated this after an i.p. EGCG treatment of 3 mg/kg/day during 3 weeks in a LPS-induced memory impairment mouse model of AD [82]. We also found marked therapeutic effects of free EGCG in APP/PS1 mice using MWM and NOR behavioural test. However, overall, EGCG formulated as EGCG/AA NPs led to even better therapeutic outcome than the free drug alone. Significantly, improvements were found in spatial learning and memory (MWM test). Furthermore, NOR test also showed that EGCG/AA NPs treatment of APP/PS1 mice restored the recognition memory and enhanced cognitive process far more than free EGCG, reaching scores comparable to those of the WT group.

Improvement in brain function clearly had cytological and biochemical basis. EGCG reduced neuroinflammation and neurodegeneration in agreement with published data [16]. However, we found

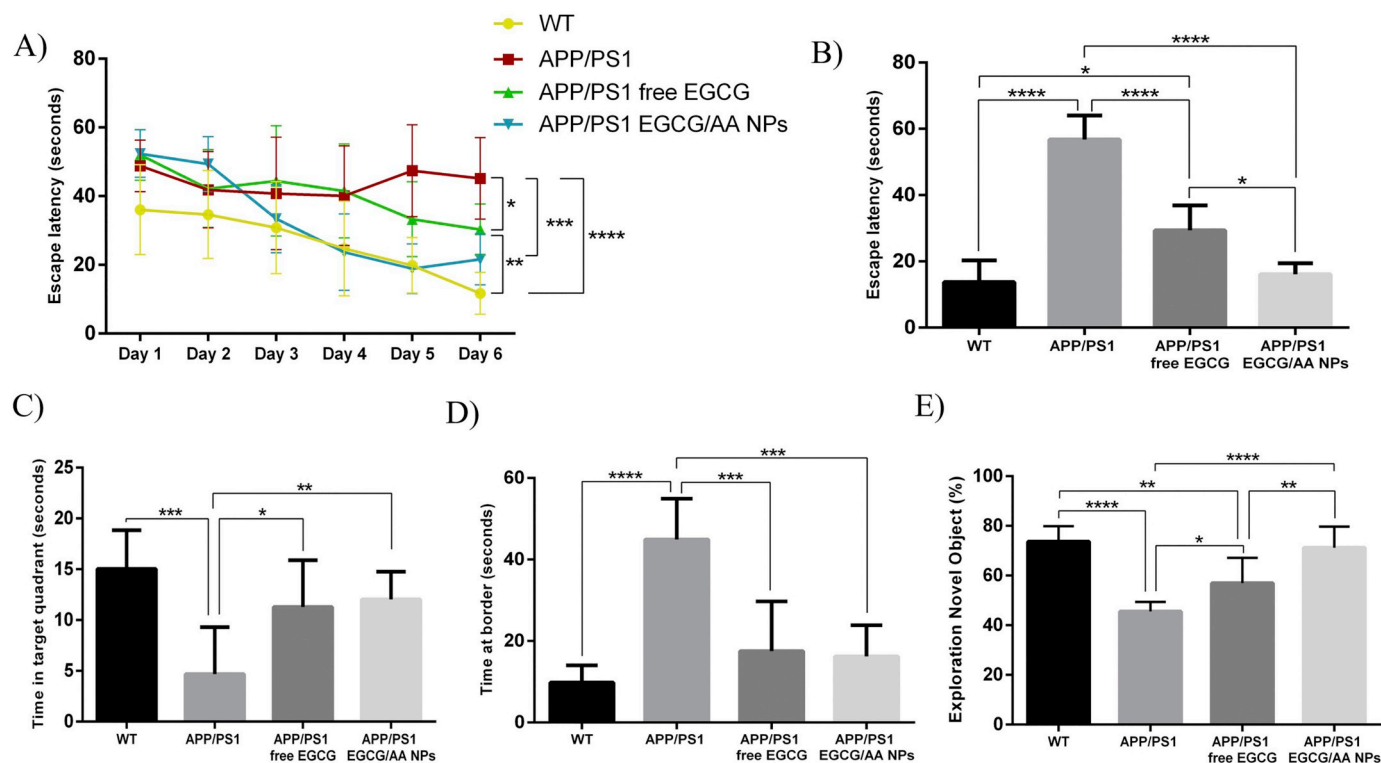


**Fig. 7.** Behavioural tests results. 3 months-old APP/PS1 mice were orally treated with EGCG/AA NPs or free EGCG 40 mg/kg/day for 3 months and then subjected to MWM and NOR tests. (A, B) Histograms shows the escape latency of learning process (statistics at the end of the training phase) (A) and of the test day (B) of WT, non-treated APP/PS1 and treated APP/PS1 mice. (C, D) Histograms show the time expended in the target quadrant (C) and the time expended at border area (D) the test day. (E) Histograms show the time percentage of investigation of the novel object by WT, non-treated APP/PS1 and treated APP/PS1 mice in the NOR test. ANOVA analysis of data is included in the table S3 of the Supplementary material.

even greater EGCG anti-neuroinflammatory activity, as well as a significant decline in the accumulation of A $\beta$  plaques, when EGCG was supplied as EGCG/AA NPs. These findings were in accordance with those obtained by Li et al., which showed that A $\beta$  deposits were reduced by 60% in the frontal cortex and 52% in the hippocampus after 3 months of treatment of EGCG 20 mg/kg/day by oral gavage in an APP transgenic mice [83].

We also found a strong increase in SYN staining following treatment of APP/PS1 mice with EGCG/AA NPs, indicating protection of synapses and increase of synaptogenesis. This correlated well with the cognitive improvement exhibited in behavioural tests. Many studies have demonstrated that small increases in the levels of A $\beta$ 42 peptide lead to permanent synaptic function impairment and neuroinflammatory responses [84]. Indeed, the high level of both soluble and insoluble A $\beta$ 42 peptide in APP/PS1 mice was significantly reduced following EGCG/AA NPs, but not free drug treatment.

## 5. Conclusions

In summary, the current work demonstrates the improvement of EGCG stability and effectiveness when loaded in PEGylated PLGA NPs within an antioxidant environment. EGCG/AA NPs were able to increase drug permanence in blood stream and brain tissue, reduce the A $\beta$  plaques burden, A $\beta$ 42 peptide levels and neuroinflammation, and enhance synaptogenesis, memory and learning process. All these facts contributed to a significant reduction of cognitive impairment in APP/PS1 mice. Based on these findings, we propose EGCG/AA NPs as a novel, safe and suitable therapeutic alternative for the treatment of AD.

## Financial support

This work was supported by the Spanish Ministry of Science and

Innovation (MAT 2014-59134-R, SAF2017-84283-R and PI2016/01), CB06/05/0024 (CIBERNED) and the European Regional Development Funds. AC<sup>a,b</sup>, ME<sup>a,b</sup>, and MLG<sup>a,b</sup> belong to 2017SGR-1477. ME<sup>c,d,e</sup>, CA<sup>f</sup>, and AC<sup>c,d</sup> belong to 2014SGR-525.

## Conflict of interest

None of the authors have any conflicts of interest including any financial, personal or other relationships with other people or organizations. All authors have reviewed the contents of the manuscript being submitted, approved its contents and validated the accuracy of the data.

## Acknowledgements

Authors acknowledge the support of the Spanish Ministry of Science and Innovation and European Regional Development Funds. The first author, AC, acknowledges the financial support of the Generalitat de Catalunya for the PhD scholarship FI-DGR (CVE-DOGC-B-14206020-2014). JHC acknowledges the financial support of the British Heart Foundation (FS/16/26/32193). Prof Giuseppe Battaglia (UCL) is thanked for helpful discussions during the preparation of this manuscript.

## Appendix A. Supplementary data

Supplementary data to this article can be found online at <https://doi.org/10.1016/j.jconrel.2019.03.010>.

## References

- [1] J. Cummings, R. Isaacson, F. Schmitt, D. Velting, A practical algorithm for managing Alzheimer's disease: what, when, and why? *Ann. Clin. Transl. Neurol.* 2 (3)

- (2015) 307–323.
- [2] Association A, Alzheimer's disease facts and figures, *Alzheimers Dement.* 13 (4) (2017) 325–373.
- [3] C. Ferri, M. Prince, C. Brayne, H. Brodaty, L. Fratiglioni, K. Hall, et al., Global prevalence of dementia: a Delphi consensus study, *Lancet* 366 (9503) (2010) 2112–2117.
- [4] M. Prince, A. Comas-Herrera, M. Knapp, M. Guerchet, M. Karagiannidou, World Alzheimer Report 2016: Improving Healthcare for People Living with Dementia, (2016).
- [5] C. Ballard, S. Gauthier, A. Corbett, C. Brayne, D. Aarsland, E. Jones, Alzheimer's disease, *Lancet* 377 (9770) (2011) 1019–1031.
- [6] R. Anand, K. Dip, A. Ali, *Neuropharmacology therapeutics of Alzheimer's disease: past, present and future*, *Neuropharmacology* 76 (2014) 27–50.
- [7] Y. Liu, F. Liu, I. Grundke-igbal, K. Iqbal, C. Gong, Deficient brain insulin signalling pathway in Alzheimer's disease, *J. Pathol.* 225 (2011) 54–62.
- [8] G.B. Frisoni, M. Boccardi, F. Barkhof, K. Blennow, S. Cappa, K. Chiotis, et al., Policy view strategic roadmap for an early diagnosis of Alzheimer's disease based on biomarkers, *Lancet Neurol.* 16 (2017) 661–676.
- [9] J. Swallow, Expectant futures and an early diagnosis of Alzheimer's disease: Knowing and its consequences, *Soc. Sci. Med.* 184 (2017) 57–64.
- [10] J. Cummings, G. Lee, T. Mortsdorf, A. Ritter, K. Zhong, Alzheimer's disease drug development pipeline: 2017, *Alzheimers Dement.* 3 (3) (2017) 367–384.
- [11] K. Kumar, A. Kumar, R.M. Keegan, R. Deshmukh, Recent advances in the neurobiology and neuropharmacology of Alzheimer's disease, *Biomed. Pharmacother.* 98 (2018) 297–307.
- [12] J. Cummings, P.S. Aisen, B. Dubois, L. Frölich, Jones R.W. Jr, et al., Drug development in Alzheimer's disease: the path to 2025, *Alzheimers Res. Ther.* 8 (39) (2016) 1–12.
- [13] H.L. Schmidt, A. Garcia, A. Martins, P.B. Mello-carpes, F.P. Carpes, Green tea supplementation produces better neuroprotective effects than red and black tea in Alzheimer-like rat model, *Food Res. Int.* 100 (2017) 442–448.
- [14] C. Braicu, M.R. Ladomery, V.S. Chedea, A. Irimie, The relationship between the structure and biological actions of green tea catechins, *Food Chem.* 141 (3) (2013) 3282–3289.
- [15] A. Chowdhury, J. Sarkar, T. Chakraborti, P.K. Pramanik, S. Chakraborti, Protective role of epigallocatechin-3-gallate in health and disease: a perspective, *Biomed. Pharmacother.* 78 (2016) 50–59.
- [16] M. Cascella, S. Bimonte, M. Muzio, V. Schiavone, A. Cuomo, The efficacy of Epigallocatechin-3-gallate (green tea) in the treatment of Alzheimer's disease: an overview of pre-clinical studies and translational perspectives in clinical practice, *Infect. Agents Cancer* 12 (36) (2017) 1–7.
- [17] R. de la Torre, S. de Sola, G. Hernandez, M. Farré, J. Pujol, J. Rodriguez, et al., Safety and efficacy of cognitive training plus epigallocatechin-3-gallate in young adults with Down's syndrome (TESDAD): a double-blind, randomised, placebo-controlled, phase 2 trial, *Lancet Neurol.* 15 (8) (2016) 801–810.
- [18] M. Younes, P. Aggett, F. Aguilar, R. Crebelli, B. Dusemund, M. Filipi, et al., Scientific opinion on the safety of green tea catechins, *EFSA J.* 16 (4) (2018) 5239.
- [19] H.J. Wobst, A. Sharma, M.I. Diamond, E.E. Wanker, J. Bieschke, The green tea polyphenol (–) -epigallocatechin gallate prevents the aggregation of tau protein into toxic oligomers at substoichiometric ratios, *FEBS Lett.* 589 (1) (2015) 77–83.
- [20] J.C. Wei, H. Huang, W. Chen, C. Huang, C. Peng, C. Lin, Epigallocatechin gallate attenuates amyloid  $\beta$ -induced inflammation and neurotoxicity in EOC 13.31 microglia, *Eur. J. Pharmacol.* 770 (2016) 16–24.
- [21] S.A. Mandel, T. Amit, L. Kalfon, L. Reznichenko, O. Weinreb, Youdim MBH, Cell signaling pathways and iron chelation in the neurorestorative activity of green tea polyphenols: special reference to Epigallocatechin Gallate (EGCG), *J. Alzheimers Dis.* 15 (2008) 211–222.
- [22] M. Awasthi, S. Singh, V.P. Pandey, U.N. Dwivedi, Alzheimer's disease: an overview of amyloid beta dependent pathogenesis and its therapeutic implications along with in silico approaches emphasizing the role of natural products, *J. Neurol. Sci.* 361 (2016) 256–271.
- [23] A. Granja, I. Frias, A.R. Neves, M. Pinheiro, S. Reis, Therapeutic potential of Epigallocatechin Gallate nanodelivery systems, *Biomed. Res. Int.* 17 (2017) 1–15.
- [24] O. Krupkova, S.J. Ferguson, K. Wuerz-Kozak, Stability of (–)-epigallocatechin gallate and its activity in liquid formulations and delivery systems, *J. Nutr. Biochem.* 37 (2016) 1–12.
- [25] W. Zhang, Y. Wu, H. Dong, J. Yin, H. Zhang, H. Wu, et al., Sparks fly between ascorbic acid and iron-based nanozymes: a study on Prussian blue nanoparticles, *Colloids Surf. B: Biointerfaces* 163 (2018) 379–384 (Accepted manuscript).
- [26] S. Dey, B. Bishayi, Killing of *S. aureus* in murine peritoneal macrophages by ascorbic acid along with antibiotics Chloramphenicol or Ofloxacin: correlation with inflammation, *Microb. Pthog.* 115 (2018) 239–250.
- [27] C. Saraiva, C. Praça, R. Ferreira, T. Santos, L. Bernardino, Nanoparticle-mediated brain drug delivery: overcoming blood – brain barrier to treat neurodegenerative diseases, *J. Control. Release* 235 (2016) 34–47.
- [28] A.O. Elzoghby, A.L. Hemasa, M.S. Freag, Hybrid protein-inorganic nanoparticles: from tumor-targeted drug delivery to cancer imaging, *J. Control. Release* 243 (2016) 303–322.
- [29] C.Y. Wong, H. Al-salami, C.R. Dass, Potential of insulin nanoparticle formulations for oral delivery and diabetes treatment, *J. Control. Release* 264 (2017) 247–275.
- [30] El-Say KM, El-Sawy HS. Polymeric nanoparticles: promising platform for drug delivery. *Int. J. Pharm.* 2017;528(1–2):675–91.
- [31] B. Bahrami, M. Hojjat-farsangi, H. Mohammadi, E. Anvari, Nanoparticles and targeted drug delivery in cancer therapy, *Immunol. Lett.* 190 (2017) 64–83.
- [32] S. Sharma, A. Parmar, S. Kori, R. Sandhir, PLGA-based nanoparticles: a new paradigm in biomedical applications, *TrAC Trends Anal. Chem.* 80 (2015) 30–40.
- [33] A. Kolate, D. Baradia, S. Patil, I. Vhora, G. Kore, A. Misra, PEG - a versatile conjugating ligand for drugs and drug delivery systems, *J. Control. Release* 192 (2014) 67–81.
- [34] M.M. El-Hammadi, Á.V. Delgado, C. Melguizo, J.C. Prados, J.L. Arias, Folic acid-decorated and PEGylated PLGA nanoparticles for improving the antitumor activity of 5-fluorouracil, *Int. J. Pharm.* 516 (1–2) (2017) 61–70.
- [35] T. Freytag, A. Dashevsky, L. Tillman, G.E. Hardee, R. Bodmeier, Improvement of the encapsulation efficiency of oligonucleotide-containing biodegradable microspheres, *J. Control. Release* 69 (1) (2000) 197–207.
- [36] K.S. Soppimath, T.M. Aminabhavi, A.R. Kulkarni, W.E. Rudzinski, Biodegradable polymeric nanoparticles as drug delivery devices, *J. Control. Release* 70 (1–2) (2001) 1–20.
- [37] J.F. Fangueiro, A.C. Calpena, B. Clares, T. Andreani, M.A. Egea, F.J. Veiga, et al., Biopharmaceutical evaluation of epigallocatechin gallate-loaded cationic lipid nanoparticles (EGCG-LNs): in vivo, in vitro and ex vivo studies, *Int. J. Pharm.* 502 (1–2) (2016) 161–169.
- [38] J.F. Fangueiro, A. Parra, A.M. Silva, M.A. Egea, E.B. Souto, M.L. Garcia, et al., Validation of a high performance liquid chromatography method for the stabilization of epigallocatechin gallate, *Int. J. Pharm.* 475 (1–2) (2014) 181–190.
- [39] E. Vega, M.A. Egea, M.L. Garduño-Ramírez, M.L. García, E. Sánchez, M. Espina, et al., Flurbiprofen PLGA-PEG nanospheres: role of hydroxy- $\beta$ -cyclodextrin on ex vivo human skin permeation and in vivo topical anti-inflammatory efficacy, *Colloids Surf. B: Biointerfaces* 110 (2013) 339–346.
- [40] A. Cano, M. Etcheto, M. Espina, C. Auladell, A.C. Calpena, J. Folch, et al., Epigallocatechin-3-gallate loaded PEGylated-PLGA nanoparticles: a new anti-seizure strategy for temporal lobe epilepsy, *Nanomedicine* 14 (4) (2018) 1073–1085.
- [41] Hudson N, Powner MB, Sarker MH, Burgoyne T, Campbell M, Ockrim ZK et al. Differential apicobasal VEGF signaling at vascular blood-neural barriers. *Dev. Cell.* 2014;30(5):541–52.
- [42] E. Horisawa, K. Kubota, I. Tuboi, K. Sato, H. Yamamoto, H. Takeuchi, et al., Size-dependency of DL-lactide/glycolide copolymer particulates for intra-articular delivery system on phagocytosis in rat synovium, *Pharm. Res.* 19 (2) (2002) 5–6.
- [43] C. Lautenschläger, C. Schmidt, C. Lehr, D. Fischer, A. Stallmach, PEG-functionalized microparticles selectively target inflamed mucosa in inflammatory bowel disease, *Eur. J. Pharm. Biopharm.* 85 (3) (2013) 578–586.
- [44] C.M. Warboys, O.B. Toh, P.A. Fraser, Role of NADPH oxidase in retinal microvascular permeability increase by RAGE activation, *Invest. Ophthalmol. Vis. Sci.* 50 (3) (2009) 1319–1328.
- [45] M. Etcheto, E. Sánchez-lópez, L. Pons, O. Busquets, Dexibuprofen prevents neurodegeneration and cognitive decline in APPswe/PS1dE9 through multiple signaling pathways, *Redox Biol.* 13 (2017) 345–352.
- [46] M.L. Mata-Bilbao, E. Roura, O. Jáuregui, C. Torre, R.M. Lamuela-Reventós, A new LC/MS/MS rapid and sensitive method for the determination of green tea catechins and their metabolites in biological samples, *J. Agric. Food Chem.* 55 (2007) 8857–8863.
- [47] L. Chen, M. Lee, H.E. Li, C.S. Yang, Absorption, distribution, and elimination of tea polyphenols in rats abstract, *Drug Metab. Dispos.* 25 (9) (1997) 0–5.
- [48] R. Zhang, G. Xue, S. Wang, L. Zhang, C. Shi, X. Xie, Novel object recognition as a facile behavior test for evaluating drug effects in APP/PS1 Alzheimer's disease mouse model, *J. Alzheimers Dis.* 31 (2012) 801–812.
- [49] D. Porquet, A. Camins, I. Ferrer, A.M. Canudas, J. Valle, Del. Amyloid and tau pathology of familial Alzheimer's disease APP/PS1 mouse model in a senescence phenotype background, *Am. Aging Assoc.* 37 (2015) 1–17.
- [50] R. Radhakrishnan, H. Kulhari, D. Pooja, S. Gudem, S. Bhargava, R. Shukla, et al., Encapsulation of biophenolic phytochemical EGCG within lipid nanoparticles enhances its stability and cytotoxicity against cancer, *Chem. Phys. Lipids* 198 (2016) 51–60.
- [51] J. Xiong, Y. Wang, Q. Xue, X. Wu, Synthesis of highly stable dispersions of nano-sized copper particles using L-ascorbic acid, *Green Chem.* 13 (2011) 900–904.
- [52] R. Singh, P. Kesharwani, N.K. Mehra, S. Singh, S.J.N. Banerjee, Development and characterization of folate anchored Saquinavir entrapped PLGA nanoparticles for anti-tumor activity, *Drug Dev. Ind. Pharm.* 4 (2015) 1888–1901.
- [53] G. Ho, S. Beom, J. Lee, C. Weon, Mechanisms of drug release from advanced drug formulations such as polymeric-based drug-delivery systems and lipid nanoparticles, *J. Pharm. Investig.* 0 (0) (2017) 0.
- [54] S. Proniuk, B. Liederer, J. Blanchard, Preformulation study of Epigallocatechin Gallate, a promising antioxidant for topical skin Cancer prevention, *J. Pharm. Sci.* 91 (2002) 111–116.
- [55] Guidance for Industry, Nonsterile Semisolid Dosage Forms. Scale-Up and Post-approval Changes: Chemistry, Manufacturing, and Controls; In Vivo Release Testing and In Vivo Bioequivalence Documentation, Food and Drug Administration (FDA). Center for Drug Evaluation and Research (CDER). SUPAC-SS, May 1997 (Internet), <http://www.fda.gov/cder/guidance>.
- [56] OECD Guideline for the testing of chemical (428), Organization for Economic Cooperation and Development (OECD/OECD) (Internet), April 2004. <https://ntp.niehs.nih.gov/iccvm/supdocs/feddocs/oecd/oecd428-508.pdf>.
- [57] Development and validation of in vitro release testing methods for semisolid formulations, Particle Sciences - Technical Brief, vol. 10, 2009, pp. 1–6 (Internet), [https://www.particlesciences.com/docs/technical\\_briefs/TB\\_10.pdf](https://www.particlesciences.com/docs/technical_briefs/TB_10.pdf).
- [58] J. Kreuter, Drug delivery to the central nervous system by polymeric nanoparticles: what do we know? *Adv. Drug Deliv. Rev.* 71 (2014) 2–14.
- [59] Y. Zhou, Z. Peng, E.S. Seven, R.M. LeBlanc, Crossing the blood-brain barrier with nanoparticles, *J. Control. Release* 270 (2018) 290–303.
- [60] C. Sze, J.C. Troncoso, C. Kawas, P. Mouton, D.L. Price, L.J. Martin, Loss of presynaptic vesicle protein synaptophysin in hippocampus correlates with cognitive decline in Alzheimer's disease, *J. Neurophatol. Exp. Neurol.* 56 (8) (1997) 933–944.

- [61] P. Eikelenboom, V. Exel, J.J.M. Hoozemans, Neuroinflammation – an early event in both the history and pathogenesis of Alzheimer's disease, *Neurodegener. Dis.* 7 (2010) 38–41.
- [62] U.K. Hanisch, H. Kettenmann, Microglia: active sensor and versatile effector cells in the normal and pathologic brain, *Nat. Neurosci.* 10 (2007) 1387–1394.
- [63] R.G.M. Morris, P. Garrud, J.N.P. Rawlins, J. O'Keefe, Place navigation impaired in rats with hippocampal lesions, *Nature* 297 (1982) 681–683.
- [64] S.A. Salem, N.M. Hwei, A. Bin Saim, C.C. Ho, I. Sagap, R. Singh, et al., Polylactic-co-glycolic acid mesh coated with fibrin or collagen and biological adhesive substance as a prefabricated, degradable, biocompatible, and functional scaffold for regeneration of the urinary bladder wall, *J. Biomed. Mater. Res.* 101 (8) (2013) 2237–2247.
- [65] L. Li, C. Sabliov, PLA/PLGA nanoparticles for delivery of drugs across the blood-brain barrier, *Nanotechnol. Rev.* 2 (3) (2013) 241–257.
- [66] E.A. Nance, G.F. Woodworth, K.A. Sailor, T.Y. Shih, Q. Xu, G. Swaminathan, et al., A dense poly(ethylene glycol) coating improves penetration of large polymeric nanoparticles within brain tissue, *Sci. Transl. Med.* 4 (149) (2012) 149ra119.
- [67] H. Yuan, C.Y. Chen, G.H. Chai, Y.Z. Du, F.Q. Hu, Improved transport and absorption through gastrointestinal tract by PEGylated solid lipid nanoparticles, *Mol. Pharm.* 10 (5) (2013) 1865–1873.
- [68] W. Sun, C. Xie, H. Wang, Y. Hu, Specific role of polysorbate 80 coating on the targeting of nanoparticles to the brain, *Biomaterials* 25 (2004) 3065–3071.
- [69] T. Ohishi, S. Goto, P. Monira, M. Isemura, Anti-inflammatory action of green tea, *Anti Inflamm. Anti Allergy Agents Med. Chem.* 15 (2) (2016) 74–90.
- [70] M. Ellulu, A. Rahmat, I. Patimah, H. Khaza'ai, Y. Abed, Effect of vitamin C on inflammation and metabolic markers in hypertensive and/or diabetic obese adults: a randomized controlled trial, *Drug Des. Dev. Ther.* 9 (2015) 3405–3412.
- [71] J.M. Anderson, M.S. Shive, Biodegradation and biocompatibility of PLA and PLGA microspheres, *Adv. Drug Deliv. Rev.* 28 (1997) 5–24.
- [72] B. Semete, L. Booyesen, Y. Lemmer, L. Kalombo, L. Katata, J. Verschoor, et al., In vivo evaluation of the biodistribution and safety of PLGA nanoparticles as drug delivery systems, *Nanomedicine* 6 (5) (2010) 662–671.
- [73] J. Park, T. Utsumi, Y.-E. Seo, Y. Deng, A. Satoh, Y. Iwakiri, Cellular distribution of injected PLGA-nanoparticles in the liver, *Nanomedicine* 12 (5) (2016) 1365–1374.
- [74] D.J. Hines, D.L. Kaplan, Poly (lactic-co-glycolic acid) controlled release systems: experimental and modelling insights, *Crit. Rev. Ther. Drug Carrier Syst.* 30 (3) (2013) 257–276.
- [75] S. Md, M. Ali, S. Baboota, J.K. Sahni, A. Bhatnagar, J. Ali, Preparation, characterization, in vivo biodistribution and pharmacokinetic studies of donepezil-loaded PLGA nanoparticles for brain targeting, *Drug Dev. Ind. Pharm.* 40 (2) (2014) 278–287.
- [76] T. Chen, C. Li, Y. Li, X. Yi, R. Wang, S.M. Lee, et al., Small-sized mPEG-PLGA nanoparticles of Schisantherin A with sustained release for enhanced brain uptake and anti-parkinsonian activity, *ACS Appl. Mater. Interfaces* 9 (11) (2017) 9516–9527.
- [77] M. Silva-Abreu, A.C. Calpena, P. Andrés-Benito, E. Aso, I.A. Romero, D. Roig-Carles, et al., PPAR agonist-loaded PLGA-PEG nanocarriers as a potential treatment for Alzheimer's disease: in vitro and in vivo studies, *Int. J. Nanomedicine* 13 (2018) 5577–5590.
- [78] Y. Yamazaki, T. Kanekiyo, Blood-brain barrier dysfunction and the pathogenesis of Alzheimer's disease, *Mol. Sci.* 18 (2017) 1–19.
- [79] E. Zenaro, G. Piacentino, G. Constantin, The blood-brain barrier in Alzheimer's disease, *Neurobiol. Dis.* 107 (2017) 41–56.
- [80] A.M. Minogue, R.S. Jones, R.J. Kelly, C.L. McDonald, T.J. Connor, M.A. Lynch, Age-associated dysregulation of microglial activation is coupled with enhanced blood-brain barrier permeability and pathology in APP/PS1 mice, *Neurobiol. Aging* 35 (2014) 1442–1452.
- [81] J.B. Vaidyanathan, T. Walle, Cellular uptake and efflux of the tea flavonoid (–) epicatechin-3-gallate in the human intestinal cell line Caco-2, *J. Pharmacol. Exp. Ther.* 307 (2) (2003) 745–752.
- [82] Y. Lee, D. Choi, Y. Yun, S. Bae, K. Oh, J. Tae, Epigallocatechin-3-gallate prevents systemic inflammation-induced memory deficiency and amyloidogenesis via its anti-neuroinflammatory properties, *J. Nutr. Biochem.* 24 (1) (2013) 298–310.
- [83] Q. Li, M. Gordon, J. Tan, Oral administration of green tea epigallocatechin-3-gallate (EGCG) reduces amyloid beta deposition in transgenic mouse model of Alzheimer's disease, *Exp. Neurol.* 198 (2006) 576.
- [84] C. Haass, D.J. Selkoe, Soluble protein oligomers in neurodegeneration: lessons from the Alzheimer's amyloid  $\beta$ -peptide, *Nature* 8 (2007) 101–112.

## 8.4 Literature review and appraisal on alternative neurotoxicity testing methods

Stefan Masjosthusmann<sup>1</sup>, Marta Barenys<sup>1</sup>, Mohamed El-Gamal<sup>1</sup>, Lieve Geerts<sup>3</sup>, Laura Gerosa<sup>2</sup>, Adriana Gorreja<sup>2</sup>, **Britta Kühne**<sup>1</sup>, Natalia Marchetti<sup>2</sup>, Julia Tigges<sup>1</sup>, Barbara Viviani<sup>3</sup>, Hilda Witters<sup>3</sup>, Ellen Fritsche<sup>1</sup>

<sup>1</sup> IUF -Leibniz Research Institute for Environmental Medicine, Auf'm Hennekamp 50, 40225 Düsseldorf, Germany

<sup>2</sup> Università degli Studi di Milano (UMIL), Dipartimento di Scienze Farmacologiche e Biomolecolari -DiSFeB, Via Balzaretti 9, 20133 Milan, Italy

<sup>3</sup> Flemish Institute for Technological Research (VITO), Environmental Risk & Health, Boeretang 200, B-2400 Mol, Belgium

|                       |   |
|-----------------------|---|
| Journal               | EFSA Supporting publication   |
| Impact Factor         | No Impact Factor [OA]   |
| Type of authorship    | Co-author   |
| Status of publication | Published: EFSA supporting publication 15 (2018) EN-1410<br>DOI: 10.2903/sp.efsa.2018.EN-1410 |

### Notice:

The publication (Masjosthusmann et al., 2018a) is with 125 pages very extensive, therefore only the first three pages are presented in this thesis. The reader is invited to read the freely accessible online version: <https://efsa.onlinelibrary.wiley.com/doi/abs/10.2903/sp.efsa.2018.EN-1410>

## Summary

The goal of this review was the evaluation of information on assessment methods in the field of alternative neurotoxicity (NT) testing. We therefore performed a systematic and comprehensive collection of scientific literature (in English) from the past 27 years until mid of 2017 on state of the art alternative testing methods including in vitro test methods, in silico methods and alternative non-mammalian models. This review identified a variety of test methods that have the ability to predict NT of chemicals based on predefined key NT endpoint categories (27). Those endpoint categories were derived from the Mode of Action (MoA) of known human neurotoxicants. Pre-evaluated MoAs of human neurotoxicants allowed the identification of performance characteristics with regard to the ability of a test system to correctly predict a chemical effect on an endpoint category. The most predictive in vitro model that covers a large variety of endpoint categories are primary rodent cells or tissues. Human based systems derived from induced pluripotent stem cells (iPSC) are promising and warrant human relevance. There is however not yet sufficient data on these models to demonstrate their suitability to reliably substitute primary rodent cells for NT testing purposes. Test methods for glia toxicity are rare and glia endpoint categories are clearly underrepresented. Therefore, a focus for future method development should be placed on glia, astrocytes, oligodendrocytes and microglia based models, preferably in a co-culture set up. The review on in silico methods, resulted into 54 QSARs publications, relevant for NT, of which 39 on blood brain barrier (BBB) permeation. The QSARs available in the publications were developed from data on drugs and chemicals, but there appears a limited set of experimental data for chemicals and pesticides on blood-brain barrier passage. The evaluation of NT methods using alternative whole organism approaches demonstrated a majority of data for *C. elegans* (nematode species), represented with high true prediction (96%). The main endpoint category was inhibition of cholinergic transmission, with specific endpoints for AChE activity and motor activity, the latter confirming the added value of a whole organism approach among alternative models. Though *D. rerio*, the zebrafish model appeared a promising model for DNT studies with numerous advantages, it was poorly evaluated for NT endpoints. Next to the need for standardized protocols using *C. elegans* as a test organism, the zebrafish model needs further exploration for NT relevant endpoints. In conclusion, a NT alternative test battery covering identified and relevant MoA for NT is recommended. Therefore, test methods with relevant controls and standard operation procedures have to be set up for covering most important MoA. To link the human in vitro testing to rodent in vivo studies and validate the stem cell-derived systems, it is advised to include rodent primary cultures into the studies. For more complex, behavioural readout, effects in alternative organisms should be combined with electrophysiological assessments in vitro.



APPROVED: 13 April 2018

doi:10.2903/sp.efsa.2018.EN-1410

## Literature review and appraisal on alternative neurotoxicity testing methods

<sup>1</sup>Stefan Masjosthusmann, <sup>1</sup>Marta Barenys, <sup>1</sup>Mohamed El-Gamal, <sup>3</sup>Lieve Geerts, <sup>2</sup>Laura Gerosa, <sup>2</sup>Adriana Gorreja, <sup>1</sup>Britta Kühne, <sup>2</sup>Natalia Marchetti, <sup>1</sup>Julia Tigges, <sup>2</sup>Barbara Viviani, <sup>3</sup>Hilda Witters, <sup>1</sup>Ellen Fritsche

<sup>1</sup>IUF - Leibniz Research Institute for Environmental Medicine, Auf'm Hennekamp 50, 40225 Düsseldorf, Germany

<sup>2</sup>Università degli Studi di Milano (UMIL), Dipartimento di Scienze Farmacologiche e Biomolecolari - DiSFeB, Via Balzaretti 9, 20133 Milan, Italy

<sup>3</sup>Flemish Institute for Technological Research (VITO), Environmental Risk & Health, Boeretang 200, B-2400 Mol, Belgium

### ABSTRACT

The goal of this review was the evaluation of information on assessment methods in the field of alternative neurotoxicity (NT) testing. We therefore performed a systematic and comprehensive collection of scientific literature (in English) from the past 27 years until mid of 2017 on state of the art alternative testing methods including in vitro test methods, *in silico* methods and alternative non-mammalian models. This review identified a variety of test methods that have the ability to predict NT of chemicals based on predefined key NT endpoint categories (27). Those endpoint categories were derived from the Mode of Action (MoA) of known human neurotoxicants. Pre-evaluated MoAs of human neurotoxicants allowed the identification of performance characteristics with regard to the ability of a test system to correctly predict a chemical effect on an endpoint category. The most predictive in vitro model that covers a large variety of endpoint categories are primary rodent cells or tissues. Human based systems derived from induced pluripotent stem cells (iPSC) are promising and warrant human relevance. There is however not yet sufficient data on these models to demonstrate their suitability to reliably substitute primary rodent cells for NT testing purposes. Test methods for glia toxicity are rare and glia endpoint categories are clearly underrepresented. Therefore, a focus for future method development should be placed on glia, astrocytes, oligodendrocytes and microglia based models, preferably in a co-culture set up. The review on *in silico* methods, resulted into 54 QSARs publications, relevant for NT, of which 39 on blood brain barrier (BBB) permeation. The QSARs available in the publications were developed from data on drugs and chemicals, but there appears a limited set of experimental data for chemicals and pesticides on blood-brain barrier passage. The evaluation of NT methods using alternative whole organism approaches demonstrated a majority of data for *C. elegans* (nematode species), represented with high true prediction (96%). The main endpoint category was inhibition of cholinergic transmission, with specific endpoints for AChE activity and motor activity, the latter confirming the added value of a whole organism approach among alternative models. Though *D. rerio*, the zebrafish model appeared a

promising model for DNT studies with numerous advantages, it was poorly evaluated for NT endpoints. Next to the need for standardized protocols using *C. elegans* as a test organism, the zebrafish model needs further exploration for NT relevant endpoints. In conclusion, a NT alternative test battery covering identified and relevant MoA for NT is recommended. Therefore, test methods with relevant controls and standard operation procedures have to be set up for covering most important MoA. To link the human in vitro testing to rodent *in vivo* studies and validate the stem cell-derived systems, it is advised to include rodent primary cultures into the studies. For more complex, behavioural readout, effects in alternative organisms should be combined with electrophysiological assessments in vitro.

© European Food Safety Authority, 2018

**KEY WORDS:** literature review, neurotoxicity, in vitro, in silico, alternative organism, mode of action

**Question number:** EFSA-Q- 2015-00822

**Correspondence:** pesticides.ppr@efsa.europa.eu

**Disclaimer:** the present document has been produced and adopted by the bodies identified above as authors. This task has been carried out exclusively by the authors in the context of a contract between the European Food Safety Authority and the authors, awarded following a tender procedure. The present document is published complying with the transparency principle to which the Authority is subject. It may not be considered as an output adopted by the Authority. The European Food Safety Authority reserves its rights, view and position as regards the issues addressed and the conclusions reached in the present document, without prejudice to the rights of the authors.

**Suggested citation:** Masjosthusmann S, Barenys M, El-Gamal M, Geerts L, Gerosa L, Gorreja A, Kühne B, Marchetti N, Tigges J, Viviani B, Witters H, Fritsche H, 2018. Literature review and appraisal on alternative Neurotoxicity testing methods. EFSA supporting publication 2018:EN-1410. 125 pp. doi:10.2903/sp.efsa.2018.EN-1410

**ISSN:** 2397-8325

© European Food Safety Authority, 2018

Reproduction is authorised provided the source is acknowledged.

## Table of contents

|  |    |
|--|----|
| Abstract.....  | 1  |
| Terms of reference as provided by [requestor].....                             | 5  |
| 1. Project Summary.....  | 6  |
| 1.1. Background .....  | 6  |
| 1.2. Review Question and Objectives.....                                       | 8  |
| 2. Methodology.....  | 9  |
| 2.1. Compound selection and mode-of-action analyses.....                       | 9  |
| 2.2. Search strategy.....  | 11 |
| 2.2.1. 'Grey' literature search .....  | 13 |
| 2.3. Selection .....   | 14 |
| 2.3.1. Selection based on title and abstract .....                             | 14 |
| 2.3.2. Selection based on full text.....                                       | 16 |
| 2.3.3. Selection of 'grey' literature .....                                    | 18 |
| 2.4. Assessment of methodological quality .....                                | 18 |
| 2.5. Data Collection.....  | 20 |
| 3. Results and Discussion.....   | 23 |
| 3.1. <i>In vitro</i> .....   | 23 |
| 3.1.1. Grey literature search.....   | 55 |
| 3.2. Cell based blood brain barrier models.....                                | 56 |
| 3.3. <i>In silico</i> .....  | 61 |
| 3.3.1. Introduction: .....   | 61 |
| 3.3.2. Models on blood-brain-barrier (BBB) permeation and neurotoxicity: ..... | 62 |
| 3.3.3. Grey literature search: .....   | 65 |
| 4. Readiness analyses.....   | 79 |
| 5. Summary.....  | 82 |
| 6. Conclusion .....  | 84 |
| 7. Summary of recommendations .....  | 85 |
| 7.1. <i>General</i> .....  | 85 |
| 7.2. <i>In vitro</i> .....   | 85 |
| 7.3. <i>Alternative organisms</i> .....  | 86 |
| 7.4. <i>In silico</i> .....  | 87 |
| 7.5. Possible EFSA follow-up activities.....                                   | 87 |

## 8.5 Summary of short stay abroad

### Report

11.01.2022

**Britta Anna Kühne**

Research stage at the IUF - Leibniz Research Institute for Environmental Medicine Düsseldorf, Germany from 01.10.2021 – 31.12.2021, financially supported by a grant for short stays from the Montcelimar Foundation 2021.

#### **Evaluation of the neurodevelopmental safety of plasticizers present in an artificial placenta system: A study in human neurospheres.**

Keywords: developmental neurotoxicity (DNT), Human cell-based testing battery, 3D *in vitro* neurosphere system, artificial placenta system, hazard assessment of plasticizer

##### **1. Initial objectives**

**Main objective:** To characterize and prevent human fetal brain injury produced by plasticizing compounds included in an artificial placental system. To bring safe biomedical devices to the clinical stage.

##### **Specific objectives:**

1. To characterize possible adverse effects induced by classical and alternative plasticizing compounds (Table 1) over basic neurogenesis mechanisms in human NPCs growing as neurospheres: cell viability, proliferation, migration, and oligodendrocyte (OL) differentiation.
2. To rank the potency of the chosen plasticizer according to their respective benchmark concentration (BMC) across all tested neurodevelopmental endpoints by applying the Toxicological Priority Index (ToxPi GUI)(Gangwal et al., 2012) and to select the most innocuous alternative plasticizers.
3. To identify the BMC<sub>50</sub> values of OL differentiation inhibition induced by the described plasticizing compounds. To analyze the gene expression of certain OL markers in human NPCs exposed to the calculated BMC<sub>50</sub> using RT-qPCR. To integrate these results in the potency ranking (ToxPi GUI) and adapt it accordingly.

## 2. Changes and justification

1.

- i. I tested one more alternative plasticizer as previously proposed, the adipate Di(2-ethylhexyl)adipate (DEHA, green in table 1).
- ii. The testing battery of basic neurogenesis mechanisms in human NPCs growing as neurospheres included the assays:

Proliferation assay:

- Cytotoxicity (LDH assay), Viability testing (CTB assay), BrdU incorporation, proliferation area

Differentiation assay:

- Cytotoxicity (LDH assay), Viability testing (CTB assay), Migration distance after 3 and 5 days, nuclei counting, OL differentiation, neuronal differentiation, total and average neurite length, number of branching points, neurite count

2. No changes

3. To analyze the gene expression of certain markers in human NPCs, I exposed human NPCs to the solvent control and three selected concentrations of the plasticizers (0.74, 6.67 and 20  $\mu$ M). RNA samples were collected after two-time points: 12 hours and 60 hours of cultivation. RT-qPCR could not be performed for two reasons: (1) previous tasks were more extensive than planned and (2) material was missing due to delivery problems. The qRT-PCR will be performed in January - February 2022 from a colleague at the IUF Düsseldorf.

*Table 3 Classical and alternative plasticizers. Scientific Committee of the European Commission on Emerging and Newly Identified Health Risks. Used in medical devices, medical tubing's, infusion equipment's, blood bags.*

| COMPOUND FAMILY                | COMPOUND NAME                  | SYNONYM | CAS       |
|--------------------------------|--------------------------------|---------|-----------|
| <b>CLASSICAL PLASTICIZER</b>   |                                |         |           |
| Phthalates                     | Bis(2-ethylhexyl) phthalate    | DEHP    | 117-81-7  |
| <b>ALTERNATIVE PLASTICIZER</b> |                                |         |           |
| Phthalates                     | Di(2-ethylhexyl) terephthalate | DEHT    | 6422-86-2 |
| Trimellitates                  | Trioctyltrimellitate           | TOTM    | 3319-31-1 |
| Adipates                       | Di(2-ethylhexyl)adipate        | DEHA    | 103-23-1  |

### 3. Summary of research stage

In this study, I have characterized possible adverse effects on neurodevelopment produced by plasticizing compounds included in the biomaterials of an artificial placental system. An increasing number of premature babies admitted to neonatal intensive care units (NICUs) suffer under neurological disabilities. The main form of brain damage is periventricular leukomalacia (PVL) or white matter injury (WMI) in its diffuse form, which is associated with a selective vulnerability of OL progenitors (Calafat et al., 2004). Thus, it was important to discover if the selected plasticizer may adversely interfere with the OL lineage to avoid a potential second hit to vulnerable babies admitted to the artificial placenta system. The classical plasticizer DEHP is the most used phthalate in medical devices and tubing and causes the most severe reproductive and developmental toxicity in experimental and preliminary epidemiological studies (Shea, 2003; Van Vliet et al., 2011) compared to other plasticizers (Scientific Committee on Emerging and Newly-Identified Health Risks, 2016). However, studies are very limited, and little is known about the mode of action (MoA) from plasticizers during neurodevelopment (Ejaredar et al., 2015; Radke et al., 2020). Hence, we aimed to find a suitable substitution for DEHP in medical devices and tubing. Therefore, human neural progenitor cells (hNPCs) growing as neurospheres were exposed to 1 classical (DEHP) and 3 alternative plasticizers (DEHT, TOTM, DEHA; table 1) and cell viability, cytotoxicity, proliferation, migration, OL, and neuronal differentiation were assessed. Finally, a potency ranking was issued to select the most innocuous plasticizers and select the materials conforming an artificial placenta system accordingly, with the overarching goal to bring a safe artificial placenta system to the pre-clinical stage.

By applying the human-based DNT in vitro test battery, we rank the plasticizers according to their potency. At first, we distinguished between general cytotoxic and DNT-specific hits and revealed that all tested compounds had DNT-specific effects without affecting cell viability. By determining the BMC20 values, we unravelled the most sensitive endpoints: Neurite length and % of OLs. Neurite length was adversely affected (not significant) by all tested compounds, while DEHT was the least potent one. DEHT and TOTM significantly reduced the percentage of OLs, whereas DEHP did insignificantly reduce the % of OLs and DEHA did not affect the % of OLs. However, the approach of the 'most sensitive endpoints'

did not include the number of disturbed endpoints, therefore we applied the Toxicological Priority Index (ToxPi) tool. This platform incorporates exposure data of all tested endpoints for chemical prioritization and calculates the ToxPi score. The ToxPi score is a numerical index that can be used for ranking, which is more flexible for prioritization than an absolute threshold. By applying the ToxPi tool, our study revealed DEHA as the least hazardous for neurodevelopment, and DEHP as the most hazardous one of all tested plasticizers:

DEHP > DEHT > TOTM > DEHA

For future application it is crucial to move from hazard to risk assessment by including the chemical specific exposure scenario. For example DEHA has a threefold greater potential to leach from medical devices relative to DEHP due to its lipophilic properties (Van Vliet et al., 2011). Whereas TOTM and DEHT leach significantly less compared to DEHP (Scientific Committee on Emerging and Newly-Identified Health Risks, 2016; Van Vliet et al., 2011). For a comprehensive risk assessment of the tested plasticizers, future studies should consider chemicals physical properties, free cellular concentrations as well as physiologically based biokinetic (PBBK) to better predict the compound related effect.

Overall, this study demonstrates that a human cell based DNT in vitro battery is a promising approach to prioritize compounds for hazard assessment and future risk assessment. Based on our results, DEHA is the best candidate of all tested plasticizers for the substitution of DEHP in the artificial placenta system.

#### **4. Material and Methods**

See “working plan Montcelimar Britta Kühne”

#### **5. Results**

##### **5.1. Evaluation of the effects of different plasticizers on neurodevelopment**

###### **5.1.1. DEHP**

The human neurosphere model was used to evaluate the possible adverse effects of plasticizing compounds on viability, proliferation, migration, OL, and neuronal differentiation. The classical plasticizer DEHP did not reduce the viability of proliferating NPCs neither it was cytotoxic in all tested concentrations. The increase of the proliferating area was not affected by DEHP, while the BrdU incorporation was significantly decreased after exposing 0.74 µM

DEHP in a concentration-dependent manner (Fig 1). DEHP exposure to NPCs under differentiation conditions did not show a cytotoxic effect nor disturbed the viability in all tested concentrations. The migration distance after 3 or 5 days was not affected with increasing concentration of DEHP, nor the percentage of nuclei in the migration area. The % of OLs reduced insignificantly (BMC20 = 8.6) as well as the % of neurons (BMC20 = 23.57). The total and average neurite length and the number of branching points were slightly decreased with increasing DEHP concentrations (BMC20 = 3.0; BMC20 = 2.8), while the neurite count remained unaffected (Fig. 2).

### **5.1.2. DEHT**

The alternative plasticizer DEHT did not show a cytotoxic effect on proliferating NPCs, also the viability measured by metabolic activity was not reduced in all tested concentrations. BrdU incorporation was not reduced, whereas the increase of proliferation area was significantly reduced after exposure to the highest tested concentration (20  $\mu$ M, BMC20 = 4.98, Fig. 3). DEHT exposure to differentiating NPCs did not show a cytotoxic effect, nor significantly reduced the viability. The migration distance after 3 and 5 days and the percentage of nuclei in the migration area were not altered with increasing concentration of DEHT. The OL percentage decreased significantly after 20  $\mu$ M DEHT exposure (BMC20 = 3.3), whereas the % of neurons was insignificantly reduced (BMC20 = 13.18). The total and average neurite length (BMC20 = 10.45; 12.89) slightly decreased with increasing concentrations, while the number of branching points and neurite count was not affected (Fig. 4).

### **5.1.3. TOTM**

The exposure to TOTM to proliferating NPCs did neither affect the cytotoxicity nor the viability in all tested concentrations. BrdU incorporation was significantly reduced exposing 20  $\mu$ M TOTM (BMC20 = 2.23), while the proliferation area was not adversely affected (Fig. 5). Under differential conditions, the OL % decreased significantly at a concentration of 6.67  $\mu$ M TOTM (BMC20 = 4.9), while no cytotoxic effect was detected. The migration distance and percentage of nuclei in the migration area were not disturbed. The percentage of neurons was not significantly altered (BMC20 = 18.59) but showed a high deviation between neurospheres obtained from different genders (data not shown). The endpoint neurite length was reduced with increasing concentrations of TOTM but not significant (total neurite length BMC20 = 2.7), while the number of branching points and neurite count remained unaffected (Fig. 6).



#### 5.1.4. DEHA

The alternative plasticizer DEHA did not affect the viability or cytotoxicity of proliferating NPCs. BrdU was not significantly reduced, however with an effective concentration of 11.88  $\mu\text{M}$ . The diameter increase of proliferating neurospheres was not affected (BMC20 = 27.68, Fig. 7). The exposure of DEHA to differentiating NPCs had no cytotoxic effect or disturbed the viability. The migration distance after 3 and 5 days did not alter after DEHA exposure, but the number of nuclei had a large deviation between experiments, here further investigations have to be performed. The OL and neuron percentage was not reduced by DEHA exposure. The total and average neurite length was slightly decreased with increasing concentrations of DEHA, while the number of branching points and neurite count was not affected (Fig. 8).

#### 5.2. Ranking of plasticizers

The six individual test methods (proliferation, cytotoxicity test, viability test, migration, OL, and neuronal differentiation) assess the effects of the tested plasticizers on processes that are specific for brain development. To distinguish if the plasticizers cause a DNT-specific or a general cytotoxic effect, cell viability and/or cytotoxicity was always determined in the same assay. For concentration-response curves, a sigmoidal curve fit was applied using GraphPad Prism 8.2.1. Statistical significance was calculated using one-way ANOVA with Bonferroni's post hoc tests ( $p \leq 0.05$ ). BMC20 and lower and upper confidence interval (CI) were calculated with GraphPad Prism 8.2.1. Finally, endpoints were classified as DNT-specific when the CI of cytotoxicity/ viability did not overlap with the CI of the endpoint-specific curve. All tested plasticizers did not show a cytotoxic/viability effect in all tested concentrations, and therefore all compound effects were classified as DNT-specific (Table 2). The color code of table 2 signifies the most sensitive endpoint for each plasticizer in red. Neurite length was in 3 of 4 compounds the most sensitive endpoint, followed by the % of OLs (3/4), proliferation by BrdU incorporation (2/4) and proliferation by area (1/4). For relative toxicological ranking and hierarchical clustering, the BMC20 values of the tested plasticizer were integrated and visualized by using the Toxicological Priority Index Graphical User Interface (ToxPi GUI) version 2.3. The BMC20 values across the data set of each endpoint were scaled from 0 to 1, while 1 represents the lowest BMC and therefore the most potent compound. Then, the ToxPi Tool hierarchically clusters the plasticizing compounds according to their potency and assay hit pattern. According to the ToxPi score, the potency ranking of the plasticizers was: DEHP > DEHT > TOTM > DEHA (Fig. 9).

## DEHP

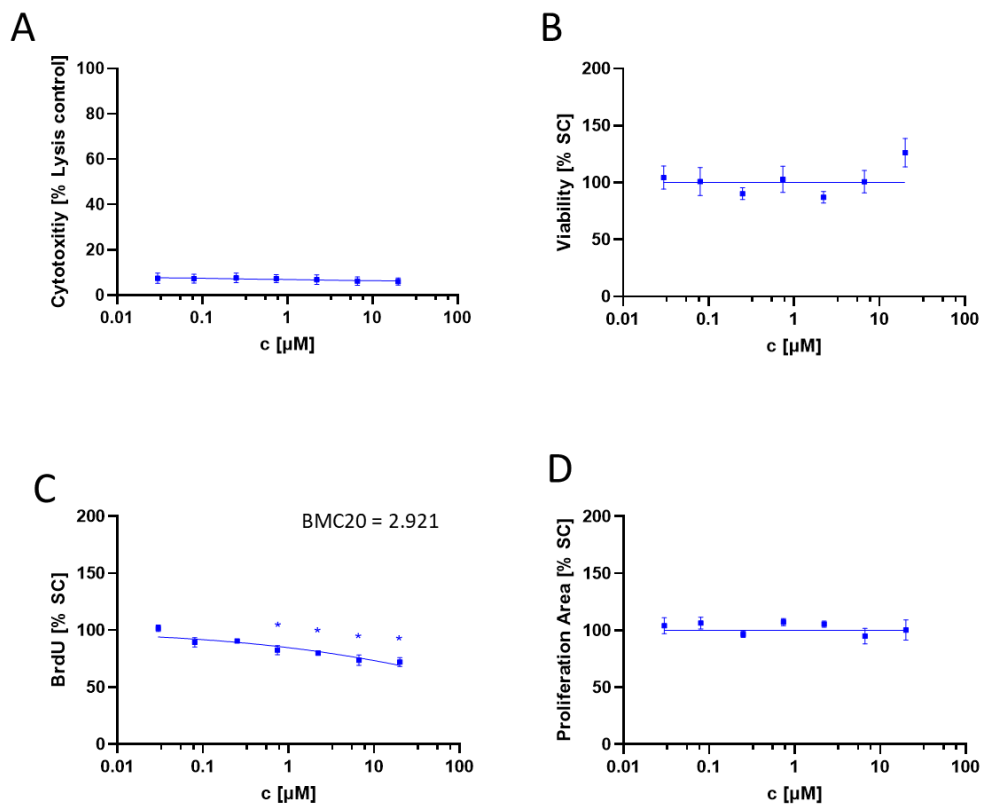


**Figure 8 “Neurosphere Assay” under proliferating conditions.** Human neuronal progenitor cells were exposed to the classical plasticizer DEHP in a serial dilution (20µM 1:3) with a range of seven concentrations and solvent control (SC). Analysis was performed after 3 days *in vitro*. (A) Cytotoxicity measured by LDH release, (B) cell viability determined by metabolic activity, (C) BrdU incorporation [% SC], (D) proliferation area determined by diameter increase. The BMC20 is indicated for endpoints showing a dose-response effect. All endpoints were evaluated in 4 neurospheres/condition in at least 3 independent experiments. Mean  $\pm$  SEM in logarithmic scale; \*:  $p < 0.05$  vs SC.

## DEHP

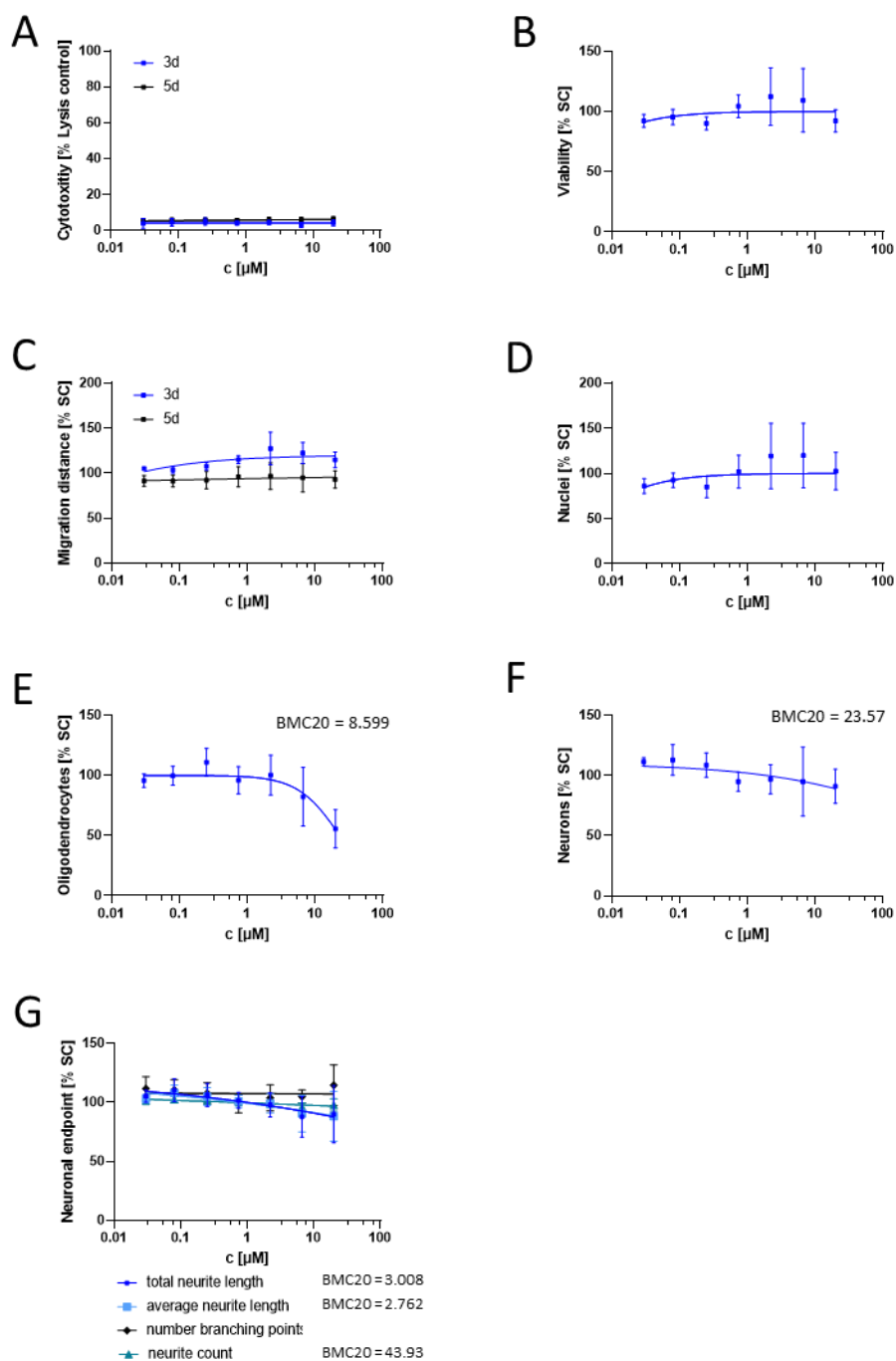


**Figure 9 “Neurosphere Assay” under differentiating conditions.** Human neuronal progenitor cells (NPCs) were exposed to the classical plasticizer DEHP in a serial dilution (20 $\mu\text{M}$  1:3) with a range of seven concentrations and solvent control (SC). Migration and cytotoxicity were measured after 3 and 5 days in vitro. Viability and differentiation analysis was performed after 5 days in vitro. (A) Cytotoxicity measured by LDH release after 3 and 5 days in culture, (B) cell viability determined by metabolic activity, (C) migration distance [ $\mu\text{m}$ ] after 3 and 5 days, (D) nuclei in [% SC], (E) Oligodendrocyte differentiation [% SC], (F) Neuronal differentiation [% SC], (G) Neuronal endpoints [% SC]: total and average neurite length, number of branching points, neurite count. The BMC20 is indicated for endpoints showing a dose-response effect. All endpoints were evaluated in 5 neurospheres/condition in at least 3 independent experiments. Mean  $\pm$  SEM in logarithmic scale; \*:  $p < 0.05$  vs SC.

# DEHT

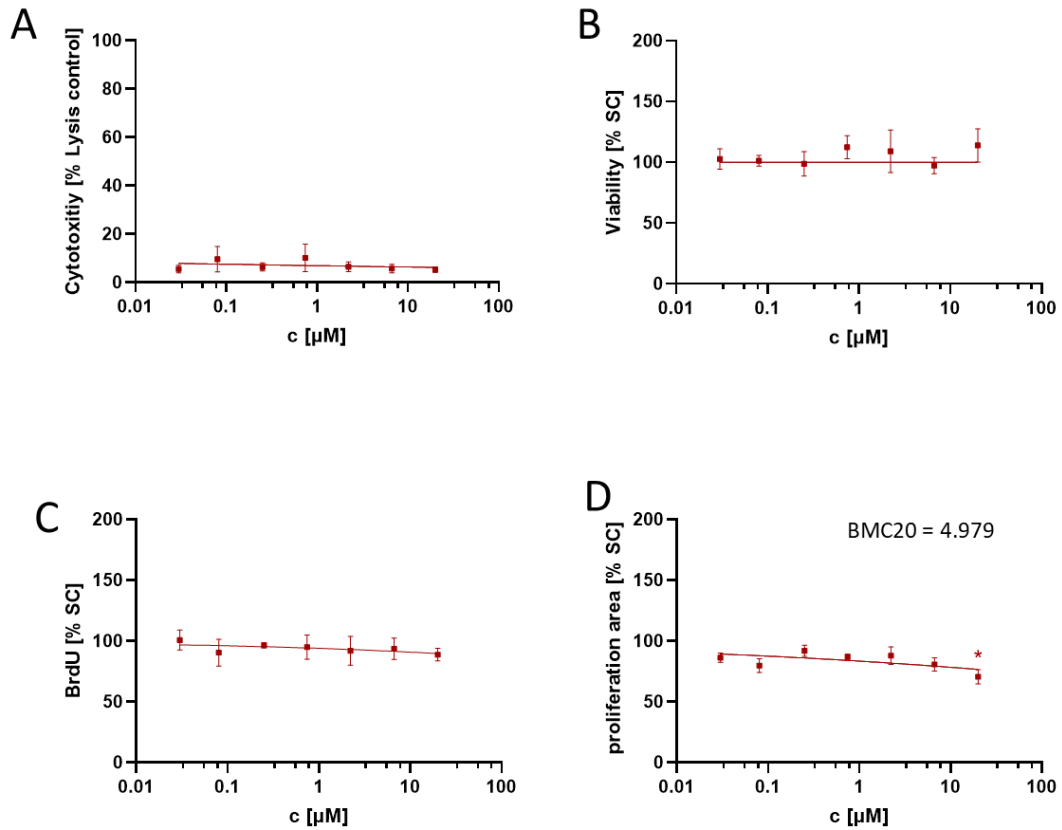


**Figure 10** “Neurosphere Assay” under proliferating conditions. Human neuronal progenitor cells were exposed to the alternative plasticizer DEHT in a serial dilution (20μM 1:3) with a range of seven concentrations and solvent control (SC). Analysis was performed after 3 days in vitro. (A) Cytotoxicity measured by LDH release, (B) cell viability determined by metabolic activity, (C) BrdU incorporation [% SC], (D) proliferation area determined by diameter increase. The BMC20 is indicated for endpoints showing a dose-response effect. All endpoints were evaluated in 4 neurospheres/condition in at least 3 independent experiments. Mean ± SEM in logarithmic scale; \*:  $p < 0.05$  vs SC.

## DEHT

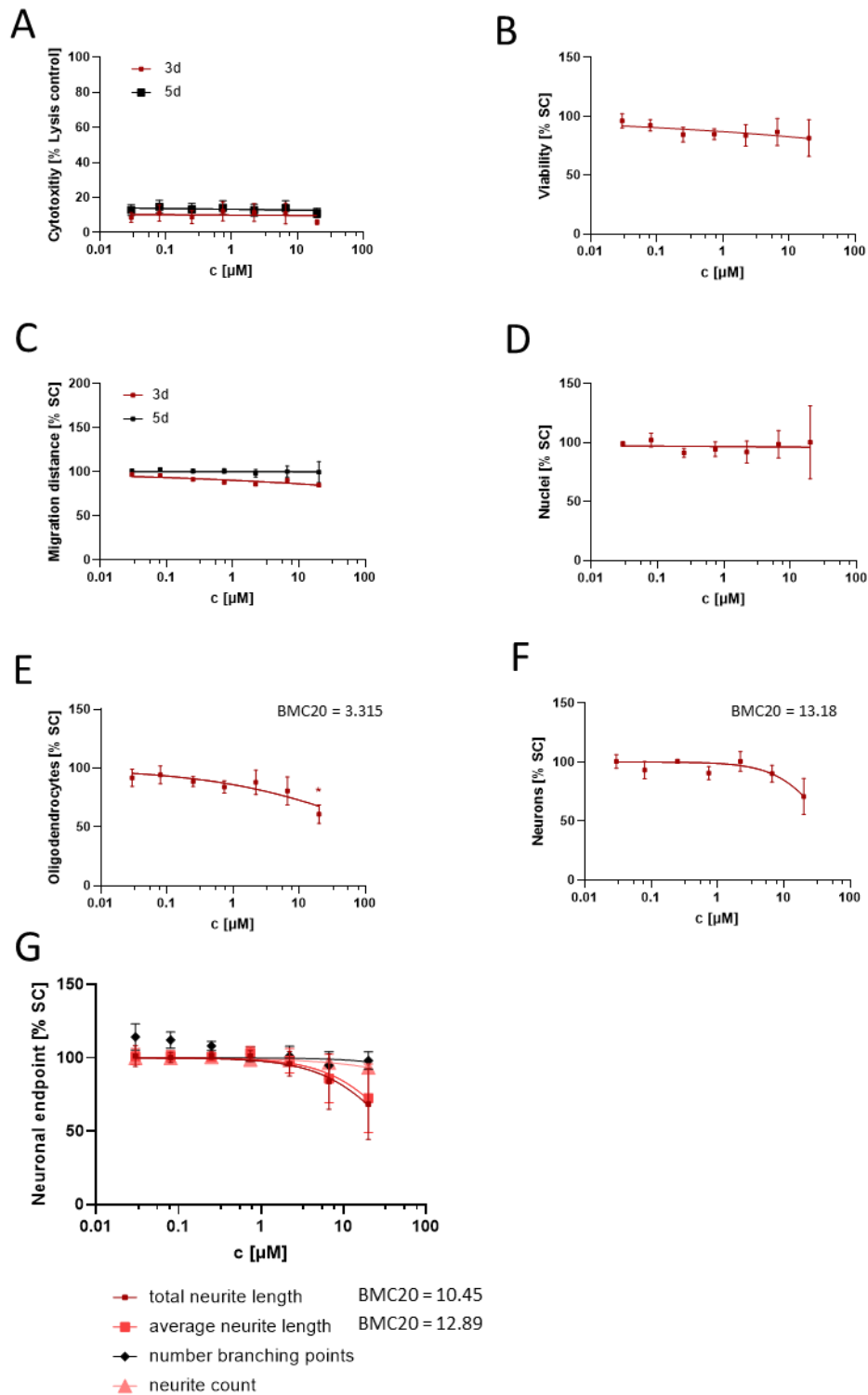


**Figure 11 “Neurosphere Assay” under differentiating conditions.** Human neuronal progenitor cells (NPCs) were exposed to the alternative plasticizer DEHT in a serial dilution (20μM 1:3) with a range of seven concentrations and solvent control (SC). Migration and cytotoxicity were measured after 3 and 5 days in vitro. Viability and differentiation analysis was performed after 5 days in vitro. (A) Cytotoxicity measured by LDH release after 3 and 5 days in culture, (B) cell viability determined by metabolic activity, (C) migration distance [μm] after 3 and 5 days, (D) nuclei in [% SC], (E) Oligodendrocyte differentiation [% SC], (F) Neuronal differentiation [% SC], (G) Neuronal endpoints [% SC]: total and average neurite length, number of branching points, neurite count. The BMC20 is indicated for endpoints showing a dose-response effect. All endpoints were evaluated in 5 neurospheres/condition in at least 3 independent experiments. Mean ± SEM in logarithmic scale; \*:  $p < 0.05$  vs SC.

# TOTM

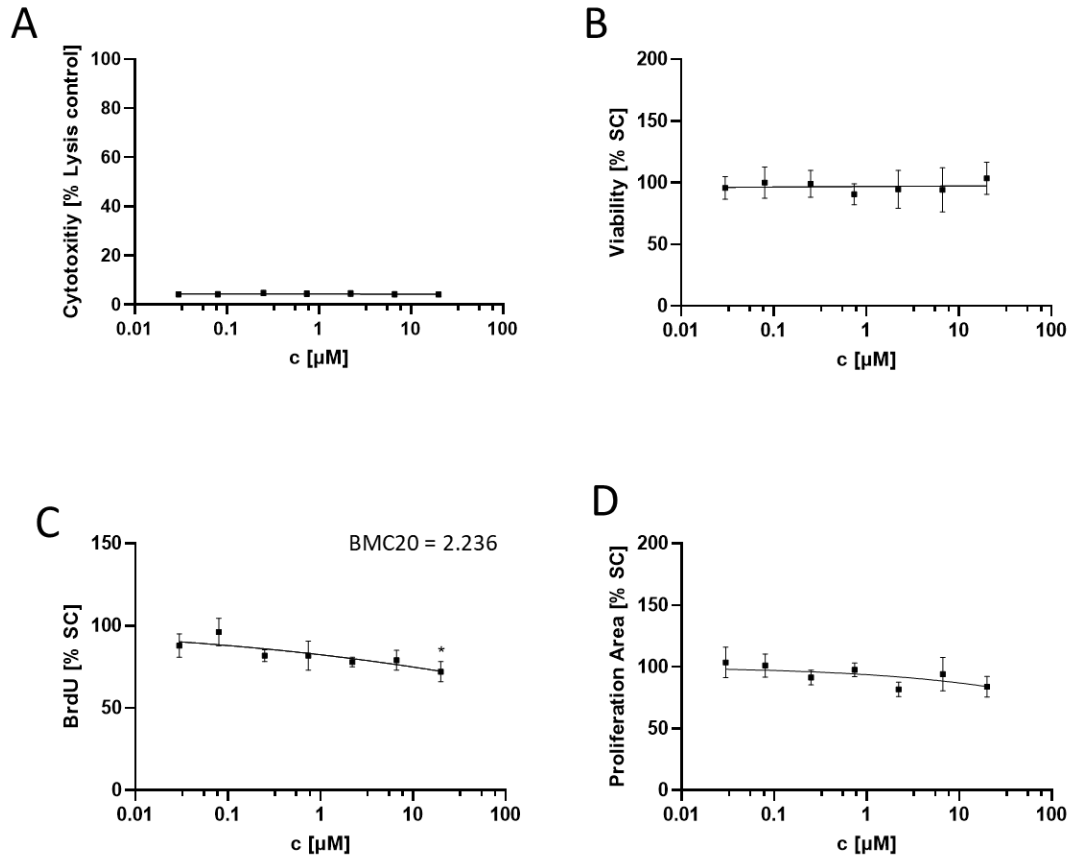


**Figure 12 “Neurosphere Assay” under proliferating conditions.** Human neuronal progenitor cells were exposed to the alternative plasticizer TOTM in a serial dilution (20µM 1:3) with a range of seven concentrations and solvent control (SC). Analysis was performed after 3 days *in vitro*. (A) Cytotoxicity measured by LDH release, (B) cell viability determined by metabolic activity, (C) BrdU incorporation [% SC], (D) proliferation area determined by diameter increase. The BMC20 is indicated for endpoints showing a dose-response effect. All endpoints were evaluated in 4 neurospheres/condition in at least 3 independent experiments. Mean ± SEM in logarithmic scale; \*:  $p < 0.05$  vs SC.

## TOTM

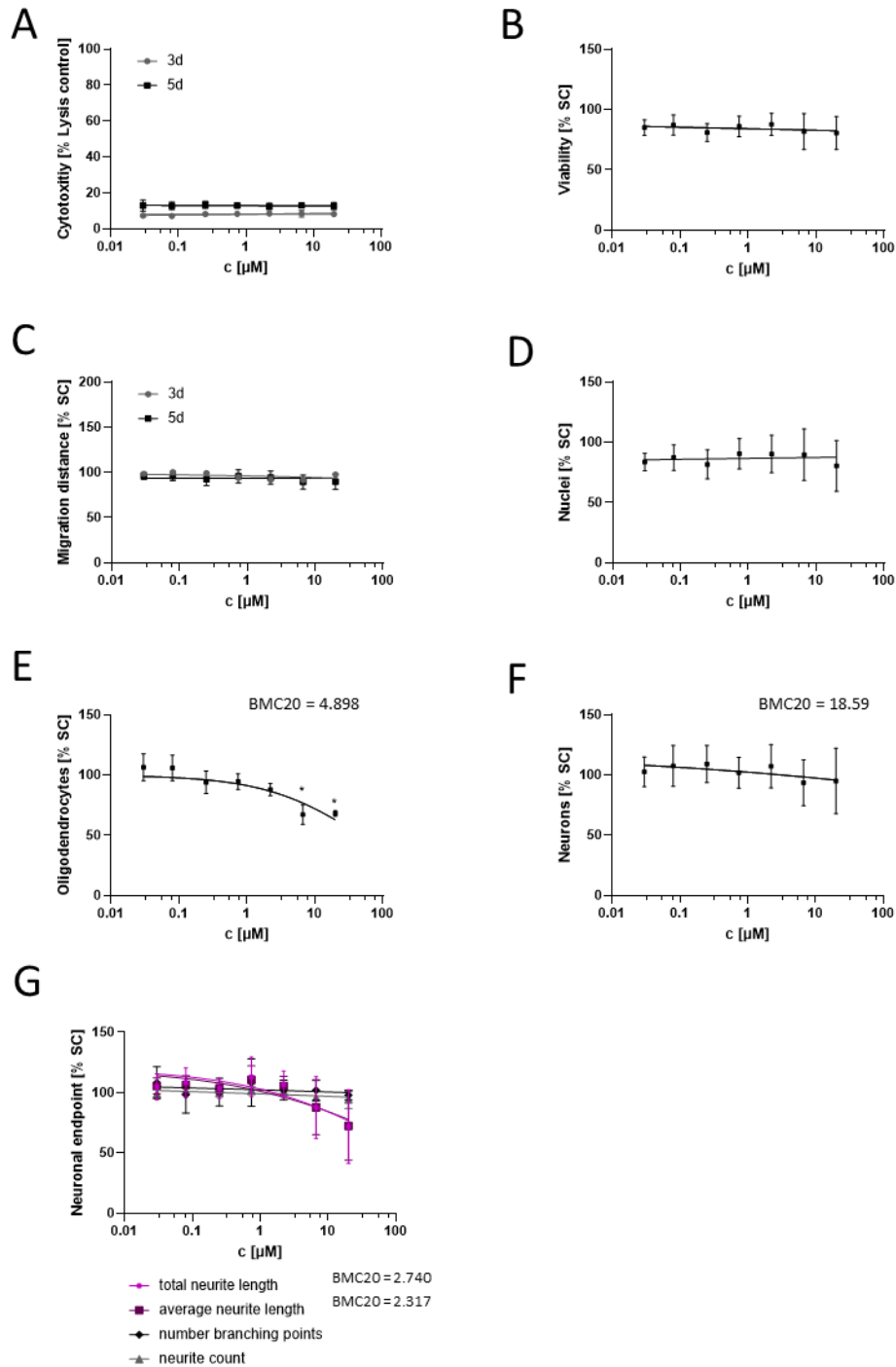


**Figure 13 “Neurosphere Assay” under differentiating conditions.** Human neuronal progenitor cells (NPCs) were exposed to the alternative plasticizer TOTM in a serial dilution (20  $\mu\text{M}$  1:3) with a range of seven concentrations and solvent control (SC). Migration and cytotoxicity were measured after 3 and 5 days *in vitro*. Viability and differentiation analysis was performed after 5 days *in vitro*. (A) Cytotoxicity measured by LDH release after 3 and 5 days in culture, (B) cell viability determined by metabolic activity, (C) migration distance [ $\mu\text{m}$ ] after 3 and 5 days, (D) nuclei in [% SC], (E) Oligodendrocyte differentiation [% SC], (F) Neuronal differentiation [% SC], (G) Neuronal endpoints [% SC]: total and average neurite length, number of branching points, neurite count. The BMC20 is indicated for endpoints showing a dose-response effect. All endpoints were evaluated in 5 neurospheres/condition in at least 3 independent experiments. Mean  $\pm$  SEM in logarithmic scale; \*:  $p < 0.05$  vs SC.

# DEHA

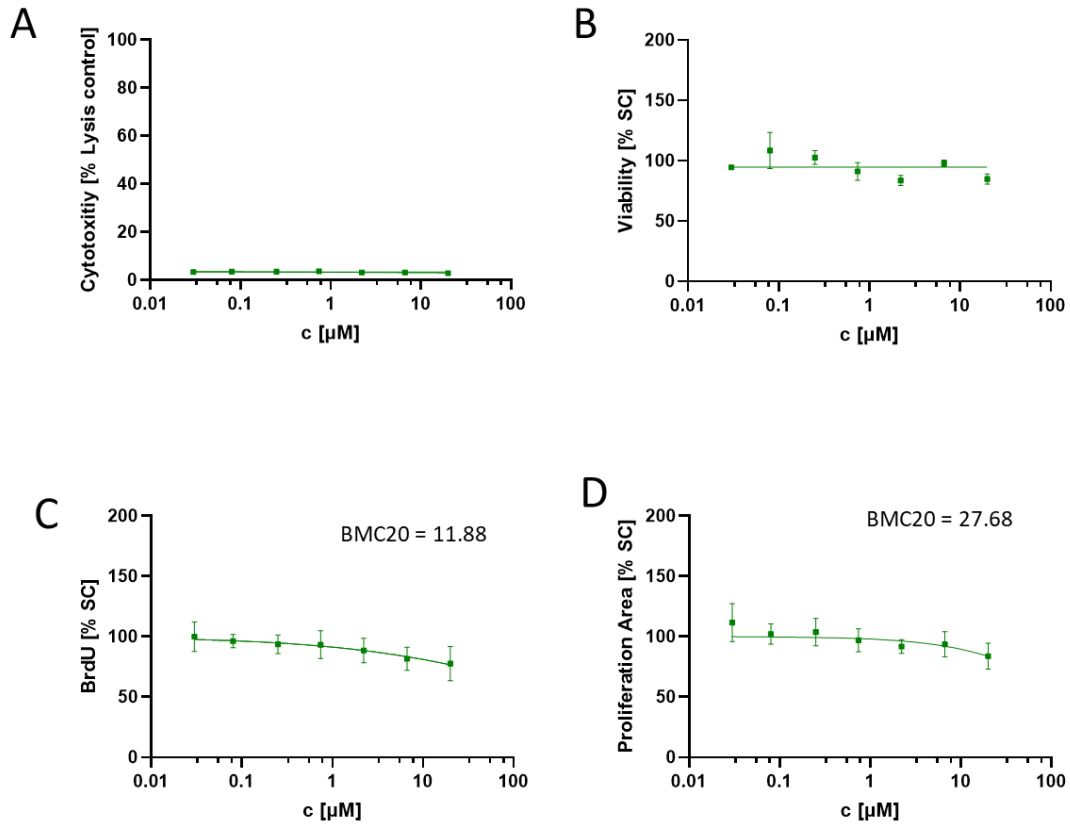


**Figure 14 “Neurosphere Assay” under proliferating conditions.** Human neuronal progenitor cells were exposed to the alternative plasticizer DEHA in a serial dilution (20µM 1:3) with a range of seven concentrations and solvent control (SC). Analysis was performed after 3 days in vitro. (A) Cytotoxicity measured by LDH release, (B) cell viability determined by metabolic activity, (C) BrdU incorporation [% SC], (D) proliferation area determined by diameter increase. The BMC20 is indicated for endpoints showing a dose-response effect. All endpoints were evaluated in 4 neurospheres/condition in at least 3 independent experiments. Mean  $\pm$  SEM in logarithmic scale; \*:  $p < 0.05$  vs SC.



# DEHA

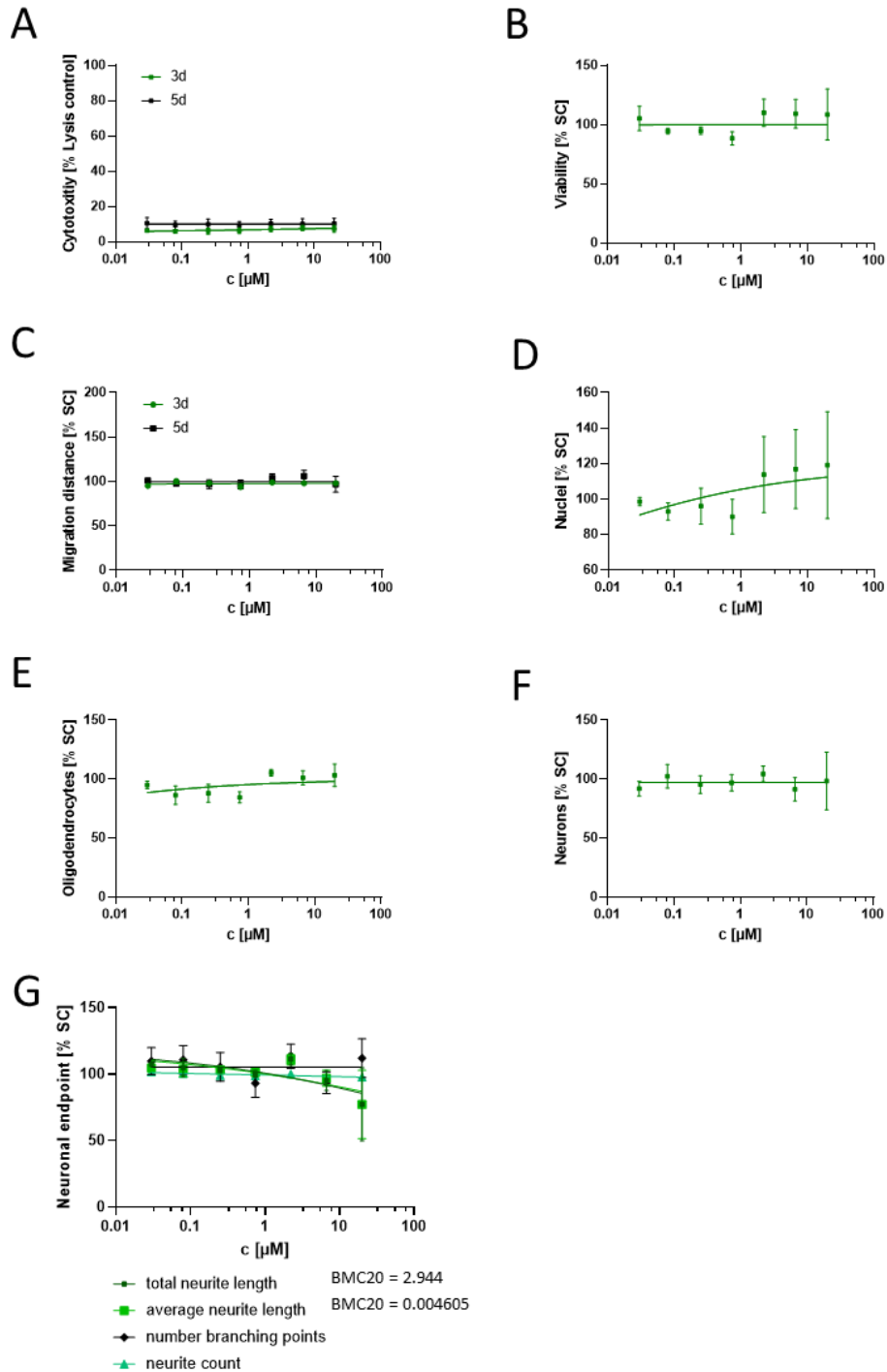
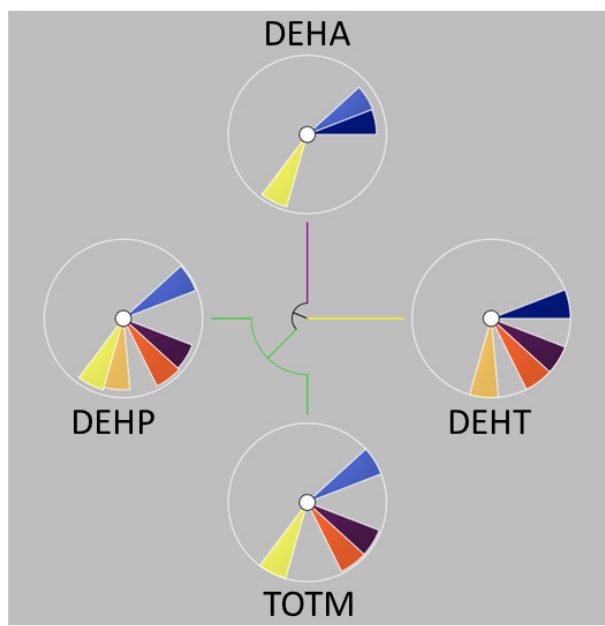


**Figure 15 “Neurosphere Assay” under differentiating conditions.** Human neuronal progenitor cells (NPCs) were exposed to the alternative plasticizer DEHA in a serial dilution (20μM 1:3) with a range of seven concentrations and solvent control (SC). Migration and cytotoxicity were measured after 3 and 5 days in vitro. Viability and differentiation analysis was performed after 5 days in vitro. (A) Cytotoxicity measured by LDH release after 3 and 5 days in culture, (B) cell viability determined by metabolic activity, (C) migration distance [μm] after 3 and 5 days, (D) nuclei in [% SC], (E) Oligodendrocyte differentiation [% SC], (F) Neuronal differentiation [% SC], (G) Neuronal endpoints [% SC]: total and average neurite length, number of branching points, neurite count. The BMC20 is indicated for endpoints showing a dose-response effect. All endpoints were evaluated in 5 neurospheres/condition in at least 3 independent experiments. Mean ± SEM in logarithmic scale; \*:  $p < 0.05$  vs SC.

**Table 2** BMC20s [ $\mu\text{M}$ ] across the DNT in vitro testing battery calculated with the best fit model using GraphPad Prism 8.2.1. All hits are DNT-specific. The colors red to green specifies the most sensitive endpoints to the least sensitive endpoints.

| <b>BMC20 [<math>\mu\text{M}</math>]</b> | <b>DEHP</b> | <b>DEHT</b> | <b>TOTM</b> | <b>DEHA</b> |
|---|-------------|-------------|-------------|-------------|
| <i>LDH 72h</i>                          | -           | -           | -           | -           |
| <i>LDH 120h</i>                         | -           | -           | -           | -           |
| <i>CTB 120h</i>                         | -           | -           | -           | -           |
| <i>Migration distance 72h</i>           | -           | -           | -           | -           |
| <i>Migration distance 120h</i>          | -           | -           | -           | -           |
| <i>Neurite count</i>                    | 43.93       | 12.89       | -           | -           |
| <i>Neurite length</i>                   | 3.01        | 10.45       | 2.74        | 2.94        |
| <i>Neuronal migration</i>               | -           | -           | -           | -           |
| <i>Number of branching points</i>       | -           | -           | -           | -           |
| <i>% of neurons</i>                     | 23.57       | 13.18       | 18.59       | -           |
| <i>Number of nuclei</i>                 | -           | -           | -           | -           |
| <i>% of oligodendrocytes</i>            | 8.60        | 3.32        | 4.90        | -           |
| <i>Oligodendrocyte migration</i>        | -           | -           | -           | -           |
| <i>Proliferation by area</i>            | -           | 4.98        | -           | 27.68       |
| <i>Proliferation by BrdU</i>            | 2.92        | -           | 2.24        | 11.88       |
| <i>Proliferation LDH</i>                | -           | -           | -           | -           |
| <i>Proliferation CTB</i>                | -           | -           | -           | -           |



| Ranking | Plasticizer | ToxPi Score |
|---------|-------------|-------------|
| 1       | DEHP        | 0.2749      |
| 2       | DEHT        | 0.2353      |
| 3       | TOTM        | 0.2317      |
| 4       | DEHA        | 0.1575      |

| Endpoint                   | Color        |
|----------------------------|--------------|
| proliferation by area      | Dark Blue    |
| proliferation by brdu      | Blue         |
| proliferation ctb          | Cyan         |
| proliferation ldh          | Blue         |
| glia migration 72h         | Dark Green   |
| glia migration 120h        | Dark Green   |
| neuronal migration         | Light Green  |
| oligo. migration           | Bright Green |
| ldh 72h                    | Dark Red     |
| ldh 120h                   | Red          |
| ctb 120h                   | Pink         |
| neurite length             | Yellow       |
| neurite count              | Orange       |
| number of branching points | Orange       |
| number of neurons          | Red-Orange   |
| number of oligodendrocytes | Dark Purple  |
| number of nuclei           | Light Purple |





## DECLARACIÓ D'ORIGINALITAT

Jo, .....Britta Anna Kühne , matriculat al programa de doctorat ...en Biomedicina... de la Universitat de Barcelona declaro que la tesi titulada “Safety and efficacy investigations for new prenatal neuroprotective therapies. Applications in a model of intrauterine growth restriction (IUGR)” és original, que la investigació que vaig realitzar compleix els codis ètics i les bones practiques i que la tesi no inclou plagi. Soc conscient i accepto per escrit que la meva tesi se sotmetrà al procés adequat per provar l’originalitat dels meus resultats.

Data 22 de Juliol de 2022





### CONFIRMACIÓ D'ORIGINALITAT

Declaro que la tesi titulada "Safety and efficacy investigations for new prenatal neuroprotective therapies. Applications in a model of intrauterine growth restriction (IUGR)" presentada pel Sr./a ..Britta Anna Kühne, sota la meva supervisió, compleix els codis ètics i les bones pràctiques i no tinc coneixement de que s'hagi produït cap plagi.

Data 21 de Juliol de 2022

(signatura)

Nom i cognoms

MARTA BARENYES ESPADALER

(signatura)

Nom i cognoms

Dr. Miriam Illa

